

Special Issue Reprint

Cellular and Molecular Mechanisms in Immune Regulation

Edited by Fábio Rinaldo Santori and Natalia B. Ivanova

mdpi.com/journal/cells



Cellular and Molecular Mechanisms in Immune Regulation

Cellular and Molecular Mechanisms in Immune Regulation

Guest Editors

Fábio Rinaldo Santori Natalia B. Ivanova



Guest Editors

Fábio Rinaldo Santori Natalia B. Ivanova

Center for Molecular Department of Biochemistry

Medicine and Molecular Biology University of Georgia University of Georgia

Athens, GA Athens, GA

USA USA

Editorial Office MDPI AG Grosspeteranlage 5 4052 Basel, Switzerland

This is a reprint of the Special Issue, published open access by the journal *Cells* (ISSN 2073-4409), freely accessible at: https://www.mdpi.com/journal/cells/special_issues/RT7P6M9Y9M.

For citation purposes, cite each article independently as indicated on the article page online and as indicated below:

Lastname, A.A.; Lastname, B.B. Article Title. Journal Name Year, Volume Number, Page Range.

ISBN 978-3-7258-5805-7 (Hbk) ISBN 978-3-7258-5806-4 (PDF) https://doi.org/10.3390/books978-3-7258-5806-4

© 2025 by the authors. Articles in this book are Open Access and distributed under the Creative Commons Attribution (CC BY) license. The book as a whole is distributed by MDPI under the terms and conditions of the Creative Commons Attribution-NonCommercial-NoDerivs (CC BY-NC-ND) license (https://creativecommons.org/licenses/by-nc-nd/4.0/).

Contents

Fabio R. Santori and Natalia B. Ivanova First Edition Special Issue on "Cellular and Molecular Mechanisms in Immune Regulation" Reprinted from: Cells 2025, 14, 1614, https://doi.org/10.3390/cells14201614
Borros Arneth
Molecular Mechanisms of Immune Regulation: A Review
Reprinted from: Cells 2025, 14, 283, https://doi.org/10.3390/cells14040283
Valeria Lodde, Ignazio Roberto Zarbo, Gabriele Farina, Aurora Masia, Paolo Solla, Ilaria Campesi, et al.
Identification of hsa_circ_0018905 as a New Potential Biomarker for Multiple Sclerosis Reprinted from: Cells 2024, 13, 1668, https://doi.org/10.3390/cells13191668 29
Soo Yeun Sim, In-Cheol Baek, Won Kyoung Cho, Min Ho Jung, Tai-Gyu Kim and Byung-Kyu Suh
Immune Gene Expression Profiling in Individuals with Turner Syndrome, Graves' Disease, and
a Healthy Female by Single-Cell RNA Sequencing: A Comparative Study
Reprinted from: Cells 2025, 14, 93, https://doi.org/10.3390/cells14020093 50
Aldo Ferreira-Hermosillo, Paola Santana-Sánchez, Ricardo Vaquero-García, Manuel R. García-Sáenz, Angélica Castro-Ríos, Adriana K. Chávez-Rueda, et al.
Circulating T Cell Subsets in Type 1 Diabetes
Reprinted from: Cells 2025, 14, 48, https://doi.org/10.3390/cells14010048
Jiani Xing, Takese McKenzie and Jian Hu
Lipid-Laden Microglia: Characterization and Roles in Diseases
Reprinted from: Cells 2025, 14, 1281, https://doi.org/10.3390/cells14161281
Takumi Memida, Guoqin Cao, Elaheh Dalir Abdolahinia, Sunniva Ruiz, Shengyuan Huang, Sahar Hassantash, et al.
B10 Promotes Polarization and Pro-Resolving Functions of Bone Marrow Derived Macrophages
(BMDM) Through PD-1 Activation Reprinted from: <i>Cells</i> 2025 , <i>14</i> , 860, https://doi.org/10.3390/cells14120860
Sohrab Ahmadivand, Robert Fux and Dušan Palić
Role of T Follicular Helper Cells in Viral Infections and Vaccine Design
Reprinted from: Cells 2025, 14, 508, https://doi.org/10.3390/cells14070508
Islam Eljilany, Sam Coleman, Aik Choon Tan, Martin D. McCarter, John Carpten, Howard Colman, et al.
Differential Infiltration of Key Immune T-Cell Populations Across Malignancies Varying by
Immunogenic Potential and the Likelihood of Response to Immunotherapy
Reprinted from: Cells 2024, 13, 1993, https://doi.org/10.3390/cells14201614
Tyler H. Montgomery, Anuj P. Master, Zeng Jin, Qiongyu Shi, Qin Lai, Rohan Desai, et al. Tissue-Resident Memory T Cells in Cancer Metastasis Control
Reprinted from: Cells 2025, 14, 1297, https://doi.org/10.3390/cells14161297
Antonia Peter, Morgane Vermeulen, Mats Van Delen, Amber Dams, Stefanie Peeters,
Hans De Reu, et al.
Physiological Oxygen Levels in the Microenvironment Program Ex Vivo-Generated
Conventional Dendritic Cells Toward a Tolerogenic Phenotype
Reprinted from: Cells 2025, 14, 736, https://doi.org/10.3390/cells14100736

Gelare Ghajar-Rahimi, Nabiha Yusuf and Hui Xu	
Ultraviolet Radiation-Induced Tolerogenic Dendritic Cells in Skin: Insights and Mechanisms	
Reprinted from: Cells 2025, 14, 308, https://doi.org/10.3390/cells14040308	:13





Editorial

First Edition Special Issue on "Cellular and Molecular Mechanisms in Immune Regulation"

Fabio R. Santori * and Natalia B. Ivanova *

Center for Molecular Medicine, University of Georgia, 325 Riverbend Road, Athens, GA 30602, USA * Correspondence: fabio.santori@uga.edu (F.R.S.); natalia.ivanova@uga.edu (N.B.I.)

In 1974, Niels K. Jerne proposed one of the first theories of immunoregulation [1]. Indeed, in his prescient paper he projected that the decades of 1970–1990 would be centered on systemic immune regulation mediated by cells cooperating with each other in multicellular networks [1]. It has been suggested that this self-regulating network of immune cells would function as an "immune sensory brain" that interprets changes in the body epitope repertoire recognized by the antigen-specific receptors of B and T cells [2]. Treating the immune system as an "immune sensory brain" suggests that it is flexible and that it could be "trained" to respond to specific stimuli and learn from its experiences. This could lead to changes in "immune sensory perception" and interpretation of bodily states. In practical terms it would mean that we could train the immune system to recognize tumors as targets for removal. This would include tumors that are naturally not immunogenic, such as those characterized as immune deserts [3].

Jerne's predictions are now coming to fruition. The importance of immunoregulation to medicine was recognized by the 2025 Nobel Prize in Medicine and Physiology awarded to Mary E. Brunknow, Fred Ramsdell and Shimon Sakaguchi. Although we are still analyzing the regulation of the immune system in parts, with T cells, B cells and macrophages being mostly studied separately, one could foresee that the next few decades will see an explosion of systemic multi-cellular network approaches being used in the study and treatment of cancer, autoimmune diseases, allergies and infections. The first edition of the Special Issue on "Cellular and Molecular Mechanisms in Immune Regulation" reflects the current state of the field of immune regulation and its movement towards a systemic multi-cellular approach.

As an opening note, we start with a systematic review of the latest advances in the molecular mechanisms of immune regulation by Dr. Arneth [4], which is followed by the work of Lodde and colleagues which analyzes the use of circular RNAs as potential biomarkers of immune function in multiple sclerosis [5]. The article by Sim and colleagues explores the effect of X chromosome loss (Turner syndrome) on immunoregulation [6]. Despite the small sample of their patient cohort, their results are intriguing, suggesting that at least 43 immunoregulatory genes may be affected by the loss of chromosome X. We are looking forward to larger studies that will strengthen and expand these results.

The next focus of the Special Issue is on autoimmunity, and the article by Ferreira-Hermosillo and colleagues provides us a glimpse of circulating T cell subsets in Type 1 diabetes [7]. The role of lipid biosynthesis and catabolism in immune regulation is highlighted in the review by Jiani Xing, Takese Mckenzie and Jian Hu, where the authors focus on the role of lipid-laden microglia in inflammation that accompanies neurodegenerative diseases as well as the healing processes following spinal cord injuries and strokes [8]. The article by Memida and colleagues explores the role of IL-10-producing regulatory B cells in

the generation of M2 anti-inflammatory macrophages [9]. The review by Sorab Ahmadivand, Robert Fux and Dušan Palič highlights recent advances in the field of immune cell communication focusing on the interaction of T follicular helper cells and B cells in viral infections and vaccine design [10]. The role of immune regulation in cancer is explored by two research articles. Eljilany and colleagues et al. [11] report the analyses of immune populations in patients with ovarian, bladder, pancreatic cancer and melanoma. Indeed, these authors report a beneficial effect of the increase of tissue resident memory T cells (TRMs) in the therapeutic outcome of patients treated with immune checkpoint inhibitors. This leads us to the review by Montgomery and colleagues [12] on the role of TRMs in the control of metastasis. TRMs are, indeed, a promising avenue for cancer therapy in metastatic disease. However, our models are currently limited to lung metastasis and more studies are needed to evaluate and promote the role of TRMs in the treatment of metastasis in brain, bone marrow and liver [12].

The Special Issue concludes with two articles highlighting the interactions between the environment and immune system, specifically on the role of oxygen tension and ultraviolet light (UV). The key is to understand how the homeostasis between organism and immune system is maintained with a changing environment. Here, the role of oxygen plays a key role. The work by Peter and colleagues [13] focuses on the role of oxygen and suggests that under physiological tissue concentrations of oxygen (4% O_2 , normoxia), dendritic cells shift towards a tolerogenic phenotype which contrasts with a pro-inflammatory phenotype observed under hyperoxia (21% O_2) or hypoxia (<2% O_2) [14]. Similarly, the skin in our body is in constant contact with light. UV light can cause mutations and dimerization of DNA but it is also required for production of vitamin D. The review by Gelare Ghajar-Rahimi, Nabiha Yusuf and Hui Xu [15] highlights the recent advances in our understanding of the role and mechanism by which UV can promote a tolerogenic phenotype in dendritic cell populations in the skin. The authors suggest that the tolerogenic effect of UV has both beneficial and pathologic aspects; thus, a delicate balance is necessary to maintain bodily homeostasis.

The first edition of the Special Issue on "Cellular and Molecular Mechanisms in Immune Regulation" gives a glimpse of the multi-cellular immunoregulatory networks implicated in autoimmune diseases, infection and cancer, as well as during normal interactions with the environment. Many topics were left unexplored, such as the regulation of pain and sensory nerve endings during immune responses, the interplay between the nervous system and the development of the immune system during ontogeny. We expect to cover many of these topics in the upcoming second edition of "Cellular and Molecular Mechanisms in Immune Regulation".

Conflicts of Interest: The authors declare no conflict of interest.

List of Contributions:

- 1. Arneth, B. Molecular Mechanisms of Immune Regulation: A Review. *Cells* **2025**, *14*, 283. https://doi.org/10.3390/cells14040283.
- 2. Lodde, V.; Zarbo, I.R.; Farina, G.; Masia, A.; Solla, P.; Campesi, I.; Delogu, G.; Muroni, M.R.; Tsitsipatis, D.; Gorospe, M.; et al. Identification of hsa_circ_0018905 as a New Potential Biomarker for Multiple Sclerosis. *Cells* **2024**, *13*, 1668. https://doi.org/10.3390/cells13191668.
- 3. Sim, S.Y.; Baek, I.C.; Cho, W.K.; Jung, M.H.; Kim, T.G.; Suh, B.K. Immune Gene Expression Profiling in Individuals with Turner Syndrome, Graves' Disease, and a Healthy Female by Single-Cell RNA Sequencing: A Comparative Study. *Cells* **2025**, *14*, 93. https://doi.org/10.3 390/cells14020093.
- 4. Ferreira-Hermosillo, A.; Santana-Sanchez, P.; Vaquero-Garcia, R.; Garcia-Saenz, M.R.; Castro-Rios, A.; Chavez-Rueda, A.K.; Gomez-Diaz, R.A.; Chavez-Sanchez, L.; Legorreta-Haquet, M.V. Circulating T Cell Subsets in Type 1 Diabetes. *Cells* **2025**, *14*, 48. https://doi.org/10.3390/cells14010048.

- 5. Xing, J.; McKenzie, T.; Hu, J. Lipid-Laden Microglia: Characterization and Roles in Diseases. *Cells* **2025**, *14*, 1281. https://doi.org/10.3390/cells14161281.
- Memida, T.; Cao, G.; Dalir Abdolahinia, E.; Ruiz, S.; Huang, S.; Hassantash, S.; Shindo, S.; Okamoto, M.; Yamashita, S.; Nakamura, S.; et al. B10 Promotes Polarization and Pro-Resolving Functions of Bone Marrow Derived Macrophages (BMDM) Through PD-1 Activation. *Cells* 2025, 14, 860. https://doi.org/10.3390/cells14120860.
- 7. Ahmadivand, S.; Fux, R.; Palic, D. Role of T Follicular Helper Cells in Viral Infections and Vaccine Design. *Cells* **2025**, *14*, 508. https://doi.org/10.3390/cells14070508.
- 8. Eljilany, I.; Coleman, S.; Tan, A.C.; McCarter, M.D.; Carpten, J.; Colman, H.; Naqash, A.R.; Puzanov, I.; Arnold, S.M.; Churchman, M.L.; et al. Differential Infiltration of Key Immune T-Cell Populations Across Malignancies Varying by Immunogenic Potential and the Likelihood of Response to Immunotherapy. *Cells* **2024**, *13*, 1993. https://doi.org/10.3390/cells13231993.
- 9. Montgomery, T.H.; Master, A.P.; Jin, Z.; Shi, Q.; Lai, Q.; Desai, R.; Zhang, W.; Maharjan, C.K.; Kolb, R. Tissue-Resident Memory T Cells in Cancer Metastasis Control. *Cells* **2025**, *14*, 1297. https://doi.org/10.3390/cells14161297.
- Peter, A.; Vermeulen, M.; Van Delen, M.; Dams, A.; Peeters, S.; De Reu, H.; Marei, W.F.A.; Berneman, Z.N.; Cools, N. Physiological Oxygen Levels in the Microenvironment Program Ex Vivo-Generated Conventional Dendritic Cells Toward a Tolerogenic Phenotype. *Cells* 2025, 14, 736. https://doi.org/10.3390/cells14100736.
- 11. Ghajar-Rahimi, G.; Yusuf, N.; Xu, H. Ultraviolet Radiation-Induced Tolerogenic Dendritic Cells in Skin: Insights and Mechanisms. *Cells* **2025**, *14*, 308. https://doi.org/10.3390/cells14040308.

References

- 1. Jerne, N.K. Towards a network theory of the immune system. Ann. Immunol. 1974, 125C, 373–389.
- 2. Santori, F.R. The immune system as a self-centered network of lymphocytes. *Immunol. Lett.* **2015**, *166*, 109–116. [CrossRef] [PubMed]
- 3. Combes, A.J.; Samad, B.; Tsui, J.; Chew, N.W.; Yan, P.; Reeder, G.C.; Kushnoor, D.; Shen, A.; Davidson, B.; Barczak, A.J.; et al. Discovering dominant tumor immune archetypes in a pan-cancer census. *Cell* **2022**, *185*, 184–203.e119. [CrossRef] [PubMed]
- 4. Arneth, B. Molecular Mechanisms of Immune Regulation: A Review. Cells 2025, 14, 283. [CrossRef] [PubMed]
- 5. Lodde, V.; Zarbo, I.R.; Farina, G.; Masia, A.; Solla, P.; Campesi, I.; Delogu, G.; Muroni, M.R.; Tsitsipatis, D.; Gorospe, M.; et al. Identification of hsa_circ_0018905 as a New Potential Biomarker for Multiple Sclerosis. *Cells* **2024**, *13*, 1668. [CrossRef] [PubMed]
- 6. Sim, S.Y.; Baek, I.C.; Cho, W.K.; Jung, M.H.; Kim, T.G.; Suh, B.K. Immune Gene Expression Profiling in Individuals with Turner Syndrome, Graves' Disease, and a Healthy Female by Single-Cell RNA Sequencing: A Comparative Study. *Cells* **2025**, *14*, 93. [CrossRef] [PubMed]
- 7. Ferreira-Hermosillo, A.; Santana-Sanchez, P.; Vaquero-Garcia, R.; Garcia-Saenz, M.R.; Castro-Rios, A.; Chavez-Rueda, A.K.; Gomez-Diaz, R.A.; Chavez-Sanchez, L.; Legorreta-Haquet, M.V. Circulating T Cell Subsets in Type 1 Diabetes. *Cells* 2025, 14, 48. [CrossRef] [PubMed]
- 8. Xing, J.; McKenzie, T.; Hu, J. Lipid-Laden Microglia: Characterization and Roles in Diseases. *Cells* **2025**, *14*, 1281. [CrossRef] [PubMed]
- 9. Memida, T.; Cao, G.; Dalir Abdolahinia, E.; Ruiz, S.; Huang, S.; Hassantash, S.; Shindo, S.; Okamoto, M.; Yamashita, S.; Nakamura, S.; et al. B10 Promotes Polarization and Pro-Resolving Functions of Bone Marrow Derived Macrophages (BMDM) Through PD-1 Activation. *Cells* **2025**, *14*, 860. [CrossRef] [PubMed]
- 10. Ahmadivand, S.; Fux, R.; Palic, D. Role of T Follicular Helper Cells in Viral Infections and Vaccine Design. *Cells* **2025**, *14*, 508. [CrossRef] [PubMed]
- 11. Eljilany, I.; Coleman, S.; Tan, A.C.; McCarter, M.D.; Carpten, J.; Colman, H.; Naqash, A.R.; Puzanov, I.; Arnold, S.M.; Churchman, M.L.; et al. Differential Infiltration of Key Immune T-Cell Populations Across Malignancies Varying by Immunogenic Potential and the Likelihood of Response to Immunotherapy. *Cells* **2024**, *13*, 1993. [CrossRef] [PubMed]
- 12. Montgomery, T.H.; Master, A.P.; Jin, Z.; Shi, Q.; Lai, Q.; Desai, R.; Zhang, W.; Maharjan, C.K.; Kolb, R. Tissue-Resident Memory T Cells in Cancer Metastasis Control. *Cells* 2025, 14, 1297. [CrossRef] [PubMed]
- 13. Peter, A.; Vermeulen, M.; Van Delen, M.; Dams, A.; Peeters, S.; De Reu, H.; Marei, W.F.A.; Berneman, Z.N.; Cools, N. Physiological Oxygen Levels in the Microenvironment Program Ex Vivo-Generated Conventional Dendritic Cells Toward a Tolerogenic Phenotype. *Cells* 2025, 14, 736. [CrossRef] [PubMed]

- 14. Peter, A.; Berneman, Z.N.; Cools, N. Cellular respiration in dendritic cells: Exploring oxygen-dependent pathways for potential therapeutic interventions. *Free Radic. Biol. Med.* **2025**, 227, 536–556. [CrossRef] [PubMed]
- 15. Ghajar-Rahimi, G.; Yusuf, N.; Xu, H. Ultraviolet Radiation-Induced Tolerogenic Dendritic Cells in Skin: Insights and Mechanisms. *Cells* **2025**, *14*, 308. [CrossRef] [PubMed]

Disclaimer/Publisher's Note: The statements, opinions and data contained in all publications are solely those of the individual author(s) and contributor(s) and not of MDPI and/or the editor(s). MDPI and/or the editor(s) disclaim responsibility for any injury to people or property resulting from any ideas, methods, instructions or products referred to in the content.





Review

Molecular Mechanisms of Immune Regulation: A Review

Borros Arneth 1,2

- ¹ Institute of Laboratory Medicine and Pathobiochemistry, Hospital of the Universities of Giessen and Marburg UKGM, Philipps University Marburg, Baldingerst 1, 35043 Marburg, Germany; borros.arneth@staff.uni-marburg.de
- Institute of Laboratory Medicine and Pathobiochemistry, Hospital of the Universities of Giessen and Marburg UKGM, Justus Liebig University Giessen, Feulgenstr. 12, 35392 Giessen, Germany

Abstract: Background: The immune system must carefully balance fighting pathogens with minimization of inflammation and avoidance of autoimmune responses. Over the past ten years, researchers have extensively studied the mechanisms regulating this delicate balance. Comprehending these mechanisms is essential for developing treatments for inflammatory conditions. Aim: This review aims to synthesize knowledge of immunoregulatory processes published from 2014–2024 and to highlight discoveries that provide fresh perspectives on this complex balance. Methods: The keywords "molecular mechanisms", "immune regulation", "immune signaling pathways", and "immune homeostasis" were used to search PubMed for articles published between 2014 and 2024, with a preference for articles published in the past three years. Results: Recent research has pinpointed the impact of factors such as cytokine signaling, T-cell regulation, epigenetic regulation, and immunometabolism on immune function. Discussion: New research highlights the intricate interactions between the immune system and other molecular elements. A key area of interest is the impact of non-coding RNAs and metabolic pathways on the regulation of immune responses. Conclusions: Exploring the mechanisms by which the immune system is regulated will provide new avenues for developing treatments to address autoimmune and inflammatory conditions.

Keywords: immune checkpoints; cytokine signaling; epigenetic modifications; non-coding RNAs; regulatory T cells (Tregs)

1. Introduction

The immune system has to strike a careful balance between tolerance to self-antigens and defense against infections. Precise molecular mechanisms that control immune activation and avoid excessive or inappropriate immunological responses are responsible for achieving this equilibrium. The topic of immune regulation is broad and complex, involving many different processes, including sirtuins, autophagy, inflammasome activation, mitochondrial function, post-translational changes, miRNA-mediated epigenetic control, and TLR signaling. Because immune regulation is so broad, it is not possible to adequately examine every facet in a single paper. Therefore, the main processes that are essential for preserving immunological homeostasis are the subject of this review. These mechanisms include immunometabolism, cytokine signaling, immune checkpoints, regulatory T cells, and epigenetic changes.

Research on these regulatory systems has evolved significantly over the past ten years, exposing the intricate interactions among metabolic and epigenetic changes, cellular checkpoints, and signaling pathways. Although these mechanisms are intricately interrelated, many parts are still poorly understood. In order to present a current analysis of the

molecular mechanisms of immune regulation, this systematic review integrates findings from the literature published between 2014 and 2024. It highlights new findings, their interactions, and their potential therapeutic applications in the treatment of autoimmune diseases, inflammatory conditions, and immune-related disorders.

2. Historical Perspectives on Immune Regulation

The control of the immune system has been an area of immense interest among scientists for nearly half a century. Research has traced some of the roots of modern understanding of immunity to very few initial observations. The main landmarks in this field comprise identifying antibodies, acknowledging their specificity, and discovering lymphocytes and their capacity for immune reactions [1]. The first discoveries in immune regulation included tolerance and autoimmunity, some early theories being Burnet's clonal selection theory in the 1950s, which explained the immune system's self-recognition [2]. These formed the basis for further investigations into how an immune response is initiated, regulated, and terminated.

Nevertheless, several questions remain unanswered despite these advancements. For instance, how is tolerance in terms of immunity sustained when there are intricacies in microenvironments, and what molecular markers guarantee the stability of the regulatory systems? Altogether, these questions are evidence of the continuous need to investigate the fundamental mechanisms of immune regulation further.

Deeper Historical and Mechanistic Analysis

Tregs were discovered in the 1990s and are a specialized subset of a cluster of differentiation 4 (CD4) T cells recognized to be constitutionally pivotal for immunologic tolerance and autoimmunity suppression [3]. Established through the T-cell-specific transcription factor, FOXP3, Tregs use pathways such as cytokines, metabolites, and cell contacts to modulate immune responses [3]. Interleukin-10 appeared on the scene in the late 1990s, and this cytokine was found to inhibit the synthesizing and promoting of proinflammatory cytokines, mostly in macrophages and dendritic cells, thereby preventing further tissue injury [4]. Likewise, the discovery further advanced regulation in the early 2000s by providing a novel layer of immune regulation through maintaining characterization as regulatory non-coding RNA that controls target mRNA stability and translation.

Functionally, FOXP3 modulates Treg function regarding the secretions of the immuno-suppressive cytokines such as Interleukin (IL-10) and transforming growth factor beta (TGF-β), which are important in immune tolerance [3]. Protein IL-10 interacts with its receptor expressed on target cells through binding, activating the Janus kinase/signal transducers and activators of transcription (JAK/STAT) signal transduction pathway to control inflammation response [5]. miRNAs, including miR-146 and miR-155 have important regulation functions [4], in which miR-146 reduces NF-κB signaling through targeting Interleukin-1 receptor-associated kinase (IRAKI) and tumor necrosis factor receptor-associated factor 6 (TRAF6) [6,7], and miR155 affects cytokine production through regulation of Suppressor of Cytokine Signaling 1 (SOCS1) level [8,9]. Other anti-miRs, including miR-21 and miR-223, control immune reactions related to T-cell activation and macrophage polarization, correspondingly [10,11]. These mechanisms demonstrate how miRNAs modulate immune responses by integrating their regulatory role throughout all immune cell types.

Nevertheless, there remain many questions unanswered. For instance, since the discovery of miRNAs, the complex interaction between these molecules and other regulating molecules in various immune scenarios has yet to be fully established. Furthermore, the contribution of other recently discovered non-coding molecules, including lncRNAs, in the regulation of the immune system remains largely unknown, indicating potential future

development in immune-related research. Knowledge of such mechanisms is vital to the formulation of new approaches to treating diseases related to immune dysregulation.

3. Recent Developments in Immune Regulation

In recent decades, considerable advances have been made in previously unresolved questions. Breakthroughs such as identifying definite regulatory molecules, including the transcription factor forkhead box P3 (FOXP3) in Tregs and microRNAs, have highlighted the complex pathways used to control the immune system [3]. For instance, FOX transcription factors, such as FOXP3, are essential for Treg development and function and are important for immune regulation [3]. Likewise, microRNAs (miRNAs) and other non-coding RNAs have been identified as exerting critical control of cytokine signaling and differentiation of immune cells. Examples of such specific miRNAs that have been reported to directly modulate the immune system and thus influence health and disease include miR 146a and miR 155 [4].

The discovery of immunometabolism has greatly revolutionized this category. Recent discoveries of key molecules such as FOXP3 in Tregs and miRNAs in the past decade have highlighted the complexity of the immunosuppressive process [3]. For example, glycolysis sustains the high energy needs of effector T cells during an immune response, while oxidative phosphorylation is important for Tregs' suppressing function [7]. Their metabolic preferences thus illustrate dynamically the interdependence of cellular energetic states with immune regulation.

The rapid advancement in single-cell technologies and high-throughput sequencing has accelerated further discoveries in this area. Such tools allow researchers to dissect the heterogeneity of immune cell populations and uncover novel regulatory molecules for new perspectives on immune regulation with unprecedented resolution. Such innovations enhance our understanding and provide promising avenues for precision medicine in immune-related disorders.

4. Technical and Philosophical Impacts

These recent findings have profound technical and philosophical implications for immunology. Technically, these findings add new molecular targets for therapeutic intervention, especially for diseases related to immune dysregulation. Such instances are found in autoimmune conditions, chronic inflammatory disorders, and even the hyperinflammatory state observed in severe cases of COVID-19 cytokine storms, which call for much-needed novel approaches for immunomodulation.

In a philosophical manner, the expanded understanding of immune regulation challenges previous views of immunity as a binary system of defense, underlining the intricacy of immune tolerance and activation as interdependent processes requiring sensitive molecular orchestration. This notion increases our appreciation of the intricacies within the immune system and points toward the need for a systems approach in studying and manipulating immune responses.

5. Description of the Immune System: Composition and Function

The immune system is a sophisticated network that keeps the body self-tolerant while protecting it against infections. Adaptive immunity and innate immunity are its two primary branches. Innate immunity offers primary, non-specific protection through physical barriers (such as mucosa and skin), soluble molecules (including cytokines and complement proteins), and immune cells (such as neutrophils, macrophages, and innate killer cells). In particular, innate immunity acts as the first line of protection and bridges adaptive immunity via the presentation of antigens by dendritic cells.

Adaptive immunity grows over time and is quite particular. It involves T cells, such as cytotoxic T cells (which target infected cells) and helper T cells (which coordinate responses), as well as B cells (which produce antibodies). Regulatory T cells (Tregs) are the aspects of CD4+, and form the central part of the immune regulation; Tregs are crucial for preventing autoimmunity by reducing the intensity of immune responses [12].

Important molecules like chemokines, cytokines, and co-stimulatory signals bridge communication between adaptive and innate immunity, establishing a balance in immune response. Modulating mechanisms such as regulatory T cells bring about tolerance and homeostasis, closely aligning to the focus of my research.

6. Mechanisms of Immunological Modulation and an Explanation of the Processes

By striking a balance between immune activation and suppression, immune regulatory systems preserve homeostasis and avert autoimmune disorders and excessive inflammation. Important mechanisms include sirtuins, autophagy, inflammasome activation, mitochondrial function, post-translational changes, Toll-like receptor (TLR) signaling, and microRNAs (miRNAs) in epigenetics [13–16].

To avoid overreactions from the immune system, autophagy breaks down infections and damaged organelles. Multiprotein complexes known as inflammasomes alter innate immunity by activating inflammatory cytokines such as IL-1β. Energy metabolism and T-cell activation are influenced by mitochondrial activity, whereas sirtuins, which are NAD+dependent enzymes, control inflammation and stress reactions. Immune signaling pathways are refined by post-translational changes like phosphorylation and ubiquitination.

In epigenetics, miRNAs influence immune cell differentiation by suppressing mRNA, which regulates gene expression. When pathogens are detected by TLR signaling, adaptive immune responses and cytokine production are triggered. Together, these systems guarantee tissue healing, pathogen protection, and immunological tolerance. Autoimmunity, metabolic diseases, and chronic inflammation are caused by dysregulation, underscoring the necessity of precise immunological modulation [17].

6.1. Immune Regulatory Processes

6.1.1. Autophagy

Autophagy is a process of cellular breakdown that maintains immunological homeostasis by eliminating damaged proteins and organelles. It controls inflammation, pathogen removal, and antigen presentation. Chronic inflammation, autoimmune disorders, and compromised immune surveillance in cancer and infections are all impacted by autophagy dysfunction [18–21].

6.1.2. Inflammasome Activation

Multiprotein complexes called inflammasomes identify threats and infections, triggering caspase-1 to release IL-1 β and IL-18. Inflammatory reactions are triggered by this. Dysregulated inflammasome activity affects tissue homeostasis and innate immune defense, which in turn leads to chronic inflammation, metabolic problems, and autoimmune illnesses [21].

6.1.3. Mitochondrial Function

Reactive oxygen species (ROS) and ATP produced by mitochondria control immunological responses by affecting immune cell activation, differentiation, and death. Mitochondria dysfunction impairs pathogen defense, increases autoimmunity, and causes inflammation. Additionally, they are crucial for immune cell metabolic reprogramming [22].

6.1.4. Role of Sirtuins

NAD+-dependent deacetylases known as sirtuins control immunological function by means of longevity, inflammatory suppression, and metabolic adaptability. They alter the polarization of macrophages, the generation of cytokines, and T-cell differentiation. Autoimmune diseases, age-related immunological dysfunction, and chronic inflammation are all associated with sirtuin dysregulation [22].

6.1.5. Post-Translational Modifications

PTMs, such as acetylation, phosphorylation, and ubiquitination, adjust protein stability, location, and activity to fine-tune immunological signals. They control immunological tolerance, antigen presentation, and cytokine signaling. Defective pathogen responses, inflammatory illnesses, and immune evasion in cancer are all influenced by aberrant PTMs [23–25].

6.1.6. MicroRNAs in Epigenetics and TLR Signaling

By directing mRNAs towards translational repression or destruction, microRNAs (miRNAs) control the expression of immunological genes. They shape innate and adaptive immunity by influencing TLR signaling and epigenetic changes. By affecting immunological homeostasis, dysregulated miRNAs play a role in cancer, infections, and autoimmune disorders [26–29].

6.2. Impacts of These Mechanisms and Their Relationship to Innate and Adaptive Immune Systems

The regulatory mechanisms of the immune system, especially those involving regulatory T cells (Tregs), are crucial for preserving immunological homeostasis and averting overreactions or detrimental immune reactions. Tregs lower the likelihood of chronic inflammation and autoimmune responses by suppressing immune cell overactivation. By inhibiting effector T cells (adaptive) and modifying antigen-presenting cells (innate), they serve as a link between innate and adaptive immunity, guaranteeing balanced reactions.

These systems are essential for immune defense cooperation. A specialized, long-lasting defense is tailored by adaptive immunity, whereas innate immunity starts responses and exposes adaptive cells to antigens. My emphasis on molecular immune regulation is closely related to the regulatory pathways that guarantee the regulation of this interaction, avoiding collateral harm and preserving tolerance to self-antigens. These pathways include cytokine signaling and Tregs.

7. Function and Dysfunction of Regulatory T Cells

Regulatory T cells (Tregs) are mainly characterized by representations of CD25, CD4, and FoxP3 transcription factors. Tregs play an important role in preventing autoimmunity and establishing a balance in immune homeostasis. Specifically, the regulatory T cells restrict immunological responses by preventing effector T cells, dendritic cells, and other immune cells from proliferating and producing cytokines. The representation of immune checkpoint molecules such as CTLA-4, production of regulatory cytokines like TGF- β and IL-10, and regulation of metabolic pathways via molecules such as CD73 and CD39 are the various techniques in which suppression occurs [30–33]. Furthermore, during inflammation and injury, Tregs preserve tissue homeostasis, guaranteeing a well-balanced immune response that lessens collateral damage. In specialized tissues like the skin and gut, where the immune system is continuously interacting with external antigens, they are especially important.

Treg dysfunction manifests in a vast spectrum of illnesses. Exaggerated immune responses caused by deficiencies in Treg function or numbers frequently result in au-

toimmune illnesses such as multiple sclerosis, systemic lupus erythematosus, and type 1 diabetes. FoxP3 gene mutation processes can result in acute immunopathologies, such as polyendocrinopathy, dysregulation of immunity, X-linked syndrome (IPEX), and enteropathy [34,35]. On the other hand, an overactive Treg population can severely inhibit immune responses, which can worsen chronic infections and aid in cancer tumor immune evasion. For example, cytotoxic T cells can be inhibited by Tregs in the tumor microenvironment, allowing the tumor to grow. Tregs' ability to balance and change between pro- and anti-inflammatory states is essential to their function. To restore immunological balance in disease situations, treatment techniques that target Tregs must be developed with an understanding of these dynamics.

Interactions Between Regulatory T Cells

The interplay between suppressor T cells encompasses both microenvironment modulation and direct cellular interactions. Effector T cells communicate with Tregs through cell-to-cell interaction controlled by molecules such as CTLA-4, which reduces the regulation of costimulatory signals that present antigens [16]. Additionally, they generate cytokines that reduce inflammation and immune cell recruitment, like IL-10. By upsetting the stability of other Tregs, dysregulated Tregs cause FoxP3 expression to decline and a change toward an effector phenotype. The immunological landscape is shaped by this intricate interaction, which affects both health and disease outcomes.

8. Materials and Methods

A thorough search of the literature was done to find publications in the PubMed database. Molecular mechanisms, immunological regulation, immune signaling pathways, cytokine signaling, and immune homeostasis were among the keywords used to find relevant articles. With an emphasis on those released within the last three years, publications from 2014–2024 were included. In particular, the inclusion criteria called for studies that provide fresh proof of immunity-related molecular regulation. As a result, 75 papers were chosen for this review. Figure 1 provides an overview of the literature selection procedure.

8.1. Study Design and Methodology

Using a systematic review methodology based on PRISMA criteria, this paper examines recent developments in molecular immune modulation. Database searches were used to find pertinent studies, which were then vetted by full-text reviews and filtered by title and abstract. Studies that looked into immune regulation mechanisms, namely immunological homeostasis, cytokine signaling, or immune pathways, and were published between 2014 and 2024, with an emphasis on the last three years, were included. Peer-reviewed papers from respectable journals were the only ones taken into account. Duplicate records, inadequate molecular data, and non-mammalian studies unless pertinent were among the exclusion criteria. The results advance our knowledge of immune system control by offering fresh perspectives on important immunological mechanisms.

8.2. Data Collection and Analysis

To reduce bias, data extraction was carried out separately by two reviewers. The study's goals, methods, main conclusions, and important findings were all methodically gathered and organized in a structured spreadsheet. Any disagreements among the reviewers were settled by dialogue or by consulting a third party. Trends in immune regulation research were assessed using a qualitative method for data synthesis. Based on their main areas of interest, such as immunological homeostasis, cytokine signaling pathways, and molecular immune interactions, the studies were grouped. Analysis of the results revealed new ideas, parallels, and inconsistencies in the literature.

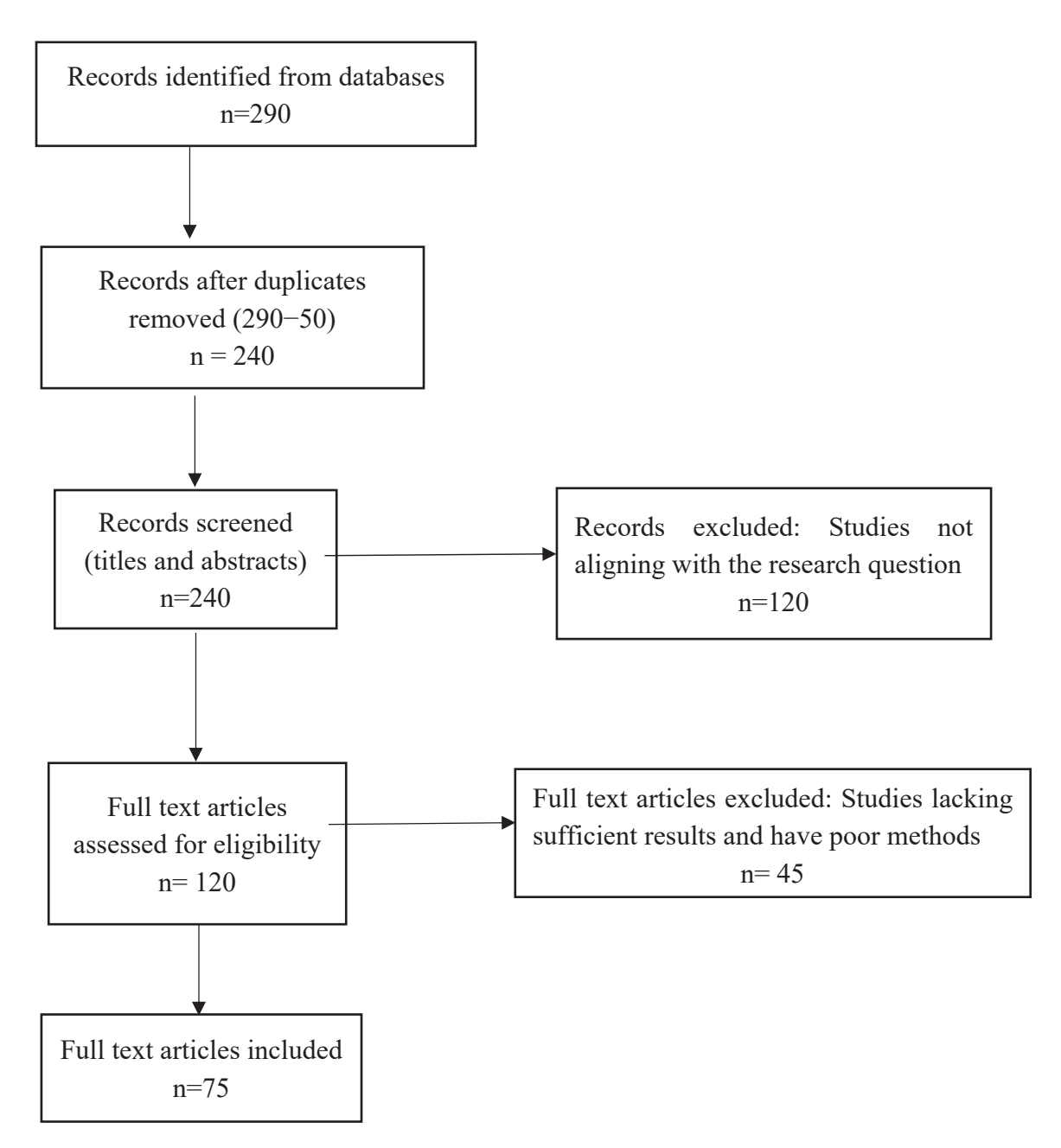


Figure 1. PRISMA flow diagram.

9. Review Themes

The six themes discussed in this review include T-cell and Checkpoint Regulation, Epigenetic Regulation, Cytokine Signaling Pathways, Suppressor T Cells, Immunometabolism, and Regulatory T Cells. In a review of the molecular mechanism of immune regulation, there is a connection between these themes. Cytokine signaling pathways are considered the main communication avenue for the immune system, interfacing responses between adaptive and innate immunity. Cytokines such as TGF- β and IL-2 are crucial for the function and differentiation of suppressive T cells and Tregs, preventing inflammation and improving immune tolerance. Besides, cytokines impact the representation of checkpoint molecules like CTLA-4 and PD-1, which regulate the activity of T-cells and establish a balance in the immune system [36–39]. This is a crucial interaction underscoring the importance of signaling pathways in improving cellular immune responses.

There is a close relationship between the functions of suppressor T cells and regulatory T cells (Tregs) concerning the modulation of immune activity. Regulatory cells suppress re-

sponses of effector T cells and foster tolerance through the production of cell-to-cell contact or cytokines [40]. On the other hand, suppressor T cells employ distinct techniques, like disruption of metabolism or direct cytolysis, to downgrade activation of immune function. Histone acetylation and DNA methylation are two examples of the complex epigenetic changes that control both cell types and guarantee their stability and functionality in a variety of physiological and pathological circumstances. For instance, FoxP3, a master regulator of Tregs, is tightly regulated by epigenetics, which connects immunological function and cellular growth. Therefore, a common framework for these subjects is provided by the interaction of various biological systems and how they are regulated.

By illustrating how metabolic changes impact immune control, immunometabolism connects these processes. Regulatory T cells depend on oxidative phosphorylation when executing suppressive tasks. On the other hand, effector cells rely on glycolysis for faster proliferation. Gene expression and immunological function are linked to cellular energy levels by epigenetic regulators, which frequently react to metabolic stimuli [41–44]. These themes come together to show a delicate yet well-organized web of signaling, control, and metabolic adaptation that is essential for preserving immunological homeostasis and treating dysfunction in illnesses like cancer and autoimmune diseases. This interwoven story highlights the common structure that underlies these disparate ideas.

10. Results

10.1. Cytokine Signaling Pathways

Among the critical factors implicated in immune system regulation, cytokines are key, particularly in mediating information flow from one immune cell to another. However, not all cytokines participate in such regulation. The specific cytokines that have been identified as key include interleukin (IL)-10, IL-17, and IL-23. In particular, IL-10 plays an important role in immune system regulation: this anti-inflammatory cytokine prevents damage to vital tissues by limiting inflammatory responses. Notably, IL-10 directly suppresses macrophage activation while inhibiting pro-inflammatory cytokine production [12,13].

In contrast, IL-17 plays a unique role in stimulating inflammatory responses in autoimmune diseases such as psoriasis and arthritis [14,15]. IL-17 is responsible for promoting neutrophil infiltration and activating the inflammatory processes observed in autoimmune diseases [16,18]. Thus, the competition between pro-inflammatory and anti-inflammatory cytokines is pivotal to immunity.

IL-23, another vital cytokine involved in immune regulation, has been implicated in T helper 17 (Th17) generation [19] and proliferation [20]. Th17 cells are involved in inflammatory disorders such as Crohn's disease and multiple sclerosis; thus, targeting IL-23 has emerged as a therapeutic approach for these conditions [21,22]. Exploring the mechanisms by which these cytokines are regulated will offer insights into how they contribute to maintaining a healthy immune system and increase our understanding of disease processes.

The discussion of diversified functions of the cytokine interleukin-6 (IL-6) focuses on its multiple anti-inflammatory and pro-inflammatory functions in the roles of the immune system. The results of this study underscore the crucial function of interleukin-6 (IL-6) as an element with diversified function in the modulation of the immune response, especially in the pathogenesis of autoimmune diseases and inflammation [45–48]. High levels of IL-6 were associated with autoimmune and inflammatory diseases, underscoring its centrality in the progression of these diseases. In addition, the study highlighted the therapeutic abilities of IL-6 inhibitors, including siltuximab and tocilizumab, in addressing autoimmune diseases, cytokine release syndrome, and hyperinflammation induced by COVID-19. Moreover, pathways that target IL-6 signaling, such as JAK or STAT, showed effectiveness

in mitigating inflammatory responses. These results demonstrate the significance of establishing a balance in IL-6 regulation to reduce severe effects while capitalizing on its therapeutic promise in various immune-mediated conditions.

It is crucial to target specific pathways and immune cells to foster cancer immunotherapy. It has been demonstrated that Th2 cells, which are controlled by cytokines such as IL-25 and IL-33, stimulate tumorigenesis and metastasis, and that pharmacological inhibition successfully prevents tumor growth. Th17 cells have been shown to decrease anti-tumor immunity in colorectal cancer (CRC), indicating context-dependent targeting techniques, despite their favorable effects in certain malignancies, such as melanoma [49]. In preclinical settings, activating B cells with substances like CD40 stimulation and CpG-ODN demonstrated promise in improving T-cell responses and lowering tumor burden. On the other hand, Breg cells are involved in immunosuppressive tumor microenvironments (TMEs), and preclinical research showed promise in inhibiting them using substances like resveratrol and LXA4. Together, these results demonstrate the dual function of inflammation in cancer and support the use of specialized strategies to alter immune responses to enhance treatment results. In a variety of physiological and pathological settings, cytokine signaling pathways play a crucial role as immunological communication mediators, coordinating the equilibrium between inflammation and tolerance [50].

10.2. T-Cell and Checkpoint Regulation

Adaptive immunity is a complex mechanism that involves interplay among various components, including T cells, that are critical for maintaining homeostasis through regulatory processes. Recent research has focused on adaptive immunity, emphasizing immune checkpoints such as programmed cell death ligand (PD-1/PD-L1) and cytotoxic T-lymphocyte-associated protein 4 (CTLA-4). These factors are critical because they prevent autoimmunity and help achieve and maintain immune tolerance [23–25]. The PD-1 receptor expressed on T cells interacts with PD-L1 and PD-L2 on antigen-presenting cells (APCs) to hinder T-cell activation [26–28]. The PD-1/PD-L1 axis is essential for maintaining tolerance and thus safeguarding against tissue harm during inflammation.

CTLA-4 is another checkpoint molecule that hinders T-cell activation by competing with CD28 for binding to B7 ligands on APCs [29–31]. This competition leads to decreases in stimulatory signaling and T-cell proliferation.

Research has shown that additional immune checkpoint proteins—T-cell immunoglobulin, mucin-domain containing-3 (TIM-3) and Lymphocyte Activation Gene 3 (LAG-3)—regulate T-cell activity. TIM-3 has been shown to suppress the Th1 cell-specific response, resulting in the production of regulatory T cells (Tregs) [32–34]. LAG-3 suppresses T-cell activation through interactions with MHC class II molecules to restrict T-cell activation while decreasing cytokine synthesis [35,36]. Studying these immune checkpoints will contribute to understanding immunity and produce potential therapeutic approaches in oncology and autoimmunity.

Oncogenic pathways, inflammatory signaling, and epigenetic mechanisms influence the regulation of CTLA-4 expression and PD-L1 at the Ribonucleic Acid (RNA) level, fostering a version of immunity in cancer [47]. The emergence of FN-γ is a vital inducer of PD-L1 through the pathways of JAK-STAT-IRF1. However, other cytokines such as IL-17 and IL-6 foster the expression of PD-L1 via various signaling cascades. Additionally, PD-L1 transcription is dynamically modulated by oncogenic pathways such as MAPK, EGRF, and PI3K-AKT, fostering suppression of immunity. Moreover, miRNA and m6A methylation are among epigenetic regulators that post-transcriptionally impact the expression of PD-L1. In general, these mechanisms underscore the intricacy of the regulation of

immune checkpoints, providing crucial therapeutic targets to foster the effectiveness of immunotherapy [47].

CD8+ T-cells perform a crucial role in protecting the body against tumors and improving the role of immune checkpoint inhibitors (ICIs) [48]. The process of activating T-cells involves various important steps; determination of the type of antigen, migration, and effector stages. The components of immune checkpoints such as PD-1 and CTLA-4 modulate the T-cells activation process [38]. ICI resistance is associated with disruption of migration of T-cells, antigen presentation, and functions of effectors. Besides, suppressive immune cells, compromised chemokine signals, and reduced expression of MHC foster resistance. Combination therapeutic techniques targeting these processes are under research. Therefore, the complex interaction between immune checkpoint pathways and T-cell activation highlights the importance of these pathways in regulating immunological responses and offers a possible treatment option for immune-related illnesses [50].

10.3. Mechanisms of Immune Regulation

10.3.1. Regulatory T Cells: Mechanisms of Regulation

Tregs play an important role in immune tolerance by suppressing other immune cells to prevent autoimmunity [3]. Cytokines such as IL-2 are critical for the development, proliferation, and regulation of Tregs. Tregs are characterized by the expression of FoxP3, a transcription factor involved in cell development and function [3]. Treg stability is also controlled by metabolic processes, such as fatty acid oxidation (FAO) under low-fat conditions [7]. Signals derived from tumor necrosis factor receptor (TNFR) and inhibitory receptors, including CTLA-4, stringently modulate Treg function and prevent the overactivation that can cause tissue-damaging inflammation [29–31].

PRMT5 and its similar pathways play a crucial role in immunosuppression and Treg cell function. In essence, PRMT5, via its control reciprocal of the recruitment of STAT3/STAT5 and FOXP3, is important in influencing the differentiation of Th17 and the maintenance of Treg activity. Conditional deletion of PRMT5 plays a critical role in the disruption of Treg cells' suppressive functions, causing phenotypes that resemble autoimmune factors. In addition, in breast cancer models, PRMT5 inhibitors foster antitumor immunity [51–53]. Moreover, Treg cells induce suppression via various techniques, such as extracellular vesicle (EV) communication, metabolic modulation, production of cytolysis (including IL-10, TGF- β , and IL-35), and perforin/granzyme-mediated cytolysis. These results underscore the therapeutic potentials of PRMT5 in the modulation of Treg functions during cancer and autoimmune settings.

Various regulatory mechanisms and functional subsets of T cells play a crucial role in boosting Treg immune function and tolerance. In particular, Th9 cells, with the influence of IRF4 and PU.1, remain undiscussed as a distinct lineage. Trl cells, defined by the production of IL-10, depend on factors like c-Maf and Blimp 1 but do not have firm lineage markers. Tregs possess Th-like characteristics under inflammation conditions, including ROR γ t and T-bet expressions, affecting their suppression and migration. Innate lymphoid cells and $\gamma\delta$ T cells play important functions in primary immune responses; ILCs resemble Th subsets and, like $\gamma\delta$ T cells, release IL-17. These results highlight the complex balance of tolerance, immunity, and the requirement for further studies to evaluate therapeutic targets. With their many functions in preserving tolerance and averting autoimmunity, regulatory T cells continue to be at the forefront of immunological regulation, offering a fundamental basis for comprehending and regulating immune homeostasis [54–56].

10.3.2. Suppressor T Cells: Mechanisms of Regulation

Suppressor T cells include subsets such as Tr1 cells that suppress immune responses through contact with cytokine-producing cells and are thus critical for immune regulation [3]. Unlike Tregs, suppressor T cells are not dependent on FoxP3 but often produce the immunosuppressive cytokines IL-10 and TGF- β [3]. The regulation of suppressor T-cell number and activity depends on the microenvironment, such as the presence of inflammatory cytokines and metabolic factors. Suppressor T cells are modulated through surface molecules such as PD-1 and LAG-3, which help maintain their suppressive function in inflamed tissues and prevent overactive immunity [35,36].

Moreover, regulatory T-CELLS (Treg cells) perform a critical role in immune regulation because of their dynamic effector and trafficking mechanisms. The study determined that chemokine receptors such as GPR15, CCR6, and CXCR4 are crucial in guiding T-cells to barrier tissues such as intestines, skin, and bone marrow; these receptors control the immune response and foster tolerance [54]. Specific subsets, including follicular T-cells, modulate T and B helper cells through specialized techniques. The ability of Treg cells to sustain tolerance of peripheral immunity is associated with their timely thymic egress, pre-activated state, and environmental adaptations. These results foster the understanding of the crucial role of Treg cells in immune response.

Treg cells perform a crucial role in tissue repair, immune regulation, and disease progression in various contexts, including autoimmunity, cancer, pregnancy, aging, and chronic infection [57]. Overactivity or dysfunction of Treg cells is associated with the progression of cancer, autoimmune diseases, and impaired efficacy of vaccines. Treg accumulates in aging, but depicts compromised functionality, resulting in inflame-aging, dysregulation of immunity, vulnerability to infections, tumor growth, and development of autoimmune diseases. The study highlights the intricacy of Treg, environmental, and tissue-specific conditions, stressing their multiple functions as critical contributors to pathological processes and protectors of immune homeostasis. The knowledge of the diversity of Treg cells provides crucial therapeutic techniques [58].

Suppressor T cells (Tregs) employ various techniques to regulate antitumor immune response. Tregs hinder effector T cell activation by interfering with costimulatory signaling through the use of cytotoxic T lymphocyte antigen 4 (CTLA-4) [48]. They can dominate IL-2 consumption thanks to their high-affinity receptor for IL-2, which promotes their accumulation in the tumor microenvironment (TME) at the expense of effector T cells. Tregs further reduce antitumor immunity by secreting immunosuppressive cytokines such as TGF- β , IL-10, and IL-35 [51]. Additionally, Tregs take advantage of metabolic changes that enable them to flourish in the nutrient-poor TME, including oxidative phosphorylation and fatty acid consumption. These complex processes make immunotherapies like PD-1 blockage less effective, underscoring the possibility of using Treg targeting as a tactic to improve cancer therapy. By preserving immunological balance and showing therapeutic promise in the management of immune-mediated illnesses, suppressor T cells provide an excellent example of the intricacy of immune regulation [59].

10.3.3. Epigenetic Regulation

It is becoming apparent that epigenetic changes are critical modulators of immunity. Epigenetic mechanisms, such as DNA methylation, histone modifications, and non-coding RNAs (ncRNAs), impact gene expression in immune cells [37–39]. DNA methylation can either suppress or increase immune-related gene expression, depending on the context [40]. Irregular DNA methylation patterns are linked to conditions such as systemic lupus erythematosus (SLE) and rheumatoid arthritis [41,42]. Histone modifications, such as acetylation and methylation, also impact gene expression. Histone acetylation is linked

to open chromatin and an active transcription state, whereas methylation can result in either activation or repression of gene expression based on the particular histone residue. Enzymes that modify histones at the level of gene expression play a role in modulating the immune response.

Additional mechanisms of epigenetic regulation have also been reported in immune cells. Epitranscriptomics has revealed that N6-methyladenosine (m6A) is involved in the stability and translation of immune-related mRNAs. Proteins within chromatin remodeling complexes, including switch/sucrose nonfermenting (SWI/SNF), regulate T-cell differentiation and macrophage activation by controlling access to immune-related genes. Knowledge of these epigenetic regulators highlights the complex regulation of gene expression related to the immune system, and the data offer new insights into the dysregulation of immune responses in disease.

MicroRNAs (miRNAs) constitute a long-term defense system. For example, miRNAs such as miR-146A and miR-155 actively influence the immune response by targeting key signaling molecules. Research has demonstrated that miR-146A can inhibit NF-κB signaling by targeting TRAF6 and IRAKI to dampen the production of inflammatory cytokines [5,43]. Similarly, miR-155 contributes to inflammation by targeting the suppressor of cytokine signaling (SOCS), which leads to an increase in inflammatory cytokine production.

The other miRNAs involved in immune regulation include miR-21, which controls T-cell activation through PTEN and whose expression is regulated by Tim-3; miR-223, which regulates macrophage polarization in inflammation; miR-181b, which plays a role in adjusting T-cell sensitivity; and miR-125b, which regulates cytokines by influencing pro-inflammatory signaling molecules. These miRNAs, by functioning as key regulators of immune and inflammatory processes, represent how ncRNAs impact the immune response.

lncRNAs play a role in controlling the immune system, as evidenced by the impact of the lncRNA NeST on interferon-gamma levels through interactions with chromatin modifiers to shape the development of Th1 cells [44]. The dysregulation of ncRNAs can lead to autoimmune and inflammatory issues, indicating the necessary role of such factors in the normal function of the immune system. Although some advancements have been made, many aspects of epigenetic regulation, including how ncRNAs, chromatin remodelers, and RNA modifications interact, remain poorly understood.

In immune evasion, progression of tumors, and therapy resistance, epigenetics plays a critical role. Tumor-infiltrating Treg cells have significantly high levels of H3K27 and EZH2, triggering immunosuppressive environments, and CCR6-CCL20 pathways produce Th17 cells that complicate the prognosis [58]. The gut microbiome affects cancer immunotherapy and Treg cell recruitment, especially through compounds like butyrate. Through epigenetic processes, cancer stem cells (CSCs) enhance tumor recurrence and metastasis by promoting intratumoral heterogeneity (ITH) and immune resistance. Although there are still issues, clinical trials show that epigenetic medications that target DNMT, EZH2, and HDAC have anticancer potential [50]. One promising approach to cancer treatment is the combination of immunotherapy and epigenetic modification [60].

MicroRNAs (miRNAs) and long non-coding RNAs (lncRNAs) play a key role in regulating liver disease, especially non-alcoholic steatohepatitis (NASH) and hepatocellular carcinoma (HCC). While lncRNA-ROR encourages HCC metastasis, lncRNAs such as lnc-DILC inhibit the growth of liver cancer stem cells. Although the processes are still unknown, lncRNAs such as lnc18q22.2 affect hepatocyte survival and the oxidative stress response in NASH. In Kupffer cells (KCs), miRNAs regulate inflammation [59]. For example, miR-155 decreases NFκB-driven signaling, while miR-192-5p increases inflammation by intercellular communication. LXR agonists, vitamin D receptor activators, and Hippo pathway modulators are examples of therapeutic targets that have shown promise in re-

ducing the inflammation, fibrosis, and metabolic dysregulation linked to NASH. Therefore, a dynamic layer of immune control is provided by epigenetic alterations, which emphasize the possibility of modifying gene expression to alter immune responses in conditions including cancer, autoimmune illness, and others.

The functions of several microRNAs (miRNAs) in immune regulation, together with their targets, impacted cell types, and pathways, are displayed in Table 1. While miR-155 promotes the production of cytokines, miR-146a inhibits inflammation through NF-kB. While miR-223 and miR-222 control macrophage polarization, miR-21 and miR-10a encourage the formation of Tregs and immunological tolerance. miR-150 regulates B/T cell development, while miR-181 increases T-cell receptor sensitivity. Together, these miRNAs affect immunological responses, inflammation, and tolerance, which in turn affects immune-mediated diseases, disease progression, and immune homeostasis.

Table 1. miRNAs involved in immune regulation.

miRNA	Role in Immune Regulation	Target(s)	Acts on Cell Type(s)	Pathway/Function	References
miR-146a	Suppresses inflammation via NF-кВ signaling	TRAF6, IRAK1	Macrophages, T-cells	Negative feedback on inflammation	[5,43]
miR-155	Promotes inflammation by enhancing cytokine production	SOCS1, SHIP1	T-cells, B-cells	Enhances Th1/Th17 responses	[5,43]
miR-21	Regulates T-cell activation and promotes Treg development	PTEN, PDCD4	Tregs	Facilitates immune tolerance	[55,56]
miR-223	Controls macrophage polarization	NFI-A, STAT3	Macrophages	Balances pro/anti-inflammatory phenotypes	[57,58]
miR-181	Enhances T-cell receptor sensitivity	Multiple phosphatases	T-cells	Modulates TCR signaling threshold	[59]
miR-125b	Modulates proinflammatory cytokines	TNF, IL-6	Macrophages, T-cells	Downregulates cytokine storms	[60]
miR-150	Regulates differentiation of B and T cells	c-Myb	B-cells, T-cells	Promotes memory B-cell and Treg development	[61,62]
miR-10a	Promotes Treg stability and suppressive function	Bcl-6, NF-кВ	Tregs	Maintains immune homeostasis	[63]
miR-29a	Suppresses Th1 responses and IFN-γ production	T-bet, Eomes	CD4+ T-cells	Balances Th1/Th2 responses	[64]
miR-27a	Enhances Th17 differentiation by targeting inhibitors of IL-6 signaling	Runx1, Foxp3	CD4+ T-cells (Th17)	Facilitates inflammatory autoimmunity	[65]
miR-31	Promotes Th1 and Th17 differentiation while limiting Treg development	RhoA	T-cells	Enhances inflammatory response	[66]
miR-326	Enhances Th17 cell differentiation	Ets-1	Th17 cells	Drives autoimmune responses	[67]
miR-150-5p	Modulates natural killer cell activity	Myb	NK cells	Regulates NK cytotoxicity	[68]
miR-26a	Regulates TGF-β signaling and Treg homeostasis	SMAD1, SMAD4	Tregs	Promotes immune tolerance	[69]
miR-124	Reduces microglial activation and neuroinflammation	STAT3, C/EBP-α	Microglia	Suppresses neuroinflammatory diseases	[70]
miR-34a	Induces apoptosis and modulates macrophage polarization	Bcl-2, SIRT1	Macrophages	Enhances antitumor immunity	[71]
miR-15b	Regulates cytokine production and T-cell apoptosis	BCL2, STAT3	T-cells, B-cells	Modulates immune responses in infections	[72]

Table 1. Cont.

miRNA	Role in Immune Regulation	Target(s)	Acts on Cell Type(s)	Pathway/Function	References
miR-221	Suppresses T-cell proliferation and migration	p27kip1	CD8+ T-cells	Restricts cytotoxic T-cell overactivation	[73]
miR-146b	Enhances Treg suppressive capacity	TRAF6, STAT1	Tregs	Reinforces NF-κB inhibition	[74]
miR-106a	Inhibits Th1 differentiation and cytokine secretion	IL-10, STAT3	T-cells	Promotes Th2 skewing	[75]
miR-142	Modulates dendritic cell maturation and Treg differentiation	APC gene family	Dendritic cells, Tregs	Coordinates antigen presentation	[76]
miR-181c	Controls mitochondrial metabolism in activated T-cells	COX1, COX2	T-cells	Maintains energy balance during activation	[77]
miR-222	Balances macrophage M1/M2 polarization	NF-κB, STAT6	Macrophages	Regulates tissue repair and inflammation	[78]

10.3.4. Immunometabolism

Immunometabolism is the process whereby immune cells undergo metabolic changes—activation, differentiation, and function—to fulfill necessary biological roles. Signaling pathways that affect metabolic processes, such as glycolysis, oxidative phosphorylation (OXPHOS), and fatty acid metabolism, are intricately associated with fluctuations in the immune response. These metabolic processes and pathways create energy-dependent and inflammatory environments for immune cells.

Immunometabolism plays an important role in fostering immune functions by bringing immunity and metabolism, emphasizing how metabolic processes improve systemic health and immune cell function [60]. The bidirectional connection between metabolism and immunological responses is one of the main discoveries; metabolic reprogramming affects tissue homeostasis, macrophage activity, and T and B cell activation. Immune states are influenced by environmental signals like nutrition and metabolic processes including lipid metabolism and glycolysis in situations like obesity, cancer, and inflammation. Complex networks within and between cells have been revealed by advances in computational and experimental methods. Potential treatment approaches for cancer, metabolic disorders, and immune-mediated diseases are presented by this knowledge [60].

Microphage metabolism is greatly influenced by viral infections, thus the need for various pathways including lipid metabolism, glycolysis, and amino acid. Viral replication is associated with increased glycolysis in HIV, Dengue, and SARS-CoV-2 infections, with different levels of glycolytic intermediates depending on the stage of infection and macrophage state. Viral survival and immune responses are supported by lipid metabolism, which is regulated by signaling pathways such as MyD88 and TRIF [70]. Cholesterol is essential for viral entry and inflammation, particularly during SARS-CoV-2 infection [61]. Amino acid metabolism, specifically glutamine and arginine, supports viral replication and immune modulation. These findings point to metabolic reprogramming as a possible therapeutic target in viral infections.

Homeostatic regulation is an important process in immunometabolism because it helps establish a balance in immune cell functionality. mTORC1 is a key regulator that controls autophagy and anabolic activities according to nutrition availability [62]. Lipid and glucose metabolism is influenced by SREBPs and LKB1, which impacts T cell differentiation and proliferation. Immune cell metabolism is disturbed by the tumor microenvironment; T cell activity is hampered by glucose deprivation, but fatty acid intake meets energy requirements. Through tryptophan depletion, NAD metabolism, and immunosuppressive metabolites, the CD38 and IDO pathways further control immunological responses, affecting T cell function and promoting immune tolerance. These processes highlight the

intricate relationship between immunity and metabolism. Therefore, the new discipline of immunometabolism provides novel insights into immune regulation and possible targets for therapeutic approaches by exposing the significant influence of metabolic reprogramming on immune cell function.

10.4. Cellular Interaction

10.4.1. Effector T Cells

Effector T cells predominantly utilize glycolysis for energy generation, biosynthesis upon activation, and cytokine secretion. Potential functional glycolytic genes include HK2, PFKFB3, and MYC, which regulate glycolytic flux. This flux enables rapid adenosine triphosphate (ATP) generation, even under the hypoxic conditions often found in inflamed tissues, helping fulfill the high energy requirements of proliferative and functional effector T cells [63,64].

10.4.2. Tregs

Tregs depend on the OXPHOS and FAO pathways for their suppressive functions. Peroxisome proliferator-activated receptor gamma coactivator 1-alpha (PPARGC1A) and FOXP3 are crucial for the metabolic preference of Tregs for OXPHOS and FAO [63,65]. FAO permits Tregs to function under the low-glucose conditions present in chronic inflammation [64,66].

10.4.3. Macrophage Polarization

Polarized macrophages differ in their metabolic behavior depending on their state. M1 macrophages rely on glycolysis for their pro-inflammatory functions, and the genes required for these functions are activated by hypoxia-inducible factor 1 alpha (HIF1A) and lactate dehydrogenase A (LDHA). Conversely, M2 macrophages support OXPHOS and FAO through the adipogenic factor peroxisome proliferator-activated receptor gamma (PPAR γ) and the carcinogenic factor ATP citrate lyase (ACLY) to execute restorative and anti-inflammatory effects [65,66].

10.4.4. Key Signaling Pathways

The mechanistic targets of rapamycin (mTOR) and AMP-activated protein kinase (AMPK) pathways, a cellular energy sensor responsible for the maintenance of energy homeostasis, represent important regulators of immunometabolism. mTOR, encoded by MTOR, promotes glycolytic pathways and effector T-cell function. Conversely, AMPK, encoded by PRKAA1, is involved in various catabolic processes, such as FAO, and maintains Treg stability [63,64]. Dysregulation of the mTOR and AMPK pathways leads to immune imbalance in various autoimmune diseases and metabolic disorders [65,66].

Key immune regulatory mechanisms, their corresponding genes, regulators, impacted cell types, and functions are displayed in Table 2. IL6, IL10, and TGFB1 are involved in cytokine signaling, which uses pro- and anti-inflammatory cytokines to balance inflammation. FOXP3 and IL2RA control regulatory T cells (Tregs), which reduce immunological responses and increase tolerance. Histone acetylation and DNA methylation are two mechanisms by which epigenetic changes, such as HDAC9 and DNMT3A, affect T-cell and macrophage development. Together, these systems control immune responses, preserving immunological homeostasis and avoiding dysregulation [58,59].

Table 2. Summary of key immune regulatory mechanisms.

No.	Mechanism	Gene(s) Involved	Regulators (Effect)	Acts on Cell Type(s)	Pathway/Function	References
1	Cytokine Signaling	IL6, IL10, TGFB1	IL-6 (pro-inflammatory), IL-10 (anti-inflammatory), TGF-β (anti-inflammatory)	T-cells, macrophages	Balances inflammation and immune suppression	[18–20]
2	Immune Checkpoints	PDCD1, CTLA4	PD-1 (inhibits T-cell activation), CTLA-4 (inhibits co-stimulation)	T-cells, APCs	Maintains self-tolerance and prevents autoimmunity	[23–28]
3	Regulatory T Cells (Tregs)	FOXP3, IL2RA	FoxP3 (essential for Treg development), TGF-β (induces Tregs), IL-2 (promotes Treg survival)	Tregs	Suppresses immune responses and promotes tolerance	[12–14]
4	Suppressor T Cells	IL10, TGFB1, CTLA4	IL-10 (anti-inflammatory), TGF-β (anti-inflammatory), CTLA-4 (blocks costimulation)	Tr1 cells, Tregs	Inhibits effector T-cell activation and inflammatory responses	[15–17]
5	Epigenetic Modifications	HDAC9, DNMT3A	Histone acetylation (activates genes), DNA methylation (silences genes)	T-cells, macrophages	Regulates immune cell differentiation and function	[37–42]
5a	Non-Coding RNAs	MIR146A, MIR155	miR-146a (anti-inflammatory), miR-155 (pro-inflammatory)	T-cells, B-cells, macrophages	Modulates cytokine signaling, TCR activation, and inflammation	[43–45]
6	Immunometabolism	MTOR, PRKAA1	mTOR (promotes effector T-cell activation), AMPK (enhances Treg activity)	Tregs, effector T-cells, macrophages	Links metabolic states to immune cell function	[46–49]
7	Apoptosis	BCL2, FAS	Bcl-2 (anti-apoptotic), Fas (pro-apoptotic)	T-cells, B-cells	Eliminates autoreactive or excess immune cells	[50–52]
8	Antigen Presentation	HLA-DRA, CD74	MHC-II (presents antigens), CD74 (regulates antigen loading)	Dendritic cells, macrophages	Initiates adaptive immune responses	[53–55]
9	Oxidative Stress	NOX2, SOD2	NOX2 (pro-oxidative), SOD2 (antioxidative)	Macrophages, neutrophils	Modulates inflammation and pathogen elimination	[56–58]
10	Autophagy	ATG5, ATG7	Beclin-1 (pro-autophagic), mTOR (inhibits autophagy)	T-cells, macrophages	Maintains immune homeostasis and antigen presentation	[59–61]
11	Complement System	C3, C5AR1	C3 (pro-inflammatory), C5a receptor (enhances inflammation)	Neutrophils, macrophages	Bridges innate and adaptive immunity	[62–64]

Immune regulatory mechanisms, their flaws, related illnesses, and pathophysiological effects are presented in Table 3. By encouraging inflammation, cytokine signaling abnormalities, like increased IL-6, are linked to rheumatoid arthritis and cytokine storms. Autoimmunity results from FOXP3 mutations that affect Treg function. Autoimmune tolerance is upset by epigenetic changes and mTOR hyperactivity, leading to metabolic and autoimmune illnesses. Because impaired autophagy decreases pathogen clearance, it plays a role in neurological illnesses and Crohn's disease. These processes show how a variety of disease disorders are caused by immunological dysregulation [60–62].

Table 3. Health conditions associated with dysfunction in immune regulation processes.

No.	Mechanism	Defect Type	Associated Disease(s)/Condition(s)	Pathophysiology/Impact	References
1	Cytokine Signaling	Elevated IL-6	Rheumatoid arthritis, cytokine storm	Promotes excessive inflammation, tissue damage, and autoimmunity	[32,33]
2	Immune Checkpoints	PD-1/CTLA-4 inhibition	Cancer, autoimmune disorders	Failure to inhibit T-cell activity leads to autoimmunity; inhibition helps tumor evasion	[34–36]
3	Regulatory T Cells (Tregs)	FOXP3 mutation (loss of function)	Autoimmune polyendocrinopathy, IPEX syndrome	Impaired Treg development causes unregulated effector T-cell responses	[28,29]
4	Suppressor T Cells	Low IL-10/TGF-β levels	Chronic inflammatory diseases, Crohn's disease	Reduced suppression of inflammatory responses leads to persistent inflammation	[30,31]
5	Epigenetic Modifications	Aberrant DNA methylation patterns	Multiple sclerosis, systemic lupus erythematosus	Dysregulated gene expression disrupts immune tolerance and promotes autoimmunity	[37–39]
6	Non-Coding RNAs	Dysregulated miRNA expression	Autoimmune diseases, inflammatory conditions	Misregulation of miRNAs alters cytokine signaling and immune cell activation	[43–45]
7	Immunometabolism	mTOR hyperactivity	Obesity, metabolic syndrome, type 2 diabetes	Increased effector T-cell activation and reduced Treg function worsen metabolic inflammation	[46,48,49]
8	Oxidative Stress	Excessive ROS production	Atherosclerosis, chronic obstructive pulmonary disease (COPD)	Oxidative stress damages tissues and promotes chronic inflammation	[50–52]
9	Autophagy	Impaired autophagy pathway	Neurodegenerative diseases, Crohn's disease	Reduces clearance of pathogens and cellular debris, increasing inflammatory responses	[53–55]
10	Complement System	Uncontrolled complement activation	Paroxysmal nocturnal hemoglobinuria, lupus	Overactivation amplifies tissue injury and autoantibody-mediated damage	[56–58]

11. Discussion

Recently, there has been an increasing focus on deciphering the regulatory functions of ncRNAs in immune regulation. In vitro studies have revealed that miRNAs regulate cytokine levels and immune cell differentiation [67,68]. For example, there is evidence indicating that miR-146a is involved in regulating the responses to inflammation by targeting the NF-kB signaling pathway [69]. Additionally, similar to miRNAs, lncRNAs can regulate immune responses by interacting with chromatin modifiers and modulating the expression of immune-related genes [70,71]. Epigenetic regulation has been identified as a major determinant of immune balance [72]. Future research is needed to clarify how these mechanisms connect and contribute to immune homeostasis under normal and pathological conditions. New immune regulators, including DNA methyltransferases and histone-modifying enzymes, have also been identified [73]. These regulators influence the accessibility of immune-related genes that direct immune cell differentiation and functionality. For example, DNA methylation is involved in controlling the expression of genes encoding cytokines, and its dysregulation is implicated in diseases such as SLE and rheumatoid arthritis [74].

11.1. Control of Immune Responses by MicroRNA

The influence of microRNAs (miRNAs) on the regulation of immune response is manifested in their impact on crucial immune cell functions and signaling pathways (Table 1). For instance, in inflammatory responses, miR-146a and miR-155 have opposite effects, with miR-146a suppressing inflammation and miR-155 boosting it. These results emphasize how crucial post-transcriptional regulation is for maintaining a balance between

tolerance and immune activation. Furthermore, miR-223 and miR-181 have an impact on T-cell receptor sensitivity and macrophage polarization, respectively, indicating their role in adaptive immunity. Therapeutic approaches aimed at dysregulated immune responses in autoimmune and inflammatory illnesses can be improved by an understanding of these molecular regulators.

11.2. Molecular Processes Controlling the Immune System

Table 2 lists a number of interrelated biological pathways, such as cytokine signaling, immunological checkpoints, and epigenetic alterations, that control immune regulation. Immune homeostasis is directly impacted by cytokine-mediated signaling, including IL-6 and TGF- β , which either stimulate or inhibit inflammation. While suppressor T cells use IL-10 and TGF- β signaling to promote immunological tolerance, regulatory T cells (Tregs), which are identified by their expression of FOXP3, are essential in preventing autoimmunity. Furthermore, immune gene expression is modulated by epigenetic mechanisms such as DNA methylation and histone acetylation, underscoring the complex regulation of immunological responses. These results imply that immune regulation is a multifaceted, intricate process that can be modulated therapeutically.

11.3. Immune Mechanism Dysregulation in Disease

Diseases linked to abnormalities in cytokine signaling, immunological checkpoints, and metabolic pathways clearly exhibit the pathogenic effects of immune dysregulation (Table 3). The negative consequences of excessive inflammation are highlighted by the fact that cytokine storm syndromes and rheumatoid arthritis are characterized by an overproduction of IL-6. Similarly, cancer and autoimmune illnesses are influenced by immune checkpoint malfunction, specifically with regard to PD-1 and CTLA-4. Immune abnormalities, as observed in multiple sclerosis and lupus, are further aggravated by dysregulated miRNA expression and epigenetic changes. Metabolic disorders are also linked to abnormal immunometabolism, including mTOR hyperactivity. These results highlight the need for tailored treatments that restore immunological balance in illness settings.

11.4. Immunometabolism and Immunotolerance

Several studies have described the phenomenon by which metabolic reprogramming controls immune functions [75,76]. In general, metabolic pathways such as glycolysis and FAO contribute to the differentiation and activation of T cells and macrophages [77]. In addition to playing an active role in cell fate, these metabolic pathways support various cellular processes by supplying the energy and biochemicals essential for cell functions. For example, effector T cells use glycolysis instead of OXPHOS since considerable energy is required for proliferation and cytokine production [66-72]. This metabolic reprogramming allows effector T cells to function under the hypoxic and high-energy-demand conditions common to inflamed tissues. In contrast, Tregs require fatty acids and OXPHOS for their suppressive functions. Therefore, Tregs remain stable even under low-glucose concentrations, as is common in chronic inflammatory diseases. The metabolic plasticity of the T cell is a fundamental that allows a particular immune response to the inflammatory situation and microenvironment. This interaction between immunometabolic pathways and other regulatory elements, such as epigenetic modifications and immune checkpoints, remains one of the most important areas for further research. It has to be underlined that in several diseases, many of the mechanisms described here may coexist and contribute to the disease pathogenesis. This cumulative effect highlights the complexity of disease etiology and the interplay between molecular pathways.

Studies on metabolism and the immune system have provided new potential approaches for disease management. Modifying immune responses by targeting metabolic

pathways, such as the mTOR and AMPK pathways, is useful in conditions governed by autoimmunity and inflammation. mTOR, for example, controls T-cell activation, differentiation, and metabolic programming contingent on nutrient status. In autoimmune diseases, immune cell activity is often excessive; therefore, mTOR inhibition can potentially limit effector T-cell-associated inflammation [75]. In contrast, the activation of AMPK simultaneously favors catabolic pathways, Treg stability, and pro-inflammatory activity [78]. Therefore, it may be possible to therapeutically influence these metabolic pathways in autoimmune inflammatory diseases. Future studies should further elucidate the exact mechanisms by which immunometabolic signaling is modulated to refine treatment strategies in disease settings in which metabolic dysregulation plays a major role.

11.5. Implications for Therapy and Illness

Numerous illnesses, including infections, cancer, autoimmune disorders, and chronic inflammation, are exacerbated by the dysregulation of immunological regulatory systems. In diseases like rheumatoid arthritis and inflammatory bowel disease, excessive inflammation is caused by improper inflammasome activation, whereas aberrant autophagy affects antigen presentation and results in autoimmunity. Mitochondrial failure promotes metabolic disorders and immunological fatigue by changing the metabolism of immune cells.

By regulating inflammatory responses and immunological tolerance in aging and neurodegenerative disorders, sirtuin targeting has therapeutic potential. Post-translational changes impact the results of cancer immunotherapy by controlling cytokine signaling and immunological checkpoints. In autoimmune and infectious disorders, microRNAs function as biomarkers and therapeutic targets for immune regulation [59].

The goal of precision medicine techniques such as gene-editing technology, biologics, and small-molecule inhibitors is to reestablish immunological homeostasis. Cancer treatment is being revolutionized by personalized immunotherapies including adoptive cell therapy and checkpoint inhibitors. Comprehending these pathways facilitates the development of innovative therapeutic approaches for the efficient treatment of immune-related illnesses.

12. Review Question

Research on immunological modulation should continue to be shaped in the future by combining historical viewpoints with current discoveries. Addressing unresolved issues and opening the door for novel therapeutic approaches against immune-mediated illnesses require such an integrative strategy. In this area, one important unanswered question is how exactly regulatory T cells (Tregs) preserve immunological homeostasis without pathologically suppressing protective immune responses. Tregs are well-known for their ability to prevent autoimmunity, but when they malfunction or become overactive, they can cause autoimmune illnesses or compromise anti-tumor immunity, creating a delicate balance that is difficult to achieve [58].

The interaction between regulatory Tregs and other regulatory cells, like epigenetic modification and cytokines, is not well-understood. Addressing this intricacy needs a precise evaluation of the effects of metabolic and environmental factors on Treg stability and functionality. For instance, understanding the chemical signals that dictate whether Tregs inhibit or allow immunological responses may provide fresh perspectives on how to modify these cells for therapeutic ends. Molecular, epigenetic and immunometabolic viewpoints might be combined in an integrated manner to show how these pathways interact to affect Treg behavior. To fill in existing knowledge gaps and meet new clinical

demands, these discoveries have the potential to greatly influence the creation of focused strategies for modifying Tregs in the context of cancer, autoimmunity, and transplantation.

12.1. Limitations of the Study

This study has several drawbacks that should be recognized. First, bias may be introduced by differences in study design, sample size, and methodology among various sources, even if a large body of the literature was examined. Furthermore, the majority of research focuses on certain immune regulation pathways, which prevents a thorough integration of all molecular mechanisms. Direct experimental validation of results is also limited by the dependence on secondary data. Furthermore, because of publication lag, new findings in immune regulation may not be fully represented, especially in fields like immunometabolism and non-coding RNAs. For a more comprehensive understanding, future research should use a standardized methodology and more recent data.

12.2. Future of the Study

Future studies should integrate multi-omics techniques, such as transcriptomics, proteomics, and metabolomics, to deepen our understanding of molecular immune modulation. Examining how immunological checkpoints, regulatory T cells, and epigenetic changes interact to cause disease progression may help identify new targets for treatment. Furthermore, investigating the ways in which environmental factors impact immune regulation could improve personalized medical strategies. Translating research into successful treatments will require clinical trials assessing immunomodulatory medicines that target important biological pathways. Last but not least, developments in machine learning and artificial intelligence may improve predictive modeling, making it easier to spot immune dysregulation trends in a range of illnesses.

13. Conclusions

The healthcare industry has learned new things about cellular-level molecular immunomodulatory mechanisms within the past decade. Epigenetic regulation, immunometabolism, cytokines, and immune checkpoints are some of the fundamental immunological components that preserve immunological homeostasis. Given their dynamic connections, these elements point to a fresh perspective on how immune systems react to shifts in homeostasis and disease conditions. Therefore, developing novel treatment strategies that alter these molecular targets may be beneficial in the management of inflammatory and autoimmune processes as well as the diseases that result from them. In the treatment of immune-related illnesses, developments in precision medicine—where treatments are customized based on a patient's genetic and molecular profile—are showing promise. Highly targeted therapies have become possible due to their capacity to target particular molecules involved in immune responses, such as immunological checkpoints or miRNAs.

Additionally, modifying immune regulatory systems could result in less harmful and more effective treatments, improving the general standard of care for individuals with long-term illnesses. This is especially important in conditions like autoimmune illnesses, when immunological tolerance is compromised, and cancer, where immune evasion is a major factor in tumor growth. Promising results may be obtained from novel therapeutic approaches that try to improve or restore immune function. For the development of next-generation medicines, especially for diseases like cancer, autoimmunity, and chronic inflammatory disorders, further investigation into the molecular basis of immune control will be essential. In the end, these developments could lead to better patient outcomes, more individualized treatment plans, and more long-term strategies for treating immunological

dysfunctions. Immunomodulation treatments have a promising future ahead of them, with increasing potential to revolutionize the management and treatment of immune-related illnesses.

Funding: This research received no external funding.

Institutional Review Board Statement: Not applicable.

Informed Consent Statement: Not applicable.

Data Availability Statement: All data are available from the text or can be passed on by the author upon request.

Conflicts of Interest: The authors declare no conflicts of interest.

References

- Cooper, M.D.; Miller, J.F. Discovery of 2 distinctive lineages of lymphocytes, T cells and B cells, as the basis of the adaptive immune system and immunologic function: 2019 Albert Lasker Basic Medical Research Award. *JAMA* 2019, 322, 1247–1248. [CrossRef] [PubMed]
- 2. Silverstein, A.M. The curious case of the 1960 Nobel Prize to Burnet and Medawar. *Immunology* **2016**, *147*, 269–274. [CrossRef] [PubMed]
- 3. Kempkes, R.W.; Joosten, I.; Koenen, H.J.; He, X. Metabolic pathways involved in regulatory T cell functionality. *Front. Immunol.* **2019**, *10*, 2839. [CrossRef]
- 4. Saraiva, M.; Vieira, P.; O'garra, A. Biology and therapeutic potential of interleukin-10. *J. Exp. Med.* **2019**, 217, e20190418. [CrossRef] [PubMed]
- 5. Hu, Q.; Bian, Q.; Rong, D.; Wang, L.; Song, J.; Huang, H.S.; Zeng, J.; Mei, J.; Wang, P.Y. JAK/STAT pathway: Extracellular signals, diseases, immunity, and therapeutic regimens. *Front. Bioeng. Biotechnol.* **2023**, *11*, 1110765. [CrossRef] [PubMed]
- 6. Zhou, C.; Zhao, L.; Wang, K.; Qi, Q.; Wang, M.; Yang, L.; Sun, P.; Mu, H. MicroRNA-146a inhibits NF-κB activation and pro-inflammatory cytokine production by regulating IRAK1 expression in THP-1 cells. *Exp. Ther. Med.* **2019**, *18*, 3078–3084. [CrossRef]
- 7. Goswami, T.K.; Singh, M.; Dhawan, M.; Mitra, S.; Emran, T.B.; Rabaan, A.A.; Mutair, A.A.; Alawi, Z.A.; Alhumaid, S.; Dhama, K. Regulatory T cells (Tregs) and their therapeutic potential against autoimmune disorders–Advances and challenges. *Hum. Vaccines Immunother.* 2022, 18, 2035117. [CrossRef] [PubMed]
- 8. Gaytán-Pacheco, N.; Ibáñez-Salazar, A.; Herrera-Van Oostdam, A.S.; Oropeza-Valdez, J.J.; Magaña-Aquino, M.; Adrián López, J.; Monárrez-Espino, J.; López-Hernández, Y. miR-146a, miR-221, and miR-155 are involved in inflammatory immune response in severe COVID-19 patients. *Diagnostics* **2022**, *13*, 133. [CrossRef]
- 9. Ye, J.; Guo, R.; Shi, Y.; Qi, F.; Guo, C.; Yang, L. miR-155 regulated inflammation response by the SOCS1-STAT3-PDCD4 axis in atherogenesis. *Mediat. Inflamm.* **2016**, *2016*, *8060182*. [CrossRef] [PubMed]
- 10. Sheedy, F.J. Turning 21: Induction of miR-21 as a key switch in the inflammatory response. Front. Immunol. 2015, 6, 19. [CrossRef]
- 11. Nguyen, M.A.; Hoang, H.D.; Rasheed, A.; Duchez, A.C.; Wyatt, H.; Cottee, M.L.; Graber, T.E.; Susser, L.; Robichaud, S.; Berber, İ.; et al. miR-223 exerts translational control of proatherogenic genes in macrophages. *Circ. Res.* **2022**, *131*, 42–58. [CrossRef]
- 12. Steen, E.H.; Wang, X.; Balaji, S.; Butte, M.J.; Bollyky, P.L.; Keswani, S.G. The role of the anti-inflammatory cytokine interleukin-10 in tissue fibrosis. *Adv. Wound Care* **2020**, *9*, 184–198. [CrossRef] [PubMed]
- 13. Kessler, B.; Rinchai, D.; Kewcharoenwong, C.; Nithichanon, A.; Biggart, R.; Hawrylowicz, C.M.; Bancroft, G.J.; Lertmemongkolchai, G. Interleukin 10 inhibits proinflammatory cytokine responses and killing of Burkholderia pseudomallei. *Sci. Rep.* **2017**, 7, 42791. [CrossRef] [PubMed]
- 14. Kuwabara, T.; Ishikawa, F.; Kondo, M.; Kakiuchi, T. The role of IL-17 and related cytokines in inflammatory autoimmune diseases. *Mediat. Inflamm.* **2017**, 2017, 3908061. [CrossRef] [PubMed]
- 15. Bernardini, N.; Skroza, N.; Tolino, E.; Mambrin, A.; Anzalone, A.; Balduzzi, V.; Colapietra, D.; Marchesiello, A.; Michelini, S.; Proietti, I.; et al. IL17 and its role in inflammatory, autoimmune, and oncological skin diseases: State of art. *Int. J. Dermatol.* **2020**, 59, 406–411. [CrossRef]
- 16. Huangfu, L.; Li, R.; Huang, Y.; Wang, S. The IL-17 family in diseases: From bench to bedside. *Signal Transduct. Target. Ther.* **2023**, 8, 402. [CrossRef]
- 17. Mills, K.H. IL-17 and IL-17-producing cells in protection versus pathology. Nat. Rev. Immunol. 2023, 23, 38–54. [CrossRef]
- 18. Sun, L.; Wang, L.; Moore, B.B.; Zhang, S.; Xiao, P.; Decker, A.M.; Wang, H.L. IL17: Balancing protective immunity and pathogenesis. *J. Immunol. Res.* **2023**, 2023, 3360310. [CrossRef] [PubMed]

- 19. Gaffen, S.L.; Jain, R.; Garg, A.V.; Cua, D.J. IL-23-IL-17 immune axis: Discovery, mechanistic understanding, and clinical testing. Nature reviews. *Immunology* **2014**, *14*, 585. [CrossRef] [PubMed]
- 20. Bunte, K.; Beikler, T. Th17 cells and the IL-23/IL-17 axis in the pathogenesis of periodontitis and immune-mediated inflammatory diseases. *Int. J. Mol. Sci.* **2019**, 20, 3394. [CrossRef] [PubMed]
- 21. Zambrano-Zaragoza, J.F.; Romo-Martínez, E.J.; Durán-Avelar, M.D.; García-Magallanes, N.; Vibanco-Pérez, N. Th17 cells in autoimmune and infectious diseases. *Int. J. Inflamm.* **2014**, 2014, 651503. [CrossRef] [PubMed]
- Zhao, J.; Lu, Q.; Liu, Y.; Shi, Z.; Hu, L.; Zeng, Z.; Tu, Y.; Xiao, Z.; Xu, Q. Th17 cells in inflammatory bowel disease: Cytokines, plasticity, and therapies. J. Immunol. Res. 2021, 2021, 8816041. [CrossRef]
- 23. Zhang, P.; Wang, Y.; Miao, Q.; Chen, Y. The therapeutic potential of PD-1/PD-L1 pathway on immune-related diseases: Based on the innate and adaptive immune components. *Biomed. Pharmacother.* **2023**, *167*, 115569. [CrossRef] [PubMed]
- 24. Buchbinder, E.I.; Desai, A. CTLA-4 and PD-1 pathways: Similarities, differences, and implications of their inhibition. *Am. J. Clin. Oncol.* **2016**, 39, 98–106. [CrossRef] [PubMed]
- 25. Ghosh, C.; Luong, G.; Sun, Y. A snapshot of the PD-1/PD-L1 pathway. J. Cancer 2021, 12, 2735. [CrossRef] [PubMed]
- 26. Chen, R.Y.; Zhu, Y.; Shen, Y.Y.; Xu, Q.Y.; Tang, H.Y.; Cui, N.X.; Jiang, L.; Dai, X.M.; Chen, W.Q.; Lin, Q.; et al. The role of PD-1 signaling in health and immune-related diseases. *Front. Immunol.* **2023**, *14*, 1163633. [CrossRef]
- 27. Zhao, Y.; Harrison, D.L.; Song, Y.; Ji, J.; Huang, J.; Hui, E. Antigen-presenting cell-intrinsic PD-1 neutralizes PD-L1 in cis to attenuate PD-1 signaling in T cells. *Cell Rep.* **2018**, 24, 379–390. [CrossRef] [PubMed]
- 28. Gutic, B.; Bozanovic, T.; Mandic, A.; Dugalic, S.; Todorovic, J.; Stanisavljevic, D.; Dugalic, M.G.; Sengul, D.; Detanac, D.A.; Sengul, I.; et al. Programmed cell death-1 and its ligands: Current knowledge and possibilities in immunotherapy. *Clinics* 2023, 78, 100177. [CrossRef] [PubMed]
- 29. Kim, G.R.; Choi, J.M. Current understanding of cytotoxic T lymphocyte antigen-4 (CTLA-4) signaling in T-cell biology and disease therapy. *Mol. Cells* **2022**, *45*, 513–521. [CrossRef] [PubMed]
- 30. Babamohamadi, M.; Mohammadi, N.; Faryadi, E.; Haddadi, M.; Merati, A.; Ghobadinezhad, F.; Amirian, R.; Izadi, Z.; Hadjati, J. Anti-CTLA-4 nanobody as a promising approach in cancer immunotherapy. *Cell Death Dis.* **2024**, *15*, 17. [CrossRef] [PubMed]
- 31. Hossen, M.M.; Ma, Y.; Yin, Z.; Xia, Y.; Du, J.; Huang, J.Y.; Huang, J.J.; Zou, L.; Ye, Z.; Huang, Z. Current understanding of CTLA-4: From mechanism to autoimmune diseases. *Front. Immunol.* **2023**, *14*, 1198365. [CrossRef] [PubMed]
- 32. Cai, L.; Li, Y.; Tan, J.; Xu, L.; Li, Y. Targeting LAG-3, TIM-3, and TIGIT for cancer immunotherapy. *J. Hematol. Oncol.* **2023**, *16*, 101. [CrossRef] [PubMed]
- 33. Sauer, N.; Janicka, N.; Szlasa, W.; Skinderowicz, B.; Kołodzińska, K.; Dwernicka, W.; Oślizło, M.; Kulbacka, J.; Novickij, V.; Karłowicz-Bodalska, K. TIM-3 as a promising target for cancer immunotherapy in a wide range of tumors. *Cancer Immunol. Immunother.* 2023, 72, 3405–3425. [CrossRef] [PubMed]
- 34. Anderson, A.C.; Joller, N.; Kuchroo, V.K. Lag-3, Tim-3, and TIGIT: Co-inhibitory receptors with specialized functions in immune regulation. *Immunity* **2016**, *44*, 989–1004. [CrossRef] [PubMed]
- 35. Ruffo, E.; Wu, R.C.; Bruno, T.C.; Workman, C.J.; Vignali, D.A. Lymphocyte-activation gene 3 (LAG3): The next immune checkpoint receptor. *Semin. Immunol.* **2019**, 42, 101305. [CrossRef] [PubMed]
- 36. He, Y.; Rivard, C.J.; Rozeboom, L.; Yu, H.; Ellison, K.; Kowalewski, A.; Zhou, C.; Hirsch, F.R. Lymphocyte-activation gene-3, an important immune checkpoint in cancer. *Cancer Sci.* **2016**, *107*, 1193–1197. [CrossRef] [PubMed]
- 37. Bure, I.V.; Nemtsova, M.V.; Kuznetsova, E.B. Histone modifications and non-coding RNAs: Mutual epigenetic regulation and role in pathogenesis. *Int. J. Mol. Sci.* **2022**, *23*, 5801. [CrossRef]
- 38. Mazzone, R.; Zwergel, C.; Artico, M.; Taurone, S.; Ralli, M.; Greco, A.; Mai, A. The emerging role of epigenetics in human autoimmune disorders. *Clin. Epigenetics* **2019**, *11*, 34. [CrossRef] [PubMed]
- 39. Wei, J.W.; Huang, K.; Yang, C.; Kang, C.S. Non-coding RNAs as regulators in epigenetics. *Oncol. Rep.* **2017**, *37*, 3–9. [CrossRef] [PubMed]
- 40. Lanata, C.M.; Chung, S.A.; Criswell, L.A. DNA methylation 101: What is important to know about DNA methylation and its role in SLE risk and disease heterogeneity. *Lupus Sci. Med.* **2018**, *5*, e000285. [CrossRef]
- 41. Hedrich, C.M.; Mäbert, K.; Rauen, T.; Tsokos, G.C. DNA methylation in systemic lupus erythematosus. *Epigenomics* **2017**, *9*, 505–525. [CrossRef] [PubMed]
- 42. Alarcón-Riquelme, M.E. The heterogeneity of systemic lupus erythematosus: Looking for a molecular answer. *Rev. Colomb. Reumatol.* **2021**, *28*, 31–38. [CrossRef]
- 43. Saba, R.; Sorensen, D.L.; Booth, S.A. MicroRNA-146a: A dominant, negative regulator of the innate immune response. *Front. Immunol.* **2014**, *5*, 578. [CrossRef] [PubMed]
- 44. Sigdel, K.R.; Cheng, A.; Wang, Y.; Duan, L.; Zhang, Y. The emerging functions of long non-coding RNA in immune cells: Autoimmune diseases. *J. Immunol. Res.* **2015**, 2015, 848790. [CrossRef] [PubMed]

- 45. Aliyu, M.; Zohora, F.T.; Anka, A.U.; Ali, K.; Maleknia, S.; Saffarioun, M.; Azizi, G. Interleukin-6 cytokine: An overview of the immune regulation, immune dysregulation, and therapeutic approach. *Int. Immunopharmacol.* **2022**, *111*, 109130. [CrossRef] [PubMed]
- 46. Zhang, H.; Dai, Z.; Wu, W.; Wang, Z.; Zhang, N.; Zhang, L.; Zeng, W.J.; Liu, Z.; Cheng, Q. Regulatory mechanisms of immune checkpoints PD-L1 and CTLA-4 in cancer. *J. Exp. Clin. Cancer Res.* **2021**, 40, 184. [CrossRef] [PubMed]
- 47. Nagasaki, J.; Ishino, T.; Togashi, Y. Mechanisms of resistance to immune checkpoint inhibitors. *Cancer Sci.* **2022**, *113*, 3303–3312. [CrossRef]
- 48. Grover, P.; Goel, P.N.; Greene, M.I. Regulatory T cells: Regulation of identity and function. *Front. Immunol.* **2021**, 12, 750542. [CrossRef] [PubMed]
- 49. Dong, C. Cytokine regulation and function in T cells. Annu. Rev. Immunol. 2021, 39, 51–76. [CrossRef] [PubMed]
- 50. Dikiy, S.; Rudensky, A.Y. Principles of regulatory T cell function. *Immunity* 2023, 56, 240–255. [CrossRef] [PubMed]
- 51. Rocamora-Reverte, L.; Melzer, F.L.; Würzner, R.; Weinberger, B. The complex role of regulatory T cells in immunity and aging. *Front. Immunol.* **2021**, *11*, 616949. [CrossRef] [PubMed]
- 52. Yang, Y.; Wang, Y. Role of epigenetic regulation in plasticity of tumor immune microenvironment. *Front. Immunol.* **2021**, 12, 640369. [CrossRef] [PubMed]
- 53. Chi, H. Immunometabolism at the intersection of metabolic signaling, cell fate, and systems immunology. *Cell. Mol. Immunol.* **2022**, *19*, 299–302. [CrossRef] [PubMed]
- 54. Gauthier, T.; Chen, W. Modulation of macrophage immunometabolism: A new approach to fight infections. *Front. Immunol.* **2022**, 13, 780839. [CrossRef] [PubMed]
- 55. Zhao, H.; Wu, L.; Yan, G.; Chen, Y.; Zhou, M.; Wu, Y.; Li, Y. Inflammation and tumor progression: Signaling pathways and targeted intervention. *Signal Transduct. Target. Ther.* **2021**, *6*, 263. [PubMed]
- 56. Koyama, S.; Nishikawa, H. Mechanisms of regulatory T cell infiltration in tumors: Implications for innovative immune precision therapies. *J. Immunother. Cancer* **2021**, *9*, e002591. [CrossRef] [PubMed]
- 57. Belk, J.A.; Daniel, B.; Satpathy, A.T. Epigenetic regulation of T cell exhaustion. *Nat. Immunol.* **2022**, 23, 848–860. [CrossRef] [PubMed]
- 58. Bennett, H.; Troutman, T.D.; Sakai, M.; Glass, C.K. Epigenetic regulation of kupffer cell function in health and disease. *Front. Immunol.* **2021**, *11*, 609618. [CrossRef]
- 59. Xu, R.; He, X.; Xu, J.; Yu, G.; Wu, Y. Immunometabolism: Signaling pathways, homeostasis, and therapeutic targets. *MedComm* **2024**, *5*, e789. [CrossRef] [PubMed]
- 60. Ménoret, S.; Tesson, L.; Remy, S.; Gourain, V.; Sérazin, C.; Usal, C.; Guiffes, A.; Chenouard, V.; Ouisse, L.H.; Gantier, M.; et al. CD4+ and CD8+ regulatory T cell characterization in the rat using a unique transgenic Foxp3-EGFP model. *BMC Biol.* **2023**, *21*, 8. [CrossRef]
- 61. López-Nevado, M.; González-Granado, L.I.; Ruiz-García, R.; Pleguezuelo, D.; Cabrera-Marante, O.; Salmón, N.; Blanco-Lobo, P.; Domínguez-Pinilla, N.; Rodríguez-Pena, R.; Sebastián, E.; et al. Primary immune regulatory disorders with an autoimmune lymphoproliferative syndrome-like phenotype: Immunologic evaluation, early diagnosis and management. *Front. Immunol.* **2021**, 12, 671755. [CrossRef] [PubMed]
- 62. Tekguc, M.; Wing, J.B.; Osaki, M.; Long, J.; Sakaguchi, S. Treg-expressed CTLA-4 depletes CD80/CD86 by trogocytosis, releasing free PD-L1 on antigen-presenting cells. *Proc. Natl. Acad. Sci. USA* **2021**, *118*, e2023739118. [CrossRef] [PubMed]
- 63. Erber, J.; Herndler-Brandstetter, D. Regulation of T cell differentiation and function by long non-coding RNAs in homeostasis and cancer. *Front. Immunol.* **2023**, *14*, 1181499. [CrossRef]
- 64. Menk, A.V.; Scharping, N.E.; Moreci, R.S.; Zeng, X.; Guy, C.; Salvatore, S.; Bae, H.; Xie, J.; Young, H.A.; Wendell, S.G.; et al. Early TCR signaling induces rapid aerobic glycolysis enabling distinct acute T cell effector functions. *Cell Rep.* **2018**, 22, 1509–1521. [CrossRef]
- 65. Rangel Rivera, G.O.; Knochelmann, H.M.; Dwyer, C.J.; Smith, A.S.; Wyatt, M.M.; Rivera-Reyes, A.M.; Thaxton, J.E.; Paulos, C.M. Fundamentals of T cell metabolism and strategies to enhance cancer immunotherapy. *Front. Immunol.* **2021**, *12*, 645242. [CrossRef]
- 66. Viola, A.; Munari, F.; Sánchez-Rodríguez, R.; Scolaro, T.; Castegna, A. The metabolic signature of macrophage responses. *Front. Immunol.* **2019**, *10*, 1462. [CrossRef] [PubMed]
- 67. Liu, Y.; Xu, R.; Gu, H.; Zhang, E.; Qu, J.; Cao, W.; Huang, X.; Yan, H.; He, J.; Cai, Z. Metabolic reprogramming in macrophage responses. *Biomark. Res.* **2021**, *9*, 1. [CrossRef] [PubMed]
- 68. Chakraborty, C.; Sharma, A.R.; Sharma, G.; Lee, S.S. The interplay among miRNAs, major cytokines, and cancer-related inflammation. *Mol. Ther. Nucleic Acids* **2020**, 20, 606–620. [CrossRef] [PubMed]
- 69. Artimovič, P.; Špaková, I.; Macejková, E.; Pribulová, T.; Rabajdová, M.; Mareková, M.; Zavacká, M. The ability of microRNAs to regulate the immune response in ischemia/reperfusion inflammatory pathways. *Genes Immun.* **2024**, 25, 277–296. [CrossRef] [PubMed]

- 70. Gilyazova, I.; Asadullina, D.; Kagirova, E.; Sikka, R.; Mustafin, A.; Ivanova, E.; Bakhtiyarova, K.; Gilyazova, G.; Gupta, S.; Khusnutdinova, E.; et al. MiRNA-146a—A key player in immunity and diseases. *Int. J. Mol. Sci.* 2023, 24, 12767. [CrossRef] [PubMed]
- 71. Statello, L.; Guo, C.J.; Chen, L.L.; Huarte, M. Gene regulation by long non-coding RNAs and its biological functions. *Nat. Rev. Mol. Cell Biol.* **2021**, 22, 96–118. [CrossRef]
- 72. Martinez-Castillo, M.; MElsayed, A.; López-Berestein, G.; Amero, P.; Rodríguez-Aguayo, C. An overview of the immune modulatory properties of long non-coding RNAs and their potential use as therapeutic targets in cancer. *Non-Coding RNA* **2023**, *9*, 70. [CrossRef] [PubMed]
- 73. Chen, S.; Yang, J.; Wei, Y.; Wei, X. Epigenetic regulation of macrophages: From homeostasis maintenance to host defense. *Cell. Mol. Immunol.* **2020**, *17*, 36–49. [CrossRef] [PubMed]
- 74. Yang, J.; Xu, J.; Wang, W.; Zhang, B.; Yu, X.; Shi, S. Epigenetic regulation in the tumor microenvironment: Molecular mechanisms and therapeutic targets. *Signal Transduct. Target. Ther.* **2023**, *8*, 210. [CrossRef] [PubMed]
- 75. Li, J.; Li, L.; Wang, Y.; Huang, G.; Li, X.; Xie, Z.; Zhou, Z. Insights into the role of DNA methylation in immune cell development and autoimmune disease. *Front. Cell Dev. Biol.* **2021**, *9*, 757318. [CrossRef] [PubMed]
- 76. Biswas, S.K. Metabolic reprogramming of immune cells in cancer progression. *Immunity* 2015, 43, 435–449. [CrossRef]
- 77. Hu, T.; Liu, C.H.; Lei, M.; Zeng, Q.; Li, L.; Tang, H.; Zhang, N. Metabolic regulation of the immune system in health and diseases: Mechanisms and interventions. *Signal Transduct. Target. Ther.* **2024**, *9*, 268. [CrossRef] [PubMed]
- 78. Almeida, L.; Lochner, M.; Berod, L.; Sparwasser, T. Metabolic pathways in T cell activation and lineage differentiation. *Semin. Immunol.* **2016**, *28*, 514–524. [CrossRef]

Disclaimer/Publisher's Note: The statements, opinions and data contained in all publications are solely those of the individual author(s) and contributor(s) and not of MDPI and/or the editor(s). MDPI and/or the editor(s) disclaim responsibility for any injury to people or property resulting from any ideas, methods, instructions or products referred to in the content.





Article

Identification of *hsa_circ_0018905* as a New Potential Biomarker for Multiple Sclerosis

Valeria Lodde ¹, Ignazio Roberto Zarbo ^{2,3}, Gabriele Farina ³, Aurora Masia ^{2,4}, Paolo Solla ^{2,3}, Ilaria Campesi ¹, Giuseppe Delogu ¹, Maria Rosaria Muroni ², Dimitrios Tsitsipatis ⁵, Myriam Gorospe ⁵, Matteo Floris ¹ and Maria Laura Idda ^{1,*}

- Department of Biomedical Sciences, University of Sassari, 07100 Sassari, Italy; vlodde@uniss.it (V.L.); icampesi@uniss.it (I.C.); giuseppe@uniss.it (G.D.); mfloris@uniss.it (M.F.)
- Department of Medicine, Surgery and Pharmacy, University of Sassari, 07100 Sassari, Italy; irzarbo@uniss.it (I.R.Z.); masia.aurora@tiscali.it (A.M.); psolla@uniss.it (P.S.); mrmuroni@uniss.it (M.R.M.)
- Unit of Clinical Neurology, AOU, 07100 Sassari, Italy; gabriele.farina@aouss.it
- Department of Medical Sciences and Public Health, University of Cagliari, 09042 Cagliari, Italy
- Laboratory of Genetics and Genomics, National Institute on Aging Intramural Research Program, National Institutes of Health, Baltimore, MD 21224, USA; dimitrios.tsitsipatis@nih.gov (D.T.); gorospem@grc.nia.nih.gov (M.G.)
- * Correspondence: mlidda1@uniss.it

Abstract: Multiple sclerosis (MS) is a demyelinating autoimmune disease characterized by early onset, for which the interaction of genetic and environmental factors is crucial. Dysregulation of the immune system as well as myelinization-de-myelinization has been shown to correlate with changes in RNA, including non-coding RNAs. Recently, circular RNAs (circRNAs) have emerged as a key player in the complex network of gene dysregulation associated with MS. Despite several efforts, the mechanisms driving circRNA regulation and dysregulation in MS still need to be properly elucidated. Here, we explore the panorama of circRNA expression in PBMCs purified from five newly diagnosed MS patients and five healthy controls (HCs) using the Arraystar Human circRNAs microarray. Experimental validation was then carried out in a validation cohort, and a possible correlation with disease severity was tested. We identified 64 differentially expressed circRNAs, 53 of which were downregulated in PBMCs purified from MS compared to the HCs. The discovery dataset was subsequently validated using qRT-PCR with an independent cohort of 20 RRMS patients and 20 HCs. We validated seven circRNAs differentially expressed in the RRMS group versus the HC group. hsa circ 0000518, hsa circ 0000517, hsa circ 0000514, and hsa circ 0000511 were significantly upregulated in the MS group, while hsa_circ_0018905, hsa_circ_0048764, and hsa_circ_0003445 were significantly downregulated; Among them, the expression level of hsa_circ_0018905 was significantly decreased in patients showing a higher level of disability and in progressive forms of MS. We described the circRNAs expression profile of PBMCs in newly diagnosed MS patients and proposed hsa_circ_0018905 as potential MS biomarker.

Keywords: circular RNAs; multiple sclerosis; biomarkers; new diagnosis; immune regulation

1. Introduction

Multiple sclerosis (MS) is an early-onset complex demyelinating autoimmune disease of the central nervous system (CNS) characterized by chronic inflammation, neuronal loss, and axonal damage [1]. Clinically, MS has been classified into four main categories based on disease progression: clinically isolated syndrome (CIS); relapsing–remitting MS (RRMS), comprising 80% of patients; primary progressive MS (PPMS); and secondary progressive MS (SPMS) [2].

Recent data indicate that the frequency of MS follows a general north–south gradient, with the prevalence of MS tending to be higher further away from the equator. Exceptions include specific populations, such as the Sardinians, characterized by having among the highest MS prevalence in the world despite its geographical localization [3]. Indeed, the prevalence of MS in Sardinia is about 361/100,000 inhabitants and the peculiar genetic background of Sardinians could partly explain this record [4].

Furthermore, it is widely accepted by the scientific community that genetic background alone is not enough to trigger disease onset, and that genetic, environmental, and epigenetic factors interact to drive MS pathogenesis [5,6]. The results from genome-wide association studies (GWAS) have identified HLA-DRB1*15:01 as one of the most prominent factors influencing MS onset; in addition, more than 236 HLA-independent genetic variants have been associated with an increased risk of MS. Most of the identified variants alter regulatory non-coding regions and influence gene expression. In general, genomic studies suggested a plethora of loci and genes with small effects on autoimmunity risk, mainly implicated in immunological (both innate and adaptive) and neurological pathways [7,8]. Environmental factors, such as vitamin D deficiency, Epstein–Barr virus (EBV), smoking, and obesity, have also been linked to MS onset [4].

Despite the fact that the underlying causes of MS are still not well understood, recently a relevant role of non-coding RNA (ncRNA) and RNA processing was identified as a key component of the molecular mechanisms potentially involved in MS pathogenesis [9]. Additionally, due to their molecular features, ncRNAs have also been suggested as new biomarkers for MS [10]. Circular RNAs (circRNAs) are a class of ncRNAs that have a unique closed-loop structure, making them more resistant than linear RNAs to degradation by ribonucleases (RNases) [11]. Notably, the type of circRNAs and their abundance vary depending on the developmental stage, tissue, age, and disease stage. According to their biogenesis, circRNAs can be categorized as exonic circRNAs (ecircRNAs), circular intronic circRNAs (ciRNAs), and exonic-intronic circRNAs (ElciRNAs) [11]. It is now widely acknowledged that circRNAs play crucial roles in cell proliferation and apoptosis, as well as in cell cycle regulation and regulation of immune cells and cytokines production [12]. Of note, circRNAs are predominantly found in the cytoplasm, but many are also localized and enriched in synapses and play significant roles in synaptic plasticity and neuronal functions [13]. Finally, circRNAs can influence the pathophysiology of several diseases through different functions, including acting as binding substrates for microRNAs (miRNAs) and RNA-binding proteins (RBPs), as well as by functioning as regulators of transcription, mRNA metabolism, and translation [14].

Accumulating evidence reveals that circRNAs elicit prominent roles in pathologies and play a key role at the interface of the immune system and CNS. One of the first identified dysregulated circRNA in MS patients was <code>hsa_circ_0106803</code>, which originates from the GSDMB gene. <code>Hsa_circ_0106803</code> was shown to be upregulated in peripheral blood mononuclear cells (PBMCs) of RRMS patients as compared to healthy controls (HCs) [15]. Later, Iparraguirre and colleagues detected 406 differentially expressed circRNAs through a microarray analysis on leucocytes of four RRMS patients and four HCs; <code>hsa_circ_0005402</code> and <code>hsa_circ_0035560</code>, two downregulated circRNAs derived from the <code>ANXA2</code> gene, were then validated [16]. Next, the enrichment of circRNAs in the MS transcriptome was studied and a circRNA derived from the MS-associated <code>STAT3</code> gene was identified [9]. In addition to genetic variants, mechanisms influencing circRNA expression levels, including epigenetic factors and regulatory networks involving other linear lncRNAs, have been proposed [17,18].

Importantly, the levels of expressed circRNAs can be influenced by disease progression and associated therapies. Therefore, we decided to study circRNAs differentially expressed in PBMCs from five newly diagnosed MS patients and five HCs. Using the Arraystar Human Circular RNA Array, we identified 64 differentially expressed circRNAs (11 upregulated and 53 downregulated) in MS compared to the HCs. Evidence gained

from experimental validation revealed that *hsa_circ_0018905* may be used as a new blood biomarker for MS.

2. Materials and Methods

2.1. Study Design

Whole-blood samples were collected from a total of 54 subjects enrolled in the study: 34 patients diagnosed with MS, and 20 HCs, consisting of age- and sex-matched individuals. The study was designed and organized to have three different cohorts: (i) a discovery cohort comprised of 5 newly diagnosed MS patients, who had no comorbidities and did not receive any pharmacological treatment, and 5 HCs matched for age and sex; (ii) a validation cohort, consisting of 20 adults diagnosed with MS with no comorbidities and who did not receive any treatment, and 20 HCs matched for age and sex; and (iii) a third cohort of MS patients with mild and severe disease, consisting of 8 RRMS patients newly diagnosed with Expanded Disability Status Scale (EDSS) < 4.5, 6 RRMS patients with EDSS > 4.5, and 8 SPMS patients with EDSS > 4.5 (Supplemental Figure S1). All MS patients were recruited from the University Hospital of Sassari (Italy). Total RNA, derived from PBMCs, was isolated as described below and used for the initial microarray analysis (discovery cohort) and validation steps ((ii) and (iii)) using reverse transcription (RT) followed by quantitative (q) PCR.

2.2. RNA Extraction

PBMCs were purified using 15 mL of blood collected using Vacutainer CPT tubes (BD) from each donor following the manufacturer's instructions. Total RNA from PBMCs was then isolated using the RNeasy Mini Kit (Qiagen, Hilden, Germany). Human serum was obtained from patients and volunteers and processed as follows. Briefly, vacutainers containing clot activator were rested upright for 60 min to allow RBCs to clot. The RBC clot was subsequently pelleted by centrifugation at $1000 \times g$ for 10 min and serum was collected. The collected supernatant was then centrifuged at $5000 \times g$ for 10 min to pellet cell fragments and other debris. Serum samples were pooled and stored in 200 μ L aliquots at -80 °C prior to analysis. RNA from serum was subsequently isolated using miRNeasy Serum/Plasma Advanced kit (Qiagen, Hilden, Germany) following the manufacturer's guidelines.

2.3. RNA Digestion, Amplification, Labeling, and Hybridization

Total RNA extracted from the discovery cohort was used for microarray analysis. Sample labeling and array hybridization were performed according to the manufacturer's protocol (Arraystar Inc., Rockville, MD, USA). Briefly, total RNA was digested with RNase R (Epicentre, Inc., Madison, WI, USA) to remove linear RNAs and enrich in circular RNAs. Then, the enriched circular RNA pool was transcribed into fluorescent cRNA utilizing the random priming method, and then amplified (Arraystar Super RNA Labeling Kit; Arraystar). The labeled cRNAs were purified using the RNeasy Mini Kit (Qiagen, Hilden, Germany). The concentration and specific activity of the labeled cRNAs (pmol Cy3/µg cRNA) were measured by NanoDrop ND-1000; 1 µg of each labeled cRNA was fragmented by adding 5 µL Blocking Agent and 1 µL of Fragmentation Buffer, then heated the mixture at 60 °C for 30 min. Finally, 25 μL of Hybridization buffer was added to dilute the labeled cRNA, and 50 µL of hybridization solution was dispensed into the gasket slide and assembled to the circRNA expression microarray slide. The slides were incubated for 17 h at 65 °C in an Agilent Hybridization Oven. The hybridized arrays were washed, fixed, and scanned using the Agilent Scanner G2505C (Agilent Technologies, Santa Clara, CA, USA).

2.4. Reverse Transcription (RT)-Quantitative (q)PCR Analysis

First-strand cDNA synthesis was performed using Maxima reverse transcriptase (Thermo Fisher, Waltham, MA, USA) and random hexamers. The generated cDNA was diluted tenfold and used as a template for RT-qPCR analysis using SYBR Green mix (Kapa

Biosystems, Wilmington, MA, USA). Relative levels of RNA were calculated using the $2^{-\Delta\Delta Ct}$ method and the levels of *GAPDH mRNA* were used for normalization. Results are reported using the fold induction value (FI) as compared to the control (CTR). Gene-specific primer pairs are listed in Table 1.

Table 1. Gene-specific primer pairs.

RT-(q)PCR Primers	Primer Sequences (5'-3')
hsa_circ_0000518	FW: CATGCCTACATTGCCCCAGA
	RV: CAGACCTTCCCAAGGGACAT
hsa_circ_0000517	FW: GGGAGGTGAGTTCCCAGAG
	RV: CAGGGAGAGCCCTGTTAGG
hsa_circ_0000514	FW: GAGCTTGGAACAGACTCACG
	RV: CATCTCCTGCCCAGTCTGA
hsa_circ_0000511	FW: CCTCCTTTGCCGGAGCTT
	RV: GGTCCACGGCATCTCCTG
hsa_circ_0006853	FW: TGAGTTCAATGGCTGAGGTG
	RV: GTTCCAAGCTCCGGCAAA
hsa_circ_0111998	FW: CAGCACTCCACAGCATCCACTA
	RV: TCCATTTCAATGGTAGCCTGCA
hsa_circ_0018905	FW: TGTTTGTGACCTCCCTCTCC
	RV: CTTCATCCTTCAGCCACACA
hsa_circ_0048764	FW: AAGCTGCTGCCAAGAAAGAC
	RV: ATCCTCCAACCTGCACAGAG
hsa_circ_0003445	FW: AGGAGCAGGAGCTGGAGAA
	RV: GTGCTGGGCATGTGGTTC
RPPH1	FW: CTGTCACTCCACTCCATGT
	RV: TTCTCTGGGAACTCACCTCC
LYLPLAL1	FW: CTGCCCAGAACACCTTGAATC
	RV: TCCTGTTCTTGATGCCAC
SAMD8	FW: TATGATCTCCGGTCTCCTCT
	RV: TGTCACTGTTGTAGCCCATCT
RPL36	FW: GACCAAACACCAAGTTCGT
	RV: TAAATTTGAGGGCCCGTTTGT
HDAC4	FW: AAAACGCAGCACAGTTCCC
	RV: GTCATCTTTGGCGTCGTACA
GAPDH	FW: ATTTGGTCGTATTGGGCGCC
	RV: TTGAGGTCAATGAAGGGGTC

2.5. Prediction of circRNA-miRNA and circRNA-RBP Interactions

The spliced sequences of the validated circRNAs were provided as input in the prediction tool miRanda software (v3.3a) to identify circRNA-associated miRNAs [19]. The RBPs potentially binding to circRNAs were predicted by the Circular RNA Interactome (CircInteractome, https://circinteractome.nia.nih.gov/, accessed on 15 January 2024) based on CLIP data sets [20].

2.6. CircRNA-microRNA-mRNA Network

Bioinformatic analyses were performed to identify potential miRNA targets for each differentially expressed circRNA using miRanda software v3.3a [19]. We also speculated on the biological functions of each circRNA by prediction analysis of proteins potentially affected by putative regulatory networks of circRNA-miRNA-mRNA. The interactions of miRNAs and mRNAs were identified using mirTarBase software (release 9.0 beta) [21]. Finally, we selected the interaction of miRNAs and MS-associated genes described in GWAS analysis from the International Multiple Sclerosis Genetics Consortium [6]. Cytoscape v3.9.0 [22] was then utilized to visualize circRNA-miRNA networks.

2.7. Statistical Analysis

Hybridized arrays were scanned, and images were imported into Agilent Feature Extraction software (version 11.0.1.1) for raw data extraction. Quantile normalization of raw data and subsequent data processing were performed using the R software (version 4.4.1) package (Arraystar). After quantile normalization of the raw data, low-intensity filtering was performed, and circRNAs that had flags in at least 1 out of 12 samples in "P" or "M" ("All Targets Value") were retained for further analyses. CircRNAs with absolute fold changes ≥ 1.5 and p-value ≤ 0.05 between the MS and HC samples were selected as significantly differentially expressed. Hierarchical clustering analysis based on expression levels of differentially expressed circRNAs was performed using Java Treeview (Stanford University School of Medicine, Stanford, CA, USA). In the scatter plot depicting the circRNA expression, the horizontal lines represent the medians.

2.8. Statistics and Data Representation

Roc curves have been generated using the pROC package available in the R software (version 4.4.1). Data were presented as the means \pm standard deviations, and all experimental data were analyzed using GraphPad Prism 9 (GraphPad Software, La Jolla, CA, USA). Differences in RNA levels among groups were evaluated using a two-tailed Student's t-test, and $p \le 0.05$ was considered statistically significant.

3. Results

3.1. Analysis of circRNAs Expressed in MS Patients Using circRNA Arrays

To explore the levels of expressed circRNAs in healthy individuals and newly diagnosed RRMS patients, we performed a microarray analysis of the circRNAs present in PBMCs using the Arraystar Human Circular RNA Array. We enrolled five RRMS and five HC age- and sex-matched subjects in the discovery cohort (Table 2). To mitigate potential confounding variables in the analysis, all donors were negative for comorbidity and did not receive drug treatment. To avoid effects of geographic origin, all the enrolled individuals were from Sardinia, with at least three grandparents of Sardinian ethnicity. For the validation step, the cohort was extended as described below (Table 2).

The Arraystar circRNAs Array was designed to identify 13,617 circRNAs, which were analyzed using the Agilent Feature Extraction software. Differential expression analysis identified a total of 64 dysregulated circRNAs in MS patients at the time of diagnosis, as compared to the HCs, of which 11 were upregulated and 53 were downregulated (Figure 1A). A complete list of dysregulated circRNAs is available in Supplemental Table S1. Hierarchical clustering revealed differentially expressed circRNAs between the MS and HCs; as expected, there was a prevalence of downregulated circRNAs in MS patients (Figure 1A,B). Notably, using the differentially expressed circRNAs, we were able to classify individuals as either MS or HC (Figure 1B).

The expression levels of circRNAs showing the most significant difference between the MS and HCs in the discovery cohort are reported in Figure 1C. $Hsa_circ_0000518$ was found to be the most upregulated (FI = 2.3; p = 0.00073), while $hsa_circ_0003596$ was the most downregulated (FI = 3.4; p = 0.006). Most of the upregulated circRNAs originate from the parental gene RPPH1 which encodes an lncRNA component of the ribonuclease P RNA;

interestingly, the lncRNA *RPPH1* has been associated with MS and circRNAs at different levels [16,23] (Figure 1C).

Table 2. Main characteristics of the individuals enrolled in the study.

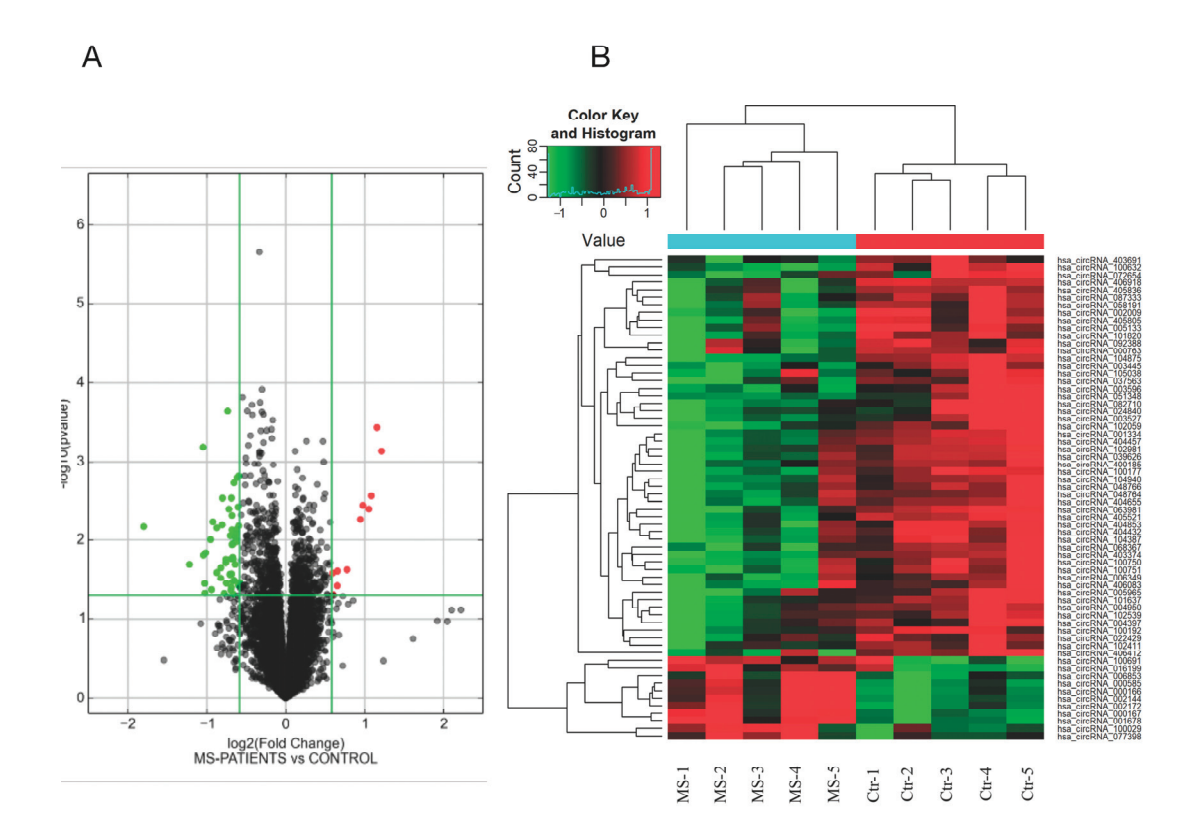
Discovery Set	НС	MS
No. tot	5	5
Female	3	3
Male	2	2
Age, yrs, mean \pm SD	34.8 ± 12.49	34.8 ± 12.49
Disease duration, mean \pm SD	na	at diagnosis
EDSS, mean \pm SD	na	2.3 ± 1.01
Validation Set	НС	MS
No. tot	20	20
Female	10	12
Male	10	8
Age, yrs, mean \pm SD	48.75 ± 15.71	43.3 ± 14.23
Disease duration, mean \pm SD	na	3.21 ± 3.89
EDSS, mean \pm SD	na	2.5 ± 0.81
MS Type		RRMS

Abbreviations: SD, standard deviation; EDSS, Expanded Disability Status Scale; RRMS, relapsing–remitting MS; na, not applicable.

The identified differentially expressed circRNAs were distributed on all chromosomes, with chromosome 1 containing the highest number of circRNAs (seven total) (Supplemental Figure S2). Some upregulated circRNAs were generated by genes located at chromosome 14, while downregulated circRNAs were generated by genes located at several chromosomes, with chromosomes 1, 11, and 19 containing the highest number (Figure 2A–C). Interestingly, the majority of the identified circRNAs mapped within exons, with the upregulated circRNAs belonging to sense overlapping (64%) and exonic (36%) circRNA classes, while downregulated circRNAs were mainly exonic (87%) (Figure 2B–D).

3.2. Validation of circRNA Expression Profiles by RT-qPCR

To validate the circRNA candidates identified by the microarray analysis, we performed RT-qPCR-mediated detection of circRNAs using divergent primers (Table 1) and samples from the validation cohort (Table 2) composed of 12 female and 8 male RRMS patients, and 20 HCs (10 female and 10 male); none of the patients or HC individuals received any drug treatment. The expression trend of the selected circRNAs was consistent with the microarray results: RT-qPCR data revealed that $hsa_circ_0000518$ (FI = 1.63; p = 0.003), $hsa_circ_0000517$ (FI = 3.93; $p = 6.66 \times 10^{-7}$), $hsa_circ_0000514$ (FI = 1.45; p = 0.004), and $hsa_circ_0000511$ (FI = 1.65; p = 0.005) were significantly upregulated in the MS group as compared with the HCs, with hsa_circ_0000517 showing the highest upregulation. Moreover, hsa_circ_0018904 (FI = 0.39; $p = 4.38 \times 10^{-16}$), hsa_circ_0048764 (FI = 0.51; $p = 1.82 \times 10^{-8}$), and $hsa_circ_0003445$ (FI = 0.61; $p = 2.84 \times 10^{-9}$) were significantly downregulated in the validation cohort. No significant difference in the expression levels of hsa_circ_0006853 or hsa_circ_0011998 was found between the MS and HCs (Figure 3A). Next, we examined the relative abundance of the parental linear transcript for each host gene. In contrast to the upregulation of the cognate circRNAs, the levels of RPPH1 did not significantly change in samples from MS patients compared to HCs, suggesting post-transcriptional regulation of the four circRNAs analyzed. By contrast, for the downregulated transcripts, we observed a coherent change in expression among circRNAs and corresponding linear transcripts (Figure 3B).



С

circRNA	p-value	FC (abs)	Reg.	circRNA_type	Chr	GeneSymbol
hsa_circ_0000518	0.0007	2.3194	ир	sense overlapping	14	RPPH1
hsa_circ_0000517	0.0004	2.2269	up	sense overlapping	14	RPPH1
hsa_circ_0000514	0.0027	2.1197	up	sense overlapping	14	RPPH1
hsa_circ_0000511	0.0040	2.0750	up	sense overlapping	14	RPPH1
hsa_circ_0000515	0.0036	1.9685	up	sense overlapping	14	RPPH1
hsa_circ_0000512	0.0054	1.9260	up	sense overlapping	14	RPPH1
hsa_circ_0006853	0.0236	1.7126	up	sense overlapping	14	RPPH1
hsa_circ_0003596	0.0067	3.4813	down	exonic	9	COL5A1
hsa_circ_0111998	0.0204	2.3296	down	sense overlapping	1	XLOC_000566
hsa_circ_0018905	0.0007	2.0673	down	exonic	10	SAMD8
hsa_circ_0051348	0.0155	2.0611	down	exonic	19	LOC390940
hsa_circ_0002356	0.0356	2.0384	down	exonic	19	CAPNS1
hsa_circ_406083	0.0469	2.0339	down	intronic	20	TASP1
hsa_circ_406412	0.0144	2.0203	down	intronic	3	RFC4
hsa_circ_0037563	0.0099	1.9352	down	exonic	16	SRRM2
hsa_circ_0048764	0.0424	1.9190	down	exonic	19	RPL36
hsa_circ_0003445	0.0059	1.8969	down	exonic	2	HDAC4

Figure 1. Differentially expressed circRNAs in MS patients versus HCs, circRNA array analysis. **(A)** Volcano plots, used to visualize up- and downregulated genes across MS samples as compared to HCs. The red (up) and green (down) dots in the plot represent the significative differentially expressed circRNAs. **(B)** Clustered heatmap of the differentially expressed circRNAs showing the relationships among the expression levels of samples. Upregulation is shown in red, and downregulation is in green. **(C)** Table showing the list of circRNAs differentially expressed, depicting the top 7 upregulated and 10 downregulated.

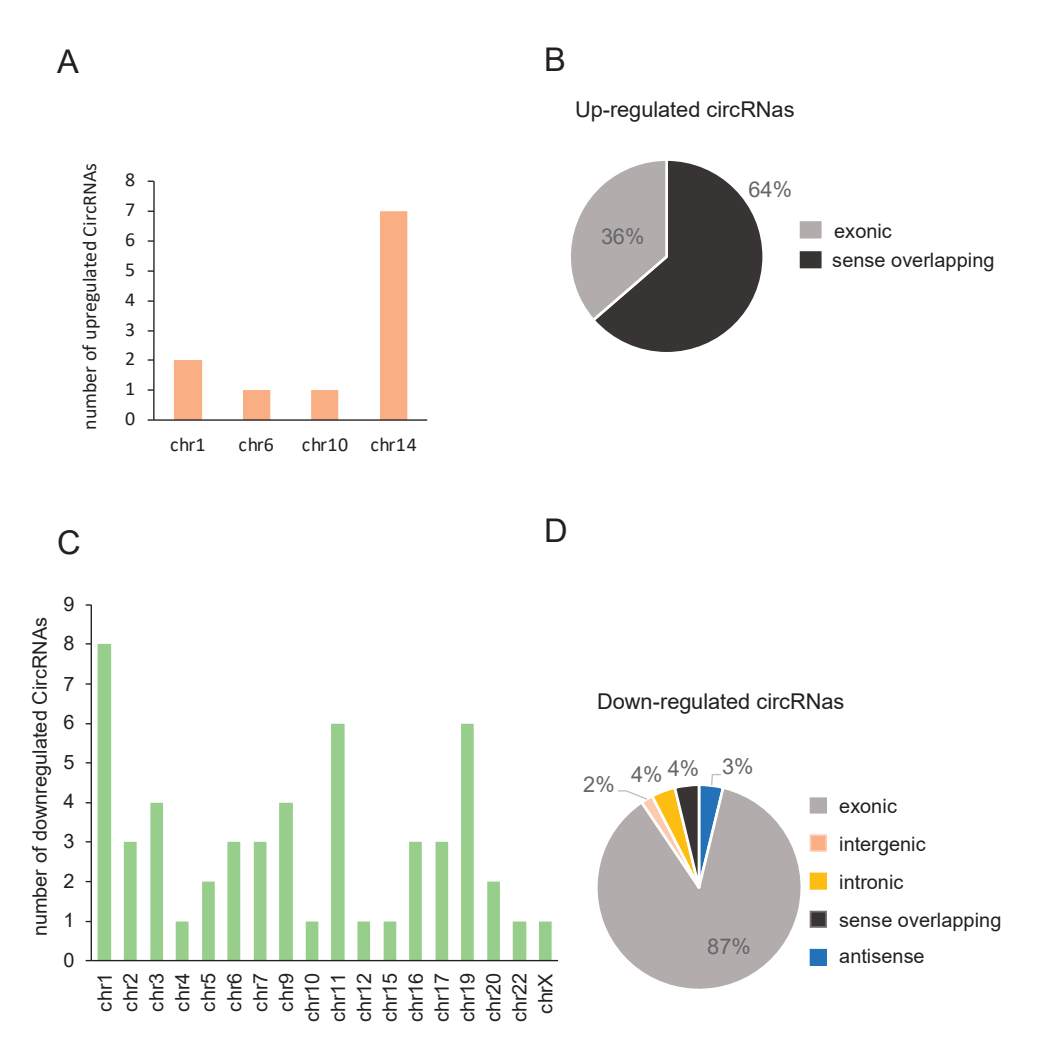
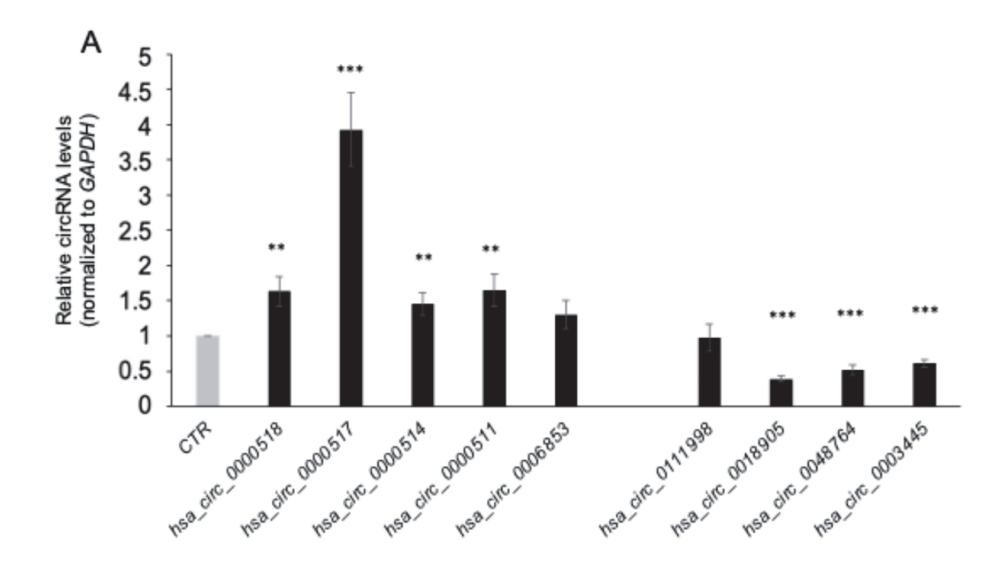


Figure 2. Characteristics of the circRNAs identified in PBMCs of MS patients versus HCs. (**A**) Distribution of significantly upregulated circRNAs according to the chromosomal location. (**B**) Class distribution of upregulated circRNAs based on the genomic origins. (**C**) Distribution of significantly downregulated circRNAs according to the chromosomal location. (**D**) Class distribution of downregulated circRNAs based on the genomic origins.

3.3. PBMC circRNA Expression Correlation with Serum

PBMCs are present in blood, where they actively release extracellular vesicles (EVs) containing several classes of ncRNAs, including circRNAs. Thus, we decided to check whether the differentially expressed circRNAs can be detected in serum, and whether the levels of the circRNAs detected in PBMCs may be reflected in serum EVs. Therefore, serum was isolated and quickly stored at $-80\,^{\circ}$ C; RNA was then isolated and measured using RT-qPCR analysis. The levels of the circRNAs <code>hsa_circ_0000518</code>, <code>hsa_circ_0000514</code>, <code>hsa_circ_0000511</code>, and <code>hsa_circ_0006853</code> increased in serum purified from MS patients compared to HCs, in line with the observation in PBMCs; <code>hsa_circ_0000517</code> was not detected in serum. In contrast, the levels in serum of <code>hsa_circ_0111998</code>, <code>hsa_circ_0018904</code>, <code>hsa_circ_0048764</code>, and <code>hsa_circ_0003445</code> were not influenced by disease status (Figure 4A) in serum samples. Interestingly, we also analyzed the linear mRNA and observed that all mRNAs analyzed could be detected in serum, and that <code>LYPLAL1</code> and <code>SAMD8</code> mRNAs are slightly but significantly more abundant in serum isolated from MS patients (Figure 4B).



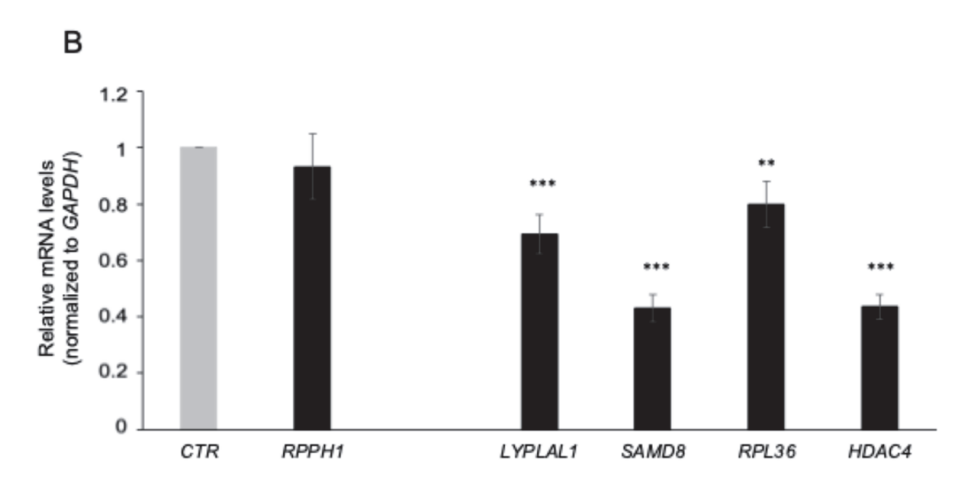


Figure 3. Validation of the circRNAs identified in PBMCs of MS patients versus HCs. Expression levels in PBMCs of five upregulated and four downregulated circRNAs (**A**) and the corresponding cognate linear mRNAs (**B**) were measured by qPCR analysis. The levels of circRNAs and mRNAs were normalized to *GAPDH mRNA* levels. Data are the means and standard deviation (+SD) from at least three independent experiments. ** p < 0.01, *** p < 0.001.

3.4. Identification of the miRNA and RBP Targets and circRNA-miRNA-mRNA Network

Highly abundant circRNAs have been shown to function as 'sponges' to sequester miRNAs and RBPs, and in turn regulate gene expression [24]. Accordingly, a miRNA target prediction program, miRanda, was used to identify in silico potential miRNA binding sites within the sequence of the circRNAs; many miRNAs were identified to have predicted miRNA response elements (MREs), and the five top-scoring miRNAs (based on the miRanda "max score") are listed (Figure 5A). For the upregulated circRNAs, an overlap on the listed miRNAs can be observed due to the common parental gene, *RPPH1*. To identify candidate RBPs interacting with the selected circRNAs, we used CircInteractome, a web tool that was developed to identify RBP-binding sites on circRNA sequences using CLIP-seq datasets from various sources [20]. Several RBPs have been identified to have potential binding sites in circRNAs. On average, circRNAs have seven different binding sites for different RBPs, and among them, the Argonaute family and FUS are the most highly represented and potentially interact with 70% of the identified and validated circRNAs (Figure 5B). The circRNA *hsa_circ_0048764* had the highest number of binding sites for RBPs in accordance with its greater length (1333 bp, with 73 binding sites).

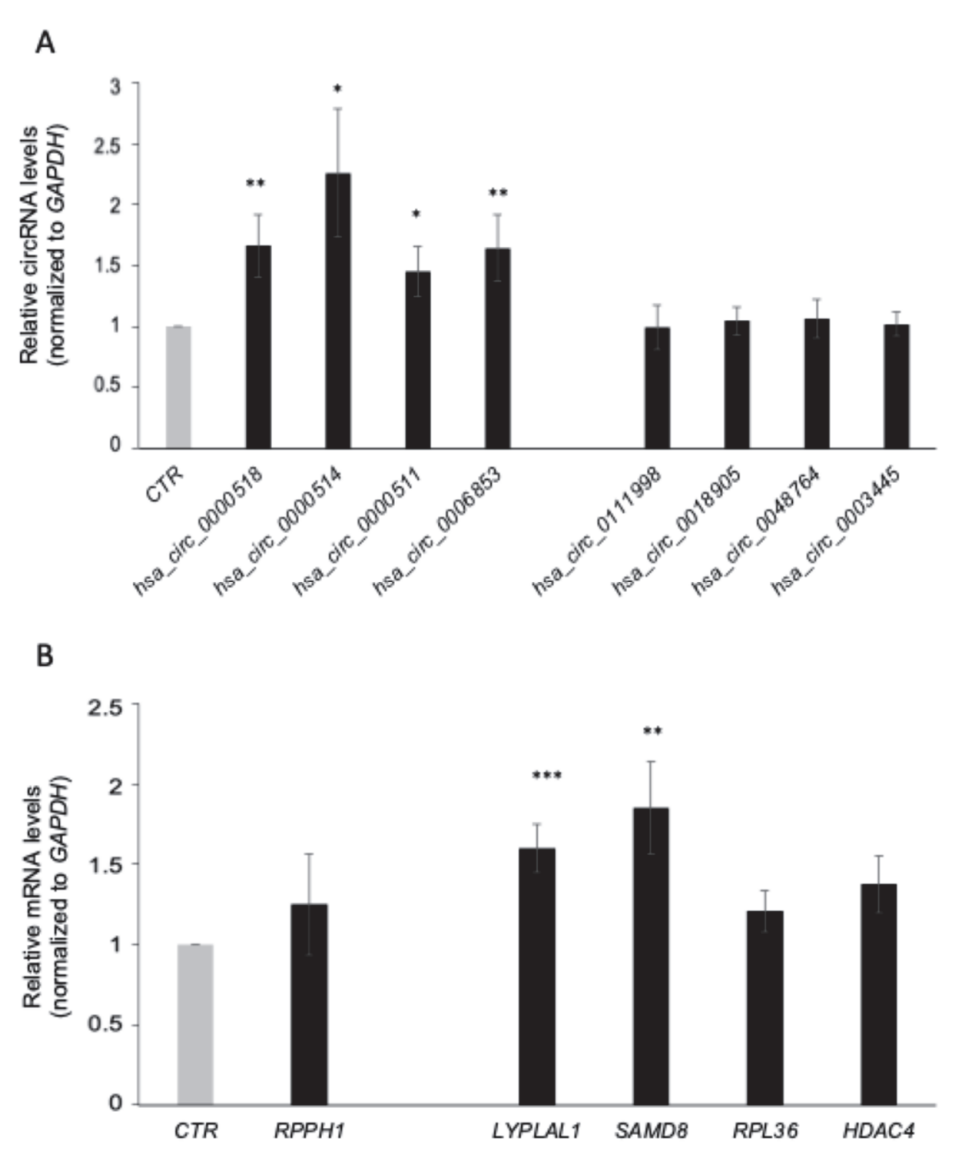


Figure 4. Validation of the circRNAs in serum of MS patients versus HCs. The levels in serum of five upregulated and four downregulated circRNAs (**A**) and the corresponding mRNAs (**B**) were measured by qPCR analysis. The levels of circRNAs and mRNAs were normalized to *GAPDH mRNA* levels. Data are the means and standard deviation (+SD) from at least three independent experiments. * p < 0.05, ** p < 0.01, *** p < 0.001.

Next, we decided to study the circRNA-miRNA-mRNA network and used the identified miRNAs to search for potential mRNA targets affected by the dysregulation of the identified circRNA. mRNA targets were selected using the list of candidate genes generated by the International Multiple Sclerosis Genetics Consortium [6]. Combining the information described above (circRNA, miRNA, and mRNA) and the mirTarBase interface [21], we constructed a putative circRNA-miRNA-mRNA network underlying dysregulated pathways in MS patients. As presented in Figure 6A, regulatory networks generated from the five validated upregulated circRNAs are predicted to result in altered expression of key proteins associated with the MS pathogenesis, namely CXCR4, FOXP1, and RREB1. Specifically, hsa_circ_0000518, hsa_circ_0000517, and hsa_circ_0000511 may bind to different miRNAs that regulate the same gene RREB1 (Ras-responsive element-binding protein 1) which is a risk gene for MS; recent evidence identified a key role of RREB1 as a positive regulator of many genes essential for neuron survival in mammalian brain [25]. The network generated using data from the downregulated circRNAs (Figure 6B) comprised three circRNA-miRNA-mRNA axes predicted to control the abundance of pivotal proteins

in MS pathogenesis, such as STAT3, ZFP36L1, and IKF3. This network highlights a key role of the miRNA-4270, which might be sponged by hsa_circ_0048764, and may affect the expression of the SLCO30A7, STAT3, ZFP36L1, and VCAM1 mRNAs. The protein encoded by ZFP36L1 (zinc finger protein 36-C3H-type-like 1) mRNA participates in mRNA degradation and translational repression. It limits the expression of a number of critical proteins involved in the regulation of immune function [26] and has been associated with several autoimmune diseases [27-29]. hsa_circ_0018905 and hsa_circ_0003445 bind miRNA-6727-3p and miRNA-612 to potentially affect the expression of IKZF3 (proteins Aiolos and Ikaros), which regulate lymphoid and myeloid cell development as well as immune homeostasis, in particular maturation and differentiation of B cells. Interestingly, IKZF3 was found to be upregulated in PBMCs of patients with MS during the relapse phase [30]. Notably, several circRNAs, including the upregulated hsa_circ_0000518 and hsa_circ_0000517, as well as the downregulated hsa_circ_0048764 and hsa_circ_0003445, may interact with distinct miRNAs that influence the expression of the PLEC gene, an essential gene in maintaining tissue integrity and elasticity in the brain [31]. Whether these predicted regulatory paradigms materialize in MS requires dedicated studies in which the copy numbers of each participating component of the complex (circRNA-miRNA-mRNA) are carefully measured, the physical interactions between the various RNAs are evaluated, and gain- and loss-of-function experiments are carried out to validate the proposed regulatory events.

3.5. PBMC circRNA Expression and Correlation with Disease Severity

To assess the potential implication of the identified circRNAs in the pathophysiology of the disease, we decided to evaluate the correlation between the expression of circRNA candidates and disease severity. We thus performed RT-qPCR analysis using a different cohort consisting of eight newly diagnosed RRMS patients with EDSS < 4.5, six RRMS patients with EDSS > 4.5, and eight SPMS patients with EDSS > 4.5 (Table 3).

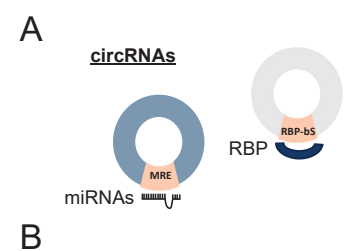
Table 3. Main characteristics of the individuals enrolled in the second step of the validation process.

Disease Type	RRMS Edss < 4.5	RRMS Edss > 4.5	SPMS Edss > 4.5
No. tot	8	6	8
Female	6	5	4
Male	2	1	4
Age, yrs, mean \pm SD	34.5 ± 11.95	64.3 ± 3.8	67.4 ± 7.2
Disease duration, mean \pm SD	at diagnosis	25.8 ± 16.6	27.4 ± 12.1
EDSS, mean \pm SD	2.3 ± 0.51	6 ± 0.70	6.3 ± 0.51

Abbreviations: SD, standard deviation; EDSS, Expanded Disability Status Scale; RRMS, relapsing–remitting MS; SPMS, secondary progressive MS.

The expression levels of $hsa_circ_0000511$ (FI = 0.73; p = 0.004 for RR EDSS > 4.5, FI = 0.62; p = 0,005 for SP EDSS > 4.5) and $hsa_circ_0018905$ (FI = 0.58; p = 0.0004 for RR EDSS > 4.5, FI = 0.70; p = 0.01 for SP EDSS > 4.5) were significantly lower in RRMS and SPMS with EDSS > 4.5 as compared with RRMS with EDSS < 4.5, thus showing a decrease in the target circRNAs with the increase in MS-related functional impairment. In contrast, $hsa_circ_0003445$ was significantly upregulated in RRMS with EDSS > 4.5 compared to RRMS with EDSS < 4.5, but significantly downregulated in SPMS with EDSS > 4.5. No significant difference was found in the expression levels of the other circRNAs analyzed (Figure 7A). We also examined the relative abundance of the cognate mRNAs for each circRNA and found a significant downregulation of SAMD8 and RPL36 mRNAs in RRMS with EDSS > 4.5, and RPL36 mRNA in SPMS as compared to RRMS with EDSS < 4.5. Interestingly, the coherent downregulation of $hsa_circ_0018905$ with MS functional impairment could drive alterations of the protein SMAD8 produced by the same parental gene. Additional analyses are needed to clarify this point. The RNAs transcribed

from the parental genes (*HDAC4* mRNA and *RPPH1*) showed no significant difference (Supplemental Figure S3).



circRNA	miRNA
	upregulated circRNA
hsa_circ_0000518	hsa-miR-328-3p, hsa-miR-127-5p, hsa-miR-7845-5p, hsa-miR-326, hsa-miR-4700-3p
hsa_circ_0000517	hsa-miR-127-5p, hsa-miR-326, hsa-miR-3191-5p, hsa-miR-1296-5p, hsa-miR-4518
hsa_circ_0000514	hsa-miR-615-5p, hsa-miR-4695-5p, hsa-miR-663a, hsa-miR-3173-3p, hsa-miR-296-5p
hsa_circ_0000511	hsa-miR-615-5p, hsa-miR-4695-5p, hsa-miR-663a, hsa-miR-512-5p, hsa-miR-3173-3p
hsa_circ_0006853	hsa-miR-4695-5p, hsa-miR-512-5p, hsa-miR-3173-3p, hsa-miR-7974, hsa-miR-3680-5p
	down regulated circRNA
hsa_circ_0018905	hsa-miR-6727-3p, hsa-miR-4732-5p, hsa-miR-4769-3p, hsa-miR-4722-3p, hsa-miR-8073
hsa_circ_0048764	hsa-miR-4739, hsa-miR-4270, hsa-miR-12128, hsa-miR-6847-5p, hsa-miR-6879-5p
hsa_circ_0003445	hsa-miR-1299, hsa-miR-6805-5p, hsa-miR-6842-3p, hsa-miR-6836-5p, hsa-miR-323a-5p

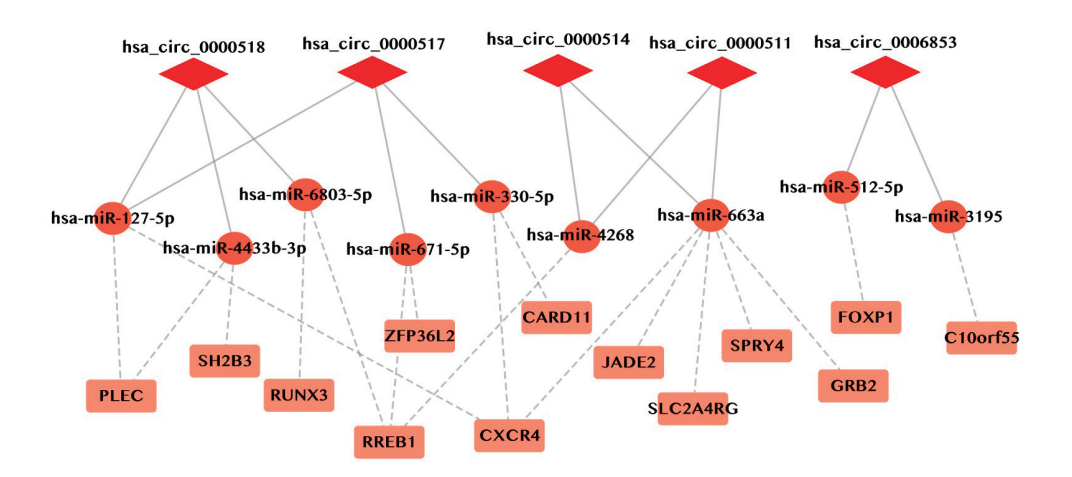
_	
	7
•	

Upregulated circRNAs	RBPs	binding site
hsa_circ_0000518	AGO1	1
	AGO2	3
	AGO3	1
	CAPRIN1	1
	DGCR8	1
	FMRP	3
	FUS	1
	FXR2	1
	HuR	1
	LIN28A	1
	LIN28B	1
hsa_circ_0000517	FUS	1
	LIN28A	1
	LIN28B	1
hsa_circ_0000514	AGO1	1
	AGO2	2
	DGCR8	1
	FMRP	2
	FUS	2
	HuR	1
hsa_circ_0000511	AGO1	1
	AGO2	2
	C170RF85	1
	DGCR8	1
	FMRP	2
	FUS	2
	HuR	1
hsa_circ_0006853	AGO1	1
	C17ORF85	1
	FMRP	1

Downregulated circRNAs	RBPs	binding site
hsa_circ_0018905	AGO1	1
	AGO2	6
	EIF4A3	13
	FMRP	24
	FUS	1
	HuR	4
	IGF2BP1	2
	IGF2BP2	2
	IGF2BP3	2
	PTB	1
	ZC3H7B	2
hsa_circ_0048764	AGO1	3
	AGO2	12
	AGO3	1
	C22ORF28	5
	CAPRIN1	3
	DGCR8	2
	EIF4A3	6
	EWSR1	2
	FMRP	8
	HuR	6
	IGF2BP1	3
	IGF2BP2	2
	IGF2BP3	3
	LIN28A	6
	LIN28B	3
	METTL3	4
	PTB	1
	SFRS1	2
	TAF15	1
hsa_circ_0003445	EIF4A3	2

Figure 5. Identification of the miRNAs and RBP Targets. (**A**) Schematic representation of circR-NAs with putative miRNA binding site (MRE) and RNA-binding protein binding site (RBP-bs). (**B**,**C**) Tables showing list of human circRNA identified from our studies and target miRNAs and interacting RNA-binding proteins as determined by analysis performed using miRanda and circInteractome, respectively.

Α



В

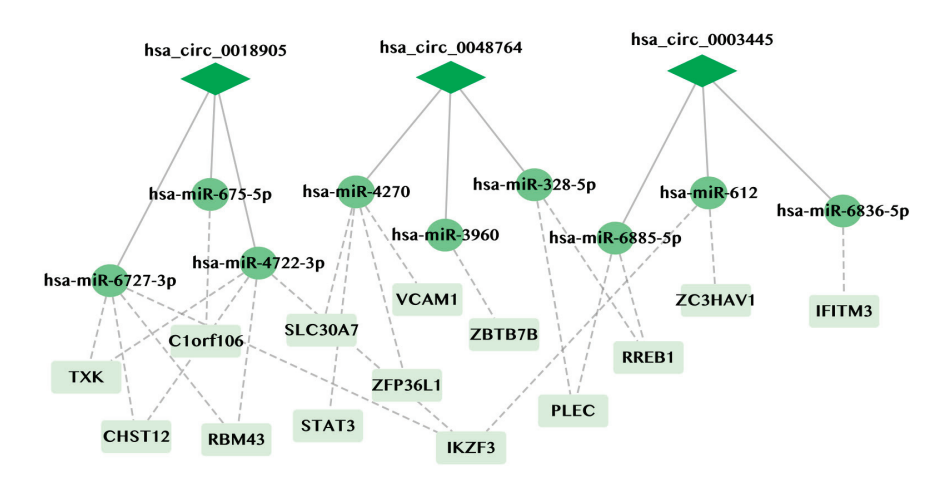
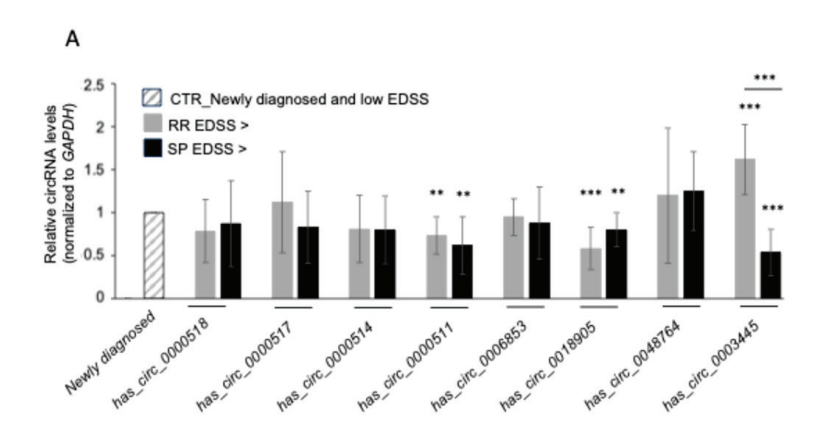


Figure 6. Network of circRNA-miRNA-mRNA for MS-associated genes. **(A)** Network of upregulated circRNAs and **(B)** downregulated circRNAs. CircRNAs are represented as red or green diamonds, miRNAs as red or green circles, and mRNAs as light red or light green rectangles. Red represents network generated from upregulated circRNAs and green from downregulated circRNAs.

To assess whether the differentially expressed circRNAs, which were differentially expressed in severe MS, could be candidate biomarkers for MS, we assessed the predictive value of $hsa_circ_0018905$ and $hsa_circ_0003445$ by employing the ROC curve analysis and using the Cq value for each circRNA. The results reported in Figure 7B showed that the area under the curve (AUC) is significant (p < 0.0002) for $hsa_circ_0003445$, with an AUC value of 0.83 (95% CI: 0.706–0.83), with a sensitivity of 90% and a specificity of 70%. For $hsa_circ_0018905$, we observed an AUC value of 0.948 (95% CI: 0.884–0.948) ($p = 5.1 \times 10^{-8}$), a sensitivity of 90%, and a specificity of 80%.



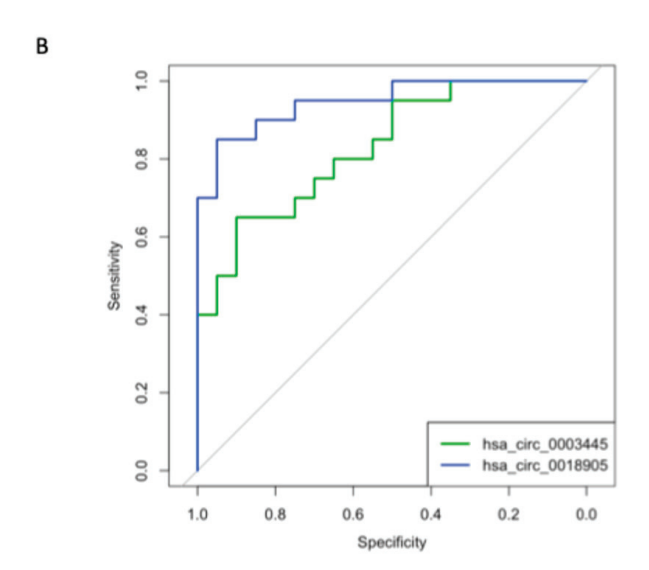


Figure 7. Validation of the circRNA expression in PBMCs and correlation with disease severity. **(A)** Expression levels in PBMCs of five upregulated and three downregulated circRNAs in MS with different disease severity measured by RT-qPCR analysis. The levels of circRNAs were normalized to GAPDH mRNA levels. **(B)** Receiver operating characteristic (ROC) curve of differentially expressed circRNAs in MS vs. HCs. Green line, $hsa_circ_0003445$ and blue line, $hsa_circ_0018905$. Data are represented as the means and standard deviation (+SD) from at least three independent experiments. ** p < 0.01, *** p < 0.001.

4. Discussion

Using circRNA microarray analysis, we discovered circRNAs differentially expressed in PBMCs of newly diagnosed MS patients as compared to HCs. The analysis identified 64 differentially expressed circRNAs, of which 11 circRNAs were upregulated and 53 were downregulated. Among the 64 differentially expressed circRNAs, 7 circRNAs were experimentally validated as dysregulated in the MS population using PBMCs from an independent validation cohort (hsa_circ_0000518, hsa_circ_0000517, hsa_circ_0000514, and hsa_circ_0000511 were confirmed to be upregulated, whereas hsa_circ_0018905, hsa_circ_0048764, and hsa_circ_003445 were confirmed to be downregulated). Due to their exceptional stability and high abundance in body fluids and EVs, circRNAs are considered promising biomarker candidates for non-invasive testing in clinical samples, including serum, plasma, saliva, urine, and cerebrospinal fluid. Interestingly, four of the validated circRNAs were also identified and validated in serum isolated from the blood of MS patients (hsa_circ_0000518, hsa_circ_0000514, hsa_circ_0000511, and hsa_circ_0006853). Notably, two circRNAs were confirmed to be downregulated in MS patients after all the validation steps, even when the disease course changed, as shown by a higher score using the EDSS and/or

SP status; in particular, <code>hsa_circ_0018905</code> and <code>hsa_circ_003445</code> were observed to remain downregulated with worsening of the disease severity (from low to high EDSS and/or from RR-to-SP status). In this context, our finding is likely correlated with the different stages of the pathophysiological process. In most cases, the development of disability leading to reduced ambulatory capacity and consequent high EDSS is indeed associated with neurodegenerative processes. Conversely, the profile of patients with lower EDSS is typically characterized by a predominance of active focal inflammation.

All the upregulated circRNAs identified are transcribed from the RPPH1 gene; RPPH1 is the RNA component of the RNase P ribonucleoprotein, an endoribonuclease that participates in tRNA maturation [32]. Upregulation of the circRNAs generated from the RPPH1 locus was validated in both PBMCs and serum (Figures 3 and 4) but was not observed in cross-sectional data analyzing changes in disease status (Figure 7). The role of this locus, and in particular of the hsa_circ_0000518 and hsa_circ_0000517, was previously described in MS [16]. Furthermore, RPPH1 was recently identified as one of the top differentially expressed RNAs implicated in RNA processing in the B-cell transcriptome of MS patients [23]. In this context, alteration of the circRNAs expression encoded from the RPPH1 gene (e.g., hsa_circ_0000518 and hsa_circ_0000517) described by our data may affect RPPH1 expression, thus influencing RNA processing in the B-cell and consequently B cell functions; indeed, circRNAs are well-known regulators of their linear parental gene through a preferential modulation of the parental gene transcription [33]. Of note, it has been observed by Jiang and colleagues that hsa_circ_0000518 promotes macrophage/microglia M1 Polarization via the FUS/CaMKKβ/AMPK pathway to aggravate MS [34]. Further studies analyzing circRNA expression using a single-cells approach are needed to clarify the expression and role of each identified circRNA in the context of MS disease.

In general, *RPPH1* has been [35,36] involved in the inflammatory pathogenesis of diabetic nephropathy and in the proliferation of breast cancer cells. It has also been reported to have a role in the pathogenesis of Alzheimer's disease (AD), where upregulation of *RPPH1* in AD mice was linked to increased expression of CDC42, promoting the formation of dendritic spines in hippocampal neurons [37], whereas *RPPH1* overexpression increased cell viability and inhibited apoptosis in A β -induced SK-N-SH cells [38]. While different studies suggest the role of *RPPH1* in the onset of different diseases, including MS, the exact function and mechanism underlying the role of *RPPH1* remain to be elucidated.

The validated circRNAs showing reduced abundance in MS were transcribed from different host genes—SAMD8, RPL36, and HDAC4. The mRNA encoding SAMD8 (Sphingomyelin synthase-related protein 1), and hsa_circ_00018905 were both downregulated in PBMCs of MS patients, and they remained downregulated despite changes in disease status (Figure 7 and Supplemental Figure S3) Furthermore, ROC analysis identified hsa_circ_00018905 as a new promising candidate biomarker for MS. SAMD8 is an ERresident ceramide phosphoethanolamine (CPE) synthase and a suppressor of ceramidemediated apoptosis in cultured cells; it was predicted to enable ceramide cholinephosphotransferase activity as well as sphingomyelin synthase activity, and it is involved in ceramide biosynthetic and regulation of ceramide biosynthetic processes [39,40]. Sphingomyelin is present in all cell membranes and also regulates inflammatory signaling and immune cell function; therefore, it may have a role in the pathophysiology of inflammatory disorders, including MS [41,42]. SAMD8 has been already associated with neurodegenerative conditions like Huntington's and AD while elevated SAMD8 expression in the brain raises questions regarding its possible role in neurodegenerative disorders that still need to be properly elucidated [40]. Regarding hsa_circ_00018905, no data are available today, and additional studies are necessary to elucidate how dysregulation is induced in MS samples and how it affects disease progression.

The RPL36 (Ribosomal Protein L36) gene from which *hsa_circ_0048764* is transcribed was mainly studied in glioma pathogenesis. It has been reported that downregulation of *RPL36* mRNA can inhibit cell proliferation and induce cell cycle arrest in glioma through STAT1. Analyzing expression data of common genes, Macrophage Migration Inhibitory

Factor signaling dysregulation of the RPL36 has been found to be associated with MS [43,44]. However, the molecular and pathological connections with the disease have not been identified until now. Additionally, hsa_circ_0048764 studies are still in their infancy and no connections have been identified with MS. Finally, for the transcripts generated by the HDAC4 gene, we observed a downregulation in PBMCs for both HDAC4 mRNA and hsa_circ_003445. Interestingly, the downregulation is maintained in the SP form of MS, but is not present when analyzing samples purified from patients with RRMS and higher EDSS. Hsa_circ_003445 is also indicated as a possible biomarker for MS by ROC curve analysis (Figure 7A,B). HDAC4 encodes the histone deacetylase 4, a protein involved in histone modifications and highly abundant in the brain [45]. HDAC4 may play a role in neuronal plasticity, and there is some evidence that HDAC inhibitors lessen the neuropathy in mice used as MS models (EAE) [46]. Furthermore, emerging evidence suggests epigenetic modifications have a role in affecting the risk of MS [47]. While studying differentially methylated regions in case/control cohorts focusing on progressive MS, Maltby and colleagues found that genes HTR2A, SLC17A9, and HDAC4 were differentially methylated between MS and control individuals [48]. Additionally, RNA sequencing analysis from different brain regions, at different stages of differentiation, uncovered thousands of highly abundant circRNAs in neurons, including hsa_circ_0003445 [49]. To sum up, we confirm the dysregulation of circRNAs that are generated from the RPPH1 gene in MS and identify new circRNAs dysregulated with the disease. Of note, all of them are generated from genes that have been implicated, at different levels, with the regulation of immune functions, one of the critical components of MS. Considering the functions of circRNA, one can expect that the dysregulation of the indicated circRNAs may affect the functions of the linear parental gene, altering immune regulation.

CircRNAs are emerging as important regulators of the immune system, significantly influencing immune cell development and differentiation, which are strongly linked to the onset and progression of autoimmune diseases [50]. Functionally, circRNAs can influence the activation and activity of various immune cells (e.g., T cells, B cells, and macrophages), thereby fine-tuning immune responses [51]. CircRNAs are also involved in the regulation of cytokines production and essential signaling pathways related to immune responses [52]. Investigating the expression profiles of circRNAomes in B cells, T cells, and monocytes, Nicolet et al. identified significant differences in circRNA expression among different immune cells. Interestingly, this study highlighted hundreds of circRNAs that exhibit cell type-specific expression suggesting the involvement in the regulation or maintenance of specific cell functions [53]. Additionally, during hematopoietic differentiation, lymphocytes displayed the highest circRNA expression levels, reflecting a greater abundance rather than diversity. For instance, circ-FNDC3B showed the highest expression in natural killer cells, while circ-ELK4, circ-MYBL1, and circ-SLFN12L were predominantly expressed in T cells and natural killer cells. Moreover, Maass et al. examined circRNA expression profiles across 20 human tissues closely associated with various diseases. They demonstrated that many circRNAs exhibit tissue-specific expression, potentially linked to the clinical phenotypes and underlying mechanisms of human diseases [54].

Concerning the circRNAs differentially expressed in MS and identified in this report, no studies have analyzed the expression pattern in the immune cells population except for *hsa_circ_0000518*, as mentioned above, which has been deeply studied in macrophages in the context of MS. In their manuscript, Zhang et al. analyzed circRNA expression in macrophages under M1 (interferon-γ and LPS-induced) and M2 (IL4-induced) polarization conditions. *Hsa_circ_0000518* has been observed to be upregulated in the cerebrospinal fluid and peripheral blood of MS patients. Additionally, interfering with *hsa_circ_0000518* expression in vitro led to reduced FUS expression, promoted the polarization of LPS-activated HMC3 cells towards the M2 type, and alleviated CNS injury in an experimental autoimmune encephalomyelitis (EAE) mouse model, indicating that *hsa_circ_0000518* might be a potential therapeutic target for MS [34]. CircRNAs exert their functions as miRNA and RNA binding sponges that affect cell regulation at various levels. This regulatory

process is implicated in various vital biological functions, such as the differentiation and survival of brain cells and the modulation of various immune processes including B-cell function, a key element of the MS pathology. In this regard, our analysis (Figures 5 and 6) predicted that hsa_circ_0000518 and hsa_circ_0000517 may sponge miR-326, a microRNA highly abundant in active MS lesions in comparison with inactive lesions or normal brain white matter which was found to be upregulated during relapse phases in RRMS [55]. Functionally, miRNA-326 promotes T helper 17 cell differentiation and phagocytosis of myelin, and has been shown to be the target for the therapeutic inhibition of disease in mice used to study autoimmune encephalomyelitis [55]. CircRNAs may also bind to and sequester RBPs, affecting the interactions with other RNAs, thus modulating translation and RNA stability [56,57]. Jiayi et al. found that the RBP HuR and miR-29a controlled the production of cystatin F, a crucial inhibitor of papain-like lysosomal cysteine proteinases that plays a pivotal role in demyelination and remyelination. Reduced levels of both HuR and cystatin F were observed in the core regions of MS plaques compared to the border zone, implying a potential connection between decreased HuR levels and cystatin F mRNA instability, leading to exacerbated demyelination in MS patients [58]. In this context, even if the copies per cell of hsa_circ_0000518, hsa_circ_0000514, and hsa_circ_0000511 are not known, the upregulation of these circRNAs may lead to the sequestration of HuR, possibly at a localized level, in turn exacerbating the demyelination process.

Several studies have now demonstrated that non-coding RNAs, including circRNAs and miRNAs, have been implicated in the development of MS at different levels. Indeed, circRNAs can interact with miRNAs, influencing their specific mRNA targets' levels and shaping the so-called competing endogenous RNAs (ceRNA) network. Thus, we also investigated the circRNA-miRNA-mRNA network for MS risk-associated genes identified by the International Multiple Sclerosis Genetics Consortium [6]. Although ceRNA analysis must be considered with caution, after considering the intracellular stoichiometry of the regulatory RNAs, the possibility that some MS-associated circRNAs could regulate MS pathogenesis deserves closer scrutiny. For example, we showed a deregulation of the immune system, including T cell proliferation and differentiation (e.g., STAT3, TXK, and CXCR4) and neurodegeneration (e.g., FOXP1 and PLEC). Alterations in circRNA-miRNAmRNA network might provide microenvironmental changes that modulate MS progression, such as hsa_circ_0000518 and hsa_circ_0000517 (upregulated), as well as hsa_circ_0048764 and hsa_circ_0003445 (downregulated), which were predicted to bind the different miRNAs that regulate the same gene, PLEC. PLEC encodes the cytoskeleton plectin protein, which is present in numerous tissues, including nervous tissue, and is involved in maintaining tissue integrity and elasticity [59]. Furthermore, Orton et al. observed consistent differences in PLEC gene expression in MS patients with different disease severity, reporting upregulation of PLEC in severe MS cases [60].

Until now, few studies have explored the relationship between circRNAs and MS. Among these, only two studies share similarities with ours: those by [16] and [30] I conducted a microarray analysis on PBMCs from four RRMS patients compared to four HCs and identified 406 differentially expressed circRNAs, with the top two upregulated, <code>has_circ_0000518</code> and <code>hsa_circ_0000517</code>, being consistent with our findings [16]. On the other hand, Zurawska et al. performed a microarray analysis on PBMCs isolated from MS patients during the relapse and remission phases and compared them with HCs [30]. However, these previous studies did not employ newly diagnosed patients, and the differences among them could be explained by heterogeneity due to disease progression and specific therapeutic interventions used by patients. Furthermore, our study, as well as the other described above [16,30], is characterized by an important limitation: the discovery dataset is small. In our study, for example, five MS samples vs. five HCs were used. Further studies should be carried out to characterize the expression profile and function of circulating circRNAs in a more extended dataset.

Although there is growing evidence highlighting the significant involvement of circRNAs in regulating immune cell functions and the CNS [61–63], their specific role(s) in

the development of MS remain largely unexplored, with only a limited number of studies investigating this aspect. Our study focused on the expression profiles of circRNAs in MS patients at the moment of diagnosis, before therapy, improving our understanding of the role of circRNAs during the first phases of MS pathogenesis. However, to date, no direct link through genetic association with MS has been reported for the identified genes (*RPPH1, SAMD8, RPL36*, and *HDAC4*), thus suggesting a role for the encoded circRNAs as biomarkers, rather than in the causal biology of disease. In sum, for the first time, we have studied the expression profile of more than 13,000 circRNAs in MS patients at the time of diagnosis, linking circRNAs to MS, and highlighting for the first time a possible role for *hsa_circ_0018905* as a biomarker for MS.

Supplementary Materials: The following supporting information can be downloaded at: https://www.mdpi.com/article/10.3390/cells13191668/s1, Figure S1: Overview of the workflow and different cohorts used in the study; Figure S2: CircRNAs chromosome distribution; Figure S3: Validation of the circRNAs parental linear transcript in PBMCs of MS patients with different disease severity. Table S1: Complete list of dysregulated circRNAs.

Author Contributions: M.L.I. and I.R.Z. organized and participated in the sample collection. V.L., G.F., A.M., G.D. and M.R.M. contributed to the sample collection. V.L. and M.L.I. designed and performed the experiment. I.C., G.D., M.R.M., P.S. and D.T. provided technical support. D.T., I.C. and M.G. provided expertise and critical feedback. V.L. and M.F. performed statistical analysis. M.F., I.R.Z. and M.L.I. conceived the study. V.L. and M.L.I. wrote the first draft of the manuscript. All authors have read and agreed to the published version of the manuscript.

Funding: The study was supported by the Italian Foundation for Multiple Sclerosis—FISM (Grant N. 2021/S/2).

Institutional Review Board Statement: The study was conducted in accordance with the Declaration of Helsinki, and approved by the Institutional Review Board (or Ethics Committee) of Ethical Review Boards of ATS Sardegna (Prot. N° 177/20021/EX2492/CE, Sassari 26/01/2021). Patient data and samples were coded anonymously to ensure confidentiality during sample processing and data analysis.

Informed Consent Statement: Informed consent was obtained from all subjects involved in the study.

Data Availability Statement: All data needed to evaluate the conclusions in the paper are present in the paper and in the Supplementary Materials.

Acknowledgments: We thank all the patients and volunteers who generously participated in this study. We would also like to thank all the medical doctors, nurses, and students who contributed to the realization of this study.

Conflicts of Interest: The authors report no conflicts of interest.

References

- 1. Shah, A.; Panchal, V.; Patel, K.; Alimohamed, Z.; Kaka, N.; Sethi, Y.; Patel, N. Pathogenesis and management of multiple sclerosis revisited. *Dis.-A-Mon.* **2023**, *69*, 101497. [CrossRef]
- 2. Sand, I.K. Classification, diagnosis, and differential diagnosis of multiple sclerosis. *Curr. Opin. Neurol.* **2015**, *28*, 193–205. [CrossRef] [PubMed]
- 3. Frau, J.; Coghe, G.; Lorefice, L.; Fenu, G.; Cocco, E. Infections and Multiple Sclerosis: From the World to Sardinia, From Sardinia to the World. *Front. Immunol.* **2021**, 12, 728677. [CrossRef] [PubMed]
- 4. Urru, S.A.M.; Antonelli, A.; Sechi, G.M.; MS Working Group. Prevalence of multiple sclerosis in Sardinia: A systematic cross-sectional multi-source survey. *Mult. Scler. J.* **2019**, *26*, 372–380. [CrossRef] [PubMed]
- 5. Olsson, T.; Barcellos, L.F.; Alfredsson, L. Interactions between genetic, lifestyle and environmental risk factors for multiple sclerosis. *Nat. Rev. Neurol.* **2016**, *13*, 25–36. [CrossRef]
- 6. International Multiple Sclerosis Genetics Consortium. Multiple sclerosis genomic map implicates peripheral immune cells and microglia in susceptibility. *Science* **2019**, *365*, eaav7188. [CrossRef]
- 7. Steri, M.; Orrù, V.; Idda, M.L.; Pitzalis, M.; Pala, M.; Zara, I.; Sidore, C.; Faà, V.; Floris, M.; Deiana, M.; et al. Overexpression of the cytokine BAFF and autoimmunity risk. *N. Engl. J. Med.* **2017**, *376*, 1615–1626. [CrossRef]
- 8. Mohammed, E.M. Environmental Influencers, MicroRNA, and Multiple Sclerosis. *J. Cent. Nerv. Syst. Dis.* **2020**, 12, 1179573519894955. [CrossRef] [PubMed]

- 9. Paraboschi, E.M.; Cardamone, G.; Soldà, G.; Duga, S.; Asselta, R. Interpreting Non-coding Genetic Variation in Multiple Sclerosis Genome-Wide Associated Regions. *Front. Genet.* **2018**, *9*, 647. [CrossRef]
- 10. Mohammed, E.M. Circular RNA in Multiple Sclerosis: Pathogenicity and Potential Biomarker Development: A Systematic Review. *Epigenetics Insights* **2023**, *16*, 25168657231213195. [CrossRef]
- 11. Li, H.; Ma, X.; Li, H. Intriguing circles: Conflicts and controversies in circular RNA research. *Wiley Interdiscip. Rev. RNA* **2019**, 10, e1538. [CrossRef] [PubMed]
- 12. Liu, S.; Guo, X.Y.; Shang, Q.J.; Gao, P. The biogenesis, biological functions and modification of Circular RNAs. *Exp. Mol. Pathol.* **2023**, *131*, 104861. [CrossRef] [PubMed]
- 13. Hanan, M.; Soreq, H.; Kadener, S. CircRNAs in the brain. RNA Biol. 2016, 14, 1028–1034. [CrossRef] [PubMed]
- 14. Herman, A.B.; Tsitsipatis, D.; Gorospe, M. Integrated lncRNA function upon genomic and epigenomic regulation. *Mol. Cell* **2022**, 82, 2252–2266. [CrossRef] [PubMed]
- 15. Cardamone, G.; Paraboschi, E.M.; Rimoldi, V.; Duga, S.; Soldà, G.; Asselta, R. The characterization of *GSDMB* splicing and backsplicing profiles identifies novel isoforms and a circular rna that are dysregulated in multiple sclerosis. *Int. J. Mol. Sci.* **2017**, 18, 576. [CrossRef] [PubMed]
- 16. Iparraguirre, L.; Muñoz-Culla, M.; Prada-Luengo, I.; Castillo-Triviño, T.; Olascoaga, J.; Otaegui, D. Circular RNA profiling reveals that circular RNAs from ANXA2 can be used as new biomarkers for multiple sclerosis. *Hum. Mol. Genet.* **2017**, *26*, 3564–3572. [CrossRef]
- 17. Holdt, L.M.; Stahringer, A.; Sass, K.; Pichler, G.; Kulak, N.A.; Wilfert, W.; Kohlmaier, A.; Herbst, A.; Northoff, B.H.; Nicolaou, A.; et al. Circular non-coding RNA ANRIL modulates ribosomal RNA maturation and atherosclerosis in humans. *Nat. Commun.* **2016**, 7, 12429. [CrossRef] [PubMed]
- 18. Ferreira, H.J.; Esteller, M. Non-coding RNAs, epigenetics, and cancer: Tying it all together. *Cancer Metastasis Rev.* **2018**, 37, 55–73. [CrossRef] [PubMed]
- 19. Enright, A.J.; John, B.; Gaul, U.; Tuschl, T.; Sander, C.; Marks, D.S. Enright-2003-Genomebiol. Pdf. Genome Biol. 2003, 5, R1.
- 20. Dudekula, D.B.; Panda, A.C.; Grammatikakis, I.; De, S.; Abdelmohsen, K.; Gorospe, M. CircInteractome: A web tool for exploring circular RNAs and their interacting proteins and microRNAs. *RNA Biol.* **2016**, *13*, 34–42. [CrossRef] [PubMed]
- 21. Huang, H.-Y.; Lin, Y.-C.; Cui, S.; Huang, Y.; Tang, Y.; Xu, J.; Bao, J.; Li, Y.; Wen, J.; Zuo, H.; et al. miRTarBase update 2022: An informative resource for experimentally validated miRNA–target interactions. *Nucleic Acids Res.* 2021, 50, D222–D230. [CrossRef] [PubMed]
- 22. Shannon, P.; Markiel, A.; Ozier, O.; Baliga, N.S.; Wang, J.T.; Ramage, D.; Amin, N.; Schwikowski, B.; Ideker, T. Cytoscape: A software environment for integrated models. *Genome Res.* 1971, 13, 426. [CrossRef]
- 23. Hecker, M.; Fitzner, B.; Boxberger, N.; Putscher, E.; Engelmann, R.; Bergmann, W.; Müller, M.; Ludwig-Portugall, I.; Schwartz, M.; Meister, S.; et al. Transcriptome alterations in peripheral blood B cells of patients with multiple sclerosis receiving immune reconstitution therapy. *J. Neuroinflamm.* 2023, 20, 181. [CrossRef]
- 24. Ikeda, Y.; Morikawa, S.; Nakashima, M.; Yoshikawa, S.; Taniguchi, K.; Sawamura, H.; Suga, N.; Tsuji, A.; Matsuda, S. CircRNAs and RNA-Binding Proteins Involved in the Pathogenesis of Cancers or Central Nervous System Disorders. *Non-Coding RNA* **2023**, 9, 23. [CrossRef]
- 25. Griffin, E.N.; Jucius, T.; Sim, S.-E.; Harris, B.S.; Heinz, S.; Ackerman, S.L. RREB1 regulates neuronal proteostasis and the microtubule network. *Sci. Adv.* **2024**, *10*, eadh3929. [CrossRef]
- 26. Perga, S.; Montarolo, F.; Martire, S.; Berchialla, P.; Malucchi, S.; Bertolotto, A. Anti-inflammatory genes associated with multiple sclerosis: A gene expression study. *J. Neuroimmunol.* **2015**, 279, 75–78. [CrossRef]
- 27. Grant, S.F.; Qu, H.-Q.; Bradfield, J.P.; Marchand, L.; Kim, C.E.; Glessner, J.T.; Grabs, R.; Taback, S.P.; Frackelton, E.C.; Eckert, A.W.; et al. Follow-up analysis of genome-wide association data identifies novel loci for type 1 Diabetes. *Diabetes* **2009**, *58*, 290–295. [CrossRef] [PubMed]
- 28. Perdigones, N.; Martín, E.; Robledo, G.; Lamas, J.R.; Taxonera, C.; Díaz-Rubio, M.; de la Concha, E.G.; López-Nevot, M.A.; García, A.; Gómez-García, M.; et al. Study of chromosomal region 5p13.1 in Crohn's disease, ulcerative colitis, and rheumatoid arthritis. *Hum. Immunol.* 2010, 71, 826–828. [CrossRef]
- 29. Medici, M.; Porcu, E.; Pistis, G.; Teumer, A.; Brown, S.J.; Jensen, R.A.; Rawal, R.; Roef, G.L.; Plantinga, T.S.; Vermeulen, S.H.; et al. Identification of Novel Genetic Loci Associated with Thyroid Peroxidase Antibodies and Clinical Thyroid Disease. *PLoS Genet.* **2014**, *10*, e1004123. [CrossRef]
- 30. Zurawska, A.E.; Mycko, M.P.; Selmaj, I.; Raine, C.S.; Selmaj, K.W. Multiple Sclerosis. *Neurol.-Neuroimmunol. Neuroinflamm.* **2021**, 8, e1041. [CrossRef]
- 31. Potokar, M.; Jorgačevski, J. Plectin in the central nervous system and a putative role in brain astrocytes. *Cells* **2021**, *10*, 2353. [CrossRef] [PubMed]
- 32. Evans, D.; Marquez, S.M.; Pace, N.R. RNase P: Interface of the RNA and protein worlds. *Trends Biochem. Sci.* **2006**, *31*, 333–341. [CrossRef]
- 33. Wang, H.; Gao, X.; Yu, S.; Wang, W.; Liu, G.; Jiang, X.; Sun, D. Circular RNAs regulate parental gene expression: A new direction for molecular oncology research. *Front. Oncol.* **2022**, *12*, 947775. [CrossRef] [PubMed]

- 34. Jiang, F.; Liu, X.; Cui, X.; Hu, J.; Wang, L.; Xue, F.; Guo, S.; Wang, X. Circ_0000518 Promotes Macrophage/Microglia M1 Polarization via the FUS/CaMKKβ/AMPK Pathway to Aggravate Multiple Sclerosis. Neuroscience 2022, 490, 131–143. [CrossRef] [PubMed]
- 35. Zhang, P.; Sun, Y.; Peng, R.; Chen, W.; Fu, X.; Zhang, L.; Peng, H.; Zhang, Z. Long non-coding RNA Rpph1 promotes inflammation and proliferation of mesangial cells in diabetic nephropathy via an interaction with Gal-3. *Cell Death Dis.* **2019**, *10*, 526. [CrossRef]
- 36. Liang, Z.X.; Liu, H.S.; Wang, F.W.; Xiong, L.; Zhou, C.; Hu, T.; He, X.W.; Wu, X.J.; Xie, D.; Wu, X.R.; et al. LncRNA RPPH1 promotes colorectal cancer metastasis by interacting with TUBB3 and by promoting exosomes-mediated macrophage M2 polarization. *Cell Death Dis.* 2019, *10*, 829. [CrossRef] [PubMed]
- 37. Cai, Y.; Sun, Z.; Jia, H.; Luo, H.; Ye, X.; Wu, Q.; Xiong, Y.; Zhang, W.; Wan, J. Rpph1 upregulates CDC42 expression and promotes hippocampal neuron dendritic spine formation by competing with miR-330-5p. *Front. Mol. Neurosci.* **2017**, *10*, 27. [CrossRef]
- 38. Gu, R.; Wang, L.; Tang, M.; Li, S.-R.; Liu, R.; Hu, X. LncRNA Rpph1 protects amyloid-β induced neuronal injury in SK-N-SH cells via miR-122/Wnt1 axis. *Int. J. Neurosci.* **2019**, *130*, 443–453. [CrossRef]
- 39. Tafesse, F.G.; Vacaru, A.M.; Bosma, E.F.; Hermansson, M.; Jain, A.; Hilderink, A.; Somerharju, P.; Holthuis, J.C.M. Sphingomyelin synthase-related protein SMSr is a suppressor of ceramide-induced mitochondrial apoptosis. *J. Cell Sci.* **2013**, 127, 445–454. [CrossRef]
- 40. Cabukusta, B.; Nettebrock, N.T.; Kol, M.; Hilderink, A.; Tafesse, F.G.; Holthuis, J.C. Ceramide phosphoethanolamine synthase SMSr is a target of caspase-6 during apoptotic cell death. *Biosci. Rep.* **2017**, *37*, BSR20170867. [CrossRef]
- 41. Filippatou, A.G.; Moniruzzaman, M.; Sotirchos, E.S.; Fitzgerald, K.C.; Kalaitzidis, G.; Lambe, J.; Vasileiou, E.; Saidha, S.; Prince, J.L.; Haughey, N.; et al. Serum ceramide levels are altered in multiple sclerosis. *Mult. Scler. J.* **2020**, 27, 1506–1519. [CrossRef] [PubMed]
- 42. Podbielska, M.; Hogan, E. Molecular and immunogenic features of myelin lipids: Incitants or modulators of multiple sclerosis? *Mult. Scler. J.* **2009**, *15*, 1011–1029. [CrossRef] [PubMed]
- 43. Cavalli, E.; Mazzon, E.; Basile, M.S.; Mangano, K.; Di Marco, R.; Bramanti, P.; Nicoletti, F.; Fagone, P.; Petralia, M.C. Upregulated expression of macrophage migration inhibitory factor, its analogue D-dopachrome tautomerase, and the CD44 receptor in peripheral CD4 T cells from clinically isolated syndrome patients with rapid conversion to clinical defined multiple sclerosis. *Medicina* **2019**, *55*, 667. [CrossRef]
- 44. Alaya, F.; Baraket, G.; Adediran, D.A.; Cuttler, K.; Ajiboye, I.; Kivumbi, M.T.; Sitharam, N.; Awe, O.I. Multiple Sclerosis Stages and their Differentially Expressed Genes: A Bioinformatics Analysis. *bioRxiv* 2024. [CrossRef]
- 45. Grozinger, C.M.; Hassig, C.A.; Schreiber, S.L. Three proteins define a class of human histone deacetylases related to yeast Hda1p. *Proc. Natl. Acad. Sci. USA* **1999**, *96*, 4868–4873. [CrossRef]
- 46. Camelo, S.; Iglesias, A.H.; Hwang, D.; Due, B.; Ryu, H.; Smith, K.; Gray, S.G.; Imitola, J.; Duran, G.; Assaf, B.; et al. Transcriptional therapy with the histone deacetylase inhibitor trichostatin A ameliorates experimental autoimmune encephalomyelitis. *J. Neuroimmunol.* 2005, 164, 10–21. [CrossRef] [PubMed]
- 47. He, H.; Hu, Z.; Xiao, H.; Zhou, F.; Yang, B. The tale of histone modifications and its role in multiple sclerosis. *Hum. Genom.* **2018**, 12, 31. [CrossRef]
- 48. Maltby, V.E.; Lea, R.A.; Burnard, S.; Xavier, A.; Van Cao, T.; White, N.; Kennedy, D.; Groen, K.; Sanders, K.A.; Seeto, R.; et al. Epigenetic differences at the HTR2A locus in progressive multiple sclerosis patients. *Sci. Rep.* **2020**, *10*, 22217. [CrossRef]
- 49. Rybak-Wolf, A.; Stottmeister, C.; Glažar, P.; Jens, M.; Pino, N.; Giusti, S.; Hanan, M.; Behm, M.; Bartok, O.; Ashwal-Fluss, R.; et al. Circular RNAs in the Mammalian Brain Are Highly Abundant, Conserved, and Dynamically Expressed. *Mol. Cell* **2015**, *58*, 870–885. [CrossRef]
- 50. Zhou, Z.; Sun, B.; Huang, S.; Zhao, L. Roles of circular RNAs in immune regulation and autoimmune diseases. *Cell Death Dis.* **2019**, *10*, 503. [CrossRef]
- 51. Carlos-Reyes, Á.; Romero-Garcia, S.; Contreras-Sanzón, E.; Ruiz, V.; Prado-Garcia, H. Role of Circular RNAs in the Regulation of Immune Cells in Response to Cancer Therapies. *Front. Genet.* **2022**, *13*, 823238. [CrossRef]
- 52. Chen, X.; Yang, T.; Wang, W.; Xi, W.; Zhang, T.; Li, Q.; Yang, A.; Wang, T. Circular RNAs in immune responses and immune diseases. *Theranostics* **2019**, *9*, 588–607. [CrossRef]
- 53. Gaffo, E.; Boldrin, E.; Molin, A.D.; Bresolin, S.; Bonizzato, A.; Trentin, L.; Frasson, C.; Debatin, K.-M.; Meyer, L.H.; Kronnie, G.T.; et al. Circular RNA differential expression in blood cell populations and exploration of circRNA deregulation in pediatric acute lymphoblastic leukemia. *Sci. Rep.* **2019**, *9*, 14670. [CrossRef]
- 54. Maass, P.G.; Glažar, P.; Memczak, S.; Dittmar, G.; Hollfinger, I.; Schreyer, L.; Sauer, A.V.; Toka, O.; Aiuti, A.; Luft, F.C.; et al. A map of human circular RNAs in clinically relevant tissues. *J. Mol. Med.* **2017**, *95*, 1179–1189. [CrossRef]
- 55. Junker, A.; Hohlfeld, R.; Meinl, E. The emerging role of microRNAs in multiple sclerosis. *Nat. Rev. Neurol.* **2010**, *7*, 56–59. [CrossRef]
- 56. Zang, J.; Lu, D.; Xu, A. The interaction of circRNAs and RNA binding proteins: An important part of circRNA maintenance and function. *J. Neurosci. Res.* **2018**, *98*, 87–97. [CrossRef]
- 57. Lodde, V.; Floris, M.; Zoroddu, E.; Zarbo, I.R.; Idda, M.L. RNA-binding proteins in autoimmunity: From genetics to molecular biology. *Wiley Interdiscip. Rev. RNA* **2023**, *14*, e1772. [CrossRef]

- 58. Li, J.; Durose, W.W.; Ito, J.; Kakita, A.; Iguchi, Y.; Katsuno, M.; Kunisawa, K.; Shimizu, T.; Ikenaka, K. Exploring the factors underlying remyelination arrest by studying the post-transcriptional regulatory mechanisms of cystatin F gene. *J. Neurochem.* **2020**, *157*, 2070–2090. [CrossRef]
- 59. Kiritsi, D.; Tsakiris, L.; Schauer, F. Plectin in Skin Fragility Disorders. Cells 2021, 10, 2738. [CrossRef]
- 60. Orton, S.M.; Sangha, A.; Gupta, M.; Martens, K.; Metz, L.M.; de Koning, A.P.J.; Pfeffer, G. Expression of risk genes linked to vitamin D receptor super-enhancer regions and their association with phenotype severity in multiple sclerosis. *Front. Neurol.* **2022**, 13, 1064008. [CrossRef]
- 61. Najafi, S.; Zarch, S.M.A.; Majidpoor, J.; Pordel, S.; Aghamiri, S.; Rasul, M.F.; Asemani, Y.; Vakili, O.; Mohammadi, V.; Movahedpour, A.; et al. Recent insights into the roles of circular RNAs in human brain development and neurologic diseases. *Int. J. Biol. Macromol.* 2023, 225, 1038–1048. [CrossRef]
- 62. Zhang, Y.; Luo, J.; Yang, W.; Ye, W.-C. CircRNAs in colorectal cancer: Potential biomarkers and therapeutic targets. *Cell Death Dis.* **2023**, *14*, 353. [CrossRef]
- 63. Lodde, V.; Murgia, G.; Simula, E.R.; Steri, M.; Floris, M.; Idda, M.L. Long noncoding RNAs and circular RNAs in autoimmune diseases. *Biomolecules* **2020**, *10*, 1044. [CrossRef]

Disclaimer/Publisher's Note: The statements, opinions and data contained in all publications are solely those of the individual author(s) and contributor(s) and not of MDPI and/or the editor(s). MDPI and/or the editor(s) disclaim responsibility for any injury to people or property resulting from any ideas, methods, instructions or products referred to in the content.





Article

Immune Gene Expression Profiling in Individuals with Turner Syndrome, Graves' Disease, and a Healthy Female by Single-Cell RNA Sequencing: A Comparative Study

Soo Yeun Sim 1 , In-Cheol Baek 2,* , Won Kyoung Cho 3,* , Min Ho Jung 4 , Tai-Gyu Kim 5 and Byung-Kyu Suh 1

- Department of Pediatrics, Seoul St. Mary's Hospital, College of Medicine, The Catholic University of Korea, Seoul 06591, Republic of Korea; sooyeunsim8@gmail.com (S.Y.S.); suhbk@catholic.ac.kr (B.-K.S.)
- ² Catholic Hematopoietic Stem Cell Bank, College of Medicine, The Catholic University of Korea, Seoul 06591, Republic of Korea
- Department of Pediatrics, St. Vincent's Hospital, College of Medicine, The Catholic University of Korea, Seoul 16247, Republic of Korea
- Department of Pediatrics, Yeouido St. Mary's Hospital, College of Medicine, The Catholic University of Korea, Seoul 07345, Republic of Korea; jmhpe@catholic.ac.kr
- Department of Microbiology, College of Medicine, The Catholic University of Korea, Seoul 06591, Republic of Korea; kimtg@catholic.ac.kr
- * Correspondence: icbaek@catholic.ac.kr (I.-C.B.); wendy626@catholic.ac.kr (W.K.C.)

Abstract: Turner syndrome (TS) can be determined by karyotype analysis, marked by the loss of one X chromosome in females. However, the genes involved in autoimmunity in TS patients remain unclear. In this study, we aimed to analyze differences in immune gene expression between a patient with TS, a healthy female, and a female patient with Graves' disease using single-cell RNA sequencing (scRNA-seq) analysis of antigen-specific CD4(+) T cells. We identified 43 differentially expressed genes in the TS patient compared with the healthy female and the female patient with Graves' disease. Many of these genes have previously been suggested to play a role in immune system regulation. This study provides valuable insights into the differences in immune-related gene expression between TS patients, healthy individuals, and those with autoimmune diseases.

Keywords: Turner syndrome; X chromosome inactivation; autoimmunity; gene expression; single-cell RNA analysis

1. Introduction

Turner syndrome (TS) is one of the two relatively common forms of female X chromosome aneuploidy, marked by distinctive physical traits such as short stature, gonadal dysgenesis, neck-webbing, and cardiovascular and renal malformation, while in many cases an increased incidence of autoimmune disease is also observed [1,2]. A recent Danish nationwide study reported a rising incidence of TS, suggesting a birth incidence of 1 in 1700 live-born females [3]. In South Korea, the TS prevalence was 7.84 per 100,000 females and a shorter life expectancy of women with TS than the general female population was reported [4]. The etiology behind the phenotypic variability in Turner syndrome is complex and not fully understood. The mechanism by which the absence of an X chromosome determines the characteristics of TS is poorly understood [5]. Traditionally, the TS phenotype has been explained by X chromosome monosomy, where the missing or structurally altered second X chromosome results in altered regulation of gene expressions that are normally present in two copies in individuals with two intact X chromosomes [6].

However, recent studies have suggested that X chromosome variation not only affects the expression level of genes of the X chromosome, but also impacts the expression of genes on other chromosomes [7]. Hence, while the deleted gene on the missing second X chromosome may individually influence the TS phenotype, the additive effects of genes on other chromosomes might also play a role [8]. These effects could result from changes in gene expression regulation, potentially prompted by epigenetic factors, contributing to the phenotypic variability of the TS phenotype [5].

Graves' disease (GD) predominantly affects females, drawing significant attention to the underlying sexual dimorphism in immune response [9,10]. The adaptive immune response plays an important role in the pathogenesis of GD, characterized by a Th2-biased response and a strong focus on antibody production [11,12]. T cells are vital components of the adaptive immune response within the lymphoid system, constituting approximately three-quarters of all lymphocytes. CD4(+) T cells, specifically, play a critical role in pathogen clearance, autoimmune disease regulation, and the elimination of pathogenic cells [13]. Furthermore, distinct CD4(+) T cell subsets produce different cytokine profiles, protecting against various pathogens and mediating immune pathologies. GATA3, a key transcription factor, is involved in the Th2 differentiation, leading to eosinophils, mast cells, and IgEproducing B cell activations [14]. CD4(+) T cells have been associated with the pathogenesis of various autoimmune diseases, including thyroid disorders such as autoimmune thyroid disease (AITD) [15]. Some suggest that the impact of X chromosome inactivation escape and skewing toward autoimmune diseases could be explained by the reactivation and loss of mosaicism hypothesis [16]. In this genome-wide association study (GWAS), GPR174/ITM2A on the X chromosome was recognized as the second most potent AITD-susceptible gene following HLA [17].

Autoimmune diseases represent a significant health concern in Turner syndrome. The most frequently reported autoimmune risk in TS patients is thyroid dysfunction, with thyroperoxidase (Anti-TPO) antibodies detected in 48% of TS patients, compared with 13% in the general population [18–20]. In TS, an increased relative risk of diabetes has been reported, demonstrating its significant health burden [21]. The X chromosome harbors approximately 1000 genes, including those encoding receptors and associated proteins, immune-related proteins, as well as factors involved in transcriptional and translational regulation. Defects in certain X chromosome-linked genes are associated with various immune system abnormalities, including issues with immunoglobulin production and the regulation of T cell and B cell functions. These abnormalities have been linked to the clinical characteristics of Turner syndrome, highlighting their potential to induce specific features of TS [22,23]. Bianchi et al. proposed that haploinsufficiency of immune-related genes on the X chromosome may contribute to the development of autoimmune diseases [24]. However, previous studies on altered gene expressions in TS patients have reported controversial results [25]. While some suggest that genetic variations in numerous immune-related genes on the X chromosomes are linked to sex-based differences in immune response and higher prevalence of certain diseases in females, others have argued for the reactivation and loss of mosaicism hypothesis [16,26,27].

Despite breakthroughs and advances in technology, our knowledge of sex chromosome aneuploidies and the genetic regulations of Turner syndrome remains limited. To uncover key immune gene expression patterns associated with each condition, we performed single-cell RNA sequencing (scRNA-seq) analysis to compare CD4(+) T cell immune profiling among three individuals: one with complete monosomy X Turner syndrome (45, X), representing haploinsufficiency of the X chromosome; a healthy female (46, XX); and a female with Graves' disease (46, XX), serving as a representative of a normal karyotype female with an autoimmune condition.

2. Materials and Methods

2.1. Subjects and Human Blood Samples

This study was approved by the Institutional Review Board (IRB) of the Catholic University of Korea (IRB Number: KC23TISI0193). All participants provided written informed consent prior to participation in this study. Peripheral blood mononuclear cell (PBMC) samples were obtained from one healthy female (HF, 46, XX) volunteer, one patient diagnosed with Turner syndrome (TS, 45, X), and one patient diagnosed with Graves' disease (GD, 46, XX). TS was diagnosed based on chromosome analysis. GD was diagnosed through thyroid assessment, including high radioactive iodine intake, clinical symptoms of hyperthyroidism, positive thyroid stimulating hormone (TSH) receptor antibodies, and elevated thyroid hormone levels. PBMCs were isolated using Ficoll-Hypaque (GE Healthcare, Chicago, IL, USA). An AutoMacs Pro separator (Miltenyi Biotec, Bergisch Gladbach, Germany) was used to isolate CD4(+) T cells via magnetic microbeads. Flow cytometric analysis confirmed the purity of the CD4(+) T cells [28].

2.2. Single-Cell Library Preparation

CD4(+) T cells gated single-cell RNA sequencing was performed for peripheral blood mononuclear cells isolated from blood samples of a patient with Turner syndrome (45, XO), a heathy female (46, XX), and a female with Graves' disease (46, XX). The Chromium Single Cell Gene Expression Solution with Chromium Single Cell 3' GEM, Library and Gel Bead Kit v2 (10xGenomics, Pleasanton, CA, USA) was used for library preparation and processing following the manufacturer's specification. The 10x Genomics system with rapid droplet-based encapsulation of single cells uses a gel bead in emulsion (GEM) approach. Each GEM contains a single cell, a gel bead with barcoded oligonucleotides, and reverse transcription regents. Isolated CD4 T (+) cells were suspended in a master mix solution. A LUNA-FLtm Automated Fluorescence Cell Counter (Logos Biosystems, Anyang, Republic of Korea) was used to select cells with viability between 70% and 90%. These cells were then loaded into a well of the channel of a Single Cell A chip. Next, gel beads and partitioning oil were added to another channel well. A Chromium Controller (10x Genomics) lysed single cells and dissolved gel beads to release identically barcoded oligonucleotides for cDNA synthesis. By dividing a thousand of the cells into a nanoliter-scale GEM, all DNA molecules shared a 10-fold barcode. Each cell and transcript were uniquely barcoded with a unique molecular identifier (UMI). The cDNA used for sequencing was generated according to the manufacturer's protocol. Transcripts were then amplified to the barcoded cDNA using a thermocycler (Macrogen Inc., Seoul, Republic of Korea). The products were purified and concentrated by PCR to generate a final cDNA library. The purified libraries were quantified using qPCR and assessed using TapeStation 4200 (Agilent Technologies, Inc., Santa Clara, CA, USA). Libraries were sequenced on an Illumina HiSeq 4000 (Macrogen Inc.) according to the read length [29].

2.3. Data Collection

Cell Ranger Single Cell v2.1.1 software (10x Genomics), an analysis pipeline, was used for processing the sequenced data, including barcode processing, UMI, gene counting, and mapping [30]. Using Cell Ranger's mkfastq, raw BCL files were demultiplexed into FASTQ files [31]. FASTQ files were transferred to BAM (Binary Alignment Map) format. Differential gene expression between cell groups was analyzed using the negative binomial exact test (sSeq method) implemented in the Cell Ranger program. Cell Ranger compares the identified cell clusters to each other to determine genes highly expressed in a cluster with respect to other clusters. A total of 13,739 cells were processed in Og-NSCs (3D_cellRanger), with an average 39,181 reads and 2353 genes per cell. Only reads uniquely mapped to the

transcriptome were included for UMI counting in the Cell Ranger, with the UMI count per cell serving as the unit of gene expression. The Loupe Browser (10x Genomics) was further used for clustering and visualization of the dataset. The Louvain algorithm was used to identify the cell type and clustering [32]. The cells were further clustered by Th2 for subclassification analysis [14,33]. The clustering algorithm partitions the pre-computed neighbor graph into modules, which are clusters of cells. Cells with similar gene expression profiles were placed close to each other while those with differences were placed further apart. The estimated number of cells was performed by 'cellranger count'. The number of barcodes associated with cell-containing partitions was estimated based on the distribution of barcode UMI count. Briefly, the cellranger count fetches FASTQ files from the cellranger mkfastq and performs sorting, filtering, barcode counting, and UMI counting. Using a chromium cellular barcode, a feature barcode matrix is generated, clusters are determined, and gene expression analysis is performed. The count pipeline can receive input through multiple sequencing runs on the same GEM well. The selector count also processes feature barcode data along with gene expression readings [34].

2.4. Statistical Analysis

Gene expression levels were normalized and adjusted using the global-scaling normalization method 'LogNormalize' in Seurat v3.1 [35,36]. This method normalizes expression measurements for each cell by dividing by the total expression, multiplying by a scale factor (default: 10,000), and applying a log transformation to the resulting values. Uniform Manifold Approximation and Projection (UMAP) analysis was employed for dimension reduction and batch correction was performed using Anchors and Canonical Correlation Analysis (CCA) in Seurat 3.1. Differential expression analysis was conducted using the Wilcoxon rank-sum test, with *p*-values adjusted for multiple comparisons using the Benjamini–Hochberg correction in the Loupe Browser [37,38].

3. Results

3.1. Participants

One healthy female (HF, 46, XX) volunteer, one patient diagnosed with Turner syndrome (TS, 45, X), and one patient diagnosed with Graves' disease (GD, 46, XX) donated peripheral blood mononuclear cell (PBMC) samples for this study. The baseline characteristics of study subjects are presented in Table 1. PBMCs of study subjects were further analyzed based on CD4(+) T cell distributions (Figure 1).

Table 1. Characteristics of subjects.

	TS	HF	GD
Subjects			
Sex	F	F	F
Anthropometric data at blood sampling			
Height (cm)	143	163	162
Weight (kg)	47	55	68
BMI (kg/m^2)	22.98	20.70	25.91
Age at enrollment (years)	24	43	17
Age at diagnosis (years)	5	N/A	16
Goiter	negative	negative	positive
Free T4 (fT4) at diagnosis, 0.85–1.86 ng/dL	WNL (T4)	WNL	6.38
TSH at diagnosis, 0.17–4.05 mIU/L	WNL	WNL	< 0.01
TSHR Ab positive at diagnosis	N/A	negative	positive
Clinically evident TAO (NOSPECS class II or higher), n (%)	negative	negative	positive

Table 1. Cont.

	TS	HF	GD
Clusters of cells			
Cluster total	1913	1018	1761
Th2 GATA3 positive	493	334	441
Estimated number of cells *	2150	1031	1909

Data are presented as mean \pm Standard Deviations (SD) or n (%). TS, Turner syndrome; HF, healthy female; GD, Graves' disease; N/A, Not applicable; TSH, thyroid stimulating hormone; TSHR Ab, TSH receptor antibody; TAO, thyroid associated ophthalmopathy; WNL, within normal range. * Estimation by 'cellranger count' described in Section 2.

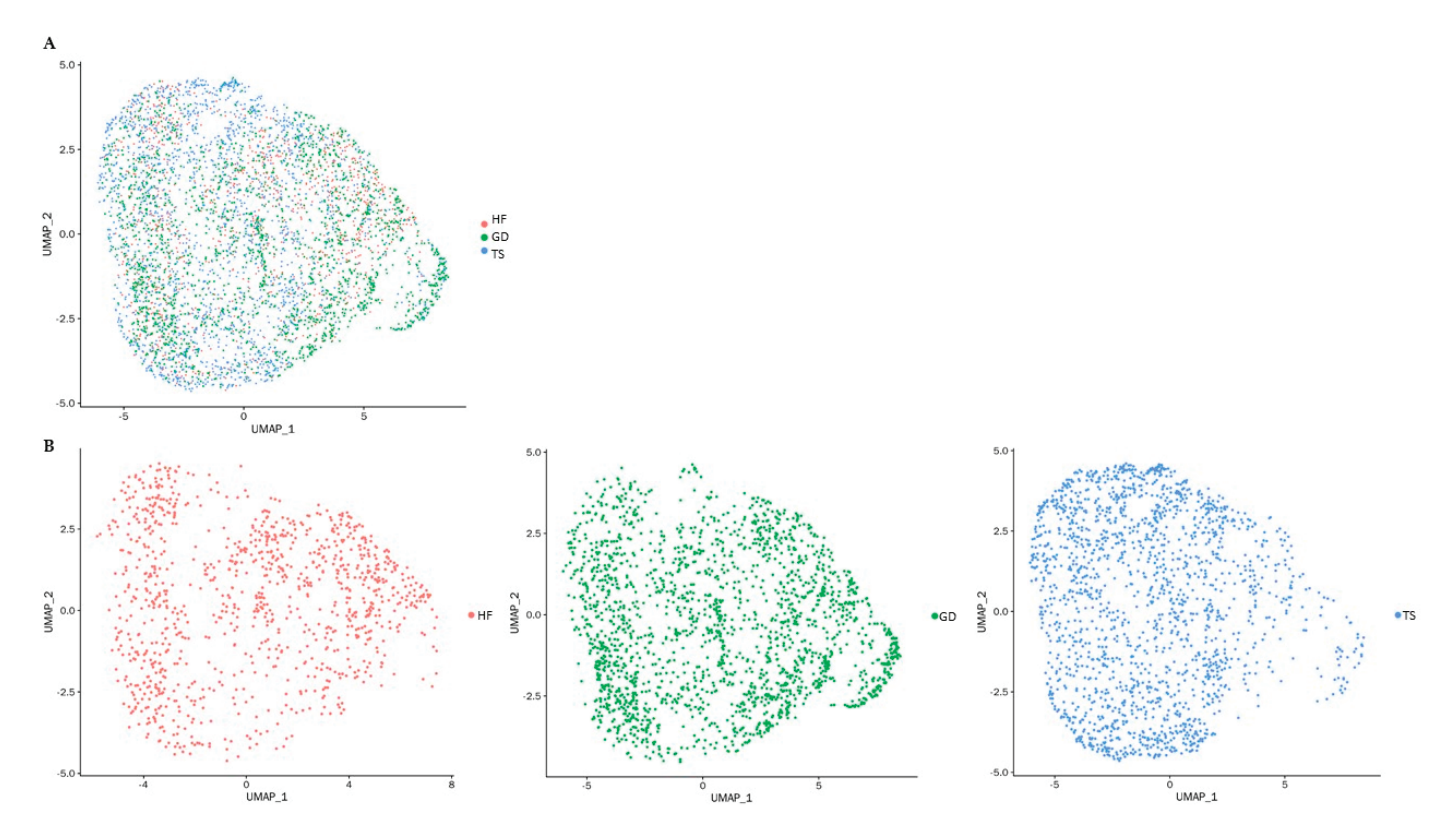


Figure 1. UMAP presentation of single-cell RNA sequencing of PBMCs. Each dot represents one of the CD4(+) T cells; **(A)** UMAP plot colored by study subjects: cells are represented based on three different groups indicated in red, green, and blue, respectively; **(B)** UMAP plot of individual study subjects: CD4(+) T cells of a healthy female (HF) are represented in red; CD4(+) T cells of a patient with Graves' disease (GD) are represented in blue; CD4(+) T cells of a patient with Turner syndrome (TS) are represented in green.

3.2. Single-Cell Gene Expression Differences Between Turner Syndrome and Healthy Female

CD4(+) T cells gated single-cell RNA-sequencing was used to conduct a detailed comparison of gene expression patterns between a Turner syndrome patient, a healthy female, and a female with Graves' disease. A total of 718 differentially expressed genes (DEGs, p < 0.05) between TS and a healthy female control were identified. Table 2 represents the top 30 most significantly differentially expressed genes, sorted by the level of significance. Subsequent analysis of CD4(+) T cells was carried out by gating the results with *GATA3* expression to distinguish significant gene expressions in Th2 cells in a patient with TS compared with an HF. The top 30 significant genes are shown in Table 3.

Table 2. Significant differences in single-cell gene expression profiles of a patient with TS compared with an HF.

Gene Symbol	Log2 Fold Change (TS/HF)	<i>p-</i> Value	Gene Title	Gene Location	Ensembl *
XIST	-10.572	3.03×10^{-106}	X inactive specific transcript	Xq13.2	ENSG00000229807
OVCH1-AS1	7.379	1.08×10^{-35}	OVCH1 antisense RNA 1	12p11.22	ENSG00000257599
SLC35F1	4.377	1.25×10^{-33}	Solute carrier family 35, member F1	6q22.2	ENSG00000196376
AL592183.1	6.288	1.57×10^{-33}	-	-	ENSG00000273748
FMN1	4.794	2.26×10^{-32}	Formin 1	15q13.3	ENSG00000248905
AC068279.2	-8.045	2.77×10^{-31}	-	2p11.2	ENSG00000287763
MYOM2	4.921	2.01×10^{-27}	Myomesin 2	8p23.3	ENSG00000036448
CALHM6	-5.436	7.25×10^{-24}	Family with sequence similarity 26, member F	6q22.1	ENSG00000188820
MTRNR2L1	3.478	1.78×10^{-22}	MT-RNR2-like 1	17p11.2	ENSG00000256618
GZMH	5.995	3.83×10^{-22}	Granzyme H	14q12	ENSG00000100450
GNLY	6.773	4.23×10^{-21}	Granulysin	2p11.2	ENSG00000115523
SHROOM1	-3.373	4.42×10^{-17}	Shroom family member 1	5q31.1	ENSG00000164403
PPP1R2C	-7.610	2.88×10^{-16}	PPP1R2 family member C	Xp11.3	ENSG00000102055
C1orf21	5.161	2.68×10^{-15}	Chromosome 1 open reading frame 21	1q25.3	ENSG00000116667
ABO	6.364	4.75×10^{-15}	ABO, alpha 1-3-N- acetylgalactosaminyltransferase and alpha	9q34.1	ENSG00000175164
OVCH1	5.050	1.54×10^{-14}	1-3-galactosyltransferase Ovochymase 1	12p11.22	ENSG00000187950
FGFBP2	5.269	2.26×10^{-14}	Fibroblast growth factor binding protein 2	4p15.32	ENSG00000137441
NKG7	3.470	2.28×10^{-14}	Natural killer cell group 7 sequence	19q13.41	ENSG00000105374
TSIX	-5.571	2.28×10^{-14}	TSIX transcript, XIST antisense RNA	Xq13.2	ENSG00000270641
PLEK	3.875	1.51×10^{-13}	Pleckstrin	2p14	ENSG00000115956
C2orf74	2.885	1.08×10^{-12}	Chromosome 2 open reading frame 74	2p15	ENSG00000237651
AL672277.1	-6.101	1.20×10^{-11}	-	Xp22.33	ENSG00000237531
ADTRP	-2.401	4.76×10^{-11}	Androgen-dependent TFPI-regulating protein	6p24.1	ENSG00000111863
LINC02254	3.218	6.27×10^{-11}	-	15q26.2	ENSG00000259664
SEMA4A	-2.710	8.19×10^{-11}	Semaphorin 4A	1q22	ENSG00000196189
LINC01952	-2.431	1.47×10^{-10}	- -	7p13	ENSG00000234183
AC004854.2	-2.414	1.62×10^{-10}	-	7p13	ENSG00000272768
H2AFX	-1.904	2.24×10^{-10}	H2A histone family, member X	11q23.3	ENSG00000188486
FHIT	-1.850	1.96×10^{-9}	Fragile histidine triad	3p14.2	ENSG00000189283
DUSP4	-2.408	2.22×10^{-9}	Dual specificity phosphatase 4	8p12	ENSG00000120875

 $[\]hbox{* Ensembl: https://grch37.ensembl.org/Homo_sapiens (accessed on 10 October 2024).}\\$

Table 3. Significant differences in single-cell gene expression profiles of Th2 cells in a patient with TS compared with an HF.

Gene Symbol	Log2 Fold Change (TS/HF)	<i>p-</i> Value	Gene Title	Gene Location	Ensembl *
XIST	-8.682	2.00×10^{-50}	X inactive specific transcript	Xq13.2	ENSG00000229807
SLC35F1	4.138	4.76×10^{-20}	Solute carrier family 35, member F1	6q22.2	ENSG00000196376
FMN1	4.792	4.76×10^{-20}	Formin 1	15q13.3	ENSG00000248905
OVCH1-AS1	7.455	1.27×10^{-17}	OVCH1 antisense RNA 1	12p11.22	ENSG00000257599

Table 3. Cont.

Gene Symbol	Log2 Fold Change (TS/HF)	<i>p</i> -Value	Gene Title	Gene Location	Ensembl *
МҮОМ2	5.568	3.23×10^{-16}	Myomesin 2	8p23.3	ENSG00000036448
AL592183.1	5.178	1.10×10^{-15}	-	-	ENSG00000273748
MTRNR2L1	3.067	1.81×10^{-11}	MT-RNR2-like 1	17p11.2	ENSG00000256618
AC068279.2	-6.160	6.34×10^{-9}	-	-	ENSG00000287763
AC004854.2	-2.826	1.56×10^{-7}	-	-	ENSG00000272768
P2RY8	-1.898	1.85×10^{-7}	Purinergic receptor P2Y, G-protein coupled, 8	Xp22.33	ENSG00000182162
CALHM6	-4.979	1.08×10^{-6}	Calcium homeostasis modulator family member 6	6q22.1	ENSG00000188820
MIDN	-1.773	6.26×10^{-6}	Midnolin	19p13.3	ENSG00000167470
H2AFX	-1.931	7.41×10^{-6}	H2A histone family, member X	11q23.3	ENSG00000188486
AC008569.1	-1.797	2.83×10^{-5}	-	-	ENSG00000267379
PPP1R2C	-6.345	2.83×10^{-5}	Protein phosphatase 1, regulatory (inhibitor) subunit 2 pseudogene 9	Xp11.3	ENSG00000102055
CRYBB2	-4.295	2.92×10^{-5}	Crystallin beta B2	22q11.23	ENSG00000244752
SHROOM1	-3.324	3.37×10^{-5}	Shroom family member 1	5q31.1	ENSG00000211732
SEMA4A	-2.882	4.87×10^{-5}	Semaphorin 4A	1q22	ENSG00000101103
RGCC	-1.543	6.60×10^{-5}	Regulator of cell cycle ABO, alpha 1-3-N-	13q14.11	ENSG00000102760
ABO	4.870	7.35×10^{-5}	acetylgalactosaminyltransferase and alpha	9q34.2	ENSG00000175164
C2orf74	2.624	9.18×10^{-5}	1-3-galactosyltransferase Chromosome 2 open reading frame 74	2p15	ENSG00000237651
HLA-DRB5	-2.902	1.75×10^{-4}	Major histocompatibility complex, class II, DR beta 5	6p21.32	ENSG00000198502
ADTRP	-2.487	2.05×10^{-4}	Androgen-dependent TFPI-regulating protein	6p24.1	ENSG00000111863
GADD45G	-2.232	2.18×10^{-4}	Growth arrest and DNA-damage-inducible, gamma	9q22.2	ENSG00000130222
GADD45B	-1.515	2.27×10^{-4}	Growth arrest and DNA-damage-inducible, beta	19p13.3	ENSG00000099860
CDKN1A	-1.819	2.29×10^{-4}	Cyclin-dependent kinase inhibitor 1A	6p21.2	ENSG00000124762
LINC02254	3.420	2.29×10^{-4}	-	15q26.2	ENSG00000259664
DUSP4	-2.390	2.38×10^{-4}	Dual specificity phosphatase 4	8p12	ENSG00000120875
DUSP2	-1.494	3.94×10^{-4}	Dual specificity phosphatase 2	2q11.2	ENSG00000158050
AP001160.1	-1.902	$4.38 imes 10^{-4}$	-	-	ENSG00000256690

^{*} Ensembl: https://grch37.ensembl.org/Homo_sapiens.

3.3. Single-Gene Expression Differences Between Turner Syndrome and a Female with Graves' Disease

There were 1574 differentially expressed genes (DEGs, p < 0.05) between the Turner syndrome patient and the female patient with Graves' disease. The top 30 most significantly differentially expressed genes are shown in Table 4. Significant differences in single-cell gene expression profiles of Th2 cells in a patient with TS compared with a patient with GD were identified by gaiting the results with GATA3 expression (Table 5).

Table 4. Significant differences in single-cell gene expression profiles of a patient with TS compared with a patient with GD.

Gene Symbol	Log2 Fold Change (TS/GD)	<i>p</i> -Value	Gene Title	Gene Location	Ensembl *
XIST	-10.871	3.82×10^{-94}	X inactive specific transcript	Xq13.2	ENSG00000229807
AC105402.3	-7.110	6.65×10^{-93}	-	2q23.1	ENSG00000231079
OVCH1-AS1	5.334	3.34×10^{-36}	OVCH1 antisense RNA 1	12p11.22	ENSG00000257599
MYOM2	4.690	1.49×10^{-32}	Myomesin 2	8p23.3	ENSG00000036448
UTS2	5.357	2.00×10^{-32}	Urotensin 2	1p36.23	ENSG00000049247
HLA-DQB1	5.452	9.76×10^{-28}	HLA-DQB1 antisense RNA 1	6p21.32	ENSG00000179344
CCR6	3.794	4.83×10^{-27}	Chemokine (C-C motif) receptor 6	6q27	ENSG00000112486
PTGER2	3.658	5.00×10^{-25}	Prostaglandin E receptor 2	14q22.1	ENSG00000125384
TSIX	-6.267	2.33×10^{-24}	TSIX transcript, XIST antisense RNA	Xq13.2	ENSG00000270641
AIF1	-3.035	6.13×10^{-23}	Allograft inflammatory factor 1	6p21.33	ENSG00000204472
AL121935.1	3.828	6.51×10^{-22}	-	6q27	ENSG00000284825
NRCAM	-3.658	1.32×10^{-20}	Neuronal cell adhesion molecule ABO blood group	7q31.1	ENSG00000091129
ABO	6.056	2.16×10^{-20}	(transferase A, alpha 1-3-N-acetylgalactosaminyltransferase; transferase B, alpha 1-3-galactosyltransferase)	9p34.1	ENSG00000175164
GZMK	3.363	7.84×10^{-20}	Granzyme K	5q11.2	ENSG00000113088
ARHGEF10	-3.967	7.84×10^{-20}	Rho guanine nucleotide exchange factor (GEF) 10	8p23.3	ENSG00000104728
MYBL1	3.034	1.05×10^{-19}	MYB proto-oncogene like 1	8q13.1	ENSG00000185697
CALHM6	-4.911	1.15×10^{-19}	Calcium homeostasis modulator family member 6	6q22.1	ENSG00000188820
RPS26	2.641	1.82×10^{-19}	Ribosomal protein S26	12q13.2	ENSG00000197728
GREM2	5.193	3.48×10^{-19}	Gremlin 2, DAN family BMP antagonist	1q43	ENSG00000180875
NFKBID	-3.060	2.13×10^{-18}	Nuclear factor of kappa light polypeptide gene enhancer in B-cells inhibitor, delta	19q13.12	ENSG00000167604
EGR1	-3.644	1.70×10^{-17}	Early growth response 1	5q31.2	ENSG00000120738
MIR155HG	-3.011	1.78×10^{-17}	MIR155 host gene	21q21.3	ENSG00000234883
RASGRP3	-3.044	1.93×10^{-17}	RAS guanyl releasing protein 3	2p22.3	ENSG00000152689
MTRNR2L1	2.647	3.63×10^{-17}	MT-RNR2-like 1	17p11.2	ENSG00000256618
SGK1	-2.563	9.54×10^{-17}	Serum/glucocorticoid regulated kinase 1	6q23.2	ENSG00000118515
TAF4B	-2.547	1.56×10^{-16}	TATA-box binding protein associated factor 4b	18q11.2	ENSG00000141384
GNLY	4.384	2.02×10^{-16}	Granulysin	2p11.2	ENSG00000115523
CFH	3.345	2.33×10^{-16}	Complement factor H	1q31.3	ENSG00000000971
AC103591.3	-2.648	9.13×10^{-16}	-	1p31.1	ENSG00000273338
HLA-DQA2	6.853	9.58×10^{-16}	Major histocompatibility complex, class II, DQ alpha 2	6p21.32	ENSG00000237541

^{*} Ensembl: https://grch37.ensembl.org/Homo_sapiens.

Table 5. Significant differences in single-cell gene expression profiles of Th2 cells in a patient with TS compared with a patient with GD.

Gene Symbol	Log2 Fold Change (TS/GD)	<i>p-</i> Value	Gene Title	Gene Location	Ensembl *
AC105402.3	-7.194	4.36×10^{-60}	-	-	ENSG00000231079
XIST	-9.058	1.75×10^{-47}	X inactive specific transcript	Xq13.2	ENSG00000229807
MYOM2	5.730	1.16×10^{-19}	Myomesin 2	8p23.3	ENSG00000036448
OVCH1-AS1	6.255	5.39×10^{-19}	OVCH1 antisense RNA 1	12p11.22	ENSG00000257599
AIF1	-3.349	1.46×10^{-16}	Allograft inflammatory factor 1	6p21.33	ENSG00000204472
CCR6	3.846	8.59×10^{-16}	Chemokine (C-C motif) receptor 6	6q27	ENSG00000112486
RPS26	2.624	4.35×10^{-15}	Ribosomal protein S26	12q13.2	ENSG00000197728
UTS2	5.219	2.28×10^{-14}	Urotensin 2	1p36.23	ENSG00000049247
MIR181A1HG	-3.142	6.48×10^{-12}	MIR181A1 host gene	1q32.1	ENSG00000229989
GREM2	6.964	1.42×10^{-11}	Gremlin 2, DAN family BMP antagonist	1q43	ENSG00000180875
ARHGEF10	-4.897	1.99×10^{-11}	Rho guanine nucleotide exchange factor (GEF) 10	8p23.3	ENSG00000104728
MYBL1	3.148	1.99×10^{-11}	MYB proto-oncogene like 1	8q13.1	ENSG00000185697
PTGER2	3.031	6.15×10^{-11}	Prostaglandin E receptor 2	14q22.1	ENSG00000125384
MTRNR2L1	2.645	1.69×10^{-10}	MT-RNR2-like 1	17p11.2	ENSG00000256618
HLA-DQB1	5.067	1.78×10^{-10}	Major histocompatibility complex, class II, DQ beta 1	6p21.32	ENSG00000179344
NFKBID	-3.401	1.78×10^{-10}	NFKB inhibitor delta WAS protein homolog	19q13.12	ENSG00000167604
WHAMM	-2.236	2.62×10^{-10}	associated with actin, golgi membranes and microtubules	15q25.2	ENSG00000156232
TSIX	-6.009	3.04×10^{-10}	TSIX transcript, XIST antisense RNA	Xq13.2	ENSG00000270641
NRCAM	-3.700	4.58×10^{-10}	neuronal cell adhesion molecule	7q31.1	ENSG00000091129
EGR1	-3.853	4.73×10^{-10}	Early growth response 1	5q31.2	ENSG00000120738
RASGRP3	-2.966	6.59×10^{-10}	RAS guanyl releasing protein 3	2p22.3	ENSG00000152689
SGK1	-2.434	1.01×10^{-9}	Serum/glucocorticoid regulated kinase 1	6q23.2	ENSG00000118515
AC103591.3	-2.805	3.14×10^{-9}	-	-	ENSG00000273338
AL121935.1	3.566	7.31×10^{-9}	-	-	ENSG00000284825
TAF4B	-2.438	7.72×10^{-9}	TATA-box binding protein associated factor 4b	18q11.2	ENSG00000141384
CHKA	-2.280	1.20×10^{-8}	Choline kinase alpha	11q13.2	ENSG00000110721
CRIP2	2.598	1.20×10^{-8}	Cysteine-rich protein 2	14q32.33	ENSG00000182809
AC008569.1	-2.192	1.20×10^{-8}	- -	-	ENSG00000267379
JUN	-1.974	2.06×10^{-8}	Jun proto-oncogene	1p32.1	ENSG00000177606
EZH2	-2.361	3.66×10^{-8}	Enhancer of zeste homolog 2	7q36.1	ENSG00000106462

 $[*] Ensembl: https://grch37.ensembl.org/Homo_sapiens.\\$

We identified 43 overlapping genes (30 up-expressed and 13 down-expressed genes) in Turner syndrome compared with a healthy control female and a female with Graves' disease (Figures 2 and 3). XIST, PPP1R2C, CALHM6, AL672277.1, TSIX, SHROOM1, ADTRP, JUND,

^{3.4.} Differentially Expressed Genes in Turner Syndrome Compared with Healthy Female and Graves' Disease Female

SGK1, CHKA, AO008569.1, MAP7D2, and AIF1 were down-expressed genes in TS compared with both the healthy female and the female patient with Graves' disease. The following 30 overlapping genes were up-expressed in TS: ABO, OVCH1-AS1, GZMB, GNLY, MYOM2, LERFS, OVCH1, C1orf21, FGFBP2, LINC02084, GPRC5D-AS1, AC107223.1, MTRNR2L1, AC104041.1, CPNE8, GZMK, LTK, MSC-AS1, GZMA, CCL5, SYT11, CEBPD, PTPRM, CST7, PZP, LINC00892, A2M, HPGD, PPP2R2B, and LINC00612.

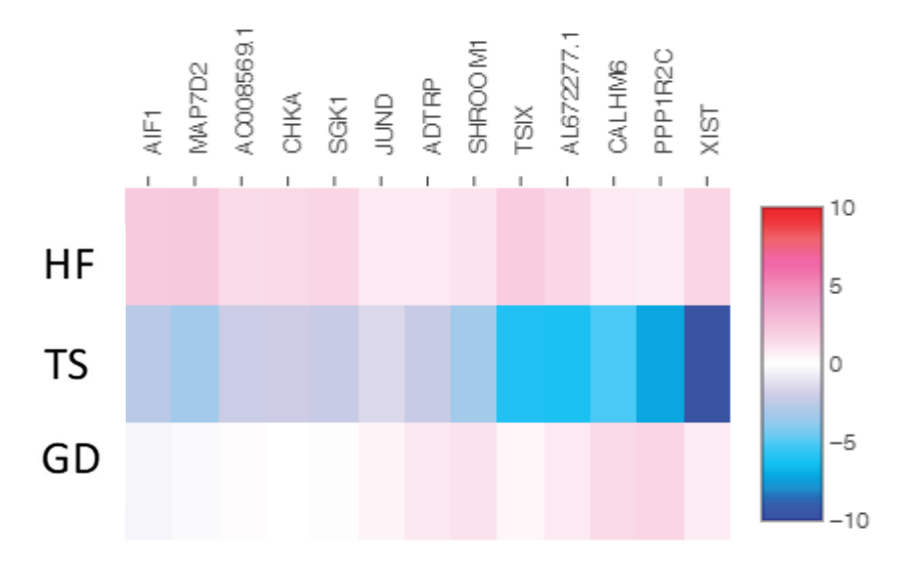


Figure 2. The heatmap of thirteen shared down-expressed genes in a patient with TS compared with both an HF and a patient with GD. Values are presented on a Log2 scale.

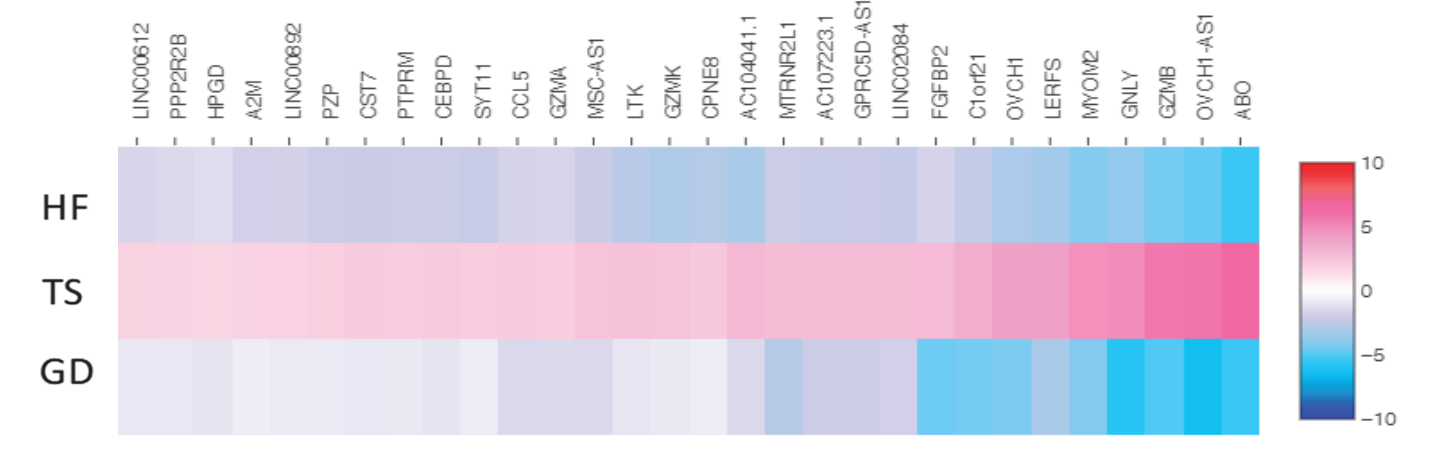


Figure 3. The heatmap of thirty shared up-expressed genes in a patient with TS compared with both an HF and a patient with GD. Values are presented on a Log2 scale.

Of those overlapping genes, the following 13 genes were down-expressed in the Turner syndrome patient compared with the healthy female control: *XIST*, *TSIX*, *SHROOM1*, *SGK1*, *PPP1R2C*, *MAP7D2*, *JUND*, *CHKA*, *CALHM6*, *AL672277.1*, *AIF1*, *ADTRP*, and *AC008569.1* (Figure 4). On the contrary, *OVCH1-AS*, *SYT11*, *PZP*, *PTPRM*, *PPP2R2B*, *OVCH1*, *MYOM2*, *MTRNR2L1*, *MSC-AS1*, *LTK*, *LINC02084*, *LINC00892*, *LINC00612*, *LERFS*, *HPGD*, *GZMK*, *GZMB*, *GZMA*, *GPRC5D-AS1*, *GNLY*, *FGFBP2*, *CST7*, *CPNE8*, *CEBPD*, *CCL5*, *C1orf21*, *AC107223.1*, *AC104041.1*, *ABO*, and *A2M* were up-expressed genes in the TS patient (Figure 5).

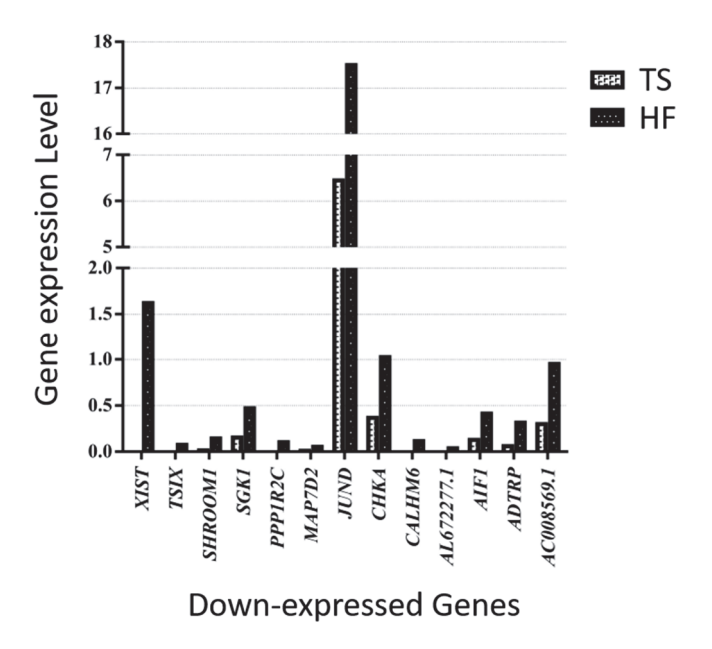


Figure 4. Thirteen down-expressed genes in a patient with TS compared with an HF.

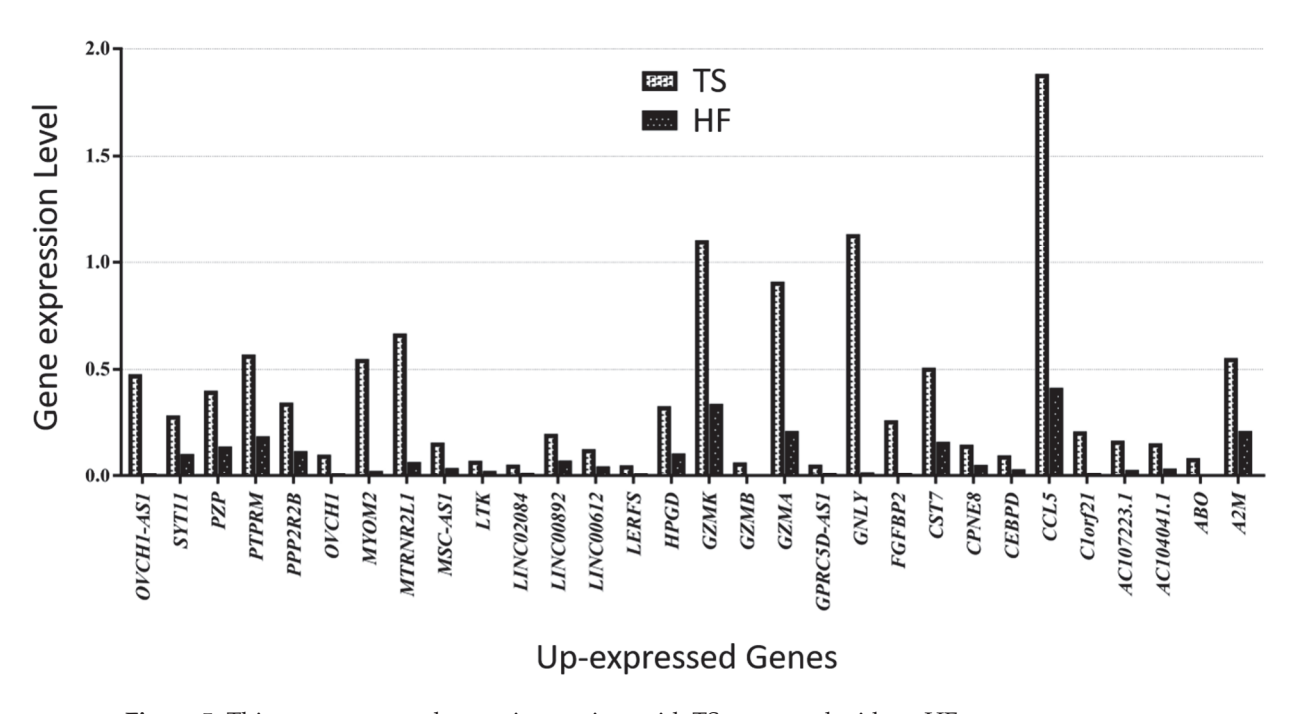


Figure 5. Thirty up-expressed genes in a patient with TS compared with an HF.

Similarly, 13 genes (XIST, TISX, SHROOM1, SGK1, PPP1R2C, MAP7D2, JUND, CHKA, CALHM6, AL672277.1, AIF1, ADTRP, and AC008569.1) were down-expressed in the Turner syndrome patient compared with the Graves' disease patient (Figure 6). OVCH1-AS1, SYT11, PZP, PTPRM, PPP2R2B, OVCH1, MYOM2, MTRNR2L1, MSC-AS1, LTK, LINC02084, LINC00892, LINC00612, LERFS, HPGD, GZMK, GZMB, GZMA, GPRC5D-AS1, GNLY, FGFBP2, CST7, CPNE8, CEBPD, CCL5, C1orf21, AC107223.1, AC104041.1, ABO, and A2M were the genes up-expressed in the TS patient compared with the Graves' disease patient (Figure 7).

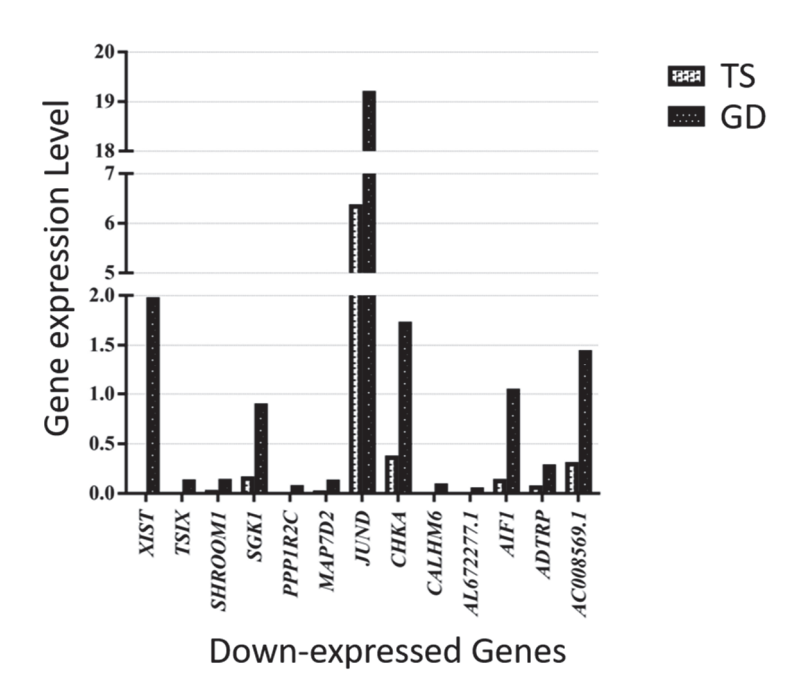


Figure 6. Thirteen down-expressed genes in a patient with TS compared with a female patient with GD.

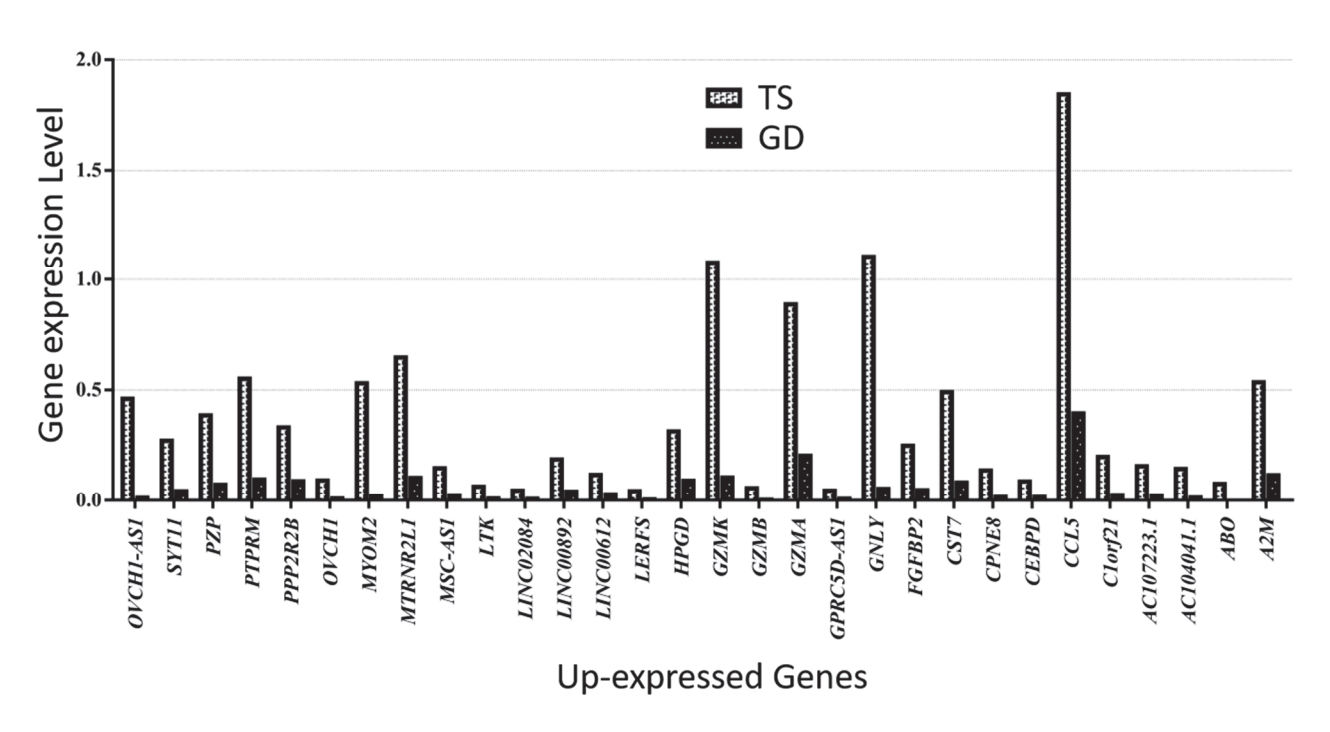


Figure 7. Thirty up-expressed genes in a patient with TS compared with a female patient with GD.

4. Discussion

To the best of our knowledge, this is the first study to apply CD4(+) T cells gated single-cell RNA sequencing of peripheral blood mononuclear cell samples to identify differentially expressed genes in a Turner syndrome patient compared with a healthy female and a female patient with Graves' disease. Graves' disease, a female-predominant condition, exhibits adaptive immune response biased towards CD4(+) T cells. Therefore, in this study CD4(+) T cell immune profiling for an individual with compete monosomy X Turner syndrome (45, X), a female patient with GD (46, XX with autoimmune disease) and a healthy female (46, XX) was conducted. The thyroid function of the TS patient and the healthy female was within the normal range, whereas the GD patient showed initial

diagnostic results consistent with hyperthyroidism. In the overall clustering analysis with UMAP plots, we presented the CD4(+) T cells from all three subjects and identified significant differences in gene expression profiles across the groups. The top 100 significantly differentially expressed genes are provided in the Supplementary Materials (Supplementary Tables S1–S4). Among these, 43 genes were differentially expressed in TS compared with both the healthy female and the patient with Graves' disease, with 30 genes being up-expressed and 13 genes being down-expressed. Notably, *XIST*, a gene known to initiate X chromosome inactivation to balance the X chromosome-related gene expression, was significantly down-expressed in TS compared with both the GD patient and the healthy female, consistent with previous findings [24,39–41]. These results further support that the observed differences are specific to TS, underscoring the unique transcriptional profile of monosomy X. Additionally, they provide insights into the potential implications of these gene expression changes for immune system function when compared with healthy individuals and those with autoimmune disorders.

A recent guideline updated in 2024 reported that women with Turner syndrome face a significantly increased risk of autoimmunity, with a 61% lifetime prevalence [21]. Various studies have documented immunological alterations in TS patients, suggesting that the rise in autoimmunity shown in TS is multifactorial. In 2020, Wang et al. conducted a bioinformatic analysis of the Gene Expression Omnibus (GEO) dataset GSE46687, which included 26 TS patients (16 with a maternally inherited X chromosome and 10 with a paternally inherited X chromosome) and 10 healthy females. They identified 85 differentially expressed genes in TS patients, focusing primarily on gene expression differences between TS patients and controls, with secondary consideration of the parental origin of the X chromosome. The authors further reported that these genes were most significantly associated with the hematological and immune systems [40]. Consistent with their findings, our single-cell RNA sequencing study identified that many of the up-expressed genes in the TS patient are documented to have links to immune responses. Following their approach, we performed additional gene expression analysis of the GEO dataset (GSE46687), identifying 30 overlapping differentially expressed genes consistent with our single-cell RNA sequencing findings, including XIST, TSIX, SHROOM1, ADTRP, JUND, SGK1, CHKA, MAP7D2, AIF1, ABO, OVCH1-AS1, GZMB, GNLY, MYOM2, Clorf21, FGFBP2, CPNE8, GZMK, LTK, MSC-AS1, GZMA, CCL5, SYT11, CEBPD, PTPRM, CST7, PZP, A2M, HPGD, and PP2R2B. Most importantly, XIST and TSIX emerged as the most significantly down-expressed genes, mirroring the results from our study. While the precise roles of these genes in TS remain unclear, previous research has suggested that many of the 43 identified genes are linked to various immune pathways.

Different innate and humoral immune responses between females and males have been well-documented by others [42]. Females with increased expression of immune-related genes and enhanced immune response are known to be more susceptible to autoimmune diseases and malignancies than males [13]. Female T and B cells have been proposed to explain the increase of female immune response to infection. Among these, CD4(+) T cells are recognized as pivotal contributors to adaptive immunity, playing a crucial role not only in eliminating pathogens, but also in regulating autoimmune diseases and targeting pathogenic cells such as cancer cells [43]. The X chromosome harbors a significant number of genes associated with immune function and thus X chromosome inactivation in females, along with genes evading this inactivation, have been speculated to contribute to the diversity of immune responses [43]. Others have suggested that the major histocompatibility complex (MHC), located in the long arm of the X chromosome, may explain the difference in immunogenic profiles observed in TS [39]. Moreover, some studies suggest that the X chromosome retains genes important for epigenetic regulation [44,45]. Zheng et al. further

suggested that expression changes of autosomal genes may be due to the ripple effects of the X chromosome genes through their influence on regulatory expression networks [7]. While the etiology of autoimmunity in TS remains unclear, various differentially expressed genes found in our study appear to be linked to immune responses.

The X chromosome plays a crucial role in ensuring balanced genetic expression between sexes as one X chromosome is randomly silenced through X chromosome inactivation, a process regulated by the X-active specific transcript gene (*XIST*), a non-coding RNA located on the X chromosome. *TSIX*, an antisense RNA to the *XIST* gene, was also down-expressed in TS. Both *XIST* and *TSIX* have been associated with incremental expression levels in X chromosome dosage, when comparing females with 45, X, 46, XX, and 47, XXX karyotypes [46]. These findings suggest that X chromosome dosage may influence various TS phenotypes. In our single-cell RNA sequencing study, the universal expression of the *XIST* gene can function as a positive control, and its lower expression level in TS suggests that X inactivation is absent, validating the accuracy of the research. Furthermore, the lack of X chromosome inactivation in TS may influence autoimmunity, not only through immune-related genes on the X chromosome but also through the lack of X chromosome inactivation and its effects on broader immunogenetic effects [18].

The *SGK1* gene, located on chromosome 6 (6q23.2), encodes serum/glucocorticoid-regulated kinase 1, which has been reported to participate in the development of several human diseases, including cervical cancer, pulmonary fibrosis, Alzheimer's disease, and type 2 diabetes mellitus [47]. Recent studies have also highlighted its involvement in immune and inflammatory regulatory functions and its role in various diseases such as inflammatory bowel diseases, multiple sclerosis, and sepsis [48]. The *JUND* gene on chromosome 19 (19p13.11) has been reported to regulate lymphocyte proliferation and T helper cell cytokine expression [49]. The *AIF1* gene (6p21.33) is known to be induced by cytokines and interferon to activate macrophage activation and T lymphocytes [50].

Among the up-expressed genes, the GNLY gene, located on chromosome 2 (2p11.2), encodes the granulysin that is present in the cytotoxic granules of T cells. Elevated expression of GNLY in tissue and serum has been associated with infections, autoimmune disease, transplant rejection, and graft-versus-host reactions. Patients with severe immunodeficiency have been reported to have very low GNLY serum levels [51,52]. Additionally, the GZMB gene, located on chromosome 14 (14q12), encodes proteins for natural killer (NK) cells and cytotoxic T lymphocytes. These genes, known as cytotoxic genes, are highly expressed in T cells with roles in the immune system. A recent study has suggested that elevated expression of GNLY and GZMB may facilitate the rapid resolution of SARS-CoV-2 infection by promoting direct cytotoxicity [53]. The GZMK and GZMA genes, located on chromosome 5 (5q11.2), are also related to cytotoxic effector expression. Granzyme K is believed to be low in cord blood, suggesting that it might be upregulated with immune experience [54]. Granzyme A expression has been associated with cytotoxic activity against tumor or virus-infected cells as well as the stimulation of several immune cell types [55]. The PPP2R2B gene, located on chromosome 5 (5q32), has been reported to protect against organ damage caused by activated T cells in chronic inflammation and systemic autoimmune diseases [56]. Additionally, a study has identified this gene as a robust tumor suppressor, playing an important role in anti-tumor immune response. In breast cancer, PPP2R2B expression was strongly associated with immune check point inhibitor genes such as BZMA, PRF1, and IFNG, suggesting that downregulation of PPP2R2B could take part in tumor immune evasion [57]. The CCL5 gene located on chromosome 17 (17q12) is known to be involved in immunoregulatory and inflammatory processes [58,59]. CCL5 is induced during inflammation and plays a crucial role in recruiting activated effector T cells and generating memory T cells [60]. The CEBPD gene found on chromosome 8

(8q11.21) encodes CCAAT/enhance-binding protein delta, a key transcription factor that regulates genes involved in immune and inflammatory responses [61]. The *CST7* gene on chromosome 20 (20p11.21) encodes cystatin F protein that regulates the cytotoxicity of natural killer (NK) cells [62]. Previously, *CST7* has also been associated with CD4(+) T cell and CD8 (+) T cell activation in liver cancer [10].

The MYOM2 gene on chromosome 8 (8p23.3) encodes a protein expressed in cardiac and skeletal muscles. Chen et al. found MYOM2 to be one of the differentially expressed genes in natural killer cells and that it is enriched in biological pathways associated with HIV replication [63]. The FGFBP2 gene encodes a protein known to be involved in cytotoxic lymphocyte-mediated immunity (chromosome 4, 4p15.32). The CPNE8 gene encoding a calcium-dependent protein is on chromosome 12 (12q12). Recent studies have indicated that CPNE8 is highly correlated with monocytes, macrophages, and neutrophils, suggesting its potential involvement in immune-related pathways [64]. The LTK gene on chromosome 15 (15q15.1) encodes leukocyte tyrosine kinase, which is involved in controlling pathways of cell growth and differentiation [65]. Previous studies have found that LTK is expressed in B lymphocyte precursor cells, and its gain-of-function is associated with the pathogenesis of systemic lupus erythematosus pathogenesis through upregulating self-reactive B cells [66]. The PZP gene encodes PZP protein, which is highly expressed in late pregnancy and plays a role in immune regulation during pregnancy [67]. Located on chromosome 12 (12p13.31), the PZP expression level is positively correlated with macrophage and neutrophil levels to regulate the tumor immune microenvironment of hepatocellular carcinoma [68]. The A2M gene is located on chromosome 12 (12p13.31) and has been associated with the activation of neutrophil migration, promoting cell division of macrophages and immunemediated pathways in humans [69]. Further, this gene encodes a protease inhibitor and cytokine transporter involved in proteolysis, as well as cellular immunity and defense mechanisms [70].

Nevertheless, this study has several limitations. Using single-cell RNA sequencing, we identified differentially expressed genes in a Turner syndrome patient, a healthy female volunteer, and a patient with Graves' disease. In studies involving individuals with rare conditions, the sample size is often limited due to patient availability and financial constraints. While the small sample size may limit broader generalizability and interpretive value, the scRNA-seq technology provides high-resolution gene expression profiling even with limited samples, lending robustness to our findings [71,72]. Furthermore, while the number of genes that differed between the three subjects were relatively small when the top 100 significantly differentially expressed genes were analyzed, genes related to X-inactivation exhibited much lower expression levels in TS, as expected (Supplementary Figure S1A,B). Aside from the prominent X-linked genes, most observed gene expression differences may not be directly attributed to Turner syndrome, as the study does not account for potential variability arising from differences. Nonetheless, despite these limitations, our study highlights distinct and consistent differences in the expression of TS-specific genes such as XIST and TSIX, which are central to our conclusions. These findings align with the known mechanisms of X chromosome haploinsufficiency in TS, supporting the notion that the observed patterns are not solely attributable to variability among 46,XX individuals. However, while their statistical significance is evident, their clinical significance requires further validation. Additionally, this study focused specifically on CD4(+) T cells from PBMCs to explore differentially expressed genes potentially related to immune function in TS patients. While this approach provided valuable insights, it inherently limited the scope of our findings. Examining a broader range of cell types and tissues would offer a more comprehensive understanding of systemic immune changes in TS. Furthermore, despite our efforts to match the study subjects as closely as possible, there were unavoidable

differences in patient characteristics, such as age, height, weight, ABO blood type, and parity. A more controlled study design would strengthen the comparability of future analyses. Nonetheless, many genes identified in our study may be associated with immune responses, although their precise roles in the autoimmune mechanisms of Turner syndrome remain to be clarified. Future studies incorporating larger sample sizes and additional controls will be critical to further validate our findings and enhance their interpretive value. Expanding the analysis to include additional cell types and tissues will also provide more comprehensive insights into the immunogenetic mechanisms underlying TS.

5. Conclusions

In this study, we used CD4(+) T cells gated single-cell RNA sequencing of peripheral blood mononuclear cell samples from a Turner syndrome patient, a healthy female, and a patient with Graves' disease to identify differentially expressed genes. As anticipated, the XIST gene was down-expressed in the TS patient (46, X) compared with both the healthy female and the patient with Graves' disease, who retained two X chromosomes. Thus, our findings may attest for the haploinsufficiency of the X chromosome in the TS patient. Furthermore, we identified 43 overlapping genes in the TS patient compared with the healthy female and the patient with Graves' disease, many of which were previously linked to immune system functions. While a direct causal inference between these genes and the pathogenesis of TS cannot yet be made, they may serve as potential targets for future studies. These findings offer valuable insights into the differences in genes related to the immune system in TS compared with healthy individuals and those with autoimmune diseases.

Supplementary Materials: The following supporting information can be downloaded at: https://www.mdpi.com/article/10.3390/cells14020093/s1, Table S1: Significantly up expressed genes in TS compared with HF; Table S2: Significantly down expressed genes in TS compared with GD; Table S4: Significantly down expressed genes in TS compared with GD; Figure S1: (A) The triangle diagram illustrating the number of genes with significant differential expression between each pair of subjects (Turner syndrome, TS; Graves' disease patient, GD; healthy female, HF); (B) The radar plots depicting the relative expression levels of the 43 genes with the most significant differences in a patient with TS compared with both an HF and a patient with GD. The expression values are normalized and plotted on a scale from 0 to the maximum expression level observed across the three subjects.

Author Contributions: Conceptualization, S.Y.S. and W.K.C.; methodology, S.Y.S., I.-C.B., W.K.C. and T.-G.K.; investigation, I.-C.B. and W.K.C.; resources; I.-C.B., M.H.J. and B.-K.S.; writing—original draft, S.Y.S. and W.K.C.; writing—review and editing, S.Y.S., I.-C.B., T.-G.K., M.H.J., B.-K.S. and W.K.C.; funding acquisition, S.Y.S. and W.K.C.; supervision, M.H.J., B.-K.S., I.-C.B., T.-G.K. and W.K.C. All authors have read and agreed to the published version of the manuscript.

Funding: This study was supported by the National Research Foundation of Korea (NRF) grant funded by the Korean government (MSIT) (RS-2022-NR072562) and by the Korean Society of Pediatric Endocrinology Grant (2023-01).

Institutional Review Board Statement: This study was approved by the Institutional Review Board (IRB) of the Catholic University of Korea (IRB Number: KC23TISI0193).

Informed Consent Statement: Informed consent was obtained from all subjects involved in the study.

Data Availability Statement: All the data analyzed in this study are not publicly available for the privacy of the research participants but are available from the corresponding author upon reasonable request.

Acknowledgments: We thank Jin Sun Kong for providing technical support for MacrogenTM.

Conflicts of Interest: The authors declare no conflicts of interest.

References

- 1. Zenaty, D.; Laurent, M.; Carel, J.C.; Léger, J. Turner Syndrome: What's new in medical care? Arch. Pediatr. 2011, 18, 1343–1347.
- 2. Park, S.Y.; Kim, S.J.; Lee, M.; Lee, H.I.; Kwon, A.; Suh, J.; Song, K.; Chae, H.W.; Joo, B.; Kim, H.S. Neurocognitive and psychosocial profiles of children with Turner syndrome. *Ann. Pediatr. Endocrinol. Metab.* **2023**, *28*, 258–266. [CrossRef] [PubMed]
- 3. Berglund, A.; Viuff, M.H.; Skakkebaek, A.; Chang, S.; Stochholm, K.; Gravholt, C.H. Changes in the cohort composition of turner syndrome and severe non-diagnosis of Klinefelter, 47,XXX and 47,XYY syndrome: A nationwide cohort study. *Orphanet J. Rare Dis.* 2019, 14, 16. [CrossRef] [PubMed]
- 4. Kim, S.E.; Park, S.H.; Han, K.; Cho, W.K.; Suh, B.K.; Park, Y.G. Population Prevalence, Cancer Risk, and Mortality Risk of Turner Syndrome in South Korean Women Based on National Health Insurance Service Data. *Yonsei Med. J.* 2022, 63, 991–998. [CrossRef] [PubMed]
- 5. Álvarez-Nava, F.; Lanes, R. Epigenetics in Turner syndrome. Clin. Epigenet. 2018, 10, 45. [CrossRef] [PubMed]
- 6. Ogata, T.; Matsuo, N. Turner syndrome and female sex chromosome aberrations: Deduction of the principal factors involved in the development of clinical features. *Hum. Genet.* **1995**, *95*, 607–629. [CrossRef] [PubMed]
- 7. Zhang, X.; Hong, D.; Ma, S.; Ward, T.; Ho, M.; Pattni, R.; Duren, Z.; Stankov, A.; Bade Shrestha, S.; Hallmayer, J.; et al. Integrated functional genomic analyses of Klinefelter and Turner syndromes reveal global network effects of altered X chromosome dosage. *Proc. Natl. Acad. Sci. USA* **2020**, *117*, 4864–4873. [CrossRef]
- 8. Olson, L.E.; Richtsmeier, J.T.; Leszl, J.; Reeves, R.H. A chromosome 21 critical region does not cause specific Down syndrome phenotypes. *Science* **2004**, *306*, 687–690. [CrossRef]
- 9. Ngo, S.T.; Steyn, F.J.; McCombe, P.A. Gender differences in autoimmune disease. *Front. Neuroendocrinol.* **2014**, *35*, 347–369. [CrossRef] [PubMed]
- 10. Yan, Z.; Lijuan, Y.; Yinhang, W.; Yin, J.; Jiamin, X.; Wei, W.; Yuefen, P.; Shuwen, H. Screening and analysis of RNAs associated with activated memory CD4 and CD8 T cells in liver cancer. *World, J. Surg. Oncol.* **2022**, 20, 2. [CrossRef]
- 11. Stassi, G.; De Maria, R. Autoimmune thyroid disease: New models of cell death in autoimmunity. *Nat. Rev. Immunol.* **2002**, 2, 195–204. [CrossRef]
- 12. Tomer, Y. Mechanisms of autoimmune thyroid diseases: From genetics to epigenetics. *Annu. Rev. Pathol.* **2014**, *9*, 147–156. [CrossRef] [PubMed]
- 13. Schurz, H.; Salie, M.; Tromp, G.; Hoal, E.G.; Kinnear, C.J.; Möller, M. The X chromosome and sex-specific effects in infectious disease susceptibility. *Hum. Genom.* **2019**, *13*, 2. [CrossRef]
- 14. O'Garra, A.; Gabrysova, L. Transcription Factors Directing Th2 Differentiation: Gata-3 Plays a Dominant Role. *J. Immunol.* **2016**, 196, 4423–4425. [CrossRef]
- 15. Janyga, S.; Marek, B.; Kajdaniuk, D.; Ogrodowczyk-Bobik, M.; Urbanek, A.; Buldak, L. CD4+ cells in autoimmune thyroid disease. *Endokrynol. Pol.* **2021**, *72*, 572–583. [CrossRef]
- 16. Libert, C.; Dejager, L.; Pinheiro, I. The X chromosome in immune functions: When a chromosome makes the difference. *Nat. Rev. Immunol.* **2010**, *10*, 594–604. [CrossRef]
- 17. Zhao, S.X.; Xue, L.Q.; Liu, W.; Gu, Z.H.; Pan, C.M.; Yang, S.Y.; Zhan, M.; Wang, H.N.; Liang, J.; Gao, G.Q.; et al. Robust evidence for five new Graves' disease risk loci from a staged genome-wide association analysis. *Hum. Mol. Genet.* **2013**, 22, 3347–3362. [CrossRef] [PubMed]
- 18. Mortensen, K.H.; Cleemann, L.; Hjerrild, B.E.; Nexo, E.; Locht, H.; Jeppesen, E.M.; Gravholt, C.H. Increased prevalence of autoimmunity in Turner syndrome--influence of age. *Clin. Exp. Immunol.* **2009**, *156*, 205–210. [CrossRef]
- 19. Radetti, G.; Mazzanti, L.; Paganini, C.; Bernasconi, S.; Russo, G.; Rigon, F.; Cacciari, E. Frequency, clinical and laboratory features of thyroiditis in girls with Turner's syndrome. The Italian Study Group for Turner's Syndrome. *Acta Paediatr.* **1995**, *84*, 909–912. [CrossRef]
- 20. Trovo de Marqui, A.B. Turner syndrome and genetic polymorphism: A systematic review. *Rev. Paul. Pediatr.* **2015**, *33*, 364–371. [CrossRef] [PubMed]
- 21. Gravholt, C.H.; Andersen, N.H.; Christin-Maitre, S.; Davis, S.M.; Duijnhouwer, A.; Gawlik, A.; Maciel-Guerra, A.T.; Gutmark-Little, I.; Fleischer, K.; Hong, D.; et al. Clinical practice guidelines for the care of girls and women with Turner syndrome. *Eur. J. Endocrinol.* **2024**, 190, G53–G151.
- 22. Cacciari, E.; Masi, M.; Fantini, M.P.; Licastro, F.; Cicognani, A.; Pirazzoli, P.; Villa, M.P.; Specchia, F.; Forabosco, A.; Franceschi, C.; et al. Serum immunoglobulins and lymphocyte subpopulations derangement in Turner's syndrome. *J. Immunogenet.* **1981**, *8*, 337–344. [CrossRef] [PubMed]
- 23. Thrasher, B.J.; Hong, L.K.; Whitmire, J.K.; Su, M.A. Epigenetic Dysfunction in Turner Syndrome Immune Cells. *Curr. Allergy Asthma Rep.* **2016**, *16*, 36. [CrossRef] [PubMed]
- 24. Bianchi, I.; Lleo, A.; Gershwin, M.E.; Invernizzi, P. The X chromosome and immune associated genes. *J. Autoimmun.* **2012**, *38*, J187–J192. [CrossRef] [PubMed]

- 25. Cho, W.K. Lifelong medical challenges and immunogenetics of turner syndrome. *Clin. Exp. Pediatr.* **2024**, *67*, 560. [CrossRef] [PubMed]
- 26. Fish, E.N. The X-files in immunity: Sex-based differences predispose immune responses. *Nat. Rev. Immunol.* **2008**, *8*, 737–744. [CrossRef]
- 27. Dai, R.; Ahmed, S.A. Sexual dimorphism of miRNA expression: A new perspective in understanding the sex bias of autoimmune diseases. *Ther. Clin. Risk Manag.* **2014**, *10*, 151–163.
- 28. Hyun, Y.S.; Lee, Y.H.; Jo, H.A.; Baek, I.C.; Kim, S.M.; Sohn, H.J.; Kim, T.G. Comprehensive Analysis of CD4(+) T Cell Response Cross-Reactive to SARS-CoV-2 Antigens at the Single Allele Level of HLA Class II. *Front. Immunol.* **2021**, 12, 774491. [CrossRef]
- 29. Arsenio, J. Single-Cell Transcriptomics of Immune Cells: Cell Isolation and cDNA Library Generation for scRNA-Seq. *Methods Mol. Biol.* **2020**, 2184, 1–18.
- 30. Wu, S.Z.; Al-Eryani, G.; Roden, D.L.; Junankar, S.; Harvey, K.; Andersson, A.; Thennavan, A.; Wang, C.; Torpy, J.R.; Bartonicek, N.; et al. A single-cell and spatially resolved atlas of human breast cancers. *Nat. Genet.* **2021**, *53*, 1334–1347. [CrossRef]
- 31. Chen, X.; Yang, Z.; Chen, W.; Zhao, Y.; Farmer, A.; Tran, B.; Furtak, V.; Moos, M., Jr.; Xiao, W.; Wang, C. A multi-center cross-platform single-cell RNA sequencing reference dataset. *Sci. Data* **2021**, *8*, 39. [CrossRef] [PubMed]
- 32. Seth, S.; Mallik, S.; Bhadra, T.; Zhao, Z. Dimensionality Reduction and Louvain Agglomerative Hierarchical Clustering for Cluster-Specified Frequent Biomarker Discovery in Single-Cell Sequencing Data. *Front. Genet.* **2022**, *13*, 828479. [CrossRef] [PubMed]
- 33. Kanhere, A.; Hertweck, A.; Bhatia, U.; Gokmen, M.R.; Perucha, E.; Jackson, I.; Lord, G.M.; Jenner, R.G. T-bet and GATA3 orchestrate Th1 and Th2 differentiation through lineage-specific targeting of distal regulatory elements. *Nat. Commun.* **2012**, *3*, 1268. [CrossRef] [PubMed]
- 34. Zhang, S.; Wang, Y.; Li, H.; Zhi, H.; Zhai, X.; Ruan, W.; Zhang, S.; Xu, X.; Wu, H. Tongmai Zhuke decoction restrains the inflammatory reaction of macrophages for carotid artery atherosclerosis by up-regulating lincRNA-Cox2. *Biotechnol. Genet. Eng. Rev.* 2023, 40, 1758–1773. [CrossRef]
- 35. Hao, Y.; Hao, S.; Andersen-Nissen, E.; Mauck, W.M., 3rd; Zheng, S.; Butler, A.; Lee, M.J.; Wilk, A.J.; Darby, C.; Zager, M.; et al. Integrated analysis of multimodal single-cell data. *Cell* 2021, 184, 3573–3587.e3529. [CrossRef] [PubMed]
- 36. Stuart, T.; Butler, A.; Hoffman, P.; Hafemeister, C.; Papalexi, E.; Mauck, W.M., 3rd; Hao, Y.; Stoeckius, M.; Smibert, P.; Satija, R. Comprehensive Integration of Single-Cell Data. *Cell* **2019**, *177*, 1888–1902.e1821. [CrossRef]
- 37. Benjamini, Y.; Hochberg, Y. Controlling the False Discovery Rate: A Practical and Powerful Approach to Multiple Testing. *J. R. Stat. Society. Ser. B (Methodol.)* **1995**, *57*, 289–300. [CrossRef]
- 38. Goeman, J.J.; Solari, A. Multiple hypothesis testing in genomics. Stat. Med. 2014, 33, 1946–1978. [CrossRef] [PubMed]
- 39. Larizza, D.; Calcaterra, V.; Martinetti, M. Autoimmune stigmata in Turner syndrome: When lacks an X chromosome. *J. Autoimmun.* **2009**, *33*, 25–30. [CrossRef] [PubMed]
- 40. Wang, H.; Zhu, H.; Zhu, W.; Xu, Y.; Wang, N.; Han, B.; Song, H.; Qiao, J. Bioinformatic Analysis Identifies Potential Key Genes in the Pathogenesis of Turner Syndrome. *Front. Endocrinol.* **2020**, *11*, 104. [CrossRef] [PubMed]
- 41. Massingham, L.J.; Johnson, K.L.; Scholl, T.M.; Slonim, D.K.; Wick, H.C.; Bianchi, D.W. Amniotic fluid RNA gene expression profiling provides insights into the phenotype of Turner syndrome. *Hum. Genet.* **2014**, *133*, 1075–1082. [CrossRef] [PubMed]
- 42. Klein, S.L.; Flanagan, K.L. Sex differences in immune responses. Nat. Rev. Immunol. 2016, 16, 626–638. [CrossRef]
- 43. Li, H.; Liu, Y.; Wang, X.; Yu, S.; Huang, H.; Shen, X.; Zhang, Q.; Hong, N.; Jin, W. Exploring the dynamics and influencing factors of CD4 T cell activation using single-cell RNA-seq. *iScience* **2023**, *26*, 107588. [CrossRef] [PubMed]
- 44. Viuff, M.; Skakkebaek, A.; Nielsen, M.M.; Chang, S.; Gravholt, C.H. Epigenetics and genomics in Turner syndrome. *Am. J. Med. Genet. C Semin. Med. Genet.* 2019, 181, 68–75. [CrossRef]
- 45. Trolle, C.; Nielsen, M.M.; Skakkebaek, A.; Lamy, P.; Vang, S.; Hedegaard, J.; Nordentoft, I.; Orntoft, T.F.; Pedersen, J.S.; Gravholt, C.H. Widespread DNA hypomethylation and differential gene expression in Turner syndrome. *Sci. Rep.* **2016**, *6*, 34220. [CrossRef]
- 46. Nielsen, M.M.; Trolle, C.; Vang, S.; Hornshoj, H.; Skakkebaek, A.; Hedegaard, J.; Nordentoft, I.; Pedersen, J.S.; Gravholt, C.H. Epigenetic and transcriptomic consequences of excess X-chromosome material in 47,XXX syndrome-A comparison with Turner syndrome and 46,XX females. Am. J. Med. Genet. C Semin. Med. Genet. 2020, 184, 279–293. [CrossRef] [PubMed]
- 47. Han, X.; Ren, J.; Lohner, H.; Yakoumatos, L.; Liang, R.; Wang, H. SGK1 negatively regulates inflammatory immune responses and protects against alveolar bone loss through modulation of TRAF3 activity. *J. Biol. Chem.* **2022**, 298, 102036. [CrossRef] [PubMed]
- 48. Bian, X.; Xue, H.; Jing, D.; Wang, Y.; Zhou, G.; Zhu, F. Role of Serum/Glucocorticoid-Regulated Kinase 1 (SGK1) in Immune and Inflammatory Diseases. *Inflammation* 2023, 46, 1612–1625. [CrossRef]
- 49. Meixner, A.; Karreth, F.; Kenner, L.; Wagner, E.F. JunD regulates lymphocyte proliferation and T helper cell cytokine expression. *EMBO J.* **2004**, *23*, 1325–1335. [CrossRef] [PubMed]

- 50. Liu, X.; Zhang, D.; Hu, J.; Xu, S.; Xu, C.; Shen, Y. Allograft inflammatory factor 1 is a potential diagnostic, immunological, and prognostic biomarker in pan-cancer. *Aging* **2023**, *15*, 2582–2609. [CrossRef] [PubMed]
- 51. Ogawa, K.; Takamori, Y.; Suzuki, K.; Nagasawa, M.; Takano, S.; Kasahara, Y.; Nakamura, Y.; Kondo, S.; Sugamura, K.; Nakamura, M.; et al. Granulysin in human serum as a marker of cell-mediated immunity. *Eur. J. Immunol.* **2003**, *33*, 1925–1933. [CrossRef] [PubMed]
- 52. Tewary, P.; Yang, D.; de la Rosa, G.; Li, Y.; Finn, M.W.; Krensky, A.M.; Clayberger, C.; Oppenheim, J.J. Granulysin activates antigen-presenting cells through TLR4 and acts as an immune alarmin. *Blood* **2010**, *116*, 3465–3474. [CrossRef] [PubMed]
- 53. Zhang, J.Y.; Wang, X.M.; Xing, X.; Xu, Z.; Zhang, C.; Song, J.W.; Fan, X.; Xia, P.; Fu, J.L.; Wang, S.Y.; et al. Single-cell landscape of immunological responses in patients with COVID-19. *Nat. Immunol.* **2020**, *21*, 1107–1118. [CrossRef] [PubMed]
- 54. Duquette, D.; Harmon, C.; Zaborowski, A.; Michelet, X.; O'Farrelly, C.; Winter, D.; Koay, H.F.; Lynch, L. Human Granzyme K Is a Feature of Innate T Cells in Blood, Tissues, and Tumors, Responding to Cytokines Rather than TCR Stimulation. *J. Immunol.* 2023, 211, 633–647. [CrossRef]
- 55. Shimizu, K.; Yamasaki, S.; Sakurai, M.; Yumoto, N.; Ikeda, M.; Mishima-Tsumagari, C.; Kukimoto-Niino, M.; Watanabe, T.; Kawamura, M.; Shirouzu, M.; et al. Granzyme A Stimulates pDCs to Promote Adaptive Immunity via Induction of Type I IFN. *Front. Immunol.* **2019**, *10*, 1450. [CrossRef] [PubMed]
- 56. Madera-Salcedo, I.K.; Sánchez-Hernández, B.E.; Svyryd, Y.; squivel-Velázquez, M.; Rodríguez-Rodríguez, N.; Trejo-Zambrano, M.I.; García-González, H.B.; Hernández-Molina, G.; Mutchinick, O.M.; Alcocer-Varela, J.; et al. PPP2R2B hypermethylation causes acquired apoptosis deficiency in systemic autoimmune diseases. JCI Insight 2019, 5, e126457. [CrossRef]
- 57. Li, Z.; Li, Y.; Wang, X.; Yang, Q. PPP2R2B downregulation is associated with immune evasion and predicts poor clinical outcomes in triple-negative breast cancer. *Cancer Cell Int.* **2021**, *21*, 13. [CrossRef]
- 58. Lapteva, N.; Huang, X.F. CCL5 as an adjuvant for cancer immunotherapy. *Expert. Opin. Biol. Ther.* **2010**, *10*, 725–733. [CrossRef] [PubMed]
- 59. Huffman, A.P.; Lin, J.H.; Kim, S.I.; Byrne, K.T.; Vonderheide, R.H. CCL5 mediates CD40-driven CD4+ T cell tumor infiltration and immunity. *JCI Insight* **2020**, *5*, e137263. [CrossRef] [PubMed]
- 60. Ortiz, B.D.; Krensky, A.M.; Nelson, P.J. Kinetics of transcription factors regulating the RANTES chemokine gene reveal a developmental switch in nuclear events during T-lymphocyte maturation. *Mol. Cell Biol.* **1996**, *16*, 202–210. [CrossRef] [PubMed]
- 61. Chuang, C.-H.; Wang, W.-J.; Li, C.-F.; Ko, C.-Y.; Chou, Y.-H.; Chuu, C.-P.; Cheng, T.-L.; Wang, J.-M. The combination of the prodrugs perforin-CEBPD and perforin-granzyme B efficiently enhances the activation of caspase signaling and kills prostate cancer. *Cell Death Dis.* **2014**, *5*, e1220. [CrossRef] [PubMed]
- 62. Sawyer, A.J.; Garand, M.; Chaussabel, D.; Feng, C.G. Transcriptomic Profiling Identifies Neutrophil-Specific Upregulation of Cystatin F as a Marker of Acute Inflammation in Humans. *Front. Immunol.* **2021**, *12*, 634119. [CrossRef] [PubMed]
- 63. Chen, Y.; Li, X.; Liu, S.; Ao, W.; Lin, J.; Li, Z.; Wu, S.; Ye, H.; Han, X.; Li, D. An atlas of immune cell transcriptomes in human immunodeficiency virus-infected immunological non-responders identified marker genes that control viral replication. *Chin. Med. J.* 2023, 136, 2694–2705. [CrossRef]
- 64. Zhang, P.; Cao, X.; Guan, M.; Li, D.; Xiang, H.; Peng, Q.; Zhou, Y.; Weng, C.; Fang, X.; Liu, X.; et al. CPNE8 Promotes Gastric Cancer Metastasis by Modulating Focal Adhesion Pathway and Tumor Microenvironment. *Int. J. Biol. Sci.* 2022, 18, 4932–4949. [CrossRef] [PubMed]
- 65. Chen, K.; Zhu, C.Y.; Bai, J.Y.; Xiao, F.; Tan, S.; Zhou, Q.; Zeng, L. Identification of feature genes and key biological pathways in immune-mediated necrotizing myopathy: High-throughput sequencing and bioinformatics analysis. *Comput. Struct. Biotechnol. J.* **2023**, *21*, 2228–2240. [CrossRef]
- 66. Li, N.; Nakamura, K.; Jiang, Y.; Tsurui, H.; Matsuoka, S.; Abe, M.; Ohtsuji, M.; Nishimura, H.; Kato, K.; Kawai, T.; et al. Gain-of-function polymorphism in mouse and human Ltk: Implications for the pathogenesis of systemic lupus erythematosus. *Hum. Mol. Genet.* 2004, *13*, 171–179. [CrossRef] [PubMed]
- 67. Cater, J.H.; Kumita, J.R.; Zeineddine Abdallah, R.; Zhao, G.; Bernardo-Gancedo, A.; Henry, A.; Winata, W.; Chi, M.; Grenyer, B.S.F.; Townsend, M.L.; et al. Human pregnancy zone protein stabilizes misfolded proteins including preeclampsia- and Alzheimer's-associated amyloid beta peptide. *Proc. Natl. Acad. Sci. USA* 2019, 116, 6101–6110. [CrossRef] [PubMed]
- 68. Su, L.; Zhang, G.; Kong, X. Prognostic Significance of Pregnancy Zone Protein and Its Correlation with Immune Infiltrates in Hepatocellular Carcinoma. *Cancer Manag. Res.* **2020**, *12*, 9883–9891. [CrossRef]
- 69. Vandooren, J.; Itoh, Y. Alpha-2-Macroglobulin in Inflammation, Immunity and Infections. *Front. Immunol.* **2021**, *12*, 803244. [CrossRef]
- 70. Huang, H.; Hara, A.; Homma, T.; Yonekawa, Y.; Ohgaki, H. Altered expression of immune defense genes in pilocytic astrocytomas. *J. Neuropathol. Exp. Neurol.* **2005**, *64*, 891–901. [CrossRef] [PubMed]

- 71. Slovin, S.; Carissimo, A.; Panariello, F.; Grimaldi, A.; Bouché, V.; Gambardella, G.; Cacchiarelli, D. Single-Cell RNA Sequencing Analysis: A Step-by-Step Overview. *Methods Mol. Biol.* **2021**, 2284, 343–365. [PubMed]
- 72. Haque, A.; Engel, J.; Teichmann, S.A.; Lönnberg, T. A practical guide to single-cell RNA-sequencing for biomedical research and clinical applications. *Genome Med.* **2017**, *9*, 75. [CrossRef] [PubMed]

Disclaimer/Publisher's Note: The statements, opinions and data contained in all publications are solely those of the individual author(s) and contributor(s) and not of MDPI and/or the editor(s). MDPI and/or the editor(s) disclaim responsibility for any injury to people or property resulting from any ideas, methods, instructions or products referred to in the content.





Article

Circulating T Cell Subsets in Type 1 Diabetes

Aldo Ferreira-Hermosillo ¹, Paola Santana-Sánchez ², Ricardo Vaquero-García ², Manuel R. García-Sáenz ³, Angélica Castro-Ríos ⁴, Adriana K. Chávez-Rueda ², Rita A. Gómez-Díaz ⁵, Luis Chávez-Sánchez ² and María V. Legorreta-Haquet ²,*

- Unidad de Investigación en Enfermedades Endócrinas de la UMAE Hospital de Especialidades, Centro Médico Nacional Siglo XXI, Instituto Mexicano del Seguro Social, Mexico City 06720, Mexico; aferreira@endocrinologia.org.mx
- Unidad de Investigación Médica en Inmunología, de la UMAE Hospital de Pediatría, Centro Médico Nacional Siglo XXI, Instituto Mexicano del Seguro Social, Mexico City 06720, Mexico; pao-ss@live.com.mx (P.S.-S.); ricardo-michelle@hotmail.com (R.V.-G.); akarina_chavez@yahoo.com.mx (A.K.C.-R.); luis_chz@hotmail.com (L.C.-S.)
- Servicio de Endocrinología, de la UMAE Hospital de Especialidades, Centro Médico Nacional Siglo XXI, Instituto Mexicano del Seguro Social, Mexico City 06720, Mexico; manuel.gsm@hotmail.com
- ⁴ Unidad de Investigación en Epidemiología Clínica de la UMAE Hospital de Pediatría, Centro Médico Nacional Siglo XXI, Instituto Mexicano del Seguro Social, Mexico City 06720, Mexico; angelica.castror@imss.gob.mx
- Unidad de Investigación en Epidemiología Clínica de la UMAE Hospital de Especialidades, Centro Médico Nacional Siglo XXI, Instituto Mexicano del Seguro Social, Mexico City 06720, Mexico; ritagomezdiaz@yahoo.com.mx
- * Correspondence: vileha14@yahoo.com.mx; Tel.: +52-5556276943

Abstract: Type 1 diabetes (T1D) is a complex disease driven by the immune system attacking the insulin-producing beta cells in the pancreas. Understanding the role of different T cell subpopulations in the development and progression of T1D is crucial. By employing flow cytometry to compare the characteristics of T cells, we can pinpoint potential indicators of treatment response or therapeutic inefficacy. Our study reveals elevated prolactin (PRL) levels in T1D patients, along with a decreased production of key cytokines. Additionally, PD1 appears to play a significant role in T1D. Notably, PRL levels correlate with an earlier disease onset and a specific T cell phenotype, hinting at the potential influence of PRL. These findings highlight the need for further research to identify promising cellular targets for more effective and tailored therapies.

Keywords: type 1 diabetes; PD1; PRL; T cells

1. Introduction

Immune system activation is essential for pathogen control and disease prevention, but regulatory mechanisms are required to avoid immunopathology caused by overactive immune responses. Immune tolerance is a crucial mechanism that prevents immune responses against the body's own antigens. However, an increase in the development of autoimmune diseases has been observed in recent years. These diseases are caused by harmful inflammatory responses involving innate immunity and autoreactive pathogenic T and B cells. T cells play a central role in regulating and initiating these responses. Therefore, understanding the mechanisms involved in autoimmune diseases and the therapeutic strategies being developed to restore immune tolerance is essential for determining the causes of autoimmune diseases such as type 1 diabetes (T1D).

According to the 2022 International Diabetes Federation report, 62% of newly diagnosed cases of T1D are individuals over the age of 20 [1]. This indicates that the de-

velopment of T1D is significantly influenced by a complex interaction of environmental factors [2,3] involving the microbiome, genome, metabolism, and immune system. T1D is caused by the autoimmune destruction of pancreatic β -cells, leading to almost complete insulin deficiency resulting in hyperglycemia, and is associated with the inflammation and infiltration of lymphocytes [4,5].

At present, the standard treatment for T1D is insulin; however, it is not effective for many people in terms of optimally controlling glucose levels. Research in the field of T1D has led to the exploration of various therapies, including gene therapy, stem cells, and immunotherapy, which offer promise for personalized treatment. Recent clinical trials have focused on immune agents, such as the anti-CD3 antibody teplizumab, as well as agents that are believed to impact beta cells directly, such as verapamil. However, none of these agents have resulted in long-term disease remission [6]. As a result, new therapeutic approaches are being actively sought, even though they have not had the expected safety. For example, the use of PD-1/PD-L1-blocking antibodies has been approved for the treatment of more than 15 different types of cancer. However, it is important to note that up to 37% of patients treated with these antibodies develop immune-related adverse events, including T1D [7].

Programmed cell death protein-1 (PD-1; CD279) is a 55 kDa protein belonging to the immunoglobulin superfamily. It is a critical regulator of the adaptive immune system [8], and is expressed on the surface of activated T and B cells [7] upon chronic exposure to antigens in various infectious processes, autoimmune diseases, and cancer [9]. The interaction of PD-1 with its ligand, PDL-1, has an immunosuppressive effect on T cells through decreasing TCR signal transduction via its ITIM and ITAM motifs [10]. Studies have shown that a deficiency of PD-1 or PD-L1 results in profoundly accelerated autoimmunity [11]. Furthermore, PD-1 single nucleotide polymorphisms (SNPs) have been shown to increase the risk of developing T1D in several populations [12–14], suggesting that, at least in a subset of patients, PD-1 plays a key role in maintaining islet tolerance. Therefore, assessing the expression of this molecule in the different subpopulations of peripheral blood T cells could constitute a fundamental tool for predicting and monitoring T1D.

Although PD-1 is characterized as an inhibitory marker, several effector T cell populations are characterized by high expression of this marker. Among the various T cell subpopulations, PD1 is a marker generally associated with follicular T cells (Tfh) [15,16], regulatory T cells (Tregs), and exhausted T cells (Tex) [17], which are implicated in the progression of autoimmune diseases and possibly associated with the development of TD1. Follicular T cells represent the CD4+ T cell subset capable of supporting antibody production by B cells and the induction of immunoglobulin isotype switching [18], circulating Tfh cells (cTfh), involves memory CD4+ T cells that express CXCR5, but have low or absent BCL6 [19]. These cells are associated with a wide range of autoimmune diseases. Although there is no clear association with autoantibody production in T1D, Tfh cells from diabetic mice transferred the disease in a mouse model, and a Tfh cell signature has been identified in autoimmune diabetes, suggesting that this population could be used as a biomarker and potentially targeted for T1D interventions [20]; meanwhile, the increases in insulin-specific antigen cTfh cells [21] and activated cTfh cells (PD1hi) were significant in children with new-onset T1D or at risk for T1D [22].

On the other hand, chronic inflammation and high antigenic persistence identified in autoimmune diseases can lead to a state of cellular exhaustion. Exhausted T cells lose their normal functions, such as producing cytokines, killing cells, and multiplying, and start expressing multiple co-inhibitory receptors (CTLA-4, PD-1, LAG-3, TIM3, and TIGIT). This exhaustion happens when T cells are constantly exposed to an antigen. Recent findings have suggested that exhausted T cells might be linked to a better prognosis in T1D [23]. In addition, there are two relevant subtypes of T cells in T1D: central memory

(CM; CD45RO+CCR7+) and effector memory (EM; CD45RO+CCR7-) T cells. Memory T cells can hold onto their protective function against familiar threats for many years without needing to be reminded of those threats [24]. Some studies have also found that memory T cells, particularly CD8+ T cells, have anti-tumor capabilities [25]. Also, memory T cells are thought to be one of the main contributors to the development of autoimmune diseases.

Moreover, it is well known that hormones such as prolactin (PRL) influence cellular responses. PRL is a hormone that stimulates cell growth and insulin production and may also enhance the development of blood vessels in pancreatic islets [26]. Additionally, PRL can function as a cytokine, influencing immune responses in various immune cell populations. However, its role in regulating the immune system is still controversial [27].

Research aiming to find effective treatments for T1D has shown that PRL treatment can enhance the engraftment and function of transplanted pancreatic islets, and it may prevent diabetes in patients treated with streptozotocin [28]. Nevertheless, the exact role of PRL in T1D remains unclear, and further studies are necessary for clarification, thus contributing to the discovery of new therapeutic strategies for the prognosis and monitoring of the development of T1D.

The main goal of this study is to analyze the different profiles of T cell subtypes and their potential association with serum PRL levels. We describe the frequency of exhausted T cells, Tfh cells, and memory T cells in patients with T1D to understand how hormonal factors and dysfunctional cellular responses could accelerate the development of autoimmunity.

2. Materials and Methods

A cross-sectional case-control study was developed to identify T cell subtype profiles associated with TD1. The cases group included patients with a diagnosis of T1D according to the criteria of the American Diabetes Association (ADA): those with clinical symptoms (polyuria, polydipsia and loss of unexplained weight, and ketoacidosis), biochemical data (fasting blood glucose ≥ 126 mg/dL, confirmed on a different day or blood glucose at any time of the day ≥ 200 mg/dL without considering the time of the last meal), requires the application of insulin for its treatment and had one or more markers of autoimmunity against the beta cell (e.g., antiGAD65, anti-IA2/-IA2ß or anti-Znt8), and without a history of neoplastic, chronic inflammatory disease or active infectious process. The control group included healthy 25- to 44-year-old volunteers without diabetes and without a history of a neoplasm, chronic inflammatory disease, or active infectious process.

2.1. Control Group

Healthy 25 to 44-year-old volunteers were selected, without diabetes and without a history of a neoplasm, chronic inflammatory disease, or active infectious process.

2.2. Sample Selection

A sample of 28 cases and 29 controls were randomly selected from patients treated in the T1D Clinic of the Endocrinology Service at the Hospital de Especialidades, Centro Médico Nacional Siglo XXI, a tertiary referral center. Group size estimates were based upon a power calculation to minimally yield an 80% chance to detect a significant difference in the respective parameter of $p \le 0.05$ between the relevant groups.

2.3. Reagents and Antibodies

A human prolactin ELISA kit (Fine Test, Wuhan, China) was used.

2.4. Blood Samples

Blood samples were collected from patients diagnosed with T1D and from healthy individuals. The samples were collected in tubes with K2 EDTA and without anticoagulant. From the anticoagulated blood, peripheral blood mononuclear cells (PBMCs) were separated using Lymphoprep (Axis-Shield, Liverpool, UK). The PBMCs were then recovered from the interface and washed three times with PBS (pH 7.4). Plasma was separated by centrifugation and kept for the determination of plasma PRL levels. The serum was also separated by centrifugation and stored at $-20\,^{\circ}\text{C}$ for the determination of cytokines.

2.5. Biochemical Determinations

Laboratory results were obtained from the Central Laboratory at UMAE Hospital de Especialidades, C.M.N. Siglo XXI, IMSS. Briefly, a 6 mL blood sample was centrifuged at $3150 \times g$ for 15 min, and the serum was divided into two aliquots. Glucose, cholesterol, c-HDL, and triglycerides were analyzed with a commercially available kit (COBAS 2010 Roche Diagnostics, Indianapolis, IN, USA) using photocolorimetry with a Roche Modular P800 spectrophotometer (2010 Roche Diagnostics, Indianapolis, IN, USA). c-HDL samples were treated with enzymes modified with polyethylene glycol and dextran sulfate and analyzed using the same photocolorimetric technique. Glycated hemoglobin (HbA1c) was evaluated through turbidimetric immunoanalysis (COBAS 2010 Roche Diagnostics, Indianapolis, IN, USA). Low-density lipoprotein cholesterol (c-LDL) was calculated with the Friedewald formula, c-LDL (mg/dL) = CT mg/dL – (c-HDL mg/dL + triglycerides mg/dL/5), if triglycerides were <400 mg/dL.

2.6. Plasma PRL Levels

Prolactin in plasma was measured using a human PRL (Prolactin) ELISA kit (FineTest, Wuhan, China).

2.7. Serum Cytokine Levels

The levels of the cytokines IL-2, IFN γ , IL-4, IL-17, IL-10, IL-6, TNF- α , sFAS, sFAS-L, Granzymes A and B, perforin, and granulysin were determined in previously frozen sera using the Multi-analyte Flow Assay Kit (Biolegend, San Diego, CA, USA), according to the manufacturer's instructions. To determine serum concentrations, the samples were analyzed on an MACS Quant X cytometer (Myltenyi Biotech, Santa Barbara, CA, USA).

2.8. Spectral Flow Cytometry

PBMCs were isolated from T1D patients and healthy donors via density centrifugation using Lymphoprep (Axis-Shield, Liverpool, UK). The PBMCs were recovered from the interface and washed three times with PBS (pH 7.4). The PBMCs were then stained with specific combinations of backbone antibody panels from the T cell subtype (Anti-human CD3-BV650 (OKT3), CD4-PE/F810 (SK3), CD8-APC/F810 (SK1), CD45RO-BV570 (UCHL1), CCR7-BV711 (G043H7), TIGIT-BV480 (A5153G), CTLA-4-PE (BNI3), LAG-3-BV785 (11C3C65), CXCR5-PE/F700 (J252D4), PD1SpkR718 (A17188B), and ICOS-PE (C398.4A), (Biolegend, San Diego, CA, USA)), for 20 min at 4 °C in the dark, and Ghost Dye, an amine reactive viability dye (Cytek® Biosciences, San Diego, CA, USA), according to the manufacturer's instructions. The cells were then washed three times with PBS, fixed with 2% paraformaldehyde, and analyzed using a Cytek® Aurora system cytometer (Cytek® Biosciences, San Diego, CA, USA).

2.9. Statistical Analysis

A descriptive and comparative analysis of the clinical characteristics of the groups was performed. Results are presented as mean (SD) or as percentages, where appropriate, for

normally distributed data, and Student's t-test for unpaired values was used to compare means between independent groups and the non-parametric Wilcoxon signed-ranks test, and the Mann–Whitney U tests were used to compare medians, mainly due to the sample size. A p-value of \leq 0.05 was considered significant with a 95% CI.

To assess the relationship between T1D evolution time and cellularity, we conducted a Pearson correlation analysis to examine linear relationships. Additionally, we performed a nonparametric Spearman correlation test using a Bonferroni-adjusted significance level. We presented a two-way dispersion graph along with its polytomous adjustment. When necessary, we conducted a stratified analysis based on prolactin levels, categorizing them into normoprolactinemic and hyperprolactinemic groups. Prolactin levels were evaluated during the study and classified as normoprolactinemic (serum PRL levels < 20 ng/mL) or hyperprolactinemic (serum PRL levels > 20 ng/mL). Evolutionary time was defined as the duration between the sample collection date and the date of T1D diagnosis. For the control group, diagnosis time zero was designated.

Analyses were performed using GraphPad Prism 10 (La Jolla, CA, USA) and the Stata software (Version 11.0; Stata Corp., College Station, TX, USA).

2.10. Ethical Considerations

The study was approved by the Human Ethics and Medical Research Committee of the Mexican Institute of Social Security (IMSS) with register R-2018-785-074 and was conducted according to the guidelines of the Declaration of Helsinki. Informed consent was obtained from all patients and healthy donors.

3. Results

3.1. Demographic Characteristics of the Study Population

In this cross-sectional study, adult patients (age \geq 18 years) diagnosed with T1D and age-matched healthy controls were included. All participants gave their consent to participate and donated a blood sample (10 mL). A total of 28 patients with T1D and 29 healthy controls were included. Of the total participants, 56% were female and 43% were male, with an average age of 30 years.

As part of the characterization of the groups, serum levels of prolactin, HbA1c%, and glucose were measured and compared, with statistically significant differences ($p \le 0.05$) observed between the patient and control groups. Because it is a group with T1D, their glucose and HbA1c levels are higher than the control group: glucose (87 \pm 6.4 mg/dL vs. 172 ± 100 mg/dL) and HbA1c (5.2 \pm 0.43% vs. 8.7 \pm 2.0%). Likewise, increased serum PRL levels were observed in the patients compared to healthy controls (16.2 \pm 13.90 ng/mL vs. 5.19 ± 3.47 ng/mL; Table 1, Figure 1a). It should be noted that, although our group of patients was mostly comprised of women when performing the differential analysis of serum PRL concentrations between men and women, we did not find that gender influenced an increase in serum PRL concentration (T1D male 16.08 ± 13.3 ng/mL vs. T1D female $17.75 \pm 14.70 \, \text{ng/mL}$ and healthy male $4.75 \pm 2.42 \, \text{ng/mL}$ vs. healthy female $4.92 \pm 3.65 \text{ ng/mL}$). A Spearman correlation analysis showed that there was a weak positive correlation between serum prolactin levels and %HbA1c (r = 0.3411, p = 0.038). This may indicate the relevance of the hormonal role, particularly of PRL, in the development and progression of the disease. The difference in PRL level expression between healthy donors and T1D patients could be a protective response to the pathology's inherent damage or an alarming signal. An increase in serum PRL levels could be related to damage generation.

Table 1. Demographic characteristics.

Characteristic	Healthy (n = 29)	T1D (n = 28)	Total (n = 57)	p Value
Sex—no. (%)				0.047
Male	16 (55.2%)	9 (32.14%)	25 (43.85%)	
Female	13 (44.8%)	19 (67.86%)	32 (56.15%)	
Age group—no.	29.8 (25-44)	32.03 (18-43)	30.63 (18-44)	0.024
Serum PRL (ng/mL)	5.19 ± 3.47	16.2 ± 13.90		0.007 *
HbA1c %	5.2 ± 0.43	8.7 ± 2.0		<0.001 *
Serum Glucose (mg/mL)	87 ± 6.4	172 ± 100		0.014 *
Waist circumference	90.54 ± 17.65	83.61 ± 9.87		0.325
Body-mass index (kg/m ²)	25.42 ± 5.21	25.21 ± 3.65		0.731
≥30.0: obese	7 (24.14%)	4 (14.28%)	11 (19.29%)	
Age onset (years)		15.0 ± 8.11		
Duration of diabetes (years)		17.0 ± 8.68		

Values represented as mean \pm SD. $p \le 0.05$ was considered statistically significant (*). PRL: Prolactin. HbA1c %: Percentage of glycated hemoglobin.

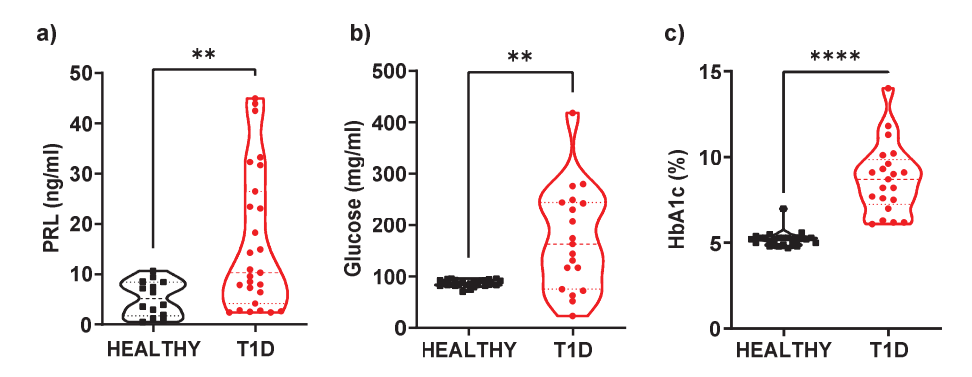


Figure 1. Serum levels of prolactin, glucose, and glycosylated hemoglobin. Quantification of serum levels of PRL glucose and HbA1 were compared between the patients with T1D and healthy controls. The results indicated significantly increased expression of (a) PRL (p = 0.007), (b) Glucose (p < 0.014), and (c) HbA1c (p < 0.0001) in T1D patients compared to healthy controls. Data are presented as mean \pm standard division (SD). (Healthy controls, n = 29, PE women, n = 28). p < 0.05 is considered statistically significant (** $p \le 0.01$, **** $p \le 0.0001$).

We found no differences regarding body mass index or waist circumference between the groups.

As we noticed an increase in serum levels of PRL, we decided to assess the hormonal profile of the study population. Although the role of hormones in autoimmunity is well-documented, our results did not show significant differences in the serum concentrations of hormones, such as estradiol, follicle-stimulating hormone (FSH), and free T4, contrary to our expectations. However, we observed a statistically significant increase in TSH (p = 0.031) in the group of patients with T1D compared to the control group. We also found higher testosterone levels in the control group, but all hormone levels were within normal ranges [27] (see Table 2). Table 2 provides mean, standard deviation, median, and interquartile range values for both study groups.

Table 2. Hormonal profile.

Group	Con	ıtrol	T1I	OM .	Cont	trol	T1	DM	
Statistics	Mean	SD	Mean	SD	Median	IQR a	p50	IQR a	Control vs. T1DM
Estradiol (pg/mL)	82.0	92.3	77.5	52.1	42.6	69.6	60.0	72.9	0.794
Testosterone (ng/dL)	403.3	302.9	199.7	282.1	468.6	500.3	36.3	477.7	0.034
FSH (MU/mL)	5.2	3.7	5.5	4.2	3.9	4.4	4.4	3.2	0.513
LH (MU/mL)	6.9	9.6	6.8	4.9	4.8	3.4	4.7	7.8	0.751
TSH (MU/mL)	2.0	0.8	2.6	1.5	1.8	1.1	2.9	3.1	0.031
T4 (ng/mL)	1.3	0.2	1.9	2.8	1.3	0.2	1.3	0.3	0.641

Values represented as mean \pm SD and median \pm IQR (q75-q25). $p \le 0.05$ was considered statistically significant. FSH = Follicle-stimulating hormone, LH = Luteinizing Hormone. TSH = Thyroid stimulating hormone (thyrotropin), T4 = Thyroxine 4. * Two-sample Kolmogorov–Smirnov test for equality of distribution functions. a: IQR = (q75-q25).

3.1.1. Serological Features of the Study Population

When comparing the biochemical profiles, we did not find any significant differences between the two groups. From Table 3, it can be observed that the serum uric acid concentration was statistically significantly higher in the control group (6.18 \pm 1.89 vs. 4.10 ± 1.10 mg/dL). This difference could be due to a less careful diet in the control group. However, the mean for both groups fell within the normal limits reported by the American Board of Internal Medicine: ABIM Laboratory Test Reference Ranges—January 2024 [29].

Table 3. Biochemical profile.

	Healthy (n = 22)	T1D (n = 24)	p Value
Cholesterol (mg/dL)	179.9 ± 34.59	166.6 ± 36.97	0.28
cHDL (mg/dL)	48.81 ± 9.125	48.75 ± 8.779	0.785
cLDL (mg/dL)	107.1 ± 28.24	93.66 ± 34.58	0.219
Triglycerides (mg/dL)	121.1 ± 81.13	111.6 ± 52.51	0.657
Uric acid (mg/dL)	6.181 ± 1.899	4.100 ± 1.107	< 0.001
Creatinine (mg/dL)	81.99 ± 92.30	281.1 ± 847.1	0.621

Values represented as mean \pm SD. $p \le 0.05$ was considered statistically significant. cHDL: High-density lipoprotein cholesterol, cLDL: Low-density lipoprotein cholesterol.

To further characterize our study population, we also determined serum cytokine levels to establish the predominant pro- or anti-inflammatory patterns in each group. We used an assay based on pre-coated beads with antibodies and flow cytometry to determine serum levels of various cytokines, such as IL-2, IL-4, IL-10, IL-6, TNF- α , sFAS, sFAS-L, Granzymes A and B, IFN γ , IL-17, perforin, and granulysin.

Our results showed that the healthy control group had elevated levels of certain cytokines, such as IL-17 (27.69 \pm 20.5 vs. 18.05 ± 9.8 pg/mL), perforin (4651 \pm 1970 vs. 3493 ± 1126 pg/mL), and granulysin (7668 \pm 2177 vs. 6103 ± 2007 pg/mL), when compared to the group of patients with DM1 (Figure 2a–c). We did not observe significant differences for the rest of the cytokines determined, although, in all cases, the concentrations of cytokines tended to be higher in the control group. This could be due to a potential state of immune system exhaustion in patients with T1D due to antigenic persistence, given the chronic nature of the disease.

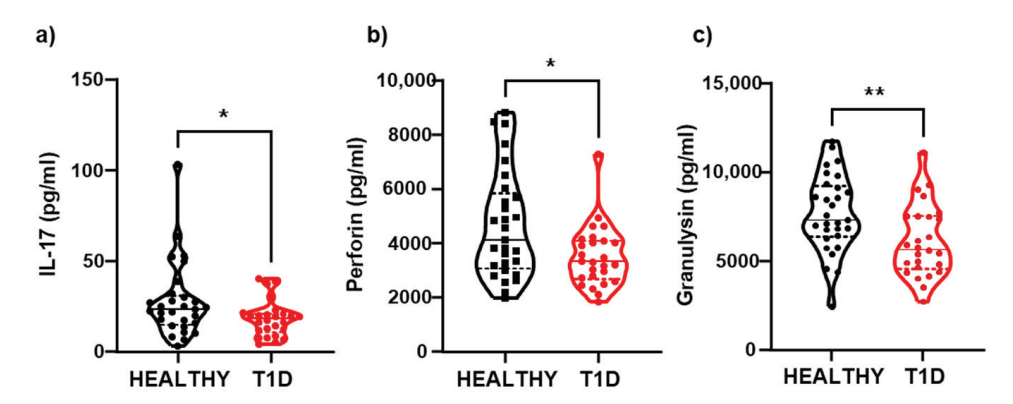


Figure 2. Serum levels of cytokines. Quantification of cytokine serum levels using flow cytometry. Serum cytokine levels were compared between patients with T1D and healthy controls. The results showed significantly increased expression of (a) IL-17 (p = 0.028), (b) Perforin (p < 0.028), and (c) Granulysin (p < 0.008) in healthy controls compared to T1D patients. Data is presented as mean \pm standard deviation (SD). (Healthy controls, n = 29; T1D patients, n = 28). p < 0.05 was considered statistically significant (* $p \le 0.05$, ** $p \le 0.01$).

3.1.2. Immunophenotype

To understand the relevance of T cells, we decided to examine the immune status of our groups by analyzing the cellular phenotypes of circulating T cell subsets, particularly focusing on follicular T cells, exhausted T cells, and different memory T cell populations. We used spectral flow cytometry to determine the percentages and absolute numbers of these T cell subsets from peripheral blood mononuclear cells, following the analysis strategy shown in Figure 3.

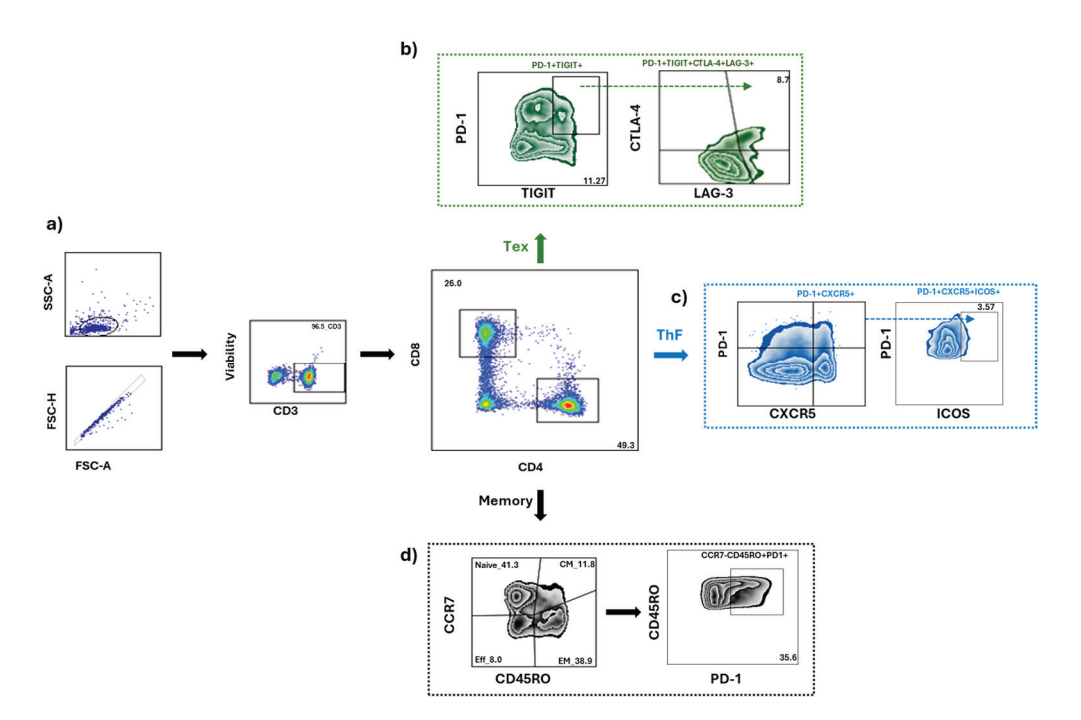


Figure 3. Circulating T cells. (a) Flow cytometry analysis strategy to gate on T cells. FSC-H vs. FSC-A plot was used to exclude doublets; lymphocytes were gated on the FSC-A vs. SSC-A plot, and live cells were gated in the Ghost Dye negative (Viability) and CD3-BV650+. From living T cells, we selected the CD4+ or CD8+ gate, and using the pre-designed panels from each T cell subtype, we selected the following markers: (b) Exhausted T cells (CD4+TIGIT+PD1+LAG3+CTLA-4+ or CD8+TIGIT+PD1+LAG3+CTLA-4+). (c) Follicular T cells (CD4+CXCR5+PD1+ICOS+ or CD8+CXCR5+PD1+ICOS+) (d) Memory T cells (CD4+CD45RO±CCR7±).

There were no significant differences in the percentages (Figure 4a,b) or absolute numbers (Figure 4c,d) of follicular T cells between the two groups. However, we observed a statistically significant increase in the number of exhausted CD8+ T cells in the group of patients with T1D compared to healthy controls (312.0 \pm 205.7 vs. 27.73 \pm 21.35 cells/µL) (Figure 4h).

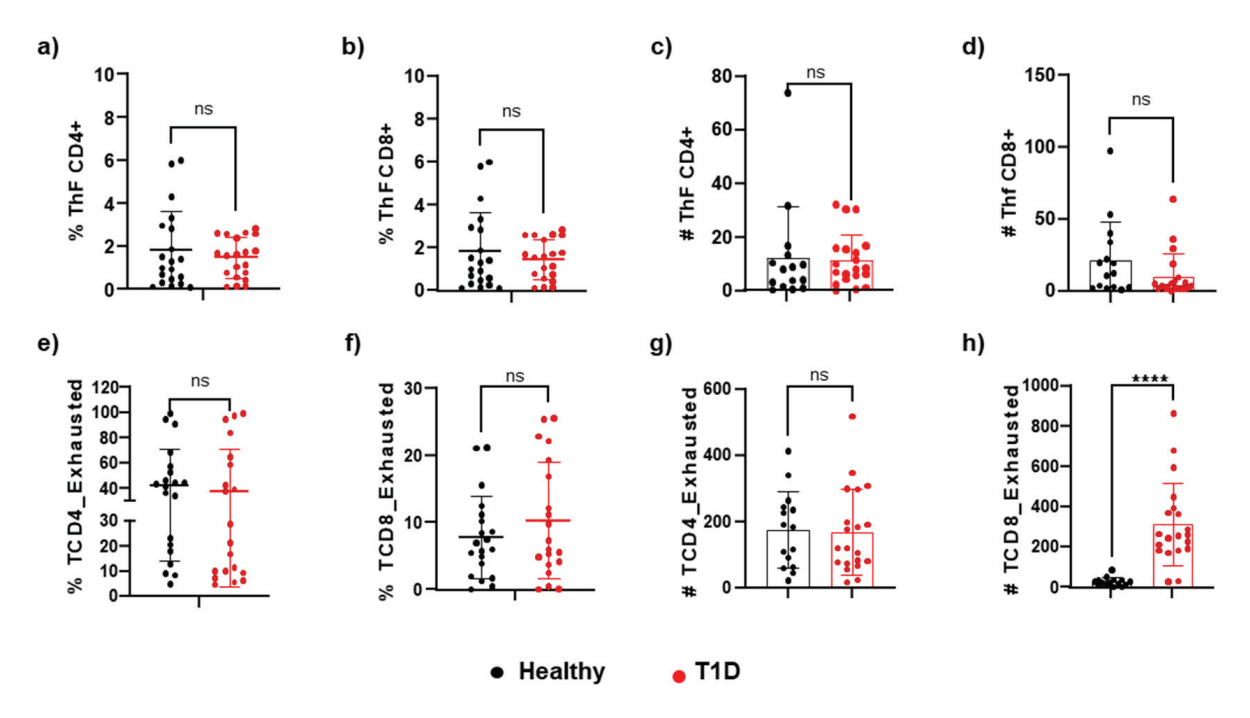


Figure 4. Comparison of frequencies of CD4/CD8 among live CD3+. (a–d) follicular T (CD4+CXCR5+PD1+ICOS+ or CD8+CXCR5+PD1+ICOS+), and (e–h) exhausted T (CD4+TIGIT+ PD1+LAG3+CTLA-4+ or CD8+TIGIT+PD1+ LAG3+CTLA-4+). These are shown as proportions or absolute numbers of circulating T cells in T1D and healthy controls. p < 0.05 was considered statistically significant (**** $p \le 0.0001$).

We examined if there were cellular changes in the memory cell fraction by calculating the percentage and number of CD4+ T cells or CD8+ T cells with specific phenotypes. We considered effector memory cells (CD45RO+CCR7-), central memory cells (CD4+CD45RO+CCR7+), effector cells (CD45RO-CCR7-), and naive cells (CD45RO-CCR7+). Our findings are presented in Figure 5a–p. Overall, we did not observe significant differences in the memory T cell compartment, except for an increase in the naive CD4+ T cell subpopulation in the T1D patient group compared to healthy individuals (82.18 \pm 49.02 vs. 65.69 \pm 36.32 cells/µL). We noted that peripheral naive T cells can be largely sustained by homeostatic expansion and tonic T cell receptor (TCR) signaling.

As there were no noteworthy differences in the T cell subtypes assessed, we sought to determine whether there was a functional difference in these cells beyond just numerical variations. We specifically focused on analyzing the expression levels of PD-1, an important immune checkpoint that negatively regulates the stability and integrity of T cell immune function, in the CD4+ T or CD8+ T cell subpopulations that we previously examined (Thf, memory T, and exhausted T).

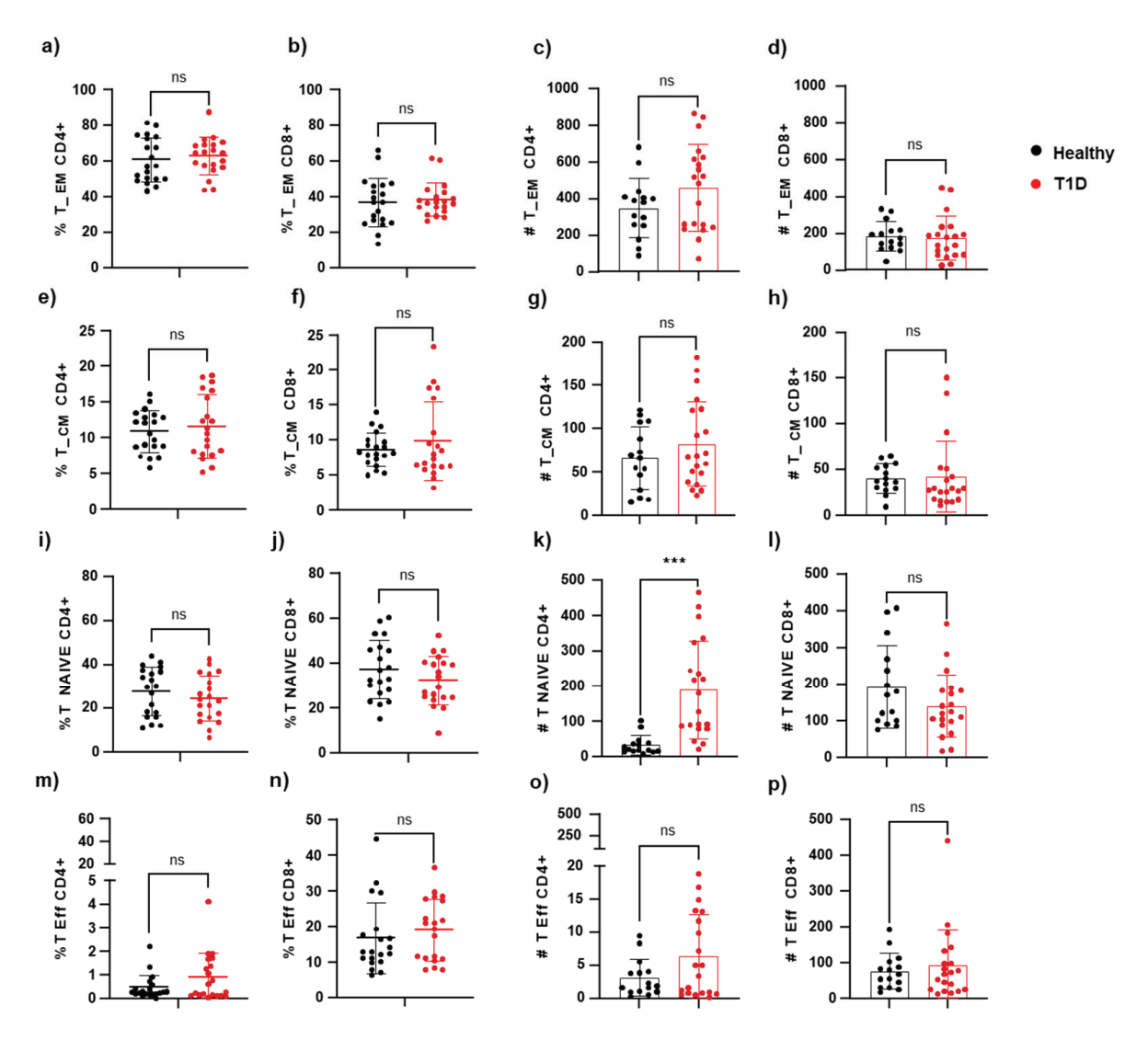


Figure 5. Comparison of the frequencies of CD4/CD8 among live CD3+ cells, TCD4+ or T CD8+. (a–d) effector memory (CD45RO+CCR7-), (e–h) central memory (CD4+CD45RO+CCR7+), (i–l) naive (CD45RO-CCR7+), and (m–p) effector (CD45RO-CCR7-) T cells are shown as proportions (left) or absolute numbers (right) of circulating T cells in T1D and healthy controls. p < 0.05 was considered statistically significant (*** $p \le 0.001$).

As seen in Figure 6, there was a difference in the expression of PD1 between the memory T cell subpopulations. There was a statistically significant increase in PD1 expression in the T1D patient group, compared to the control group, in central memory CD4+ T cells (5.45 ± 3.67 vs. 2.35 ± 1.68 cells/µL), effector memory (159.4 ± 82.63 vs. 101.8 ± 68.54 cells/µL), and effector (2.19 ± 2.89 vs. 0.5141 ± 0.6044 cells/µL). This might indicate an attempt to restore balance in a system that is overactivated by autoimmune antigen persistence (Figure 6a,c,e). On the other hand, in CD8+ T cells, there was a statistically significant decrease in the central memory cell compartment in patients with T1D compared to the group of healthy individuals (20.87 ± 8.414 vs. 12.68 ± 11.88 cells/µL) (Figure 6b).

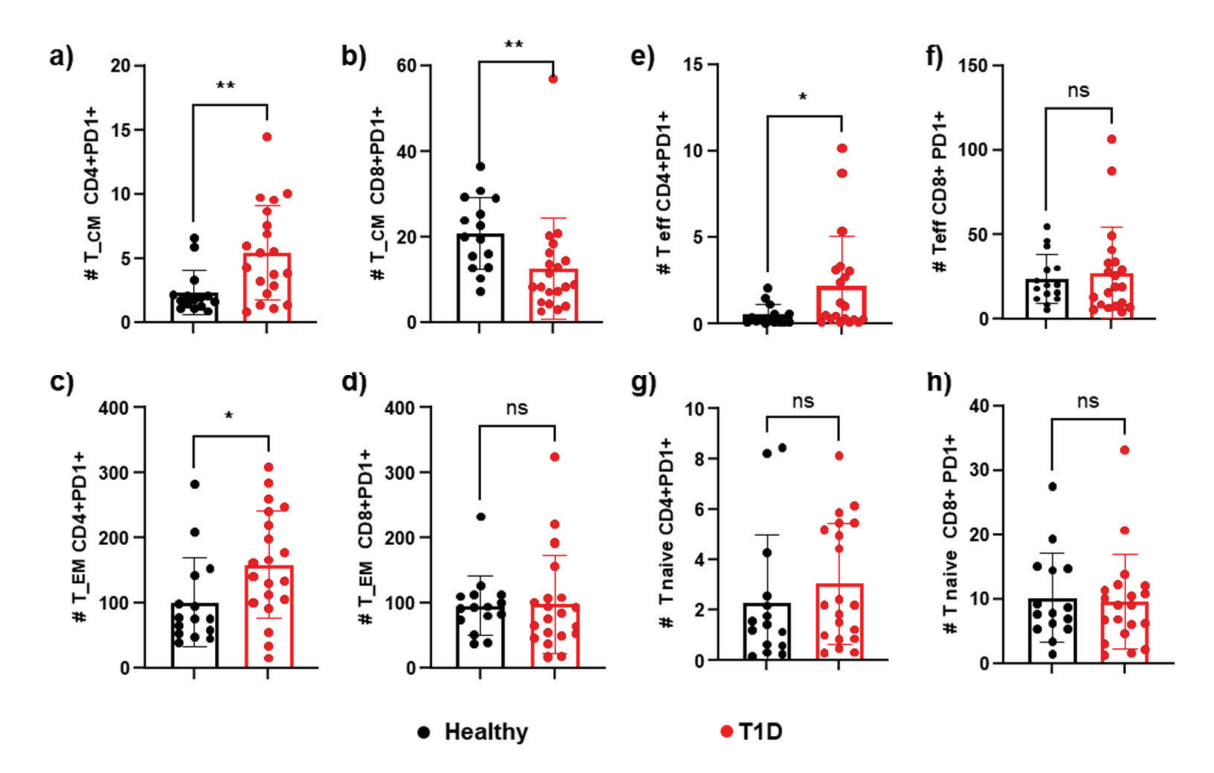


Figure 6. Comparison of frequencies of TCD4+ or T CD8+PD1+ between those of (a,b) central memory (CD4+CD45RO+CCR7+), (c,d) effector memory (CD4+CD45RO+CCR7-), (e,f) effectors (CD45RO-CCR7-), and (g,h) naïve (CD45RO-CCR7+) are shown as the absolute number of circulating T cells in T1D and healthy controls. p < 0.05 was considered statistically significant (* $p \le 0.05$, ** $p \le 0.01$).

To analyze the relationships between cell populations and serum prolactin concentrations during the progression of T1D, we performed a Pearson correlation analysis (for linear relationships) and a Spearman rank analysis (for non-linear relationships). These analyses were stratified based on the level of prolactin control. The significance level of the correlation was assessed using the Bonferroni-adjusted statistical test.

Prolactin was evaluated at the time of the blood study and categorized as normoprolactinemia (serum PRL levels < 20 ng/mL) or hyperprolactinemia (serum PRL levels > 20 ng/mL). The evolution time was calculated as the duration between the date of sample collection and the date of T1D diagnosis confirmation. For the control group of individuals without diabetes, a diagnosis time of zero was specified.

In Figure 7, the scatter plots illustrate the relationship between serum PRL levels and diagnosis time of T1D. In the hyperprolactinemic group, there was a strong negative correlation (r = -0.5667) between PRL levels and time since diagnosis, although it was not statistically significant. This suggests a potential involvement of prolactin in the etiopathogenesis of T1D. Conversely, in normoprolactinemic patients, there was a weak positive correlation (r = 0.3436, p = 0.050*) between serum PRL levels and the time of diagnosis.

The analysis of the correlation between serum prolactin levels and time was also performed for all T cell subpopulations, revealing a strong negative correlation for CD8_CM_PD1 (r = -0.6355, p = 0.0026 *) (Figure 7b), a weak negative correlation for CD8_NAIVE (r = -0.4849, p = 0.0289) (Figure 7d), a strong positive correlation for CD8_Exhausted (r = 0.500, p = 0.024 *) (Figure 7e), and a strong negative correlation for CD8_Thf (r = -0.7580, p = 0.0001 *) (Figure 7f), in the normoprolactinemic group.

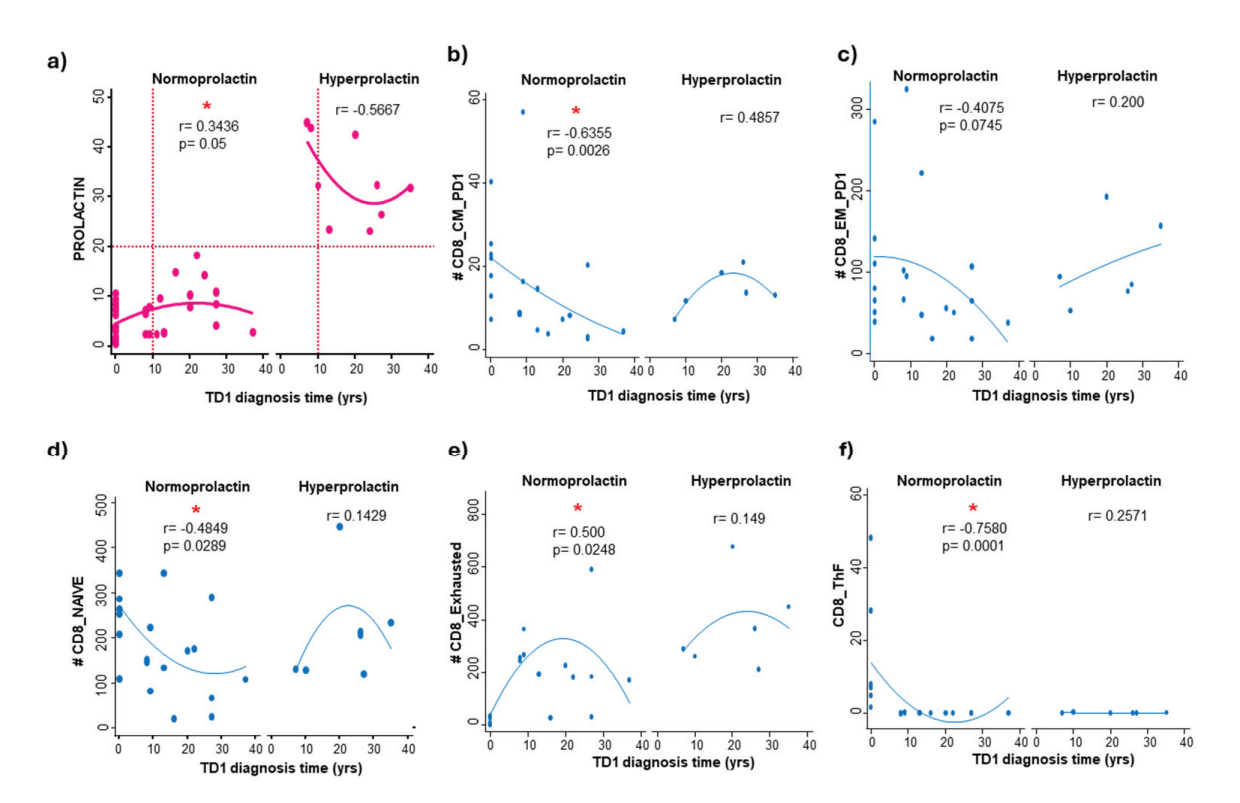


Figure 7. Two-way dispersion graph: prolactin and CD4 vs. TD1 diagnosis time (a) Spearman's correlations_ TD1 diagnosis time and prolactin levels: NP r = 0.3436, p = 0.050 *, HP r = -0.5667, ns. (b) TD1 diagnosis time and CD8-CM: NP r = -0.6355, p = 0.0026 *, HP r = 0.4857, ns. (c) TD1 diagnosis time and CD8-EM_PD1: NP r = -0.4075, ns HP r = 0.200, ns (d) TD1 diagnosis time and CD8_NAIVE: NP r = -0.4849, p = 0.0289 * HP r = 0.1429, ns. (e) TD1 diagnosis time and CD8_Exhausted: NP r = 0.500, p = 0.024 *. HP r = 0.200, ns. (f) TD1 diagnosis time and CD8_ThF = -0.7580, p = 0.0001 *. HP r = 0.2571, ns. HP = Hyperprolactin, NP = Normoprolactin.

Significant correlations were not found in the hyperprolactinemic group. However, this group tends to increase cellular levels concerning the diagnosis time. This difference may warrant further investigation in the search for distinguishing markers that can help track the progression of the disease.

It is important to note that correlation does not imply causality, but we believe that this approach could help identify prognostic or monitoring markers in these patients.

Due to the complexity of the autoimmunity phenomenon and the variation in cellular profiles among patients with T1D, further study of these cellular subpopulations is necessary to confirm the identified profiles and evaluate the results associated with each patient group.

4. Discussion

The measurement of HbA1c is an important diagnostic tool for diseases, serving as the primary indicator of glycemic control. It correlates with the clinical picture and can predict the development of complications [30]. Due to the T1D, the patient group had significantly higher levels of HbA1c and glucose compared to the control group; this may indicate inadequate glycemic control and a predisposition to clinical complications [31]. However, other biochemical parameters of the patient group did not indicate metabolic or renal alterations, and we were unable to establish associations between the presence of obesity or overweight and the evaluated biochemical and cellular parameters.

In terms of the hormonal profile, we found a direct relationship between serum levels of PRL and HbA1c. Although the majority of the patients with T1D were women, there was

no difference in the profile of steroid and thyroid hormones between the study populations, even when data were grouped according to gender.

Prolactin, a hormone secreted in the anterior pituitary, is involved in various physiological processes such as lactation, metabolism, or immunoregulation [32]. Increased levels of prolactin have been reported in various autoimmune diseases and were observed in the group of patients in this study, suggesting potential effects on the activation and secretion of cytokines in immune cells [33]. However, at present, there is insufficient evidence for the participation of this hormone in the pathophysiology of T1D.

Given the pivotal role of T cells in the development of T1D, it is crucial to further investigate the potential alterations in the various T cell populations. However, this is a challenging task due to the inherent complexity of these cells. For instance, autoreactive T cells have specific characteristics that make it challenging to develop biomarkers for T cells in diabetes, such as their low frequency in peripheral blood and their minimal response to the peptide-MHC complex. Furthermore, healthy individuals carrying MHC molecules associated with a risk for T1D may have autoreactive T cells that are quantitatively and functionally similar to those of patients with T1D [34]. Additionally, during activation, CD4+ T cells undergo less efficient metabolic reprogramming in aerobic glycolysis, similar to highly proliferative cancer cells. To limit tumor growth in cancer, glycolytic inhibitors are used, and this strategy has also been employed to suppress T cell responses in autoimmune diseases such as systemic lupus erythematosus, multiple sclerosis, and rheumatoid arthritis. However, the modulation of T cell metabolism in the context of T1D remains an underexplored therapeutic opportunity [35]. Multiple mechanisms are involved in maintaining peripheral immune tolerance. Immune checkpoint inhibitors play a vital role in immune tolerance by downregulating the immune system. Among these, PD-1 and PD-L1 are essential for the termination of immune responses. The PD1/PDL1 pathway induces immune system tolerance by promoting the development of Tregs and suppressing effector T cell responses [36].

In this study, the frequency and number of different CD4+ and CD8+ T cell subpopulations were evaluated to search for prognostic markers and their associations with the broad spectrum of clinical manifestations of the disease. Knowledge of the phenotype and function of cells is a fundamental tool in the search for new therapeutic approaches. The obtained results revealed discrete changes in the phenotype of T cell subpopulations and some effector molecules such as PD1. PD1 leads a highly relevant pathway due to its inhibitory functions in chronic viral infections and tumors and has special relevance in the context of autoimmunity. It is known that the use of PD-1 antagonist monoclonal antibodies is a therapeutic alternative in various neoplasia that has presented favorable effects in different clinical phases [37]. However, cases of spontaneous development of T1D in patients have been reported, with the rapid development of ketoacidosis and formation of autoantibodies in almost half of the patients who presented T1D [38,39]. In fact, dual use of antibodies against CTLA-4 and PD-1 or PD-L1 has been associated with an increased risk of developing T1D (hazard ratio [HR] = 1.62), compared to the use of anti-PD-L1 or anti-PD-1 alone [38]. Therefore, the association of this molecule with pathology is relevant.

In patients with T1D, the population of exhausted CD8 T cells is increased compared to that in healthy individuals. This increase could be due to the persistence of antigens as a result of the chronic nature of the disease. This highlights exhausted T cells as an important profile to monitor the development or progression of T1D. CD8+ cells have the ability to release antimicrobial and cytolytic molecules, such as granulysin and perforin, during infectious and autoimmune processes, contributing to the maintenance of inflammation [40–42]. However, studies in mice have shown that perforin's cytolytic activity leads to the destruction of β cells [43]. When comparing the serum levels of these molecules and pro- and

anti-inflammatory cytokines in T1D patients and healthy individuals, our results indicated significantly lower levels of perforin and granulysin in the T1D patient group. This suggests that constant antigen presentation during the autoimmune process may cause an exhausted state, resulting in a decrease in effector response capacity, such as the secretion of granules and proinflammatory cytokines [44,45]. Furthermore, there is also a significant decrease in IL-17—a pro-inflammatory cytokine—in patients with T1D, which is consistent with the increase in exhausted CD8+ T cells.

Our findings indicated an increase in the expression of CD8+ TIGIT+ potentially exhausted, while cells CD4+ TIGIT+ did not show a similar increase. The rise in the frequency of CD8+ exhausted T cells has been linked to slower disease progression. Furthermore, it has been observed that patients with T1D who responded effectively to teplizumab (CD3) treatment had a higher percentage of partially exhausted CD8+ EOMES+ KLRG1+ TIGIT+ T cells [46].

Regarding serum PRL levels, in cases where prolactin levels are normal, serum PRL remains consistent regardless of the age at diagnosis. Additionally, patients with normal prolactin levels showed minor levels of naive T CD8+ cells, effector memory cells, central memory cells, and ThF cells, which seem to be linked to early ages at diagnosis.

It is known that hyperprolactinemia has been associated with the development of various autoimmune diseases, such as systemic lupus erythematosus, potentially affecting disease activity. Research from both clinical and experimental studies indicates that the impact of prolactin on metabolism and the immune response varies based on its levels in the blood. Some studies suggest that prolactin has a protective effect. In contrast, others indicate that it could act as a pro-inflammatory factor, leading to harmful metabolic and immune changes associated with hyperprolactinemia.

PRL's role is still controversial. It has been shown in some human or rat experiments to stimulate glucose-dependent insulin secretion, insulin gene transcription, and β -cell proliferation [47,48]. Conversely, in some people, poor insulin secretion has been linked to chronic hyperprolactinemia [49,50]. Further research is required to better understand how excess or deficiency of PRL affects metabolic changes and to look into the possibility of using PRL as a therapeutic target.

Currently, there is insufficient information regarding the connection between PRL and T1D. Research, including our own, would facilitate a more in-depth exploration of the potential role of the hormone PRL in T1D. Regarding the correlation analyses, while we understand the necessity for a larger sample size and more extensive analysis, these methods could be adapted and employed in prediction or therapeutic monitoring models. Specifically, we could investigate the relationships between serum prolactin levels and CD8 T cell subtypes (e.g., naïve or follicular) in order to better monitor and understand the progression of T1D.

The study's strengths include the generation of knowledge in a fertile field that is challenging due to the limited experimental information available in the literature. Thus, there is a need to propose new analytical approaches that could lead to innovative strategies for monitoring T1D. This could involve considering the dual character of PRL as a growth factor with immunomodulatory activity and exploring the combination of hormonal and immunological approaches. It is important to acknowledge that extensive research in this field. The use of spectral flow cytometry as a powerful tool for analyzing cellular populations offers the possibility of multivariate analysis, allowing us to construct marker panels that could potentially be useful as prognostic or therapeutic sufficiency markers. As for the weaknesses of the study, we can mention the limited number of patients and controls. However, as an initial approach, we obtained a general overview of the cellular populations ex vivo, which provides a basis for further study through functional analysis

of these cellular subtypes in evaluating autoreactive responses. The reported phenotypic observations justify future specific studies on the impacts of the observed expression levels.

5. Conclusions

The presence of follicular T cells in both T1D patients and control subjects suggests that this cell type may not play a crucial role in the clinical course of T1D. However, differences in the frequencies of exhausted T cells indicate their potential connection to the development or progression of T1D, making them promising targets for therapeutic interventions. Our study demonstrated that the expression of immune checkpoints in the peripheral blood differs in patients with T1D when compared to healthy individuals, implying a potential suboptimal adaptation of the immune response. This underscores the importance of exploring the potential clinical applications of PD-1 manipulation in the context of autoimmunity. We cannot dismiss the possible impact of PRL on the response of memory T cells.

As a result, further immunological assessments of the phenotype and function of relevant T cell subtypes are essential for more accurate prediction, monitoring, and classification of patients with T1D. The ultimate goal is to explore how signaling pathways involving PD-1 could be harnessed to modulate the immune response and potentially prevent or treat autoimmune diseases such as T1D.

Author Contributions: Conceptualization, M.V.L.-H., A.F.-H. and R.A.G.-D.; methodology, P.S.-S., R.V.-G. and M.R.G.-S.; validation, M.V.L.-H.; formal analysis A.C.-R.; resources, L.C.-S.; data curation, A.C.-R.; writing—original draft preparation, A.F.-H., R.V.-G. and P.S.-S.; writing—review and editing, supervision, M.V.L.-H.; funding acquisition, M.V.L.-H. and A.K.C.-R. All authors have read and agreed to the published version of the manuscript.

Funding: This research was supported by Instituto Mexicano del Seguro Social (grant number R-2018-785-074 and R-2023-785-028).

Institutional Review Board Statement: All studies were approved by Comisión Nacional de Investigación Científica, Coordinación de Investigación en Salud, Centro Médico Nacional Siglo XXI, IMSS (protocol number R-2018-785-074).

Informed Consent Statement: Informed consent was obtained from all subjects involved in the study.

Data Availability Statement: The data presented in this study are available on request from the corresponding author.

Conflicts of Interest: The authors declare no conflicts of interest.

References

- 1. International Diabetes Federation. *IDF Diabetes Atlas*, 10th ed.; International Diabetes Federation: Brussels, Belgium, 2021.
- 2. Fröhlich-Reiterer, E.E.; Rosenbauer, J.; Bechtold-Dalla Pozza, S.; Hofer, S.E.; Schober, E.; Holl, R.W.; DPV-Wiss Study Group; German BMBF Competence Networks Diabetes mellitus and Obesity. Predictors of increasing BMI during the course of diabetes in children and adolescents with type 1 diabetes: Data from the German/Austrian DPV multicentre survey. *Arch. Dis. Child.* **2014**, *9*, 738–743. [CrossRef] [PubMed]
- 3. Schwandt, A.; Hermann, J.M.; Rosenbauer, J.; Boettcher, C.; Dunstheimer, D.; Grulich-Henn, J.; Kuss, O.; Rami-Merhar, B.; Vogel, C.; Holl, R.W.; et al. Longitudinal Trajectories of Metabolic Control From Childhood to Young Adulthood in Type 1 Diabetes From a Large German/Austrian Registry: A Group-Based Modeling Approach. *Diabetes Care* 2017, 40, 309–316. [CrossRef]
- 4. Priya, G.; Kalra, B.; Grewal, E.; Dardi, I. Premarriage Counseling in Type 1 Diabetes. *Indian J. Endocrinol. Metab.* **2018**, 22, 123–131. [CrossRef] [PubMed]
- 5. DiMeglio, L.A.; Evans-Molina, C.; Oram, R.A. Type 1 diabetes. Lancet 2018, 391, 2449–2462. [CrossRef] [PubMed]
- 6. Carr, A.L.J.; Evans-Molina, C.; Oram, R.A. Precision medicine in type 1 diabetes. *Diabetologia* **2022**, *65*, 1854–1866. [CrossRef] [PubMed]

- 7. Tucker, C.G.; Dwyer, A.J.; Fife, B.T.; Martinov, T. The role of programmed death-1 in type 1 diabetes. *Curr. Diab Rep.* **2021**, 21, 20. [CrossRef] [PubMed]
- 8. Freeman, G.J.; Long, A.J.; Iwai, Y.; Bourque, K.; Chernova, T.; Nishimura, H.; Fitz, L.J.; Malenkovich, N.; Okazaki, T.; Byrne, M.C.; et al. Engagement of the PD-1 Immunoinhibitory Receptor by a Novel B7 Family Member Leads to Negative Regulation of Lymphocyte Activation. *J. Exp. Med.* **2000**, *192*, 1027–1034. [CrossRef]
- 9. Sharpe, A.H.; Pauken, K.E. The diverse functions of the PD1 inhibitory pathway. Nat. Rev. Immunol. 2018, 18, 153–167. [CrossRef]
- 10. Arasanz, H.; Gato-Cañas, M.; Zuazo, M.; Ibañez-Vea, M.; Breckpot, K.; Kochan, G.; Escors, D. PD1 signal transduction pathways in T cells. *Oncotarget* 2017, 8, 51936–51945. [CrossRef]
- 11. Wang, J.; Yoshida, T.; Nakaki, F.; Hiai, H.; Okazaki, T.; Honjo, T. Establishment of NOD-Pdcd1^{-/-} mice as an efficient animal model of type I diabetes. *Proc. Natl. Acad. Sci. USA* **2005**, *102*, 11823–11828. [CrossRef] [PubMed]
- 12. Ni, R.; Ihara, K.; Miyako, K.; Kuromaru, R.; Inuo, M.; Kohno, H.; Hara, T. PD-1 gene haplotype is associated with the development of type 1 diabetes mellitus in Japanese children. *Hum. Genet.* **2007**, *121*, 223–232. [CrossRef]
- 13. Pizarro, C.; García-Díaz, D.F.; Codner, E.; Salas-Pérez, F.; Carrasco, E.; Pérez-Bravo, F. PD-L1 gene polymorphisms and low serum level of PD-L1 protein are associated to type 1 diabetes in Chile. *Diabetes/Metab. Res. Rev.* **2014**, *30*, 761–766. [CrossRef] [PubMed]
- 14. Nielsen, C.; Hansen, D.; Husby, S.; Jacobsen, B.; Lillevang, S. Association of a putative regulatory polymorphism in the PD-1 gene with susceptibility to type 1 diabetes. *Tissue Antigens* **2003**, *62*, 492–497. [CrossRef] [PubMed]
- 15. Good-Jacobson, K.L.; Szumilas, C.G.; Chen, L.; Sharpe, A.H.; Tomayko, M.M.; Shlomchik, M.J. PD-1 regulates germinal center B cell survival and the formation and affinity of long-lived plasma cells. *Nat. Immunol.* **2010**, *11*, 535–542. [CrossRef] [PubMed] [PubMed Central]
- 16. Shi, J.; Hou, S.; Fang, Q.; Liu, X.; Liu, X.; Qi, H. PD-1 Controls Follicular T Helper Cell Positioning and Function. *Immunity* **2018**, 49, 264–274.e4. [CrossRef] [PubMed]
- 17. Freeman, G.J.; Wherry, E.J.; Ahmed, R.; Sharpe, A.H. Reinvigorating exhausted HIV-specific T cells via PD-1-PD-1 ligand blockade. *J. Exp. Med.* 2006, 203, 2223–2227. [CrossRef]
- 18. Crotty, S. T follicular helper cell biology: A decade of discovery and diseases. Immunity 2019, 50, 1132–1148. [CrossRef] [PubMed]
- 19. Chevalier, N.; Jarrossay, D.; Ho, E.; Avery, D.T.; Ma, C.S.; Yu, D.; Sallusto, F.; Tangye, S.G.; Mackay, C.R. CXCR5 expressing human central memory CD4 T cells and their relevance for humoral immune responses. *J. Immunol.* **2011**, *186*, 5556–5568. [CrossRef] [PubMed]
- 20. Kenefeck, R.; Wang, C.J.; Kapadi, T.; Wardzinski, L.; Attridge, K.; Clough, L.E.; Heuts, F.; Kogimtzis, A.; Patel, S.; Rosenthal, M.; et al. Follicular helper T cell signature in type 1 diabetes. *J. Clin. Investig.* **2015**, 125, 292–303. [CrossRef] [PubMed]
- 21. Serr, I.; Fürst, R.W.; Ott, V.B.; Scherm, M.G.; Nikolaev, A.; Gökmen, F.; Kälin, S.; Zillmer, S.; Bunk, M.; Weigmann, B.; et al. miRNA92a targets KLF2 and the phosphatase PTEN signaling to promote human T follicular helper precursors in T1D islet autoimmunity. *Proc. Natl. Acad. Sci. USA* **2016**, *113*, E6659–E6668. [CrossRef] [PubMed]
- 22. Viisanen, T.; Ihantola, E.-L.; Näntö-Salonen, K.; Hyöty, H.; Nurminen, N.; Selvenius, J.; Juutilainen, A.; Moilanen, L.; Pihlajamäki, J.; Veijola, R.; et al. Circulating CXCR5+PD-1+ICOS+ Follicular T Helper Cells Are Increased Close to the Diagnosis of Type 1 Diabetes in Children With Multiple Autoantibodies. *Diabetes* 2017, 66, 437–447. [CrossRef] [PubMed]
- 23. Kwong, C.J.; Selck, C.; Tahija, K.; McAnaney, L.J.; Le, D.V.; Kay, T.W.; E Thomas, H.; Krishnamurthy, B. Harnessing CD8+T-cell exhaustion to treat type 1 diabetes. *Immunol. Cell Biol.* **2021**, *99*, 486–495. [CrossRef] [PubMed]
- 24. Gattinoni, L.; E Speiser, D.; Lichterfeld, M.; Bonini, C. T memory stem cells in health and disease. *Nat. Med.* **2017**, 23, 18–27. [CrossRef] [PubMed]
- 25. Liu, Q.; Sun, Z.; Chen, L. Memory T cells: Strategies for optimizing tumor immunotherapy. *Protein Cell* **2020**, *11*, 549–564. [CrossRef] [PubMed]
- Ramirez-Hernandez, G.; Adan-Castro, E.; Diaz-Lezama, N.; Ruiz-Herrera, X.; de la Escalera, G.M.; Macotela, Y.; Clapp, C. Global Deletion of the Prolactin Receptor Aggravates Streptozotocin-Induced Diabetes in Mice. Front. Endocrinol. 2021, 12, 619696.
 [CrossRef]
- 27. Legorreta-Haquet, M.V.; Santana-Sánchez, P.; Chávez-Sánchez, L.; Chávez-Rueda, A.K. The effect of prolactin on immune cell subsets involved in SLE pathogenesis. *Front. Immunol.* **2022**, *13*, 1016427. [CrossRef]
- 28. Hyslop, C.M.; Tsai, S.; Shrivastava, V.; Santamaria, P.; Huang, C. Prolactin as an Adjunct for Type 1 Diabetes Immunotherapy. Endocrinology 2016, 157, 150–165. [CrossRef] [PubMed]
- 29. American Boardof Internal Medicine. *ABIM Laboratory Test Reference Ranges–January* 2024; American Boardof Internal Medicine: Philadelphia, PA, USA, 2024.
- 30. Sherwani, S.I.; Khan, H.A.; Ekhzaimy, A.; Masood, A.; Sakharkar, M.K. Significance of HbA1c Test in Diagnosis and Prognosis of Diabetic Patients. *Biomark. Insights* **2016**, *11*, BMI-S38440. [CrossRef] [PubMed]

- 31. Antonio-Villa, N.E.; García-Tuomola, A.; Almeda-Valdes, P.; Vidrio-Velázquez, M.; Islas-Ortega, L.; Madrigal-Sanromán, J.R.; Zaballa-Lasso, C.; Martínez-Ramos-Méndez, A.; De la Garza-Hernández, N.E.; Bustamante-Martínez, J.F.; et al. Glycemic control, treatment and complications in patients with type 1 diabetes amongst healthcare settings in Mexico. *Diabetes Res. Clin. Pract.* 2021, 180, 109038. [CrossRef]
- 32. Shelly, S.; Boaz, M.; Orbach, H. Prolactin and autoimmunity. Autoimmun. Rev. 2012, 11, A465–A470. [CrossRef]
- 33. Chavezrueda, K.; Hérnández, J.; Zenteno, E.; Leanosmiranda, A.; Legorretahaquet, M.; Blancofavela, F. Identification of prolactin as a novel immunomodulator on the expression of co-stimulatory molecules and cytokine secretions on T and B human lymphocytes. *Clin. Immunol.* **2005**, *116*, 182–191. [CrossRef] [PubMed]
- 34. Culina, S.; Lalanne, A.I.; Afonso, G.; Cerosaletti, K.; Pinto, S.; Sebastiani, G.; Kuranda, K.; Nigi, L.; Eugster, A.; Østerbye, T.; et al. Islet-reactive CD8+ T-cell frequencies in the pancreas but not blood distinguish type 1 diabetes from healthy donors. *Sci. Immunol.* **2018**, *3*, eaao4013. [CrossRef] [PubMed]
- 35. Pearce, E.L.; Poffenberger, M.C.; Chang, C.-H.; Jones, R.G. Fueling Immunity: Insights into Metabolism and Lymphocyte Function. *Science* **2013**, 342, 1242454. [CrossRef]
- 36. Keir, M.E.; Butte, M.J.; Freeman, G.J.; Sharpe, A.H. PD-1 and its ligands in tolerance and immunity. *Annu. Rev. Immunol.* **2008**, 26, 677–704. [CrossRef] [PubMed]
- 37. Sun, G.; Liu, H.; Shi, X.; Tan, P.; Tang, W.; Chen, X.; Sun, G.; Yang, W.; Kong, X.; Zheng, Z.; et al. Treatment of patients with cancer using PD-1/PD-L1 antibodies: Adverse effects and management strategies (Review). *Int. J. Oncol.* 2022, 60, 74. [CrossRef]
- 38. Chen, X.; Affinati, A.H.; Lee, Y.; Turcu, A.F.; Henry, N.L.; Schiopu, E.; Qin, A.; Othus, M.; Clauw, D.; Ramnath, N.; et al. Immune Checkpoint Inhibitors and Risk of Type 1 Diabetes. *Diabetes Care* 2022, 45, 1170–1176. [CrossRef] [PubMed]
- 39. Zhang, R.; Cai, X.-L.; Liu, L.; Han, X.-Y.; Ji, L.-N. Type 1 diabetes induced by immune checkpoint inhibitors. *Chin. Med. J.* **2020**, 133, 2595–2598. [CrossRef] [PubMed]
- 40. Jiang, W.-Y.; Raychaudhuri, S.K.; Krensky, A.M. Lesional T cells and dermal dendrocytes in psoriasis plaque express increased levels of granulysin. *J. Am. Acad. Dermatol.* **2004**, *51*, 1006–1008. [CrossRef]
- 41. Stegelmann, F.; Bastian, M.; Swoboda, K.; Bhat, R.; Kiessler, V.; Krensky, A.M.; Roellinghoff, M.; Modlin, R.L.; Stenger, S. Coordinate expression of CC chemokine ligand 5, granulysin, and perforin in CD8+ T cells provides a host defense mechanism against Mycobacterium tuberculosis. *J. Immunol.* 2005, 175, 7474–7483. [CrossRef] [PubMed]
- 42. Fogagnolo, L.; Soares, T.C.B.; Senna, C.G.; Souza, E.M.; Blotta, M.H.S.L.; Cintra, M.L. Cytotoxic granules in distinct subsets of cutaneous lupus erythematosus. *Clin. Exp. Dermatol.* **2014**, *39*, 835–839. [CrossRef] [PubMed]
- 43. Trivedi, P.; Graham, K.L.; Krishnamurthy, B.; Fynch, S.; Slattery, R.M.; Kay, T.W.H.; E Thomas, H. Perforin facilitates beta cell killing and regulates autoreactive CD8+ T-cell responses to antigen in mouse models of type 1 diabetes. *Immunol. Cell Biol.* **2016**, 94, 334–341. [CrossRef] [PubMed]
- 44. Wherry, E.J.; Kurachi, M. Molecular and cellular insights into T cell exhaustion. *Nat. Rev. Immunol.* **2015**, *15*, 486–499. [CrossRef] [PubMed]
- 45. Wherry, E.J. T cell exhaustion. *Nat. Immunol.* **2011**, *12*, 482–489. [CrossRef]
- 46. Long, S.A.; Thorpe, J.; DeBerg, H.A.; Gersuk, V.; Eddy, J.A.; Harris, K.M.; Ehlers, M.; Herold, K.C.; Nepom, G.T.; Linsley, P.S. Partial exhaustion of CD8 T cells and clinical response to teplizumab in new-onset type 1 diabetes. *Sci. Immunol.* **2016**, *1*, eaai7793. [CrossRef] [PubMed]
- 47. Brelje, T.C.; Scharp, D.W.; E Lacy, P.; Ogren, L.; Talamantes, F.; Robertson, M.; Friesen, H.G.; Sorenson, R.L. Effect of homologous placental lactogens, prolactins, and growth hormones on islet b-cell division and insulin secretion in rat, mouse, and human islets: Implication for placental lactogen regulation of islet function during pregnancy. *Endocrinology* **1993**, *132*, 879–887. [CrossRef] [PubMed]
- 48. Petryk, A.; Fleenor, D.; Driscoll, P.; Freemark, M. Prolactin induction of insulin gene expression: The roles of glucose and glucose transporter-2. *J. Endocrinol.* **2000**, *164*, 277–286. [CrossRef] [PubMed]
- 49. Kim, S.Y.; Sung, Y.A.; Ko, K.S.; Cho, B.Y.; Lee, H.K.; Koh, C.S.; Min, H.K. Direct relationship between elevated free testosterone and insulin resistance in hyperprolactinemic women. *Korean J. Intern. Med.* **1993**, *81*, 8–14. [CrossRef]
- 50. Foss, M.C.; Paula, F.J.A.; Paccola, G.M.G.F.; Piccinato, C.E. Peripheral glucose metabolism in human hyperprolactinaemia. *Clin. Endocrinol.* **1995**, 43, 721–726. [CrossRef]

Disclaimer/Publisher's Note: The statements, opinions and data contained in all publications are solely those of the individual author(s) and contributor(s) and not of MDPI and/or the editor(s). MDPI and/or the editor(s) disclaim responsibility for any injury to people or property resulting from any ideas, methods, instructions or products referred to in the content.





Review

Lipid-Laden Microglia: Characterization and Roles in Diseases

Jiani Xing 1,2,†, Takese McKenzie 1,3,† and Jian Hu 1,2,3,4,*

- Department of Cancer Biology, The University of Texas MD Anderson Cancer Center, Houston, TX 77054, USA; jxing1@mdanderson.org (J.X.); ttmckenzie@mdanderson.org (T.M.)
- ² Cancer Biology Graduate Program, The University of Texas MD Anderson Cancer Center UTHealth Houston Graduate School of Biomedical Sciences, Houston, TX 77030, USA
- Neuroscience Graduate Program, The University of Texas MD Anderson Cancer Center UTHealth Houston Graduate School of Biomedical Sciences, Houston, TX 77030, USA
- ⁴ Cancer Neuroscience Program, The University of Texas MD Anderson Cancer Center, Houston, TX 77030, USA
- * Correspondence: jhu3@mdanderson.org; Tel.: +1-7137945238
- [†] These authors contributed equally to this work.

Abstract: Microglia are resident phagocytes of the central nervous system that play an essential role in brain development and homeostasis. When the intracellular lipid content exceeds the metabolic capacity of microglia, lipid droplets accumulate, giving rise to a distinct population termed lipid-laden microglia (LLMs). LLMs have been implicated in various neuroinflammatory and neurodegenerative diseases, functioning as both regulators/indicators of inflammation and potential therapeutic targets. This review summarizes the current research on LLMs, focusing on disease-specific regulators and functions, protective roles, interactions with neighboring cells, and advances in diagnostic and analytical tools. We also discuss the blurred distinction between LLMs and macrophages, inconsistent terminology, and major knowledge gaps across different disease contexts. Deciphering the composition, formation, and dynamics of lipid droplets in microglia is critical for uncovering how microglial states shift under diverse pathological stimuli. A clearer view of these mechanisms may reveal novel roles of LLMs and open new avenues for therapeutic intervention.

Keywords: lipid droplets; microglia; neurodegeneration; lipid metabolism; lipid droplet analytical tools

1. Introduction

From unicellular organisms to humans, lipids are essential biomolecules that serve as structural components, energy reservoirs, and signaling mediators in cells [1]. For many years, lipid droplets (LDs) were believed to be inert fat particles used to store energy. However, accumulating evidence has redefined LDs as dynamic, endoplasmic reticulum (ER)-derived organelles involved in lipid metabolism, stress response, and signal transduction [2]. LDs contribute to lipid and energy homeostasis and participate in modulating ER stress, oxidative stress, and various signaling pathways [3,4]. Their biogenesis and structural features appear to be conserved across species and cell types [5]. Structurally, LDs contain a neutral lipid core—mainly triacylglycerols, diacylglycerols, monoacylglycerols, and cholesteryl esters (CEs)—encased in a phospholipid monolayer embedded with proteins such as perilipin (PLIN) and seipin [5,6].

The observation of glial lipid accumulation dates to 1907, when Alois Alzheimer described such changes in the brains of dementia patients [7]. Decades later, in the 1970s,

lipid-laden macrophages—termed "foamy macrophages"—were identified as markers of immune dysfunction in atherosclerotic lesions [8]. Since then, the view of LD accumulation as a mere byproduct has been replaced by recognizing its role as a disease marker and active player in central nervous system (CNS) dysfunction. Notably, LD accumulation in microglia has been implicated in various neuroinflammatory and neurodegenerative diseases. Microglia are phagocytes that play an essential role in brain development and homeostasis. The accumulation of LDs in microglia is disease-specific and can be triggered by various pathological stimuli, such as lipopolysaccharide, long-chain fatty acids, brain injury, aging, amyloid-beta (A β), and even tauopathy neurons [9]. These triggers activate distinct signaling pathways, contributing to diverse microglial phenotypes and functional states. This review highlights recent progress in the characterization, regulation, and function of microglia with lipid droplets across diseases—including neurodegeneration, cancer, and metabolic disorders—and discusses their emerging diagnostic value and therapeutic potential.

2. Lipid-Laden Microglia in the Context of Microglial Heterogeneity

Microglia are the resident phagocytes of the central nervous system that promote homeostasis. Unlike monocyte-derived macrophages, microglia originate from the embryonic yolk sac and migrate into the neural tube, where they undergo maturation [10]. Initially, microglia were categorized into M1 and M2 states. The M1 state was proinflammatory and neurotoxic, while the M2 phase was anti-inflammatory and neuroprotective [11]. However, the field has now acknowledged that microglia cannot be categorized into two distinct states because these cells are highly dynamic, and their function is highly contextdependent [12]. Microglia are known to acquire diverse functional states during development and disease [12]. Homeostatic microglia survey the brain environment, phagocytose debris, and secrete regulatory cytokines. These microglia are characterized by markers such as P2RY12 and TMEM119 [12]. Microglial states are dynamic as microglia transition from a homeostatic state to different functional states in disease, aging, and injury, giving rise to microglial heterogeneity [12]. This diversity ranges from disease-associated microglia (DAM) found in Alzheimer's Disease to white matter-associated microglia (WAM) in demyelination and aging. These states are characterized by the expression of specific gene signatures; for example, DAMs express markers such as Clec7a and APOE. Together, this shows that the role and state of microglia are highly heterogeneous and context-dependent.

Over the years, studies have identified the distinct accumulation of lipid droplets in a subpopulation of phagocytes across various disease models. In studies on demyelination, these cells are referred to as "foamy phagocytes," which describes cells with a bubbly, lipidrich appearance near demyelinated plaques [13]. Originally identified in atherosclerotic lesions, foamy phagocytes indicate that cells have engulfed excessive lipids—particularly cholesterol and cholesteryl esters—leading to the formation of LDs. [8,14]. These LDenriched cells are considered a hallmark of atherosclerosis [15]. While phagocytes such as macrophages dominate the foamy cell population, other cell types (e.g., microglia, smooth muscle cells, and endothelial cells) can also become foamy [14]. Microglia are the resident phagocytes of the brain, and recently, studies have characterized the presence of LD accumulating in microglia in the brain. More recently, the term "lipid dropletaccumulating microglia" (LDAM) was introduced to describe a subtype of microglia in aged and Alzheimer's Disease (AD) brains that accumulate triglyceride-rich LDs and display impaired phagocytosis and heightened oxidative stress [6]. In other studies, terms like "lipid droplet-rich microglia (LDRM)" are used interchangeably with 'foamy microglia' and 'lipid-laden microglia', adding to the terminological ambiguity [16-19]. While extensive efforts have been made to characterize microglial functional states, other than the

accumulation of lipids, very little is known about the gene expression profile of microglia with extensive LDs. Lipid metabolism genes regulate the formation of LDs, and many genes involved in lipid metabolism are dysregulated across multiple microglial phenotypes, including DAMs [12]. Outside of AD and aging, whether lipid droplet-rich microglia represent a unique microglial subtype or a continuum of a pre-existing microglial subtype has yet to be fully elucidated. For this review, we have adopted the umbrella term "lipid-laden microglia" (LLM) to collectively describe microglia with intracellular LD accumulation, regardless of disease trigger or lipid species. While this generalization facilitates discussion, it underscores the urgent need for future studies to classify LLM subtypes based on their molecular triggers, functional phenotypes, gene expression, and lipidomic profiles.

3. Molecular and Analytical Tools for Detecting Lipid Droplets in Microglia

3.1. Traditional Detection Methods (Staining and Labeling)

The traditional method of detecting LDs in cells relies on staining intracellular neutral lipids using lipophilic dyes like Oil Red O (ORO), Sudan Black B, BODIPY, and Nile Red. ORO and Sudan Black B staining, in combination with conventional wide-field trans-illumination microscopy, have been widely used to visualize LD morphology [20,21]. The traditional ORO staining protocol was later refined by reducing the staining time to 1 min and the fixation time to 10 min, achieving a clearer visualization of LDs in over 90% of macrophages [21]. The use of 60% isopropanol during both infiltration and destaining enhanced lipid penetration and minimized background staining, improving imaging quality [21]. Oxidized low-density lipoprotein (oxLDL) is internalized by microglia and macrophages via scavenger receptors and accumulates in phagolysosomes, promoting the transformation of these cells into foamy phenotypes under ischemic conditions [22]. DiI, a lipophilic and non-toxic fluorescent dye, can be conjugated to oxLDL (DiI-oxLDL) and detected by confocal microscopy or flow cytometry. This approach enables quantitative analysis of oxLDL uptake and subsequent LD accumulation, offering a functional tool for studying the formation of lipid-laden cells [21].

However, ORO and Sudan Black B staining are restricted to fixed samples and highly sensitive to preparation conditions, making them time-consuming and less reproducible [20]. In contrast, BODIPY and Nile Red are lipophilic fluorescent dyes with high specificity and photostability, which are suitable for both live and fixed cell imaging. While the autofluorescence of lipofuscin (480–695 nm) partially overlaps with the emission of BODIPY 493/503 (\sim 505 nm), it is demonstrated that lipofuscin requires longer exposure times (5–10 s) to become visible, whereas BODIPY imaging requires only \sim 750 ms of exposure [23]. This difference minimizes interference and validates BODIPY as a reliable LD marker in microglia [23]. Nile Red displays polar-sensitive spectral shifts, changing from yellow (580 nm) for neutral lipids to red (628 nm) for polar lipids. These spectral properties can be both a challenge and an opportunity: while the color change complicates quantitative imaging, it can also indicate a change in the composition of the LDs [20].

Another widely used approach to visualize LDs across a broad size range is electron microscopy, including transmission and scanning electron microscopy (TEM and SEM). These techniques provide a subcellular resolution ranging down to <10 nm, allowing for the precise visualization of LD localization and their spatial relationships with other intracellular structures [20]. In TEM, a beam of high-energy electrons (80–300 keV) is transmitted through ultrathin tissue sections. The small electron wavelengths enable resolution at the angstrom scale. As primary electrons interact with the sample, they reveal the internal ultrastructure in detail. Due to its superior spatial resolution, TEM is a valuable tool for studying microglial LDs. It has been used to detect LDs in various pathological conditions,

such as Alzheimer's disease (AD), multiple sclerosis (MS), and spinal cord injury (SCI). Under pathological stress, microglia can acquire a distinct ultrastructural phenotype known as dark microglia, characterized by electron-dense cytoplasm and nuclear condensation [24]. In TEM images, LDs in these cells appear as bright, spherical structures enclosed by a single membrane. It has been shown that single dark microglia can contain up to 100 LDs [25]. Given the ability of TEM to resolve the microglial ultrastructure, it is an indispensable tool for characterizing LLMs.

Furthermore, confocal fluorescence microscopy combined with immunohistochemistry is widely used to detect intracellular LDs and their associated proteins, such as seipin, PEX30, and members of the PLIN family [26]. While these traditional techniques are straightforward, cost-effective, and widely accessible, they generally require the chemical fixation or staining of cells, limiting their ability to monitor dynamic LD behavior under physiological conditions. Moreover, excess fluorescent dye can result in nonspecific labeling and potentially interfere with cellular lipid metabolism [27].

3.2. Label-Free Methods

Given the limitations of label-dependent methods—including fixation requirements, staining artifacts, photobleaching, and spectral overlap—label-free imaging techniques are gaining attention for studying LDs in a more physiologically relevant manner. For example, synchrotron-based micro-Fourier transform infrared (microFTIR) spectroscopy can be employed to analyze foamy cells derived from RAW264.7 macrophages [28]. This technique enabled the detection of lipid content and efflux in response to experimental treatments without the need for fluorescent or chemical labeling [28]. At the single-cell level, coherent anti-Stokes Raman scattering (CARS) microscopy and stimulated Raman scattering (SRS) microscopy offer high-throughput, label-free, non-invasive, and chemically specific imaging by detecting the intrinsic vibrational frequencies of molecular bonds, particularly C-H stretches in lipids. Notably, studies show that under comparable imaging conditions, CARS can provide superior spatial resolution relative to SRS [27,29], while SRS offers improved signal linearity and quantification. Another emerging label-free technique is holotomography, also known as optical diffraction tomography (ODT), which reconstructs three-dimensional (3D) images based on refractive index differences between LDs and the cytoplasm [30]. ODT allows for real-time, live-cell 3D imaging of LD volume, number, distribution, and total lipid content.

Recently, the emergence of artificial intelligence has opened new avenues for exploring LDs using label-free imaging approaches. Coupling ODT with a deep learning-based virtual labeling framework allows for the simultaneous prediction of multiple fluorescent markers from a single refractive index scan, achieving the real-time, label-free 4D tracking of LDs in live cells [31]. Overall, the label-free methods avoid many drawbacks of traditional staining techniques, such as phototoxicity, photobleaching, and nonspecific labeling [32]. They offer a powerful and precise platform for investigating lipid metabolism, dynamics, and storage in single live cells with minimal perturbation. Both the label-dependent and label-free tools discussed in this section are summarized in Table 1, along with their respective advantages and disadvantages.

Table 1. Advantages and disadvantages of emerging tools for detecting and analyzing lipid droplets in microglia.

Tools	Principles	Advantages	Disadvantages			
Label-dependent approaches (invasive)						
Sudan Black B; ORO ¹	Lipophilic diazo dyes	Classical stains for visualizing neutral lipids; inexpensive	Only for fixed cells; requires freshly prepared and sensitive to preparation conditions			
Dil-oxLDL	Lipophilic, non-toxic fluorescent dye DiI attached to oxidized LDL to trace LDL uptake	Useful for studying the uptake and trafficking of LDL in live cells	Not a direct LDs marker; needs to be combined with other LDs dye for study			
BODIPY; Nile Red	Lipophilic fluorescent molecules	Both have high specificity and photostability for LDs; can be applied to both live and fixed cells; Nile Red is a polar-sensitive fluorescent molecule	May have non-specific binding to other lipid-rich membranes like mitochondrial and nuclear membranes			
TEM ² ; SEM ³	Electron beam imaging	Better preservation of cellular structures	Cannot be used for live and dynamic imaging; requires cell-fixing			
	Label-free app	roaches (non-invasive)				
Synchrotron-based microFTIR spectroscopy	Lipid-characteristic infrared absorption spectra	Monitors lipid content and efflux without labeling	Complex and expensive setup for detecting LDs			
CARS microscopy ⁴ ; SRS Microscopy ⁵	Measures molecular specific vibrational frequency	Label-free, real-time, live-cell imaging; high spatial resolution	CARS can achieve higher spatial resolution than SRS; however, SRS provides superior quantification and eliminates the non-resonant background that can interfere with signal specificity in CARS.			
ODT ⁶	Based on the RI differences between LDs and cytoplasm	Label-free, live-cell, 3D imaging; can track LD volume, number, and distribution	Low dynamic range			
ODT + RI2FL Deep Learning Model	Enables label-free tracking of LD dynamics over time with high temporal resolution	Predicts LD dynamics in live cells without photobleaching; long-term 4D tracking	AI training dataset required			

 $^{^1}$ Oil Red O (ORO). 2 Transmission electron microscopy (TEM). 3 Scanning electron microscopy (SEM). 4 Coherent anti-Stokes Raman-scattering microscopy (CARS microscopy). 5 Stimulated Raman-scattering microscopy (SRS microscopy). 6 Optical diffraction tomography (ODT).

4. Lipid-Laden Microglia Formation in Aging

Aging is one of the strongest risk factors for many neurodegenerative diseases [33]. It causes the dysfunction of cells and is characterized by various hallmarks, including telomere attrition, genomic instability, epigenetic alterations, altered intercellular communication, stem cell exhaustion, cellular senescence, mitochondrial dysfunction, dysregulated nutrient sensing, and loss of proteostasis [33]. Microglia, a key cell type important for regulating brain homeostasis, are also dysregulated during aging [34]. Aging also induces the dysregulation of microglial function and lipid metabolism; therefore, it is reasonable to infer potential alterations in LLMs during aging [34]. Earlier, a significant increase in lipid-laden cells in the aged brain was found using ORO staining [35]. Recently, a pioneering study was published, reporting a striking buildup of LDs in microglia in aged mouse and human brains [6], termed Lipid Droplet-Accumulating Microglia (LDAM). LDAMs are characterized as having defective phagocytosis, increased proinflammatory cytokine

secretion, and elevated levels of reactive oxygen species. These characteristics implicate LDAMs as possible instigators of dysfunction during aging.

Studies have sought to identify specific mediators of increased microglial reactivity with aging and focused on sialic acid-binding immunoglobulin-like lectin-11 (SIGLEC-11), a human microglial surface receptor that dampens microglial inflammatory pathways [36]. Expressing human SIGLEC-11 in mice and examining these mice at 6 and 24 months old, they found reduced LLM numbers, neuronal loss, and the expression of proinflammatory genes, suggesting that SIGLEC-11 attenuated neuroinflammation and the formation of LLM with age.

Lifestyle factors, especially diet, are modifiable aspects that can affect aging. A high-fat diet promotes inflammation and perturbs lipid metabolism, and its consumption is increased in older adults [37]. To assess the impact of diet on brain function during aging, aged mice were fed with a high-fat diet [38]. A significant increase in neutral lipid content, assessed by BODIPY and microglial lipid load, was observed in these mice. Microglia in the hippocampus were also more activated, as seen by an increase in CD68 immunoreactivity. Furthermore, another study shows that PPAR agonists were able to reduce microglial LDs and partially restored microglial function [39]. Together, these studies highlight that, during aging, the burden of LLMs increases, and these microglia tend to be more proinflammatory, thus possibly driving dysfunction.

5. Lipid-Laden Microglia in CNS Neurodegeneration

Neurodegeneration refers to the chronic progressive decline in the central nervous system [40]. Microglia, which constitute about 10% of the brain's cells and serve as its resident immune cells, are key mediators of neurodegeneration [41]. In this section, we summarize the current literature detailing the role of LLM in neurodegenerative diseases.

5.1. Alzheimer's Disease

AD is one of the most common forms of dementia and a leading cause of death and disability in the elderly worldwide [42]. The key hallmarks of AD include the aggregation of A β plaques, hyperphosphorylation of tau, neuronal loss, and neuroinflammation [43]. Some of the strongest genetic risk factors for AD include mutations in *APOE* and *TREM2*, which are microglia-enriched genes that regulate lipid metabolism [43]. Given the importance of lipid metabolism in the formation of LLMs, it is expected that LLMs are present in AD.

LDAMs, defined by the expression of the LD-associated enzyme acyl-CoA synthetase long-chain (*ACSL*), were recently found in the AD brain [44]. *ACSL1+* microglia were more abundant in AD patients with the *APOE4/4* genotype, and carrying the E4 mutation in the *APOE* gene has been identified as one of the most significant risk factors for the development of late-onset AD [45]. The abundance of LD-laden *ACSL1+* microglia in *APOE4/4* brains suggests that dysfunction in *APOE* lipid metabolism could drive the formation of LDAMs in AD. Additionally, *APOE4/4* iPSC-derived microglia that contain LDs induce tau hyperphosphorylation and neuronal apoptosis, highlighting the detrimental nature of these microglia.

TREM2 is a myeloid cell receptor that is significantly upregulated in microglia associated with amyloid plaques [46,47]. TREM2 has also been defined as a key activator of the disease-associated microglia found around plaques [47]. The presence of the TREM2-R47H variant is also associated with an increased risk for the development of AD [48]. Claes et al. addressed the effect of the TREM2-R47H mutation on LD formation in AD by transplanting TREM2-R47H iPSC-derived microglia into a chimeric AD mouse model. In vitro, these

microglia displayed an accumulation of LDs; however, in vivo, the opposite was found. This suggests that LD accumulation occurs secondary to *TREM2* mutation.

In addition to specific genetic risk factors, LDAMs can be mediated by changes in the brain environment due to AD pathology. Prakash et al. [49] demonstrated that $A\beta$ exposure induces the formation of LDs in microglia in a proximity-driven manner in AD. Similarly to previous reports, these microglia exhibited defective $A\beta$ phagocytosis. The study suggests that the accumulation of LDs is mediated by changes in the microglial lipid composition through decreasing free fatty acids and increasing triacylglycerols. Inhibiting diacylglycerol O-acyltransferase 2, an enzyme that converts free fatty acids to triacylglycerols, promoted microglial $A\beta$ phagocytosis and reduced neuronal damage.

Additionally, the inhibition of fat storage-inducing transmembrane protein (FIT2) reduced LD formation and improved the microglial phagocytosis of A β plaques [50]. In assessing the formation of LDs in AD microglia, Sha et al. [51] utilized the 3xTg AD mouse model, which has both amyloid and tau pathology. The LDs in AD microglia were regulated through the TRPV1–PKM2–SREBP1 axis. PMK2 and SREBP1, which are particularly enriched in microglia, were upregulated in the 3xTg mice, accompanied by increased LD formation in these mice. In this study, it was established that treating AD mice with capsaicin increased microglial phagocytic function through the inhibition of PKM2 dimerization and reduction in SREBP1 activation, which in turn increased TRPV1 activation. These findings suggest that modulating microglial lipid droplet formation is a potential therapeutic for AD.

Complement C3a receptor (C3aR), which is predominantly expressed in microglia, was also found to be a regulator of lipid accumulation in AD mice [52]. In the amyloid precursor protein (APP) AD mouse model, microglia shifted to a high-C3aR-expressing subpopulation, and the deletion of C3aR attenuated LD accumulation in microglia. Using an in vitro cell culture system with BV2 immortalized microglial cells, Li et al. [53] showed that Aβ treatment directly induced the formation of LDs. This profile was strongly correlated with the increased expression of the lipid metabolism gene *ANGPTL4*. Additionally, others have uncovered a unique regulation of neuronal activity by LD-accumulating microglia [54]. Human-derived microglia expressing the *APOE4* allele were found to have an accumulation of LDs. These microglia had a weak response to neuronal activity. Exposing neurons to conditioned media from *APOE4* LLMs also led to a significant decrease in neuronal calcium transients.

These results support the AD environment and lipid metabolism genes as key drivers of LD accumulation in microglia. Given the role of LD-accumulating microglia in AD, researchers have tried to therapeutically target them. Comerota et al. [55] utilized oleoylethanolamide, a health span-promoting endogenous lipid amide, as a therapeutic agent in chronically inflamed $5 \times \text{FAD}$ mice [56]. Oleoylethanolamide was able to specifically reduce LD formation in the microglia through a PPAR α -dependent mechanism. A study by Wu et al. also demonstrated how the modulation of microglial lipid metabolism through fasting could alter LD formation in AD [50]. APP/PS1 mice that underwent intermittent fasting demonstrated decreased accumulation of LDs in the microglia. These microglia also showed increased A β phagocytosis and a more amoeboid shape. Intermittent fasting also improved cognitive function, as measured by the Barnes maze and Y maze.

Overall, an abundance of studies have shown that LD accumulation in microglia is a predominant feature of AD. The accumulation of LDs in AD causes these microglia to become defective, exhibiting reduced phagocytosis and increased proinflammatory signals. The formation of LLMs in AD is influenced by genetic risk factors such as *APOE4* and

TREM2-R47H mutations. Additionally, perturbations in lipid metabolism genes such as *ACSL*, *DGAT2*, and *FIT2* also significantly contribute to the formation of LLMs.

5.2. Tauopathies

Tauopathies refer to a diverse group of neurodegenerative diseases that are characterized by the abnormal accumulation of tau in the brain. Tau is a microtubule-associated protein that functions by binding to tubulin, promoting its polymerization and stabilization to form microtubules [57]. Tauopathies are classified into two subsets: primary and secondary [57]. Primary tauopathies refer to diseases where tau deposition is the predominant feature. Secondary tauopathies refer to diseases where another upstream factor drives the deposition of tau. Tauopathies include AD, Pick's disease, and progressive supranuclear palsy. The predominant clinical features of tauopathies are progressive aphasia, cognitive deficits, and movement disorders.

The accumulation of tau leads to chronic neuroinflammation in the brain. Li et al. [58] utilized Raman scattering (SRS) microscopy to visualize the brains of mice with tauopathy and observed the striking accumulation of LDs in phagocytes, marked by ionized calciumbinding adaptor molecule 1 (Iba1) and CD68. These LDs originated from neurons, which were subsequently transferred to phagocytes in the mouse hippocampus. These phagocytes with LDs had features like LDAMs found in AD. The study found that LD accumulation in microglia in the presence of tau results in defective phagocytosis and the secretion of proinflammatory cytokines. While many studies have used Iba1 and CD68 to mark microglial cells, these markers are also expressed in monocyte-derived macrophages [59], which have functional roles in tauopathies [60].

On assessing publicly available RNA sequencing data on tauopathy human brains, Li et al. found a striking dysregulation of genes involved in LD formation, including PLIN2, GPAT1, and ABCA1. Neuronal AMP-activated protein kinase (AMPK), a master regulator of energy homeostasis, was also significantly downregulated, and its depletion in iPSC neurons co-cultured with BV2 microglia promoted the accumulation of LD in microglia. Tau in the presence of microglia was also found to directly increase the abundance of phospholipids and sphingolipids, thus facilitating the accumulation of LDs [61]. Additionally, a study published by Xu et al. [62] further delineated the role of LD-accumulating microglia in tauopathy. They characterized the role of the autophagy gene Atg7 in microglia/ macrophages using a Cx3CR1 promoter-driven conditional knockout mouse model and cultured BV2 immortalized microglial cell line. The disruption of autophagy caused by Atg7 depletion shifted microglia to a proinflammatory state with heightened LD accumulation. In addition, Atg7-depleted microglia also promoted the spread of tau in neurons [62]. Together, these findings indicate that tau can directly induce LD formation in microglia, which is detrimental to the microglia. They also highlight the dynamics of microglia, whereby LD formation can be induced by adjacent tau-laden neurons and dysfunction in intrinsic microglia autophagy.

5.3. Demyelinating Diseases

Demyelination refers to the pathological loss of myelin, a lipid-rich structure in the nervous system [63]. Myelin comprises about 70% lipids, including cholesterol, phospholipid, and glycolipid [63]. The phagocytosis of lipid-rich myelin by phagocytes leads to the acquisition of a foamy phenotype. This foamy phenotype is characterized by the presence of LDs rich in cholesteryl esters surrounded by a phospholipid monolayer. Most of the published literature has focused on LD accumulation in Multiple Sclerosis (MS) and Krabbe's disease; therefore, we summarize the findings on these demyelinating diseases below.

MS is the most common primary demyelinating neurodegenerative disease, affecting over 2 million people worldwide. It is characterized by focal demyelinating lesions in the brain and spinal cord that lead to motor and neurological impairments [64]. The lesions are characterized by the accumulation of LD-laden foamy phagocytes, infiltrating T-cells, neuronal loss, and damaged myelin. Studies have also shown that microglia are not the only phagocytes present in the lesions, as monocyte-derived macrophages also infiltrate from the periphery. However, MS involves demyelination of the CNS; therefore, microglia, the resident phagocytes of the CNS, are thought to have a predominant role.

In a study characterizing early MS plaques, 60% of phagocytes marked by EBM11 (CD68) expressed nucleoside diphosphatase activity, a microglial marker [65]. This indicates that microglia are the main phagocytes in early MS and thus play an important role in disease progression. While this study has delineated the origin of the main phagocytes in MS, very few studies have made a clear distinction between the role of yolk sac-derived microglia and monocyte-derived macrophages. This is highlighted in a study where the term 'microglia' was used to define the entire population of phagocytes in the MS demyelinating lesion [66]. Therefore, there is a need for future research to clearly distinguish the contribution of lipid droplets in microglia and macrophages to MS pathology.

Given the prevalence of foamy phagocytes in MS pathology, researchers have characterized their regulators. One study found that Chitinase 1 (CHIT1) is mostly expressed by lipid-laden microglia/macrophages in active postmortem MS lesions [67]. CHIT1 is an enzyme that facilitates the degradation of chitin-containing pathogens. CHIT1 expression was correlated with the transition of microglia/macrophages to a more activated state and associated with foam cell differentiation. Additionally, CHIT1 cerebrospinal fluid (CSF) levels correlated positively with later disability. Together, these data suggest that CHIT1 produced by lipid-laden microglia/macrophages is a potential biomarker for disability progression in MS.

In addition, CSF levels of neurofilament light chain (NfL) were also strongly correlated with the proportion of MS patient lesions containing foamy microglia/macrophages [68]. The active lesions with foamy microglia/macrophages also had a higher proportion of axonal damage, suggesting increased neurodegeneration. Conversely, CSF NfL levels were negatively correlated with the proportions of inactive and remyelinating lesions. Together, this study suggested that the presence of foamy microglia/macrophages may be a driver of neurodegeneration, and CSF NfL could be a biomarker of foamy microglia/macrophage-driven lesion activity and disease progression in MS.

The uptake of myelin drives the formation of foamy microglia, and scavenger receptors bind to and facilitate the phagocytosis of myelin. Hendrickx et al. [69] characterized changes in the expression of the scavenger receptors CXCL16, SR-AI/II, FcyFRIII, and LRP-1 in the chronic active lesions of microglia of MS patients [69]. These microglia were defined by the expression of HLA-DR, Iba1, and CD68 [58]. The scavenger receptors were specifically upregulated in the foamy microglia at the rims of chronic active MS lesions, suggesting that they mediate early phagocytosis and the formation of foamy microglia during demyelination. The dynamics of these foamy microglia are also regulated by several players during demyelination. Using the lysolecithin mouse model of demyelination, Ma et al. [70] showed that miR-223 regulated the degradation of LDs through lipophagy in microglia. Microglia were characterized using Iba1 staining and transmission electron microscopy imaging. Specifically, miR-223 enhanced autophagy, thereby reducing LD accumulation in microglia by inhibiting cathepsin B. Together, this inhibited the formation of LLM during demyelination.

In a case of demyelination induced by ischemia, Low-Density Lipoprotein (LDL) promoted lipid accumulation in microglia [71]. Microglia activated by LDL were shown to

be detrimental by promoting the breakdown of the blood-brain barrier and ischemic demyelination. PLIN2, a surface marker of LDs highly expressed in lipid-laden microglia/macrophages in many demyelination diseases, helps LDs escape from degradation, which impairs the remyelination process. PLIN2 deficiency reduced inflammation signals and accelerated remyelination, providing new insight into the treatment of demyelinating disease with LDs accumulation [72]. These studies together highlight the strong correlation between key proteins expressed during the formation of LLMs and disease progression in MS.

Disrupted lipid metabolism directly affects the formation of LLMs; therefore, researchers have targeted this dysmetabolism to alter microglial profiles. A demyelinating disease characterized by LLMs and macrophages is Krabbe's disease. This disease is caused by loss-of-function mutations in galactosylceramidase, which results in neuroinflammation, demyelination, and neurodegeneration [73]. Aisenberg and colleagues showed the paramount role of microglia in Krabbe's disease [74] by demonstrating that the replacement of galactosylceramidase-mutated microglia with healthy microglia was able to attenuate disease progression in mice. This highlights the role that LLMs play in promoting neurodegeneration.

On the other hand, others have demonstrated that promoting the formation of LLMs can help prevent demyelination [55]. They treated a rodent model of inflammatory injury with UCM1341, a compound that inhibits fatty acid amide hydrolase and activates melatonin receptors. These targets have been previously shown to have potential for treating neuroinflammation-driven neuropathological states. UCM1341 stimulated the formation of lipid-laden microglia/macrophages and attenuated demyelination. The protective role of LDs was also demonstrated by the identification of *TREM2* as a key mediator of LD formation expressed in microglia and macrophages. The loss of *TREM2* led to a disruption in LD formation, increased ER stress, and reduced remyelination [75]. This study indicated that microglia/macrophages clear the excess lipid from myelin breakdown by generating LDs in a *TREM2*-dependent way, which is a necessary process.

Overall, lipid-laden microglia/macrophages are a key defining feature of demyelinating lesions. They have cholesterol-rich LDs from the phagocytosis of myelin and are initially beneficial for disease recovery through the clearance of damaged myelin. However, the chronic presence of foamy microglia/macrophages is linked to increased demyelination. Regulators of foamy phagocyte formation include enzymes (CHIT1), scavenger receptors (CXCL16), and microRNAs (miR-223). The expression of some of these markers in the CSF has been used as a biomarker for disease progression. A key deficit in the field of demyelination is the lack of a functional distinction between lipid-laden microglia and macrophages. Common markers that are widely used include Cx3CR1 and Iba1, which are unable to differentiate between microglia and macrophages. Future studies could address this by incorporating microglia-specific deletion of lipid metabolic genes and microglia-specific markers such as P2Y purinoceptor 12 (P2RY12).

6. Lipid-Laden Microglia in CNS Injury

Central Nervous System (CNS) injury refers to an insult to the brain or spinal cord that results in neuronal dysfunction and disability. As the resident immune cells of the brain, microglia represent one of the first responders to CNS injury. Here, we summarize the role of LLM in spinal cord injury and traumatic brain injury, the two most studied CNS injuries in the literature.

6.1. Spinal Cord Injury

Spinal Cord Injury (SCI) affects millions worldwide and has devastating consequences, including impaired motor and nerve function, chronic pain, and severely reduced quality of life [76]. The pathology of SCI includes necrotic cell death, the accumulation of myelin debris, the activation of microglia, and the infiltration of macrophages [77,78]. The spinal cord is a part of the CNS composed of long, parallel neuronal axons wrapped with myelin [77]. SCI results in damage to myelin, which is subsequently cleared by resident microglia and macrophages to attenuate neuroinflammation. The phagocytosis of cholesterol-rich myelin results in the formation of LDs and the induction of the foamy microglial/macrophage state. The accumulation of LDs in microglia is a prevalent feature of SCI [78]. The presence of LDs in microglia during SCI has been characterized utilizing CARS microscopy, a technique that is superior for visualizing myelin and lipid bodies in biological tissue [77]. Using this technique in a rat model of SCI, LLMs were successfully detected in inflammatory SCI lesions.

Recently, work has been carried out to characterize the regulators of microglial LDs in SCI. Ou et al. [78] utilized the hemicontusion SCI model established by using an impactor tip to form a contusion at the C5 lamina in the mouse spinal cord. Using TEM coupled with TMEM119 as the marker to specifically label microglia, they identified that LDs were predominantly accumulated in microglia in the epicenter of the injury. RNA sequencing of the injured spinal cord revealed a significant upregulation in pathways such as microglial cell activation, phagocytosis, and lipid homeostasis. ATP-binding cassette transporter A1 (ABCA1) was one of the most significantly upregulated genes involved in lipid metabolism. Interestingly, a unique axis between microRNA-223 (miR-223) and ABCA1 was identified as a regulator of microglial LDs [78]. Overexpression of miR-223 promoted the expression of ABCA1 in microglia and enhanced the clearance of myelin debris and LDs. This work specifically demonstrated that the accumulation of LLMs in response to SCI is regulated in a lipid metabolism-dependent manner through ABCA1.

The glucocorticoid receptor (GR), an evolutionarily conserved nuclear steroid receptor, has also recently been implicated in the regulation of LLMs in SCI [79]. Given that glucocorticoids have anti-inflammatory properties and promote recovery after SCI, Madalena and colleagues tested the effect of depleting GR in microglia. Surprisingly, they found that the depletion of GR impaired LD accumulation and myelin phagocytosis, thus dampening the formation of foamy microglia/macrophages marked by Cx3CR1. Together, their findings suggest that GR may be an early regulator of microglial lipid-sensing and phagocytosis.

APOE has long been established as a dominant regulator of lipid metabolism during neurodegeneration. APOE is the most abundant lipoprotein in the CNS, primarily expressed by microglia and astrocytes, and plays a key role in cholesterol metabolism [80]. In SCI, APOE is a top-upregulated gene in microglia [81]. Additionally, polymorphisms in the human APOE gene are strongly associated with chronic pain in SCI [82]. Tansley et al. utilized single-cell RNA sequencing to demonstrate that APOE's regulation of lipid metabolism may directly affect microglial inflammatory functions. Specifically, following the phagocytosis of cholesterol-rich myelin debris, APOE promotes the efflux of cholesterol, which accumulates in LDs in microglia. This study showed that APOE regulation of LDs in foamy microglia can directly perturb the microglial inflammatory profile. To further assess the role of APOE in LLMs in SCI, Yao et al. [81] performed cervical spinal cord hemi-contusion on APOE-/- mice. Interestingly, APOE-/- mice demonstrated increased microglial LDs and dense lysosomal material in microglia, as visualized by transmission electron microscopy. These mutant mice also had worsened neurological dysfunction, neuroinflammation, and demyelination. These findings agree with the study by Tansley and

colleagues, which highlights *APOE* as a key regulator of microglial LDs and inflammation following SCI.

Lipophagy refers to the specific autophagic breakdown of LDs [83]. Given the active role of LLMs, which contain excessive LDs, in SCI progression and resolution, it is likely that regulators of lipophagy can impact the function of LLMs. A study by Wang and colleagues aimed to characterize the role of CD36 in microglial lipophagy [84]. CD36 is a fatty acid translocase that negatively regulates autophagy. Wang et al. [84] established a mouse model of SCI by performing laminectomy at T9-T10 vertebrae, followed by moderate compression injury. They found that microglia with excessive LDs, identified by TEM and Iba1 immunoreactivity, displayed an elevated proinflammatory response, which eventually triggered pyroptosis. These microglia also displayed an increase in the expression of CD36 and breakdown of lipophagy. Conversely, the treatment of mice with sulfo-N-succinimidyl oleate sodium, a CD36 inhibitor, enhanced lipophagy, LD degradation, and SCI recovery. Thus, CD36 regulates lipophagy in microglia following SCI by promoting the uptake of fatty acids. Additionally, Yao et al. [25] utilized a temporal ultrastructural approach to provide thorough characterizations of the molecular changes following SCI. Using this approach, they identified novel epigenetic regulators of LD accumulation in microglia. Specifically, they found that a key feature of chronic SCI was the increase in cholesterol and m6A methylation in LD-accumulating monocytes and microglia.

Taken together, these studies show that LLMs are key regulators of SCI. In addition, the research in the field thus far has shown that there are diverse regulators of the accumulation of LDs in microglia following SCI, including lipoproteins such as *APOE*, microRNAs such as miR-233, and even methylation of lipid genes.

6.2. Traumatic Brain Injury

Traumatic brain injury (TBI) occurs when an external mechanical force causes an acquired insult to the brain, leading to temporary or permanent impairment [85]. Zambusi et al. [86] found that, in postmortem cortical brain tissues from patients with TBI, microglial activation was correlated with the accumulation of LDs and TAR DNA-binding protein of 43 kDa (TDP-43+) condensates. The study investigated microglial dynamics in TBI using the zebra fish. Unlike mammals, zebra fish have extensive regenerative potential. Using a stab wound, a zebra fish TBI model was established by destroying the telencephalic hemispheres and 4C4 immunostaining was used to specifically mark microglia. In this study, they also identified a unique injury-induced microglial state characterized by the accumulation of LDs and TDP-43+ condensates, validating the results they found in humans. Interestingly, this state was transient as microglia spontaneously returned to a homeostatic state. This transition was mediated by Granulin as Granulin-deficient microglia were unable to resolve LD accumulation, prolonged microglia activation, and reduced neurogenesis. These findings also directly show that TBI induces the formation of LLMs.

Furthermore, Sridharan et al. [87] provided insights on the role of LLMs in TBI. Following TBI in a mouse model, they observed increased mitochondrial fission accompanied by increased levels of mitochondrial fission 1 protein (Fis1). Pharmacologically preventing Fis1 binding to its partner, dynamin-related protein 1 (Drp1), prevented mitochondrial impairment, microglial activation, and LD formation, which attenuated cognitive impairment and neurodegeneration. These findings suggest that in the context of TBI, LLMs may be pathological and regulated by mitochondrial energy dynamics.

Overall, in TBI, LLM represents a response to injury. This response is mediated by lipid and mitochondrial proteins. If left unmonitored, this response could lead to neurodegeneration. This indicates that, in TBI, the strict regulation of LLM is necessary for injury resolution.

7. Lipid-Laden Microglia in Glioblastoma

Glioblastoma (GBM) is the most lethal malignant brain tumor in adults, with an average survival duration of 12 to 14 months [88]. This malignancy lives within a complex tumor microenvironment, where tumor-associated microglia/macrophages (TAMs) play a central role in promoting tumor progression, immune evasion, and therapy resistance [89]. TAMs are heterogeneous populations including both resident microglia and monocyte-derived macrophages recruited from the circulation. These two cell types differ in their developmental origin, spatial localization, and immunological functions. Despite these distinctions, TAMs collectively constitute the most abundant non-neoplastic cell population in the GBM microenvironment, accounting for up to one-third of all tumor-associated cells [90]. However, challenges remain in clearly distinguishing microglia from macrophages in human GBM [89]. As a result, many studies refer to these cells collectively as TAMs and analyze them as a unified population, even though their ontological and functional roles in tumor biology are distinct.

LD accumulation is increasingly recognized as a hallmark of various diseases, including GBM. These LDs play an important role in cancer immunosuppression, drug resistance, aggressiveness, and crosstalk with other cell types in the tumor microenvironment [91]. LD-laden glioma cells augment the secretion of vascular endothelial growth factor (VEGF) and hepatocyte growth factor (HGF), which induces tumor vascularization, glioma-associated microglia/macrophage recruitment, and functional alternations [92]. These recruited microglia/macrophages subsequently undergo functional reprogramming and contribute to the establishment of a highly immunosuppressive microenvironment. This immunosuppressive state not only supports tumor progression but also impairs the efficacy of conventional therapies and correlates with poor patient prognosis [92,93].

Beyond tumor cells themselves, accumulating evidence now reveals that LD enrichment also occurs in immune cells within the GBM microenvironment, particularly in TAMs. Governa et al. [94] characterized a population of macrophages with abundant LDs in human GBM that they called tumor-associated foam cells (TAFs). These cells constitute up to 40% of the total TAM population in GBM. TAFs accumulate LDs through the uptake of extracellular vesicles released by GBM cells, which contributes to their pro-tumorigenic phenotype. Gene set enrichment analysis and immunostaining revealed that the majority of TAFs originate from bone marrow-derived monocytes, while only ~20% are resident microglia.

In parallel, Kloosterman et al. [95] identified a distinct subpopulation of lipid-laden tumor-associated macrophage (TAM), including both brain-resident microglia and infiltrating monocyte-derived macrophages, that are enriched specifically in mesenchymal-like GBM tumors. These cells exhibit an immunosuppressive phenotype marked by elevated CD39 and PD-L1 expression and reduced MHC-II levels. Functionally, they engulf myelin debris from the tumor microenvironment and export lipids to mesenchymal-like GBM cells via an LXR/ABCA1-dependent mechanism, supporting tumor metabolic demands and enhancing proliferation [95,96]. Interestingly, another study reported that the treatment of GBM with a combination of rapamycin and hydroxychloroquine induces substantial LD accumulation in TAMs [97]. Contrary to earlier findings that linked LD accumulation with impaired phagocytic capacity [6], these rapamycin and hydroxychloroquine-induced lipid-laden TAMs displayed increased phagocytosis ability and more proinflammatory phenotype. This discrepancy underscores the context-dependent nature of LD function in immune cells and highlights the need to better understand how lipid metabolism modulates microglial and macrophage behavior in the tumor setting [6,97].

Collectively, LDs play an important role in both tumor cells and TAMs in their tumor microenvironment. LDs are increasingly proposed as novel biomarkers and potential therapeutic targets, particularly in the context of immunometabolic reprogramming and

anti-inflammatory strategies for GBM. Current evidence suggests that most lipid-laden TAMs in GBM are derived from bone marrow-derived macrophages rather than resident microglia [95]. However, the line between tumor-associated microglia and tumor-associated macrophages is blurred in many studies due to the lack of a clear distinction between the two populations in brain tumors. The precise contribution of LLMs to brain tumors remains poorly defined and warrants further investigation.

8. Lipid-Laden Microglia in Obesity and Diabetes

Metabolic disorders like obesity and diabetes are increasingly recognized as not only peripheral health concerns but also systemic diseases that contribute to neurodegeneration, depression, and anxiety [98]. Clinical studies show that patients with diabetes have a two-fold higher risk of experiencing diabetes-associated cognitive impairment [99]. One study reported that obesity results in the accumulation of senescent glial cells (mostly astrocytes and microglia) in the lateral ventricle, a region critical for adult neurogenesis [100]. These cells establish the phenotype of excessive LD accumulation, termed 'accumulation of lipids in senescence' (ALISE). ALISE glial cells were associated with reduced neurogenesis and the prevalence of anxiety. Remarkably, pharmacological or genetic clearance of these senescent cells restored neurogenic potential and alleviated anxiety, which suggests a promising therapeutic avenue for neuropsychiatric disorders [100].

As a risk factor for neurodegenerative disorders, type 2 diabetes mellitus (T2DM) causes LD accumulation in microglial cells in the hippocampus but not in neurons in mice [101]. These LDs colocalized with *TREM*1—a microglia-specific inflammatory amplifier. This buildup of *TREM*1 enhanced neuroinflammation by activating the NLRP3 inflammasome, thereby exacerbating cognitive deficits in T2DM [102]. Together, these studies highlight the emerging role of LLM in mediating neuroinflammation, impaired neurogenesis, and cognitive decline in metabolic disorders such as obesity and diabetes.

9. Sex Differences and Environmental Effects

Beyond disease-associated triggers, the formation of LLMs is also influenced by biological sex and environmental exposures. Although relatively understudied, emerging evidence suggests that LLM formation exhibits sex-dependent patterns. For instance, there is a study that characterized the sex-dependent response to demyelination in microglia of progranulin-deficient mice [103]. Heterozygous mutations in the *GRN* gene lead to haploinsufficiency of progranulin, which is one of the most common genetic causes of frontotemporal lobar degeneration (FTLD). In male mice, progranulin-deficient microglia accumulate LDs and lipofuscin, increase ROS, and decrease mitochondrial respiration, but these mechanisms are not observed in female mice [103]. These sex-dependent alterations are also consistent with the postmortem analysis of FTLD patients with *GRN* mutations, though the underlying molecular mechanisms remain unclear [103].

Lee et al. [104] further reported that in their tauopathy mouse models, circadian nuclear receptor REV-ERB α depletion in microglia reduced tau uptake, upregulated inflammatory signaling, impaired lipid metabolism, and caused LD accumulation in microglia. This was observed in male mice but not in female mice [104]. Similarly, another study showed that Atg5-mediated autophagy prevents excessive LD accumulation in microglia during AD-related stress, with a notable sex difference [105]. In this case, however, loss of Atg5 in microglia in response to A β stimulation enhanced LD accumulation and activation more in female mice than in male mice, suggesting that both autophagic regulation and sex play key roles in modulating microglial lipid homeostasis [105].

Environmental exposures can also lead to LLM formation. Lead pollution, a world-wide public health issue, is associated with neurodegenerative diseases, among others. A

recent study showed that lead exposure also disrupts microglial lipid metabolism by damaging lipophagy, which induces LD accumulation, and fatty acid oxidation in microglia [106].

Collectively, these studies suggest that LLM formation is not only the consequence of disease triggers but also affected by intrinsic and extrinsic factors like sex and environmental toxins. These variables should also be considered in future studies in this field.

10. Conclusions

In conclusion, as the resident immune cells of CNS, microglia can undergo profound metabolic and functional reprogramming under stress, resulting in the accumulation of intracellular LDs and the formation of LLM. LLM represent a dynamic and multifaceted cellular phenotype that arises across a wide spectrum of physiological and pathological contexts—from aging and neurodegeneration to brain tumors, metabolic dysfunction, injury, sex difference, and environmental exposures. As an emerging hallmark of neuron inflammation, unresolved LLMs are frequently associated with dysfunctional phagocytosis, heightened proinflammatory signaling, and disease progression in various neurodegenerative diseases.

However, emerging evidence reveals that LD accumulation in microglia is a double-edged sword. In some acute stress conditions, such as demyelination or stroke, LLMs may play a transiently protective role, with LDs supporting neuroprotection by activating anti-inflammatory states, promoting repair mechanisms, and clearing debris. Modulating LD dynamics in microglia may therefore offer novel therapeutic strategies. Overall, current evidence suggests that the role of LD formation is dynamic and context-dependent: while moderate LD accumulation at specific stages can be protective, impaired clearance leading to chronic, excessive LD buildup can drive microglial dysfunction.

Additionally, advancements in both label-dependent and label-free imaging technologies have greatly enhanced our ability to track and study LLMs, offering new insight into their dynamics, distribution, and cross-talk with other cells in the CNS. Together, these findings are reshaping our understanding of LLMs and inspiring the development of novel therapeutic strategies.

11. Future Directions

Although significant progress has been made in identifying their triggers, signaling pathways, and characteristics of LLMs by various tools, the field still lacks a unified classification framework based on nomenclature, lipid composition, origin, and functional state. Terms such as 'foamy microglia', "lipid droplet-accumulating microglia" (LDAMs), and 'lipid-laden microglia' are often used interchangeably across different disease contexts, even though these microglial subtypes frequently share similar functional impairments. A standardized and systematic nomenclature is essential for advancing the field. Moreover, the influence of sex and other extrinsic factors on LLMs remains underexplored, and more systematic investigation is needed to achieve a comprehensive understanding.

The lipid composition of LDs in LLMs may vary depending on the inducing condition. A comprehensive classification of LLM subtypes based on lipid content remains lacking, limiting our understanding of their functional heterogeneity. Another persistent challenge in the field is distinguishing LLMs and lipid-laden macrophages. Although both contribute to neurodegeneration, they differ in origin: microglia are CNS-resident immune cells derived from yolk sac progenitors, whereas macrophages are monocyte-derived and infiltrate the CNS during disease. This distinction becomes particularly blurred in conditions like GBM, where both populations coexist within the tumor microenvironment. Furthermore, many studies have focused predominantly on lipid-laden macrophages,

especially in diseases like MS. Future studies should therefore more clearly differentiate between macrophages and microglia to ensure accurate functional attribuation.

Surprisingly, LD accumulation in microglia remains poorly characterized in certain neurodegenerative diseases, such as Parkinson's disease. While lipid dysregulation in neurons has received considerable attention, it is increasingly recognized that neuronal lipid imbalance can indirectly promote LD accumulation in microglia. Future studies that focus on characterizing LDs in microglia, alongside neurons, may offer deeper insights into the mechanisms underlying neurodegeneration.

Moving forward, a deeper understanding of LLM biology could enable the development of targeted strategies to modulate microglial lipid metabolism in a context-specific manner—ultimately opening new therapeutic avenues for a broad range of disorders.

Author Contributions: Conceptualization, J.X., T.M.; writing—original draft preparation, J.X., T.M.; writing—review and editing, J.X., T.M., J.H.; All authors have read and agreed to the published version of the manuscript.

Funding: This research received no external funding.

Data Availability Statement: No new data were created or analyzed in this study.

Acknowledgments: We thank the MD Anderson Cancer Center Research Medical Library for providing editorial support. J.H. is supported by The University of Texas Rising STARs Award, the Sidney Kimmel Scholar Award, the Sontag Foundation Distinguished Scientist Award, and the Sabin Foundation. T.M. is supported by the NIA F99/K00 (1F99AG088439-01), President's Research Scholarship, John J. Kopchick Research Fellowship, Larry Deaven Ph.D. Fellowship in Biomedical Sciences, Dee S. and Patricia Osborne Endowed Scholarship in Neuroscience, Marilyn and Frederick R. Lummis, Jr., Fellowship Dean's Excellence Scholarship, and the Roberta M and Jean M Worsham Endowed Fellowship.

Conflicts of Interest: The authors declare no conflicts of interest.

References

- 1. Sunshine, H.; Iruela-Arispe, M.L. Membrane lipids and cell signaling. Curr. Opin. Lipidol. 2017, 28, 408–413. [CrossRef]
- 2. Fujimoto, T.; Parton, R.G. Not just fat: The structure and function of the lipid droplet. *Cold Spring Harb. Perspect. Biol.* **2011**, 3, a004838. [CrossRef]
- 3. Olzmann, J.A.; Carvalho, P. Dynamics and functions of lipid droplets. Nat. Rev. Mol. Cell Biol. 2019, 20, 137–155. [CrossRef]
- 4. Welte, M.A.; Gould, A.P. Lipid droplet functions beyond energy storage. *Biochim. Biophys. Acta Mol. Cell Biol. Lipids* **2017**, *1862 Pt B*, 1260–1272. [CrossRef]
- 5. Pereira-Dutra, F.S.; Teixeira, L.; Costa, M.F.d.S.; Bozza, P.T. Fat, fight, and beyond: The multiple roles of lipid droplets in infections and inflammation. *J. Leukoc. Biol.* **2019**, *106*, 563–580. [CrossRef]
- 6. Marschallinger, J.; Iram, T.; Zardeneta, M.; Lee, S.E.; Lehallier, B.; Haney, M.S.; Pluvinage, J.V.; Mathur, V.; Hahn, O.; Morgens, D.W.; et al. Lipid-droplet-accumulating microglia represent a dysfunctional and proinflammatory state in the aging brain. *Nat. Neurosci.* 2020, 23, 194–208. [CrossRef]
- 7. Alzheimer, A.; Stelzmann, R.A.; Schnitzlein, H.N.; Murtagh, F.R. An English translation of Alzheimer's 1907 paper, "Uber eine eigenartige Erkankung der Hirnrinde". *Clin. Anat.* 1995, 8, 429–431. [CrossRef]
- 8. Fowler, S.D.; Mayer, E.P.; Greenspan, P. Foam cells and atherogenesis. Ann. N. Y. Acad. Sci. 1985, 454, 79–90. [CrossRef]
- 9. Khatchadourian, A.; Bourque, S.D.; Richard, V.R.; Titorenko, V.I.; Maysinger, D. Dynamics and regulation of lipid droplet formation in lipopolysaccharide (LPS)-stimulated microglia. *Biochim. Biophys. Acta* **2012**, *1821*, 607–617. [CrossRef]
- 10. Wurm, J.; Konttinen, H.; Andressen, C.; Malm, T.; Spittau, B. Microglia Development and Maturation and Its Implications for Induction of Microglia-Like Cells from Human iPSCs. *Int. J. Mol. Sci.* **2021**, 22, 3088. [CrossRef]
- 11. Guo, S.; Wang, H.; Yin, Y. Microglia Polarization From M1 to M2 in Neurodegenerative Diseases. *Front. Aging Neurosci.* **2022**, 14, 815347. [CrossRef] [PubMed]
- 12. Paolicelli, R.C.; Sierra, A.; Stevens, B.; Tremblay, M.E.; Aguzzi, A.; Ajami, B.; Amit, I.; Audinat, E.; Bechmann, I.; Bennett, M.; et al. Microglia states and nomenclature: A field at its crossroads. *Neuron* 2022, *110*, 3458–3483. [CrossRef] [PubMed]
- 13. Grajchen, E.; Hendriks, J.J.A.; Bogie, J.F.J. The physiology of foamy phagocytes in multiple sclerosis. *Acta Neuropathol. Commun.* **2018**, *6*, 124. [CrossRef]

- 14. Yamamoto, S.; Masuda, T. Lipid in microglial biology—from material to mediator. Inflamm. Regen. 2023, 43, 38. [CrossRef]
- 15. Zhu, Y.; Choi, D.; Somanath, P.R.; Zhang, D. Lipid-Laden Macrophages in Pulmonary Diseases. Cells 2024, 13, 889. [CrossRef]
- Wei, W.; Lattau, S.S.J.; Xin, W.; Pan, Y.; Tatenhorst, L.; Zhang, L.; Graf, I.; Kuang, Y.; Zheng, X.; Hao, Z.; et al. Dynamic Brain Lipid Profiles Modulate Microglial Lipid Droplet Accumulation and Inflammation Under Ischemic Conditions in Mice. Adv. Sci. 2024, 11, e2306863. [CrossRef]
- 17. Wei, W.; Zhang, L.; Xin, W.; Pan, Y.; Tatenhorst, L.; Hao, Z.; Gerner, S.T.; Huber, S.; Juenemann, M.; Butz, M.; et al. TREM2 regulates microglial lipid droplet formation and represses post-ischemic brain injury. *Biomed. Pharmacother.* **2024**, *170*, 115962. [CrossRef]
- 18. Arbaizar-Rovirosa, M.; Pedragosa, J.; Lozano, J.J.; Casal, C.; Pol, A.; Gallizioli, M.; Planas, A.M. Aged lipid-laden microglia display impaired responses to stroke. *EMBO Mol. Med.* **2023**, *15*, e17175. [CrossRef]
- 19. van der Vliet, D.; Di, X.; Shamorkina, T.M.; Pavlovic, A.; van der Vliet, I.A.C.M.; Zeng, Y.; Macnair, W.; van Egmond, N.; Chen, J.Q.A.; van den Bosch, A.M.R.; et al. Foamy microglia link oxylipins to disease progression in multiple sclerosis. *bioRxiv* 2024. [CrossRef]
- 20. Daemen, S.; van Zandvoort, M.; Parekh, S.H.; Hesselink, M.K.C. Microscopy tools for the investigation of intracellular lipid storage and dynamics. *Mol. Metab.* **2016**, *5*, 153–163. [CrossRef]
- 21. Xu, S.; Huang, Y.; Xie, Y.; Lan, T.; Le, K.; Chen, J.; Chen, S.; Gao, S.; Xu, X.; Shen, X.; et al. Evaluation of foam cell formation in cultured macrophages: An improved method with Oil Red O staining and DiI-oxLDL uptake. *Cytotechnology* **2010**, *62*, 473–481. [CrossRef]
- 22. Zbesko, J.C.; Stokes, J.; Becktel, D.A.; Doyle, K.P. Targeting foam cell formation to improve recovery from ischemic stroke. *Neurobiol. Dis.* **2023**, *181*, 106130. [CrossRef]
- 23. Maiyo, B.K.; Loppi, S.H.; Morrison, H.W.; Doyle, K.P. Assessment and Quantification of Foam Cells and Lipid Droplet-Accumulating Microglia in Mouse Brain Tissue Using BODIPY Staining. *Bio Protoc.* **2024**, *14*, e5107. [CrossRef]
- 24. Bisht, K.; Sharma, K.P.; Lecours, C.; Sanchez, M.G.; El Hajj, H.; Milior, G.; Olmos-Alonso, A.; Gomez-Nicola, D.; Luheshi, G.; Vallieres, L.; et al. Dark microglia: A new phenotype predominantly associated with pathological states. *Glia* **2016**, *64*, 826–839. [CrossRef]
- 25. Yao, X.Q.; Chen, J.Y.; Garcia-Segura, M.E.; Wen, Z.H.; Yu, Z.H.; Huang, Z.C.; Hamel, R.; Liu, J.H.; Shen, X.; Huang, Z.P.; et al. Integrated multi-omics analysis reveals molecular changes associated with chronic lipid accumulation following contusive spinal cord injury. *Exp. Neurol.* **2024**, *380*, 114909. [CrossRef]
- 26. Kim, H.; Oh, S.; Lee, S.; Lee, K.S.; Park, Y. Recent advances in label-free imaging and quantification techniques for the study of lipid droplets in cells. *Curr. Opin. Cell Biol.* **2024**, *87*, 102342. [CrossRef]
- 27. Zhang, C. Coherent Raman scattering microscopy of lipid droplets in cells and tissues. *J. Raman Spectrosc.* **2023**, *54*, 988–1000. [CrossRef]
- 28. Xie, B.; Njoroge, W.; Dowling, L.M.; Sule-Suso, J.; Cinque, G.; Yang, Y. Detection of lipid efflux from foam cell models using a label-free infrared method. *Analyst* **2022**, *147*, 5372–5385. [CrossRef]
- 29. Cao, C.; Zhou, D.; Chen, T.; Streets, A.M.; Huang, Y. Label-Free Digital Quantification of Lipid Droplets in Single Cells by Stimulated Raman Microscopy on a Microfluidic Platform. *Anal. Chem.* **2016**, *88*, 4931–4939. [CrossRef]
- 30. Kim, K.; Lee, S.; Yoon, J.; Heo, J.; Choi, C.; Park, Y. Three-dimensional label-free imaging and quantification of lipid droplets in live hepatocytes. *Sci. Rep.* **2016**, *6*, 36815. [CrossRef]
- 31. Jo, Y.; Cho, H.; Park, W.S.; Kim, G.; Ryu, D.; Kim, Y.S.; Lee, M.; Park, S.; Lee, M.J.; Joo, H.; et al. Label-free multiplexed microtomography of endogenous subcellular dynamics using generalizable deep learning. *Nat. Cell Biol.* **2021**, 23, 1329–1337. [CrossRef]
- 32. Yu, Y.; Ramachandran, P.V.; Wang, M.C. Shedding new light on lipid functions with CARS and SRS microscopy. *Biochim. Biophys. Acta* **2014**, *1841*, 1120–1129. [CrossRef]
- 33. Hou, Y.; Dan, X.; Babbar, M.; Wei, Y.; Hasselbalch, S.G.; Croteau, D.L.; Bohr, V.A. Ageing as a risk factor for neurodegenerative disease. *Nat. Rev. Neurol.* **2019**, *15*, 565–581. [CrossRef]
- 34. Li, X.; Li, Y.; Jin, Y.; Zhang, Y.; Wu, J.; Xu, Z.; Huang, Y.; Cai, L.; Gao, S.; Liu, T.; et al. Transcriptional and epigenetic decoding of the microglial aging process. *Nat. Aging* **2023**, *3*, 1288–1311. [CrossRef]
- 35. Shimabukuro, M.K.; Langhi, L.G.; Cordeiro, I.; Brito, J.M.; Batista, C.M.; Mattson, M.P.; Mello Coelho, V. Lipid-laden cells differentially distributed in the aging brain are functionally active and correspond to distinct phenotypes. *Sci. Rep.* **2016**, *6*, 23795. [CrossRef]
- 36. Abou Assale, T.; Afrang, N.; Wissfeld, J.; Cuevas-Rios, G.; Klaus, C.; Linnartz-Gerlach, B.; Neumann, H. Neuroprotective role of sialic-acid-binding immunoglobulin-like lectin-11 in humanized transgenic mice. *Front. Neurosci.* **2024**, *18*, 1504765. [CrossRef]
- 37. Uranga, R.M.; Bruce-Keller, A.J.; Morrison, C.D.; Fernandez-Kim, S.O.; Ebenezer, P.J.; Zhang, L.; Dasuri, K.; Keller, J.N. Intersection between metabolic dysfunction, high fat diet consumption, and brain aging. *J. Neurochem.* **2010**, *114*, 344–361. [CrossRef]

- 38. Zhuang, H.; Yao, X.; Li, H.; Li, Q.; Yang, C.; Wang, C.; Xu, D.; Xiao, Y.; Gao, Y.; Gao, J.; et al. Long-term high-fat diet consumption by mice throughout adulthood induces neurobehavioral alterations and hippocampal neuronal remodeling accompanied by augmented microglial lipid accumulation. *Brain Behav. Immun.* 2022, 100, 155–171. [CrossRef]
- 39. Loving, B.A.; Tang, M.; Neal, M.C.; Gorkhali, S.; Murphy, R.; Eckel, R.H.; Bruce, K.D. Lipoprotein Lipase Regulates Microglial Lipid Droplet Accumulation. *Cells* **2021**, *10*, 198. [CrossRef]
- 40. Burgunder, J.M. Neurodegeneration. IUBMB Life 2003, 55, 291. [CrossRef]
- 41. Colonna, M.; Butovsky, O. Microglia Function in the Central Nervous System During Health and Neurodegeneration. *Annu. Rev. Immunol.* **2017**, *35*, 441–468. [CrossRef]
- 42. Better M, A. 2024 Alzheimer's disease facts and figures. Alzheimers Dement. 2024, 20, 3708–3821. [CrossRef]
- 43. Lane, C.A.; Hardy, J.; Schott, J.M. Alzheimer's disease. Eur. J. Neurol. 2018, 25, 59–70. [CrossRef]
- 44. Haney, M.S.; Palovics, R.; Munson, C.N.; Long, C.; Johansson, P.K.; Yip, O.; Dong, W.; Rawat, E.; West, E.; Schlachetzki, J.C.M.; et al. APOE4/4 is linked to damaging lipid droplets in Alzheimer's disease microglia. *Nature* **2024**, *628*, 154–161. [CrossRef]
- 45. Jansen, W.J.; Ossenkoppele, R.; Knol, D.L.; Tijms, B.M.; Scheltens, P.; Verhey, F.R.; Visser, P.J.; Amyloid Biomarker Study, G.; Aalten, P.; Aarsland, D.; et al. Prevalence of cerebral amyloid pathology in persons without dementia: A meta-analysis. *JAMA* 2015, 313, 1924–1938. [CrossRef]
- 46. Jiang, T.; Tan, L.; Zhu, X.C.; Zhang, Q.Q.; Cao, L.; Tan, M.S.; Gu, L.Z.; Wang, H.F.; Ding, Z.Z.; Zhang, Y.D.; et al. Upregulation of TREM2 ameliorates neuropathology and rescues spatial cognitive impairment in a transgenic mouse model of Alzheimer's disease. *Neuropsychopharmacology* **2014**, *39*, 2949–2962. [CrossRef]
- 47. Keren-Shaul, H.; Spinrad, A.; Weiner, A.; Matcovitch-Natan, O.; Dvir-Szternfeld, R.; Ulland, T.K.; David, E.; Baruch, K.; Lara-Astaiso, D.; Toth, B.; et al. A Unique Microglia Type Associated with Restricting Development of Alzheimer's Disease. *Cell* 2017, 169, 1276–1290.E17. [CrossRef]
- 48. Jonsson, T.; Stefansson, H.; Steinberg, S.; Jonsdottir, I.; Jonsson, P.V.; Snaedal, J.; Bjornsson, S.; Huttenlocher, J.; Levey, A.I.; Lah, J.J.; et al. Variant of TREM2 associated with the risk of Alzheimer's disease. N. Engl. J. Med. 2013, 368, 107–116. [CrossRef]
- 49. Prakash, P.; Manchanda, P.; Paouri, E.; Bisht, K.; Sharma, K.; Rajpoot, J.; Wendt, V.; Hossain, A.; Wijewardhane, P.R.; Randolph, C.E.; et al. Amyloid-beta induces lipid droplet-mediated microglial dysfunction via the enzyme DGAT2 in Alzheimer's disease. *Immunity* 2025, 58, 1536–1552.E8. [CrossRef]
- 50. Wu, L.; Zhao, Y.; Gong, X.; Liang, Z.; Yu, J.; Wang, J.; Zhang, Y.; Wang, X.; Shu, X.; Bao, J. Intermittent Fasting Ameliorates beta-Amyloid Deposition and Cognitive Impairment Accompanied by Decreased Lipid Droplet Aggregation Within Microglia in an Alzheimer's Disease Model. *Mol. Nutr. Food Res.* 2025, 69, e202400660. [CrossRef]
- 51. Sha, X.; Lin, J.; Wu, K.; Lu, J.; Yu, Z. The TRPV1-PKM2-SREBP1 axis maintains microglial lipid homeostasis in Alzheimer's disease. *Cell Death Dis.* **2025**, *16*, 14. [CrossRef]
- 52. Gedam, M.; Comerota, M.M.; Propson, N.E.; Chen, T.; Jin, F.; Wang, M.C.; Zheng, H. Complement C3aR depletion reverses HIF-1alpha-induced metabolic impairment and enhances microglial response to Abeta pathology. *J. Clin. Invest.* **2023**, 133, e167501. [CrossRef]
- 53. Li, N.; Wang, X.; Lin, R.; Yang, F.; Chang, H.C.; Gu, X.; Shu, J.; Liu, G.; Yu, Y.; Wei, W.; et al. ANGPTL4-mediated microglial lipid droplet accumulation: Bridging Alzheimer's disease and obesity. *Neurobiol. Dis.* **2024**, 203, 106741. [CrossRef]
- 54. Victor, M.B.; Leary, N.; Luna, X.; Meharena, H.S.; Scannail, A.N.; Bozzelli, P.L.; Samaan, G.; Murdock, M.H.; von Maydell, D.; Effenberger, A.H.; et al. Lipid accumulation induced by APOE4 impairs microglial surveillance of neuronal-network activity. *Cell Stem Cell* 2022, 29, 1197–1212.E8. [CrossRef]
- 55. Cammarota, M.; Ferlenghi, F.; Vacondio, F.; Vincenzi, F.; Varani, K.; Bedini, A.; Rivara, S.; Mor, M.; Boscia, F. Combined targeting of fatty acid amide hydrolase and melatonin receptors promotes neuroprotection and stimulates inflammation resolution in rats. *Br. J. Pharmacol.* **2023**, *180*, 1316–1338. [CrossRef]
- 56. Comerota, M.M.; Gedam, M.; Xiong, W.; Jin, F.; Deng, L.; Wang, M.C.; Wang, J.; Zheng, H. Oleoylethanolamide facilitates PPARalpha and TFEB signaling and attenuates Abeta pathology in a mouse model of Alzheimer's disease. *Mol. Neurodegener.* **2023**, *18*, 56. [CrossRef]
- 57. Kovacs, G.G. Tauopathies. Handb. Clin. Neurol. 2017, 145, 355–368. [CrossRef]
- 58. Li, Y.; Munoz-Mayorga, D.; Nie, Y.; Kang, N.; Tao, Y.; Lagerwall, J.; Pernaci, C.; Curtin, G.; Coufal, N.G.; Mertens, J.; et al. Microglial lipid droplet accumulation in tauopathy brain is regulated by neuronal AMPK. *Cell Metab.* **2024**, *36*, 1351–1370.E8. [CrossRef]
- 59. Hopperton, K.E.; Mohammad, D.; Trépanier, M.O.; Giuliano, V.; Bazinet, R.P. Markers of microglia in post-mortem brain samples from patients with Alzheimer's disease: A systematic review. *Mol. Psychiatry* **2018**, *23*, 177–198. [CrossRef]
- 60. Drieu, A.; Du, S.; Kipnis, M.; Bosch, M.E.; Herz, J.; Lee, C.; Jiang, H.; Manis, M.; Ulrich, J.D.; Kipnis, J.; et al. Parenchymal border macrophages regulate tau pathology and tau-mediated neurodegeneration. *Life Sci. Alliance* **2023**, *6*, e202302087. [CrossRef]

- 61. Olesova, D.; Dobesova, D.; Majerova, P.; Brumarova, R.; Kvasnicka, A.; Kouril, S.; Stevens, E.; Hanes, J.; Fialova, L.; Michalicova, A.; et al. Changes in lipid metabolism track with the progression of neurofibrillary pathology in tauopathies. *J. Neuroinflammation* **2024**, *21*, 78. [CrossRef]
- 62. Xu, Y.; Propson, N.E.; Du, S.; Xiong, W.; Zheng, H. Autophagy deficiency modulates microglial lipid homeostasis and aggravates tau pathology and spreading. *Proc. Natl. Acad. Sci. USA* **2021**, *118*, e2023418118. [CrossRef]
- 63. Poitelon, Y.; Kopec, A.M.; Belin, S. Myelin Fat Facts: An Overview of Lipids and Fatty Acid Metabolism. *Cells* **2020**, *9*, 812. [CrossRef]
- 64. Walton, C.; King, R.; Rechtman, L.; Kaye, W.; Leray, E.; Marrie, R.A.; Robertson, N.; La Rocca, N.; Uitdehaag, B.; van der Mei, I.; et al. Rising prevalence of multiple sclerosis worldwide: Insights from the Atlas of MS, third edition. *Mult. Scler.* **2020**, *26*, 1816–1821. [CrossRef]
- 65. Li, H.; Cuzner, M.L.; Newcombe, J. Microglia-derived macrophages in early multiple sclerosis plaques. *Neuropathol. Appl. Neurobiol.* **1996**, 22, 207–215. [CrossRef]
- 66. de Boer, A.; van den Bosch, A.M.R.; Mekkes, N.J.; Fransen, N.L.; Dagkesamanskaia, E.; Hoekstra, E.; Hamann, J.; Smolders, J.; Huitinga, I.; Holtman, I.R. Disentangling the heterogeneity of multiple sclerosis through identification of independent neuropathological dimensions. *Acta Neuropathol.* 2024, 147, 90. [CrossRef]
- 67. Belien, J.; Swinnen, S.; D'Hondt, R.; Verdu de Juan, L.; Dedoncker, N.; Matthys, P.; Bauer, J.; Vens, C.; Moylett, S.; Dubois, B. CHIT1 at diagnosis predicts faster disability progression and reflects early microglial activation in multiple sclerosis. *Nat. Commun.* 2024, 15, 5013. [CrossRef]
- 68. van den Bosch, A.; Fransen, N.; Mason, M.; Rozemuller, A.J.; Teunissen, C.; Smolders, J.; Huitinga, I. Neurofilament Light Chain Levels in Multiple Sclerosis Correlate With Lesions Containing Foamy Macrophages and With Acute Axonal Damage. *Neurol. Neuroimmunol. Neuroinflamm.* 2022, 9, e1154. [CrossRef]
- 69. Hendrickx, D.A.E.; van Eden, C.G.; Schuurman, K.G.; Hamann, J.; Huitinga, I. Staining of HLA-DR, Iba1 and CD68 in human microglia reveals partially overlapping expression depending on cellular morphology and pathology. *J. Neuroimmunol.* **2017**, 309, 12–22. [CrossRef]
- 70. Ma, H.; Ou, Z.L.; Alaeiilkhchi, N.; Cheng, Y.Q.; Chen, K.; Chen, J.Y.; Guo, R.Q.; He, M.Y.; Tang, S.Y.; Zhang, X.; et al. MiR-223 enhances lipophagy by suppressing CTSB in microglia following lysolecithin-induced demyelination in mice. *Lipids Health Dis.* **2024**, 23, 194. [CrossRef]
- 71. Zhou, L.Q.; Chu, Y.H.; Dong, M.H.; Yang, S.; Chen, M.; Tang, Y.; Pang, X.W.; You, Y.F.; Wu, L.J.; Wang, W.; et al. Ldl-stimulated microglial activation exacerbates ischemic white matter damage. *Brain Behav. Immun.* **2024**, *119*, 416–430. [CrossRef]
- 72. Loix, M.; Wouters, E.; Vanherle, S.; Dehairs, J.; McManaman, J.L.; Kemps, H.; Swinnen, J.V.; Haidar, M.; Bogie, J.F.J.; Hendriks, J.J.A. Perilipin-2 limits remyelination by preventing lipid droplet degradation. *Cell. Mol. Life Sci.* 2022, 79, 515. [CrossRef]
- 73. Orsini, J.J.; Escolar, M.L.; Wasserstein, M.P.; Caggana, M. Krabbe Disease. In *GeneReviews* (®); Adam, M.P., Feldman, J., Mirzaa, G.M., Pagon, R.A., Wallace, S.E., Amemiya, A., Eds.; University of Washington: Seattle, WA, USA, 1993.
- 74. Aisenberg, W.H.; O'Brien, C.A.; Sangster, M.; Yaqoob, F.; Zhang, Y.; Temsamrit, B.; Thom, S.; Gosse, L.; Chaluvadi, S.; Elfayomi, B.; et al. Direct microglia replacement reveals pathologic and therapeutic contributions of brain macrophages to a monogenic neurological disease. *Immunity* 2025, 58, 1254–1268.E9. [CrossRef]
- 75. Gouna, G.; Klose, C.; Bosch-Queralt, M.; Liu, L.; Gokce, O.; Schifferer, M.; Cantuti-Castelvetri, L.; Simons, M. TREM2-dependent lipid droplet biogenesis in phagocytes is required for remyelination. *J. Exp. Med.* **2021**, *218*, e20210227. [CrossRef]
- 76. Anjum, A.; Yazid, M.D.; Fauzi Daud, M.; Idris, J.; Ng, A.M.H.; Selvi Naicker, A.; Ismail, O.H.R.; Athi Kumar, R.K.; Lokanathan, Y. Spinal Cord Injury: Pathophysiology, Multimolecular Interactions, and Underlying Recovery Mechanisms. *Int. J. Mol. Sci.* 2020, 21, 7533. [CrossRef]
- 77. Tamosaityte, S.; Galli, R.; Uckermann, O.; Sitoci-Ficici, K.H.; Koch, M.; Later, R.; Schackert, G.; Koch, E.; Steiner, G.; Kirsch, M. Inflammation-related alterations of lipids after spinal cord injury revealed by Raman spectroscopy. *J. Biomed. Opt.* **2016**, 21, 61008. [CrossRef] [PubMed]
- 78. Ou, Z.; Cheng, Y.; Ma, H.; Chen, K.; Lin, Q.; Chen, J.; Guo, R.; Huang, Z.; Cheng, Q.; Alaeiilkhchi, N.; et al. miR-223 accelerates lipid droplets clearance in microglia following spinal cord injury by upregulating ABCA1. *J. Transl. Med.* 2024, 22, 659. [CrossRef] [PubMed]
- 79. Madalena, K.M.; Brennan, F.H.; Popovich, P.G. Genetic deletion of the glucocorticoid receptor in Cx(3)cr1(+) myeloid cells is neuroprotective and improves motor recovery after spinal cord injury. *Exp. Neurol.* **2022**, *355*, 114114. [CrossRef]
- 80. Mahley, R.W. Central Nervous System Lipoproteins: ApoE and Regulation of Cholesterol Metabolism. *Arter. Thromb. Vasc. Biol.* **2016**, *36*, 1305–1315. [CrossRef]
- 81. Yao, X.Q.; Chen, J.Y.; Yu, Z.H.; Huang, Z.C.; Hamel, R.; Zeng, Y.Q.; Huang, Z.P.; Tu, K.W.; Liu, J.H.; Lu, Y.M.; et al. Bioinformatics analysis identified apolipoprotein E as a hub gene regulating neuroinflammation in macrophages and microglia following spinal cord injury. *Front. Immunol.* 2022, *13*, 964138. [CrossRef]

- 82. Tansley, S.; Uttam, S.; Urena Guzman, A.; Yaqubi, M.; Pacis, A.; Parisien, M.; Deamond, H.; Wong, C.; Rabau, O.; Brown, N.; et al. Single-cell RNA sequencing reveals time- and sex-specific responses of mouse spinal cord microglia to peripheral nerve injury and links ApoE to chronic pain. *Nat. Commun.* **2022**, *13*, 843. [CrossRef]
- 83. Schott, M.B.; Rozeveld, C.N.; Weller, S.G.; McNiven, M.A. Lipophagy at a glance. *J. Cell Sci.* **2022**, *135*, jcs259402. [CrossRef] [PubMed]
- 84. Wang, B.N.; Du, A.Y.; Chen, X.H.; Huang, T.; Mamun, A.A.; Li, P.; Du, S.T.; Feng, Y.Z.; Jiang, L.Y.; Xu, J.; et al. Inhibition of CD36 ameliorates mouse spinal cord injury by accelerating microglial lipophagy. *Acta Pharmacol. Sin.* **2025**, *46*, 1205–1220. [CrossRef] [PubMed]
- 85. Capizzi, A.; Woo, J.; Verduzco-Gutierrez, M. Traumatic Brain Injury: An Overview of Epidemiology, Pathophysiology, and Medical Management. *Med. Clin. N. Am.* **2020**, *104*, 213–238. [CrossRef]
- 86. Zambusi, A.; Novoselc, K.T.; Hutten, S.; Kalpazidou, S.; Koupourtidou, C.; Schieweck, R.; Aschenbroich, S.; Silva, L.; Yazgili, A.S.; van Bebber, F.; et al. TDP-43 condensates and lipid droplets regulate the reactivity of microglia and regeneration after traumatic brain injury. *Nat. Neurosci.* **2022**, 25, 1608–1625. [CrossRef]
- 87. Sridharan, P.S.; Koh, Y.; Miller, E.; Hu, D.; Chakraborty, S.; Tripathi, S.J.; Kee, T.R.; Chaubey, K.; Vázquez-Rosa, E.; Barker, S.; et al. Acutely blocking excessive mitochondrial fission prevents chronic neurodegeneration after traumatic brain injury. *Cell Rep. Med.* 2024, *5*, 101715. [CrossRef]
- 88. Davis, M.E. Glioblastoma: Overview of Disease and Treatment. Clin. J. Oncol. Nurs. 2016, 20 (Suppl. 5), S2-S8. [CrossRef]
- 89. Buonfiglioli, A.; Hambardzumyan, D. Macrophages and microglia: The cerberus of glioblastoma. *Acta Neuropathol. Commun.* **2021**, *9*, 54. [CrossRef]
- 90. Choi, J.; Stradmann-Bellinghausen, B.; Yakubov, E.; Savaskan, N.E.; Regnier-Vigouroux, A. Glioblastoma cells induce differential glutamatergic gene expressions in human tumor-associated microglia/macrophages and monocyte-derived macrophages. *Cancer Biol. Ther.* 2015, 16, 1205–1213. [CrossRef] [PubMed]
- 91. Cruz, A.L.S.; Barreto, E.A.; Fazolini, N.P.B.; Viola, J.P.B.; Bozza, P.T. Lipid droplets: Platforms with multiple functions in cancer hallmarks. *Cell Death Dis.* **2020**, *11*, 105. [CrossRef]
- 92. Offer, S.; Menard, J.A.; Perez, J.E.; de Oliveira, K.G.; Indira Chandran, V.; Johansson, M.C.; Bang-Rudenstam, A.; Siesjo, P.; Ebbesson, A.; Hedenfalk, I.; et al. Extracellular lipid loading augments hypoxic paracrine signaling and promotes glioma angiogenesis and macrophage infiltration. *J. Exp. Clin. Cancer Res.* **2019**, *38*, 241. [CrossRef]
- 93. Zhang, L.; Zhou, Y.; Yang, Z.; Jiang, L.; Yan, X.; Zhu, W.; Shen, Y.; Wang, B.; Li, J.; Song, J. Lipid droplets in central nervous system and functional profiles of brain cells containing lipid droplets in various diseases. *J. Neuroinflamm.* 2025, 22, 7. [CrossRef]
- 94. Governa, V.; de Oliveira, K.G.; Bång-Rudenstam, A.; Offer, S.; Cerezo-Magaña, M.; Li, J.; Beyer, S.; Johansson, M.C.; Månsson, A.-S.; Edvardsson, C. Protumoral lipid droplet–loaded macrophages are enriched in human glioblastoma and can be therapeutically targeted.pdf. *Sci. Transl.* **2024**, *16*, eadk1168. [CrossRef] [PubMed]
- 95. Kloosterman, D.J.; Erbani, J.; Boon, M.; Farber, M.; Handgraaf, S.M.; Ando-Kuri, M.; Sanchez-Lopez, E.; Fontein, B.; Mertz, M.; Nieuwland, M.; et al. Macrophage-mediated myelin recycling fuels brain cancer malignancy. *Cell* **2024**, *187*, 5336–5356.E30. [CrossRef] [PubMed]
- 96. Pang, L.; Zhou, F.; Chen, P. Lipid-Laden Macrophages Recycle Myelin to Feed Glioblastoma. *Cancer Res.* **2024**, *84*, 3712–3714. [CrossRef]
- 97. Hsu, S.P.C.; Chen, Y.C.; Chiang, H.C.; Huang, Y.C.; Huang, C.C.; Wang, H.E.; Wang, Y.S.; Chi, K.H. Rapamycin and hydroxychloroquine combination alters macrophage polarization and sensitizes glioblastoma to immune checkpoint inhibitors. *J. Neurooncol.* **2020**, *146*, 417–426. [CrossRef]
- 98. Grigsby, A.B.; Anderson, R.J.; Freedland, K.E.; Clouse, R.E.; Lustman, P.J. Prevalence of anxiety in adults with diabetes: A systematic review. *J. Psychosom. Res.* **2002**, *53*, 1053–1060. [CrossRef]
- 99. Hui, Y.; Xu, Z.; Li, J.; Kuang, L.; Zhong, Y.; Tang, Y.; Wei, J.; Zhou, H.; Zheng, T. Nonenzymatic function of DPP4 promotes diabetes-associated cognitive dysfunction through IGF-2R/PKA/SP1/ERp29/IP3R2 pathway-mediated impairment of Treg function and M1 microglia polarization. *Metabolism* **2023**, *138*, 155340. [CrossRef]
- 100. Ogrodnik, M.; Zhu, Y.; Langhi, L.G.P.; Tchkonia, T.; Kruger, P.; Fielder, E.; Victorelli, S.; Ruswhandi, R.A.; Giorgadze, N.; Pirtskhalava, T.; et al. Obesity-Induced Cellular Senescence Drives Anxiety and Impairs Neurogenesis. *Cell Metab.* **2019**, 29, 1061–1077.e8. [CrossRef] [PubMed]
- 101. Seferi, G.; Mjones, H.S.; Havik, M.; Reiersen, H.; Dalen, K.T.; Nordengen, K.; Morland, C. Distribution of lipid droplets in hippocampal neurons and microglia: Impact of diabetes and exercise. *Life Sci. Alliance* **2024**, 7, e202302239. [CrossRef] [PubMed]
- 102. Li, Q.; Zhao, Y.; Guo, H.; Li, Q.; Yan, C.; Li, Y.; He, S.; Wang, N.; Wang, Q. Impaired lipophagy induced-microglial lipid droplets accumulation contributes to the buildup of TREM1 in diabetes-associated cognitive impairment. *Autophagy* **2023**, *19*, 2639–2656. [CrossRef]
- 103. Zhang, T.; Feng, T.; Wu, K.; Guo, J.; Nana, A.L.; Yang, G.; Seeley, W.W.; Hu, F. Progranulin deficiency results in sex-dependent alterations in microglia in response to demyelination. *Acta Neuropathol.* 2023, 146, 97–119. [CrossRef] [PubMed]

- 104. Lee, J.; Dimitry, J.M.; Song, J.H.; Son, M.; Sheehan, P.W.; King, M.W.; Travis Tabor, G.; Goo, Y.A.; Lazar, M.A.; Petrucelli, L.; et al. Microglial REV-ERBalpha regulates inflammation and lipid droplet formation to drive tauopathy in male mice. *Nat. Commun.* 2023, 14, 5197. [CrossRef] [PubMed]
- 105. Tang, X.; Walter, E.; Wohleb, E.; Fan, Y.; Wang, C. ATG5 (autophagy related 5) in microglia controls hippocampal neurogenesis in Alzheimer disease. *Autophagy* **2024**, 20, 847–862. [CrossRef] [PubMed]
- 106. Hu, M.; Zhang, J.; Wu, J.; Su, P. Lead exposure induced lipid metabolism disorders by regulating the lipophagy process in microglia. *Environ. Sci. Pollut. Res. Int.* **2023**, *30*, 125991–126008. [CrossRef] [PubMed]

Disclaimer/Publisher's Note: The statements, opinions and data contained in all publications are solely those of the individual author(s) and contributor(s) and not of MDPI and/or the editor(s). MDPI and/or the editor(s) disclaim responsibility for any injury to people or property resulting from any ideas, methods, instructions or products referred to in the content.





Article

B10 Promotes Polarization and Pro-Resolving Functions of Bone Marrow Derived Macrophages (BMDM) Through PD-1 Activation

Takumi Memida, Guoqin Cao, Elaheh Dalir Abdolahinia, Sunniva Ruiz, Shengyuan Huang, Sahar Hassantash, Satoru Shindo, Motoki Okamoto, Shohei Yamashita, Shin Nakamura, Maiko Suzuki, Toshihisa Kawai and Xiaozhe Han *

Department of Oral Science and Translational Research, College of Dental Medicine, Nova Southeastern University, 3301 South University Drive, Fort Lauderdale, FL 33314, USA; tmemida@nova.edu (T.M.); guoqin416@163.com (G.C.); edalirab@nova.edu (E.D.A.); sruiz4@nova.edu (S.R.); dentisthsy@foxmail.com (S.H.); shassantash@outlook.com (S.H.); sshindo1@nova.edu (S.S.); mokamoto@nova.edu (M.O.); syamashi@nova.edu (S.Y.); shinnakamura06@okayama-u.ac.jp (S.N.); msuzuki@nova.edu (M.S.); tkawai@nova.edu (T.K.)

* Correspondence: xhan@nova.edu

Abstract: Regulatory B cells (B regs) are immune cells that help suppress excessive inflammatory responses by interacting with other immune components. Among them, B-10 cells are known for their strong immunoregulatory function. This study focused on how B-10 cells influence macrophage phenotype and function through the PD-1 signaling pathway. To investigate this, B-10 cells derived from mouse spleens were co-cultured with bone marrow-derived macrophages (BMDMs) from either wild-type (WT) or PD-1 knockout (PD-1 KO) mice, using both direct contact and Transwell setups. The findings indicated that direct co-culture with B-10 cells significantly promoted the polarization of macrophages towards the anti-inflammatory M2 type, characterized by increased expression of surface markers (F4/80⁺, CD206⁺, CD163⁺), higher levels of PD-1, and upregulation of M2-related genes (IL-1ra, IL-10, Arg-1, IL-6, and CCL1). These macrophages also exhibited enhanced phagocytic activity and greater secretion of specialized pro-resolving mediator (SPMs) like RvD2 and 15-epi LXA4. In contrast, these effects were reduced when B-10 cells were cultured indirectly or when PD-1 was absent. These findings suggest that B-10 cells promote anti-inflammatory macrophage activity primarily through PD-1 signaling, offering insights into potential therapeutic approaches for controlling inflammation.

Keywords: regulatory B cell; B10 cells; macrophage; PD-1; SPMs

1. Introduction

The regulatory B cells (B regs) have been studied for inhibiting excessive inflammation through immunoregulatory cytokines [1]. Notably, Interleukin-10 (IL-10) secreting B regs, termed B10 cells (B-10), exhibit pivotal roles in regulating immune responses through IL-10 production [2–4]. The previous article has shown that B-10 inhibits CD8⁺ T cell proliferation, and B-10 effector cell function can be enhanced through cognate interaction with CD4⁺ T cells via MHC classIIand CD40 [5].

Macrophages are also known to be leading players in regulating the inflammatory state [6,7]. Generally, the pro-inflammatory macrophage (M1 phenotype) features pro-inflammatory mediators production, which hold out against microbial pathogens and activate the adaptive immune response [8]. In contrast, pro-resolving macrophage (M2 phenotype) polarizes to prevent the host from excessive inflammatory response and to facilitate the tissue repair process [6]. Macrophages also contribute critically to inflammation

resolution through the phagocytic activity of neutrophils in apoptosis and the secretion of specialized pro-resolving mediators (SPMs) [9,10]. SPMs are synthesized from dietary polyunsaturated fatty acids (PUFAs) via lipoxygenase (LOX) and cyclooxygenase 1 and 2 (COX-1/2) [11] and contribute to the resolution of the inflammatory response. Emerging evidence has indicated that SPMs such as LipoxinA4 (LXA4) [12], ResolvinD1, D2 (RvD1 [13], RvD2 [14]), and ResolvinE1 (RvE1) [15] enhance the ability of the macrophage to clear apoptotic cells [16]. It is now recognized that enhancing pro-resolving function in the inflammatory microenvironment is crucial to tissue repair and regeneration [17].

We have already reported that B-10-rich CD1dhi CD5+ B cells led to a significant decrease in inflammatory response and alveolar bone loss in a murine periodontitis model [18,19]. Moreover, we have described that the adaptation of B-10 cells treated with LPS and CpG in mice was infiltrated with more B-10 cells in the periodontium, promoting anti-inflammatory responses [20]. However, it remained unclear whether and how B-10 cells play a role in the inflammatory resolution through B-10-macrophage interaction. To elucidate the interaction between B-10 and macrophages, we explored the potential ligand-receptor connection between the two cell types. Interestingly, human CD19⁺CD24⁺CD38⁺ B cells, a subset of B regs, exhibit elevated programmed cell deathligand 1 (PD-L1) expression [21]. On the other hand, programmed cell death 1 (PD-1), an immune checkpoint receptor, is expressed on regulatory T cells, B cells, dendritic cells, and macrophages and is well known for its inhibitory role in immune responses, including those related to cancer and autoimmune diseases [22,23]. Recently, it has been observed that PD-1-expressing macrophages display M2 function [24]. PD-L1/PD-1 axis represents a key ligand-receptor signaling pathway involved in negative immune regulation [25]. Thus, the crosstalk between PD-L1-expressing B-10 and PD-1-expressing macrophages may contribute to their pro-resolving functions via PD-L1/PD-1 engagement. Understanding how this pathway contributes to macrophage-mediated resolution of inflammation could provide valuable insight into the development of targeted therapies for chronic inflammatory and autoimmune diseases. In this context, B-10 cells, which produce IL-10 and express PD-L1, may be an attractive tool for cell-based immunotherapy. Thus, B-10 cell-based therapy could represent a novel and precise strategy for controlling pathological inflammation through macrophage-directed immune regulation.

In the present study, we investigated whether B-10 could potentiate macrophage proresolving function through PD-L1/PD-1 ligation. Our findings demonstrate that B-10 enhanced M2-type macrophage polarization, upregulated PD-1 expression, and pro-resolving functions such as phagocytic activity and specific SPM production. Such promotion of macrophage pro-resolving functions requires cell–cell contact, particularly via PD-1 activation.

2. Materials and Methods

2.1. Animals

Wild-type (WT) (C57BL/6) and PD-1 knockout (PD-1 KO) mice (B6.Cg-pdcd1tm1.1Shr/J) were obtained from Jackson Laboratory (Bar Harbor, ME, USA) and used in this study (6–8 weeks old). All mice were housed under specific pathogen-free conditions in cages equipped with air circulation systems. The animals were maintained at a temperature of 71 degrees Fahrenheit with $50 \pm 20\%$ relative humidity and exposed to a 14 h light and 10 h dark cycle. A standard rodent chow diet was provided. The use of laboratory animals in this study was approved by the IACUC of Nova Southeastern University.

2.2. Splenocyte Isolation and Culture

WT mice were sacrificed using a CO₂ chamber, and their spleens were harvested in cold PBS. Splenocytes were mechanically dissociated using a glass syringe plunger and metal mesh. The cell suspension was centrifuged at $300 \times g$ for 5 min at room temperature (RT). Red blood cells were lysed using ACK Lysing Buffer (Gibco, Grand Island, NY, USA), with a 5 min incubation at RT. The lysate was filtered through a 40 μ m cell strainer. After another centrifugation at $300 \times g$ for 5 min at room temperature (RT), the cell pellet was then resuspended in IMDM (Gibco, Grand Island, NY, USA) supplemented with 10% fetal bovine serum, 50 μ M 2-mercaptoethanol (Gibco, Grand Island, NY, USA). To produce IL-10 in B cells, splenocytes were treated with Porphyromonas gingivalis lipopolysaccharide (Pg. LPS) from ATCC33277 (10 μ g/mL) (InvivoGen, San Diego, CA, USA), and CpG-TLR9 ligand (10 μ M) (InvivoGen, San Diego, CA, USA). As previously described, the isolated cells were maintained with CpG and Pg.-LPS for 48 h [18,26]. After this period, the stimulated splenocytes were utilized for subsequent B-10 cell isolation.

2.3. Bone Marrow-Derived Macrophage Isolation and Culture

Mice were euthanized by CO_2 inhalation, and the tibias and femurs were removed from WT and PD-1 KO mice. Bone marrow cells were collected by flushing the femoral and tibial bones and were cultured in DMEM (Gibco, Grand Island, NY, USA) containing 10% FBS, 1% Anti-Anti, 50 μ M 2-ME (Medium A) with the addition of m-CSF (20 ng/mL, Biolegend, San Diego, CA, USA) for 2 days. After this period, the attached cells were collected as bone marrow-derived macrophages (BMDMs) and utilized for the subsequent co-culture procedure.

2.4. B-10 Culture and Isolation

B-10 cells were isolated using an established method [18]. Following the manufacturer's protocol, B regs from wild-type (WT) mice were purified with the Regulatory B Cell Isolation Kit (Miltenyi Biotec, Cambridge, MA, USA). In brief, splenocytes were cultured with CpG-TLR9 and Pg. LPS for 48 h, supplemented with 50 ng/mL phorbol 12-myristate 13-acetate (PMA) and 500 ng/mL ionomycin during the final 5 h of stimulation. The splenic single-cell suspension was incubated at 4 °C for 10 min with a biotin–antibody cocktail targeting non-B cell markers, followed by a 15-min incubation at 4 °C with antibiotin antibody-conjugated magnetic microbeads. Cells labeled with magnetic beads were removed using LD columns (Miltenyi Biotec, Bergisch Gladbach, Germany) within the QuadroMACS Separator (Miltenyi Biotec, Bergisch Gladbach, Germany). The unlabeled fraction, enriched for CD19+ cells with >99% purity, was collected.

For further purification of the B-10 cells, splenocytes depleted of non-B cell fraction were gently mixed into cold IMDM containing Regulatory B Cell Catch Reagent and harvested on ice for 5 min. The cell suspension (per 10⁷ cells) was then transferred to warm medium (37 °C) and incubated in a sealed tube at 37 °C for 45 min, with gentle agitation every 5 min to prevent cell settling. Post-incubation, cells were incubated with PE-conjugated Regulatory B Cell Detection Antibody on ice for 10 min, after which they were incubated for 15 min at 4 °C with anti-PE antibody-conjugated magnetic microbeads. Magnetically labeled cells were isolated using LS columns (Miltenyi Biotec, Bergisch Gladbach, Germany) under the QuadroMACS Separator. The collected cells, identified as B-10 cells, had a purity of >80% and were used for co-culture experiments.

2.5. Macrophage-B-10 Co-Culture

Adherent BMDMs were harvested by scraping and suspended in 10 mL of Medium A. The cell suspension was subjected to centrifugation at $300 \times g$ for 5 min, and the cells were resuspended. The cell number was determined using a hemacytometer. Naïve-B lymphocytes or B-10 were purified from mouse splenocytes as previously mentioned. BMDMs were co-cultured with either naïve-B or B-10 cells in 12 well plates, with or without Transwell (Greiner Bio-One, Kremsmünster, Austria), at a cell ratio of 1.0×10^5 BMDMs to 5.0×10^5 naïve-B or B-10 cells. Cultures were maintained at 37 °C in a 5% CO₂ atmosphere for 48 h. Additionally, PD-1 knockout (KO) BMDMs were co-cultured with naïve-B cells or B-10 under the same conditions.

2.6. Flow Cytometry

Macrophage phenotypes and expression levels of PD-1 were assessed using flow cytometry. After co-culturing BMDM, cells were washed three times with PBS to remove the unattached cells (naïve-B lymphocytes or B-10). The experiment was performed on the isolated macrophages. BMDMs were collected and transferred to a U-bottom 96-well plate, then resuspended in PBS. The cells were stained with anti-mouse F4/80-APC, CD86-PE, CD206-PE, CD163-Brilliant Violet 421, and PD-1-PE antibodies (all from BioLegend, San Diego, CA, USA) and incubated at 4 $^{\circ}$ C for 30 min. Following staining, the cell suspension was centrifuged at $450 \times g$ for 5 min, and the supernatant was removed. After resuspension in PBS, the cell pellet was analyzed with a BD LSRFortessa X-20 flow cytometer (BD Biosciences, San Jose, CA, USA). Data analysis was performed using FlowJo software version 10.9.0 (FlowJo LLC, Ashland, OR, USA). Additionally, the representative gating strategy used in this study is shown in Supplementary Figure S2.

2.7. Western Blotting

Following the co-cultivation of BMDMs and either naïve-B lymphocytes or B-10, non-adherent cells were removed by washing three times with PBS. The experiment was conducted on the isolated macrophages. BMDMs were then lysed using lysis buffer (RIPA; Invitrogen, Carlsbad, CA, USA) in the presence of a protease inhibitor cocktail (Invitrogen, Carlsbad, CA, USA), followed by centrifugation at 15,000× g for 15 min. Protein concentrations in the collected supernatant were assessed via the BCA method. (Thermo Scientific, Waltham, MA, USA). Proteins from the lysates were separated by SDS-PAGE gels and transferred onto PVDF Transfer Stacks (Invitrogen, Carlsbad, CA, USA) using iblot 3. The membrane was blocked with 5% nonfat dry milk in TBS and probed overnight at 4 °C with primary antibodies against Anti-PD-1 IgG at a dilution of 1:250 (rabbit, PA5-20350 Invitrogen, Carlsbad, CA, USA) and anti-β-actin antibody at a dilution of 1:5000 (rabbit, 13E5, Danvers, MA, USA, Cell Signaling Technology, Danvers, MA, USA) followed by incubation with HRP-conjugated secondary antibodies. After a 5 min exposure to ECL substrate, images were acquired using an Azure C400 imaging system (Azure Biosystems, Dublin, CA, USA). Representative full gels are available in Supplementary Figure S1.

2.8. Real-Time RT-PCR

After 48 h of incubation of the BMDMs with naïve-B lymphocyte or B-10, non-adherent cells were removed by washing the BMDMs three times with PBS. The experiment was performed on isolated macrophages. Total RNA was then isolated from the BMDMs using Trizol reagent (Invitrogen, Carlsbad, CA, USA) and the PureLink RNA Mini Kit (Invitrogen, Carlsbad, CA, USA), according to the manufacturer's protocol. Reverse transcription was performed using the cDNA Synthesis Kit (Verso) (Thermo Scientific, Waltham, MA,

USA). Quantitative real-time PCR was carried out using PowerUp SYBR Green Master Mix (Applied Biosystems, Foster City, CA, USA) to assess the expression of genes including II10, II1rn, $Tgf\beta$, Vegfa, II1 β , II6, Pdcd1, Arg1, Ccl1, and Alox15. Gene expression fold changes were determined using the $\Delta\Delta$ Ct method, with Gapdh as the housekeeping gene. Primer sequences used in this study are provided in Supplementary Table S1.

2.9. Phagocytosis Assay

The phagocytosis assay was performed only on macrophages after co-culture, using pHrodo Red S. aureus BioParticles Conjugate (Invitrogen, Carlsbad, CA, USA) according to the manufacturer's instructions. In brief, pHrodo BioParticles Conjugate (25 μg/mL) was added to BMDM cultures after 48 h of co-culture, followed by a 30 min incubation at 37 °C. Phagocytosis was halted by placing the plates on ice. Unbound bioparticles were removed by washing the cells with PBS. Following detachment with StemPro Accutase (Gibco, Grand Island, NY, USA), cells were collected into round-bottom polystyrene tubes (Corning, NY, USA, Corning) and analyzed by flow cytometry using a BD LSRFortessa X-20 (San Jose, CA, USA, BD Biosciences). Imaging was performed with an EVOS M5000 system (Invitrogen, Carlsbad, CA, USA). Immunofluorescence images were acquired using a fluorescence microscope at 40× magnification. For each experimental condition, six fields per sample were randomly selected. Quantification of the fluorescence signal was analyzed using Image software (version 1.54d, National Institutes of Health, Bethesda, MD, USA). A consistent threshold was applied across all images to exclude background fluorescence. The area of fluorescence-positive signals was measured and used as an index of fluorescence intensity. Approximately 200–300 cells were analyzed per condition. To ensure reproducibility, all measurements were conducted under identical image acquisition and processing settings.

2.10. LC-MS/MS-Based Lipidomics

After a 30 min incubation of BMDMs in high-glucose DMEM supplemented with HEPES and lacking phenol-red (Gibco, Grand Island, NY, USA), both culture supernatants and cells were transferred into cryovials and promptly frozen at -80 °C for later analysis.

Each 0.85 mL aliquot was mixed with 1 ng of internal standards (dissolved in 150 μL methanol), including 15(S)-HETE-d8, 14(15)-EpETrE-d11, Resolvin D2-d5, Leukotriene B4-d4, and Prostaglandin E1-d4, to enable accurate quantification and recovery assessment. The mixtures were thoroughly vortexed and subjected to the extraction of polyunsaturated fatty acid (PUFA) metabolites using C18 solid-phase columns, following established protocols [27,28]. The QTRAP7500 system was employed for mass spectrometric detection. In brief, the pre-spiked samples were loaded onto conditioned C18 cartridges, washed sequentially with 15% aqueous methanol and hexane, then dried under vacuum. Lipid mediators were eluted using 0.5 mL of methanol, evaporated under nitrogen, and the dried residue was reconstituted in 50 μL of a 1:1 solution of methanol and 25 mM ammonium acetate. Chromatographic separation was carried out on a Sciex UHPLC system equipped with a Luna C18 column (3 μ m, 2.1 imes 150 mm). A binary solvent system was used: Solvent A (methanol: water: acetonitrile = 10.85.5, v/v) and Solvent B (methanol: water: acetonitrile = 90:5:5, v/v), both containing 0.1% ammonium acetate. The gradient elution profile for Solvent B was programmed as follows: 50% (0-1 min), ramping to 80% (1-8 min), to 95% (8–15 min), and held at 95% (15–17 min), at a flow rate of 0.2 mL/min.

Eluates were directed into the QTRAP7500's electrospray ionization source operating in negative ion mode with the following parameters: Curtain Gas at 40 psi, Ion Source Gases 1 and 2 at 40 and 70 psi, respectively, temperature at $600\,^{\circ}$ C, ion spray voltage at $-2500\,$ V, and low collision gas pressure. Lipid mediators were detected using a scheduled

multiple reaction monitoring (MRM) strategy, targeting specific precursor–product ion pairs for each analyte. Collision energy (18–35 eV) and collision cell exit potentials (7–10 V) were optimized per transition.

For structural validation, Enhanced Product Ion (EPI) scans were recorded for each analyte. Chromatograms were processed using SciexOS 3.4 software. Quantification was performed based on the signal intensities of the internal standards, which served as normalization references for analyte recovery and relative abundance.

2.11. Statistical Analysis

Statistical analysis of the data was performed using Prism version 10 (GraphPad, La Jolla, CA, USA). An unpaired t-test was used to compare the differences between two independent groups. All data were presented as mean \pm standard error (SEM). The criterion for statistical significance was p < 0.05.

3. Results

3.1. B-10 Cells Induce Macrophage Polarization Towards M2 Through Direct Cell-Cell Interaction

The ability of B-10 cells to influence macrophage polarization through direct cell-cell interaction was investigated. BMDMs were cultured with B-10 using a Transwell system to assess the role of physical contact. Transwell inserts were employed to prevent direct B-cell and macrophage interactions. Four experimental groups were established: M0 macrophages alone (M0), macrophages with naïve-B cells (M0 + B), macrophages with B-10 cells separated by Transwell (Tr M0 + B-10), and macrophages with B-10 cells in direct contact (M0 + B10). After 48 h of co-culture, the proportions of M1 macrophages (F4/80+/CD86+) and M2 macrophages (F4/80+/CD206+/CD163+) were evaluated by flow cytometry across all groups. The fraction of F4/80⁺ CD86⁺ cells showed no significant changes across all conditions (Figure 1A,B). In contrast, the proportion of F4/80⁺ CD206⁺ CD163⁺ cells in the M0 + B10 group (20.5 \pm 4.93%) was markedly elevated in comparison with the M0 (1.22 \pm 0.74%) (p < 0.05, Figure 1C,D). No appreciable changes in F4/80⁺ CD206⁺ CD163⁺ triple-positive cells were detected in the Tr M0 + B-10 or M0 + B groups relative to M0 alone. Additionally, the M0 + B-10 group ($20.5 \pm 4.93\%$) exhibited a significantly higher frequency of F4/80⁺ CD206⁺ CD163⁺ cells in comparison to the Tr M0 + B-10 group (1.72 \pm 1.11%) (p < 0.05, Figure 1C,D). These results indicate that B-10 cells enhance M2 macrophage polarization through direct cell-cell contact, without influencing M1 macrophage differentiation.

3.2. B-10 Cells Upregulate PD-1 on Macrophages via Direct Cell-Cell Interaction

We evaluated whether co-culturing BMDMs with B-10 cells could enhance PD-1 expression. PD-1 expression in BMDMs was assessed using quantitative PCR (qPCR), Western blotting, and flow cytometry. No significant changes in PD-1 protein or mRNA levels were observed in the M0 + B group compared to the M0 alone group. However, flow cytometry revealed a significant increase in PD-1 surface protein expression in the M0 + B10 group (19.2 \pm 7.70) versus the M0 alone condition (p < 0.05, Figure 2A,B). Western blotting further confirmed elevated PD-1 protein levels in the M0 + B10 group (1.62 \pm 0.20) relative to the M0-only condition (p < 0.05, Figure 2C,D). Similarly, qPCR revealed a marked increase in Pdcd1 mRNA expression in the M0 + B-10 group (5.50 \pm 1.52) compared to the M0 alone group (p < 0.05, Figure 2E). In contrast, the Transwell co-culture group (Tr M0 + B-10) did not show a significant increase in PD-1 protein levels when compared with the macrophage-only group (M0). Additionally, Pdcd1 gene expression in the Tr M0 + B-10 condition was notably decreased (0.49 \pm 0.14) relative to the M0-only condition (p < 0.05, Figure 2E). Importantly, both PD-1 gene and protein levels were considerably elevated

in the M0 + B-10 group compared to the Transwell counterpart (p < 0.05, Figure 2A–E). Collectively, these results indicate that the upregulation of PD-1 in macrophages by B-10 cells requires direct intercellular contact.

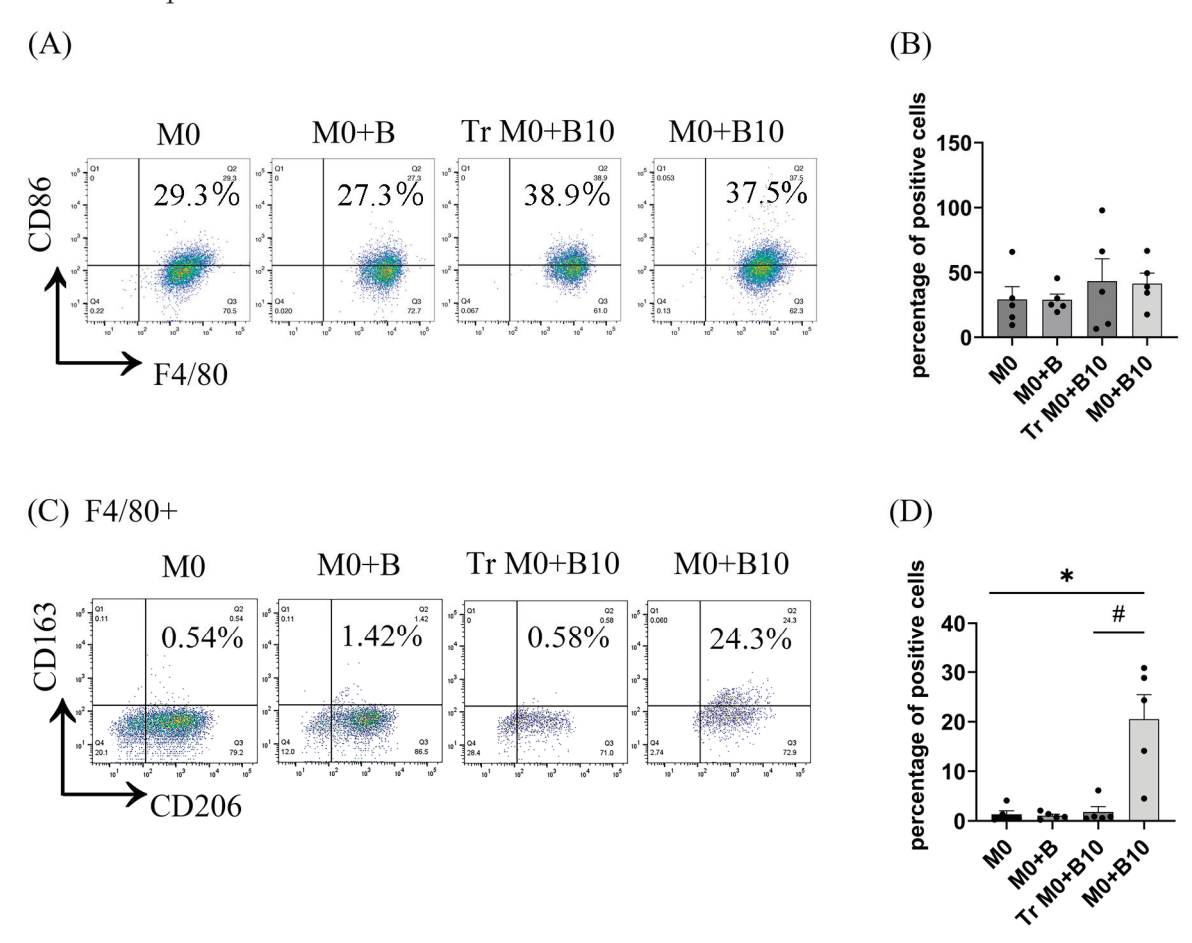


Figure 1. B-10 cells induce macrophage polarization towards M2 through direct cell–cell interaction. Bone marrow-derived macrophages (BMDMs) were harvested for 48 h with either naïve-B cells (B) or B-10 at a 1:5 ratio, either in direct contact or separated by a Transwell system (Tr). (**A,B**) The proportion of F4/80⁺ CD86⁺ cells was quantified by flow cytometry to identify the M1 phenotype. (**C,D**) The proportion of F4/80⁺ CD206⁺ CD163⁺ macrophages was evaluated by flow cytometry to identify the M2 phenotype. Experiments were independently replicated five times. Differences between groups were analyzed using an unpaired *t*-test. Data are presented as mean \pm SEM, * p < 0.05 indicates significant differences compared to M0 alone (M0 + B, Tr M0 + B10, M0 + B10), while # p < 0.05 denotes a significant difference between direct and Transwell co-culture with B10 cells. Group descriptions: M0 (macrophages cultured alone), M0 + B (macrophages with naïve-B lymphocytes), Tr M0 + B10 (macrophages with B-10 in Transwell), M0 + B10 (macrophages directly co-cultured with B-10).

3.3. B-10 Cells Enhance M2-Related Cytokines in Macrophages

Macrophages, classified into various subtypes, exhibit high plasticity and change their functional phenotypes in response to microenvironmental signals [29,30]. Notably, M2 macrophages are further subdivided into four subpopulations: M2a (IL-10⁺, IL-1ra⁺, and Arg-1⁺), M2b (IL-10⁺, CCL1⁺, IL-1 β ⁺, and IL-6⁺), M2c (IL-10⁺ and TGF- β ⁺), and M2d (IL-10⁺ and VEGF- α ⁺) [31]. As previously reported, B-10 cells promote M2 macrophage polarization through direct cell–cell contact. To explore which M2 subset-associated cytokines are upregulated in co-cultured macrophages, mRNA expression levels of *Il10* and various M2 subset markers were assessed, including *Il1rn* and *Arg1* as an M2a related marker, *Il1\beta*, *Il6*, *Ccl1* as a M2b related marker, *Tgf\beta* as a M2c related marker, and *Vegf\alpha* as a M2d related marker. No appreciable differences in cytokine expression were observed in the M0 + B

group (M0 with naïve-B lymphocytes) in comparison with the M0-only condition. In the Tr M0 + B10 group (M0 with B-10 cells separated by Transwell), Arg1 mRNA expression was significantly elevated (p < 0.05, Figure 3C). In contrast, the M0 + B10 group (M0 with B-10 cells in direct contact) exhibited significantly higher mRNA levels of Il10, Il1rn, Arg1, Il6, and Ccl1 compared to the M0 alone group (p < 0.05, p < 0.01, or p < 0.001, Figure 3A–C,E,F). Moreover, when comparing the Tr M0 + B-10 and M0 + B-10 groups, M2a related genes (Il10, Il1rn, and Arg1) and M2b related genes (Il6 and Ccl1) levels were markedly elevated in the M0 + B-10 (p < 0.05 or p < 0.001, Figure 3A–C,E,F). The present findings indicated that direct cell–cell contact was a crucial mechanism by which B-10 cells regulated the expression of M2a and M2b macrophage-related cytokines.

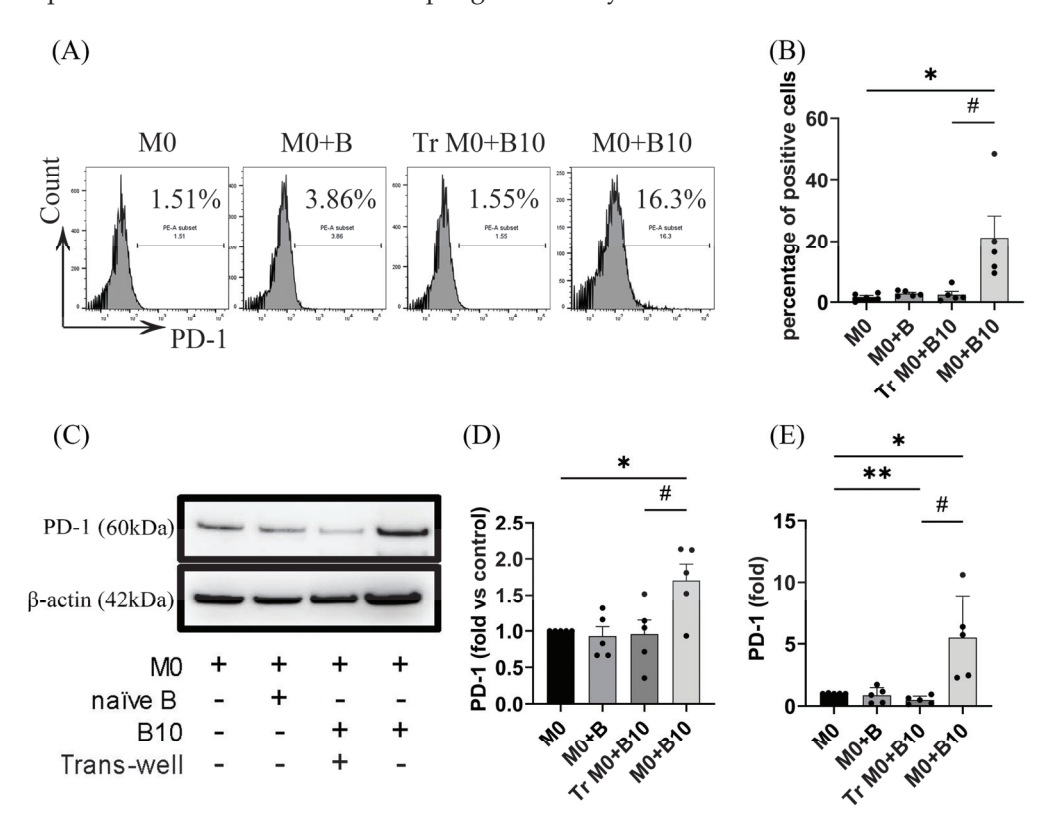


Figure 2. B-10 cells upregulate PD-1 on macrophages via direct cell–cell Interaction. Bone marrow-derived macrophages (BMDMs) were incubated with naïve-B lymphocytes (B) or B-10 (B-10) at a 1:5 ratio, either in direct contact or separated by a Transwell system (Tr), for 48 h. (**A,B**) Surface PD-1 expression on macrophages was assessed using PD-1-PE antibodies via flow cytometry. (**C,D**) PD-1 protein levels in BMDMs were quantified by immunoblotting. (**E**) *Pdcd1* gene expression in BMDMs was measured by real-time qPCR. Experiments were independently replicated five times. Group differences were evaluated using an unpaired *t*-test. Data are presented as mean value \pm SEM, * p < 0.05, ** p < 0.01 (M0 + B, Tr M0 + B-10, and M0 + B-10 compared to M0-alone respectively), # p < 0.05 (M0 + B-10 compared to Tr M0 + B-10). Group descriptions: M0 (macrophages cultured alone), M0 + B (macrophages with naïve-B lymphocytes), Tr M0 + B10 (macrophages co-cultured with B-10 cells in Transwell), M0 + B10 (macrophages directly co-cultured with B-10).

3.4. B-10 Cells Enhance Macrophage Phagocytosis Through Direct Cell-Cell Contact

Phagocytic activity, a critical pro-resolving aspect of macrophage activity, was evaluated to determine whether B-10 cells enhance this function. A phagocytosis assay was performed after co-culturing macrophages with B-10 cells. Cells were exposed to pHrodoTM Red *S. aureus* bioparticles for 30 min. Flow cytometry and immunofluorescent staining were subsequently used to assess phagocytic activity. Flow cytometry data revealed no change in the proportion of phagocytic cells in the M0 + B group. However, phagocytic activity was markedly increased in the Tr M0 + B-10 (1.20 \pm 0.15), and the M0 + B-10 (4.35 \pm 0.51)

group exhibited significantly higher phagocytic activity compared to M0 alone (0.72 ± 0.06) (p < 0.05 or p < 0.0001, Figure 4A,B). Furthermore, when comparing M0 + B-10 and Tr M0 + B-10, the M0 + B-10 group exhibited significantly higher phagocytic activity (p < 0.0001). The immunofluorescent staining results showed that the pHrodoTM bioparticles-positive cells were increased dramatically in the Tr M0 + B-10 and M0 + B-10 groups compared to the M0 alone group (p < 0.01 and p < 0.0001, Figure 4C,D). Moreover, when comparing Tr M0 + B-10 and M0 + B-10 groups, more cells were observed in the M0 + B-10 (p < 0.01, Figure 4C,D). When comparing the Tr M0 + B-10 and M0 + B-10 groups, the M0 + B-10 group displayed a higher number of positive cells (p < 0.01, Figure 4C,D). These results, supported by immunofluorescence quantification, indicate that engulfing cells were more abundant in the direct B-10 culture condition. Collectively, these results suggest that B-10 cells enhance macrophage phagocytic function, primarily through direct interaction.

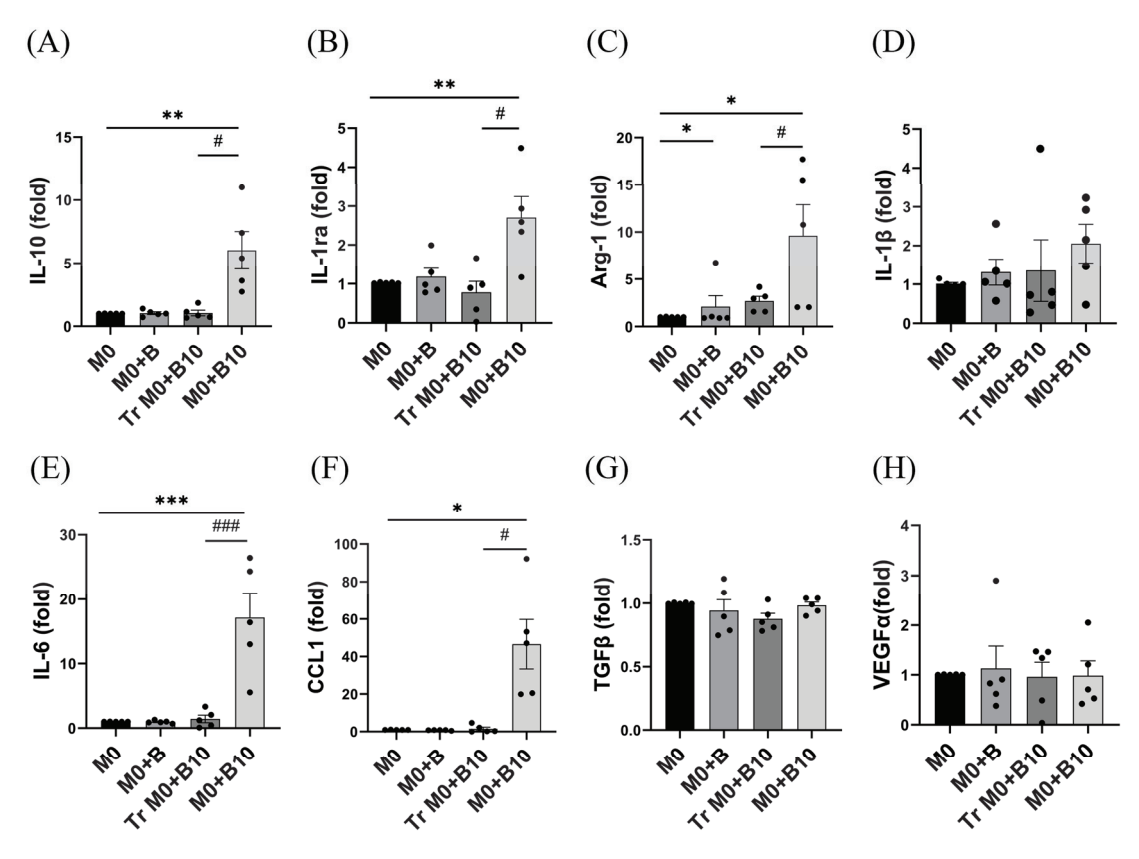


Figure 3. B-10 cells enhance M2-related cytokines in macrophages. A 48 h co-culture was conducted between BMDMs and either naïve-B lymphocytes or B-10 (1:5), using direct contact or Transwell-separated conditions. (**A–C**) Expression of M2a polarization marker (*ll10*, *ll1rn*, *Arg1*) was measured. (**D–F**) Expression of M2b-related genes (*ll1b*, *ll6*, *Ccl1*) was evaluated. (**G**) Expression of the M2c-related gene (*Tgfb*) was assessed. (**H**) Expression of the M2d-related gene (*Vegfa*) was quantified. All measurements were performed using real-time PCR. Experiments were performed independently on five separate occasions. Differences between groups were analyzed using an unpaired *t*-test. Data are presented as mean \pm SEM, * p < 0.05, *** p < 0.01, **** p < 0.001 (M0 + B, Tr M0 + B10, and M0 + B10 in comparison with the M0-only respectively), # p < 0.05, ### p < 0.001 (direct vs. Transwell co-culture). Group descriptions: M0 (macrophages cultured alone), M0 + B (macrophages with naïve-B lymphocytes), Tr M0 + B10 (macrophages with B-10 cells in Transwell), M0 + B10 (macrophages directly co-cultured with B-10 cells).

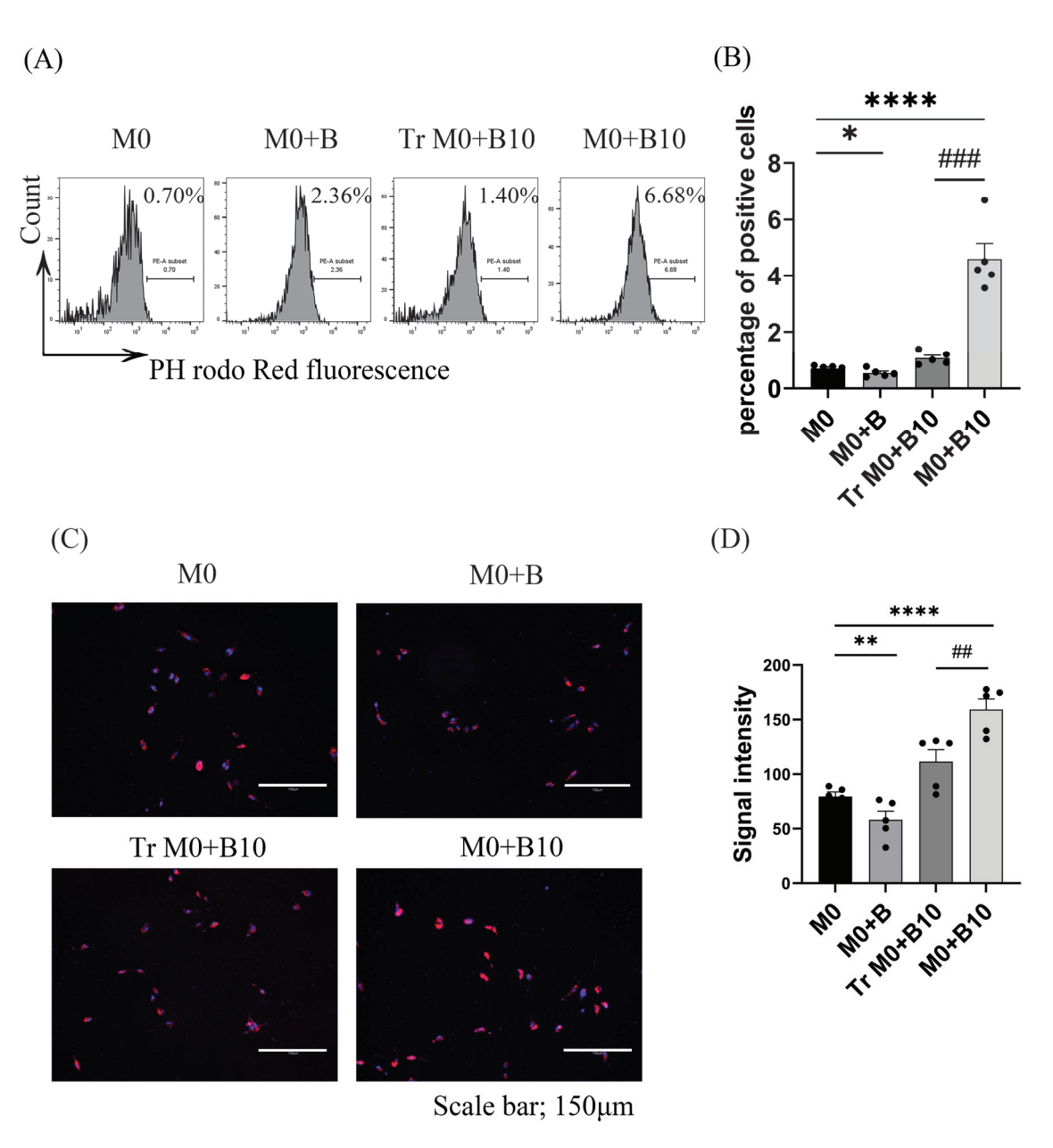


Figure 4. B-10 cells enhance macrophage phagocytosis through direct cell–cell contact. Bone marrow-derived macrophages (BMDM) were incubated with either naïve-B lymphocyte (B) or B-10 at a 1:5 ratio, either in direct contact or separated by a Transwell (Tr) system, for 48 h. Subsequently, 25 μg/mL of pH-sensitive fluorescent bioparticles was introduced into the culture medium, followed by a 30 min incubation at 37 °C. (**A**) Phagocytic cells were quantified using flow cytometry. (**B**) The proportion of pHrodoTM BioParticlesTM-positive macrophages was determined. (**C**) Representative images were captured using the EVOS M5000 imaging system. (**D**) Fluorescence intensity of the particles was measured using ImageJ software (version 1.54d). All experiments were independently replicated five times. Differences between groups were analyzed using an unpaired *t*-test. Data are presented as mean \pm SEM, * p < 0.05, ** p < 0.01, **** p < 0.001 (M0 + B, Tr M0 + B-10, and M0 + B-10 compared to M0-only respectively), ## p < 0.01, ### p < 0.001 (M0 + B-10 compared to Tr M0 + B-10). Group definitions: M0 (macrophages alone), M0 + B (M0 with naïve-B lymphocytes), Tr M0 + B10 (M0 with B-10 using Transwell), M0 + B10 (M0 with B-10 cells in direct contact).

3.5. B-10 Cells Induce M2 Macrophage Polarization from M0 Through PD-L1/PD-1 Ligation

Macrophages polarized by B-10 cells exhibited an increase in PD-1 expression and a shift towards the M2 phenotype through direct cell–cell contact. However, the specific ligand-receptor interaction involved in this process remained unclear. We then investigated

whether B-10 cells modulate the polarization of pro-resolving macrophages through PD-1 on macrophages and PD-L1 on B-10 cells. Firstly, we confirmed whether PD-1 was present in WT BMDMs and PD-1 KO BMDM. The results demonstrated that PD-1 was diminished in the PD-1 KO BMDMs (Figure 5A,B). The next experiments confirmed that PD-L1 expression on B-10 cells was enhanced by Pg.-LPS and CpG stimulation (Figure 5C,D). After 48 h of co-culture, we assessed M1 (F4/80+ CD86+) and M2 (F4/80+, CD206+, CD163+) phenotypic markers in the following groups using flow cytometry: WT M0, WT M0 + B, WT M0 + B10, PD-1 KO M0, PD-1 KO M0 + B, and PD-1 KO M0 + B10. The data revealed no consistent increase in the proportion of F4/80+ CD86+ cells in WT M0 + B or WT M0 + B10 groups versus the WT M0 condition, nor in PD-1 KO M0 + B or PD-1 KO M0 + B10 groups compared to PD-1 KO M0 alone (Figure 5E,F). While the population of F4/80⁺, CD206⁺, and CD163⁺ triple-positive cells showed no differences in WT M0 + B compared to WT M0 alone, a significant increase in F4/80+, CD206+, and CD163+ cells was observed only in the WT M0 + B10 cells group (25.63 \pm 5.18%) in comparison with the WT M0-only condition (p < 0.01, Figure 5G,H). Nonetheless, no statistically significant differences were observed in the PD-1 KO M0 + B or PD-1 KO M0 + B10 group in comparison to the PD-1 KO M0 alone group (Figure 5G,H). This suggests that the PD-L1/PD-1 axis between B-10 cells and macrophages is essential to induce M2-type macrophage polarization.

3.6. PD-1/PD-L1 Ligation Regulates the Release of Cytokines Related to Various M2 Type Macrophages

We next examined the role of PD-L1/PD-1 ligation in regulating M2-related cytokine expressions. Wild-type (WT) macrophages incubated with naïve-B cells showed no notable changes in cytokine mRNA levels in comparison to the WT M0 control. In contrast, WT BMDM cultured with B-10 displayed considerably elevated gene expression of M2a (Arg1, IL1rn, and Il10), M2b (Ccl1 and Il6) relative to the WT M0 control (p < 0.05 or p < 0.001, Figure 6A–C,E,F). Conversely, PD-1 knockout (KO) macrophages cultured with naïve-B cells exhibited a significant reduction in CCL1 mRNA levels compared to the PD-1 KO M0 control (p < 0.01, Figure 3F). In PD-1 KO macrophages cultured with B-10 cells, mRNA levels of $Tgf\beta$ and $Vegf\alpha$ were markedly reduced (p < 0.01, Figure 6G,H), whereas Il10, Il6, and Ccl1 mRNA levels were significantly elevated compared to the PD-1 KO M0 control (p < 0.05 or p < 0.01, Figure 6A,E,F). The present observations suggest the PD-L1/PD-1 interaction between B-10 cells and macrophages primarily enhances M2a-associated cytokine production, while M2b-associated cytokine expression appears unaffected by PD-L1/PD-1 signaling.

3.7. B-10 Cells Enhance Phagocytic Activity Through PD-L1/PD-1 Engagement

We explored the contribution of PD-L1/PD-1 signaling to the phagocytosis induced by B-10 in macrophages. To eliminate PD-L1/PD-1 signaling, PD-1 KO macrophages were used in the co-culture experiments. A marked increase in the proportion of phagocytic macrophages was observed in WT macrophages co-cultured with B-10 cells relative to WT M0 alone (p < 0.0001) but not under co-culture conditions of WT BMDMs and na $\ddot{\text{u}}$ elymphocytes. In contrast, co-culture of PD-1 KO BMDM with na $\ddot{\text{u}}$ elymphocytes or B-10 reduced the percentage of phagocytic cells compared to the PD-1 KO M0 control group (Figure 7A,B). These observations were further supported by imaging and quantitative analysis (p < 0.001, Figure 7C,D). Collectively, these data indicate that B-10 facilitates macrophage phagocytic ability primarily via PD-L1/PD-1 ligation.

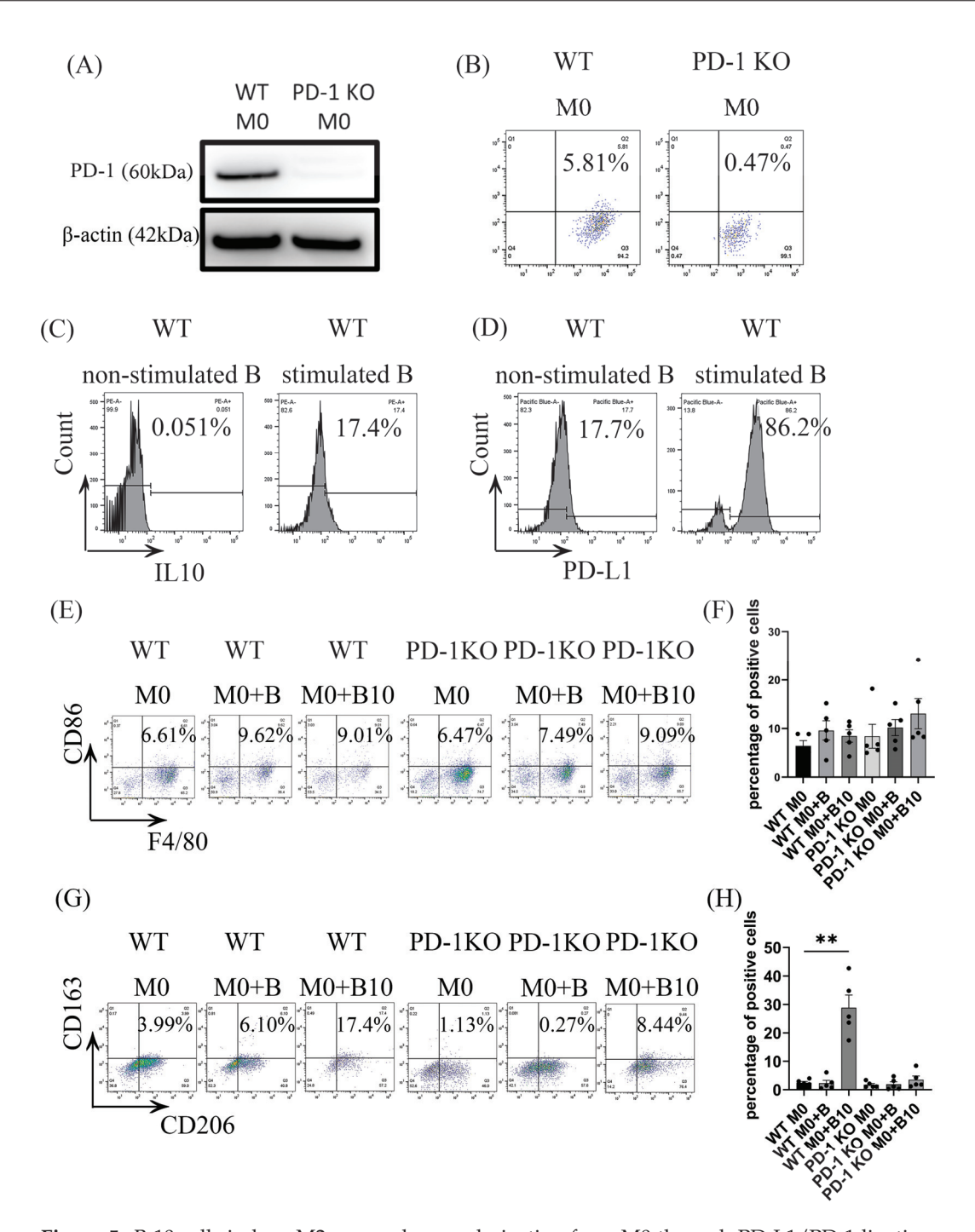


Figure 5. B-10 cells induce M2 macrophage polarization from M0 through PD-L1/PD-1 ligation. WT (C57BL/6) or PD-1 KO (B6.Cg-Pdcd1^tm1.1Shr^/J) BMDMs were cultured with B or B-10 in direct contact for 48 h. **(A)** PD-1 protein expression in WT and PD-1 KO BMDMs was quantified using Western blot analysis. **(B)** Surface PD-1 expression was assessed using flow cytometry with F4/80-APC and PD-1-PE antibodies (Q2 shows F4/80+ PD-1+ cells). **(C)** The proportion of CD19+ IL-10+ cells was measured using PE-A+ staining. **(D)** The proportion of CD19+ PD-L1+ cells was evaluated using Pacific Blue-A+ staining. **(E,F)** The proportion of F4/80+ CD86+ cells (M1 phenotype) was quantified using flow cytometry. **(G,H)** The percentage of F4/80+ CD206+ CD163+ cells (M2 phenotype) was quantified using flow cytometry. Experiments were independently replicated five times. Differences between groups were analyzed using an unpaired *t*-test. Data are presented as mean \pm SEM, ** p < 0.01 (WT M0 + B, WT M0 + B10 compared to WT M0 alone, respectively). Group definitions: WT M0 (WT macrophages alone), WT M0 + B (WT M0 with naïve-B lymphocytes), WT M0 + B10 (WT M0 with B-10), PD-1 KO M0 (PD-1 KO macrophages alone), PD-1 KO M0 + B (PD-1 KO M0 with naïve-B cells).

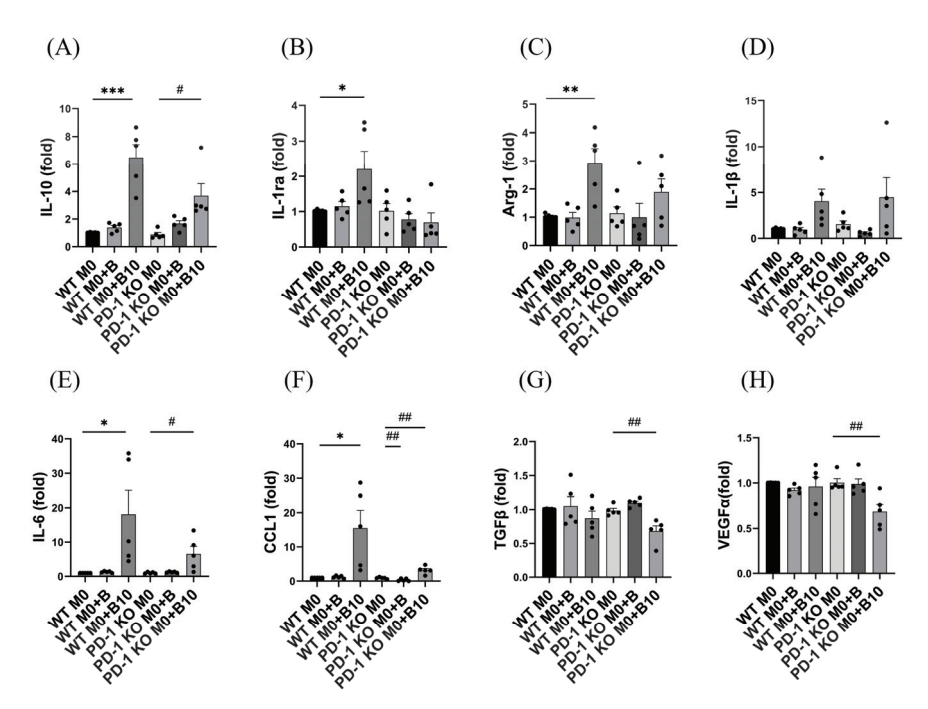


Figure 6. PD-1/PD-L1 ligation regulates the release of cytokines related to various M2-type macrophages. Bone marrow-derived macrophages (BMDMs) from wild-type C57BL/6 mice (WT M0) or PD-1 knockout mice (B6.Cg-Pdcd1tm1.1Shr/J; PD-1 KO M0) were co-cultured with naïve-B lymphocytes or B-10 for 48 h in direct contact. (**A–C**) Expression of M2a-related genes (*Il10*, *Il1rn*, *Arg1*) was quantified. (**D–F**) Expression of M2b-related genes (*Il1β*, *Il6*, *Ccl1*) was assessed. (**G**) Expression of the M2c related gene (*Tgfβ*) was evaluated. (**H**) Expression of the M2d-related gene (*Vegfα*) was measured. All measurements were performed using real-time qPCR. All experiments were conducted independently in five replicates. Differences between groups were analyzed using an unpaired *t*-test. Data are presented as mean \pm SEM, * p < 0.05, ** p < 0.01, *** p < 0.001 (WT M0 + B, WT M0 + B10 compared to WT M0 alone, respectively), # p < 0.05, ## p < 0.01 (PD-1 KO M0 + B and PD-1 KO M0 + B 10 compared to PD-1 KO M0 alone, respectively). Group definitions: WT M0 (WT macrophages alone), WT M0 + B (WT M0 with naïve-B lymphocytes), WT M0 + B10 (WT M0 with B-10 cells), PD-1 KO M0 (PD-1 KO M0 with B-10 cells).

3.8. B-10 Cells Stimulate Specialized Pro-Resolving Mediator (SPM) Synthesis via PD-L1/PD-1 Interaction

Specialized pro-resolving mediators (SPMs) are pivotal in mitigating inflammation. To assess whether B-10 cells drive SPM synthesis through PD-L1/PD-1 signaling, we analyzed lipidomics using liquid chromatography-tandem mass spectrometry (LC-MS/MS). Principal component analysis (PCA), depicted in 2D (Figure 8A) and 3D (Figure 8B) formats, revealed distinct SPM profiles between the two clusters. One cluster encompassed WT M0, WT M0 + B, PD-1 KO M0, and PD-1 KO M0 + B, while the other included WT M0 + B10 and PD-1 KO M0 + B10, with the B-10 co-culture conditions distinctly separated from others (Figure 8A,B). Heatmap analysis highlighted four SPMs—18-carboxy dinor LXB4, AT-RvD4, 15-epi LXA4, and RvD2—that were substantially higher in the presence of B-10 during co-culture compared to other groups (Figure 8C). Volcano plot analysis identified RvD2 (p < 0.05, Figure 8E,H) and 15-epi LXA4 (p < 0.05, Figure 8E,I) as dramatically upregulated in WT M0 + B-10 compared to WT M0-alone (Figure 8D-G). Notably, these elevated SPMs (RvD2 and 15-epi LXA4) were absent in PD-1 KO M0 + B and PD-1 KO M0 + B10 groups (Figure 8F,G). Furthermore, as the SPM pathway involves 15-lipoxygenase (15-LOX), we examined Alox15 gene expression. No significant changes in Alox15 mRNA levels were observed in WT M0 + B compared to WT M0 alone, but Alox15 mRNA levels showed a significant increase in WT M0 + B-10 relative to WT M0 alone (p < 0.05, Figure 8J). In contrast, no differences were detected among PD-1 KO M0, PD-1 KO M0 + B, and PD-1 KO M0 + B10 groups (Figure 8J). These findings indicate that B-10 cells promote the synthesis of RvD2 and 15-epi LXA4, as well as *Alox15* gene expression, primarily through PD-L1/PD-1 signaling.

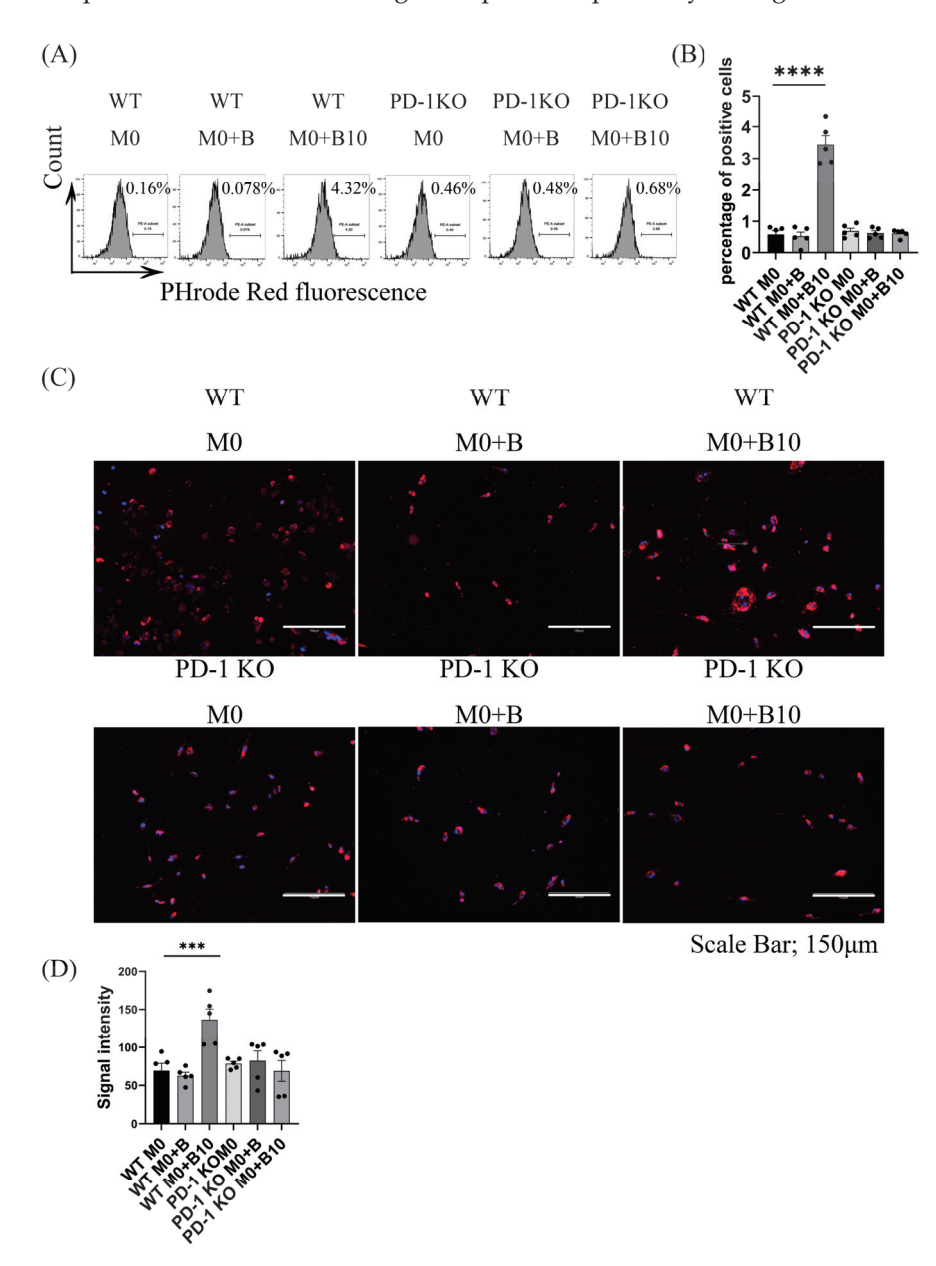


Figure 7. B-10 cells enhance phagocytic activity through PD-L1/PD-1 ligation. Bone marrow-derived macrophages (BMDMs) from wild-type C57BL/6 mice (WT M0) or PD-1 knockout mice (B6.Cg-Pdcd1^tm1.1Shr^/J; PD-1 KO M0) were co-cultured in direct contact with naïve-B lymphocytes or B-10 for 48 h. A concentration of 25 μg/mL pH-sensitive fluorescent bioparticles was applied to the culture and harvested for 30 min at 37 °C. (**A**) Phagocytic cells were evaluated using flow cytometric analysis. (**B**) The proportion of cells bearing pH-sensitive fluorescent bioparticles was determined. (**C**) Representative images were captured using the EVOS M5000 imaging system. (**D**) Fluorescence particle intensity was quantified using ImageJ software. All experiments were performed independently five times. Group differences were assessed using an unpaired *t*-test. Data are expressed as mean \pm SEM, *** p < 0.001, **** p < 0.0001 (WT M0 + B, WT M0 + B10 compared to WT M0 alone, respectively). Group designations: WT M0 (WT macrophages alone), WT M0 + B (WT macrophages with naïve-B lymphocytes), WT M0 + B10 (WT macrophages with B-10), PD-1 KO M0 (PD-1 KO macrophages with naïve-B cells), PD-1 KO M0 + B10 (PD-1 KO macrophages with B-10 cells).

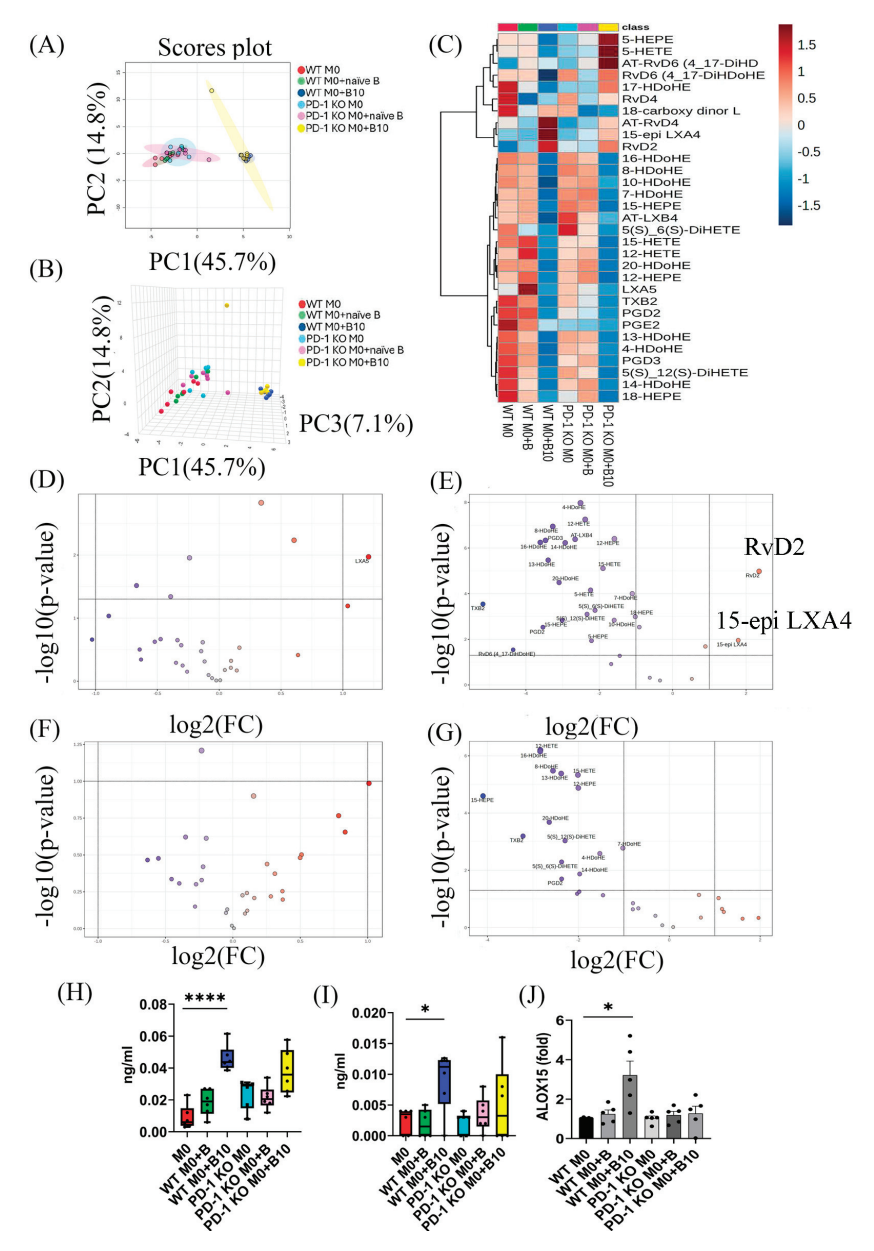


Figure 8. B-10 cells stimulate specialized pro-resolving mediator (SPM) synthesis via PD-L1/PD-1 interaction. Macrophages derived from bone marrow of wild-type C57BL/6 mice (WT M0) or PD-1 knockout mice (B6.Cg-Pdcd1tm1.1Shr/J; PD-1 KO M0) were incubated with naïve-B lymphocytes or B-10 for 48 h in direct contact. (A) Principal component analysis depicts group distinctions in 2D. (B) PCA illustrates group distinctions in 3D. Red dots represent WT M0 alone, green dots indicate WT M0 + B, blue dots signify WT M0 + B10, light blue dots denote PD-1 KO M0 alone, pink dots mark PD-1 KO M0 + B, and yellow dots indicate PD-1 KO M0 + B10. (C) Heatmap with hierarchical clustering visualizes SPM data. The color scale indicates the expression levels of SPMs, with darker colors representing higher expression. (D-G) Volcano plots combine fold change and t-tests to identify key SPM candidates. (D) WT M0 + B vs. WT M0, (E) WT M0 + B10 vs. WT M0, (F) PD-1 KO M0 + B vs. PD-1 KO M0, (G) PD-1 KO M0 + B10 vs. PD-1 KO M0. The x-axis represents log2 (fold change), and the y-axis represents -log10 (p-value). (H) Box plot quantifies RvD2 concentrations. (I) Box plot quantifies 15-epi LXA4 concentrations. (J) Expression of the Alox15 gene was quantified using real-time qPCR. Independent replication was carried out five times for each experiment. Differences between groups were analyzed using an unpaired t-test. Data are presented as mean \pm SEM, * p < 0.05, **** p < 0.0001 (WT M0 + B, WT M0 + B10 compared to WT M0 alone, respectively). Group definitions: WT M0 (WT macrophages alone), WT M0 + B (WT M0 with naïve-B lymphocytes), WT M0 + B10 (WT M0 with B-10 cells), PD-1 KO M0 (PD-1 KO macrophages alone), PD-1 KO M0 + B (PD-1 KO M0 with naïve-B cells), PD-1 KO M0 + B10 (PD-1 KO M0 with B-10 cells).

4. Discussion

The immunoregulatory role of B-10 cells is widely recognized to rely on the production of IL-10 [3,32]. Emerging research indicates that B regs regulate CD4+ T cells and T reg development through direct cell–cell interactions and cytokine-mediated pathways. Moreover, B regs have been shown to suppress CD8+ T cell expansion through specific cognate contacts [5]. These observations highlight the pivotal role of cell–cell interactions in mediating the anti-inflammatory properties of B regs. Nevertheless, the precise ligand-receptor mechanisms governing the regulatory effects of B-10 cells on macrophages remain unclear. In this study, we established that B-10 cells augment the inflammation-resolving capabilities of macrophages via PD-L1/PD-1 signaling.

To examine if a direct association between B-10 cells and macrophages is required for initiating a pro-resolving polarization state, we employed a Transwell system in co-culture experiments. Macrophages cultured in direct contact with B-10 cells exhibited increased expression of F4/80, CD206, and CD163, markers indicative of M2-type macrophages (Figure 1A–D). Furthermore, prior research has established that PD-1-expressing macrophages display M2-like surface characteristics [24]. Accordingly, we assessed PD-1 expression in macrophages. Our results revealed significantly elevated PD-1 levels in the M0 macrophage group that were co-cultured with B-10 cells (Figure 2A–E). These observations suggest that B-10 cells drive M2 macrophage polarization, marked by PD-1 expression, through direct cell–cell interactions.

In addition, in the PD-1 KO group, the percentage of M2 macrophages did not change even if co-cultured with B-10 (Figure 5A–D). Additionally, a prior study has shown that anti-PD-L1 treatment can encourage macrophages to adopt a more pro-inflammatory phenotype. Moreover, another article indicated that treating THP-1-derived macrophages with PD-L1 led to polarization toward M2-type macrophages [33]. Taken together, our results related to polarization toward M2-type macrophages align with these studies. Therefore, these findings suggest that PD-L1/PD-1 ligation between B-10 cells and macrophages plays a critical role in differentiating macrophages towards the M2 phenotype.

We then evaluated the effect of B-10 cells on M2-related macrophage cytokine expression. Macrophages are highly plastic and can change their functional phenotypes depending on microenvironmental signals. Notably, M2 macrophages are subdivided into four subpopulations: M2a, M2b, M2c, and M2d. Previous studies have shown that B-10 cells inhibit mRNA expression levels of IL-1 β and TNF- α , pro-inflammatory related cytokines [26]. In this study, IL-10 expression was significantly increased in macrophages co-cultured with B-10 cells directly, whereas this upregulation was markedly reduced when the cells were separated by a Transwell insert and in the PD-1 KO macrophage (Figures 3A and 6A). Our observation supports that direct cellular contact, especially PD-L1/PD-1 engagement, plays a more crucial role than soluble factors in promoting IL-10 production in macrophages. Although B-10 cells are known to secrete IL-10 abundantly, the finding implies that IL-10 secretion by macrophages may be selectively induced through cognitive interactions. Furthermore, the present data also showed that while Arg-1, IL-10, and IL-1ra, anti-inflammatory related cytokines, exhibited a significant increase under direct co-culture conditions with B-10 cells (Figure 3A-C), unexpectedly, IL-6, a pro-inflammatory-associated cytokine, was also expressed by macrophages after co-culture with B-10 (Figure 3E). M2b macrophages, classified as regulatory macrophages, express CCL1 and IL-10 [31]. In addition to anti-inflammatory cytokines, M2b macrophages also secrete pro-inflammatory cytokines such as IL-1 β , IL-6, and TNF- α [31,34]. M2b macrophages exhibit dual roles, contributing to both protective and pathogenic outcomes in disease contexts. Our findings suggest that IL-6 expression is associated with M2b macrophages. Furthermore, in co-cultures with PD-1 knockout (KO) macrophages, levels

of M2a-associated cytokines (IL-1ra and Arg-1) remained unchanged (Figure 6B,C), whereas M2b-related cytokines (IL-6 and CCL1) were markedly elevated (Figure 6E,F). Conversely, M2c ($TGF\beta$) and M2d ($VEGF\alpha$) cytokines were reduced (Figure 6G,H). Currently, limited data exist regarding the link between M2b macrophage differentiation and the PD-L1/PD-1 signaling pathway. Recent studies have shown that when the PD-L1/PD-1 pathway was blocked, the population of M1 macrophages and pro-inflammatory cytokines, such as IL-1 β and TNF- α , were increased [35]. However, these cytokines are expressed not only in M1 macrophages but also in M2b [31]. Furthermore, another research suggested that soluble PD-L1 secreted by trophoblast cells enhanced macrophage polarization towards the M2b phenotype, alleviating inflammation and facilitating tissue repair and tolerance [36]. Thus, PD-L1/PD-1 ligation appears necessary for the polarization toward M2a and M2b macrophages. However, our results showed that cell-cell contact could polarize macrophages to M2b, but this effect was not responsible for the PD-L1/PD-1 signaling. In this study, we demonstrated the different cytokine profile changes of M2 macrophages by using B cells. Since we utilized various co-culture systems with B cells to prevent cell-cell contact or PD-L1/PD-1 interactions, other cellular components may be involved in differentiating macrophages. Thus, these results suggested that macrophages co-cultured with B-10 cells exhibited upregulated mRNA levels of M2a, not responsible for M2b, M2c, and M2d specific genes, through PD-L1/PD-1 ligation.

Phagocytosis is recognized as a crucial mechanism in both innate and adaptive immune responses to foreign antigens, with macrophages playing a key role in promoting microbial clearance and wound debridement [37]. Recently, the function of lipid mediators (LMs) associated with the resolution of inflammation has been elucidated. These LMs, known as specialized pro-resolving mediators (SPMs), have been shown to enhance the phagocytic activity of macrophages [38]. In the current study, RvD2 and 15-epi LXA4 were identified as upregulated specific SPMs in macrophages co-cultured with B-10 cells (Figure 8C,E). Both RvD2 [39] and 15-epi LXA4 [40] are well known for their antiinflammatory and pro-resolving effects. They also stimulate macrophage phagocytosis, thereby helping to modulate excessive immune responses. The engulfing function of macrophages co-cultured with B-10 cells was markedly increased compared to other groups without Transwell or with PD-L1/PD-1 signaling (Figures 4A–D and 7A–D). These outcomes were in agreement with prior findings, which demonstrated that activation of the PD-1 pathway increased phagocytic activity [35]. In addition to direct quantification using the phagocytosis assay, the upregulation of CD163 observed in B-10-treated macrophages may further support enhanced phagocytic potential. CD163 is a well-characterized scavenger receptor involved in the uptake of apoptotic cells and hemoglobin-haptoglobin complexes, and its expression has been functionally linked to efficient clearance and inflammation resolution [41–43]. The increased levels of CD163 and the production of SPMs may indicate a coordinated transition towards pro-resolving macrophages that are capable of an efficient phagocytosis phenotype. These findings highlight a potential mechanism by which B-10 cells enhance macrophage function in the resolution phase of inflammation. Moreover, co-culturing B-10 with macrophages promoted the synthesis of RvD2 and 15-epi LXA4, which in turn activated the pro-resolving functions of macrophages. These SPMs are metabolized from DHA by 15-lipoxygenase (15-LOX). The murine enzyme 15-LOX, encoded by ALOX15, is implicated in the biosynthesis of several SPMs [44]. Previous studies have shown that the Th2 cytokines IL-4 and IL-13 are potent stimuli for the expression of 15-LOX in human monocytes [45]. As IL-4 strongly induces ALOX15 expression, 15-LOX is also recognized as an M2 macrophage marker [46]. In this study, ALOX15 gene expression in macrophages was upregulated by co-culturing with B-10 (Figure 8J). The specific SPM production (RvD2 and 15-epi LXA4) was also increased (Figure 8H,I), and phagocytic activity in macrophages was enhanced (Figures 4A–D and 7A–D). However, these results were diminished without cell–cell contact or PD-L1/PD-1 ligation. Little research has been conducted on PD-L1/PD-1 ligation and SPM production. The PD-L1/PD-1 axis is known as an immunosuppressive signal cascade, and that pathway leads to the polarization of M2-type macrophages [47]. SPMs are mainly synthesized by M2-type macrophages. Based on these results, it is suggested that B-10 cells enhanced the pro-resolving functions of macrophages, including phagocytic function and SPM secretion, through the PD-L1/PD-1 ligation.

As we described above, the reason why both M2a and M2b cytokines were upregulated was unclear. A previous study indicated that IL-10 was considered to enhance Fcy receptor expression in monocytes and increase their responsiveness to immune complexes [48]. Immune complexes are known as one of the factors that polarize M2b-type macrophages. Therefore, the possible reason is that IL-10 produced by B-10 may reflect on the production of M2b-related cytokines. However, this study did not evaluate the effects of IL-10. Moreover, the previous article suggested that, in addition to IL-10 production and PD-L1 expression, other soluble factors or costimulatory molecules might be present in the regulatory B cells, including B-10 cells [49]. Moreover, several articles have reported the existence of pro-resolution macrophages (rM) [50]. The rM possesses a hybrid phenotype of M2 or M1. These macrophages express high ALOX15 and produce pro-resolving Lipoxin [51]. Such phenotypes are similar to macrophages co-cultured with B-10 directly in this study. In addition, although the precise downstream signaling was not examined, previous studies have demonstrated that STAT3 is a common effector activated by both IL-10 and PD-1 signaling. IL-10 has been reported to induce STAT3 activation, leading to M2 polarization of macrophages [52,53]. Moreover, PD-1+ M2-like tumor-associated macrophages have been shown to exhibit STAT3-mediated immunosuppressive programming, which can be reversed by PD-L1 blockade [54]. In addition to the STAT3 pathway, recent studies have suggested that PD-1 signaling may influence macrophage function through the PI3K/Akt axis. PD-1 has been shown to recruit SHP1/2 phosphatases, suppressing the PI3K/Akt pathway, thereby promoting a proinflammatory M1-like polarization state. In a murine model of lung ischemia-reperfusion injury, the inhibition of PD-1 was reported to restore PI3K/Akt activation in alveolar macrophages, resulting in reduced M1 polarization and inflammation [55]. Although this signaling mechanism was not directly examined in the present study, it is plausible that B-10-derived PD-L1 could suppress M1 polarization of macrophages via modulation of the PI3K/Akt pathway and STAT3 activation. This hypothesis warrants further investigation to better define the intracellular signaling networks that contribute to the pro-resolving effects induced by B-10 cells. Considering our results and these findings, it remains to be determined how other regulatory molecules, in addition to IL-10 and PD-L1, affect macrophage polarization and functions by B-10 cells.

In summary, this study demonstrated that PD-L1/PD-1 engagement increased the population of PD-1+ M2 macrophages and enhanced their phagocytic activity and production of specific SPMs (RvD2 and 15-epi LXA4) in primary bone marrow-derived macrophages from mice. We reported that the interaction between Raw 264.7 cells (a mouse macrophage cell line) and B-10 polarized pro-resolving macrophages enhances pro-resolving functions through cell–cell contact and IL-10 secretion [56]. In the current study, we utilized primary bone marrow-derived macrophages. We have observed different outcomes between these two cell types. However, we consistently demonstrated how B-10 cells influence bone marrow-derived macrophages to alleviate inflammatory responses, as mentioned above. In addition, PD-L1/PD-1 ligation is an essential cell component for B-10 cells to drive the pro-resolving function on macrophages. Based on these observations, it is the potential candidate that B-10 cells, which produce IL-10 and express PD-L1, could be used as a novel immunoregulatory therapy. In particular, the ability of B-10 cells to promote macrophage

functions related to inflammation resolution may be useful for developing targeted therapies. Such cell-based approaches could be applied to control pathological inflammation in chronic inflammatory and autoimmune diseases, where immune regulation is often disrupted. Thus, a therapeutic strategy using B-10 cells may offer a precise and biologically relevant method to enhance macrophage-mediated immune resolution in the medical and dental field.

5. Conclusions

In conclusion, B-10 cells promote M2-like macrophages and enhance pro-resolving functions, such as phagocytic activity and specific SPM secretion, through PD-1 activation.

Supplementary Materials: The following supporting information can be downloaded at: https://www.mdpi.com/article/10.3390/cells14120860/s1. Figure S1.original gel images and microscope images (A, B) Original gel images corresponding to Figure 2C. (C, D) Original gel images corresponding to Figure 5A. (E) Original microscopy image corresponding to Figure 4C. (F) Original microscopy image corresponding to Figure 7C. Figure S2. Representative gating strategy for flow cytometric analysis of macrophage subsets and PD-1 expression. A sequential gating strategy was applied to identify macrophage populations and assess their polarization states. (A) Debris was excluded based on forward scatter area (FSC-A) and side scatter area (SSC-A). (B) Single cells were subsequently selected using an FSC-H versus FSC-A plot. (C) Macrophages were identified by gating F4/80+ cells. (D) Within the single-cell population, CD86 expression was analyzed in conjunction with F4/80 to define M1-like macrophages (F4/80+CD86+). (E) Within the F4/80+ population, M2-like macrophages were identified based on co-expression of CD206 and CD163. (F) PD-1 expression was also assessed within the F4/80+ gate to evaluate its expression on macrophages. Table S1. PCR primer sequences

Author Contributions: T.M.: Investigation, Writing—original draft. G.C.: Investigation. E.D.A.: Investigation. S.R.: Investigation. S.H. (Shengyuan Huang): Investigation. S.H. (Sahar Hassantash): Investigation. S.S.: Interpretation of data. M.O.: Interpretation of data. S.Y.: Interpretation of data. S.N.: Interpretation of data. S.N.: Project Administration/oversight, Conceptualization, Writing—review, editing, and revision. All authors have read and agreed to the published version of the manuscript.

Funding: Funding for this study was provided by the National Institute of Dental and Craniofacial Research (NIDCR): DE025255 (XH), DE029709 (TK), and DE027648 (MS).

Institutional Review Board Statement: All animal procedures were approved by the Animal Care and Use Committee of Nova Southeastern University (protocol code 2022.02.XH1, approved on 25 February 2022) and were carried out in accordance with institutional and national guidelines.

Informed Consent Statement: Not applicable.

Data Availability Statement: The data presented in this study are available on request from the corresponding author.

Acknowledgments: We acknowledge support from NIH grant S10OD032292, awarded to the Lipidomics Core Facility at Wayne State University.

Conflicts of Interest: The authors declare no conflicts of interest. The funders had no role in the study's design; in the collection, analyses, or interpretation of data; in the writing of the manuscript; or in the decision to publish the results.

References

- 1. Mauri, C.; Bosma, A. Immune regulatory function of B cells. Annu. Rev. Immunol. 2012, 30, 221–241. [CrossRef] [PubMed]
- 2. Mizoguchi, A.; Mizoguchi, E.; Takedatsu, H.; Blumberg, R.S.; Bhan, A.K. Chronic intestinal inflammatory condition generates IL-10-producing regulatory B cell subset characterized by CD1d upregulation. *Immunity* **2002**, *16*, 219–230. [CrossRef] [PubMed]

- 3. Fillatreau, S.; Sweenie, C.H.; McGeachy, M.J.; Gray, D.; Anderton, S.M. B cells regulate autoimmunity by provision of IL-10. *Nat. Immunol.* **2002**, *3*, 944–950. [CrossRef]
- 4. Carter, N.A.; Vasconcellos, R.; Rosser, E.C.; Tulone, C.; Muñoz-Suano, A.; Kamanaka, M.; Ehrenstein, M.R.; Flavell, R.A.; Mauri, C. Mice lacking endogenous IL-10–producing regulatory B cells develop exacerbated disease and present with an increased frequency of Th1/Th17 but a decrease in regulatory T cells. *J. Immunol.* 2011, 186, 5569–5579. [CrossRef]
- 5. Yoshizaki, A.; Miyagaki, T.; DiLillo, D.J.; Matsushita, T.; Horikawa, M.; Kountikov, E.I.; Spolski, R.; Poe, J.C.; Leonard, W.J.; Tedder, T.F. Regulatory B cells control T-cell autoimmunity through IL-21-dependent cognate interactions. *Nature* **2012**, 491, 264–268. [CrossRef]
- 6. Liu, Y.-C.; Zou, X.-B.; Chai, Y.-F.; Yao, Y.-M. Macrophage polarization in inflammatory diseases. *Int. J. Biol. Sci.* **2014**, *10*, 520. [CrossRef]
- 7. Koh, T.J.; DiPietro, L.A. Inflammation and wound healing: The role of the macrophage. *Expert Rev. Mol. Med.* **2011**, *13*, e23. [CrossRef]
- 8. Atri, C.; Guerfali, F.Z.; Laouini, D. Role of human macrophage polarization in inflammation during infectious diseases. *Int. J. Mol. Sci.* **2018**, *19*, 1801. [CrossRef] [PubMed]
- Jordan, P.M.; Werz, O. Specialized pro-resolving mediators: Biosynthesis and biological role in bacterial infections. FEBS J. 2022, 289, 4212–4227. [CrossRef]
- 10. Serhan, C.N. Pro-resolving lipid mediators are leads for resolution physiology. *Nature* **2014**, 510, 92–101. [CrossRef]
- 11. Harwood, J.L. Polyunsaturated fatty acids: Conversion to lipid mediators, roles in inflammatory diseases and dietary sources. *Int. J. Mol. Sci.* **2023**, 24, 8838. [CrossRef] [PubMed]
- 12. Prescott, D.; McKay, D.M. Aspirin-triggered lipoxin enhances macrophage phagocytosis of bacteria while inhibiting inflammatory cytokine production. *Am. J. Physiol.-Gastrointest. Liver Physiol.* **2011**, 301, G487–G497. [CrossRef] [PubMed]
- 13. Krishnamoorthy, S.; Recchiuti, A.; Chiang, N.; Yacoubian, S.; Lee, C.-H.; Yang, R.; Petasis, N.A.; Serhan, C.N. Resolvin D1 binds human phagocytes with evidence for proresolving receptors. *Proc. Natl. Acad. Sci. USA* **2010**, *107*, 1660–1665. [CrossRef] [PubMed]
- 14. Chiang, N.; de la Rosa, X.; Libreros, S.; Serhan, C.N. Novel resolvin D2 receptor axis in infectious inflammation. *J. Immunol.* **2017**, 198, 842–851. [CrossRef]
- 15. Haas-Stapleton, E.J.; Lu, Y.; Hong, S.; Arita, M.; Favoreto, S.; Nigam, S.; Serhan, C.N.; Agabian, N. Candida albicans modulates host defense by biosynthesizing the pro-resolving mediator resolvin E1. *PLoS ONE* **2007**, 2, e1316. [CrossRef]
- 16. Decker, C.; Sadhu, S.; Fredman, G. Pro-resolving ligands orchestrate phagocytosis. Front. Immunol. 2021, 12, 660865. [CrossRef]
- 17. Vannella, K.M.; Wynn, T.A. Mechanisms of organ injury and repair by macrophages. *Annu. Rev. Physiol.* **2017**, 79, 593–617. [CrossRef]
- 18. Wang, Y.; Yu, X.; Lin, J.; Hu, Y.; Zhao, Q.; Kawai, T.; Taubman, M.A.; Han, X. B10 cells alleviate periodontal bone loss in experimental periodontitis. *Infect. Immun.* **2017**, *85*, e00335-17. [CrossRef]
- 19. Yu, P.; Hu, Y.; Liu, Z.; Kawai, T.; Taubman, M.A.; Li, W.; Han, X. Local induction of B cell interleukin-10 competency alleviates inflammation and bone loss in ligature-induced experimental periodontitis in mice. *Infect. Immun.* **2017**, *85*, e00645-16. [CrossRef]
- 20. Wang, Y.; Hu, Y.; Pan, K.; Li, H.; Shang, S.; Wang, Y.; Tang, G.; Han, X. In-vivo imaging revealed antigen-directed gingival B10 infiltration in experimental periodontitis. *Biochim. Et Biophys. Acta* (*BBA*)-*Mol. Basis Dis.* **2021**, *1867*, 165991. [CrossRef]
- 21. Hasan, M.M.; Thompson-Snipes, L.; Klintmalm, G.; Demetris, A.J.; O'Leary, J.; Oh, S.; Joo, H. CD24hiCD38hi and CD24hiCD27+ human regulatory B cells display common and distinct functional characteristics. *J. Immunol.* **2019**, 203, 2110–2120. [CrossRef] [PubMed]
- 22. Liang, S.C.; Latchman, Y.E.; Buhlmann, J.E.; Tomczak, M.F.; Horwitz, B.H.; Freeman, G.J.; Sharpe, A.H. Regulation of PD-1, PD-L1, and PD-L2 expression during normal and autoimmune responses. *Eur. J. Immunol.* 2003, *33*, 2706–2716. [CrossRef] [PubMed]
- 23. Azuma, T.; Yao, S.; Zhu, G.; Flies, A.S.; Flies, S.J.; Chen, L. B7-H1 is a ubiquitous antiapoptotic receptor on cancer cells. *Blood J. Am. Soc. Hematol.* **2008**, *111*, 3635–3643. [CrossRef]
- 24. Gordon, S.R.; Maute, R.L.; Dulken, B.W.; Hutter, G.; George, B.M.; McCracken, M.N.; Gupta, R.; Tsai, J.M.; Sinha, R.; Corey, D. PD-1 expression by tumour-associated macrophages inhibits phagocytosis and tumour immunity. *Nature* **2017**, *545*, 495–499. [CrossRef]
- 25. Iwai, Y.; Hamanishi, J.; Chamoto, K.; Honjo, T. Cancer immunotherapies targeting the PD-1 signaling pathway. *J. Biomed. Sci.* **2017**, 24, 26. [CrossRef]
- 26. Cao, G.; Xu, Q.; Huang, S.; Dai, D.; Wang, J.; Li, W.; Zhao, Y.; Lin, J.; Han, X. B10 cells regulate macrophage polarization to alleviate inflammation and bone loss in periodontitis. *J. Periodontol.* **2024**, *96*, 355–368. [CrossRef]
- 27. Maddipati, K.R.; Zhou, S.-L. Stability and analysis of eicosanoids and docosanoids in tissue culture media. *Prostaglandins Other Lipid Mediat.* **2011**, *94*, 59–72. [CrossRef]

- 28. Maddipati, K.R.; Romero, R.; Chaiworapongsa, T.; Zhou, S.-L.; Xu, Z.; Tarca, A.L.; Kusanovic, J.P.; Munoz, H.; Honn, K.V. Eicosanomic profiling reveals dominance of the epoxygenase pathway in human amniotic fluid at term in spontaneous labor. *FASEB J.* **2014**, *28*, 4835. [CrossRef] [PubMed]
- 29. Mosser, D.M.; Edwards, J.P. Exploring the full spectrum of macrophage activation. Nat. Rev. Immunol. 2008, 8, 958–969. [CrossRef]
- 30. Mantovani, A.; Sozzani, S.; Locati, M.; Allavena, P.; Sica, A. Macrophage polarization: Tumor-associated macrophages as a paradigm for polarized M2 mononuclear phagocytes. *Trends Immunol.* **2002**, 23, 549–555. [CrossRef]
- 31. Wang, L.-X.; Zhang, S.-X.; Wu, H.-J.; Rong, X.-L.; Guo, J. M2b macrophage polarization and its roles in diseases. *J. Leukoc. Biol.* **2019**, *106*, 345–358. [CrossRef]
- 32. Iwata, Y.; Matsushita, T.; Horikawa, M.; DiLillo, D.J.; Yanaba, K.; Venturi, G.M.; Szabolcs, P.M.; Bernstein, S.H.; Magro, C.M.; Williams, A.D. Characterization of a rare IL-10–competent B-cell subset in humans that parallels mouse regulatory B10 cells. *Blood J. Am. Soc. Hematol.* **2011**, *117*, 530–541. [CrossRef] [PubMed]
- 33. Wei, Y.; Liang, M.; Xiong, L.; Su, N.; Gao, X.; Jiang, Z. PD-L1 induces macrophage polarization toward the M2 phenotype via Erk/Akt/mTOR. *Exp. Cell Res.* **2021**, *402*, 112575. [CrossRef]
- 34. Ito, I.; Asai, A.; Suzuki, S.; Kobayashi, M.; Suzuki, F. M2b macrophage polarization accompanied with reduction of long noncoding RNA GAS5. *Biochem. Biophys. Res. Commun.* **2017**, 493, 170–175. [CrossRef]
- 35. Zhang, Y.; Ma, L.; Hu, X.; Ji, J.; Mor, G.; Liao, A. The role of the PD-1/PD-L1 axis in macrophage differentiation and function during pregnancy. *Hum. Reprod.* **2019**, *34*, 25–36. [CrossRef] [PubMed]
- 36. Zhang, Y.-H.; Aldo, P.; You, Y.; Ding, J.; Kaislasuo, J.; Petersen, J.F.; Lokkegaard, E.; Peng, G.; Paidas, M.J.; Simpson, S. Trophoblast-secreted soluble-PD-L1 modulates macrophage polarization and function. *J. Leucoc. Biol.* **2020**, *108*, 983–998. [CrossRef]
- 37. Greenlee-Wacker, M.C. Clearance of apoptotic neutrophils and resolution of inflammation. *Immunol. Rev.* **2016**, 273, 357–370. [CrossRef] [PubMed]
- 38. Fredman, G.; Khan, S. Specialized pro-resolving mediators enhance the clearance of dead cells. *Immunol. Rev.* **2023**, *319*, 151–157. [CrossRef]
- 39. Spite, M.; Norling, L.V.; Summers, L.; Yang, R.; Cooper, D.; Petasis, N.A.; Flower, R.J.; Perretti, M.; Serhan, C.N. Resolvin D2 is a potent regulator of leukocytes and controls microbial sepsis. *Nature* **2009**, *461*, 1287–1291. [CrossRef]
- Mitchell, S.; Thomas, G.; Harvey, K.; Cottell, D.; Reville, K.; Berlasconi, G.; Petasis, N.A.; Erwig, L.; Rees, A.J.; Savill, J. Lipoxins, Aspirin-Triggered Epi-Lipoxins, Lipoxin Stable Analogues, and the Resolution of Inflammation: Stimulation of Macrophage Phagocytosis of Apoptotic Neutrophils: In Vivo. J. Am. Soc. Nephrol. 2002, 13, 2497–2507. [CrossRef]
- 41. Kneidl, J.; Löffler, B.; Erat, M.C.; Kalinka, J.; Peters, G.; Roth, J.; Barczyk, K. Soluble CD163 promotes recognition, phagocytosis and killing of Staphylococcus aureus via binding of specific fibronectin peptides. *Cell. Microbiol.* **2012**, *14*, 914–936. [CrossRef] [PubMed]
- 42. Jiao, K.; Zhang, J.; Zhang, M.; Wei, Y.; Wu, Y.; Qiu, Z.Y.; He, J.; Cao, Y.; Hu, J.; Zhu, H. The identification of CD163 expressing phagocytic chondrocytes in joint cartilage and its novel scavenger role in cartilage degradation. *PLoS ONE* **2013**, 8, e53312. [CrossRef]
- 43. Schulz, D.; Severin, Y.; Zanotelli, V.R.T.; Bodenmiller, B. In-depth characterization of monocyte-derived macrophages using a mass cytometry-based phagocytosis assay. *Sci. Rep.* **2019**, *9*, 1925. [CrossRef]
- 44. Sezin, T.; Ferreirós, N.; Jennrich, M.; Ochirbold, K.; Seutter, M.; Attah, C.; Mousavi, S.; Zillikens, D.; Geisslinger, G.; Sadik, C.D. 12/15-Lipoxygenase choreographs the resolution of IgG-mediated skin inflammation. *J. Autoimmun.* 2020, 115, 102528. [CrossRef] [PubMed]
- 45. Ivanov, I.; Kuhn, H.; Heydeck, D. Structural and functional biology of arachidonic acid 15-lipoxygenase-1 (ALOX15). *Gene* **2015**, 573, 1–32. [CrossRef] [PubMed]
- 46. Radmark, O. Formation of eicosanoids and other oxylipins in human macrophages. *Biochem. Pharmacol.* **2022**, 204, 115210. [CrossRef]
- 47. Li, W.; Wu, F.; Zhao, S.; Shi, P.; Wang, S.; Cui, D. Correlation between PD-1/PD-L1 expression and polarization in tumor-associated macrophages: A key player in tumor immunotherapy. *Cytokine Growth Factor Rev.* **2022**, *67*, 49–57. [CrossRef]
- 48. van Roon, J.; Wijngaarden, S.; Lafeber, F.P.; Damen, C.; van de Winkel, J.; Bijlsma, J.W. Interleukin 10 treatment of patients with rheumatoid arthritis enhances Fc gamma receptor expression on monocytes and responsiveness to immune complex stimulation. *J. Rheumatol.* **2003**, *30*, 648–651.
- 49. Blair, P.A.; Noreña, L.Y.; Flores-Borja, F.; Rawlings, D.J.; Isenberg, D.A.; Ehrenstein, M.R.; Mauri, C. CD19+ CD24hiCD38hi B cells exhibit regulatory capacity in healthy individuals but are functionally impaired in systemic lupus erythematosus patients. *immunity* **2010**, *32*, 129–140. [CrossRef]
- 50. Bystrom, J.; Evans, I.; Newson, J.; Stables, M.; Toor, I.; Van Rooijen, N.; Crawford, M.; Colville-Nash, P.; Farrow, S.; Gilroy, D.W. Resolution-phase macrophages possess a unique inflammatory phenotype that is controlled by cAMP. *Blood J. Am. Soc. Hematol.* **2008**, 112, 4117–4127. [CrossRef]

- 51. Stables, M.J.; Shah, S.; Camon, E.B.; Lovering, R.C.; Newson, J.; Bystrom, J.; Farrow, S.; Gilroy, D.W. Transcriptomic analyses of murine resolution-phase macrophages. *Blood J. Am. Soc. Hematol.* **2011**, *118*, e192–e208. [CrossRef] [PubMed]
- 52. Williams, L.; Bradley, L.; Smith, A.; Foxwell, B. Signal transducer and activator of transcription 3 is the dominant mediator of the anti-inflammatory effects of IL-10 in human macrophages. *J. Immunol.* **2004**, *172*, 567–576. [CrossRef] [PubMed]
- 53. Sarma, U.; Maiti, M.; Nair, A.; Bhadange, S.; Bansode, Y.; Srivastava, A.; Saha, B.; Mukherjee, D. Regulation of STAT3 signaling in IFNγ and IL10 pathways and in their cross-talk. *Cytokine* **2021**, *148*, 155665. [CrossRef] [PubMed]
- 54. Han, Z.; Wu, X.; Qin, H.; Yuan, Y.-C.; Schmolze, D.; Su, C.; Zain, J.; Moyal, L.; Hodak, E.; Sanchez, J.F. Reprogramming of PD-1+ M2-like tumor-associated macrophages with anti–PD-L1 and lenalidomide in cutaneous T cell lymphoma. *JCI Insight* 2023, 8, e163518. [CrossRef]
- 55. He, X.; Xiao, J.; Li, Z.; Ye, M.; Lin, J.; Liu, Z.; Liang, Y.; Dai, H.; Jing, R.; Lin, F. Inhibition of PD-1 alters the SHP1/2-PI3K/Akt axis to decrease M1 polarization of alveolar macrophages in lung ischemia–reperfusion injury. *Inflammation* **2023**, 46, 639–654. [CrossRef]
- 56. Memida, T.; Abdolahinia, E.D.; Cao, G.; Ruiz, S.; Huang, S.; Shindo, S.; Nakamura, S.; Lin, J.; Kawai, T.; Han, X. B10 cells promote pro-resolving macrophage function through direct cell-cell contact and IL-10 secretion in Raw 264.7 cells. *Int. Immunol.* 2025. [CrossRef]

Disclaimer/Publisher's Note: The statements, opinions and data contained in all publications are solely those of the individual author(s) and contributor(s) and not of MDPI and/or the editor(s). MDPI and/or the editor(s) disclaim responsibility for any injury to people or property resulting from any ideas, methods, instructions or products referred to in the content.





Review

Role of T Follicular Helper Cells in Viral Infections and Vaccine Design

Sohrab Ahmadivand ^{1,*}, Robert Fux ² and Dušan Palić ^{1,*}

- Faculty of Veterinary Medicine, Ludwig-Maximilians-University Munich, 80539 Munich, Germany
- Institute for Infectious Diseases and Zoonoses, Ludwig-Maximilians-University Munich, 80539 Munich, Germany; robert.fux@lmu.de
- * Correspondence: sohrab.ahmadivand@lmu.de (S.A.); d.palic@lmu.de (D.P.)

Abstract: T follicular helper (Tfh) cells are a specialized subset of CD4+ T lymphocytes that are essential for the development of long-lasting humoral immunity. Tfh cells facilitate B lymphocyte maturation, promote germinal center formation, and drive high-affinity antibody production. Our current knowledge of Tfh interactions with the humoral immune system effectors suggests that they have a critical role in supporting the immune response against viral infections. This review discusses the mechanisms through which Tfh cells influence anti-viral immunity, highlighting their interactions with B cells and their impact on antibody quality and quantity. We explore the role of Tfh cells in viral infections and examine how vaccine design can be improved to enhance Tfh cell responses. Innovative vaccine platforms, such as mRNA vaccines and self-assembling protein nanoplatforms (SAPNs), are promising strategies to enhance Tfh cell activation. Their integration and synergistic combination could further enhance immunity and Tfh responses (SAPN-RNA vaccines). In summary, we provide a comprehensive overview of the current insights into Tfh cells' role during viral infections, emphasizing their potential as strategic targets for innovative vaccine development.

Keywords: viral infections; Tfh cells; mRNA vaccine; ferritin; germinal centers; B cells

1. Introduction

Viral infections remain a global health challenge in human beings and animals due to their ability to evade immune responses, establish persistence, and undergo rapid mutation [1,2]. A robust immune response is the crucial element in countering viral infections, with T follicular helper (Tfh) cells playing a pivotal role in the generation of long-lasting immunity [3]. Tfh cells, a specialized subset of CD4+ T cells, are central to humoral immunity as they support B cell activation and promote germinal center (GC) formation and high-affinity antibody production. This process is primarily driven by CD40L-CD40 interactions and cytokines, particularly IL-21 [4]. Their role is especially crucial during viral infections, when they are essential for generating neutralizing antibodies [5–7]. In SARS-CoV-2 infections, a robust Tfh cell response is vital for protective immunity [7]. While Tfh cells promote rapid GC formation and antibody production in acute infections like influenza, their dysfunction in chronic infections such as HIV can impair immune responses and contribute to viral persistence [5,6].

The induction of Tfh cells can be influenced by factors such as species differences [8], individual characteristics [9], vaccine formulation (including adjuvants) [10,11], administration route and dose [12], and, most importantly, vaccine type and design [13], all of

which affect antigen presentation and immune activation, highlighting the challenges in developing effective vaccines against viruses.

Recent advances in vaccinology have begun to leverage the unique capabilities of Tfh cells to improve vaccine efficacy. Novel platforms such as mRNA vaccines and self-assembling protein nanocages have demonstrated significant potential to enhance Tfh responses, driving robust GC reactions and high-affinity antibody production [14,15]. mRNA vaccines against SARS-CoV-2 are an example, where their lipid nanoparticle (LNP) formulation possesses intrinsic adjuvant activity and can mediate the induction of strong Tfh cell and GC responses [16,17]. Self-assembling protein nanocages, such as ferritin, offer advantages by mimicking the size and structure of viral particles and enhancing antigen presentation and Tfh cell activation through multivalent antigen display [18,19].

Such approaches and their synergistic combination to vaccine design that involve formulations with or without adjuvants targeting Tfh cells have shown promise in enhancing immune responses against several animal and human viruses [20–22]. Moreover, they offer cross-protection against different viral strains, making them a strong candidate in explorations of a "broad-spectrum" immunity approach [10,23]. The use of adjuvants, such as TLR and STING agonists has emerged as another critical strategy for optimizing vaccine-induced Tfh responses by promoting Tfh differentiation and GC reactions through dendritic cell activation, cytokine modulation, and enhanced antigen presentation [16].

This review provides a comprehensive overview of the current understanding of Tfh cells' role in immune responses against viral infections across different species, emphasizing their interactions with B cells and significance in vaccine design. We address the potential for emerging strategies and technologies such as mRNA and self-assembling protein nanocage vaccine platforms and their synergistic combination, as well as potential adjuvants, to enhance Tfh cell responses, thereby offering insight into the development of next-generation vaccines for both human and veterinary applications.

2. T Follicular Helper Cells

2.1. Tfh Cell Characteristics and Function

T lymphocytes, a crucial component of the adaptive immune system, play diverse roles in orchestrating immune responses against pathogens, including viruses. Among them, CD4⁺ T helper (Th) cells are essential in mediating the immune system defense by providing support to other immune cells, such as CD8⁺ cytotoxic T cells and B cells [24]. Upon activation, Th cells differentiate into various subsets, each tailored to combat specific types of pathogens (Figure 1A). These subsets include Th1, Th2, Th17, and the relatively more specialized Tfh cells, each with distinct roles in immune regulation. Th1 cells support cellular immunity and IgG1 and IgG3 antibody responses, while Th2 cells assist in humoral immunity, promoting IgE production [25]. Th17 cells are integral to mucosal immunity in areas like the lung and gut, and Tfh cells are uniquely involved in supporting humoral immunity and are essential for generating high-affinity antibodies [4]. The induced immune response can be suppressed by regulatory T cells (Tregs), another subset of CD4+ T cells [4].

Tfh cells, a specialized CD4⁺ T cell lineage, provide essential help to B-lymphocytes in GCs within secondary lymphoid organs (SLOs). They facilitate B cell affinity maturation through somatic hypermutation (SHM) and class-switch recombination (CSR), leading to the production of high-affinity antibodies [4,26]. This process also promotes B cell differentiation into memory B cells and antibody-secreting cells (ASCs), including plasmablasts and plasma cells. Without interactions with Tfh cells and the GC reaction, B cells primarily produce low-affinity antibodies as short-lived plasma cells [27], (Figure 1C).

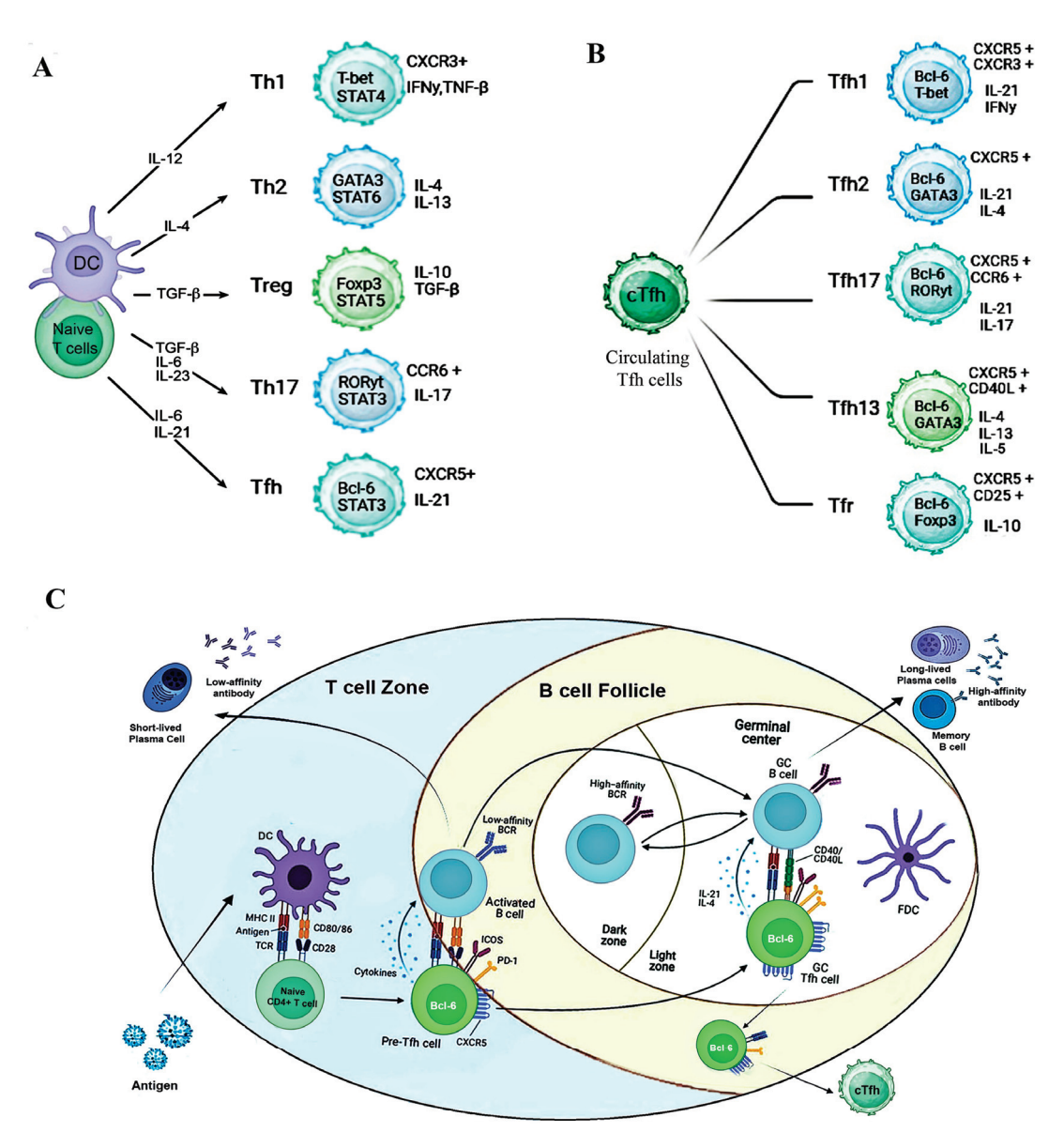


Figure 1. T follicular helper (Tfh) cell differentiation, subsets, and germinal center function. (**A**) Differentiation of T helper (Th) cell subsets. Interaction between dendritic cells (DCs) and naïve CD4⁺ T cells leads to polarization into Th1, Th2, and Th17 regulatory T cells (Tregs), and Tfh cells, driven by specific cytokines and transcription factors. (**B**) Subsets of circulating Tfh cells (cTfh). Tfh cells released into circulation (CD4⁺CXCR5⁺) are associated with distinct cytokine profiles and transcription factors such as T-bet, GATA3, RORγt, and Foxp3. (**C**) Germinal center (GC) Tfh differentiation. Naïve CD4⁺ T cells activated by DCs differentiate into pre-Tfh cells, which migrate to the T-B cell border and interact with activated B cells. In the GC, FDCs and Tfh cells (Bcl-6+, CXCR5+, PD-1+, ICOS+) promote B cell affinity maturation and differentiation into memory and long-lived plasma cells through costimulatory signals mediated by ICOS–ICOSL and CD40–CD40L interactions along with IL-4 and IL-21 cytokine secretion. Without Tfh interaction in GCs, B cells produce low-affinity antibodies as short-lived plasma cells. IL-6 is crucial for Tfh formation in animal models, but not in humans. Created with BioRender.com.

Tfh cells are characterized by the expression of the surface markers chemokine receptor 5 (CXCR5) [28], programmed cell death protein 1 (PD-1), [29], and inducible co-stimulatory molecule (ICOS), along with the transcription factor B cell lymphoma 6 (Bcl-6) [4,30]. Bcl-6 is regarded as the master regulator of the GC response, coordinating the interaction between Tfh and GC B cells, and it drives the transcriptional program that governs Tfh cell differentiation [31]. Tfh cells express CD40 Ligand (CD40L), which binds to CD40 on B

cells in GCs, providing essential signals for B cell activation, survival, and differentiation into plasma cells and memory B cells [4].

They can also co-express T-bet (Th1), GATA3 (Th2), or RORγT (Th17), giving rise to distinct subsets: cTfh1, cTfh2, and cTfh17 cells found in the blood of both mice and humans and displaying a phenotype that closely resembles that of memory T cells (Figure 1B) [32]. The origin of circulating Tfh (cTfh) cells remains elusive, although their function as effective B cell helpers is well established [33]. cTfh cells, functioning alongside Tfh cells, can promote B cell differentiation into antibody-secreting cells [33]. cTfh cells are suggested to reflect GC reactivity, which was shown in both murine and human studies post-rituximab treatment, even in the absence of GC B cells [34]. However, further investigation is needed to fully define their role in GC responses.

In human blood, cTfh cells have been characterized by high CXCR5 and PD-1 expression, low to intermediate ICOS expression, and reduced Bcl-6 expression following Ebola vaccination, suggesting that continuous antigen stimulation may sustain or enhance Bcl-6 expression and influence cTfh cell function [31,35].

However, lymphoid tissue does not appear to contain equivalent Tfh subsets. In human blood, CD4⁺CXCR5⁺ cells are further divided into distinct cTfh subpopulations (cTfh1, cTfh2, and cTfh17) based on CCR6 and CXCR3 expression, each associated with specific transcription factors and cytokine secretion (Figure 1B) [33]. The functional diversity of Tfh cell subsets plays a crucial role in supporting the class switching of GC B cells, leading to the production of different immunoglobulin types. cTfh1 cells, characterized by a CXCR3+ CCR6— pattern, are primarily involved in antiviral immunity and responses to intracellular pathogens. They produce IFN-γ and IL-21, which drive IgG2a and IgG3 class switching in B cells [33]. In contrast, cTfh2 cells, which lack CXCR3 and CCR6, secrete IL-4 and IL-21, supporting immune responses to allergens and parasitic infections by promoting B cell class switching, especially to IgE [36]. cTfh17 cells, identified by their CXCR3+CCR6+ pattern, produce IL-21 and IL-17, and play a significant role in autoimmune responses and inflammatory conditions. IL-17 production enhances T–B cell interactions, promoting switching to IgG2a and IgG3 [37].

Follicular regulatory T (Tfr) cells play a vital role in maintaining immune tolerance and controlling autoimmunity by regulating GC responses and suppressing Tfh activity, primarily through the inhibition of Bcl-6 and promotion of Blimp-1 expression. Tfr cells express Treg markers like Foxp3 and co-express Bcl-6 but lack cytokines such as IL-4, IL-21, and CD40L, which are crucial for B cell activation. However, they have no or low expression of CD25 compared to Treg cells [36,38].

Tfh-like cells have also been identified in non-lymphoid tissues, which exhibit distinct marker expression patterns compared to Tfh cells in secondary lymphoid organs [36]. A newly identified subset, Tfh13, play a role in IgE production in allergic responses [39].

NKT cells can differentiate into CXCR5+PD-1+Bcl6+ follicular helper NKT (NKTfH) cells, which engage in CD1d-mediated cognate interactions with B cells, secrete IL-21, and support germinal center responses [40]. However, it has been shown that NKT cells do not acquire the NKTfH phenotype following viral infection [41].

Tfh cells are not characterized in many species due to the lack of antibodies for markers like CXCR5 and PD-1, which are commonly used in humans, mice, and pigs. Species-specific immune differences complicate comparisons [42], highlighting the need for further research on Tfh cells across species and diseases.

2.2. Tfh Cell Differentiation

Tfh cell differentiation is a multifaceted and highly regulated process that is essential for humoral immunity, enabling the formation of GCs and the production of high-affinity

antibodies. Different stages of this process occur in distinct anatomical locations within SLOs and are influenced by specific molecular signals and cellular interactions [4,31].

Tfh cell differentiation begins with the activation of naïve CD4⁺ T cells by dendritic cells (DCs) in the T cell zone of SLOs. DCs present peptide–MHC class II complexes to T cells, triggering TCR signaling and co-stimulatory signals (e.g., B7 family: CD28-CD80/CD86). This initiates the upregulation of Bcl-6 and the differentiation into pre-Tfh cells [30]. Cytokines such as IL-6 (in animal models) and IL-21 (in both humans and animal models) activate STAT3, further enhancing Bcl-6 expression [43]. This, in turn, enables the expression of CXCR5, guiding pre-Tfh cells to migrate towards B cell follicles, where they encounter CXCL13-producing stromal cells and are poised for interaction with B cells [28].

At the T-B border, pre-Tfh cells interact with antigen-presenting B cells, reinforcing the Tfh transcriptional program. As Tfh cells mature in the germinal center, they adopt a CXCR5⁺, PD-1⁺, Bcl-6⁺ phenotype [44]. In the light zone, Tfh cells interact with B cells and follicular dendritic cells (FDCs), which present antigens to B cells, promoting survival, affinity maturation, and differentiation through CD40-CD40L and ICOS-ICOSL interactions [45]. Cytokines like IL-21 and IL-4 further support B cell maturation, with Tfh-derived IL-21 being essential for the formation and maintenance of germinal centers, as well as the development of long-lived plasma cells and memory B cells [4].

GC B cells return to the dark zone for SHM and CSR, with FDCs helping maintain the immune synapse. In the dark zone, centroblasts (activated B cells) undergo SHM and proliferation, driven by activation-induced cytidine deaminase (AID), [46].

Afterward, they migrate to the light zone, where they differentiate into centrocytes. This cycling between the dark and light zones ensures the selection of high-affinity B cells, while low-affinity or autoreactive B cells undergo apoptosis [44].

B cells also act as antigen-presenting cells (APCs) and produce cytokines like IL-6, which stabilize Tfh cell identity by promoting the expression of surface markers such as PD-1 and CXCR5. In turn, Tfh cells secrete IL-21, priming B cells for their roles in the germinal center reaction, including affinity maturation and differentiation into memory B cells and plasma cells [4,43]. IL-6 supports Tfh cell development in animal models, while IL-21 is essential for Tfh differentiation and function in both humans and animals [4].

Notably, recent evidence highlighted the role of BCR engagement in promoting GC B cell selection and differentiation into plasma blasts, despite the suppressed BCR signaling in GC B cells [47].

The differentiation of Tfh cell subsets is guided by the cytokine milieu and STAT activation [36,48]. Precursor Tfh (pre-Tfh) cells share developmental pathways with Th1, Th2, and Th17 cells. STAT1/STAT4 signaling (e.g., Type I IFN and IL-12) drives Tfh1 development, while IL-4/STAT6 promotes Tfh2 polarization but is inhibited by IL-6. Also, IL-6 and/or IL-21, and IL-23 activate STAT3 to drive Tfh17 differentiation, with RORγt aiding their specialization. ICOS signaling is also essential for Tfh17 differentiation. Most Tfr cells originate from Foxp3+ regulatory T cells (Tregs), although some can differentiate directly from naïve CD4+ T cells [48]. Tfr cells balance GC responses by producing IL-10 to support B cell growth and high-affinity antibodies while suppressing Tfh cells, GC B cells, and autoantibodies [48]. Recently, Tfh13 cells, characterized by IL-4, IL-5, and IL-13 co-production and the Th2 transcription factor GATA3, have been identified as key drivers of high-affinity IgE production [39,49].

The differentiation of Tfh cells is orchestrated by a network of transcription factors. Bcl6 plays a central role by repressing alternative CD4+ T cell fates, such as Th1, Th2, and Th17 cells, while enabling the expression of Tfh-associated genes [4]. In addition to Bcl-6, transcription factors like STAT3, TCF1, Ascl2, c-Maf, IRF4, and Batf synergize with Bcl-6 to

promote Tfh cell differentiation and sustain the Tfh phenotype [31]. These factors coordinate the expression of key Tfh markers such as CXCR5, ICOS, and PD-1, facilitating Tfh cell migration to B cell follicles and interactions with B cells [31]. Conversely, negative regulators like Blimp-1 and STAT5 inhibit Tfh differentiation by promoting alternative effector T cell pathways, maintaining immune balance, and preventing excessive or inappropriate Tfh cell differentiation. These regulators also preserve immune homeostasis by preventing Tfh overactivation or differentiation into unwanted T cell subsets [36].

While the overall process of Tfh cell differentiation is conserved, the cytokine milieu varies across species. In mice, IL-6, IL-21, and Bcl6 are essential for Tfh formation, while in humans, Tfh generation relies on TGF- β , IL-12, IL-21, IL-23, and Activin A signaling, indicating the adaptability of Tfh cells to diverse immune environments [50].

Notable species-specific adaptations are also seen in non-mammalian vertebrates and farm animals. In pig lymph nodes, a CD4+ T cell population with an ICOS+Bcl-6+CD8 α + phenotype was identified, similar to human and murine germinal center Tfh cells. Blood-derived ICOShiCD25- and ICOSdimCD25dim CD4+ T cells induced the differentiation of CD21+IgM+ B cells into Ig-secreting plasma blasts. These cells were 3- to 7-fold enriched for Tfh-related transcripts (CD28, CD40LG, IL6R, and MAF) compared to naïve CD4+ T cells, as revealed by single-cell RNA sequencing [51]. Also, differences in lymphoid structures across species, such as the bursa of Fabricius in birds [52] or the absence of lymph nodes in fish [42], further hinder the characterization and functional study of Tfh cells that is needed to support tailored vaccine strategies.

3. Role of Tfh Cells in Viral Infections

Tfh cells, defined by CXCR5, ICOS, and PD-1 surface markers, along with the transcription factor Bcl-6 and the cytokine IL-21, are indispensable for mounting effective humoral immune responses during viral infections [4]. In acute infections, they drive antibody production, whereas in chronic infections, they contribute to immune regulation and viral persistence [5,6]. Their importance has been confirmed across species, including human and animals, against various viruses [5–7]. For instance, the IgG response to the vaccinia virus is diminished by 98% in the absence of Tfh cells [53].

Research in this context has predominantly focused on bulk GC-Tfh populations due to difficulties in isolating antigen-specific cells to study infections such as HIV and SIV infections, in which Tfh cells are associated with the development of broadly neutralizing antibodies, while Tbet+ GC-Tfh cells suggest a hybrid Tfh/Th1 function, though their precise roles require further investigation [54].

Circulating Tfh cells, which represent blood-resident counterparts of GC-Tfh cells, further underscore the importance of Tfh-mediated immunity in both contexts. Among the cTfh subset, Tfh1 cells, driven by IL-12 and STAT4, produce IFN- γ and enhance IgG2a and IgG3 antibody responses, which are critical in certain viral infections [37]. Longitudinal tracking of cTfh cells also showed activation of the cTfh1 subset and ASC expansion between 10 and 20 days post-infection, with the response magnitude correlating with the neutralizing- and total antibody titers [55].

IFN- γ from Tfh1 cells promotes the expression of T-bet in B cells, aiding in antibody isotype class switching and retention of B cells in the GC dark zone for affinity maturation during viral infections like lymphocytic choriomeningitis virus (LCMV) infections [56]. However, excessive IFN- γ can suppress GC responses, as was seen in some models of Plasmodium infection, indicating a fine balance in Tfh1-mediated regulation [57].

Tfh2 cells, characterized by IL-4 and IL-13 production, are involved in class switching to IgE and IgG1, which is particularly relevant in type 2 immune responses [36]. Although not traditionally associated with viral infections, sustained IL-4 production by Tfh2 cells

can influence low-affinity antibody responses, which may contribute to viral immunity under certain conditions [56].

Tfh17 cells, producing IL-17 alongside IL-21, have been implicated in enhancing GC formation and supporting IgG2a/IgG3 switching. While their role in viral infections remains less well defined, their ability to stabilize T–B cell interactions in GCs could be significant in contexts requiring robust antibody production [37].

3.1. Tfh Cells in Acute Viral Infections

Acute viral infections rapidly induce Tfh responses, which are crucial for the production of virus-specific neutralizing antibodies. Mouse models of infections, such as LCMV, vesicular stomatitis virus (VSV), and influenza infections, have demonstrated the indispensable role of Tfh cells in protective humoral responses during acute infection. CD40L-deficient mice exhibit impaired GC formation, reduced memory B cell populations, and poor antiviral antibody production during LCMV and VSV infections [58]. Also, ICOS-deficient mice fail to generate robust GC responses during influenza infection, indicating the importance of ICOS signaling in Tfh functionality [59].

During acute viral infections, naïve CD4+ T cells differentiate into Tfh cells under the guidance of DCs and a cytokine-rich environment. Cytokines like IL-6, IL-21, and IL-27 activate STAT3 and induce the transcription factor Bcl-6, which drives Tfh lineage commitment while suppressing competing CD4+ T cell fates, including Th1, Th2, and Th17 cells [60].

Tfh differentiation is initiated through MHC-II/TCR interactions and stabilized by costimulatory signals such as ICOS and CD40L, which can be coordinated by Bcl-6, TCF-1, and mTORC2 [60]. Once differentiated, Tfh cells upregulate the chemokine receptor CXCR5, guiding them to B cell follicles. Within these follicles, primarily the IL-21-secreting Tfh cells ensure efficient GC formation and the generation of long-lived plasma cells and memory B cells. Notably, transient expression of T-bet in Tfh cells facilitates IFN- γ secretion, enhancing IgG2a class switching, especially during viral infections like influenza infections [4].

An acute Zika virus infection model in immunocompetent mice demonstrated that ZIKV elicits robust Th1-like Tfh cell and protective antibody responses. These Th1-like Tfh cells share phenotypic and transcriptomic features with both Tfh and Th1 cells but possess distinct markers and are T-bet dependent. They are essential for class switching to ZIKV-specific IgG2c antibodies and for sustaining long-term neutralizing-antibody responses, a function not performed by Th1 cells [61].

Early Tfh differentiation is linked to strong GC formation and high-affinity antibody production [56], but Tfh response kinetics are tightly regulated during acute viral infections. Early Tfh differentiation begins within 24–48 h, driven by high-affinity TCR interactions with DCs and sustained IL-6 and IL-21 signaling. IL-2 signaling, which supports Th1 differentiation, is suppressed by STAT5, promoting Tfh lineage commitment. Transcriptional regulators such as TCF-1 and Ascl2 also play key roles in early Tfh cell commitment during infections with viruses like influenza and LCMV [4].

During acute SARS-CoV-2 infection, activated cTfh cells (PD-1+ICOS+) with increased CD38 and reduced CCR7 expression peak within 14 days post-symptom onset. Spike-specific cTfh cells persist in convalescent individuals for at least 6 months, with a half-life of approximately 129 days, indicating their importance in long-term immunity [62]. The magnitude of Tfh responses is influenced by cytokines like IL-6 and/or IL-21 and the strength of the TCR signaling.

Moreover, this viral infection promotes spike-specific CXCR3+ Tfh cells, which are more persistent and better correlated with antibody responses, suggesting that prolonged

infection can support the maintenance and recall of Tfh cells [7]. Notably, cTfh1 clones show a significant overlap with CXCR3+ tonsil-derived Tfh cells [16,63].

Similarly, strong Tfh generation during influenza infection depends on the localized recognition of antigens by CD4 effector cells and the presence of continuous infection-derived signals, reinforcing the idea that sustained infection is key to driving effective Tfh responses [64]. These findings indicate that the duration and persistence of the infection are essential for inducing durable Tfh responses, providing insights for improving vaccine efficacy by replicating the continuous antigenic stimulation observed in natural infections.

3.2. Tfh Cells in Chronic Viral Infections

Chronic infections with viruses such as HIV, hepatitis C virus (HCV), and chronic LCMV present unique challenges to Tfh cells' functionality. Persistent antigenic stimulation during chronic infections skews CD4+ T cell differentiation toward the Tfh lineage, leading to increased Tfh cell frequencies. However, this expansion often comes at the cost of functionality, with chronic immune activation impairing Tfh cell support for B cells, disrupting GC dynamics, and resulting in delayed or suboptimal antibody responses [5].

In chronic LCMV infection, the loss of Th1 cells is accompanied by an increase in Tfh cells; however, these Tfh cells fail to sustain robust GC reactions, produce lower levels of IL-21, and delay neutralizing-antibody production, ultimately compromising the viral control [65]. During HCV infection, CXCR3+ cTfh cells are associated with stronger neutralizing-antibody responses, reflecting pathogen-specific influences on cTfh function [66]. During HIV infection, expanded Tfh populations contribute to polyclonal B cell activation, hypergammaglobulinemia, and defective antibody responses. Nonetheless, circulating PD-1+CXCR3-CXCR5+ memory Tfh cells remain highly functional and are associated with the development of broadly neutralizing HIV antibody responses [67]. In HIV infection, Tfh cells within GCs also evade CD8+ T cell-mediated killing and serve as latent viral reservoirs, complicating both immune clearance and therapeutic interventions [68]. Pre-Tfh cells in secondary lymphoid tissues, marked by high CCR5 expression, are particularly susceptible to this infection. These cells may transition into fully functional Tfh cells, upregulating PD-1 during chronic infections and further contributing to viral persistence [5].

Therapeutic strategies such as PD-1 blockade and recombinant IL-21 are being explored to enhance Tfh-B cell interactions and improve antibody responses in chronic infections. However, these approaches carry risks, including heightened T cell activation, which could trigger viral reactivation or promote the formation of new reservoirs within GCs [69].

Despite these challenges, Tfh cells remain crucial for vaccine efficacy against chronic viral infections. Enhancing Tfh responses through targeted therapies or vaccines could improve antibody generation to combat rapidly mutating viruses such as HIV and HCV. Understanding the transcriptional regulation of Tfh differentiation, including the roles of Bcl-6 and Blimp-1, could provide valuable insights for tailoring immune responses in chronic viral infections.

4. Targeting Tfh Cells Through Vaccine Design

4.1. Tfh Cells and Vaccines

Vaccines are effective in preventing viral infections, reducing transmission, and establishing herd immunity [70–72]. Humoral immunity, driven by high-affinity antibodies produced by B cells, is essential for vaccine efficacy [4]. Consequently, the efficient elicitation of Tfh cell responses to vaccine antigens has become a key area of research. Serological responses to influenza, yellow fever, malaria, and SARS-CoV-2 vaccines correlate with cTfh

activation, particularly those expressing markers such as CXCR5+ and ICOS+, and the Th1-polarizing conditions in these infections generally result in the predominant generation of type 1 Tfh cells [55].

Vaccine type significantly affects Tfh cell activation and overall efficacy. Live attenuated vaccines induce the strongest Tfh responses, mimicking infection, while inactivated and subunit vaccines, though safer, often require adjuvants to enhance immunogenicity [17,73]. Aligned with this, Devarajan et al. [64] have reported that a second dose of a live attenuated influenza vaccine during the effector phase can effectively replicate infection-like conditions, eliciting robust Tfh responses.

Studies on inactivated vaccines have shown that Tfh responses are typically induced only when an adjuvant is included and after administering at least three doses [73]. For example, the BBV152 vaccine, a whole-virion inactivated SARS-CoV-2 formulation, achieved this effect by incorporating a TLR 7/8 agonist molecule (IMDG) adsorbed to alum [71]. However, these findings are further complicated by safety concerns, particularly adjuvant-dependent effects associated with inactivated vaccines [74].

Despite the role of the CpG domain in DNA vaccines, the Tfh response has been shown to be further enhanced by chitosan encapsulation of a plasmid encoding the VP1 protein of coxsackievirus B3 [75]. However, the commercialization of this type of vaccine is hindered due to concerns related to genetically modified organisms [76].

Modulating the GC Tfh abundance can influence B cell recruitment and epitope-specific antibody production [77], further indicating the importance of strong CD4+ T cell responses in vaccination [5,78]. Furthermore, GC-Tfh cells rely on continuous antigen presentation for their maintenance, and adjuvants that support CD4+ T cell priming or prolong GC-Tfh cell activity can improve humoral immunity [79]. Lymph node fine needle aspirates (FNAs) offer a minimally invasive approach to assessing GC-Tfh cells and GC biology, providing insights into Tfh and GC dynamics in human and primate models [80].

Nonetheless, studying Tfh responses and the exact role of Tfh subsets in blood is challenging, as GC-Tfh cells primarily reside in lymphoid tissues [4]. Recently activated cTfh cells (CXCR5+ICOS+, Ki67+PD1hi) can be identified and are distinct from the predominant resting memory cTfh cells [81,82]. Following influenza vaccination, the frequency of influenza-specific activated cTfh cells increases, correlating with the IgG responses [82].

The subunit SARS-CoV-2 RBD vaccine, composed of the RBD protein expressed in Drosophila S2 cells and formulated with an alum adjuvant, has elicited significant antigenspecific Tfh cell responses (predominantly Tfh1 and Tfh1-17 subset responses and strong GC responses) in the lymph nodes and spleen, playing a critical role in the induced humoral responses [16]. Additionally, the magnitude of the Tfh and GC responses is crucial for the immunogenicity of these vaccines, which can be directly influenced by the vaccine dose and frequency, i.e., boosters [83].

In the case of the SARS-CoV-2 vaccine, although ICOS+CXCR5+CD4+ T cells recognized the RBD antigen by day 7 post-vaccination, indicating rapid Tfh cell activation, booster vaccination—known to modulate the magnitude of Tfh and GC responses—further enhanced Tfh activation by preferentially increasing the CXCR3+ (Tfh1 and Tfh1-17) subset over the CXCR3— (Tfh2 and Tfh17) subset in the spleen and lymph nodes [17]. A nonadjuvanted trivalent influenza vaccine increased the CXCR3+ cell frequency [66], while Tfh17 cells were induced during the rVSV-ZEBOV Ebola vaccine response [35]. Both Tfh1 and Tfh17 responses were observed in SARS-CoV-2 mRNA-LNP vaccines [84]. Additionally, Yin et al. [85] reported a shift from cTfh2 and cTfh17 to cTfh1 in low responders to the hepatitis B vaccine, further highlighting the importance of studying Tfh subsets.

Studies on influenza vaccines have shown that they primarily activate memory B cells (MBCs), enhancing antibody responses [33,86]. Recombinant RBD protein induces Tfh

cells, which effectively promotes MBC differentiation into antibody-secreting cells, unlike non-Tfh cells. Elevated IgG and IL-21 levels in Tfh-MBC co-culture supernatants after RBD stimulation suggest that Tfh cells amplify the memory B cell response. This role of Tfh cells in boosting antibody production has also been observed with other vaccines, such as papillomavirus vaccines [86].

Moreover, some vaccine platforms (such as mRNA) promote a shift from IL-4 to IFN- γ production in Tfh cells, which is associated with improved immune responses [87]. This suggests that the ability to elicit functional IFN- γ -producing Tfh cells could be also a key factor in improving vaccine efficacy.

Other innovative strategies, such as incorporating SAPNs into mRNA vaccines [88] and utilizing adjuvants, have shown promising potential in enhancing Tfh cell activation, warranting dedicated discussion to explore their mechanisms and applications in enhancing vaccine efficacy for both human and animal viruses.

4.2. RNA Vaccines: Immunity and Tfh Cell Responses in Humans and Animals

RNA vaccines, such as messenger RNA (mRNA) vaccines, have emerged as a transformative technology in vaccinology, offering rapid development and adaptability to various pathogens (Figure 2). Their scalability was notably demonstrated during the SARS-CoV-2 pandemic [89]. At the core of conventional mRNA vaccine development is the molecular design of synthetic mRNA, which incorporates critical elements to optimize stability, prevent degradation, and ensure efficient translation. Conventional mRNA vaccines are transcribed in vitro from DNA templates, with stabilization achieved through 5' capping, untranslated regions (UTRs) and poly-A tails to enhance translation and reduce degradation [90] (Figure 2A).

In addition to their success in combating SARS-CoV-2, mRNA vaccines are being explored for other viral infections and even cancer therapies. In this context, self-amplifying RNA (saRNA) platforms have emerged, offering enhanced vaccine efficiency by amplifying antigen production within cells, reducing the necessary mRNA doses, and lowering production costs [91,92]. In contrast to conventional mRNA vaccines that encode only the antigen of interest and rely entirely on the host cell machinery for translation [87], saRNA vaccines incorporate replication machinery derived from alphaviruses, including nonstructural proteins (nsP1–4), enabling intracellular RNA amplification [93] (Figure 2A). These vaccines utilize LNPs to deliver mRNA into host cells, which is then translated into antigen proteins that stimulate both humoral and cellular immune responses [94] (Figure 2C). In addition to LNPs, several alternative delivery systems under investigation include polymeric nanoparticles (PEI and chitosan) for stability, inorganic nanoparticles (gold and silica) for targeted delivery, and cell-penetrating peptides (CPPs) for direct mRNA entry into cells [95,96].

More recently, self-assembling protein nanoparticles (SAPNs) have emerged as an approach to stabilizing antigenic proteins in RNA vaccines and improve their presentation to the immune system, thereby amplifying the efficacy of the vaccines. We refer to this approach as the "SAPN-RNA vaccine" (Figure 2B). The immune responses and Tfh cell activation induced by both conventional mRNA and saRNA vaccines can be further enhanced through this incorporation [22,88] (Figure 2D).

mRNA vaccines have shown promising results in promoting adaptive immunity against various human and animal viruses. mRNA vaccines, such as Moderna mRNA-1273 and Pfizer/BioNTech BNT162b2, induce strong immune responses, including increases in memory CD4+ T cells, circulating Tfh cells, and cytotoxic T cells. Although antibody levels decrease over time, the stability of memory T and B cells supports long-term immunity. mRNA vaccines also generate superior neutralizing antibodies and have lower reacto-

genicity compared to inactivated and viral vector vaccines, offering enhanced protection against viral infections [13,97]. mRNA vaccines also induce both humoral and cellular immunity. Upon delivery, the mRNA is translated into antigens in the cytosol, leading to their degradation and presentation on MHC-I molecules, activating cytotoxic CD8+ T cells. Simultaneously, secreted or membrane-bound antigens are processed via MHC-II pathways, stimulating CD4+ T cells and promoting antibody production by B cells [98].

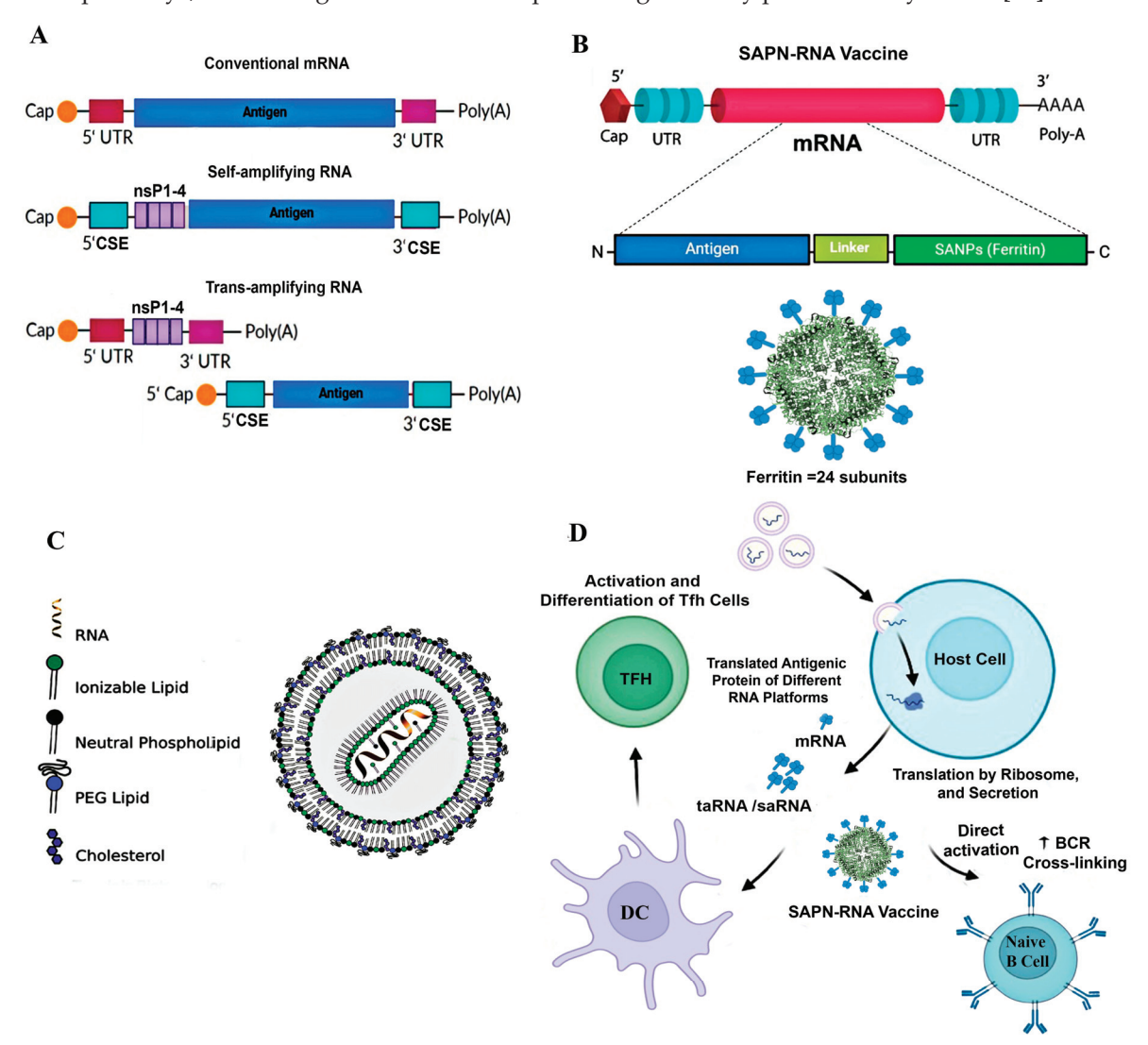


Figure 2. Design and antigen expression mechanism of various mRNA vaccine platforms. (A) Comparison of conventional mRNA, self-amplifying RNA (saRNA), and trans-amplifying RNA (taRNA) vaccine designs. (B) SAPN-RNA vaccine design: Integration of self-assembling protein nanoparticles (e.g., ferritin with 24 subunits) in mRNA vaccines for multivalent antigen display. (C) Key components of lipid nanoparticles (LNPs). (D) Mechanism of action of mRNA vaccines: SAPN-RNA vaccine directly activates naïve B cells and is efficiently processed by antigen-presenting cells, such as dendritic cells (DCs), facilitating Tfh cell activation and differentiation from CD4+ T cells by engaging PRRs, while other formulations mainly rely on LNP adjutant properties. This along with promoting multiple BCR cross-linking and its slow-release properties ensure robust, durable, and stable antibody responses at a lower dose. Cap: m7G; UTR: untranslated region; CSE: conserved sequence element; nsP1-4: alphavirus nonstructural proteins 1-4. Created with BioRender.com.

SARS-CoV-2 mRNA vaccines are an example of vaccines that promote strong Tfh cell activation and germinal center responses, leading to higher neutralizing-antibody production and the generation of long-lived plasma cells and memory B cells (Table 1). LNP formulations activate innate immune responses via pattern recognition receptors

(PRRs), such as Toll-like receptors (TLR7 (mouse and human) and TLR8 (human) that detect the presence of foreign RNA, triggering the production of type I interferons and other inflammatory cytokines [98,99]. Through this process, the ionizable lipid in the LNPs triggers the production of cytokines, such as IL-6 in mice [17]. Notably, these vaccines promote a shift from IL-4 to IFN- γ production in Tfh cells, which is associated with improved immune responses [87].

In addition to SARS-CoV-2, mRNA vaccines for other viruses, including influenza and Zika, have been developed and tested in animal models and showed similar immune responses in terms of Tfh and GC activation. For example, mRNA vaccines targeting the influenza virus in mice have been shown to activate antigen-specific Tfh cells, leading to enhanced GC responses and high titers of neutralizing antibodies, a result supported by the secretion of IL-21 [94]. The induction of robust B cell responses following influenza mRNA vaccination is closely associated with the presence of circulating hemagglutinin-specific ICOS+ PD-1+ CXCR3+ Tfh cells [100]. Similarly, an mRNA vaccine developed against the Zika virus has demonstrated that vaccination increases Tfh responses, which play a crucial role in eliciting a sustained neutralizing-antibody response, providing lasting protection against Zika infection [101].

mRNA vaccines are also gaining attention in veterinary medicine as innovative solutions for managing viral infections in farm animals [102]. However, most animal studies, including those using animal models and veterinary species, focus on GC-Tfh cells, whereas the human data predominantly relate to cTfh cells, primarily due to sampling limitations. Recent research has highlighted their ability to induce robust immune responses, including the activation of Tfh cells, mirroring their success in human medicine [12], optimizing the mRNA-B sequence for expressing the rabies virus glycoprotein (RABV-G), and evaluating its immunogenicity across various animals. A single dose of the mRNA-B-LNP vaccine induced rapid and long-lasting protective antibody responses in mice, outperforming inactivated vaccines in dogs by generating higher neutralizing-antibody titers. Two doses provided sustained humoral responses, strong Tfh and GC B cell activity, and Th1-biased cellular immunity. Additionally, the vaccine remains stable as a liquid formulation at 2–8 °C for up to two months, showcasing its practical application in veterinary medicine. Studies on zoonotic Rift Valley fever virus (RVFV) mRNA vaccines targeting various viral proteins, including Gn-head, Gn-stem, Gc, and GnGc, revealed high frequencies of GC B cells and Tfh cells in BALB/c mice, as determined by flow cytometry of inguinal lymph node cells. These immune responses were also confirmed in rhesus macaques, demonstrating the vaccine's potential for cross-species immune activation [103].

In livestock, mRNA vaccines have shown promising results against several viral diseases. These vaccines, such as those for Foot-and-Mouth Disease Virus (FMDV) [104], avian influenza [105], and Bovine Viral Diarrhea Virus (BVDV-1) [106], induce strong immune responses, including the production of virus-specific antibodies (IgY and IgA) and activation of CD4+ T cells and Tfh-like cells. These responses significantly reduce viral loads and pathology. For BVDV-1, both cap-dependent and cap-independent mRNA vaccines generate robust neutralizing-antibody titers in many species, including mice, guinea pigs, and goats. In swine, mRNA vaccines targeting African Swine Fever (ASF), and Porcine Reproductive and Respiratory Syndrome Virus (PRRSV) [107–109] have shown excellent safety and efficacy, boosted neutralizing-antibody production, and activated both CD4+ and CD8+ T cells with increased cytokine secretion. For PRRSV, GP5-mRNA vaccines also demonstrated superior immunogenicity compared to traditional vaccines [109].

Table 1. The cell responses induced by mRNA and self-assembling protein nanocage (SAPN) vaccines against viral pathogens.

Vaccine Type	Virus(es) (Antigen)	Species	Adjuvant	Tfh-Related Immune Responses	Ref(s).
mRNA	SARS-CoV-2 (Spike Protein)	Human	1	Induces strong neutralizing-antibody response and persistent cTfh cells for six months, with potent GC B and Tfh responses, including increase in Tfh1 cells after the first dose	[15, 110]
mRNA	HIV-1 (Env), ZIKV (prM-E); influenza virus (HA)	Mice and rhesus macaques	ı	Potent T follicular helper and germinal center B cell responses	[94]
mRNA	RVFV (Gn and Gc)	Mice and rhesus macaques		Induces potent GC B and Tfh cell responses $10\mathrm{days}$ after booster	[103]
saRNA	SARS-CoV-2 (RBD-TM)	Mouse, NHP, and hamster models	Alum	Robustly activated Tfh cells; cross-reactive responses against heterologous variants and VOCs, lasting at least 12 months in NHPs (Cynomolgus macaques)	[63]
Ferritin-mRNA	HIV-1 (Env)	Mice	1	Induced specific GC B cells and memory B cells in spleen. Tfh cells and GC Tfh cells were also observed in vaccinated mice	[88]
Ferritin-mRNA	SARS-CoV-2 (RBD)	Mice	1	Elicited robust titers of specific antibodies, including neutralizing antibodies with increased expression of IFN- γ and IL-4	[111]
LuS-mRNA	Rotavirus (P2-VP8*)	Mice and guinea pigs	Alum	Induced the highest specific IgG titers compared to conventional mRNA and subunit vaccines, which remained constant over time	[112]
LuS-mRNA	SARS-CoV-2 (RBD)	Mice	1	Strong neutralizing-antibody responses and protection against the Delta variant	[113]
LuS-saRNA	$HIV \left(gp120\right)$	Mice	ISCOM-like	Elicited GC B and Tfh cell responses with a balanced $\lg G1/\lg G2$ humoral immune response	[22]
Ferritin	Influenza virus (HA)	Mice and pigtail macaques	AddaVax	High antibody titers and directly activated germinal centers through a B cell-intrinsic mechanism	[114]
Ferritin	HBV (preS1 domain)	Mice	CpG-1826	SIGNR1+ dendritic and macrophage cells activated Tfh and B cells, driving strong and lasting antibody responses	[16]
Ferritin	SARS-CoV-2 (Spike Protein)	Mice	ALFQ/Alhydrogel	One dose of vaccine induced IL-21-producing spike-specific Tfh and GC B cells, S-2P-specific IgM/IgG, and robust cross-neutralizing antibodies by day 7	[10]
Encapsulin	Rotavirus (VP8*)	Mice	Alhydrogel	Induced specific IgG1, IgG2a, and neutralizing antibodies with superior immunogenicity over subunit vaccine	[115]
LuS and E2	RVFV(Gn)	Mice and lambs	TS6	Protection correlated with the induction of robust neutralizing antibodies in both species	[116]
sHSP	Antigen ovalbumin (OVA)	Mice	Alum	OVA-specific IgG1 was detectable by day 5, with strong mucosal sIgA and germinal center B and Tfh cell responses	[18]

In aquaculture, mRNA vaccines are emerging as a potential solution to viral diseases, which pose a significant challenge to the industry [117–119]. While promising for both fish [120] and crustaceans [121], mRNA vaccines face substantial challenges due to their distinct and relatively simple immune systems [42,122]. For example, fish lack germinal centers and instead rely on diffuse lymphoid tissues for B cell activation, with Tfh-like cells playing a role in supporting immune responses [42]. These findings highlight the potential of mRNA vaccines in veterinary medicine, though key aspects, such as Tfh cell responses, remain underexplored.

To further enhance immune responses and Tfh cell activation, mRNA and saRNA vaccines can be combined with molecules that activate immunostimulatory receptors, such as OX40, CD137, or CD40, or molecules that block immune checkpoints like PD-1, PD-L1, and CTLA-4. Such combinatory strategies have been shown to potentiate the efficacy of these vaccines. For instance, activating OX40 in combination with saRNA vaccines has been tested in COVID-19 models, resulting in enhanced T cell cytokine responses and improved viral clearance [123]. Similarly, combining IL-12-MOP with the BNT162b2 SARS-CoV-2 vaccine significantly boosted immune responses in animal models [124].

The SAPN-RNA approach, incorporating self-assembling protein nanocages to mRNA vaccines, offers a novel strategy to boost immunity and activate Tfh cell responses. This could allow mRNA vaccines to be more effective, potentially requiring lower doses and offering better stability, making it a promising strategy for both human and veterinary vaccines.

4.3. Self-Assembling Protein Nanocages (SAPNs) as Vaccine Platforms: Immunity and Tfh Cell Responses

Self-assembling protein nanocages (SAPNs) occur naturally in various organisms and have emerged as promising platforms for novel vaccine development (Figure 3). These nanoscale structures, ranging from 10 to 100 nm in size, closely mimic the size and shape of viruses, enabling the multivalent display of antigens in highly ordered architectures [19,21]. This design enhances their uptake and processing by antigen-presenting cells, directly activates naïve B cells, and facilitates efficient cross-linking of B cell receptors (BCRs) [19]. Like mRNA vaccines, they simulate innate immune responses through PRRs (TLR-4) engagement [125]. Moreover, SAPNs promote robust interactions with immune cells, such as Tfh cells, driving germinal center responses that are critical for generating durable and high-affinity antibody responses (Table 1).

SAPNs exhibit remarkable thermal and pH stability, monodispersity, a small and uniform size, biodegradability, biocompatibility, cost-effective mass production, pseudoreversible spontaneous assembly/disassembly, and the potential for surface conjugation [19,21,126].

Importantly, SAPNs can favor the co-delivery of antigen and adjuvant to the same immune cell, which enhances the adjuvant effects and limits off-target effects [127]. SAPNs provide versatile scaffolds capable of accommodating a range of antigens, including those from enveloped viruses via substituting lipid membranes and matrix proteins, and rescuing insoluble antigenic proteins for vaccine applications [126]. These properties address significant challenges in the stability and immunogenicity of subunit and mRNA vaccines, enabling rapid deployment during epidemics or pandemics. Several SANP-based vaccines are undergoing clinical trials [19,21,128].

Protein nanocages currently used for the development of novel vaccines include ferritin, lumazine synthase (LuS), Encapsulin, E2 protein, and small heat-shock proteins (sHSPs) (Figure 3). Each of these protein nanocages has distinct structural and immunological characteristics, allowing for the display of antigens on their surfaces through methods

such as genetic fusion, tag coupling, or chemical conjugation to the N- and/or C-terminal regions, which are compatible with both prokaryotic and eukaryotic expression systems [129].

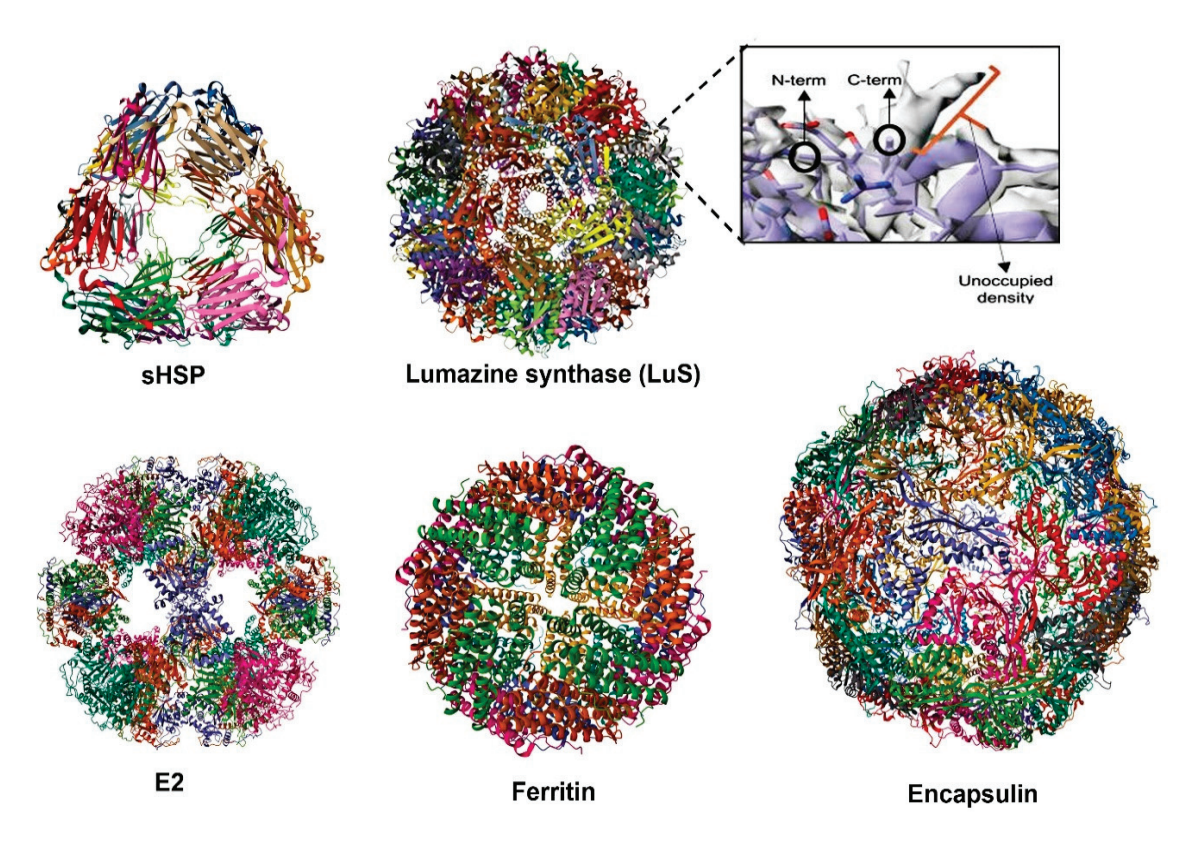


Figure 3. Schematic structures of natural self-assembling protein nanocages (SAPNs). sHSP: small heat shock protein; MjsHSP16.5 (~16.5 nm, 24-mer; PDB ID: 8WP9); lumazine synthase (~16–24 nm, 60-mer; PDB ID: 8F25) with exposed C- and N-termini on the surface; E2 Dihydrolipoyl Acetyltransferase (~24 nm, 60-mer; PDB ID: 1B5S), ferritin (12 nm, 24-mer; PDB ID: 3BVE); and Encapsulin (20–100 nm, 60-, 180-, or 240-mer; PDB ID: 3DKT). Created with BioRender.com.

SAPNs-based vaccines utilize their unique nanoscale size (typically < 50 nm) and multivalent structure to mimic viral particles, enhancing immune activation. These nanoparticles are efficiently taken up by APCs and processed through the MHC-II pathway to activate CD4+ T cells, particularly Tfh cells. Simultaneously, their small size allows for direct interaction with naïve B cells, triggering germinal center reactions critical for high-affinity antibody production [19,128]. By synergizing BCR signaling with Tfh cell help, these antigens promote the survival, positive selection, clonal expansion, and affinity maturation of GC B cells, ensuring antibody diversity while preventing apoptosis through a balanced signaling interplay [130].

Previous studies reported neglectable anti-carrier antibodies to protein nanocages, indicating no adverse effects on vaccine immunogenicity [131]. Generally, these proteins alone are non-immunogenic, and those derived from bacterial sources do not induce autoimmunity [126,132]. Some of mentioned studies highlighted the role of adjuvants in the proper induction of immunity and in effectively engaging Tfh cells to SAPN vaccines (Table 1). SAPNs can also engage MHC-I pathways, stimulating CD8+ cytotoxic T cells, which provide cellular immunity by targeting infected cells [19,21]. This dual activation of humoral and cellular immunity is further supported by innate immune responses through PRR engagement. SAPNs mimic PAMPs to activate PRRs on DCs, triggering cytokine release (e.g., IL-21), antigen presentation, and Tfh cell differentiation [125].

SAPN vaccines effectively induce neutralizing antibodies and robust Tfh cell responses, which are critical for durable and cross-protective humoral immunity against rapidly

mutating viruses. While Tfh cell responses have been extensively studied in humans and animal models, their evaluation in other species relies on indirect markers such as Tfh-associated cytokines or germinal center dynamics. Here, we describe examples of this multi-pathway mechanism of immune activation by protein nanocages.

Ferritin-based vaccines for chronic hepatitis B and SARS-CoV-2 have successfully induced efficient Tfh and GC responses [16,133]. Vaccination of mice with influenza HA–ferritin has also shown enhanced and longer-lasting GC responses in draining lymph nodes, focal deposition of the antigen in the GCs of these nodes, and increased BCR mutations in memory B cells following HA–ferritin immunization. However, no improvement in HA-specific Tfh cell responses was observed, suggesting that a highly structured and repetitive antigen array may promote germinal center formation through a B cell intrinsic mechanism independent of Tfh cell involvement [114]. IL-21 induction has been noted in response to the SARS-CoV-2 spike–ferritin vaccine, with the generation of long-lived plasma cells and the production of cross-neutralizing antibodies [10].

Similarly, lumazine synthase (LuS) and E2 nanoparticles, which are capable of presenting complex antigens, enhance Tfh cell activation by mimicking the repetitive antigenic patterns of natural pathogens, thereby facilitating optimal interactions between Tfh cells and antigen-specific B cells. However, studies using *Aquifex aeolicus* LuS have been limited to a few human pathogens, including HIV, SBV, SARS-CoV-2, and RVFV [21]. For example, a vaccine based on *A. aeolicus* LuS has been shown to protect approximately 80% of mice against a lethal dose of SBV and to produce virtually sterile immunity in cattle, even with a single dose of the vaccine [134]. The coupling of the SARS-CoV-2 spike protein with Lus has also been shown to elicit higher neutralizing responses than spike protein alone [135]. When multimerized with a rationally designed epitope (HIV-1 gp-120), LuS NPs have been found to activate both germline and mature VRC01 class B cells, which could be the basis for the broadly neutralizing antibody response to HIV-1 [136].

Recently, SARS-CoV-2 vaccine candidates were developed using an HR2-deleted glycine-capped spike (S2G Δ HR2) displayed on ferritin and E2 protein. In mice, both SAPN vaccine candidates induced high neutralizing-antibody titers and robust T cell responses, including Th1, memory CD4+, CD107a-producing cytolytic CD4+ T cell, and GM-CSF-producing CD8+ effector T cell responses, highlighting their potential as vaccine candidates [137]. The 24-meric RBD-ferritin SAPN vaccines elicited stronger neutralizingantibody responses compared to the RBD or stabilized spike (S2P) alone. However, S2GΔHR2 displayed on multilayered E2 proteins and I3-01v9 SAPNs achieved significantly higher titers, with an up to a 10-fold increase over S2P. While both ferritin and E2 protein platforms enhanced immunogenicity, the E2-based vaccine candidate showed a notable plateau in neutralizing-antibody responses after three doses, indicating the potential to reduce the dosage or number of injections without compromising efficacy [137]. This makes E2 protein an efficient platform for dose-sparing strategies, whereas ferritin provided robust baseline responses. E2 protein and LuS, with their 60-subunit structures, may have similar immunogenicity. However, compared to ferritin with 24 subunits, their larger size allows for the display of more antigen, potentially enhancing the immune responses and stability.

In this context, a subunit vaccine targeting zoonotic RVFV used the glycoprotein Gn head domain conjugated to LuS nanoparticles [116]. This vaccine candidate reduced mortality in a lethal mouse model and protected lambs, the most susceptible hosts, from viremia and clinical signs. Similarly, coupling the same subunit to E2 resulted in a vaccine candidate that was able to achieve full protection in lambs. However, to conclude that the type of SAPNs determines the immunogenicity, additional head-to-head comparisons are needed.

Encapsulin is another protein nanocage whose use in vaccines has shown effectiveness in inducing neutralizing antibodies against rotavirus, influenza, and COVID-19 (180-mer). Although Tfh cell responses were not explicitly evaluated, the vaccine candidate's ability to stimulate robust humoral immunity was evident [115,138,139].

The potential of Encapsulin from Myxococcus xanthus as a scaffold for displaying 180 copies of the monomeric receptor-binding domain (mRBD) to enhance vaccine efficacy against SARS-CoV-2 variants in mice was evaluated [139]. The nanoparticle demonstrated long-term stability and, in mice, elicited high titers of neutralizing antibodies following a single immunization. A single booster enhanced these titers by 42-fold, effectively neutralizing the alpha, beta, and delta variants of concern (VOCs) with IC50 values comparable to the wild type. This platform proved highly effective in inducing robust neutralizing antibody responses. In mice, intramuscular immunization with oil-in-water adjuvanted formulations demonstrated that Encapsulin–pH1HA10 expressed in a prokaryote system provided complete protection against both homologous (Bel 09) and heterologous (PR8) influenza viral challenges [138].

In contrast, ferritin with the same antigen attachment and formulation offered partial protection and more pronounced clinical signs. This highlights *E. coli*'s suitability for generating simpler SAPNs and suggests that the number of subunits (180 in Encapsulin compared to 24 in ferritin) may play a critical role in enhancing antibody production and improving protective efficacy. The larger number of subunits in Encapsulin may contribute to more robust immune responses, underscoring the importance of nanoparticle design in vaccine effectiveness.

For rotavirus, the encapsulated (60-mer) vaccine candidate showed enhanced stability, and notable improvements in VP8*-specific IgG, including IgG1 and IgG2a, and neutralizing antibody responses with superior immunogenicity over a subunit vaccine in mice [115]. These responses indicate a balanced Th1/Th2 immune profile and capacity to promote cell-mediated immunity that is essential for effective viral vaccines.

Small heat shock proteins (sHSPs) hold promise as vaccine platforms, as they can promote durable antibody production and robust immune responses. Intranasal administration of an OVA–sHSP formulation in mice accelerated and enhanced OVA-specific IgG1 responses, with detection as early as 5 days post-immunization [18]. The study also revealed strong mucosal sIgA titers, germinal center accumulation of B and Tfh cells, and primed lung immunity, facilitating IgG and IgA responses upon influenza virus challenge. These findings underscore the potential of sHSPs to engage Tfh cells and support effective vaccine strategies, though further exploration is warranted.

Considering the numerous advantages of SAPN platforms, such as their ability to create safe, effective, and stable vaccines suitable for mucosal immunization and oral delivery, it is imperative to evaluate and optimize the various aspects of their application. Specifically, strategies like the SpyTag/SpyCatcher system or protein-induced nanocage (PINC) technology [140] for antigen attachment and adjuvant encapsulation targeting Tfh cell activation, such as saponins and TLR agonists, could significantly enhance vaccine efficacy. Delivering adjuvants with nanocage vaccine candidates shows promise for engaging Tfh responses, promoting durable antibody production and providing cross-protection against emerging viral strains. The recent use of SAPNs in mRNA vaccines further highlights their significant role and potential in vaccinology.

4.4. Self-Assembling Protein Nanocages in RNA Vaccine Design (SAPN-RNA Vaccines)

Most viruses, including influenza, undergo rapid antigenic changes through drift and shift. Therefore, the ultimate goal is to develop a universal vaccine that offers broad protection against diverse strains and emerging pandemic threats [141].

The incorporation of SAPNs with the mRNA approach (SAPN-RNA vaccines) represents a synergistic strategy to enhance vaccine efficacy with cross-protection potential against different viral strains. SAPNs, with their multivalent antigen display and nanoscale architecture, further amplify immune responses by directly engaging B cells and facilitating germinal center formation, as well as activation of PRRs, while also reinforcing the LNP formulation for improved uptake and more efficient antigen delivery [19,128]. Based on recent studies, this approach can induce robust Tfh-mediated antibody responses at lower doses while enhancing stability, versatility, and cross-protection against evolving pathogens (Table 1). Additionally, SAPNs may extend the immune response duration of mRNA vaccines. Studies on ferritin-fused mRNA vaccines for HIV and SARS-CoV-2 demonstrated significant improvements in immune responses compared to traditional mRNA or subunit vaccines [88,111]. Ferritin-fused mRNA vaccines induced stronger Tfh cell activation and enhanced GC responses, leading to higher frequencies of GC Tfh cells and elevated IL-21 cytokine levels [88,111]. An mRNA-encoded HIV-1 Env trimer ferritin nanoparticle vaccine demonstrated an ability to elicit robust GC B cell, memory B cell, and Tfh cell responses in mice [88].

Incorporating LuS self-assembling protein nanoparticles into mRNA vaccines enhances immunogenicity by forming 60-mer nanoparticles that mimic viral structures. For SARS-CoV-2, an mRNA vaccine using LuS nanoparticles to display multivalent RBD Delta induced strong neutralizing antibody responses and provided protection against the Delta variant in mice. The platform also allows for the design of a bivalent vaccine encoding wild-type and alpha variants, demonstrating comparable antibody responses to the monovalent version, highlighting its versatility [113].

An ongoing Phase 1 clinical trial (NCT05001373) evaluating the safety and immunogenicity of LuS-based HIV mRNA vaccines is expected to provide further insights into the LuS-specific immune responses elicited in humans after repeated vaccinations. Broadly neutralizing HIV antibodies typically require high levels of somatic hypermutation and specialized germline features, presenting challenges for vaccine development. To address this, an LNP-vectored alphavirus replicon encoding the GT eOD-GT8 immunogen, fused to LuS, was used to enhance the development of broadly neutralizing responses against HIV [22]. In the clinical trial, replicon immunization induced a slight, though not statistically significant, increase in the total number of CD4+CXCR5+ Tfh cells compared to protein-based vaccines. GC Tfh cells were induced at similar levels in both groups, but replicon immunization resulted in higher upregulation of the ICOS costimulatory receptor on Tfh cells early in the immune response, indicating that replicon vaccines may induce equivalent or superior GC responses, enhancing the potential for broadly neutralizing HIV antibodies [22]. Peak Tfh responses were also observed by day 12, with a slow decay thereafter, suggesting that the incorporation of SAPNs such as Lus may help facilitate slower antigen release and extend the duration of the immune response

LuS nanocages have also been employed in the context of RNA replicon vaccines against rotavirus [112]. LuS mRNA vaccines encoding VP8* self-assemble into 60-mer nanoparticles that mimic viral structures, effectively enhancing antigen presentation. These vaccines demonstrated robust immunogenicity in rodents, eliciting both humoral and cellular immune responses. In guinea pigs, LuS-P2-VP8* consistently induced higher antibody levels than P2-VP8* mRNA over a six-month period in both monovalent and trivalent formulations targeting P8], P6], and P4] genotypes. Moreover, the mRNA vaccines generated superior virus-neutralizing antibody responses and VP8*-specific T cell responses, which were absent in the alum-adjuvanted protein vaccine groups [112]. However, despite the high levels of neutralizing antibodies, the role of Tfh cells in LuS-based mRNA vaccines remains unexplored.

4.5. Adjuvants Promote Tfh Cell Differentiation and Responses

Adjuvants are essential component of non-live vaccines as they enhance immunogenicity by activating innate immune pathways, promote GC reactions, and drive the differentiation of Tfh cells. Certain delivery materials can also act as adjuvants by mimicking the size or structure of natural pathogens, facilitating antigen uptake and presentation by APCs through PRR signaling [11]. The selection and design of adjuvants directly influence the magnitude and quality of Tfh responses, which are especially important for targeting viral pathogens [10,142].

Aluminum salts (alum), one of the most extensively used vaccine adjuvants, primarily induce the development of Th2 and Tfh cells, promoting the production and secretion of high-affinity antibodies [143]. Demonstrating superior efficacy over MF59 in certain contexts, alum enhances early germinal center formation in response to peptide–protein conjugates and improves vaccine efficacy against non-viral disorders [144]. Alum adjuvants have also been used in SAPN vaccines to engage Tfh and GC responses (Table 1). Nonetheless, concerns about the local side effects of this adjuvant, along with its limited ability to elicit robust Tfh responses, highlight the necessity for more advanced adjuvant systems to address the challenges posed by viruses [145].

Recent advancement in adjuvant technology have introduced formulations targeting immune pathways to enhance Tfh cell responses. Oil-in-water emulsions like MF59 promote Tfh differentiation via IL-6-driven expression of Bcl6, a key transcription factor, and have demonstrated success in human influenza vaccines by boosting germinal center reactions and antibody responses [146]. MontanideTM ISA 206 is another example that has shown efficacy in veterinary vaccines, such as those for PRRSV, by enhancing germinal center formation and antibody production [147]. In the context of SAPN vaccines for viruses, oil-in-water emulsions such as MF59 have been used in ferritin-based SARS-CoV-2 and HIV vaccines, as well as in Encapsulin-based IAV and EBV vaccines, while Montanide ISA201VG was used to support FMDV–ferritin vaccines [21].

Toll-like receptor (TLR) agonists are a class of adjuvants that have demonstrated significant promise in enhancing Tfh and antibody responses [148,149]. TLR4 agonists, such as monophosphoryl lipid A (MPLA), and TLR9 agonists, like CpG oligodeoxynucleotides, are more effective than alum at stimulating immune responses by activating the innate immune system using potent danger signals [11].

Moreover, TLR9 and STING agonists have been shown to synergistically enhance the SARS-CoV-2 RBD vaccine response by boosting GC B cells and modulating Tfh responses. The combination of CpG-2722 and STING ligands elicited robust GC Tfh (CD4+Bcl-6+CXCR5+ICOS+) and B cell responses in draining lymph nodes and spleens, demonstrating their cooperative potential to improve vaccine efficacy [16].

TLR7/8 agonists are another promising vaccine adjuvant due to their ability to activate APCs and enhance Th1 and Tfh responses, which are critical for viral immunity. In a non-human primate model, TLR7 adjuvantation induced robust HIV Env-specific CD4+ T cell responses, and enhanced Tfh differentiation and germinal center formation [148], while TLR8 is a key sensor of vita-PAMPs and driver of Tfh differentiation; thus, TLR7/8 agonists have potential in Tfh-skewing vaccine adjuvant strategies [149].

MPLA enhances the immune response to inactivated rabies vaccines by promoting the generation of Tfh cells, GC B cells, and plasma cells, which increases the production of RABV-specific IgG, IgG2a, IgG2b, and virus-neutralizing antibodies, indicating its potential in improving immune responses against zoonotic viruses [150]. Notably, MPLA, a key component of the adjuvants AS01 (containing QS-21, a saponin-based adjuvant) and AS04 (containing aluminum salts), has been successfully used in licensed vaccines, including AS01 for malaria [151] and AS04 for HPV [152]. AS04 induces a Th1-biased immune

response, while AS01, which also enhances Tfh cell responses, is being evaluated in vaccines targeting viral infections [153]. Saponin/MPLA nanoparticles showed greater potency than AS01B in mice and primed robust immune responses, including germinal center B cell, Tfh cell, and HIV tier 2 neutralizing antibody responses in non-human primates [154].

NKT cell-based adjuvants are an effective strategy for enhancing vaccine efficacy by promoting early cytokine production, which supports Tfh cell differentiation and B cell activation, thereby boosting humoral immunity [155]. These cells are activated by lipid antigens presented by CD1d molecules, secreting cytokines like IL-4, IL-21, and IFN- γ that strengthen the adaptive immune response [40,41]. An example is α -galactosylceramide (α -GalCer), a glycolipid that activates invariant NKT cells. In murine studies, co-administration of α -GalCer with an influenza virus vaccine enhanced germinal center reactions, leading to the production of high-affinity antibodies against the virus [156].

Another approach involves adjuvants that target mucosa-associated invariant T (MAIT) cells. There is evidence that intranasal immunization with MAIT cell agonists, combined with protein antigens like the spike RBD of SARS-CoV-2 and influenza hemagglutinin, induces protective humoral immunity and IgA production. The MAIT cell-mediated adjuvant activity is driven by CD40L-dependent dendritic cell activation and Tfh cell priming, with antibody responses comparable to those induced by the NKT cell agonist α -GalCer [157].

Comparative studies have underscored the importance of adjuvant selection in shaping Tfh responses. For instance, a malaria P27A peptide vaccine formulated with the experimental adjuvant GLA-SE elicited significantly higher circulating Tfh activation and antibody titers than alum-based formulations [145]. Similarly, the PfRH5 antigen combined with AS01 produced stronger Tfh responses compared to a heterologous viral vector prime-boost regimen [153].

Nanoencapsulation can enhance the efficacy of classical vaccines by inducing CD4+ Th17 and Tfh cell responses, which are crucial for promoting robust humoral immunity. This mechanism contributes to improved vaccine outcomes by facilitating antigen presentation and promoting germinal center formation [75].

Despite the self-adjuvant role of LNPs, some studies explored combining mRNA vaccines with traditional adjuvants, like alum, to further enhance immune activation [93,112]. mRNA vaccines encoding the HIV-1 Env trimer, in combination with ferritin NPs, induced monoclonal antibodies that neutralized diverse HIV-1 isolates, further demonstrating the potential of mRNA-LNP and SAPN platforms to stimulate potent Tfh and GC responses [88].

While SAPN vaccines enhance neutralizing-antibody production, adjuvants can help achieve complete protection by optimizing immune responses [21]. As demonstrated with the ALFQ formulation, combining MPLA and QS-21 significantly boosted antigenspecific immune responses in SARS-CoV-2–ferritin vaccine models, leading to potent polyfunctional cytokine responses and long-lived memory CD8+ T cells [10]. This lipid formulation or the different dosing regimen of this unique adjuvant can extend the duration of antigen presentation.

In chronic hepatitis B (HBV), the combination of ferritin nanoparticles and CpG-1826 enhanced Tfh cell and germinal center B cell responses, improving antibody production [15]. Similarly, squalene-based formulations like AddaVaxTM, similar to MF59, have been shown to drive extended germinal center activity and memory B cell maturation in influenza ferritin-based vaccines [114]. These adjuvants promote cytokine expression, Tfh cell recruitment, and B cell activation, aiding immune memory formation and effective antigen targeting.

Future directions in adjuvant research should focus on refining Tfh responses by modulating cytokine pathways such as IL-6 and IL-27 signaling or suppressing IL-2, which are critical for Tfh differentiation and germinal center maintenance. Innovative adjuvants like QS-21 saponins, STING agonists, and nanoparticles provide new strategies for optimizing immune responses and vaccine design. Future approaches may also incorporate IL-21 as an immune adjuvant to enhance humoral immunity and promote Tfh activation. Additionally, probiotics, whether as non-replicating vectors [158] or vaccination adjuncts, could further amplify Tfh-mediated immunity [32], particularly in mRNA and SAPN-based vaccines. These advancements in adjuvants and vaccine design hold promise for next-generation vaccines that elicit durable, high-quality immunity.

5. Challenges and Future Directions

Tfh cells are essential for generating long-lasting humoral immunity, driving B cell maturation, germinal center formation, and high-affinity antibody production, making them crucial for immune responses against viral infections. Their central role has positioned them as key targets in vaccine development aimed at enhancing antibody responses. However, several challenges remain in fully utilizing Tfh cells for immunotherapy and vaccine design.

A major challenge in evaluating Tfh cells during viral infections is their transient nature and specialized localization in secondary lymphoid tissues like lymph nodes, making them difficult to study in vivo. Their activation is regulated by a complex network of cytokines and interactions with B cells, which are context-dependent and often short-lived, complicating the ability to track and analyze Tfh cell responses during an active viral infection.

Chronic viral infections impair Tfh cell function, disrupting B cell support and leading to suboptimal antibody responses. This dysfunction, along with immune dysregulation, complicates Tfh evaluation. Identifying antigen-specific Tfh cells is challenging due to their low frequency and transient expression of markers like PD-1 and CXCR5. Advancing techniques such as single-cell RNA sequencing and spatial transcriptomics, along with developing species-specific antibodies targeting CD4+ and GC Tfh cells, will improve our understanding of Tfh cells' roles in viral infections and support vaccine development.

Circulating Tfh (cTfh) cells are key biomarkers of systemic immune responses, especially in vaccine-induced immunity. While mainly studied in humans, their heterogeneity, unclear relationship with tissue-resident Tfh cells, and dynamic fluctuations complicate their use as reliable correlates of protection. Future research should prioritize refining cTfh phenotyping, standardizing measurement protocols, and exploring their role across diverse infectious diseases and vaccine platforms, which could also enhance viral control and vaccine efficacy in veterinary species exhibiting species-specific immune variations.

Exploring vaccines that induce Tfh cell responses is critical for enhancing protective immunity against viral infections. The development of novel vaccine platforms, such as mRNA vaccines and self-assembling protein nanocages, as well as their integration into synergistic strategies like SAPN-RNA vaccines, offers promising solutions to stimulate Tfh activation and improve antibody responses. Additionally, the inclusion of targeted adjuvants may further optimize these vaccines for stronger and longer-lasting immunity. Adjuvants such as TLR agonists, saponins, and STING agonists, along with another strategy like dendritic cell mRNA vaccines, may further support post-vaccination Tfh cell function during viral infections.

In summary, the development of vaccines that engage Tfh cell responses offers significant potential to improve prevention and control strategies for viral infections in both human and veterinary medicine.

Author Contributions: S.A. drafted the manuscript and designed the diagrams. D.P. and R.F. participated in manuscript writing and editing. All authors have read and agreed to the published version of the manuscript.

Funding: This research received no external funding.

Institutional Review Board Statement: Not applicable.

Informed Consent Statement: Not applicable.

Data Availability Statement: No new data were created or analyzed in this study. Data sharing is not applicable to this article.

Conflicts of Interest: The authors declare no conflicts of interest.

References

- 1. Murphy, F.A. Epidemiology of Human and Animal Viral Diseases. *Encycl. Virol.* 2008, 140–148. [CrossRef]
- 2. Ahmadivand, S.; Weidmann, M.; El-Matbouli, M.; Rahmati-Holasoo, H. Low pathogenic strain of infectious pancreatic necrosis virus (IPNV) associated with recent outbreaks in Iranian trout farms. *Pathogens* **2020**, *9*, 782. [CrossRef]
- 3. Boyd, M.A.A.; Hoppe, A.C.; Kelleher, A.D.; Munier, C.M.L. T follicular helper cell responses to SARS-CoV-2 vaccination among healthy and immunocompromised adults. *Immunol. Cell Biol.* **2023**, *101*, 504–513. [CrossRef]
- 4. Crotty, S. T follicular helper cell biology: A decade of discovery and diseases. *Immunity* 2019, 50, 1132–1148. [PubMed]
- 5. Vella, L.A.; Herati, R.S.; Wherry, E.J. CD4+ T Cell Differentiation in Chronic Viral Infections: The Tfh Perspective. *Trends Mol. Med.* **2017**, 23, 1072–1087. [PubMed]
- 6. Koutsakos, M.; Nguyen, T.H.O.; Kedzierska, K. With a Little Help from T Follicular Helper Friends: Humoral Immunity to Influenza Vaccination. *J. Immunol.* **2019**, 202, 360–367. [CrossRef]
- 7. He, R.; Zheng, X.; Zhang, J.; Liu, B.; Wang, Q.; Wu, Q.; Liu, Z.; Chang, F.; Hu, Y.; Xie, T.; et al. SARS-CoV-2 spike-specific TFH cells exhibit unique responses in infected and vaccinated individuals. *Sig. Transduct. Target. Ther.* **2023**, *8*, 393.
- 8. Ueno, H.; Banchereau, J.; Vinuesa, C.G. Pathophysiology of T follicular helper cells in humans and mice. *Nat. Immunol.* **2015**, *16*, 142–152.
- 9. Webb, L.M.C.; Fra-Bido, S.; Innocentin, S.; Matheson, L.S.; Attaf, N.; Bignon, A.; Novarino, J.; Fazilleau, N.; Linterman, M.A. Ageing promotes early T follicular helper cell differentiation by modulating expression of RBPJ. *Aging Cell* **2021**, 20, e13295. [CrossRef]
- 10. Shrivastava, S.; Carmen, J.M.; Lu, Z.; Basu, S.; Sankhala, R.S.; Chen, W.H.; Nguyen, P.; Chang, W.C.; King, J.; Corbitt, C.; et al. SARS-CoV-2 spike-ferritin-nanoparticle adjuvanted with ALFQ induces long-lived plasma cells and cross-neutralizing antibodies. *NPJ Vaccines* **2023**, *8*, 43.
- 11. Zhao, T.; Cai, Y.; Jiang, Y.; He, X.; Wei, Y.; Yu, Y.; Tian, X. Vaccine Adjuvants: Mechanisms and Platforms. *Signal Transduct. Target. Ther.* **2023**, *8*, 283. [PubMed]
- 12. Long, J.R.; Yu, C.X.; Cao, Y.M.; Miao, Y.Q.; Sun, H.S.; Zhang, Z.; Mai, J.; Wang, X.; Mao, Y.; Li, H.; et al. A rabies mRNA vaccine provides a rapid and long-term immune response in mice. *Nano Today* **2023**, *53*, 102038. [CrossRef]
- 13. Zhang, Z.; Mateus, J.; Coelho, C.H.; Dan, J.M.; Moderbacher, C.R.; Gálvez, R.I.; Cortes, F.H.; Grifoni, A.; Tarke, A.; Chang, J.; et al. Humoral and cellular immune memory to four COVID-19 vaccines. *Cell* 2022, 185, 2434–2451. [CrossRef] [PubMed]
- 14. Mudd, P.A.; Minervina, A.A.; Pogorelyy, M.V.; Turner, J.S.; Kim, W.; Kalaidina, E.; Petersen, J.; Schmitz, A.J.; Lei, T.; Haile, A.; et al. SARS-CoV-2 mRNA vaccination elicits a robust and persistent T follicular helper cell response in humans. *Cell* **2022**, *185*, 603–613.e15. [CrossRef]
- 15. Wang, W.; Zhou, X.; Bian, Y.; Wang, S.; Chai, Q.; Guo, Z.; Wang, Z.; Zhu, P.; Peng, H.; Yan, X.; et al. Dual-targeting nanoparticle vaccine elicits a therapeutic antibody response against chronic hepatitis B. *Nat. Nanotechnol.* **2020**, *15*, 406–416. [CrossRef]
- 16. Yang, J.X.; Tseng, J.C.; Tien, C.F.; Lee, C.Y.; Liu, Y.L.; Lin, J.J.; Tsai, P.J.; Liao, H.C.; Liu, S.J.; Su, Y.W.; et al. TLR9 and STING agonists cooperatively boost the immune response to SARS-CoV-2 RBD vaccine through an increased germinal center B cell response and reshaped T helper responses. *Int. J. Biol. Sci.* 2023, 19, 2897–2913. [CrossRef]
- 17. Alameh, M.G.; Tombácz, I.; Bettini, E.; Lederer, K.; Sittplangkoon, C.; Wilmore, J.R.; Gaudette, B.T.; Soliman, O.Y.; Pine, M.; Hicks, P.; et al. Lipid nanoparticles enhance the efficacy of mRNA and protein subunit vaccines by inducing robust T follicular helper cell and humoral responses. *Immunity* 2022, 54, 2877–2892.e7. [CrossRef]
- 18. Richert, L.E.; Servid, A.E.; Harmsen, A.L.; Rynda-Apple, A.; Han, S.; Wiley, J.A.; Douglas, T.; Harmsen, A.G. A virus-like particle vaccine platform elicits heightened and hastened local lung mucosal antibody production after a single dose. *Vaccine* **2012**, *30*, 3653–3665. [CrossRef]
- 19. Ahmadivand, S.; Fux, R.; Palić, D. Ferritin Vaccine Platform for Animal and Zoonotic Viruses. Vaccines 2024, 12, 1112. [CrossRef]

- 20. Le, T.; Sun, C.; Chang, J.; Zhang, G.; Yin, X. mRNA Vaccine Development for Emerging Animal and Zoonotic Diseases. *Viruses* **2022**, *14*, 401. [CrossRef]
- 21. Lamontagne, F.; Khatri, V.; St-Louis, P.; Bourgault, S.; Archambault, D. Vaccination Strategies Based on Bacterial Self-Assembling Proteins as Antigen Delivery Nanoscaffolds. *Vaccines* **2022**, *10*, 1920. [CrossRef]
- 22. Melo, M.; Porter, E.; Zhang, Y.; Silva, M.; Li, N.; Dobosh, B.; Liguori, A.; Skog, P.; Landais, E.; Menis, S.; et al. Immunogenicity of RNA Replicons Encoding HIV Env Immunogens Designed for Self-Assembly into Nanoparticles. *Mol. Ther.* **2019**, 27, 2080–2090. [CrossRef] [PubMed]
- 23. Xiong, F.; Zhang, C.; Shang, B.; Zheng, M.; Wang, Q.; Ding, Y.; Luo, J.; Li, X. An mRNA-based broad-spectrum vaccine candidate confers cross-protection against heterosubtypic influenza A viruses. *Emerg. Microbes Infect.* **2023**, *12*, 2256422. [CrossRef]
- 24. Klarquist, J.; Cross, E.W.; Thompson, S.B.; Willett, B.; Aldridge, D.L.; Caffrey-Carr, A.K.; Xu, Z.; Hunter, C.A.; Getahun, A.; Kedl, R.M. B cells promote CD8 T cell primary and memory responses to subunit vaccines. *Cell Rep.* **2021**, *36*, 36. [CrossRef]
- 25. Dong, C. Cytokine Regulation and Function in T Cells. Annu. Rev. Immunol. 2021, 39, 51–76. [CrossRef] [PubMed]
- 26. Vinuesa, C.G.; Linterman, M.A.; Yu, D.; MacLennan, I.C.M. Follicular helper T cells. *Annu. Rev. Immunol.* **2016**, *34*, 335–368. [CrossRef] [PubMed]
- 27. Yu, D.; Walker, L.S.K.; Liu, Z.; Linterman, M.A.; Li, Z. Targeting TFH cells in human diseases and vaccination: Rationale and practice. *Nat. Immunol.* **2022**, 23, 1157–1168. [CrossRef]
- 28. Schaerli, P.; Willimann, K.; Lang, A.B.; Lipp, M.; Loetscher, P.; Moser, B. CXC chemokine receptor 5 expression defines follicular homing T cells with B cell helper function. *J. Exp. Med.* **2000**, *192*, 1553–1562. [CrossRef]
- 29. Shi, J.; Hou, S.; Fang, Q.; Liu, X.; Liu, X.; Qi, H. PD-1 controls follicular T helper cell positioning and function. *Immunity* **2018**, 49, 264–274. [CrossRef]
- Goenka, R.; Barnett, L.G.; Silver, J.S.; O'Neill, P.J.; Hunter, C.A.; Cancro, M.P.; Laufer, T.M. Cutting edge: Dendritic cell-restricted antigen presentation initiates the follicular helper T cell program but cannot complete ultimate effector differentiation. *J. Immunol.* 2011, 187, 1091–1095. [CrossRef]
- 31. Choi, J.; Crotty, S. Bcl6-Mediated transcriptional regulation of follicular helper T cells (TFH). Trends Immunol. 2021, 42, 336–349.
- 32. Ma, L.; Zhang, L.; Zhuang, Y.; Ding, Y.; Chen, J. Lactobacillus Improves the Effects of Prednisone on Autoimmune Hepatitis via Gut Microbiota-Mediated Follicular Helper T Cells. *Cell Commun. Signal.* **2022**, *20*, 83.
- 33. Morita, R.; Schmitt, N.; Bentebibel, S.E.; Ranganathan, R.; Bourdery, L.; Zurawski, G.; Foucat, E.; Dullaers, M.; Oh, S.; Sabzghabaei, N.; et al. Human blood CXCR5(+) CD4(+) T cells are counterparts of T follicular cells and contain specific subsets that differentially support antibody secretion. *Immunity* 2011, 34, 108–121. [CrossRef]
- 34. Wallin, E.F.; Jolly, E.C.; Suchánek, O.; Bradley, J.A.; Espéli, M.; Jayne, D.R.; Linterman, M.A.; Smith, K.G. Human T-follicular helper and T-follicular regulatory cell maintenance is independent of germinal centers. *Blood* **2014**, *124*, 2666–2674. [CrossRef] [PubMed]
- 35. Farooq, F.; Beck, K.; Paolino, K.M.; Phillips, R.; Waters, N.C.; Regules, J.A.; Bergmann-Leitner, E.S. Circulating follicular T helper cells and cytokine profile in humans following vaccination with the rVSV-ZEBOV Ebola vaccine. *Sci. Rep.* **2016**, *6*, 27944.
- 36. Olatunde, A.C.; Hale, J.S.; Lamb, T.J. Cytokine-skewed Tfh cells: Functional consequences for B cell help. *Trends Immunol.* **2021**, 42, 536–550. [PubMed]
- 37. Mitsdoerffer, M.; Lee, Y.; Jäger, A.; Kim, H.J.; Korn, T.; Kolls, J.K.; Cantor, H.; Bettelli, E.; Kuchroo, V.K. Proinflammatory T helper type 17 cells are effective B-cell helpers. *Proc. Natl. Acad. Sci. USA* **2010**, 107, 14292–14297.
- 38. Yao, Y.; Wang, Z.-C.; Wang, N.; Zhou, P.-C.; Chen, C.-L.; Song, J.; Sun, B. Allergen Immunotherapy Improves Defective Follicular Regulatory T Cells in Patients with Allergic Rhinitis. *J. Allergy Clin. Immunol.* **2019**, 144, 118–128.
- 39. Gowthaman, U.; Chen, J.S.; Zhang, B.; Flynn, W.F.; Lu, Y.; Song, W.; Joseph, J.; Gertie, J.A.; Xu, L.; Collet, M.A.; et al. Identification of a T follicular helper cell subset that drives anaphylactic IgE. *Science* **2019**, *365*, eaaw6433.
- 40. King, I.L.; Fortier, A.; Tighe, M.; Dibble, J.; Watts, G.F.M.; Veerapen, N.; Haberman, A.M.; Besra, G.S.; Mohrs, M.; Brenner, M.B.; et al. Invariant natural killer T cells direct B cell responses to cognate lipid antigen in an IL-21-dependent manner. *Nat. Immunol.* **2011**, *13*, 44–50.
- 41. Gaya, M.; Barral, P.; Burbage, M.; Aggarwal, S.; Montaner, B.; Warren Navia, A.; Aid, M.; Tsui, C.; Maldonado, P.; Nair, U.; et al. Initiation of antiviral B cell immunity relies on innate signals from spatially positioned NKT cells. *Cell* **2018**, *172*, 517–533.e20. [CrossRef]
- 42. Abos, B.; Wang, T.; Secombes, C.J.; Tafalla, C. Distinct modes of action of CD40L and adaptive cytokines IL-2, IL-4/13, IL-10, and IL-21 on rainbow trout IgM+ B cells. *Dev. Comp. Immunol.* **2020**, *111*, 103752. [CrossRef] [PubMed]
- 43. Eto, D.; Lao, C.; DiToro, D.; Barnett, B.; Escobar, T.C.; Kageyama, R.; Yusuf, I.; Crotty, S. IL-21 and IL-6 are critical for different aspects of B cell immunity and redundantly induce optimal follicular helper CD4 T cell (Tfh) differentiation. *PLoS ONE* **2011**, *6*, e17739. [CrossRef] [PubMed]
- 44. Yeh, C.H.; Finney, J.; Okada, T.; Kurosaki, T.; Kelsoe, G. Primary germinal center-resident T follicular helper cells are a physiologically distinct subset of CXCR5hiPD-1hi T follicular helper cells. *Immunity* **2022**, *55*, 272–289.e7. [CrossRef] [PubMed]

- 45. Liu, Z.; Liu, S.; Zhang, Y.; Zeng, W.; Wang, S.; Ji, P.; Pan, M.; Zhu, C.; Wang, Y. Distinct roles of ICOS and CD40L in human T-B cell adhesion and antibody production. *Cell. Immunol.* **2021**, *368*, 104420. [CrossRef]
- 46. Reynaud, C.A.; Weill, J.C. Predicting AID off-targets: A step forward. J. Exp. Med. 2018, 215, 721–722. [CrossRef]
- 47. Turner, J.S.; Ke, F.; Grigorova, I.L. B Cell Receptor Crosslinking Augments Germinal Center B Cell Selection when T Cell Help Is Limiting. *Cell Rep.* **2018**, 25, 1395–1403.e4. [CrossRef]
- 48. Xie, M.M.; Dent, A.L. Unexpected Help: Follicular Regulatory T Cells in the Germinal Center. *Front. Immunol.* **2018**, *9*, 1536. [CrossRef]
- 49. Chen, J.S.; Grassmann, J.D.S.; Gowthaman, U.; Olyha, S.J.; Simoneau, T.; Berin, M.C.; Eisenbarth, S.C.; Williams, A. Flow Cytometric Identification of Tfh13 Cells in Mouse and Human. *J. Allergy Clin. Immunol.* **2021**, 147, 470–483. [CrossRef]
- 50. Qin, L.; Waseem, T.C.; Sahoo, A.; Bieerkehazhi, S.; Zhou, H.; Galkina, E.V.; Nurieva, R. Insights Into the Molecular Mechanisms of T Follicular Helper-Mediated Immunity and Pathology. *Front. Immunol.* **2018**, *9*, 1884. [CrossRef]
- 51. Hoog, A.; Villanueva-Hernández, S.; Razavi, M.A.; van Dongen, K.; Eder, T.; Piney, L.; Chapat, L.; de Luca, K.; Grebien, F.; Mair, K.H.; et al. Identification of CD4+ T cells with T follicular helper cell characteristics in the pig. *Dev. Comp. Immunol.* **2022**, 134, 104462. [CrossRef] [PubMed]
- 52. Von La Roche, D.; Schumacher, M.; Kohn, M.; Trapp, J.; Schusser, B.; Rautenschlein, S.; Härtle, S. Characterization of class-switched B cells in chickens. *Front. Immunol.* **2024**, *15*, 1484288.
- 53. Xiao, N.; Eto, D.; Elly, C.; Peng, G.; Crotty, S.; Liu, Y.-C. The E3 ubiquitin ligase Itch is required for the differentiation of follicular helper T cells. *Nat. Immunol.* **2014**, *15*, 657–666. [PubMed]
- 54. Velu, V.; Mylvaganam, G.H.; Gangadhara, S.; Hong, J.J.; Iyer, S.S.; Gumber, S.; Ibegbu, C.C.; Villinger, F.; Amara, R.R. Induction of Th1-biased T follicular helper (Tfh) cells in lymphoid tissues during chronic simian immunodeficiency virus infection defines functionally distinct germinal center Tfh cells. *J. Immunol.* **2016**, *197*, 1832–1842.
- 55. Juno, J.A.; Hill, D.L. T follicular helper cells and their impact on humoral responses during pathogen and vaccine challenge. *Curr. Opin. Immunol.* **2022**, *74*, 112–117. [PubMed]
- Yusuf, I.; Kageyama, R.; Monticelli, L.; Johnston, R.J.; Ditoro, D.; Hansen, K.; Barnett, B.; Crotty, S. Germinal center T follicular helper cell IL-4 production is dependent on signaling lymphocytic activation molecule receptor (CD150). *J. Immunol.* 2010, 185, 190–202.
- 57. Carpio, V.H.; Aussenac, F.; Puebla-Clark, L.; Wilson, K.D.; Villarino, A.V.; Dent, A.L.; Stephens, R. T Helper Plasticity Is Orchestrated by STAT3, Bcl6, and Blimp-1 Balancing Pathology and Protection in Malaria. *iScience* **2020**, 23, 101310.
- 58. Borrow, P.; Tishon, A.; Lee, S.; Xu, J.; Grewal, I.S.; Oldstone, M.B.; A Flavell, R. CD40L-Deficient Mice Show Deficits in Antiviral Immunity and Have an Impaired Memory CD8+ CTL Response. *J. Exp. Med.* 1996, 183, 2129–2142. [CrossRef]
- 59. Bertram, E.M.; Tafuri, A.; Shahinian, A.; Chan, V.S.; Hunziker, L.; Recher, M.; Ohashi, P.S.; Mak, T.W.; Watts, T.H. Role of ICOS versus CD28 in Antiviral Immunity. *Eur. J. Immunol.* **2002**, *32*, 3376–3385. [CrossRef]
- 60. Huang, Q.; Hu, J.; Tang, J.; Xu, L.; Ye, L. Molecular Basis of the Differentiation and Function of Virus-Specific Follicular Helper CD4+ T Cells. *Front. Immunol.* **2019**, *10*, 249. [CrossRef]
- 61. Liang, H.; Tang, J.; Liu, Z.; Liu, Y.; Huang, Y.; Xu, Y.; Hao, P.; Yin, Z.; Zhong, J.; Ye, L.; et al. ZIKV infection induces robust Th1-like Tfh cell and long-term protective antibody responses in immunocompetent mice. *Nat. Commun.* **2019**, *10*, 3859. [CrossRef] [PubMed]
- 62. Dan, J.M.; Mateus, J.; Kato, Y.; Hastie, K.M.; Yu, E.D.; Faliti, C.E.; Grifoni, A.; Ramirez, S.I.; Haupt, S.; Frazier, A.; et al. Immunological memory to SARS-CoV-2 assessed for up to 8 months after infection. *Science* **2021**, *371*, eabf4063. [CrossRef] [PubMed]
- 63. Brenna, E.; Davydov, A.N.; Ladell, K.; McLaren, J.E.; Bonaiuti, P.; Metsger, M.; Ramsden, J.D.; Gilbert, S.C.; Lambe, T.; Price, D.A.; et al. CD4+ T Follicular Helper Cells in Human Tonsils and Blood Are Clonally Convergent but Divergent from Non-Tfh CD4+ Cells. *Cell Rep.* 2020, 30, 137–152.e5. [CrossRef]
- 64. Devarajan, P.; Vong, A.M.; Castonguay, C.H.; Kugler-Umana, O.; Bautista, B.L.; Jones, M.C.; Kelly, K.A.; Xia, J.; Swain, S.L. Strong Influenza-Induced Tfh Generation Requires CD4 Effectors to Recognize Antigen Locally and Receive Signals from Continuing Infection. *Proc. Natl. Acad. Sci. USA* **2022**, *119*, e2111064119. [CrossRef]
- 65. Harker, J.A.; Dolgoter, A.; Zuniga, E.I. Cell-Intrinsic IL-27 and gp130 Cytokine Receptor Signaling Regulates Virus-Specific CD4+ T Cell Responses and Viral Control during Chronic Infection. *Immunity* 2013, 39, 548–559. [CrossRef]
- 66. Zhang, J.; Liu, W.; Wen, B.; Xie, T.; Tang, P.; Hu, Y.; Huang, L.; Jin, K.; Zhang, P.; Liu, Z.; et al. Circulating CXCR3+ Tfh cells positively correlate with neutralizing antibody responses in HCV-infected patients. *Sci. Rep.* **2019**, *9*, 10090. [CrossRef] [PubMed]
- 67. Moysi, E.; Petrovas, C.; Koup, R.A. The role of follicular helper CD4 T cells in the development of HIV-1 specific broadly neutralizing antibody responses. *Retrovirology* **2018**, *15*, 54. [CrossRef]
- 68. Perreau, M.; Savoye, A.L.; De Crignis, E.; Corpataux, J.M.; Cubas, R.; Haddad, E.K.; De Leval, L.; Graziosi, C.; Pantaleo, G. Follicular helper T cells serve as the major CD4 T cell compartment for HIV-1 infection, replication, and production. *J. Exp. Med.* **2013**, *210*, 143–156. [CrossRef]

- 69. Day, C.L.; Kaufmann, D.E.; Kiepiela, P.; Brown, J.A.; Moodley, E.S.; Reddy, S.; Mackey, E.W.; Miller, J.D.; Leslie, A.J.; DePierres, C.; et al. PD-1 expression on HIV-specific T cells is associated with T-cell exhaustion and disease progression. *Nature* **2006**, 443, 350–354. [CrossRef]
- 70. Soltani, M.; Ahmadivand, S.; Behdani, M.; Hassanzadeh, R.; Rahmati-Holasoo, H.; Taheri-Mirghaed, A. Transcription of adaptive-immune genes upon challenge with infectious pancreatic necrosis virus (IPNV) in DNA vaccinated rainbow trout. *Int. J. Aquat. Biol.* **2016**, *4*, 353–359.
- 71. Ella, R.; Reddy, S.; Jogdand, H.; Sarangi, V.; Ganneru, B.; Prasad, S.; Das, D.; Raju, D.; Praturi, U.; Sapkal, G.; et al. Safety and immunogenicity of an inactivated SARS-CoV-2 vaccine, BBV152: Interim results from a double-blind, randomised, multicentre, phase 2 trial, and 3-month follow-up of a double-blind, randomised phase 1 trial. *Lancet Infect. Dis.* **2021**, 21, 950–961. [PubMed]
- 72. Ahmadivand, S.; Soltani, M.; Shokrpoor, S.; Rahmati-Holasoo, H.; El-Matbouli, M.; Taheri-Mirghaed, A. Cyprinid Herpesvirus 3 (CyHV-3) Transmission and Outbreaks in Iran: Detection and Characterization in Farmed Common Carp. *Microb. Pathog.* 2020, 149, 104321. [CrossRef]
- 73. Song, Y.; Wang, J.; Yang, Z.; He, Q.; Bao, C.; Xie, Y.; Sun, Y.; Li, S.; Quan, Y.; Yang, H.; et al. Heterologous booster vaccination enhances antibody responses to SARS-CoV-2 by improving Tfh function and increasing B-cell clonotype SHM frequency. *Front. Immunol.* **2024**, *15*, 1406138.
- 74. Dillard, J.A.; Taft-Benz, S.A.; Knight, A.C.; Anderson, E.J.; Pressey, K.D.; Parotti, B.; Martinez, S.A.; Diaz, J.L.; Sarkar, S.; Madden, E.A.; et al. Adjuvant-Dependent Impact of Inactivated SARS-CoV-2 Vaccines during Heterologous Infection by a SARS-Related Coronavirus. *Nat. Commun.* 2024, 15, 3738.
- 75. Zhao, H.; Yang, J.; Qian, Q.; Wu, M.; Li, M.; Xu, W. Mesenteric CD103+DCs Initiate Switched Coxsackievirus B3 VP1-Specific IgA Response to Intranasal Chitosan-DNA Vaccine Through Secreting BAFF/IL-6 and Promoting Th17/Tfh Differentiation. *Front. Immunol.* 2018, 9, 2986.
- 76. Ahmadivand, S.; Soltani, M.; Behdani, M.; Evensen, Ø.; Alirahimi, E.; Soltani, E.; Hassanzadeh, R.; Ashrafi-Helan, J. VP2 (PTA motif) encoding DNA vaccine confers protection against lethal challenge with infectious pancreatic necrosis virus (IPNV) in trout. *Mol. Immunol.* 2018, 94, 61–67. [CrossRef]
- 77. Lee, J.H.; Hu, J.K.; Georgeson, E.; Nakao, C.; Groschel, B.; Dileepan, T.; Jenkins, M.K.; Seumois, G.; Vijayanand, P.; Schief, W.R.; et al. Modulating the Quantity of HIV Env-Specific CD4 T Cell Help Promotes Rare B Cell Responses in Germinal Centers. *J. Exp. Med.* 2021, 218, e20201254.
- 78. Ahmadivand, S.; Soltani, M.; Behdani, M.; Evensen, Ø.; Alirahimi, E.; Hasanzadeh, R.; Soltani, E. Oral DNA vaccines based on CS-TPP nanoparticles and alginate microparticles confer high protection against infectious pancreatic necrosis virus (IPNV) infection in trout. *Dev. Comp. Immunol.* 2017, 74, 178–189. [CrossRef]
- 79. Baumjohann, D.; Preite, S.; Reboldi, A.; Ronchi, F.; Ansel, K.M.; Lanzavecchia, A.; Sallusto, F. Persistent Antigen and Germinal Center B Cells Sustain T Follicular Helper Cell Responses and Phenotype. *Immunity* **2013**, *38*, 596–605.
- 80. Havenar-Daughton, C.; Newton, I.G.; Zare, S.Y.; Reiss, S.M.; Schwan, B.; Suh, M.J.; Hasteh, F.; Levi, G.; Crotty, S. Normal Human Lymph Node T Follicular Helper Cells and Germinal Center B Cells Accessed via Fine Needle Aspirations. *J. Immunol. Methods* **2020**, 479, 112746.
- 81. Locci, M.; Havenar-Daughton, C.; Landais, E.; Wu, J.; Kroenke, M.A.; Arlehamn, C.L.; Su, L.F.; Cubas, R.; Davis, M.M.; Sette, A.; et al. Human Circulating PD-1+CXCR3-CXCR5+ Memory Tfh Cells Are Highly Functional and Correlate with Broadly Neutralizing HIV Antibody Responses. *Immunity* 2013, 39, 758–769. [PubMed]
- 82. Hill, D.L.; Whyte, C.E.; Innocentin, S.; Lee, J.; Dooley, J.; Wang, J.; James, E.A.; Lee, J.C.; Kwok, W.W.; Zand, M.S.; et al. Impaired HA-Specific T Follicular Helper Cell and Antibody Responses to Influenza Vaccination Are Linked to Inflammation in Humans. *eLife* 2021, 10, e70554.
- 83. Havenar-Daughton, C.; Carnathan, D.G.; Torrents de la Peña, A.; Pauthner, M.; Briney, B.; Reiss, S.M.; Wood, J.S.; Kaushik, K.; van Gils, M.J.; Rosales, S.L.; et al. Direct Probing of Germinal Center Responses Reveals Immunological Features and Bottlenecks for Neutralizing Antibody Responses to HIV Env Trimer. *Cell Rep.* **2016**, *17*, 2195–2209.
- 84. Painter, M.M.; Mathew, D.; Goel, R.R.; Apostolidis, S.A.; Pattekar, A.; Kuthuru, O.; Baxter, A.E.; Herati, R.S.; Oldridge, D.A.; Gouma, S.; et al. Rapid Induction of Antigen-Specific CD4+ T Cells Is Associated with Coordinated Humoral and Cellular Immunity to SARS-CoV-2 mRNA Vaccination. *Immunity* 2021, 54, 2133–2142.e3. [CrossRef]
- 85. Yin, M.; Xiong, Y.; Liang, D.; Tang, H.; Hong, Q.; Liu, G.; Zeng, J.; Lian, T.; Huang, J.; Ni, J. Circulating Tfh Cell and Subsets Distribution Are Associated with Low-Responsiveness to Hepatitis B Vaccination. *Mol. Med.* **2021**, *27*, 32.
- 86. Aljurayyan, A.; Puksuriwong, S.; Ahmed, M.; Sharma, R.; Krishnan, M.; Sood, S.; Davies, K.; Rajashekar, D.; Leong, S.; McNamara, P.S.; et al. Activation and Induction of Antigen-Specific T Follicular Helper Cells Play a Critical Role in Live-Attenuated Influenza Vaccine-Induced Human Mucosal Anti-Influenza Antibody Response. J. Virol. 2018, 92, e00114-18. [PubMed]
- 87. Sahin, U.; Muik, A.; Derhovanessian, E.; Vogler, I.; Kranz, L.M.; Vormehr, M.; Baum, A.; Pascal, K.; Quandt, J.; Maurus, D.; et al. COVID-19 Vaccine BNT162b1 Elicits Human Antibody and TH1 T Cell Responses. *Nature* 2020, 586, 594–599. [PubMed]

- 88. Mu, Z.; Wiehe, K.; Saunders, K.O.; Henderson, R.; Cain, D.W.; Parks, R.; Martik, D.; Mansouri, K.; Edwards, R.J.; Newman, A.; et al. mRNA-encoded HIV-1 Env trimer ferritin nanoparticles induce monoclonal antibodies that neutralize heterologous HIV-1 isolates in mice. *Cell Rep.* **2022**, *38*, 110514. [CrossRef]
- 89. Gote, V.; Bolla, P.K.; Kommineni, N.; Butreddy, A.; Nukala, P.K.; Palakurthi, S.S.; Khan, W. A Comprehensive Review of mRNA Vaccines. *Int. J. Mol. Sci.* **2023**, *24*, 2700. [CrossRef]
- 90. Son, S.; Lee, K. Development of mRNA Vaccines/Therapeutics and Their Delivery System. Mol. Cells 2023, 46, 41–47.
- 91. Schmidt, C.; Schnierle, B.S. Self-Amplifying RNA Vaccine Candidates: Alternative Platforms for mRNA Vaccine Development. *Pathogens* **2023**, 12, 138. [CrossRef] [PubMed]
- 92. Blakney, A.K.; Ip, S.; Geall, A.J. An Update on Self-Amplifying mRNA Vaccine Development. *Vaccines* **2021**, *9*, 97. [CrossRef] [PubMed]
- 93. Komori, M.; Nogimori, T.; Morey, A.L.; Sekida, T.; Ishimoto, K.; Hassett, M.R.; Masuta, Y.; Ode, H.; Tamura, T.; Suzuki, R.; et al. saRNA vaccine expressing membrane-anchored RBD elicits broad and durable immunity against SARS-CoV-2 variants of concern. *Nat. Commun.* 2023, 14, 2810. [CrossRef]
- 94. Pardi, N.; Hogan, M.J.; Porter, F.W.; Weissman, D. mRNA Vaccines-A New Era in Vaccinology. *Nat. Rev. Drug Discov.* **2018**, 17, 261–279.
- 95. Shim, M.S.; Kwon, Y.J. Stimuli-Responsive Polymers and Nanomaterials for Gene Delivery and Imaging Applications. *Adv. Drug Deliv. Rev.* **2012**, *64*, 1046–1059. [CrossRef]
- 96. Guidotti, G.; Brambilla, L.; Rossi, D. Cell-Penetrating Peptides: From Basic Research to Clinics. *Trends Pharmacol. Sci.* **2017**, *38*, 406–424. [CrossRef]
- 97. Goel, R.R.; Painter, M.M.; Apostolidis, S.A.; Mathew, D.; Meng, W.; Rosenfeld, A.M.; Lundgreen, K.A.; Reynaldi, A.; Khoury, D.S.; Pattekar, A.; et al. mRNA Vaccines Induce Durable Immune Memory to SARS-CoV-2 and Variants of Concern. *Science* 2021, 374, abm0829. [CrossRef] [PubMed]
- 98. Cagigi, A.; Loré, K. Immune Responses Induced by mRNA Vaccination in Mice, Monkeys, and Humans. *Vaccines* **2021**, *9*, 61. [CrossRef]
- 99. Verbeke, R.; Hogan, M.J.; Loré, K.; Pardi, N. Innate Immune Mechanisms of mRNA Vaccines. *Immunity* **2022**, *55*, 1993–2005. [CrossRef]
- 100. Lindgren, G.; Ols, S.; Liang, F.; Thompson, E.A.; Lin, A.; Hellgren, F.; Bahl, K.; John, S.; Yuzhakov, O.; Hassett, K.J.; et al. Induction of Robust B Cell Responses after Influenza mRNA Vaccination Is Accompanied by Circulating Hemagglutinin-Specific ICOS+PD-1+ CXCR3+ T Follicular Helper Cells. Front. Immunol. 2017, 8, 1539. [CrossRef]
- 101. Richner, J.M.; Himansu, S.; Dowd, K.A.; Butler, S.L.; Salazar, V.; Fox, J.M.; Julander, J.G.; Tang, W.W.; Shresta, S.; Pierson, T.C.; et al. Modified mRNA Vaccines Protect against Zika Virus Infection. *Cell* 2017, 168, 1114–1125.e10. [PubMed]
- 102. Fazel, F.; Doost, J.S.; Raj, S.; Boodhoo, N.; Karimi, K.; Sharif, S. The mRNA Vaccine Platform for Veterinary Species. *Vet. Immunol. Immunopathol.* **2024**, 274, 110803. [CrossRef]
- 103. Bian, T.; Hao, M.; Zhao, X.; Zhao, C.; Luo, G.; Zhang, Z.; Fu, G.; Yang, L.; Chen, Y.; Wang, Y.; et al. A Rift Valley fever mRNA vaccine elicits strong immune responses in mice and rhesus macaques. *npj Vaccines* **2023**, *8*, 164.
- 104. Pulido, M.R.; Sobrino, F.; Borrego, B.; Sáiz, M. RNA immunization can protect mice against foot-and-mouth disease virus. *Antivir. Res.* **2010**, *85*, 556–558. [PubMed]
- 105. Hajam, I.A.; Senevirathne, A.; Hewawaduge, C.; Kim, J.; Lee, J.H. Intranasally administered protein-coated chitosan nanoparticles encapsulating influenza H9N2 HA2 and M2e mRNA molecules elicit protective immunity against avian influenza viruses in chickens. *Vet. Res.* **2020**, *51*, 37. [CrossRef] [PubMed]
- 106. Huang, J.; Hu, Y.; Niu, Z.; Hao, W.; Ketema, H.; Wang, Z.; Xu, J.; Sheng, L.; Cai, Y.; Yu, Z.; et al. Preclinical Efficacy of Cap-Dependent and Independent mRNA Vaccines against Bovine Viral Diarrhea Virus-1. *Vet. Sci.* **2024**, *11*, 373. [CrossRef]
- 107. Gong, L.; Zhang, Y.; Wang, L.; Zhao, X.; Wang, L.; Qiu, X.; Yang, X.; Zhu, W.; Lv, L.; Kang, Y.; et al. Advancing vaccine development: Evaluation of a mannose-modified lipid nanoparticle-based candidate for African swine fever p30 mRNA vaccine eliciting robust immune response in mice. *Int. J. Biol. Macromol.* 2024, 270 Pt 1, 132432.
- 108. Vander Veen, R.L.; Loynachan, A.T.; Mogler, M.A.; Russell, B.J.; Harris, D.L.; Kamrud, K.I. Safety, Immunogenicity, and Efficacy of an Alphavirus Replicon-Based Swine Influenza Virus Hemagglutinin Vaccine. *Vaccine* **2012**, *30*, 1944–1950.
- 109. Zhou, L.; Wubshet, A.K.; Zhang, J.; Hou, S.; Yao, K.; Zhao, Q.; Dai, J.; Liu, Y.; Ding, Y.; Zhang, J.; et al. The mRNA Vaccine Expressing Single and Fused Structural Proteins of Porcine Reproductive and Respiratory Syndrome Induces Strong Cellular and Humoral Immune Responses in BalB/C Mice. *Viruses* 2024, 16, 544. [CrossRef]
- 110. Gupta, S.; Su, H.; Agrawal, S. Immune Response to SARS-CoV-2 Vaccine in 2 Men. *Int. Arch. Allergy Immunol.* **2022**, *183*, 350–359. [CrossRef]
- 111. Yu, T.; Zhang, C.; Xing, J.; Zhang, T.; Xu, Z.; Di, Y.; Yang, S.; Jiang, R.; Tang, J.; Zhuang, X.; et al. Ferritin-binding and ubiquitination-modified mRNA vaccines induce potent immune responses and protective efficacy against SARS-CoV-2. *Int. Immunopharmacol.* 2024, 129, 111630.

- 112. Roier, S.; Mangala Prasad, V.; McNeal, M.M.; Lee, K.K.; Petsch, B.; Rauch, S. mRNA-based VP8* nanoparticle vaccines against rotavirus are highly immunogenic in rodents. *npj Vaccines* **2023**, *8*, 190. [CrossRef] [PubMed]
- 113. Brandys, P.; Montagutelli, X.; Merenkova, I.; Barut, G.T.; Thiel, V.; Schork, N.J.; Trüeb, B.; Conquet, L.; Deng, A.; Antanasijevic, A.; et al. A mRNA Vaccine Encoding for a RBD 60-mer Nanoparticle Elicits Neutralizing Antibodies and Protective Immunity Against the SARS-CoV-2 Delta Variant in Transgenic K18-hACE2 Mice. *Front. Immunol.* 2022, 13, 912898.
- 114. Kelly, H.G.; Tan, H.X.; Juno, J.A.; Esterbauer, R.; Ju, Y.; Jiang, W.; Wimmer, V.C.; Duckworth, B.C.; Groom, J.R.; Caruso, F.; et al. Self-Assembling Influenza Nanoparticle Vaccines Drive Extended Germinal Center Activity and Memory B Cell Maturation. *JCI Insight* 2020, 5, e136653. [PubMed]
- 115. Jung, H.-G.; Jeong, S.; Kang, M.-J.; Hong, I.; Park, Y.-S.; Ko, E.; Kim, J.-O.; Choi, D.-Y. Molecular Design of Encapsulin Protein Nanoparticles to Display Rotavirus Antigens for Enhancing Immunogenicity. *Vaccines* **2024**, *12*, 1020. [CrossRef]
- 116. Wichgers Schreur, P.J.; Tacken, M.; Gutjahr, B.; Keller, M.; van Keulen, L.; Kant, J.; van de Water, S.; Lin, Y.; Eiden, M.; Rissmann, M.; et al. Vaccine Efficacy of Self-Assembled Multimeric Protein Scaffold Particles Displaying the Glycoprotein Gn Head Domain of Rift Valley Fever Virus. *Vaccines* **2021**, *9*, 301. [CrossRef]
- 117. Soltani, M.; Zamani, M.; Taheri-Mirghaed, A.; Ahmadivand, S.; Mohamdian, S.; Abdi, K.; Soltani, E. Incidence and Genetic Analysis of White Spot Syndrome Virus (WSSV) in Farmed Shrimps (*P. indicus* and *L. vannamei*) in Iran. *Bull. Eur. Assoc. Fish. Pathol.* 2018, 38, 24–34.
- 118. Ahmadivand, S.; Palić, D.; Weidmann, M. Molecular Epidemiology of Novirhabdoviruses Emerging in Iranian Trout Farms. *Viruses* **2021**, *13*, 448. [CrossRef]
- 119. Rahmati-Holasoo, H.; Ahmadivand, S.; Marandi, A.; Shokrpoor, S.; Palić, D.; Jahangard, A. Identification and Characterization of Lymphocystis Disease Virus (LCDV) from Indian Glassy Fish (*Parambassis ranga* Hamilton, 1822) in Iran. *Aquacult. Int.* **2022**, *30*, 2593–2602.
- 120. Dahl, L.O.S.; Hak, S.; Braaen, S.; Molska, A.; Rodà, F.; Parot, J.; Wessel, Ø.; Fosse, J.H.; Bjørgen, H.; Borgos, S.E.; et al. Implementation of mRNA-Lipid Nanoparticle Technology in Atlantic Salmon (*Salmo salar*). *Vaccines* **2024**, 12, 788. [CrossRef]
- 121. See, S.A.; Bhassu, S.; Tang, S.S.; Yusoff, K. Newly Developed mRNA Vaccines Induce Immune Responses in Litopenaeus vannamei Shrimps During Primary Vaccination. *Dev. Comp. Immunol.* **2024**, *1*62, 105264.
- 122. Soltani, M.; Ahmadivand, S.; Ringø, E. Chapter 11—Bacillus as Probiotics in Shellfish Culture. In *Bacillus Probiotics for Sustainable Aquaculture*; Soltani, M., Elumalai, P., Ghosh, K., Ringø, E., Eds.; Taylor & Francis': Abingdon, UK; CRC Press: Boca Raton, FL, USA, 2024; p. 280.
- 123. Duhen, R.; Beymer, M.; Jensen, S.M.; Abbina, S.; Abraham, S.; Jain, N.; Thomas, A.; Geall, A.J.; Hu, H.M.; Fox, B.A.; et al. OX40 Agonist Stimulation Increases and Sustains Humoral and Cell-Mediated Responses to SARS-CoV-2 Protein and saRNA Vaccines. *Front. Immunol.* 2022, *13*, 896310. [CrossRef]
- 124. Brook, B.; Duval, V.; Barman, S.; Speciner, L.; Sweitzer, C.; Khanmohammed, A.; Menon, M.; Foster, K.; Ghosh, P.; Abedi, K.; et al. Adjuvantation of a SARS-CoV-2 mRNA Vaccine with Controlled Tissue-Specific Expression of an mRNA Encoding IL-12p70. *Sci. Transl. Med.* 2024, 16, eadm8451. [PubMed]
- 125. Zepeda-Cervantes, J.; Ramírez-Jarquín, J.O.; Vaca, L. Interaction Between Virus-Like Particles (VLPs) and Pattern Recognition Receptors (PRRs) from Dendritic Cells (DCs): Toward Better Engineering of VLPs. Front. Immunol. 2020, 11, 1100.
- 126. Ahmadivand, S.; Krpetic, Z.; Martínez, M.M.; García-Ordoñez, M.; Roher, N.; Palić, D. Self-assembling ferritin nanoplatform for the development of infectious hematopoietic necrosis virus vaccine. *Front. Immunol.* **2024**, *15*, 1346512.
- 127. Nguyen, B.; Tolia, N.H. Protein-based antigen presentation platforms for nanoparticle vaccines. npj Vaccines 2021, 6, 70.
- 128. Pandey, K.K.; Sahoo, B.R.; Pattnaik, A.K. Protein Nanoparticles as Vaccine Platforms for Human and Zoonotic Viruses. *Viruses* **2024**, *16*, 936. [CrossRef]
- 129. Brune, K.D.; Howarth, M. New Routes and Opportunities for Modular Construction of Particulate Vaccines: Stick, Click, and Glue. *Front. Immunol.* **2018**, *9*, 1432.
- 130. Inoue, T.; Baba, Y.; Kurosaki, T. BCR Signaling in Germinal Center B Cell Selection. Trends Immunol. 2024, 45, 693–704.
- 131. Lainšček, D.; Fink, T.; Forstnerič, V.; Hafner-Bratkovič, I.; Orehek, S.; Strmšek, Ž.; Manček-Keber, M.; Pečan, P.; Esih, H.; Malenšek, Š.; et al. A Nanoscaffolded Spike-RBD Vaccine Provides Protection against SARS-CoV-2 with Minimal Anti-Scaffold Response. *Vaccines* 2021, 9, 431. [CrossRef]
- 132. Kanekiyo, M.; Wei, C.-J.; Yassine, H.M.; McTamney, P.M.; Boyington, J.C.R.; Whittle, J.R.; Rao, S.S.; Kong, W.-P.; Wang, L.; Nabel, G.J. Self-Assembling Influenza Nanoparticle Vaccines Elicit Broadly Neutralizing H1N1 Antibodies. *Nature* **2013**, 499, 102–106.
- 133. Carmen, J.M.; Shrivastava, S.; Lu, Z.; Anderson, A.; Morrison, E.B.; Sankhala, R.S.; Chen, W.H.; Chang, W.C.; Bolton, J.S.; Matyas, G.R.; et al. SARS-CoV-2 ferritin nanoparticle vaccine induces robust innate immune activity driving polyfunctional spike-specific T cell responses. *Npj Vaccines* **2021**, *6*, 151.
- 134. Aebischer, A.; Wernike, K.; König, P.; Franzke, K.; Wichgers Schreur, P.J.; Kortekaas, J.; Vitikainen, M.; Wiebe, M.; Saloheimo, M.; Tchelet, R.; et al. Development of a Modular Vaccine Platform for Multimeric Antigen Display Using an Orthobunyavirus Model. *Vaccines* 2021, 9, 651. [CrossRef] [PubMed]

- 135. Zhang, B.; Chao, C.W.; Tsybovsky, Y.; Abiona, O.M.; Hutchinson, G.B.; Moliva, J.I.; Olia, A.S.; Pegu, A.; Phung, E.; Stewart-Jones, G.B.E.; et al. A platform incorporating trimeric antigens into self-assembling nanoparticles reveals SARS-CoV-2-spike nanoparticles to elicit substantially higher neutralizing responses than spike alone. *Sci. Rep.* **2020**, *10*, 18149. [CrossRef]
- 136. He, L.; de Val, N.; Morris, C.D.; Vora, N.; Thinnes, T.C.; Kong, L.; Azadnia, P.; Sok, D.; Zhou, B.; Burton, D.R.; et al. Presenting native-like trimeric HIV-1 antigens with self-assembling nanoparticles. *Nat. Commun.* **2016**, *7*, 12041. [CrossRef] [PubMed]
- 137. He, L.; Lin, X.; Wang, Y.; Abraham, C.; Sou, C.; Ngo, T.; Zhang, Y.; Wilson, I.A.; Zhu, J. Single-component, self-assembling, protein nanoparticles presenting the receptor binding domain and stabilized spike as SARS-CoV-2 vaccine candidates. *Sci. Adv.* **2021**, 7, eabf1591. [PubMed]
- 138. Kar, U.; Khaleeq, S.; Garg, P.; Bhat, M.; Reddy, P.; Vignesh, V.S.; Upadhyaya, A.; Das, M.; Chakshusmathi, G.; Pandey, S.; et al. Comparative Immunogenicity of Bacterially Expressed Soluble Trimers and Nanoparticle Displayed Influenza Hemagglutinin Stem Immunogens. *Front. Immunol.* **2022**, *13*, 890622.
- 139. Khaleeq, S.; Sengupta, N.; Kumar, S.; Patel, U.R.; Rajmani, R.S.; Reddy, P.; Pandey, S.; Singh, R.; Dutta, S.; Ringe, R.P.; et al. Neutralizing Efficacy of Encapsulin Nanoparticles against SARS-CoV2 Variants of Concern. *Viruses* 2023, 15, 346. [CrossRef]
- 140. Sheng, Y.; Chen, Z.; Cherrier, M.V.; Martin, L.; Bui, T.T.T.; Li, W.; Lynham, S.; Nicolet, Y.; Ebrahimi, K.H. A Versatile Virus-Mimetic Engineering Approach for Concurrent Protein Nanocage Surface-Functionalization and Cargo Encapsulation. *Small* **2024**, 20, e2310913.
- 141. Langenmayer, M.C.; Luelf-Averhoff, A.T.; Marr, L.; Jany, S.; Freudenstein, A.; Adam-Neumair, S.; Tscherne, A.; Fux, R.; Rojas, J.J.; Blutke, A.; et al. Newly Designed Poxviral Promoters to Improve Immunogenicity and Efficacy of MVA-NP Candidate Vaccines against Lethal Influenza Virus Infection in Mice. *Pathogens* **2023**, *12*, 867. [CrossRef]
- 142. Riteau, N.; Radtke, A.J.; Shenderov, K.; Mittereder, L.; Oland, S.D.; Hieny, S.; Jankovic, D.; Sher, A. Water-in-Oil-Only Adjuvants Selectively Promote T Follicular Helper Cell Polarization through a Type I IFN and IL-6-Dependent Pathway. *J. Immunol.* 2016, 197, 3884–3893. [CrossRef] [PubMed]
- 143. Serre, K.; Mohr, E.; Benezech, C.; Bird, R.; Khan, M.; Caamano, J.H.; Cunningham, A.F.; Maclennan, I.C. Selective effects of NF-κB1 deficiency in CD4(+) T cells on Th2 and Tfh induction by alum-precipitated protein vaccines. *Eur. J. Immunol.* **2011**, 41, 1573–1582. [CrossRef] [PubMed]
- 144. Robinson, C.; Baehr, C.; Schmiel, S.E.; Accetturo, C.; Mueller, D.L.; Pravetoni, M. Alum adjuvant is more effective than MF59 at prompting early germinal center formation in response to peptide-protein conjugates and enhancing efficacy of a vaccine against opioid use disorders. *Hum. Vaccin. Immunother.* **2019**, *15*, 909–917. [CrossRef]
- 145. Hill, D.L.; Pierson, W.; Bolland, D.J.; Mkindi, C.; Carr, E.J.; Wang, J.; Houard, S.; Wingett, S.W.; Audran, R.; Wallin, E.F.; et al. The Adjuvant GLA-SE Promotes Human Tfh Cell Expansion and Emergence of Public TCRβ Clonotypes. *J. Exp. Med.* **2019**, 216, 1857–1873. [CrossRef] [PubMed]
- 146. Mastelic Gavillet, B.; Eberhardt, C.S.; Auderset, F.; Castellino, F.; Seubert, A.; Tregoning, J.S.; Lambert, P.H.; Siegrist, C.A. MF59 mediates its B cell adjuvanticity by promoting T follicular helper cells and germinal center responses in adult and early life. *J. Immunol.* 2015, 194, 4836–4846.
- 147. Gómez, E.A.; Rodríguez-Cariño, C.; García-Blanco, M.; Martínez-Lobo, F.J.; Mateu, E. Enhanced germinal center responses and antibody production with Montanide ISA 206 in PRRSV vaccines. *Vet. Immunol. Immunopathol.* **2023**, 254, 110550.
- 148. Liang, F.; Lindgren, G.; Sandgren, K.J.; Thompson, E.A.; Francica, J.R.; Seubert, A.; De Gregorio, E.; Barnett, S.; O'Hagan, D.T.; Sullivan, N.J.; et al. Vaccine priming is restricted to draining lymph nodes and controlled by adjuvant-mediated antigen uptake. *Sci. Transl. Med.* **2017**, *9*, eaal2094.
- 149. Dowling, D.J. Recent Advances in the Discovery and Delivery of TLR7/8 Agonists as Vaccine Adjuvants. *Immunohorizons* **2018**, 2, 185–197.
- 150. Chen, C.; Zhang, C.; Li, R.; Wang, Z.; Yuan, Y.; Li, H.; Fu, Z.; Zhou, M.; Zhao, L. Monophosphoryl-Lipid A (MPLA) is an efficacious adjuvant for inactivated rabies vaccines. *Viruses* **2019**, *11*, 1118. [CrossRef]
- 151. Olotu, A.; Fegan, G.; Wambua, J.; Nyangweso, G.; Leach, A.; Lievens, M.; Kaslow, D.C.; Njuguna, P.; Marsh, K.; Bejon, P. Seven-year efficacy of RTS, S/AS01 malaria vaccine among young African children. *N. Engl. J. Med.* **2016**, 374, 2519–2529. [CrossRef]
- 152. Garçon, N.; Morel, S.; Didierlaurent, A.; Descamps, D.; Wettendorff, M.; Van Mechelen, M. Development of an AS04-adjuvanted HPV vaccine with the adjuvant system approach. *BioDrugs* **2011**, 25, 217–226. [CrossRef]
- 153. Nielsen, C.M.; Ogbe, A.; Pedroza-Pacheco, I.; Doeleman, S.E.; Chen, Y.; Silk, S.E.; Barrett, J.R.; Elias, S.C.; Miura, K.; Diouf, A.; et al. Protein/AS01B Vaccination Elicits Stronger, More Th2-Skewed Antigen-Specific Human T Follicular Helper Cell Responses than Heterologous Viral Vectors. *Cell Rep. Med.* **2021**, *2*, 100207. [CrossRef] [PubMed]
- 154. Silva, M.; Kato, Y.; Melo, M.B.; Phung, I.; Freeman, B.L.; Li, Z.; Roh, K.; Van Wijnbergen, J.W.; Watkins, H.; Enemuo, C.A.; et al. A particulate saponin/TLR agonist vaccine adjuvant alters lymph flow and modulates adaptive immunity. *Sci. Immunol.* **2021**, *6*, eabf1152. [CrossRef] [PubMed]

- 155. Burn, O.K.; Pankhurst, T.E.; Painter, G.F.; Connor, L.M.; Hermans, I.F. Harnessing NKT Cells for Vaccination. *Oxf. Open Immunol.* **2021**, 2, iqab013. [CrossRef] [PubMed]
- 156. Driver, J.P.; de Carvalho Madrid, D.M.; Gu, W.; Artiaga, B.L.; Richt, J.A. Modulation of Immune Responses to Influenza A Virus Vaccines by Natural Killer T Cells. *Front. Immunol.* **2020**, *11*, 2172. [CrossRef]
- 157. Pankhurst, T.E.; Buick, K.H.; Lange, J.L.; Marshall, A.J.; Button, K.R.; Palmer, O.R.; Farrand, K.J.; Montgomerie, I.; Bird, T.W.; Mason, N.C.; et al. MAIT cells activate dendritic cells to promote TFH cell differentiation and induce humoral immunity. *Cell Rep.* **2023**, 42, 112310. [CrossRef]
- 158. Naderi-Samani, M.; Soltani, M.; Dadar, M.; Taheri-Mirghaed, A.; Zargar, A.; Ahmadivand, S.; Hassanzadeh, R.; Moazami Goudarzi, L. Oral Immunization of Trout Fry with Recombinant Lactococcus lactis NZ3900 Expressing G Gene of Viral Hemorrhagic Septicemia Virus (VHSV). Fish. Shellfish. Immunol. 2020, 105, 62–70. [CrossRef]

Disclaimer/Publisher's Note: The statements, opinions and data contained in all publications are solely those of the individual author(s) and contributor(s) and not of MDPI and/or the editor(s). MDPI and/or the editor(s) disclaim responsibility for any injury to people or property resulting from any ideas, methods, instructions or products referred to in the content.





Article

Differential Infiltration of Key Immune T-Cell Populations Across Malignancies Varying by Immunogenic Potential and the Likelihood of Response to Immunotherapy

Islam Eljilany ¹, Sam Coleman ², Aik Choon Tan ², Martin D. McCarter ³, John Carpten ⁴, Howard Colman ^{2,5}, Abdul Rafeh Naqash ⁶, Igor Puzanov ⁷, Susanne M. Arnold ⁸, Michelle L. Churchman ⁹, Daniel Spakowicz ¹⁰, Bodour Salhia ⁴, Julian A. Marin-Acevedo ¹¹, Shridar Ganesan ¹², Aakrosh Ratan ¹³, Craig Shriver ¹⁴, Patrick Hwu ¹, William S. Dalton ⁹, George J. Weiner ¹⁵, Jose R. Conejo-Garcia ¹⁶, Paulo Rodriguez ¹⁶ and Ahmad A. Tarhini ^{1,16},*

- Departments of Cutaneous Oncology, H. Lee Moffitt Cancer Center and Research Institute, Tampa, FL 33612, USA
- Huntsman Cancer Institute, Salt Lake City, UT 84132, USA
- University of Colorado Cancer Center, Aurora, CO 80045, USA
- Norris Comprehensive Cancer Center, University of Southern California, Los Angeles, CA 90033, USA
- Department of Neurosurgery, School of Medicine, University of Utah, Salt Lake City, UT 84132, USA
- Oklahoma University Health Stephenson Cancer Center, Oklahoma City, OK 73104, USA
- Department of Medicine, Roswell Park Comprehensive Cancer Center, Buffalo, NY 14263, USA
- ⁸ University of Kentucky Markey Cancer Center, Lexington, KY 40536, USA
- ⁹ Aster Insights, Hudson, FL 34667, USA
- Ohio State University Comprehensive Cancer Center, Columbus, OH 43210, USA
- 11 Simon Comprehensive Cancer Center, Indiana University, Indianapolis, IN 46202, USA
- Rutgers Cancer Institute of New Jersey, New Brunswick, NJ 08903, USA
- Department of Genome Sciences, School of Medicine, University of Virginia, Charlottesville, VA 22908, USA
- Murtha Cancer Center, Walter Reed National Military Medical Center, Falls Church, VA 22042-5101, USA
- Department of Internal Medicine, Carver College of Medicine, University of Iowa Health Care, Iowa City, IA 52242, USA
- Department of Immunology, H. Lee Moffitt Cancer Center and Research Institute, Tampa, FL 33612, USA
- * Correspondence: ahmad.tarhini@moffitt.org; Tel.: +1-813-745-8581

Abstract: Background: Solid tumors vary by the immunogenic potential of the tumor microenvironment (TME) and the likelihood of response to immunotherapy. The emerging literature has identified key immune cell populations that significantly impact immune activation or suppression within the TME. This study investigated candidate T-cell populations and their differential infiltration within different tumor types as estimated from mRNA co-expression levels of the corresponding cellular markers. Methods: We analyzed the mRNA co-expression levels of cellular biomarkers that define stem-like tumor-infiltrating lymphocytes (TILs), tissue-resident memory T-cells (TRM), early dysfunctional T-cells, late dysfunctional T-cells, activated-potentially anti-tumor (APA) T-cells and Butyrophilin 3A (BTN3A) isoforms, utilizing clinical and transcriptomic data from 1892 patients diagnosed with melanoma, bladder, ovarian, or pancreatic carcinomas. Real-world data were collected under the Total Cancer Care Protocol and the Avatar® project (NCT03977402) across 18 cancer centers. Furthermore, we compared the survival outcomes following immune checkpoint inhibitors (ICIs) based on immune cell gene expression. Results: In melanoma and bladder cancer, the estimated infiltration of APA T-cells differed significantly ($p = 4.67 \times 10^{-12}$ and $p = 5.80 \times 10^{-12}$, respectively) compared to ovarian and pancreatic cancers. Ovarian cancer had lower TRM T-cell infiltration than melanoma, bladder, and pancreatic ($p = 2.23 \times 10^{-8}$, 3.86×10^{-28} , and 7.85×10^{-9} , respectively). Similar trends were noted with stem-like, early, and late dysfunctional T-cells. Melanoma and ovarian expressed BTN3A isoforms more than other malignancies. Higher densities of stem-like TILs; TRM, early and late dysfunctional T-cells; APA T-cells; and BTN3A isoforms were associated with increased survival in melanoma (p = 0.0075, 0.00059, 0.013, 0.005,0.0016, and 0.041, respectively). The TRM gene signature was a moderate predictor of survival in the melanoma cohort (AUROC = 0.65), with similar findings in testing independent public datasets of ICI-treated patients with melanoma (AUROC 0.61-0.64). Conclusions: Key cellular elements related

to immune activation are more heavily infiltrated within ICI-responsive versus non-responsive malignancies, supporting a central role in anti-tumor immunity. In melanoma patients treated with ICIs, higher densities of stem-like TILs, TRM T-cells, early dysfunctional T-cells, late dysfunctional T-cells, APA T-cells, and BTN3A isoforms were associated with improved survival.

Keywords: immune cell infiltration; immune response; melanoma; RNA expression; ovarian cancer; pancreatic cancer; bladder cancer; T-cell

1. Introduction

In 2023, melanoma, ovarian, pancreatic, and bladder cancers were projected to be among the most diagnosed cancers in the United States. The survival rates over five years for these cancers show considerable variation, with notably better outcomes observed for cutaneous melanoma and bladder carcinoma. This discrepancy in survival rates is partially attributed to the effectiveness of immunotherapy treatments in managing these cancers [1]. Immune checkpoint inhibitors (ICIs) have emerged as highly effective treatments for various advanced cancers, delivering extended survival benefits [2]. Specifically, therapies targeting immune checkpoints such as cytotoxic T-lymphocyte antigen-4 (CTLA-4) and programmed death/ligand 1 (PD-1/PD-L1) have demonstrated significant benefits in treating melanoma and bladder carcinoma [2].

However, many patients fail to respond favorably to these therapies, with some experiencing early disease progression due to mechanisms that confer tumor immune resistance [2]. Furthermore, ICI activity is relatively limited in treating some cancer types like ovarian cancer and pancreatic adenocarcinoma [3]. Notably, tumor immune resistance can be primarily attributed to the distinctive features of their tumor microenvironments (TMEs), which play pivotal roles in cancer development and immune resistance mechanisms [4]. The immunogenic nature of the TME impacts tumor immune evasion through various complex mechanisms [5].

The TME represents a sophisticated ecosystem incorporating diverse cell types that interact within their architectures. Immune cells infiltrating tumors are pivotal in modulating tumor behavior and susceptibility to therapeutic interventions [6,7]. Notably, tumor antigen-specific CD8+ cytotoxic T-cells play a crucial function in anti-tumor immunity, detecting and eliminating tumor cells that express neoantigens and distinctive antigens arising from mutated gene expressions [8]. However, the tumor milieu also includes immunosuppressive cells, including regulatory T (Treg)-cells and myeloid-derived suppressor cells (MDSCs), which can foster tumor growth and facilitate immune escape by suppressing immune responses [9].

Understanding the composition and quantity of immune cells infiltrating tumors is vital for unraveling the complex dynamics of the immune response against cancer. This knowledge not only illuminates the pathways through which the immune system combats or supports cancer but also aids in evaluating the immunogenic impact of anticancer treatments. Such insights are essential for strategically developing combination therapies that can more effectively harness the immune system [5]. Since immunotherapies, including those targeting immune checkpoints, only benefit a select group of patients, analyzing immune cell infiltration in tumor samples before and during treatment offers a promising avenue for discovering new biomarkers [10].

Recent studies have highlighted specific immune cell subsets' crucial roles in enhancing or dampening the immune response in cancer patients. However, the differential infiltration of certain immune cells of increasing interest across cancers with varied immunogenic potential remains poorly understood. Therefore, this study aims to help fill this gap by examining the density of immune cell groups of interest, including stem-like tumor-infiltrating lymphocytes (TILs), tissue-resident memory (TRM) T-cells, activated-potentially anti-tumor T-cells, early dysfunctional T-cells, late dysfunctional T-cells, and Butyrophilin

3 A (BTN3A) isoforms through assessing their distinct expression across different cancer types by analyzing mRNA co-expression levels of associated cellular biomarkers. Elucidating these key immune cell populations across tumors may help guide the development of tailored treatments and combination therapies taking into account the tumors' diverse immune milieu.

2. Materials and Methods

2.1. Patient Cohort and Data Compilation

This investigation utilized a comprehensive dataset merging clinical observations and genetic expression data, nested within the Total Cancer Care (TCC) Protocol (NCT03977402; Advara IRB# Pro00014441) and the Avatar project that is conducted within the Oncology Research Information Exchange Network (ORIEN), which is a consortium of 19 cancer centers [11,12]. We utilized clinical and transcriptomic data collected from patients with melanoma (N = 232), bladder urothelial carcinoma (N = 349), ovarian cancer (N = 664) and pancreatic adenocarcinoma (N = 647), representing a spectrum from more responsive to poorly responsive to ICIs. The cohort comprised adult patients with cancer (aged 18 and above), with the study protocol encompassing the collection of tumor, blood, and/or fluid samples as part of standard clinical practice. Data collection extended from each patient's enrollment in TCC until the data cut-off for this analysis. Written informed consent was obtained from all subjects including the genetic analysis of germline and tumor DNA, alongside the perpetual aggregation of their clinical data. Adhering to the ethical guidelines in the Declaration of Helsinki, the study received approval from all participating entities' Institutional Review Boards (IRB; Advara IRB# Pro00014441, Tampa, FL, USA).

2.2. RNA Sequencing and Data Retrieval

Gene expression relevant to our research interests was interpreted through RNA sequencing, adhering to methodologies elaborated in a previously issued white paper (https://www.asterinsights.com/white-paper/renal-cell-carcinoma-rwd-data/ (accessed on12 February 2024)). The genetic expression data were sourced from the ORIEN database, necessitating the download of numerous FASTQ files for data analysis.

2.3. Quantification Analysis of RNA Gene Expression

Gene expression quantification entailed a multistep technical process, initiating with the use of Bbduk software (version 38.96) for trimming adapter sequences from the RNA-Seq reads (https://sourceforge.net/projects/bbmap/ (accessed on 13 August 2023)) [13]. This was followed by aligning the reads to the human reference genome (CRCH38/hg38) using STAR software (version 2.7.3a), available at https://github.com/alxdobin/STAR (accessed on 13 August 2023) [14]. The integrity of the RNA data was verified using the RNA-Seq Quality Control (RNA-SeQC) software (version 2.3.2), https://github.com/getzlab/rnaseqc (accessed on 13 August 2023) [15]. Expression levels were then quantified as Transcripts Per Million (TPM), utilizing the RNA-Seq by Expectation Maximization (RSEM) software (version 1.3.1), https://github.com/deweylab/RSEM (accessed on 14 August 2023) [16], followed by logarithmic transformation with +1 [log2(TPM + 1)] and batch effect adjustments via the ComBat function within the sva package (version 3.34.0), https://doi.org/10.18129/B9.bioc.sva (accessed on 14 August 2023) [17].

2.4. Generation of Gene Expression Signature Scores

Standardization of gene names was achieved using the NCBI Entrez gene number. Subsequently, the average z-score for each gene expression signature was calculated per the method described by Lee et al. [18].

2.5. Enrichment Analysis of Gene Sets

The Gene Set Enrichment Analysis (GSEA) software V.20.3.4., accessible at https://www.gsea-msigdb.org/gsea/login.jsp (accessed on 16 October 2023) [19], was

employed alongside hallmark gene sets from the Molecular Signatures Database (MSigDB) V.7.5.1., https://www.gsea-msigdb.org/gsea/msigdb (accessed on 16 October 2023) [19–21], to determine significant differences in normalized enrichment score (NES) between responders and non-responders. This analysis involved leveraging curated databases like the Kyoto Encyclopedia of Genes and Genomes (KEGG) and REACTOME for pathway enrichment comparisons. In the end, in an attempt to gain a more comprehensive understanding of the differences in cell types associated with each gene set, the TIMEx "http://timex.moffitt.org" (accessed on 9 March 2023) web portal was used to deconvolute the bulk transcriptomic data of the responder and non-responder samples [22].

2.6. Study Outcomes

The primary outcome was the mRNA co-expression levels of specific cellular biomarkers associated with defined types of T-cells, including stem-like TILs (Transcription factor 7 (TCF7), Interleukin-7 receptor (IL7R), CXCR5, CD28, and CD27), TRM T-cells (CD69 and CD103), activated-potentially anti-tumor T-cells (PD1+, CD27+, CD28+, CD137+, Glucocorticoid-induced TNFR-related+ (GITR+)), early dysfunctional T-cells (programmed death-1+ (PD-1+), C-C chemokine receptor type 5+ (CCR5+), TCF7+, T-cell immunoglobulin and mucin-domain containing-3- (Tim-3-)), late dysfunctional T-cells (PD1+, CD38+, CD39+, CD101+, TIM3+), and BTN3A isoforms (BTN3A1, BTN3A2, BTN3A3) assessed across the four cancer types of interest, thereby estimating their differential infiltration.

The secondary outcome was comparing the estimated infiltration of these T-cell types between immunotherapy responders and non-responders. For this analysis, responders were defined as those with at least 2-year survival from the initiation of immunotherapy. Therefore, non-responders were defined by overall survival (OS) < 24 months and responders by an OS \geq 24 months from the initiation of immunotherapy. Also, we estimated patients' survival probability based on the estimated infiltration of the T-cell subtypes being studied.

2.7. Validation

To validate the predictive value of each significant biomarker, we tested the predictive power of the area under the receiver operating characteristic (AUROC) of each biomarker to predict immunotherapy response in patients with melanoma who are within the OREIN dataset as well as combined data from ten available public datasets, including 672 patients (Table 1) [23–33].

Table 1. Public datasets with patients with melanoma on immunotherap

Dataset	Cohort	Treatment(s)	Pre /On/Post Treatment	Patients (N)	REF
Du	Du	Ipilimumab/Nivolumab/Pembrolizumab	Pre/On	50	[23]
G: 1	Gide_Pre_PD-1_CTLA4	Ipilimumab/Nivolumab/Pembrolizumab	Pre/On	41	[24]
Gide	Gide_Pre_PD-1	Pembrolizumab/Nivolumab	Pre/On	50	[24]
COF	GSE165278	Ipilimumab	Pre/Post	22	[25]
GSE -	GSE158403	Durvalumab	Pre/On	81	[26]
Freeman	Freeman	N/A	Pre/Post	38	[27]
Hugo	HugoLo_IPRES_2016	Pembrolizumab	Pre/On	26	[28]
Lauss	Lauss	Adoptive T-cell therapy	Pre	25	[29]
Lee	Lee	Pembrolizumab/Nivolumab	Pre/On	78	[30]
Liu	Liu	Pembrolizumab/Nivolumab	Pre/On	122	[31]

Table 1. Cont.

Dataset	Cohort	Treatment(s)	Pre /On/Post Treatment	Patients (N)	REF
Riaz	Riaz	Nivolumab	Pre/On	98	[32]
Van Allen	VanAllen_anti-CTLA4_2015	Ipilimumab	Pre	41	[33]

CTLA4: cytotoxic T-lymphocyte antigen-4, N/A: not available, No: number, PD-1: programmed death-1, Ref: references.

2.8. Statistical Analysis

The statistical analysis, conducted by SciPy 1.7.0 software, encompassed the Mann–Whitney U test to compare the median gene expression signature scores of each T-cell type among the four malignancies and the z-score of each T-cell type between immunotherapy responders and non-responders. The Kaplan–Meier analysis and the log-rank test were performed to evaluate the difference in survival probability between patients with low vs. high gene expression of each T-cell type. The AUROC was based on the z-score of immunotherapy responders and non-responders. After correction for multiple testing, which controls the false discovery rate (FDR), two-tailed or FDR-adjusted *p*-values < 0.05 or 0.02, respectively, were established as criteria for significance.

3. Results

3.1. Patients Characteristics

Table 2 summarizes the demographic and clinical characteristics of 1892 patients analyzed in our study, stratified into specific cancer categories: 232 with cutaneous melanoma, 664 with ovarian cancer, 647 with pancreatic adenocarcinoma, and 349 with bladder cancer. The collective mean \pm standard deviation (SD) age was 62 \pm 13 years, highlighting a broad age range within the cohort. There was a male predominance in three cancer types (>50%), excluding ovarian cancer. The ethnic composition was primarily non-Hispanic white, exceeding 90% across all cancer categories. Notably, cancer stages at initial diagnosis varied, with Stage III being prevalent among most cancers (about one-third), except for pancreatic adenocarcinoma, where a significant portion (approximately 54.1%) were diagnosed with Stage II. Finally, Eastern Cooperative Oncology Group (ECOG) performance status ranged from 0 (fully active) to 4 (completely disabled), with the majority at 0 or 1, indicating that in patients for whom the ECOG status was known, this trended towards better performance status across the group. Our study highlighted the distribution of histological subtypes within ovarian cancer. A significant portion, 442 cases or 66.5%, were classified as advanced epithelial tumors. The most common subtype encountered was serious cystadenocarcinoma, accounting for 44.1% (293 cases) of the study group. This was followed by adenocarcinoma and serous surface papillary carcinoma, making up 13.4% (89 cases) and 9% (60 cases) of the cases, respectively. Rarer forms, such as clear cell and mucinous adenocarcinomas, were observed in smaller numbers, with the former seen in 3.6% (24 cases) and the latter in 1.5% (10 cases) of the patient cohort. Our study on ovarian cancer histological subtypes observed that the epithelial subtype accounted for most cases, comprising 78% (n = 515). The mixed epithelial and mesenchymal subtype comprised 17% (n = 114) of the cases, while the remaining 5% (n = 35) were classified as Sex-cord stromal, germ cell, or miscellaneous types. Serous carcinoma was the most common sub-classification within the epithelial subtype, accounting for 75% (n = 387) of epithelial cases and 58% of all cases in the total sample. Additional forms of epithelial carcinomas observed in the study included endometrioid (9%, n = 48), clear cell (5%, n = 24), and mucinous (3%, n = 14). The remaining cases were classified as other carcinomas (8%, n = 40).

Table 2. Patients' demographics and characteristics.

Characteristic	Total (N = 1892)	Cutaneous Melanoma (N = 232)	Ovarian Cancer (N = 664)	Pancreatic Adenocarcinoma (N = 647)	Bladder Urothelial Carcinoma (N = 349)
Age in years Mean \pm SD	62 ± 13	59 ± 14	59 ± 13	63 ± 13	68 ± 11
Sex, n (%)					
Female	1141 (60.3)	89 (38.4)	664 (100)	301 (46.5)	87 (24.9)
Male	751 (39.7)	143 (61.6)	0 (0)	346 (53.5)	262 (75.1)
Ethnicity, n (%)					
Hispanic	94 (5.0)	9 (3.9)	39 (5.9)	32 (4.9)	14 (4.0)
Non-Hispanic	1749 (92.4)	217 (93.5)	618 (93.1)	603 (93.2)	311 (89.1)
Unknown	49 (2.6)	6 (2.6)	7 (1.1)	12 (1.9)	24 (6.9)
Race, n (%)					
African American					
American Indian or	55 (2.9)	1 (0.4)	21 (3.2)	23 (3.6)	10 (2.9)
Alaska Native	11 (0.6)	1 (0.4)	8 (1.2)	2 (0.3)	0 (0)
Asian	40 (4.0)	2 (2)	0 (1 1)	= (4.4)	2 (0.0)
Native Hawaiian or	19 (1.0)	0 (0)	9 (1.4)	7 (1.1)	3 (0.9)
Other Pacific Islander	2 (0.1)	0.(0)	2 (0.2)	0 (0)	0 (0)
White	2 (0.1)	0 (0)	2 (0.3)	0 (0)	0 (0)
Other	1757 (92.9)	226 (97.4)	610 (91.9)	601 (92.9)	320 (91.7)
Unknown	24 (1.3)	1 (0.4)	6 (0.9)	7 (1.1)	10 (2.9)
	24 (1.3)	3 (1.3)	8 (1.2)	7 (1.1)	6 (1.7)
Cancer stage at initial					
diagnosis, n (%)	202 (14.0)	2F (10.0)	07 (14 ()	117 (10 1)	42 (12 2)
Stage I	282 (14.9)	25 (10.8) 48 (20.7)	97 (14.6) 74 (11.1)	117 (18.1)	43 (12.3)
Stage II	527 (27.9)	\ /	\ /	350 (54.1)	55 (15.8)
Stage III	526 (27.8)	73 (31.5)	292 (44.0)	47 (7.3)	114 (32.7)
Stage IV Unknown	324 (17.1 193 (10.2)	43 (18.5) 43 (18.5)	129 (19.4) 72 (10.8)	77 (11.9)	75 (21.5) 42 (12.0)
Ulkliowii	193 (10.2)	43 (16.3)	72 (10.6)	36 (5.6)	42 (12.0)
Performance status (ECOG), n (%)					
0	386 (20.4)	39 (16.8)	140 (21.1)	141 (21.8)	66 (18.9)
1	282 (14.9)	11 (4.7)	117 (17.6)	114 (17.6)	40 (11.5)
2	48 (2.5)	4 (1.7)	22 (3.3)	12 (1.9)	10 (2.9)
3	8 (0.4)	1 (0.4)	4 (0.6)	1 (0.2)	2 (0.6)
Unknown	1168 (61.7)	177 (76.3	381 (57.4)	379 (58.6)	231 (66.2)

ECOG, Eastern Cooperative Oncology Group; N, number of patients; SD, standard deviation.

3.2. Differential Immune Infiltrating T-Cells Across Four Cancers

The boxplot in Figure 1 illustrates a broad range of estimated T-cell infiltration across ovarian, pancreatic, bladder, and melanoma cancer types. Notably, ovarian cancer showed the lowest median z-score in all T-cell populations, except for bladder cancer, which was lowest in the expression of BTN3A isoforms. In contrast, melanoma exhibited higher median z-scores among most T-cell populations except for TRM T-cells, which were highest in bladder cancer. Pancreatic cancer had a median z-score that was higher than ovarian and lower than melanoma or bladder cancers. The variability in expression of APA T-cells, early dysfunctional T-cells, late dysfunctional T-cells, and BTN3A-related T-cells, as indicated by the interquartile ranges (IQRs) displayed in the boxplot, was higher in melanoma, while stem-like TILs and TRM T-cells were higher in bladder cancer. On the other hand, the expression variability of all T-cell populations was narrower for ovarian cancer only. Obviously, outliers were present in all T-cell populations of the four malignancies, with several cases showing very high z-scores.

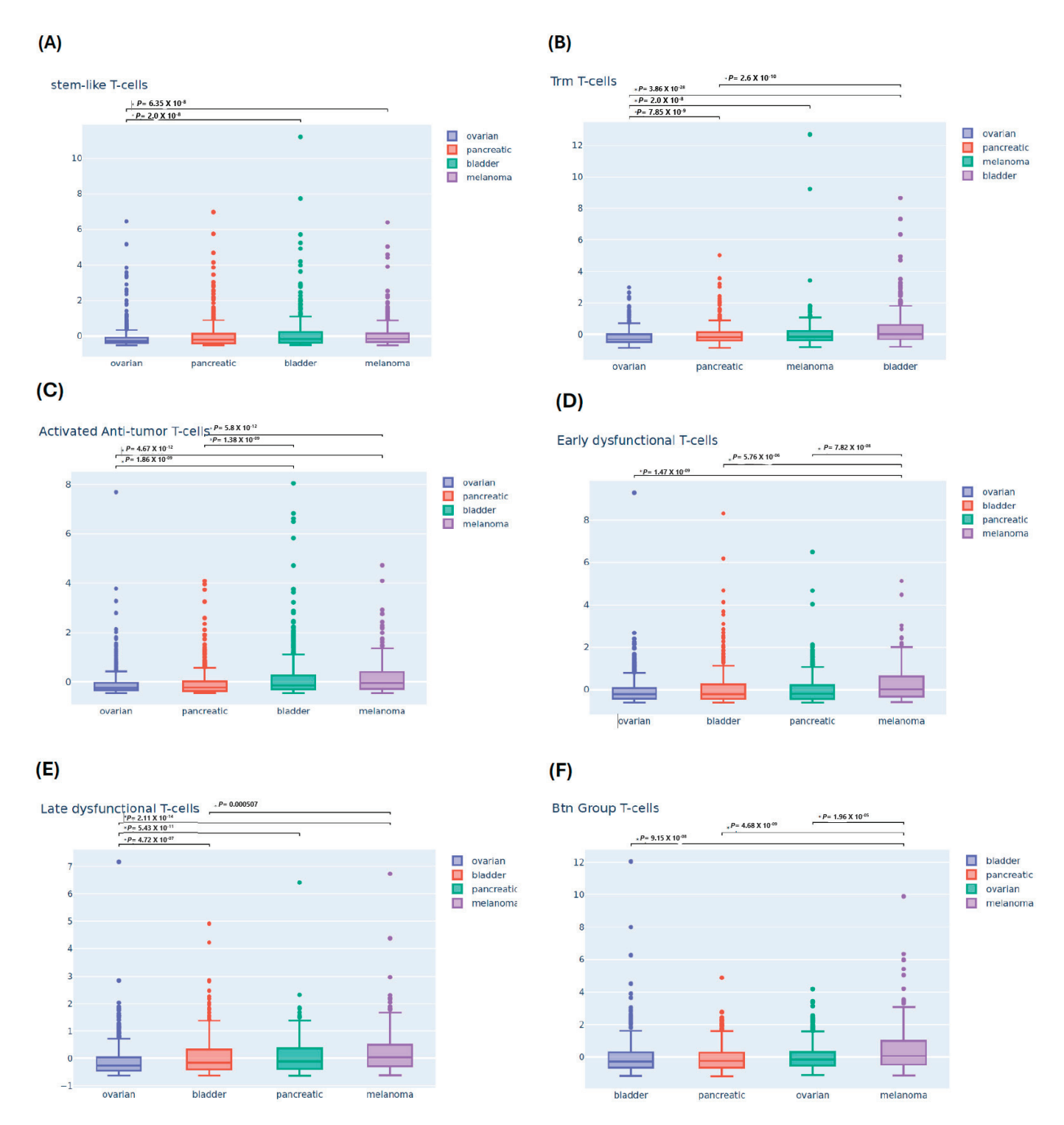


Figure 1. Gene expression of different infiltration T-cells among four malignancies. The boxplots demonstrate the gene expression levels of the signatures corresponding to the T-cell subtypes of interest as well as Butyrophilin 3 A (BTN3A) isoforms among four cancer types. The Y-axis represents gene expression value as a z-score, and the X-axis represents four cancer types: ovarian, bladder, pancreatic, and melanoma. The *p*-value threshold was 0.001. **(A)** Differential expression of stem-like tumor infiltrating lymphocytes (TILs) across four cancer types. **(B)** Expression patterns of tissue-resident memory (TRM) T-cells. **(C)** Activated-potentially anti-tumor T-cells. **(D)** Early dysfunctional T-cell. **(E)** Late dysfunctional T-cell. **(F)** Expression of Butyrophilin 3 A (BTN3A) isoforms.

As shown in Figure 1A, the ovarian cancer cohorts demonstrated a significantly lower median expression of stem-like TILs than the bladder cancer or melanoma cohorts (p-values = 2×10^{-8} or 6.35×10^{-8} , respectively). Similarly, Figure 1B demonstrates significantly lower expression of TRM T-cell expression levels with ovarian cancer compared to pancreatic, melanoma, and bladder cancers $(p = 7.852 \times 10^{-9}, p = 2.232 \times 10^{-8}, p = 2.232 \times 10^{-8})$ and 3.862×10^{-28} , respectively). A more pronounced significant difference was noted when comparing pancreatic and bladder cancers ($p = 2.62 \times 10^{-10}$). In Figure 1C, ovarian and pancreatic cancers show significantly lower expression levels of APA T-cells compared to bladder ($p = 1.862 \times 10^{-9}$ and $p = 1.382 \times 10^{-12}$, respectively) and melanoma $(p = 4.672 \times 10^{-12})$ and $p = 5.82 \times 10^{-12}$, correspondingly). Moreover, the differences in median z-scores in melanoma compared to ovarian, bladder, and pancreatic cancer $(p = 1.472 \times 10^{-9}, p = 9.762 \times 10^{-6}, \text{ and } p = 7.822 \times 10^{-8}, \text{ respectively}) \text{ were signifi-}$ cantly higher in the estimated infiltration of early dysfunction T-cells (Figure 1D). Significant differences in the expression of late dysfunction T-cells are highlighted in Figure 1E, including ovarian cancer versus bladder cancer ($p = 4.722 \times 10^{-7}$), pancreatic cancer $(p = 5.452 \times 10^{-11})$, and melanoma $(p = 2.112 \times 10^{-14})$ and also between bladder cancer and melanoma (p = 0.000507). Finally, significant differences were seen when comparing melanoma to bladder, pancreatic, and ovarian cancers ($p = 9.152 \times 10^{-8}$, $p = 4.682 \times 10^{-9}$, $p = 1.962 \times 10^{-5}$, respectively) in the expression of BTN3A isoforms.

3.3. Comparing Immune T-Cell Subtype Infiltration in Patients with Melanoma Treated with Immunetherapy and Testing Association with Survival Outcomes

We examined the differences in the expression levels of the gene signatures of interest between immunotherapy responders and non-responders in melanoma. Melanoma is known to be an immunogenic tumor with a higher likelihood of response to immunotherapy. This was supported by our results, which demonstrated the highest expression levels of most signatures in melanoma compared to the other malignancies, except for TRM T-cells in bladder cancer. In examining the expression levels of six T-cell signatures of interest between immunotherapy responder and non-responder patients with melanoma (n = 123), strong trends were seen for all, as illustrated in the boxplot analysis in Figure 2. Only TRM T-cells showed a statistically significant difference between responders and non-responders regarding the average z-score (adjusted p-value = 0.02).

This figure contains six box plots representing the average gene expression z-score distribution of stem-like tumor-infiltrating lymphocytes (TILs), tissue-resident memory (TRM) T-cells, activated-potentially anti-tumor T-cells, early dysfunctional T-cells, late dysfunctional (dys) T-cells, and Butyrophilin 3 A groups (btn grp) in patients with melanoma treated with immunotherapy. These plots are categorized by responder status: responders (Rs) defined as having OS \geq 2 years and non-responders (NRs) with OS < 2 years. Adjusted p-value < 0.05 is considered significant. Adj P.Val: adjusted p-value.

The Kaplan–Meier curves shown in Figure 3 demonstrate an association with improved survival in patients with melanoma whose tumors had high-expression levels of all six signatures tested, where significant differences were seen by the log-rank test in stem-like TILs (p = 0.0075), TRM T-cells (p = 0.0059), activated-potentially anti-tumor T-cells (p = 0.0016), early dysfunction T-cells (p = 0.013), late dysfunctions T-cells (p = 0.005), and BTN3A (p = 0.041).

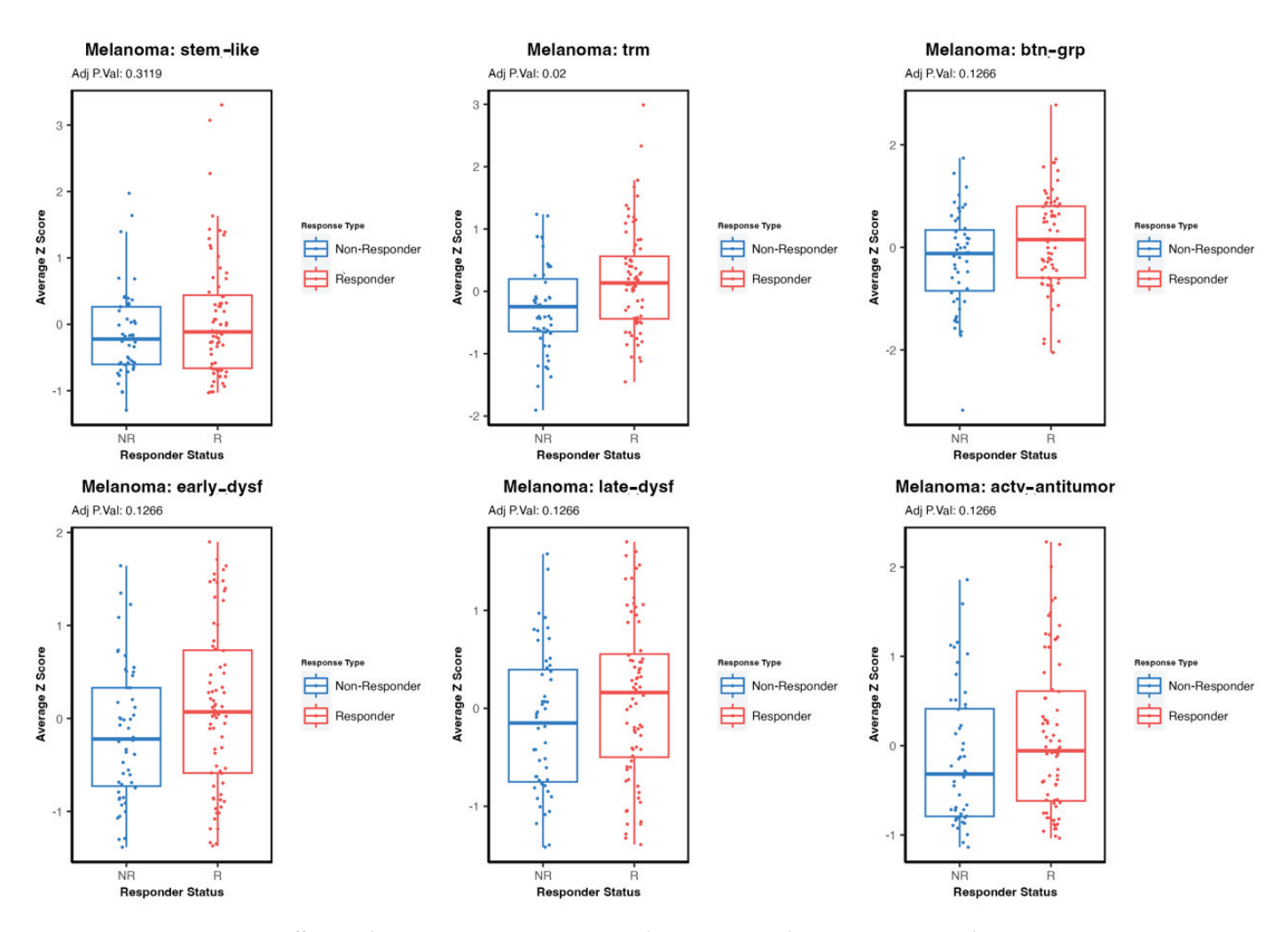


Figure 2. Differential gene expression in immunotherapy responders vs. non-responders in patients with melanoma (n = 123): a box plot analysis.

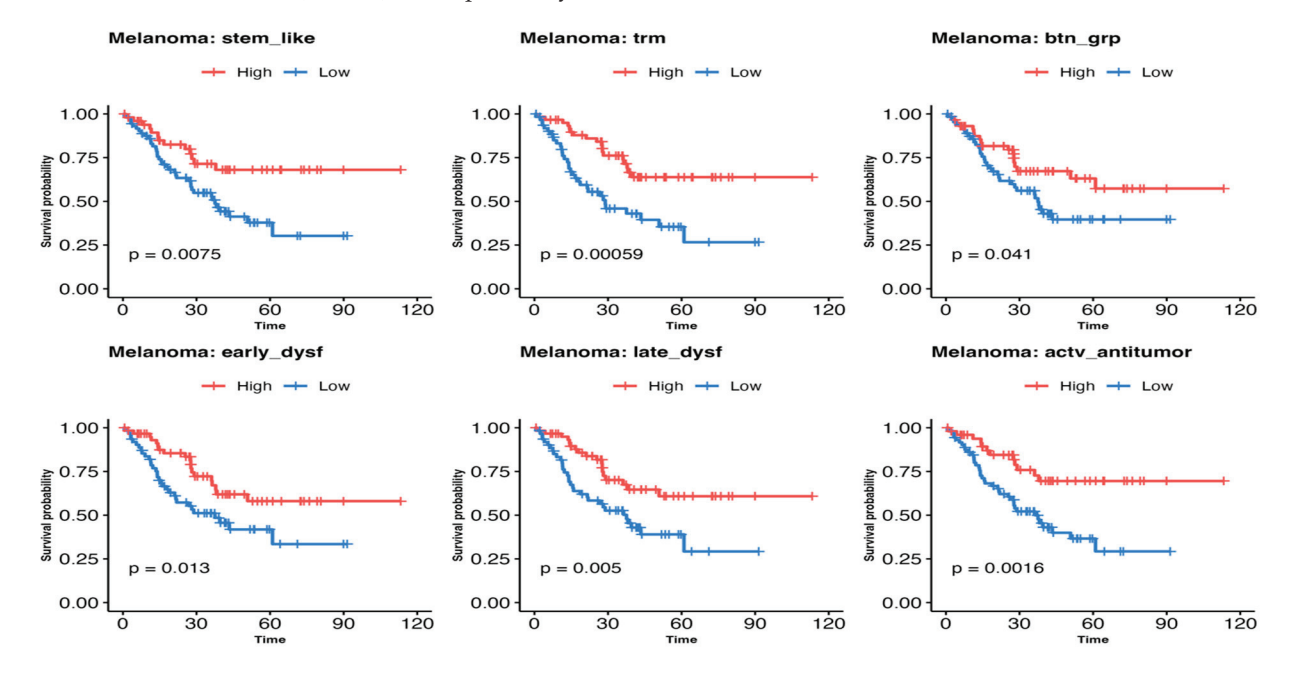


Figure 3. Survival probability of melanoma patients treated with immunotherapy (n = 123): impact of estimated T-cell subtype infiltration.

The figure shows the Kaplan–Meier survival curves, each representing the survival probability as overall survival on the Y-axis over 120 months on the X-axis for melanoma patients treated with immunotherapy. Each plot contrasts the survival probability for patients with high (Red) versus low (Blue) expression of specific T-cell gene signatures. These gene signatures included stem-like tumor-infiltrating lymphocytes (TILs), tissue-resident memory (TRM) T-cells, activated-potentially anti-tumor T-cells, early dysfunctional T-cells, late dysfunctional (dys) T-cells, and Butyrophilin 3 A groups (btn grp) genes. A p-value (p) < 0.05 was significant.

3.4. Immune Cell Infiltration Gene Expression Signature Validation

The TRM T-cell gene signature had the best AUROC as a moderate predictor (AUROC = 0.65) associated with improved survival following immunotherapy in the OREIN dataset. The AUROC of the other GE signatures ranged from 0.55 to 0.59, as shown in Table 3. These signatures had a better predictive performance when examined in the public datasets. Table 3 shows that the six gene expression signatures had similarly moderate predictive values of immunotherapy response in patients with melanoma treated with immunotherapy (AUROC = 0.61–0.64).

Table 3. The AUROC of six gene signatures in different datasets of patients with melanoma on immunotherapy.

T-Cells Populations	Stem-like TILs	TRM T-Cells	Activated- Potentially Anti-Tumor T-Cells	Early Dysfunction T-Cells	Late Dysfunction T-Cells	BTN3A Group-Related T-Cells
OREIN dataset	0.554	0.655	0.586	0.593	0.588	0.594
Public datasets *	0.633	0.605	0.633	0.619	0.638	0.625

^{*} Average AUROC. AUROC: area under the receiver operating characteristic, BTN3A: Butyrophilin 3 A groups, OREIN: Oncology Research Information Exchange Network: TILs: tumor-infiltrating lymphocytes, TRM: tissue-resident memory.

4. Discussion

Understanding the composition and prevalence of immune cells within tumors is critical for decoding the immune response to cancer and gauging the efficacy of immunotherapy regimens. Gaining such insights is paramount for developing treatments that can effectively activate the host's immune response [34]. Recent investigations have identified specific subpopulations of infiltrating T-cells that are associated with either enhanced or suppressed immune response in patients with cancer. However, the detailed abundance of these immune cells in tumors with varying immunogenic potentials remains largely unexplored [35,36]. The present study was designed to determine the diverse immune T-cell infiltrates across four cancer types by estimating the density of several immune cell groups, including stem-like TILs, TRM T-cells, activated-potentially anti-tumor T-cells, early and late dysfunctional T-cells, and BTN3A isoforms. This research evaluated the unique expression of these immune cell subsets across ovarian, bladder, and pancreatic cancers and melanoma by analyzing the mRNA co-expression levels of associated cellular biomarkers.

The selection of these specific T-cell subsets and BTN3A isoforms for analysis was rooted in their significant roles within the TME. Stem-like TILs, noted for their proliferation capacity and generation of effector T-cells within the TME, provide insights into the durability and adaptability of immune responses against tumors [37]. TRM T-cells, recognized for their prolonged tissue residency and swift antigenic response, are crucial for local tumor surveillance and correlate with more favorable clinical outcomes [38,39]. Investigating activated-potentially anti-tumor T-cells estimates the host's direct immune attempts at tumor eradication. Exploring both early and late dysfunctional T-cells offers insights into T-cell exhaustion, a significant obstacle to effective anti-tumor immunity,

suggesting pathways for therapeutic intervention to revitalize these cells [40]. Furthermore, BTN3A isoforms, which play a role in T-cell activation for tumor destruction, emphasize the potential for new regulatory mechanisms and therapeutic targets within cancer immunotherapy [41,42]. This precisely chosen array aimed to explain the complex dynamics of T-cell behavior within tumors, varying the ability to respond to immunotherapy, providing a comprehensive perspective on potential immunotherapeutic interventions, and advancing cancer treatment strategies.

The most notable result was that this comprehensive analysis reveals a broad spectrum of estimated T-cell infiltrations among solid tumors, reflecting their unique immune microenvironments and responsiveness to immunotherapy. Melanoma exhibited the highest levels of T-cell gene signature expression among the tumors studied, while ovarian cancer showed the lowest. These observations appear to mirror the distinct immunogenic profiles of these tumors and the complexity of tumor–immune cell interactions within patients diagnosed with these malignancies. Specifically, melanoma's robust immune response to ICIs, often linked to a higher mutational burden, is associated with T-cell infiltration [33,43,44]. This aligns with the understanding that a high mutational load is associated with improved immunotherapy outcomes due to the enhanced potential for neoantigen presentation and T-cell activation [29]. In contrast, the lower T-cell infiltration and gene signature expression observed in ovarian carcinoma may reflect its lower immunogenic nature or a more suppressive TME, which may present challenges for immunotherapy, supporting the need to develop combinatorial strategies that may enhance immune cell recruitment or counter immunosuppressive elements [45].

T-cell priming, activation, and the overall immune response to tumors depend heavily on the interaction between the tumor antigens and antigen-presenting cells, such as dendritic cells (DCs), along with various co-stimulatory signals within the TME [46]. In our study, we noticed T-cell gene signature expression variability, especially pronounced in bladder cancer and melanoma as indicated by the high IQR in their boxplots, which suggests significant heterogeneity in immune responses within these TMEs, which could result from multiple factors, including the diversity of mutations generating different tumor antigens, the high extent of immune cell infiltration, and the presence of suppressive mechanisms like Tregs or myeloid-derived suppressor cells (MDSCs) [47]. Also, the presence of outliers could indicate individual patients with exceptional immune profiles. At the same time, T-cell gene signature expression variability was more homogenous in ovarian cancer due to the low IQR. This could indicate a more consistent mechanism of tumor antigen presentation, low immune cell recruitment, or a lack of immune diversity in the TME due to tumor/stroma interactions, including a dense fibrotic stroma or vascular characteristics that inhibit immune penetration into the tumor core [48]. This may indicate the importance of cancer-specific approaches in designing immunotherapeutic strategies. Moreover, all examined T-cells showed outliers in the four malignancies, which could hint at a unique patient immune profile that differs from the general trend that is consistent with what is observed in clinical practice. These anomalies may be attributed to distinct genetic, environmental, or treatment-related factors that influence individual responses to immunotherapy, emphasizing the importance of personalized treatment approaches [49].

One obvious finding that emerged from the analysis is that all six predefined T-cell gene sets demonstrated higher expression in immunotherapy responders compared to non-responders, with only TRM T-cells displaying significantly higher expression in responders. This differential gene expression suggests intrinsic immunogenic characteristics of melanoma and a pivotal role of TRM T-cells in mediating effective immune responses in those benefiting from immunotherapy [50,51]. While the higher infiltration by TRM T-cells within the tumors of responders supports their recognized role in sustaining anti-tumor immunity, it raises the possibility that the observed differences may be largely attributed to an overall increase in immune cell presence in responders rather than specific, functionally distinct contributions of the individual T-cell subtypes. Consequently, identifying specific T-cell populations associated with favorable immunotherapy outcomes may lead to more

precise patient selection and treatment customization, potentially enhancing therapeutic efficacy; however, it does not provide conclusive evidence that the specific T-cell subtypes we investigated independently drive treatment response [52]. In this study, the Kaplan-Meier survival analysis suggested that patients with melanoma who had high expression levels of all T-cell GE signatures exhibited significantly better survival outcomes than those with lower expression levels. This implies that all T-cell subsets studied constitute interactive elements of a very complex immunogenic TME that ultimately drives the effective anti-tumor response. This observation also supports broadening the investigation of T-cell presence and activity within the TME in an effort to gain valuable insights that could inform the development of biomarkers for predicting immunotherapy outcomes and refining treatment strategies [53].

In the final part of this study, applying the AUROC analysis to evaluate the predictive value of the T-cell gene signatures for immunotherapy response in melanoma revealed that the TRM gene signature emerged as the most robust indicator, displaying superior predictive value. This finding further supports the pivotal role of TRM T-cells in the immune response to immunotherapy in melanoma. This is likely partly due to TRM cells' capacity for persistent tissue residency and long-term immune surveillance [54]. According to these data, we can infer that the TRM gene expression's potential as a biomarker for predicting outcomes in melanoma immunotherapy facilitates the identification of patients more likely to derive benefits from such treatments. This finding supports further exploration and validation of these gene signatures in broader patient cohorts and across different cancer types, as well as a deeper investigation into the biological mechanisms underlying these signatures. The goal is to uncover novel targets for amplifying immunotherapy efficacy, thereby advancing the field of personalized cancer treatment strategies. Still, we must point out that the observed variability in AUROC values between the OREIN and public datasets presents a complex picture that warrants further exploration. Specifically, while the TRM gene signature showed a higher AUROC in the OREIN dataset, the other biomarkers exhibited better predictive performance in the public datasets as compared to the ORIEN dataset. These observations likely reflect the specific characteristics of the ORIEN cohort, being a "real-world" dataset that reflects all comers among the patient population that presents to an oncology clinic, including broad disease characteristics, performance status, and patient demographics. By comparison, the public datasets used represent clinical trial participants who have to meet strict criteria with regard to the extent of the cancer, performance status, and other required eligibility criteria. Therefore, clinical trial participants are generally more likely to respond to immunotherapy, while "real-world" patient populations tend to be more heterogeneous and have a poorer prognosis but are also more representative of a real-world patient population. In this regard, our findings continue to suggest that TRM T-cells are more likely to play a more pivotal role as a predictive biomarker since they are also significant in the ORIEN cohort.

This study of the differential infiltration of immune cells in four types of tumors provides significant advancements to the field of oncological research, with multiple notable points. The key strength of this study is its use of a large group of patients, selected from the ORIEN database and verified using public databases, increasing the applicability and significance of its results. The study's thorough research of four different types of cancer—ovarian, pancreatic, bladder, and melanoma—contributes to a comparative assessment of the immunogenic characteristics of these malignancies. In addition, using modern RNA sequencing and bioinformatics techniques to measure mRNA co-expression levels of certain biological biomarkers linked to various immune T-cell populations is a robust methodological approach. Although this study has notable strengths, it is not devoid of limitations of the retrospective aspect of the data compilation, which, although comprehensive, may involve inherent biases associated with patient selection and data collection procedures. Moreover, we recognize that our data could be interpreted as reflecting a more generalized immune activation rather than a subtype-specific effect. Future studies using more granular methodologies, such as single-cell RNA sequencing

or spatial transcriptomics, would be valuable to determine whether these T-cell subtypes possess unique roles within the tumor microenvironment or represent components of a broader immune response and elucidate the underlying factors that influence biomarker performance and stress the importance of validating these biomarkers across multiple, diverse cohorts. We also acknowledge that our analysis is limited by the absence of matched non-cancerous control tissue data, which prevents a direct comparison of immune cell infiltration between tumor and normal tissues. Including such controls would have provided valuable insights into the extent of immune cell infiltration relative to baseline levels. Future research should consider incorporating control tissue comparisons to further elucidate the immune landscape across different malignancies, particularly in cancers like ovarian cancer, which exhibited the lowest median T-cell infiltration in our study. When looking at specific ICIs or regimens, we did not find significant differences, which is likely due to the small sample size. This represents a significant limitation, as the mechanisms of action of these ICIs differ and could influence immune cell infiltration in distinct ways. Future studies should aim to collect detailed treatment information to explore whether certain ICIs confer specific immunological advantages or disadvantages, potentially impacting therapeutic strategies and patient stratification. In addition, the interpretation of these findings must be cautiously approached due to the lack of significant p-values for most markers, which could result from various factors, including sample size, patient population variability, or the complex nature of the immune response in melanoma.

5. Conclusions

The findings indicated low expression levels of key T-cell markers, mainly in ovarian carcinoma. In contrast, they were significantly higher in melanoma, followed by bladder cancer, and moderate in pancreatic carcinoma. In melanoma patients treated with ICIs, higher densities of stem-like TILs, TRM T-cells, early dysfunctional T-cells, late dysfunctional T-cells, APA T-cells, and BTN3A isoforms were associated with improved survival, supporting a central role in anti-tumor immunity.

Author Contributions: Conceptualization, A.A.T.; Methodology, A.A.T.; Formal Analysis, A.A.T. and A.C.T.; Investigation, A.A.T.; Resources, A.A.T.; Data Curation, All authors; Writing—Original Draft Preparation, I.E. and A.A.T.; Writing—Review and Editing, All authors; Supervision, A.A.T.; Project Administration, A.A.T.; Funding Acquisition, A.A.T. All authors have read and agreed to the published version of the manuscript.

Funding: This work was supported by an ORIEN FOUNDATION NOVA (New Oncologic Visionary Award) Grant and the Community Foundation of Tampa Bay: 69-21295-01-01 (PI: A. Tarhini).

Institutional Review Board Statement: The study was conducted in accordance with the Declaration of Helsinki and approved by the Institutional Review Board (IRB; IRB# Pro00014441) of the Total Cancer Care Protocol (NCT03977402) and Avatar[®] project.

Informed Consent Statement: Written informed consent was obtained at the participating institutions from all subjects involved in the original study protocol within which this project was nested.

Data Availability Statement: All results relevant to this study are included in the article. Data are available upon reasonable requests to the corresponding author.

Conflicts of Interest: I.E., S.C., M.L.C., J.C., W.S.D., G.J.W., D.S., B.S., J.A.M.-A., S.G., A.R., C.S., A.R.N., and P.H. declare no conflicts of interest. M.M. declares contracted research grants with Merck, Taiho, and the National Comprehensive Cancer Network. IP declares Program Leader (1.2 cal months) for NIH/NCI Cancer Center Support Grant (P30CA016056); consulting with Nouscom, Iovance, Nektar, and Regeneron; and stock owner with Ideaya, Inc. H.C. declares advisory board/consultant: Best Doctors/Teladoc, Orbus Therapeutics, Bristol Meyers Squibb, Regeneron, Novocure, and PPD/Chimerix and research funding (site PI/institutional contract): Orbus, GCAR, Array BioPharma, Karyopharm Therapeutics, Nuvation Bio, Bayer, Bristol Meyer Squib, and Sumitomo Dainippon Pharma. To date, S.M.A. is a member of ASCO COI. I.M.E.N. is on the scientific advisory board of Endectra. L.L. acts as deputy editor for the Journal of Medical Physics and receives funding from NIH and DoD. J.R.C.G has stock options in Compass Therapeutics, Anixa Biosciences

and Alloy Therapeutics; receives consulting fees from Alloy Therapeutics; has intellectual property with Compass Therapeutics and Anixa Biosciences; receives licensing fees from Anixa Biosciences; and is co-founder of Cellepus Therapeutics. A.A.T. declares contracted research grants with their institution from Bristol Myers Squib, Genentech-Roche, Regeneron, Sanofi-Genzyme, Nektar, Clinigen, Merck, Acrotech, Pfizer, Checkmate, OncoSec, Scholar Rock, InflaRx GmbH, Agenus and personal consultant/advisory board fees from Bristol Myers Squibb, Merck, Easai, Instil Bio, Clinigin, Regeneron, Sanofi-Genzyme, Novartis, Partner Therapeutics, Genentech/Roche, BioNTech, Concert AI, AstraZeneca outside the submitted work.

References

- 1. Siegel, R.L.; Miller, K.D.; Wagle, N.S.; Jemal, A. Cancer statistics, 2023. CA A Cancer J. Clin. 2023, 73, 17–48. [CrossRef] [PubMed]
- 2. Ziogas, D.C.; Theocharopoulos, C.; Lialios, P.P.; Foteinou, D.; Koumprentziotis, I.A.; Xynos, G.; Gogas, H. Beyond CTLA-4 and PD-1 Inhibition: Novel Immune Checkpoint Molecules for Melanoma Treatment. *Cancers* **2023**, *15*, 2718. [CrossRef]
- 3. Bondhopadhyay, B.; Sisodiya, S.; Chikara, A.; Khan, A.; Tanwar, P.; Afroze, D.; Singh, N.; Agrawal, U.; Mehrotra, R.; Hussain, S. Cancer immunotherapy: A promising dawn in cancer research. *Am. J. Blood Res.* **2020**, *10*, 375–385. [PubMed]
- 4. Hinshaw, D.C.; Shevde, L.A. The Tumor Microenvironment Innately Modulates Cancer Progression. *Cancer Res.* **2019**, 79, 4557–4566. [CrossRef] [PubMed]
- 5. Topalian, S.L.; Taube, J.M.; Anders, R.A.; Pardoll, D.M. Mechanism-driven biomarkers to guide immune checkpoint blockade in cancer therapy. *Nat. Rev. Cancer* **2016**, *16*, 275–287. [CrossRef]
- 6. Fridman, W.H.; Pages, F.; Sautes-Fridman, C.; Galon, J. The immune contexture in human tumours: Impact on clinical outcome. *Nat. Rev. Cancer* **2012**, *12*, 298–306. [CrossRef]
- 7. Chen, D.S.; Mellman, I. Elements of cancer immunity and the cancer-immune set point. *Nature* **2017**, *541*, 321–330. [CrossRef] [PubMed]
- 8. Chen, D.S.; Mellman, I. Oncology meets immunology: The cancer-immunity cycle. *Immunity* 2013, 39, 1–10. [CrossRef] [PubMed]
- 9. Finotello, F.; Trajanoski, Z. New strategies for cancer immunotherapy: Targeting regulatory T cells. *Genome Med.* **2017**, *9*, 10. [CrossRef]
- 10. Shendure, J.; Ji, H. Next-generation DNA sequencing. Nat. Biotechnol. 2008, 26, 1135–1145. [CrossRef]
- 11. Fenstermacher, D.A.; Wenham, R.M.; Rollison, D.E.; Dalton, W.S. Implementing personalized medicine in a cancer center. *Cancer J.* 2011, 17, 528–536. [CrossRef] [PubMed]
- 12. Caligiuri, M.A.; Dalton, W.S.; Rodriguez, L.; Sellers, T.; Willman, C.L. Orien. Oncol. Issues 2016, 31, 62–66. [CrossRef]
- 13. Bushnell, B.; Rood, J.; Singer, E. BBMerge—Accurate paired shotgun read merging via overlap. *PLoS ONE* **2017**, *12*, e0185056. [CrossRef]
- 14. Dobin, A.; Davis, C.A.; Schlesinger, F.; Drenkow, J.; Zaleski, C.; Jha, S.; Batut, P.; Chaisson, M.; Gingeras, T.R. STAR: Ultrafast universal RNA-seq aligner. *Bioinformatics* **2013**, 29, 15–21. [CrossRef]
- 15. DeLuca, D.S.; Levin, J.Z.; Sivachenko, A.; Fennell, T.; Nazaire, M.D.; Williams, C.; Reich, M.; Winckler, W.; Getz, G. RNA-SeQC: RNA-seq metrics for quality control and process optimization. *Bioinformatics* **2012**, *28*, 1530–1532. [CrossRef]
- 16. Li, B.; Dewey, C.N. RSEM: Accurate transcript quantification from RNA-Seq data with or without a reference genome. *BMC Bioinform.* **2011**, *12*, 323. [CrossRef]
- 17. Johnson, W.E.; Li, C.; Rabinovic, A. Adjusting batch effects in microarray expression data using empirical Bayes methods. *Biostatistics* **2007**, *8*, 118–127. [CrossRef] [PubMed]
- 18. Lee, E.; Chuang, H.Y.; Kim, J.W.; Ideker, T.; Lee, D. Inferring pathway activity toward precise disease classification. *PLoS Comput. Biol.* **2008**, *4*, e1000217. [CrossRef]
- 19. Subramanian, A.; Tamayo, P.; Mootha, V.K.; Mukherjee, S.; Ebert, B.L.; Gillette, M.A.; Paulovich, A.; Pomeroy, S.L.; Golub, T.R.; Lander, E.S.; et al. Gene set enrichment analysis: A knowledge-based approach for interpreting genome-wide expression profiles. *Proc. Natl. Acad. Sci. USA* **2005**, *102*, 15545–15550. [CrossRef]
- 20. Liberzon, A.; Subramanian, A.; Pinchback, R.; Thorvaldsdóttir, H.; Tamayo, P.; Mesirov, J.P. Molecular signatures database (MSigDB) 3.0. *Bioinformatics* **2011**, 27, 1739–1740. [CrossRef]
- 21. Liberzon, A.; Birger, C.; Thorvaldsdóttir, H.; Ghandi, M.; Mesirov, J.P.; Tamayo, P. The Molecular Signatures Database (MSigDB) hallmark gene set collection. *Cell Syst.* **2015**, *1*, 417–425. [CrossRef]
- 22. Xie, M.; Lee, K.; Lockhart, J.H.; Cukras, S.D.; Carvajal, R.; Beg, A.A.; Flores, E.R.; Teng, M.; Chung, C.H.; Tan, A.C. TIMEx: Tumor-immune microenvironment deconvolution web-portal for bulk transcriptomics using pan-cancer scRNA-seq signatures. *Bioinformatics* **2021**, *37*, 3681–3683. [CrossRef] [PubMed]
- 23. Du, K.; Wei, S.; Wei, Z.; Frederick, D.T.; Miao, B.; Moll, T.; Tian, T.; Sugarman, E.; Gabrilovich, D.I.; Sullivan, R.J.; et al. Pathway signatures derived from on-treatment tumor specimens predict response to anti-PD1 blockade in metastatic melanoma. *Nat. Commun.* 2021, 12, 6023. [CrossRef] [PubMed]
- 24. Gide, T.N.; Quek, C.; Menzies, A.M.; Tasker, A.T.; Shang, P.; Holst, J.; Madore, J.; Lim, S.Y.; Velickovic, R.; Wongchenko, M.; et al. Distinct Immune Cell Populations Define Response to Anti-PD-1 Monotherapy and Anti-PD-1/Anti-CTLA-4 Combined Therapy. *Cancer Cell* **2019**, *35*, 238–255.e236. [CrossRef]

- Zappasodi, R.; Serganova, I.; Cohen, I.J.; Maeda, M.; Shindo, M.; Senbabaoglu, Y.; Watson, M.J.; Leftin, A.; Maniyar, R.; Verma, S.; et al. CTLA-4 blockade drives loss of T(reg) stability in glycolysis-low tumours. *Nature* **2021**, *591*, 652–658. [CrossRef] [PubMed]
- 26. Ribas, A.; Algazi, A.; Ascierto, P.A.; Butler, M.O.; Chandra, S.; Gordon, M.; Hernandez-Aya, L.; Lawrence, D.; Lutzky, J.; Miller, W.H., Jr.; et al. PD-L1 blockade in combination with inhibition of MAPK oncogenic signaling in patients with advanced melanoma. *Nat. Commun.* 2020, 11, 6262. [CrossRef]
- 27. Freeman, S.S.; Sade-Feldman, M.; Kim, J.; Stewart, C.; Gonye, A.L.K.; Ravi, A.; Arniella, M.B.; Gushterova, I.; LaSalle, T.J.; Blaum, E.M.; et al. Combined tumor and immune signals from genomes or transcriptomes predict outcomes of checkpoint inhibition in melanoma. *Cell Rep. Med.* **2022**, *3*, 100500. [CrossRef]
- 28. Hugo, W.; Zaretsky, J.M.; Sun, L.; Song, C.; Moreno, B.H.; Hu-Lieskovan, S.; Berent-Maoz, B.; Pang, J.; Chmielowski, B.; Cherry, G.; et al. Genomic and Transcriptomic Features of Response to Anti-PD-1 Therapy in Metastatic Melanoma. *Cell* **2016**, *165*, 35–44. [CrossRef]
- 29. Lauss, M.; Donia, M.; Harbst, K.; Andersen, R.; Mitra, S.; Rosengren, F.; Salim, M.; Vallon-Christersson, J.; Torngren, T.; Kvist, A.; et al. Mutational and putative neoantigen load predict clinical benefit of adoptive T cell therapy in melanoma. *Nat. Commun.* **2017**, *8*, 1738. [CrossRef]
- 30. Lee, J.H.; Shklovskaya, E.; Lim, S.Y.; Carlino, M.S.; Menzies, A.M.; Stewart, A.; Pedersen, B.; Irvine, M.; Alavi, S.; Yang, J.Y.H.; et al. Transcriptional downregulation of MHC class I and melanoma de- differentiation in resistance to PD-1 inhibition. *Nat. Commun.* 2020, 11, 1897. [CrossRef]
- 31. Liu, D.; Schilling, B.; Liu, D.; Sucker, A.; Livingstone, E.; Jerby-Arnon, L.; Zimmer, L.; Gutzmer, R.; Satzger, I.; Loquai, C.; et al. Integrative molecular and clinical modeling of clinical outcomes to PD1 blockade in patients with metastatic melanoma. *Nat. Med.* **2019**, 25, 1916–1927. [CrossRef] [PubMed]
- 32. Riaz, N.; Havel, J.J.; Makarov, V.; Desrichard, A.; Urba, W.J.; Sims, J.S.; Hodi, F.S.; Martin-Algarra, S.; Mandal, R.; Sharfman, W.H.; et al. Tumor and Microenvironment Evolution during Immunotherapy with Nivolumab. *Cell* **2017**, *171*, 934–949.e916. [CrossRef] [PubMed]
- 33. Van Allen, E.M.; Miao, D.; Schilling, B.; Shukla, S.A.; Blank, C.; Zimmer, L.; Sucker, A.; Hillen, U.; Foppen, M.H.G.; Goldinger, S.M.; et al. Genomic correlates of response to CTLA-4 blockade in metastatic melanoma. *Science* 2015, 350, 207–211. [CrossRef] [PubMed]
- 34. Maffuid, K.; Cao, Y. Decoding the Complexity of Immune-Cancer Cell Interactions: Empowering the Future of Cancer Immunotherapy. *Cancers* **2023**, *15*, 4188. [CrossRef] [PubMed]
- 35. Blessin, N.C.; Li, W.; Mandelkow, T.; Jansen, H.L.; Yang, C.; Raedler, J.B.; Simon, R.; Buscheck, F.; Dum, D.; Luebke, A.M.; et al. Prognostic role of proliferating CD8(+) cytotoxic Tcells in human cancers. *Cell Oncol.* **2021**, *44*, 793–803. [CrossRef]
- 36. Zuo, S.; Wei, M.; Wang, S.; Dong, J.; Wei, J. Pan-Cancer Analysis of Immune Cell Infiltration Identifies a Prognostic Immune-Cell Characteristic Score (ICCS) in Lung Adenocarcinoma. *Front. Immunol.* **2020**, *11*, 1218. [CrossRef]
- 37. Yi, L.; Yang, L. Stem-like T cells and niches: Implications in human health and disease. *Front. Immunol.* **2022**, *13*, 907172. [CrossRef]
- 38. Gebhardt, T.; Wakim, L.M.; Eidsmo, L.; Reading, P.C.; Heath, W.R.; Carbone, F.R. Memory T cells in nonlymphoid tissue that provide enhanced local immunity during infection with herpes simplex virus. *Nat. Immunol.* **2009**, *10*, 524–530. [CrossRef] [PubMed]
- 39. Masopust, D.; Choo, D.; Vezys, V.; Wherry, E.J.; Duraiswamy, J.; Akondy, R.; Wang, J.; Casey, K.A.; Barber, D.L.; Kawamura, K.S.; et al. Dynamic T cell migration program provides resident memory within intestinal epithelium. *J. Exp. Med.* 2010, 207, 553–564. [CrossRef]
- 40. Philip, M.; Schietinger, A. CD8(+) T cell differentiation and dysfunction in cancer. Nat. Rev. Immunol. 2022, 22, 209–223. [CrossRef]
- 41. Harly, C.; Guillaume, Y.; Nedellec, S.; Peigne, C.M.; Monkkonen, H.; Monkkonen, J.; Li, J.; Kuball, J.; Adams, E.J.; Netzer, S.; et al. Key implication of CD277/butyrophilin-3 (BTN3A) in cellular stress sensing by a major human gammadelta T-cell subset. *Blood* **2012**, 120, 2269–2279. [CrossRef] [PubMed]
- 42. Rhodes, D.A.; Stammers, M.; Malcherek, G.; Beck, S.; Trowsdale, J. The cluster of BTN genes in the extended major histocompatibility complex. *Genomics* **2001**, *71*, 351–362. [CrossRef] [PubMed]
- 43. Snyder, A.; Makarov, V.; Merghoub, T.; Yuan, J.; Zaretsky, J.M.; Desrichard, A.; Walsh, L.A.; Postow, M.A.; Wong, P.; Ho, T.S.; et al. Genetic basis for clinical response to CTLA-4 blockade in melanoma. *N. Engl. J. Med.* **2014**, *371*, 2189–2199. [CrossRef]
- 44. Rizvi, N.A.; Hellmann, M.D.; Snyder, A.; Kvistborg, P.; Makarov, V.; Havel, J.J.; Lee, W.; Yuan, J.; Wong, P.; Ho, T.S.; et al. Cancer immunology. Mutational landscape determines sensitivity to PD-1 blockade in non-small cell lung cancer. *Science* 2015, 348, 124–128. [CrossRef]
- 45. Yang, B.; Li, X.; Zhang, W.; Fan, J.; Zhou, Y.; Li, W.; Yin, J.; Yang, X.; Guo, E.; Li, X.; et al. Spatial heterogeneity of infiltrating T cells in high-grade serous ovarian cancer revealed by multi-omics analysis. *Cell Rep. Med.* **2022**, *3*, 100856. [CrossRef]
- 46. Albert, M.L.; Sauter, B.; Bhardwaj, N. Dendritic cells acquire antigen from apoptotic cells and induce class I-restricted CTLs. *Nature* **1998**, 392, 86–89. [CrossRef]
- 47. Nesseler, J.P.; Lee, M.H.; Nguyen, C.; Kalbasi, A.; Sayre, J.W.; Romero, T.; Nickers, P.; McBride, W.H.; Schaue, D. Tumor Size Matters-Understanding Concomitant Tumor Immunity in the Context of Hypofractionated Radiotherapy with Immunotherapy. *Cancers* 2020, *12*, 714. [CrossRef] [PubMed]

- 48. Hegde, P.S.; Karanikas, V.; Evers, S. The Where, the When, and the How of Immune Monitoring for Cancer Immunotherapies in the Era of Checkpoint Inhibition. *Clin. Cancer Res.* **2016**, 22, 1865–1874. [CrossRef]
- 49. Wang, R.C.; Wang, Z. Precision Medicine: Disease Subtyping and Tailored Treatment. Cancers 2023, 15, 3837. [CrossRef]
- 50. Enamorado, M.; Iborra, S.; Priego, E.; Cueto, F.J.; Quintana, J.A.; Martínez-Cano, S.; Mejías-Pérez, E.; Esteban, M.; Melero, I.; Hidalgo, A.; et al. Enhanced anti-tumour immunity requires the interplay between resident and circulating memory CD8(+) T cells. *Nat. Commun.* **2017**, *8*, 16073. [CrossRef]
- 51. Park, S.L.; Buzzai, A.; Rautela, J.; Hor, J.L.; Hochheiser, K.; Effern, M.; McBain, N.; Wagner, T.; Edwards, J.; McConville, R.; et al. Tissue-resident memory CD8(+) T cells promote melanoma-immune equilibrium in skin. *Nature* **2019**, *565*, 366–371. [CrossRef] [PubMed]
- 52. Malik, B.T.; Byrne, K.T.; Vella, J.L.; Zhang, P.; Shabaneh, T.B.; Steinberg, S.M.; Molodtsov, A.K.; Bowers, J.S.; Angeles, C.V.; Paulos, C.M.; et al. Resident memory T cells in the skin mediate durable immunity to melanoma. *Sci. Immunol.* **2017**, 2, eaam6346. [CrossRef] [PubMed]
- 53. Arnaud, M.; Chiffelle, J.; Genolet, R.; Navarro Rodrigo, B.; Perez, M.A.S.; Huber, F.; Magnin, M.; Nguyen-Ngoc, T.; Guillaume, P.; Baumgaertner, P.; et al. Sensitive identification of neoantigens and cognate TCRs in human solid tumors. *Nat. Biotechnol.* **2022**, *40*, 656–660. [CrossRef] [PubMed]
- 54. Szabo, P.A.; Miron, M.; Farber, D.L. Location, location: Tissue resident memory T cells in mice and humans. *Sci. Immunol.* **2019**, *4*, eaas9673. [CrossRef] [PubMed]

Disclaimer/Publisher's Note: The statements, opinions and data contained in all publications are solely those of the individual author(s) and contributor(s) and not of MDPI and/or the editor(s). MDPI and/or the editor(s) disclaim responsibility for any injury to people or property resulting from any ideas, methods, instructions or products referred to in the content.





Review

Tissue-Resident Memory T Cells in Cancer Metastasis Control

Tyler H. Montgomery ¹, Anuj P. Master ¹, Zeng Jin ¹, Qiongyu Shi ¹, Qin Lai ¹, Rohan Desai ¹, Weizhou Zhang ^{1,2}, Chandra K. Maharjan ^{1,*} and Ryan Kolb ^{1,2,*}

- Department of Pathology, Immunology and Laboratory Medicine, College of Medicine, University of Florida, Gainesville, FL 32610, USA; t.montgomery@ufl.edu (T.H.M.); anujmaster@ufl.edu (A.P.M.); zengjing@ufl.edu (Z.J.); qshi1@ufl.edu (Q.S.); qinlai7@gmail.com (Q.L.); rohan.desai@ufl.edu (R.D.); zhangw@ufl.edu (W.Z.)
- ² UF Health Cancer Center, University of Florida, Gainesville, FL 32610, USA
- * Correspondence: cmaharjan@ufl.edu (C.K.M.); ryankolb@ufl.edu (R.K.); Tel.: +1-352-273-6748 (C.K.M.)

Abstract: Tissue-resident memory T (TRM) cells have emerged as critical sentinels in the control of cancer metastasis, yet their precise roles across different tumor types and tissues remain underappreciated. Here, we review current insights into the mechanisms governing TRM cell seeding and retention in pre-metastatic niches, their effector functions in eliminating disseminated tumor cells, and their dynamic crosstalk with local stromal and myeloid populations. Here, we highlight evidence for organ-specific variability in TRM cell-mediated immunity, discuss strategies for therapeutically harnessing these cells—ranging from vaccination and checkpoint modulation to chemokine axis manipulation—and explore their promise as prognostic biomarkers. Finally, we outline key knowledge gaps and future directions aimed at translating TRM cell biology into targeted interventions to prevent and treat metastatic disease.

Keywords: tissue-resident memory T (TRM) cells; cancer; metastasis; cancer therapy

1. Introduction

Metastasis remains one of the largest challenges in modern cancer therapy, accounting for the vast majority of cancer-related mortality [1]. Despite this burden, our understanding of how the immune system responds to and controls metastases is still emerging. Tissue-resident memory T (TRM) cells have emerged as a distinct subset of memory T lymphocytes that are critical in tumor control and primary players in immune-checkpoint inhibitor function. Early evidence suggests that TRM cells may also play an essential role in the prevention and control of metastases. TRM biology has been heavily studied in the two decades since its identification, but its involvement specifically in metastatic seeding and progression has yet to be fully synthesized.

This review summarizes current knowledge on how TRM cells influence cancer metastasis, highlighting their core biology, metastatic control program, and clinical significance as both a prognostic biomarker and potential therapeutic target. We also discuss unanswered questions and future directions necessary to better understand TRM cell-mediated metastasis control.

2. TRM Biology Relevant to Metastasis Control

TRM cells are a non-circulating subset of memory T lymphocytes (the other known subsets are effector memory and central memory T cells) that take up long-term residence within the tissue of peripheral organs. During a tissue infection, TRM cells elicit

a rapid response to eliminate infected cells to evade a potential systemic immune reaction. Traditionally, TRM cells have been identified by their expression of CD69—an early activation marker that inhibits sphingosine-1-phosphate receptor-1 (S1PR1) to prevent tissue egress—and CD103, an integrin that binds epithelial E-cadherin to promote retention within epithelial layers [2]. Despite this, multiple studies have now shown that nearly all TRM markers, including CD69 and CD103, can vary substantially in expression by tissue type, activation state, and even disease-specific context [3–6]. Here, we limit our discussion to the emerging aspects of TRM biology most relevant to metastasis control. For a comprehensive general overview of TRM cell lineage commitment, full marker panels, and core transcriptional programs, readers are referred to several recent reviews [7–10].

Below, we focus on three key aspects of TRM biology—tissue seeding, on-site function, and microenvironment influence—that may dictate their roles in metastatic and pre-metastatic tissues and might involve relevant target pathways for future therapies (Figure 1). We then address direct mechanistic evidence demonstrating TRM cell-mediated control of metastasis in preclinical and clinical models.

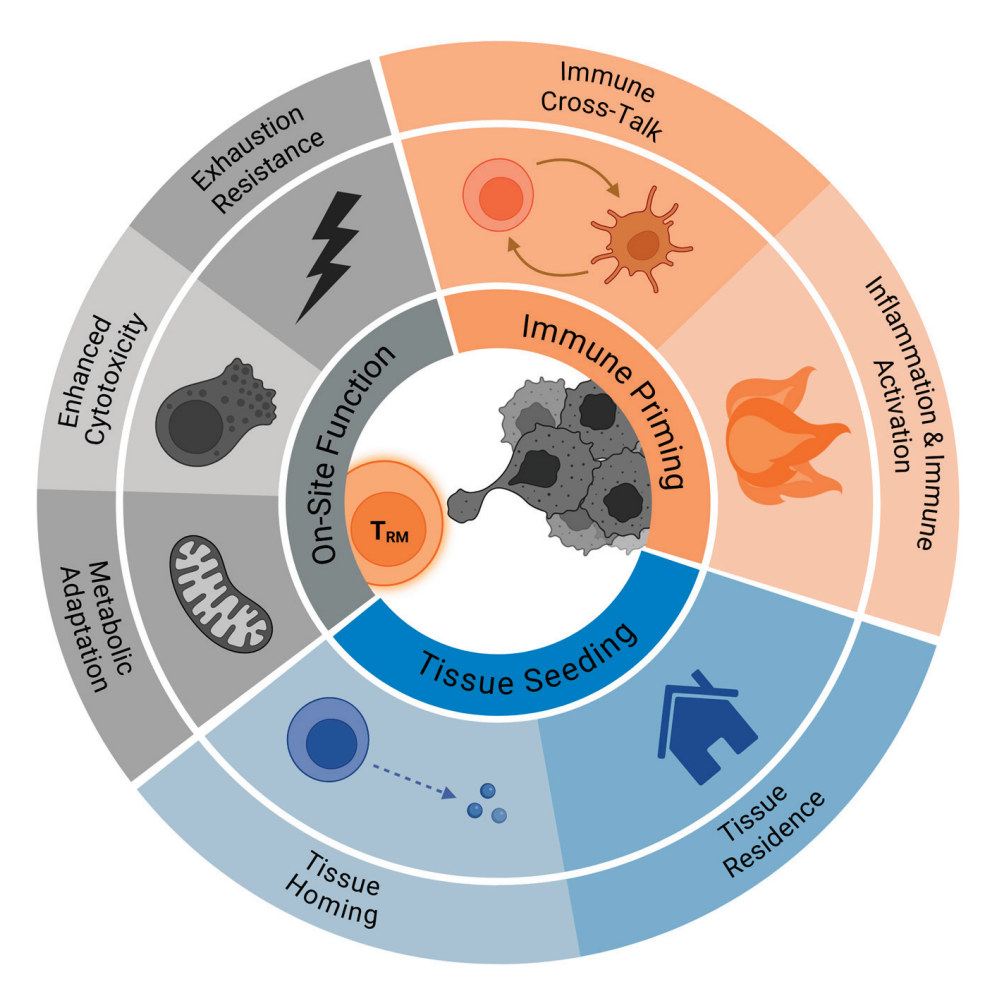


Figure 1. Relevant factors influencing TRM cell-mediated control of cancer metastasis.

2.1. Tissue Seeding and Retention of TRM Cells

The mechanisms governing how TRM cells differentiate and seed within tumors and pre-metastatic tissues remain incompletely defined, but chemokine and cytokine cues clearly shape homing, local differentiation, and durable residence. CXCR6 is a chemokine receptor and is often expressed by TRM cells and other T cell subtypes, and its roles in immunosurveillance and tissue residence are multifaceted [11,12]. Its ligand, CXCL16, can be expressed by cancer cells and antigen-presenting cells (APCs), and the interaction of

the two has been found to play a key role in recruiting and retaining TRMs in various tissue contexts (Figure 2) [12,13]. For instance, tumor-specific CXCR6 knockout (KO) T cells demonstrate greatly reduced TRM cell retention within ovarian tumors, increasing responses in blood and spleen, but reducing resident memory behavior at the primary tumor and leading to poor tumor control [14]. This suggests that CXCR6 is critical for tissue residence.

More studies have focused on the exploration of modulating CXCL16 rather than targeting CXCR6 for exerting influence on TRM cell seeding. Viral-infection models have demonstrated that epithelial-cell-derived CXCL16 establishes a chemotactic gradient to pull CXCR6+ TRM cells into the airway lumen, which can be depleted by interfering with the CXCL16-CXCR6 axis [11]. In cancer, CXCL16 may be directly targetable as monotherapy and as a therapeutic adjuvant. For example, anti-CXCL16 blockade in mouse breast cancer liberates CXCR6+ effectors from primary tumors, driving their migration and differentiation into lung TRM cells (see Section 3) and highlighting a promising target for TRM-directed therapies [15]. In Head-and-neck and lung tumor models, cancer vaccine immunization can drive local CXCL16 upregulation, CXCR6 expression on TRM precursors, and robust TRM recruitment, while impaired TRM cell seeding was observed in CXCR6deficient mice [16]. Together, these studies indicate that local CXCL16 expression in tissues by stromal or tumor cells plays a critical role in TRM attraction and residency via CXCR6 and may compete to dictate where TRM precursors localize. Moreover, emphasis on balanced interference with this axis is required when modulating homing into premetastatic niches and protecting against metastatic seeding.

Complementing this positional axis, transforming growth factor beta (TGF- β) signaling has been identified to promote T cells to adopt tissue resident phenotypes like CD103 expression and subsequent tissue retention (Figure 2) [17]. Loss of TGF- β receptor signaling sharply reduces accumulation of CD103+ TRM-like cells in pancreatic tumor models [18]. Like with CXCL16 blockade, TGF- β neutralization has also been demonstrated to cause downregulation of tissue residency markers, leading to enhanced systemic tumor immunity, secondary tumor response, and overall survival when combined with PD-L1 blockade in mice [19]. This evidence suggests that, like the CXCR6-CXCL16 axis, TGF- β modulation could offer an opportunity to influence TRM behavior to promote systemic tumor immunity and control metastasis, especially when combined with other treatments.

After establishing within target tissues, TRM cell survival depends on interfacing with a dedicated niche. In mouse melanoma models, CD11c+ dendritic cells (DCs) were found to closely cluster with CXCR6+ TRMs around hair follicles, express high CXCL16, and were required to maintain TRM cell populations [20]. Short-term DC ablation disrupted these clusters, and prolonged depletion caused them to disappear completely [20]. Other murine melanoma models showed tumor DCs presenting CXCL16 and trans-presenting IL-15 to incoming T cells in the TME, while blocking these signals led to declines in their survival [21]. While not limited to solely TRM cells, this study suggests a potential role of DC in maintenance of TRM cell populations by directly supplying CXCL16 and IL-15 signals—known to be key to TRM cell survival [21,22]. Further investigation will be needed to understand how this potential interaction between DCs and TRM cells occurs in tissues not harboring active tumors, including pre-metastatic niches. Consideration of the factors that hold and maintain TRM cell populations at tumor-relevant sites will be critical for the design of functional and lasting TRM-based therapeutics.

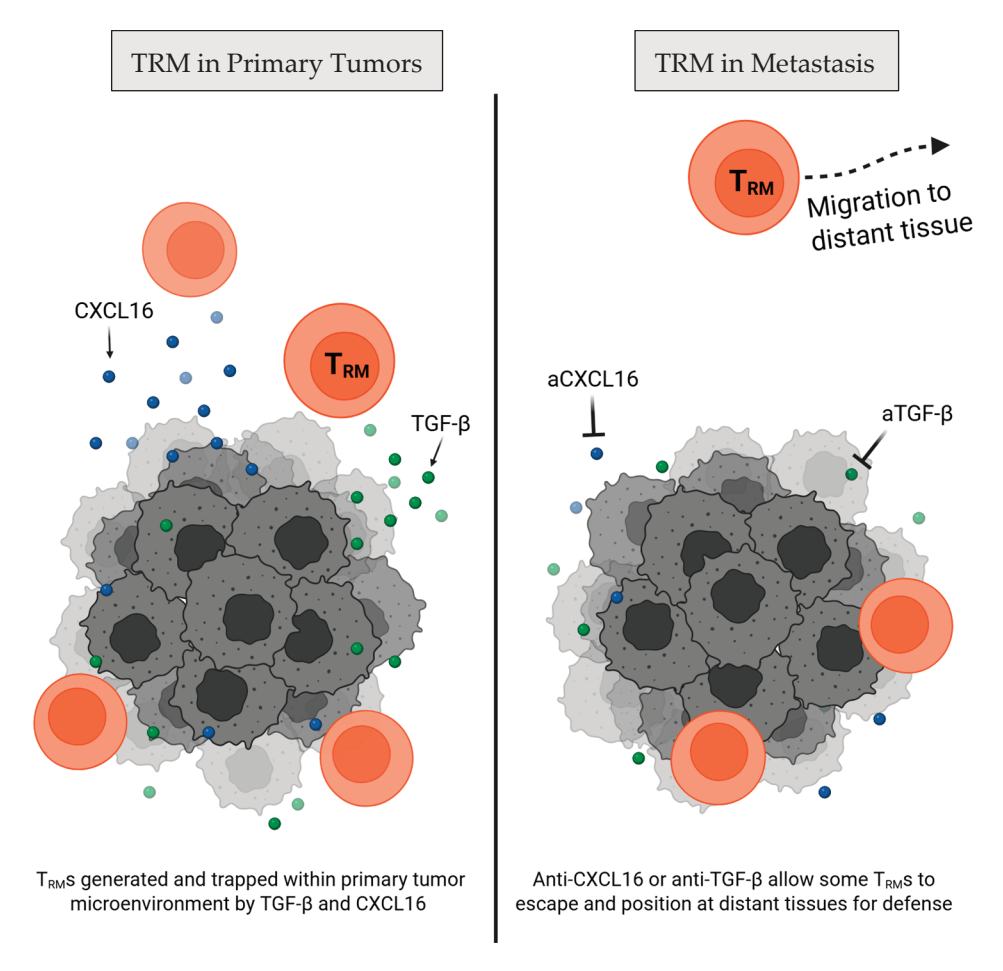


Figure 2. Retention of TRM cells at a primary tumor site is influenced by TGF- β and CXCL16 signaling. (**Left**) CXCL16-CXCR6 axis [12,13] and TGF- β signaling [17,19] promote primary tumor retention of TRM cells, while (**Right**) disruption of these pathways has been shown to induce dissemination of TRM cells into distant tissues for metastatic control [15,18,19].

2.2. On-Site TRM Cell Effector Function

TRM cells not only seed and persist in tissues but also exhibit unique functional and metabolic programs that distinguish them from circulating T cells and enable them to endure and act in hostile microenvironments, such as tumors or metastatic sites. TRM cells are distinguished by their ability to launch rapid, high-potency effector responses upon antigen encounter, an attribute that makes them especially efficient killers of tumors [23,24]. Consistently, tumor co-culture experiments have shown that TRM cells demonstrate superior tumor killing when compared to peripheral blood CD8+ T cells [25].

In order to carry out their heightened capability for targeted killing, TRM cells must survive long-term in nutrient-restricted and potentially hypoxic tissue niches, conditions that circulating T cells, which favor glycolysis, are poorly equipped to endure. To accomplish this, some TRM cells have been observed to rewire their metabolism in a tissue-dependent manner. In the lung, TRM cells take up exogenous fatty acids and rely on carnitine-palmitoyl transferase 1A (CPT1A)-mediated B-oxidation for energy [26]. Genetic or pharmacologic inhibition of CPT1A markedly reduces CD103+CD69+ TRM pools in the lung [26]. Similarly, gut TRM cells use fatty acid oxidation to fuel their homeostatic proliferation and survival, the blockage of which leads to TRM cell attrition in the intestine [27]. Beyond lipid oxidation, TRM cells in the small intestine have been found to depend on de novo cholesterol synthesis via the SREBP2-regulated mevalonate pathway. Murine models have demonstrated that this pathway—and downstream coenzyme Q production—is essential for maintaining mitochondrial membrane potential and reactive-oxygen-species

buffering in TRM cells [28]. Disruption of these features impaired TRM cell persistence and function without affecting circulating memory cells [28].

It is evident that tissue-dependent metabolism is a core part of TRM cell function, and that consideration of local microenvironment cues—including oxygen and metabolite availability—will be required for the development of TRM cell-based therapies, especially those hoping to prophylactically position TRMs to protect tissues against incoming metastasis. For applications aimed at controlling existing metastatic growths, direct metabolic profiling of TRM cells in metastatic tumors remains unexplored, although some primary tumors have been profiled [29]. Therefore, more work will need to be done to understand the specific TRM cell metabolic requirements in diverse metastatic and pre-metastatic environments.

2.3. TRM Cell and Microenvironment Crosstalk

Beyond direct killing, TRM cells serve as on-site immunological alarms, shaping the local tissue by creating an inflamed environment, promoting local T cell responses, and crosstalk with other immune cells to reinforce local and systemic antitumor responses. Mechanistic murine studies have shown that TRM cell activation triggers a cascade of crosstalk, licensing migratory dendritic cells via IFN- γ /TNF α to prime systemic circulating T cells [30] and secreting IL-2/IL-15 to recruit bystander T cells into tissues [31]. Extending these principles to human metastases, single-cell transcriptomics, and multiplex imaging of ovarian omental lesions revealed TRM cell-like clusters co-localized with granulysin+CD4+ T cells, proliferative plasmablasts, and activated macrophages, creating an intensely inflamed immune niche [32]. In viral models, TRM activation in the mouse brain was found to lead to TRM-directed local immune activation and recruitment of immune cells, further supporting their immune-directing capabilities [33]. The authors note that this feature could be harnessed to target brain tumors [33], suggesting a clear therapeutic avenue to be explored to target brain primary tumors and metastases in a TRM-mediated manner. These examples of multicellular immune collaboration illustrate how TRMs can orchestrate a local and systemic immune response that could underpin durable containment of metastases. TRM can therefore be understood as not only direct defenders but also on-site alarms which ignite local inflammation, recruit other immune cells, and promote systemic CTL responses upon antigen re-encounter. As such, TRMs are uniquely equipped and positioned to detect and contain potential metastases, thereby preventing their growth at sites distant from the primary tumor.

3. TRM Mechanistic and Phenotypic Insights

Recent studies have overturned the notion of tissue-resident memory T (TRM) cells as mere local sentinels, revealing them instead as active defenders against metastatic initiation and spread. Far from passive residents, CD8+ TRMs infiltrate pre-metastatic niches, intercept circulating tumor cells, and orchestrate a local alarm system that identifies and contains micrometastases. Mechanistic work and observations in both animal models and patient samples suggest that TRM cells may actively patrol and defend metastatic niches; understanding how they carry out these functions will be critical for designing TRM cell-targeted therapies against metastasis.

Tumor-specific TRM cells preemptively position themselves within non-lymphoid tissues to prevent metastatic seeding. In a murine 4T1 breast cancer model, pre-metastatic lungs were found to contain TRM cells with high clonotypic overlap between primary tumor T cells 3 weeks following tumor formation [15]. Further, promotion of T cell egress from the primary tumors using anti-CXCL16 by the same authors enhanced protection against lung metastasis, likely due to the boosted lung TRM cell populations, and significantly

reduced metastatic lung tumor burden in a TRM cell-mediated manner [15], suggesting the ability to functionally direct TRM cell populations. By contrast, in metastatic melanoma, lung metastatic seeding was found to be predominantly restrained by circulating memory CD8+ T cells—with little contribution from tissue-resident subsets—highlighting that TRM-mediated metastasis defense may vary markedly by cancer type even within the same organ [34]. Strikingly, targeted prime-boost vaccination with an intramuscular DNA prime followed by an intranasal influenza-vector was demonstrated to overcome this difference, converting circulatory central memory T (TCM) cells to lung-resident CD8+ TRM cells, and that alone sufficed to block melanoma and mesothelioma lung metastases in mice [35]. These data demonstrate that actively directing TRM cell seeding and accumulation offers a powerful strategy to fortify pre-metastatic niches against tumor spread.

In many tissue contexts, TRM cells show significant heterogeneity and multiple distinct populations of different origins. Despite this, the effect of tissue environment on anti-metastasis activities of TRM is just beginning to be investigated. In colorectal cancer liver metastases isolated from human samples, two main subsets of TRM cells were identified as CD103+CD69+ or CD103-CD69+ TRM [24]. Since liver TRM normally develop without TGF-β (and therefore lack CD103 expression), the presence of CD103+ TRMs suggests that the cell fate of this population could have been determined by the original tumor microenvironment [24]. This CD103+CD69+ TRM population was found to be more cytotoxic, expressed activation markers (PD-1, CD39, and CD49a), and was the only population that was associated with better liver metastasis outcomes [24]. This suggests that the metastasis seeding destination may matter less for TRM phenotype and functionality than the TME of origin, although much more research will be needed to support this theory. PD-1 expression and function also contribute to the heterogeneity of TRM phenotypes, with multiple reports implicating it as a marker of residency and activation rather than a marker of exhaustion [24,33,36,37]. Furthermore, characterization of skin TRMs revealed PD-1 to be crucial for early TRM engraftment and fate-determination by sensitizing TRMs to TGF-β [36]. PD-1 knockout in skin TRMs resulted in the loss of skin-specific transcriptional signatures such as extracellular matrix-related transcripts and adoption of a similar phenotype to PD-1 knockout TRMs from the spleen [36]. Likewise, anti-PD-1 blockade induced toxicity and impaired skin TRM cell formation [36], suggesting that PD-1 plays a very important role in TRM function in the skin. This highlights yet another aspect that can influence the heterogeneity of TRM phenotypes and responses within different organs and should be considered when developing skin-targeted TRM therapeutics.

While TRM cells have traditionally been defined as memory T cells that are resident within non-lymphoid tissues, recent evidence suggests that they can also establish long-term, non-recirculating residency in lymph nodes (LNs) following local antigen exposure [38,39]. Large numbers of CD8+CD103+CD69+ TRM cells have been observed in human melanoma-infiltrated lymph nodes through both immunofluorescence and transcriptional analysis, and these cells were found to concentrate at the tumor border [34]. In functional parabiosis experiments, only mice retaining these LN TRM cells—but not their partner mice sharing all circulating T cells—rejected direct challenge with melanoma metastases, demonstrating that LN TRM cells may suffice for metastatic protection in some contexts [34]. TRM cells frequently position themselves at the margins of emerging metastases. For instance, CD8+CD103+ TRMs have been found to cluster at the border of human melanoma metastases in the skin and lymph node [40]. Further, a recent case report of an 82-year-old melanoma patient demonstrated that an in-transit micrometastasis was densely infiltrated by CD8+CD103+ TRM cells that surrounded individual melanoma cells [41]. These spatial proximities imply that TRMs could enforce cancer-immune equilibrium even at the earliest, clinically undetectable stages of metastatic growth, which could be exploited

for therapeutic fortification against future metastases. Still, the presence alone of TRMs does not always guarantee metastatic control: in a vaginal metastatic melanoma patient, CD8+CD103+ TRM cells clustered at the margins of distant metastases and expanded following anti-PD1 therapy but were insufficient to clear the tumors due to tumor MHC-I loss [42]. Despite this failure, in vitro experiments demonstrated the ability of these cells to recognize the metastatic tumor cells and respond with stronger cytotoxicity than all other CD8+ T cell types, suggesting that in vivo TRM cell responses are likely suppressed in some contexts [42]. The maintenance of close spatial associations between metastases and TRM cells across diverse metastatic relevant organs (such as lymph nodes, lungs, and liver) suggests a clear opportunity for anti-metastatic therapies; however, more work will be needed to verify true functional interactions (like direct cell killing) between TRM and metastases beyond just spatial proximity.

Taken together, this early evidence suggests a clear potential role for TRM cells in controlling metastasis spread, seeding, and growth. While the mechanistic understanding of how TRM cells directly operate within each tissue and respond to diverse contexts and cues is still developing, our current knowledge suggests a unique opportunity for therapeutically boosting these tissue defenders to provide early protection for highly metastatic cancers.

4. TRM Therapeutic and Biomarker Implications for Metastasis Control

Although direct interventional data is still emerging, multiple lines of preclinical evidence and early clinical correlations point to tissue-resident memory T (TRM) cells both as targets for anti-metastatic therapies and as powerful biomarkers of metastatic risk and response.

4.1. Therapeutics Avenues Targeting TRM Cell Populations

Exploiting TRM cell biology for therapeutic applications has been widely suggested in both infection and cancer contexts. While most studies to date have focused on enhancing primary-tumor control, growing evidence indicates that TRM cell-based interventions can also prevent or clear metastases. Diverse strategies to manipulate TRM cell expansion, function, and trafficking at metastases are summarized in Table 1, and explored in depth below.

Vaccine-based strategies for inducing differentiation and expansion of TRM cell populations have garnered the most interest within the field, with studies recognizing their potential as a cancer therapy [43]. Prime-boost vaccination specifically has emerged as a powerful approach to preemptively seed TRM cells to protect tissues against metastasis. One study demonstrated that tumor DNA priming immunization followed by an intranasal live-attenuated influenza boost can reprogram TCM cells into CD103+CD69+ TRM cells within two days of mucosal boosting, providing robust protection against melanoma and mesothelioma lung metastases in mice [35]. In a complementary strategy, a subcutaneous prime and intranasal boost of microsphere encapsulated tumor antigen peptides generated lung TRM cell pools detectable two months post-boost that significantly reduced B16F10 melanoma nodules in the lung [44]. Extending these principles, an intranasal adenoviral vector alongside an IL-1 β adjuvant elicited high frequencies of lung TRM cells that, even in prophylactic settings, curtailed 4T1 breast cancer metastases and, when combined with focal radiotherapy, further enhanced tumor control [45]. Similarly, intranasal delivery of CpG-coated, tumor-antigen-containing nanoparticles elicited lung-resident CD8+ TRM cells that dramatically reduced 4T1 breast-cancer metastases [46]. Evidently, there are many potential technical approaches to vaccine-based strategies for boosting TRM cells; differences in potency, selectivity, and cost will need to be investigated and weighed to develop

the best therapeutic platform. Whatever the mechanism, vaccine-based approaches clearly show promise for preemptively staging TRM cells to protect tissues against metastases. Despite this potential, current evidence is limited to vaccine functionality in preventing lung metastases (likely due to the intranasal delivery method) which, although highly relevant due to the lungs being a site of frequent metastasis, calls for further investigation about efficacy of these approaches in preventing metastasis in other sites such as the lymph nodes, brain, liver, and bone.

Table 1. TRM cell boosting therapeutic strategies for potential metastasis control.

Therapy Approach	Techniques	Mechanism	Cancer Models	Key Outcome	Direct Metastasis Control Evidence
Vaccines	Prime-boost vaccination [35,44]	Intranasal attenuated influenza or boost following DNA vaccine priming promotes TRM migration and differentiation	Metastatic murine B16F10 (melanoma) and AB1 (mesothelioma)	↑ TRM cell precursors to the lung; induce TRM cell differentiation; ↑ protection against lung metastasis	High (but studies currently limited to lung metastases)
	Nasal mucosa vaccination [45,46]	Intranasal vaccination of an adenoviral vector vaccine with IL-1β adjuvant or tumor antigen containing CpG-coated nanoparticles	Metastatic mouse breast cancer (4T1)	↑ TRM cell infiltration to existing lung metastasis; prevention of metastasis; ↓ primary tumor size (*CpG-coated nanoparticles only)	Moderate (in-depth metastatic mouse models, aligns with prime-boost vaccination findings. Studies limited to lung metastases)
Chemokine & cytokine targeting	Anti-CXCL16 [15]	Neutralizes intratumoral CXCL16, allowing tumor-derived TRM cell migration to lung for metastasis protection	Murine triple negative breast cancer (4T1)	↑ Tumor-specific TRM cells defending non-tumor tissues; ↓ metastatic tumor burden in the lung	Moderate (abundant conceptual support; but direct mechanistic study limited to murine metastasis models)
Immune checkpoint blockade	Neoadjuvant anti-PD-1 (± CTLA-4 or chemotherapy) [47–49]	Enhances TRM cell function and supports systemic tumor-specific immunity	Murine ESCC; Phase III ESCC (NCT01216527) & Phase II oral-cancer (NCT02919683) cohorts	↑ CD8+CD103+ TRM cells; delayed progression; ↓ relapses; ↑ systemic anti-tumor immunity	High (abundant pre-clinical and clinical data)
Adoptive cell therapy	TGF-β- conditioned CAR-T cells [50]	Programs CAR-T into the TRM cell phenotype through exposure to TGF-β ex vivo	In vitro co-culture with pancreatic cancer cells (AsPC-1)	Proof-of-concept generation of CAR-TRM cells; ↑ primary tumor control; ↑ exhaustion resistance	Low (functional TRM cells; no direct metastasis data, only primary tumor control)
	iPSC-derived TRM cells [51]	CRISPR-edited iPSCs showing increased TRM markers and behaviors	Human cervical cancer (SiHa)	Generation of iPSC-derived TRM-like cells;↓ primary tumor growth	Low (functional TRM generation; efficacy shown against primary tumors only; no metastasis data)

Symbols ' \uparrow ' and ' \downarrow ' refer to increased and decreased, respectively.

Another emerging strategy is the manipulation of chemical signals to enhance TRM cell egress from primary tumors and promote seeding into pre-metastatic niches. Modulating chemokine gradients offers a direct way to steer TRM cell trafficking to, and increase their efficacy within metastatic niches. For instance, targeting the CXCL16-CXCR6 axis allows active redirecting of TRM cell precursors into pre-metastatic niches. In a 4T1 breast cancer model, using antibodies to neutralize intratumoral CXCL16 not only liberated CXCR6+ effector-memory cells from the primary tumor but also led to their accumulation as CD103+CD69+ TRM cells in the lungs [15]. This redistribution correlated with a marked reduction in metastatic burden when compared with IgG control mice, demonstrating a potential therapeutic approach that warrants further investigation [15]. Beyond chemokine manipulation, targeting cytokines has been shown to modulate TRM cell induction. Intranasal vaccination with a Shiga-toxin B-based mucosal vector drives lung TRM cell formation in head-and-neck and lung cancer models, but concurrent blockade of TGF-β sharply reduces CD103+CD69+ TRM frequencies and eliminates vaccine efficacy, demonstrating that in vivo TGF-β signaling is essential for generating protective TRM cells [43]. This highlights TGF-β as a critical adjuvant for therapies aimed at seeding and sustaining anti-metastatic TRM cell pools. Overall, cytokines and chemokines alike will need to be considered when attempting to direct and sustain TRM cell responses at sites of metastases, and more work will be required to identify other chemical axes that could influence TRM cell therapy success.

The therapeutic potential of TRM cells in immune checkpoint inhibitors (ICI) is the most well characterized due to the surprising finding that TRM cells are the principal responders to ICI therapy in many cancers [52,53]. Neoadjuvant ICI—treating cancer patients with ICI prior to surgical intervention—shows clear promise as an approach for metastasis prevention and control and may even outperform standard adjuvant ICI therapy in metastatic cancers [47]. Mouse studies in esophageal squamous cell carcinoma (ESCC) reveal that preventative PD-1 blockade at early ESCC stages potently increases CD8+CD103+ TRM cell infiltration, delays lesion progression, and, upon re-exposure to carcinogen, maintains TRM cell colonies that mediate prolonged survival [54]. Analysis of a clinical trial of oral cancer patients treated with anti-PD-1/CTLA-4 or neoadjuvant anti-PD-1 demonstrated that early responses to neoadjuvant ICB were mediated by preexisting TRM cells, followed by reinforcement at the tumor-site by new T cells later primed in draining LNs [49], boosting both local and systemic immunity. Enhanced combined tumor immunity of this type has consistently been suggested to be important for protection against distant metastases [49,55]. In analyses of clinical trials in esophageal squamous cancer, combined neoadjuvant chemotherapy and neoadjuvant immunotherapy show improved control of systemic tumors and consequently fewer patients developing distant metastases post-surgery when compared to patients who received just neoadjuvant chemotherapy [48,56]. In the most recent analysis, TRM cells were identified as a significant contributor to observed enhanced metastatic control in the neoadjuvant ICI-treated group and suggested as a potential prognostic factor [56]. Combined, these insights suggest that neoadjuvant ICI (with or without chemotherapy) may be one of the most promising techniques for preventing metastasis by establishing local and systemic immunity to cancer cells to enable effective therapies across a range of cancer types.

Adoptive cell therapy (ACT) approaches that seek to engineer or select for TRM-like phenotypes remain underexplored. Despite this, due to their strong cytotoxic responses, extended tissue residency, and response efficacy to ICI, TRM cells have been recognized as potential candidates for adoptive cell therapies to prevent cancer progression and spread [57]. Chimeric antigen receptor (CAR) T-cell therapy—a form of ACT in which patient T cells are genetically modified ex vivo to express a tumor-specific receptor and

then reinfused—has revolutionized cancer therapy. Despite this, CAR-T modalities have shown limited success in solid tumors, suggesting that optimization for in-tissue functionality is needed. Some authors have shown that it is possible to generate TRM-like CAR-T cells by exposing patient T cells to TGF- β alone during the engineering process, marked by upregulation of CD103, tissue residency expression patterns, and adoption of a stem-like memory state [50]. Interestingly, these engineered CAR-TRM cells were found to be resistant to exhaustion, aligning with existing knowledge about TRM cell canonical functioning in vivo [50]. Another group demonstrated the generation of hypo-immunogenic, iPSC-derived CTLs that are intrinsically enriched for TRM markers like CD103 and CD69, evade host rejection, and demonstrate robust in vitro cytotoxicity and in vivo persistence in cervical cancer models [51]. This suggests that multiple potential approaches should be explored to determine the best technique for generating ACT of TRM cell-like populations, which we propose could be used for anti-metastasis therapies. Despite these promising proofs-of-concept for designing tumor-responsive TRM cell ACTs, systemic evaluation of manufacturing conditions, homing cues, and retention signals specifically in metastatic models is still very limited. Further, metastasis control studies with TRM ACT platforms have yet to be conducted, highlighting a clear gap for future study. A deeper mechanistic understanding of TRM differentiation, seeding, and functional persistence will be essential to translate TRM-based ACT into effective anti-metastasis therapies.

The significant heterogeneity of TRMs is now well established within the field, but very little is understood about how TRMs functionally differ specifically within sites of active metastases. Further, the field lacks a clear consensus on how (or even if) metastasis-associated TRMs have specific phenotypic and molecular differences when compared with those from primary tumors or even non-cancer contexts. As such, it will be very important to consider the known aspects of TRM biology, such as homing cues (e.g., CXCR6/CXCL16), retention signals (e.g., IL-15, TGF-β), and cell-to-cell interactions (e.g., PD1-PDL1) to design therapeutics. These diverse factors (and others yet to be identified) impacting TRM function must be profiled in metastatic contexts throughout major organs of interest before any TRM-focused therapy can truly be designed in an informed manner. Existing data provides sufficient rationale for the design of TRM-based therapies, but much more work is required to understand their phenotype and behavior in diverse metastatic conditions, given that, due to their significant heterogeneity, there is likely not a single TRM therapy that will work in all metastatic cancers.

4.2. TRM Cells as a Biomarker for Metastatic Cancer

Despite tumor-infiltrating lymphocytes being, on average, associated with improved overall survival, it is increasingly recognized that total tumor-infiltrating lymphocytes count alone does not always act as a perfect prognostic signal in many cancers, spurring interest in more specific prognostic biomarkers [58]. TRM cells have been reported to consistently correlate with better patient prognosis across colorectal, lung, oral, ovarian, and breast cancers [23,24,35,59,60]. In colorectal cancer, high TRM cell density also forecasts a lower risk of liver metastasis [25], and in gastrointestinal-derived brain metastases, TRM cell abundance associates with markedly extended post-metastasis survival and even co-recruitment of tumor-infiltrating B cells [61]. High prevalence of TRM cells in metastatic lymph nodes of esophageal squamous cell carcinoma was also found to be associated with enhanced overall survival, even when compared to high-density TRM cells in the primary tumor [62]. Higher infiltration of CD8+CD103+ into metastatic lymph nodes is also associated with a favorable prognosis in gastric cancer, as well as correlating with better outcomes after adjuvant chemotherapy [63]. This evidence suggests a functional and prognostic significance beyond raw functional TRM cell numbers and highlights the

relevance of the spatial distribution of TRM cells when considering it as a prognostic factor. Beyond site-specific findings, transcriptional analyses across thousands of metastatic melanoma samples revealed that enrichment for a memory/TRM-like signature independently predicted overall survival as well as response to anti-PD-1 therapy [64].

Controversies have emerged over the validity of TRMs as true, widely applicable prognostic factors for tumor progression and metastasis control. For instance, in a study of 379 head-and-neck squamous cell carcinoma (HNSCC) cases, high density of CD8+CD103+ TRM cells in the primary tumors predicted better overall and disease-free survival, while TRM cell density in matched lymph node metastases failed to correlate with outcome, underscoring that TRM cell impact could vary by tumor site and stage [65]. Another recent study concluded that TRM cells were not the lymph node T cell population required for tumor control, and rather may simply be a good proxy for effective anti-tumor immune responses [66]. The authors suggest that this observation could stem from TGF-β signaling impairing functional response to tumors by trapping TRMs within the lymph nodes, which was found to be rescued by TGF-β signaling deletion [66]. This result aligns directly with previous mechanistic findings on the role of excessive TGF-β in impairing systemic tumor defense [19]. As such, this observation may have more to do with the specific tissue environment of tumor-draining lymph nodes (like high TGF-β concentrations), rather than speaking directly to the broad function of TRMs. Additionally, a study of non-small cell lung cancer demonstrated that TRM profiles, dynamics, and prognostic relevance change significantly with disease progression [67], reinforcing the idea that usage of TRMs as a prognostic tool could be tumor stage dependent. Together, these results suggest that the use of TRMs as prognostic markers could fail in certain environments and tumor stages, especially in contexts with strong residency signals (e.g., TGF-β) that can impair TRM function. Thus, it will be vital to more clearly establish when and where TRMs can be effectively used for cancer prognosis, and what factors can impair their proper function in controlling both metastatic and primary tumor progression.

Despite some contradictory evidence, a strong base of existing data supports TRMs as promising prognostic biomarkers for metastasis susceptibility and patient outcomes, though further human studies are needed to unravel the full mechanistic underpinnings of their protective role and limitations of their use as prognostic tools.

5. Future Directions

While the current literature offers a tantalizing snapshot of TRM cells' ability to control metastatic tissue and prevent the initial establishment of metastasis, evidence is still missing at several critical points. To convert this promise into actionable therapies, we propose four short-term research priorities: (I) better characterization of TRM-metastasis behavior in organs beyond the lung; (II) identification of TRM metabolic requirements within metastatic niches; (III) direct visualization of TRM-metastasis engagement; and (IV) testing of TRM adoptive cell therapies in metastasis models.

Existing evidence for mechanistic and therapeutic roles of TRMs against metastases heavily hinges on lung metastasis models, with only a handful of studies investigating other common metastasis sites such as the brain, lymph nodes, liver, and bone. Despite this lack of functional data, TRM density correlates with better prognosis at a range of metastatic sites, such as the liver [25], brain [61], and lymph nodes [68], which highlights a clear gap for understanding why these correlations may exist at a mechanistic level. As such, we suggest that future work should better resolve organ-specific TRM programs in significant metastasis sites. For this, utilizing a more diverse set of metastasis-generating syngeneic mouse models will be necessary, such as MC38 colon carcinoma for studying liver metastases [69] or B16F10 for lymph node metastases [70]. These models could help

better test whether TRMs can engraft and curb metastatic growth in other metastatic tissue contexts, while also providing platforms for therapeutic-focused perturbations of residency signals like CXCL16 or TGF- β . Additional studies should probe for what stage TRM cell fate is determined, and whether the local metastatic microenvironment or the original tumor microenvironment plays the biggest role in dictating the efficacy of TRM metastasis control.

Further, while TRM metabolic adaptations of the conditions at the primary tumor have been investigated, more research must be conducted within tissues with active metastases to assess potential metastasis-associated TRM metabolic adaptations. Highly multiplexed spatial transcriptomics can provide the necessary resolution for identifying not only metabolic adaptations of TRMs but also aid in the identification of local microenvironment architecture and cues that cause them to arise, such as cytokines, cellular contacts, and signaling events [71]. This level of profiling will also allow for the identification of functional heterogeneity within the tissue to determine which TRM populations are most relevant for response in each metastasis model. The specific understanding of how TRMs respond to local metastatic tissue cues will dictate the rational design of therapeutics targeted to defined metastasis sites and could help inform future TRM cell engineering efforts by optimizing their survival and function.

Direct in vivo visualization of TRM and metastatic cell contact also remains unmet and will be critical for translating TRM biology into therapeutic interventions. Various techniques are available and have even been optimized for use with TRMs previously in other contexts. Two-photon microscopy allows real-time intravital imaging of a diverse set of organs and has already been used to track interactions between primary melanoma cells and CD8+CD103+ TRMs in mice [40], which we suggest could be extended to visualize and confirm interactions between metastatic cells and TRMs. TRM-focused two-photon microscopy setups have also been applied for other metastasis-relevant organs (like the lungs) in viral contexts, which could be repurposed for future metastasis-specific experiments [72]. In parallel, multiplexed immunofluorescence techniques can map associations between TRM and metastases and have already been used to identify spatial associations between TRMs and metastatic cells in the skin and lymph nodes [40]. Applying these dynamic (two-photon) and static (multiplex immunofluorescence) setups across common metastatic sites will provide critical evidence for direct TRM positioning and engagement with active metastases and could further support hypotheses about TRM's ability to control trafficking of micrometastases.

Finally, more experiments are needed to conclusively show that TRMs generated for adoptive cell therapies (ACTs) can successfully defend against metastasis progression. The limited existing evidence on TRM-based ACTs showed success with primary tumors and tumor rechallenge [50,51], but there is still no evidence supporting their use in metastatic cancer. The most pressing task will be to establish whether engineered TRMs can home, engraft, and reduce metastatic burden in well-validated metastasis models like 4T1 breast cancer or B16F10 melanoma. Demonstration of direct interaction between engineered TRM-like cells and metastatic cells using previously mentioned imaging techniques will also greatly strengthen the rationale for TRM-based ACTs as functional in vivo tools. Although the generation of TRM-based ACTs has proven both feasible and effective in primary tumors, much more evidence will be needed before these initial platforms can be supported as a realistic means to control metastases in organs of interest like the lung, brain, and lymph nodes.

6. Conclusions and Perspectives

TRM cells functionally combine strategic tissue residency programs with potent effector functions and immune crosstalk ability that can position them as defenders against metastatic invasion of peripheral and lymphoid tissues. Preclinical models have demonstrated reduced metastatic burden in mice using a diverse array of TRM therapeutics, including vaccines, antibodies, and TRM cell engineering, and clinical observations demonstrate TRM's predictive power and direct involvement in metastatic cancer control. A separate argument for TRM cells in cancer/metastasis control is antigen-dependency; there are reports supporting cancer-antigen-specific responses and cancer-antigen-independent TRM responses. Considering the complex roles of TRM cells in immune regulation, careful consideration is required regarding antigen-dependent versus -independent TRM responses in cancer control and therapy.

Questions around optimal delivery, tissue-specific efficacy, and the full mechanisms of TRM cell metastasis control and prevention remain unanswered. Still, the converging landscape of mechanistic and translational knowledge offers a solid foundation for TRM cell-based metastasis therapies, which could reduce the large existing metastasis burden or even allow its prophylactic control.

Author Contributions: Writing, Editing, and Conceptualization: T.H.M., W.Z., R.K. and C.K.M.; writing—original draft preparation, T.H.M., A.P.M., R.K. and C.K.M.; writing—review and editing, W.Z., A.P.M., C.K.M., Q.L., Q.S., R.D., Z.J.; visualization, T.H.M., Q.L., Q.S., R.D., W.Z.; supervision, C.K.M., R.K. and W.Z.; funding acquisition, W.Z. and R.K.; Final approval of the paper: T.H.M., A.P.M., Z.J., Q.S., Q.L., R.D., R.K., C.K.M., W.Z. All authors have read and agreed to the published version of the manuscript.

Funding: This work is partially supported by the National Institute of Health grant R01CA288749 (PI: Kolb), CA269662 (W. Zhang), CA260239 (W. Zhang; D. Zhou; G. Zheng), and CA290792 (W. Zhang; G. Zheng; K.S.M. Smalley). W. Zhang was also supported by an endowment fund from the Dr. and Mrs. James Robert Spenser Family and shared resources from the UF Health Cancer Center, which is supported in part by state appropriations provided in Fla. Stat. Section 381.915 and the National Cancer Institute (Grant No. P30CA247796).

Institutional Review Board Statement: Not applicable.

Informed Consent Statement: Not applicable.

Data Availability Statement: Not applicable.

Acknowledgments: During the preparation of this manuscript, the authors used Biorender to draw illustrations.

Conflicts of Interest: The authors declare no conflicts of interest.

References

- 1. Fares, J.; Fares, M.Y.; Khachfe, H.H.; Salhab, H.A.; Fares, Y. Molecular Principles of Metastasis: A Hallmark of Cancer Revisited. Signal Transduct. Target. Ther. 2020, 5, 28. [CrossRef]
- 2. Szabo, P.A.; Levitin, H.M.; Miron, M.; Snyder, M.E.; Senda, T.; Yuan, J.; Cheng, Y.L.; Bush, E.C.; Dogra, P.; Thapa, P.; et al. Single-Cell Transcriptomics of Human T Cells Reveals Tissue and Activation Signatures in Health and Disease. *Nat. Commun.* **2019**, *10*, 4706. [CrossRef]
- 3. Crowl, J.T.; Heeg, M.; Ferry, A.; Milner, J.J.; Omilusik, K.D.; Toma, C.; He, Z.; Chang, J.T.; Goldrath, A.W. Tissue-Resident Memory CD8+ T Cells Possess Unique Transcriptional, Epigenetic and Functional Adaptations to Different Tissue Environments. *Nat. Immunol.* 2022, 23, 1121–1131. [CrossRef] [PubMed]
- 4. Kumar, B.V.; Ma, W.; Miron, M.; Granot, T.; Guyer, R.S.; Carpenter, D.J.; Senda, T.; Sun, X.; Ho, S.-H.; Lerner, H.; et al. Human Tissue-Resident Memory T Cells Are Defined by Core Transcriptional and Functional Signatures in Lymphoid and Mucosal Sites. *Cell Rep.* 2017, 20, 2921–2934. [CrossRef]

- 5. Mueller, S.N.; Mackay, L.K. Tissue-Resident Memory T Cells: Local Specialists in Immune Defence. *Nat. Rev. Immunol.* **2016**, *16*, 79–89. [CrossRef]
- 6. Evrard, M.; Becht, E.; Fonseca, R.; Obers, A.; Park, S.L.; Ghabdan-Zanluqui, N.; Schroeder, J.; Christo, S.N.; Schienstock, D.; Lai, J.; et al. Single-Cell Protein Expression Profiling Resolves Circulating and Resident Memory T Cell Diversity across Tissues and Infection Contexts. *Immunity* 2023, 56, 1664–1680.e9. [CrossRef] [PubMed]
- 7. Christo, S.N.; Park, S.L.; Mueller, S.N.; Mackay, L.K. The Multifaceted Role of Tissue-Resident Memory T Cells. *Annu. Rev. Immunol.* **2024**, 42, 317–345. [CrossRef]
- 8. Okła, K.; Farber, D.L.; Zou, W. Tissue-Resident Memory T Cells in Tumor Immunity and Immunotherapy. *J. Exp. Med.* **2021**, 218, e20201605. [CrossRef] [PubMed]
- 9. Gavil, N.V.; Cheng, K.; Masopust, D. Resident Memory T Cells and Cancer. *Immunity* 2024, 57, 1734–1751. [CrossRef]
- 10. Min, D.; Fiedler, J.; Anandasabapathy, N. Tissue-Resident Memory Cells in Antitumoral Immunity and Cancer Immunotherapy. *Curr. Opin. Immunol.* **2024**, *91*, 102499. [CrossRef]
- 11. Wein, A.N.; McMaster, S.R.; Takamura, S.; Dunbar, P.R.; Cartwright, E.K.; Hayward, S.L.; McManus, D.T.; Shimaoka, T.; Ueha, S.; Tsukui, T.; et al. CXCR6 Regulates Localization of Tissue-Resident Memory CD8 T Cells to the Airways. *J. Exp. Med.* **2019**, 216, 2748–2762. [CrossRef]
- 12. Mabrouk, N.; Tran, T.; Sam, I.; Pourmir, I.; Gruel, N.; Granier, C.; Pineau, J.; Gey, A.; Kobold, S.; Fabre, E.; et al. CXCR6 Expressing T Cells: Functions and Role in the Control of Tumors. *Front. Immunol.* **2022**, *13*, 1022136. [CrossRef] [PubMed]
- 13. Korbecki, J.; Kojder, K.; Kapczuk, P.; Kupnicka, P.; Gawrońska-Szklarz, B.; Gutowska, I.; Chlubek, D.; Baranowska-Bosiacka, I. The Effect of Hypoxia on the Expression of CXC Chemokines and CXC Chemokine Receptors-A Review of Literature. *Int. J. Mol. Sci.* 2021, 22, 843. [CrossRef]
- 14. Muthuswamy, R.; McGray, A.R.; Battaglia, S.; He, W.; Miliotto, A.; Eppolito, C.; Matsuzaki, J.; Takemasa, T.; Koya, R.; Chodon, T.; et al. CXCR6 by Increasing Retention of Memory CD8+ T Cells in the Ovarian Tumor Microenvironment Promotes Immunosurveillance and Control of Ovarian Cancer. *J. Immunother. Cancer* **2021**, *9*, e003329. [CrossRef] [PubMed]
- Christian, L.S.; Wang, L.; Lim, B.; Deng, D.; Wu, H.; Wang, X.-F.; Li, Q.-J. Resident Memory T Cells in Tumor-Distant Tissues Fortify against Metastasis Formation. Cell Rep. 2021, 35, 109118. [CrossRef] [PubMed]
- 16. Karaki, S.; Blanc, C.; Tran, T.; Galy-Fauroux, I.; Mougel, A.; Dransart, E.; Anson, M.; Tanchot, C.; Paolini, L.; Gruel, N.; et al. CXCR6 Deficiency Impairs Cancer Vaccine Efficacy and CD8+ Resident Memory T-Cell Recruitment in Head and Neck and Lung Tumors. J. Immunother. Cancer 2021, 9, e001948. [CrossRef] [PubMed]
- 17. Qiu, Z.; Chu, T.H.; Sheridan, B.S. TGF-β: Many Paths to CD103+ CD8 T Cell Residency. Cells 2021, 10, 989. [CrossRef] [PubMed]
- 18. Green, W.D.; Gomez, A.; Plotkin, A.L.; Pratt, B.M.; Merritt, E.F.; Mullins, G.N.; Kren, N.P.; Modliszewski, J.L.; Zhabotynsky, V.; Woodcock, M.G.; et al. Enhancer-Driven Gene Regulatory Networks Reveal Transcription Factors Governing T Cell Adaptation and Differentiation in the Tumor Microenvironment. *Immunity* 2025, 58, 1725–1741.e9. [CrossRef] [PubMed]
- Fay, M.; Sievers, C.; Robbins, Y.; Yang, X.; Huynh, A.; Redman, J.M.; Hodge, J.W.; Schlom, J.; Gulley, J.L.; Allen, C.T.; et al. TGF-β
 Neutralization Attenuates Tumor Residency of Activated T Cells to Enhance Systemic Immunity in Mice. iScience 2024, 27, 110520.

 [CrossRef]
- 20. Vella, J.L.; Molodtsov, A.; Angeles, C.V.; Branchini, B.R.; Turk, M.J.; Huang, Y.H. Dendritic Cells Maintain Anti-Tumor Immunity by Positioning CD8 Skin-Resident Memory T Cells. *Life Sci. Alliance* **2021**, *4*, e202101056. [CrossRef]
- Pilato, M.D.; Kfuri-Rubens, R.; Pruessmann, J.N.; Ozga, A.J.; Messemaker, M.; Cadilha, B.L.; Sivakumar, R.; Cianciaruso, C.; Warner, R.D.; Marangoni, F.; et al. CXCR6 Positions Cytotoxic T Cells to Receive Critical Survival Signals in the Tumor Microenvironment. Cell 2021, 184, 4512–4530.e22. [CrossRef]
- 22. Tieu, R.; Zeng, Q.; Zhao, D.; Zhang, G.; Feizi, N.; Manandhar, P.; Williams, A.L.; Popp, B.; Wood-Trageser, M.A.; Demetris, A.J.; et al. Tissue-Resident Memory T Cell Maintenance during Antigen Persistence Requires Both Cognate Antigen and Interleukin-15. *Sci. Immunol.* 2023, 8, eadd8454. [CrossRef] [PubMed]
- 23. Kitakaze, M.; Uemura, M.; Hara, T.; Chijimatsu, R.; Motooka, D.; Hirai, T.; Konno, M.; Okuzaki, D.; Sekido, Y.; Hata, T.; et al. Cancer-Specific Tissue-Resident Memory T-Cells Express ZNF683 in Colorectal Cancer. *Br. J. Cancer* 2023, 128, 1828–1837. [CrossRef]
- 24. Abdeljaoued, S.; Doussot, A.; Kroemer, M.; Laloy, E.; Pallandre, J.R.; El Kaddissi, A.; Spehner, L.; Ben Khelil, M.; Bouard, A.; Mougey, V.; et al. Liver Metastases of Colorectal Cancer Contain Different Subsets of Tissue-Resident Memory CD8 T Cells Correlated with a Distinct Risk of Relapse Following Surgery. Oncoimmunology 2025, 14, 2455176. [CrossRef]
- 25. Liu, S.; Wang, P.; Wang, P.; Zhao, Z.; Zhang, X.; Pan, Y.; Pan, J. Tissue-Resident Memory CD103+CD8+ T Cells in Colorectal Cancer: Its Implication as a Prognostic and Predictive Liver Metastasis Biomarker. *Cancer Immunol. Immunother.* **2024**, 73, 176. [CrossRef]
- 26. Lin, R.; Zhang, H.; Yuan, Y.; He, Q.; Zhou, J.; Li, S.; Sun, Y.; Li, D.Y.; Qiu, H.-B.; Wang, W.; et al. Fatty Acid Oxidation Controls CD8+ Tissue-Resident Memory T-Cell Survival in Gastric Adenocarcinoma. *Cancer Immunol. Res.* **2020**, *8*, 479–492. [CrossRef]

- 27. Pan, Y.; Tian, T.; Park, C.O.; Lofftus, S.Y.; Mei, S.; Liu, X.; Luo, C.; O'Malley, J.T.; Gehad, A.; Teague, J.E.; et al. Survival of Tissue-Resident Memory T Cells Requires Exogenous Lipid Uptake and Metabolism. *Nature* **2017**, 543, 252–256. [CrossRef] [PubMed]
- 28. Reina-Campos, M.; Heeg, M.; Kennewick, K.; Mathews, I.T.; Galletti, G.; Luna, V.; Nguyen, Q.; Huang, H.; Milner, J.J.; Hu, K.H.; et al. Metabolic Programs of T Cell Tissue Residency Empower Tumour Immunity. *Nature* **2023**, *621*, 179–187. [CrossRef] [PubMed]
- 29. Tsuji, T.; Matsuzaki, J.; Odunsi, K. Tissue Residency of Memory CD8+ T Cells Matters in Shaping Immunogenicity of Ovarian Cancer. *Cancer Cell* **2022**, *40*, 452–454. [CrossRef]
- 30. Menares, E.; Gálvez-Cancino, F.; Cáceres-Morgado, P.; Ghorani, E.; López, E.; Díaz, X.; Saavedra-Almarza, J.; Figueroa, D.A.; Roa, E.; Quezada, S.A.; et al. Tissue-Resident Memory CD8+ T Cells Amplify Anti-Tumor Immunity by Triggering Antigen Spreading through Dendritic Cells. *Nat. Commun.* **2019**, *10*, 4401. [CrossRef]
- 31. Behr, F.M.; Parga-Vidal, L.; Kragten, N.A.M.; van Dam, T.J.P.; Wesselink, T.H.; Sheridan, B.S.; Arens, R.; van Lier, R.A.W.; Stark, R.; van Gisbergen, K.P.J.M. Tissue-Resident Memory CD8+ T Cells Shape Local and Systemic Secondary T Cell Responses. *Nat. Immunol.* 2020, 21, 1070–1081. [CrossRef]
- 32. Olalekan, S.; Xie, B.; Back, R.; Eckart, H.; Basu, A. Characterizing the Tumor Microenvironment of Metastatic Ovarian Cancer by Single-Cell Transcriptomics. *Cell Rep.* **2021**, *35*, 109165. [CrossRef]
- 33. Musial, S.C.; Kleist, S.A.; Degefu, H.N.; Ford, M.A.; Chen, T.; Isaacs, J.F.; Boussiotis, V.A.; Skorput, A.G.J.; Rosato, P.C. Alarm Functions of PD-1+ Brain-Resident Memory T Cells. *J. Immunol.* **2024**, *213*, 1585–1594. [CrossRef]
- 34. Molodtsov, A.K.; Khatwani, N.; Vella, J.L.; Lewis, K.A.; Zhao, Y.; Han, J.; Sullivan, D.E.; Searles, T.G.; Preiss, N.K.; Shabaneh, T.B.; et al. Resident Memory CD8+ T Cells in Regional Lymph Nodes Mediate Immunity to Metastatic Melanoma. *Immunity* 2021, 54, 2117–2132.e7. [CrossRef]
- 35. Xu, H.; Yue, M.; Zhou, R.; Wang, P.; Wong, M.Y.-C.; Wang, J.; Huang, H.; Chen, B.; Mo, Y.; Tam, R.C.-Y.; et al. A Prime-Boost Vaccination Approach Induces Lung Resident Memory CD8+ T Cells Derived from Central Memory T Cells That Prevent Tumor Lung Metastasis. *Cancer Res.* 2024, 84, 3173–3188. [CrossRef]
- 36. Devi, K.S.P.; Wang, E.; Jaiswal, A.; Konieczny, P.; Kim, T.-G.; Nirschl, C.J.; Verma, A.; Liu, Y.; Milczanowski, J.; Christo, S.N.; et al. PD-1 Is Requisite for Skin TRM Cell Formation and Specification by TGFβ. *Nat. Immunol.* **2025**, *26*, 1339–1351. [CrossRef] [PubMed]
- 37. Schøller, A.S.; Nazerai, L.; Christensen, J.P.; Thomsen, A.R. Functionally Competent, PD-1+ CD8+ Trm Cells Populate the Brain Following Local Antigen Encounter. *Front. Immunol.* **2020**, *11*, 595707. [CrossRef]
- 38. Beura, L.K.; Wijeyesinghe, S.; Thompson, E.A.; Macchietto, M.G.; Rosato, P.C.; Pierson, M.J.; Schenkel, J.M.; Mitchell, J.S.; Vezys, V.; Fife, B.T.; et al. T Cells in Nonlymphoid Tissues Give Rise to Lymph-Node-Resident Memory T Cells. *Immunity* **2018**, *48*, 327–338.e5. [CrossRef] [PubMed]
- 39. Anthony, S.M.; Van Braeckel-Budimir, N.; Moioffer, S.J.; van de Wall, S.; Shan, Q.; Vijay, R.; Sompallae, R.; Hartwig, S.M.; Jensen, I.J.; Varga, S.M.; et al. Protective Function and Durability of Mouse Lymph Node-Resident Memory CD8+ T Cells. *eLife* **2021**, 10, e68662. [CrossRef] [PubMed]
- 40. Park, S.L.; Buzzai, A.; Rautela, J.; Hor, J.L.; Hochheiser, K.; Effern, M.; McBain, N.; Wagner, T.; Edwards, J.; McConville, R.; et al. Tissue-Resident Memory CD8+ T Cells Promote Melanoma-Immune Equilibrium in Skin. *Nature* 2019, 565, 366–371. [CrossRef] [PubMed]
- 41. Hochheiser, K.; Aw Yeang, H.X.; Wagner, T.; Tutuka, C.; Behren, A.; Waithman, J.; Angel, C.; Neeson, P.J.; Gebhardt, T.; Gyorki, D.E. Accumulation of CD103+ CD8+ T Cells in a Cutaneous Melanoma Micrometastasis. *Clin. Transl. Immunol.* **2019**, *8*, e1100. [CrossRef]
- 42. Pizzolla, A.; Keam, S.P.; Vergara, I.A.; Caramia, F.; Thio, N.; Wang, M.; Kocovski, N.; Tantalo, D.; Jabbari, J.; Au-Yeung, G.; et al. Tissue-Resident Memory T Cells from a Metastatic Vaginal Melanoma Patient Are Tumor-Responsive T Cells and Increase after Anti-PD-1 Treatment. *J. Immunother. Cancer* 2022, 10, e004574. [CrossRef]
- 43. Nizard, M.; Roussel, H.; Diniz, M.O.; Karaki, S.; Tran, T.; Voron, T.; Dransart, E.; Sandoval, F.; Riquet, M.; Rance, B.; et al. Induction of Resident Memory T Cells Enhances the Efficacy of Cancer Vaccine. *Nat. Commun.* 2017, 8, 15221. [CrossRef]
- 44. MacKerracher, A.; Sommershof, A.; Groettrup, M. PLGA Particle Vaccination Elicits Resident Memory CD8 T Cells Protecting from Tumors and Infection. *Eur. J. Pharm. Sci.* **2022**, *175*, 106209. [CrossRef]
- 45. Oltmanns, F.; Vieira Antão, A.; Irrgang, P.; Viherlehto, V.; Jörg, L.; Schmidt, A.; Wagner, J.T.; Rückert, M.; Flohr, A.-S.; Geppert, C.I.; et al. Mucosal Tumor Vaccination Delivering Endogenous Tumor Antigens Protects against Pulmonary Breast Cancer Metastases. *J. Immunother. Cancer* 2024, 12, e008652. [CrossRef]
- 46. Donkor, M.; Choe, J.; Reid, D.M.; Quinn, B.; Pulse, M.; Ranjan, A.; Chaudhary, P.; Jones, H.P. Nasal Tumor Vaccination Protects against Lung Tumor Development by Induction of Resident Effector and Memory Anti-Tumor Immune Responses. *Pharmaceutics* **2023**, *15*, 445. [CrossRef]

- 47. Liu, J.; Blake, S.J.; Yong, M.C.R.; Harjunpää, H.; Ngiow, S.F.; Takeda, K.; Young, A.; O'Donnell, J.S.; Allen, S.; Smyth, M.J.; et al. Improved Efficacy of Neoadjuvant Compared to Adjuvant Immunotherapy to Eradicate Metastatic Disease. *Cancer Discov.* 2016, 6, 1382–1399. [CrossRef]
- 48. Yang, H.; Liu, H.; Chen, Y.; Zhu, C.; Fang, W.; Yu, Z.; Mao, W.; Xiang, J.; Han, Y.; Chen, Z.; et al. Neoadjuvant Chemoradiotherapy Followed by Surgery Versus Surgery Alone for Locally Advanced Squamous Cell Carcinoma of the Esophagus (NEOCRTEC5010): A Phase III Multicenter, Randomized, Open-Label Clinical Trial. *J. Clin. Oncol.* 2018, 36, 2796–2803. [CrossRef] [PubMed]
- 49. Luoma, A.M.; Suo, S.; Wang, Y.; Gunasti, L.; Porter, C.B.M.; Nabilsi, N.; Tadros, J.; Ferretti, A.P.; Liao, S.; Gurer, C.; et al. Tissue-Resident Memory and Circulating T Cells Are Early Responders to Pre-Surgical Cancer Immunotherapy. *Cell* 2022, 185, 2918–2935.e29. [CrossRef] [PubMed]
- 50. Jung, I.-Y.; Noguera-Ortega, E.; Bartoszek, R.; Collins, S.M.; Williams, E.; Davis, M.; Jadlowsky, J.K.; Plesa, G.; Siegel, D.L.; Chew, A.; et al. Tissue-Resident Memory CAR T Cells with Stem-like Characteristics Display Enhanced Efficacy against Solid and Liquid Tumors. *Cell Rep. Med.* 2023, 4, 101053. [CrossRef] [PubMed]
- 51. Furukawa, Y.; Ishii, M.; Ando, J.; Ikeda, K.; Igarashi, K.J.; Kinoshita, S.; Azusawa, Y.; Toyota, T.; Honda, T.; Nakanishi, M.; et al. iPSC-Derived Hypoimmunogenic Tissue Resident Memory T Cells Mediate Robust Anti-Tumor Activity against Cervical Cancer. *Cell Rep. Med.* 2023, 4, 101327. [CrossRef] [PubMed]
- 52. Virassamy, B.; Caramia, F.; Savas, P.; Sant, S.; Wang, J.; Christo, S.N.; Byrne, A.; Clarke, K.; Brown, E.; Teo, Z.L.; et al. Intratumoral CD8+ T Cells with a Tissue-Resident Memory Phenotype Mediate Local Immunity and Immune Checkpoint Responses in Breast Cancer. *Cancer Cell* 2023, 41, 585–601.e8. [CrossRef]
- 53. Zhao, Y.; Wucherpfennig, K.W. Tissue-Resident T Cells in Clinical Response and Immune-Related Adverse Events of Immune Checkpoint Blockade. *Clin. Cancer Res.* **2024**, *30*, 5527–5534. [CrossRef] [PubMed]
- 54. Xiao, B.-Y.; Zhang, X.; Cao, T.-Y.; Li, D.-D.; Jiang, W.; Kong, L.-H.; Tang, J.-H.; Han, K.; Zhang, C.-Z.; Mei, W.-J.; et al. Neoadjuvant Immunotherapy Leads to Major Response and Low Recurrence in Localized Mismatch Repair-Deficient Colorectal Cancer. *J. Natl. Compr. Cancer Netw.* 2023, 21, 60–66.e5. [CrossRef]
- 55. Fairfax, B.P.; Taylor, C.A.; Watson, R.A.; Nassiri, I.; Danielli, S.; Fang, H.; Mahé, E.A.; Cooper, R.; Woodcock, V.; Traill, Z.; et al. Peripheral CD8+ T Cell Characteristics Associated with Durable Responses to Immune Checkpoint Blockade in Patients with Metastatic Melanoma. *Nat. Med.* 2020, 26, 193–199. [CrossRef]
- 56. Liu, A.; Liu, D.; Liu, X.; Chi, Y.; Guo, L.; Li, D.; Wang, Q.; Li, Y.; Li, Y.; Zheng, G.; et al. The Prognosis Prediction Value of CD69+ CD8+ Tissue-Resident Memory T Cell as a Novel Indicator of Pathologic Complete Response Heterogeneity Following Different Neoadjuvant Therapy Regimen in Esophageal Squamous Cell Carcinoma. *Cancer Immunol. Immunother.* 2025, 74, 147. [CrossRef]
- 57. Beumer-Chuwonpad, A.; Taggenbrock, R.L.R.E.; Ngo, T.A.; van Gisbergen, K.P.J.M. The Potential of Tissue-Resident Memory T Cells for Adoptive Immunotherapy against Cancer. *Cells* **2021**, *10*, 2234. [CrossRef]
- 58. Brummel, K.; Eerkens, A.L.; de Bruyn, M.; Nijman, H.W. Tumour-Infiltrating Lymphocytes: From Prognosis to Treatment Selection. *Br. J. Cancer* **2023**, *128*, 451–458. [CrossRef]
- 59. Anadon, C.M.; Yu, X.; Hänggi, K.; Biswas, S.; Chaurio, R.A.; Martin, A.; Payne, K.K.; Mandal, G.; Innamarato, P.; Harro, C.M.; et al. Ovarian Cancer Immunogenicity Is Governed by a Narrow Subset of Progenitor Tissue-Resident Memory T Cells. *Cancer Cell* 2022, 40, 545–557.e13. [CrossRef] [PubMed]
- 60. Ali, A.; Younas, K.; Khatoon, A.; Murtaza, B.; Ji, Z.; Akbar, K.; Tanveer, Q.; Bahadur, S.U.K.; Su, Z. Immune Watchdogs: Tissue-Resident Lymphocytes as Key Players in Cancer Defense. *Crit. Rev. Oncol. Hematol.* **2025**, 208, 104644. [CrossRef]
- 61. Ohno, M.; Kuramitsu, S.; Yamashita, K.; Nagasaka, T.; Haimoto, S.; Fujita, M. Tumor-Infiltrating B Cells and Tissue-Resident Memory T Cells as Prognostic Indicators in Brain Metastases Derived from Gastrointestinal Cancers. *Cancers* **2024**, *16*, 3765. [CrossRef]
- 62. Natsuki, S.; Tanaka, H.; Nishiyama, M.; Mori, T.; Deguchi, S.; Miki, Y.; Yoshii, M.; Tamura, T.; Toyokawa, T.; Lee, S.; et al. Prognostic Relevance of Tumor-Resident Memory T Cells in Metastatic Lymph Nodes of Esophageal Squamous Cell Carcinoma. *Cancer Sci.* 2023, 114, 1846–1858. [CrossRef]
- 63. Nishiyama, M.; Miki, Y.; Tanaka, H.; Natsuki, S.; Kuroda, K.; Yoshii, M.; Tamura, T.; Toyokawa, T.; Lee, S.; Maeda, K. Resident Memory T Cell in Metastatic Lymph Nodes Is Associated with Favorable Prognosis in Gastric Cancer Patients. *Cancer Sci.* 2025. [CrossRef] [PubMed]
- 64. Jaiswal, A.; Verma, A.; Dannenfelser, R.; Melssen, M.; Tirosh, I.; Izar, B.; Kim, T.-G.; Nirschl, C.J.; Devi, K.S.P.; Olson, W.C.; et al. An Activation to Memory Differentiation Trajectory of Tumor-Infiltrating Lymphocytes Informs Metastatic Melanoma Outcomes. *Cancer Cell* 2022, 40, 524–544.e5. [CrossRef] [PubMed]
- 65. von Witzleben, A.; Ellis, M.; Thomas, G.J.; Hoffmann, T.K.; Jackson, R.; Laban, S.; Ottensmeier, C.H. Tumor-Infiltrating CD103+ Tissue-Resident Memory T Cells and CD103-CD8+ T Cells in HNSCC Are Linked to Outcome in Primary but Not Metastatic Disease. Clin. Cancer Res. 2024, 30, 224–234. [CrossRef]

- 66. Wijesinghe, S.K.M.; Rausch, L.; Gabriel, S.S.; Galletti, G.; De Luca, M.; Qin, L.; Wen, L.; Tsui, C.; Man, K.; Heyden, L.; et al. Lymph-Node-Derived Stem-like but Not Tumor-Tissue-Resident CD8+ T Cells Fuel Anticancer Immunity. *Nat. Immunol.* 2025, 26, 1367–1383. [CrossRef] [PubMed]
- 67. Yang, L.; Yang, H.; Zhao, M.; Yuan, H.; Geng, J.; Yan, Y.; Wu, L.; Xing, L.; Yu, J.; Sun, X. Stage-Dependent Spatial Distribution and Prognostic Value of CD8+ Tissue-Resident Memory T Cells in NSCLC. NPJ Precis. Oncol. 2025, 9, 51. [CrossRef]
- 68. Natsuki, S.; Tanaka, H.; Nishiyama, M.; Deguchi, S.; Miki, Y.; Yoshii, M.; Tamura, T.; Toyokawa, T.; Lee, S.; Maeda, K. Significance of CD103+ Tissue-Resident Memory T Cells for Predicting the Effectiveness of Immune Checkpoint Inhibitors in Esophageal Cancer. *BMC Cancer* 2023, 23, 1011. [CrossRef]
- 69. Greenlee, J.D.; King, M.R. A Syngeneic MC38 Orthotopic Mouse Model of Colorectal Cancer Metastasis. *Biol. Methods Protoc.* **2022**, 7, bpac024. [CrossRef]
- 70. Breuer, C.B.; Xiong, Z.; Wang, A.; Rodriguez, G.E.; Abhiraman, G.C.; Garcia, K.C.; Reticker-Flynn, N.E. Spontaneous and Experimental Models of Lymph Node Metastasis. *Nat. Protoc.* **2025**, 1–18. [CrossRef]
- 71. Reina-Campos, M.; Monell, A.; Ferry, A.; Luna, V.; Cheung, K.P.; Galletti, G.; Scharping, N.E.; Takehara, K.K.; Quon, S.; Challita, P.P.; et al. Tissue-Resident Memory CD8 T Cell Diversity Is Spatiotemporally Imprinted. *Nature* 2025, 639, 483–492. [CrossRef] [PubMed]
- 72. van de Wall, S.; Anthony, S.M.; Hancox, L.S.; Pewe, L.L.; Langlois, R.A.; Zehn, D.; Badovinac, V.P.; Harty, J.T. Dynamic Landscapes and Protective Immunity Coordinated by Influenza-Specific Lung-Resident Memory CD8+ T Cells Revealed by Intravital Imaging. *Immunity* **2024**, *57*, 1878–1892.e5. [CrossRef] [PubMed]

Disclaimer/Publisher's Note: The statements, opinions and data contained in all publications are solely those of the individual author(s) and contributor(s) and not of MDPI and/or the editor(s). MDPI and/or the editor(s) disclaim responsibility for any injury to people or property resulting from any ideas, methods, instructions or products referred to in the content.





Article

Physiological Oxygen Levels in the Microenvironment Program Ex Vivo-Generated Conventional Dendritic Cells Toward a Tolerogenic Phenotype

Antonia Peter ^{1,*}, Morgane Vermeulen ¹, Mats Van Delen ^{1,2}, Amber Dams ¹, Stefanie Peeters ^{1,3}, Hans De Reu ^{1,4}, Waleed F. A. Marei ^{5,6}, Zwi N. Berneman ^{1,3} and Nathalie Cools ^{1,3,4}

- Laboratory of Experimental Hematology, Vaccine & Infectious Disease Institute (VAXINFECTIO), Faculty of Medicine and Health Sciences, University of Antwerp, 2610 Antwerp, Belgium
- ² Health Department, Flemish Institute for Technological Research (VITO), 2400 Mol, Belgium
- Center for Cell Therapy and Regenerative Medicine, Antwerp University Hospital, 2650 Edegem, Belgium
- Flow Cytometry and Sorting Core Facility (FACSUA), University of Antwerp, 2610 Antwerp, Belgium
- Gamete Research Centre, Laboratory of Veterinary Physiology and Biochemistry, Department of Veterinary Sciences, University of Antwerp, 2610 Antwerp, Belgium
- Department of Theriogenology, Faculty of Veterinary Medicine, Cairo University, Giza 3725005, Egypt
- * Correspondence: antonia.peter@uantwerpen.be

Abstract: Dendritic cells (DCs) are critical regulators of immune homeostasis, balancing tolerance and immunity through antigen presentation and T cell modulation. While the influence of hypoxia (<2% O₂) on DC function in pathological settings is well-documented, the impact of physiological O₂ levels remains underexplored. This study investigates the role of physioxia $(4\% O_2)$ in programming mature DCs toward a tolerogenic phenotype compared to atmospheric conditions (21% O₂) typically present in in vitro assays. DC cultures generated under 4% O2 exhibited a reduced monocyte-to-DC transformation rate, increased lactate production, a semi-mature surface marker profile, and increased surface expression of the tolerance-associated marker ILT4. T cell priming was altered only when atmospheric DCs were co-cultured under physioxia, suggesting an O_2 -dependent threshold for immunostimulatory capacity. These findings highlight the complexity of O₂-dependent mechanisms in DC-T cell interactions, revealing a delicate balance between tolerance and immunogenicity. Our results underscore the need for physiologically relevant O₂ conditions in DC research to better reflect in vivo behavior and inform immunotherapy design. Overall, this study advances understanding of how microenvironmental cues shape DC biology, with implications for immune tolerance, autoimmunity, and cancer immunotherapy.

Keywords: dendritic cells; microenvironment; oxygen; immunometabolism; dendritic-cell based immunotherapy

1. Introduction

Dendritic cells (DCs) are professional antigen-presenting cells that serve as a critical link between the innate and adaptive immune systems. Derived from CD34⁺ bone marrow-resident hematopoietic stem cells, they are strategically distributed throughout the body to perform immune surveillance and modulate immune responses [1–3]. Under homeostatic conditions, DCs capture self-antigens and harmless environmental antigens (e.g., commensal microbes, apoptotic cells) in peripheral tissues such as the skin, lungs, and gut [4]. Immature (i) DCs, characterized by high endocytic capacity, low antigen presentation capacity, low expression of co-stimulatory molecules, and minimal cytokine secretion,

present these antigens in a non-inflammatory context to T cells in secondary lymphoid organs [5-8]. This process promotes peripheral tolerance by inducing regulatory T cells (Tregs) or silencing self-reactive T cells, thereby preventing autoimmune responses. During inflammation, danger signals such as damage-associated molecular patterns (DAMPs) or pathogen-associated molecular patterns (PAMPs) trigger DCs into maturation [9-11]. This involves upregulation of antigen presentation via the major histocompatibility complex, costimulatory molecules (e.g., CD80, CD86), and chemokine receptors, enabling their efficient migration to secondary lymphoid organs [12–14]. Mature (m)DCs subsequently present processed antigens to T cells, initiating adaptive immune responses tailored to the detected pathogen [15,16]. Depending on the specific microenvironmental signals they receive, mDCs can promote tolerance or immunogenicity [17–20]. For example, in a tolerogenic context, inhibitory signals such as the programmed death-ligand (PD-L)1/2—programmed death-1 (PD-1), CD155—T cell immunoreceptor with immunoglobulin and ITIM domains (TIGIT), and CD80/CD86—cytotoxic T lymphocyte-associated protein-4 (CTLA-4) interactions, combined with secretion of anti-inflammatory cytokines (e.g., IL-10), suppress effector T cell activation and support Treg induction [21–24]. In an immunogenic context, CD80 and CD86 interact with CD28 on T cells and, in combination with pro-inflammatory cytokines like IL-12, drive effector T cell activation and differentiation, promoting robust immune responses to pathogens [25,26]. Through the integration of cytokine secretion profiles and surface marker expression, mDCs can prime Tregs for immune tolerance or activate T helper cell subsets such as Th1, Th2, and Th17 [27,28]. These subsets coordinate responses against intracellular pathogens, extracellular parasites, or mucosal infections, respectively. The ability of DCs to balance tolerance and immunogenicity is crucial for maintaining immune homeostasis, as an overactive response may lead to allergies or autoimmunity, whereas insufficient activation could result in uncontrolled infections or tumor progression. Homeostatic immune responses aim to prevent unwanted immune activation while maintaining vigilance for potential threats.

These diverse functional outcomes are mediated by different DC subsets, each of which plays a specialized role in shaping immune responses. DC subsets include conventional (c)DCs, plasmacytoid DCs, and monocyte-derived (mo)DCs [29]. cDCs are further classified into cDC1 and cDC2 based on their lineage and function, with cDC1 excelling in cross-presentation and cytotoxic T cell activation, while cDC2 specializes in activating T helper cells. pDCs play a critical role in antiviral immunity through the production of type I interferons, enhancing the immune response to viral infections. moDCs, often generated ex vivo for autologous immunotherapies, can also differentiate from monocytes in vivo under inflammatory conditions, highlighting the plasticity of the immune system and its ability to adapt to pathological states. Together, these subsets provide the functional versatility required for DCs to balance immune responses across diverse physiological and pathological scenarios.

In both health and disease, the tissue microenvironment plays a crucial role in guiding immune functions. The microenvironment is composed of various factors, including cell interactions, cytokines, nutrients, metabolites, pH, and oxygen (O_2) levels, all of which collectively influence cellular behavior and function [30–32]. In a homeostatic state, these components are tightly regulated to maintain normal tissue function and immune balance. However, in disease states such as cancer, chronic inflammation, and ischemic conditions, homeostatic mechanisms become dysregulated. This dysregulation imposes significant metabolic and physiological challenges, leading to altered immune responses and pathological outcomes [33–36]. Among the various factors in the tissue microenvironment, O_2 availability plays a pivotal role in shaping the metabolic and functional states of immune cells, including DCs. Physiological O_2 levels range from 4–14% in the blood, 3–9% in

well-vascularized tissues, and as low as 0.5% in lymphoid organs [37–41]. In contrast, atmospheric O_2 levels (21%) typically used in cell culture represent a hyperoxic state and do not reflect in vivo environments [41–48]. While the role of O_2 in the regulation of DC function has been extensively studied in pathological states such as tumors, wounds, and inflamed tissues, characterized by hypoxia (<2%) [49], its specific role in immune homeostasis remains underexplored.

This study investigates whether physiological O_2 levels (4%) program DCs toward a tolerogenic phenotype, thereby contributing to immune homeostasis. To explore the role of O_2 in DC biology, we applied 4% O_2 during the DC generation period to mimic the O_2 conditions typically encountered in peripheral tissues. We assessed the resulting cells in terms of their phenotype, mitochondrial function, and capacity to activate allogeneic T cells. Recognizing and incorporating physiologically relevant O_2 conditions into experimental designs may enhance our understanding of how DCs operate in their natural microenvironment and support the clinical translation of DC-based therapies. Ultimately, gaining deeper insights into how O_2 shapes DC biology will advance our understanding of immune responses in both health and disease.

2. Materials and Methods

2.1. Cells and Culture Conditions

Buffy coats derived from healthy donor whole blood collections were purchased from the Red Cross Flanders (Mechelen, Belgium) and processed as described previously [50], with each biological replicate, denoted as n, representing an independent donor. Peripheral blood mononuclear cells were isolated using Ficoll-Paque density gradient centrifugation (GE Healthcare, Diegem, Belgium) followed by isolation of CD14⁺ monocytes using CD14microbead-based immunomagnetic separation (CD14 reagent; Miltenyi Biotec, Leiden, The Netherlands). To generate DCs, purified CD14⁺ cells were resuspended in Iscove's Modified Dulbecco's Medium (IMDM; Thermo Fisher Scientific, Merelbeke, Belgium), supplemented with 2% human AB serum (hAB; Thermo Fisher Scientific), 250 IU/mL interleukin (IL)-4 (Miltenyi Biotec), and 200 IU/mL granulocyte-macrophage colony-stimulating factor (GM-CSF; Gentaur, Kampenhout, Belgium) at day 0 at a density of 1×10^6 cells/mL and cultured for a period of six days in culture flasks (Greiner Bio-One, Vilvoorde, Belgium). On day 4, a combination of pro-inflammatory cytokines, consisting of 1000 IU/mL IL-1β (Miltenyi Biotec), 1000 IU/mL tumor necrosis factor (TNF)-α (Miltenyi Biotec), and 2.5 µg/mL prostaglandin (PG)E₂ (Pfizer, Puurs, Belgium) was added to the culture for a 48-h maturation stimulus. Cells were incubated at 37 °C in a humidified atmosphere with 5% CO₂ under either 21% or 4% O₂, using a Whitley H45 HEPA Hypoxystation (Don Whitley Scientific, Bingley, UK) for the latter (Figure 1). On day 6, mature moDCs were harvested for additional experiments.

The fraction of CD14 $^-$ cells, comprising peripheral blood lymphocytes (PBLs), was cryopreserved for further use at a concentration of 50×10^6 cells/mL in fetal bovine serum (FBS; Thermo Fisher Scientific) supplemented with 10% dimethyl sulfoxide (DMSO; Merck Life Science, Hoeilaart, Belgium) and 4% glucose (Laboratoires Sterop, Brussel, Belgium). The aliquots were frozen in Corning CoolCell LX cell-freezing containers (Corning, Lasne, Belgium) at $-80\,^{\circ}$ C.

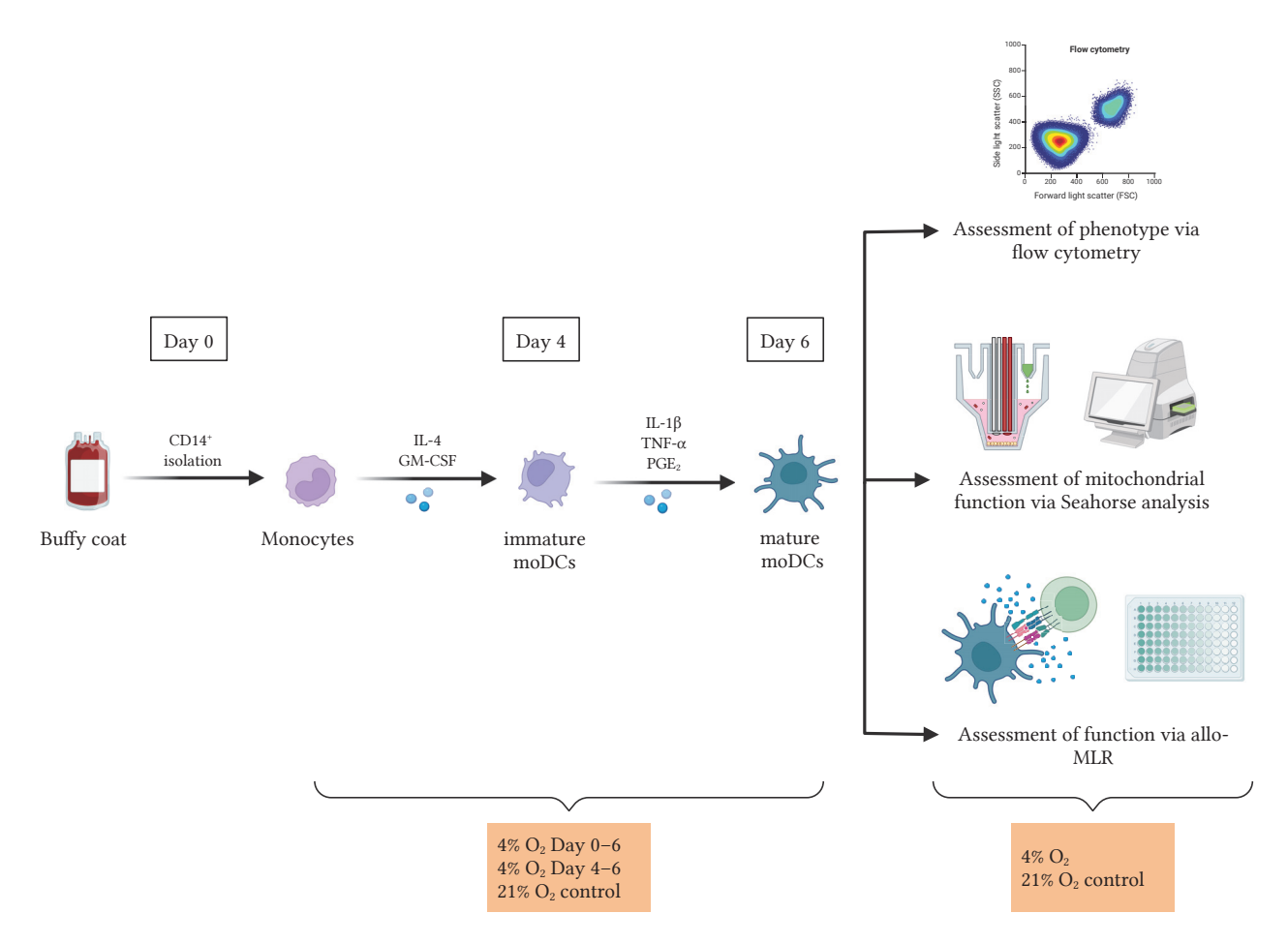


Figure 1. Workflow for the assessment of physioxic culture conditions in moDCs. DCs were differentiated from monocytes in the presence of IL-4 and GM-CSF and matured with the proinflammatory cytokines IL-1β, TNF- α , and PGE₂. Cultures were divided into three experimental groups: (1) continuous culture under 21% O₂ (atmospheric O₂ levels), (2) continuous culture under 4% O₂ (days 0–6), and (3) 4% O₂ during the maturation phase only (days 4–6). The latter was included to provide a reference for late-stage low-O₂ exposure and to support interpretation of the sustained low-O₂ exposure group. On day 6, cell phenotype was analyzed by flow cytometry, mitochondrial function was assessed using a Seahorse assay, and immunostimulatory capacity was evaluated in an allo-MLR performed at either 4% or 21% O₂. This setup was designed to better mimic the physiological O₂ levels found in human tissues. Abbreviations used: moDCs, monocyte-derived dendritic cells; IL, interleukin; GM-CSF, granulocyte-macrophage colony-stimulating factor; TNF- α , tumor necrosis factor-alpha; PGE₂, prostaglandin E₂; O₂, oxygen; allo-MLR, allogeneic mixed lymphocyte reaction.

2.2. *Immunophenotyping of DCs*

The quality of the cells was evaluated by assessing viability using flow cytometry with propidium iodide staining (Thermo Fisher Scientific) after the harvest on day 6. Additionally, DC surface marker expression was assessed through phenotypical analysis. Following a 5-min blocking step (Human TruStain FcX; BioLegend, Amsterdam, The Netherlands), cells were stained with two distinct antibody panels, both of which included a viability dye (LIVE/DEAD fixable Near-Infrared Dead Cell Stain; Thermo Fisher Scientific) and a TruStain monocyte blocker (BioLegend) to avoid unspecific binding of DCs to tandem fluorophores. The first panel was designed to assess DC identity and maturation, and contained the following fluorochrome-conjugated monoclonal antibodies: anti-CD209-phycoerythrincyanine7 (PE-Cy7; BioLegend), anti-human leukocyte antigen (HLA)-DR-Kiravia-Blue-520 (BioLegend), anti-CD14-Brilliant-Violet-711 (BV711; BioLegend), anti-CD83-BV785 (BioLegend)

gend), anti-CD80-allophycocyanin (APC, BioLegend), and anti-CD86-BV605 (BioLegend). The second panel focused on the analysis of tolerance-associated surface markers and included: anti-CD209-PE (BioLegend), anti-CD11c-PerCP/Cyanine5.5 (BioLegend), anti-B7 homolog 3 (B7-H3)-PE/Dazzle 594 (BioLegend), anti-programmed death-ligand 1 (PD-L1)-BV711 (BioLegend), anti-CD40-BV650 (BioLegend), and anti-immunoglobulin-like transcript 4 (ILT4)-APC (BioLegend). In addition, staining for ILT3 (anti-ILT3-PE; BioLegend) was performed separately in combination with the same viability dye. The concentrations used for each antibody are listed in Supplementary Table S1. Non-specific background staining was assessed using isotype-matched control antibodies or fluorescence-minus-one (FMO) controls, as appropriate. Compensations were set up with compensation beads (UltraComp eBeads Plus Compensation Beads, Thermo Fisher Scientific) according to the manufacturer's instructions. Per condition, 1×10^5 cells were washed in sheath buffer (BD FACSFlow Sheath Fluid, BD Biosciences, Erembodegem, Belgium) supplemented with 0.1% bovine serum albumin (BSA; Merck Life Science) and 0.05% sodium azide (Merck Life Science), stained in a volume of 100 µL for 15 min at 4 °C, and washed once more before data acquisition on a NovoCyte Quanteon flow cytometer (Agilent Technologies, Diegem, Belgium), collecting 10^4 events per sample based on forward scatter (FSC) and side scatter (SSC) properties. All median fluorescence intensity (MFI) and percentage expression values were calculated from viable cells, as determined by exclusion of the L/D marker. Control populations consistently exhibited >99% CD209 and HLA-DR double-positivity, confirming their DC identity. Gating strategy and representative plots for all markers are provided in Supplementary Figure S1.

In addition, Mitotracker dyes were used for mitochondrial labeling of DCs: Mitotracker Green FM fluorescein isothiocyanate (FITC), Mitotracker Red FM CMXRos PE, and MitoSOX Red PE (Table S1). Mitochondrial labeling was performed in single stains in combination with a LIVE/DEAD fixable Near-Infrared Dead Cell Stain. All Mitotracker dyes are products of Thermo Fisher Scientific. Per condition, 1×10^5 cells were washed in serum-free phosphate-buffered saline (PBS; Thermo Fisher Scientific), stained in a volume of 100 μ L for 30 min at 37 °C, and washed once more before data acquisition as described above. MFI values were directly recorded from viable cells, gated as described in Supplementary Figure S1.

2.3. Lactate Measurement

To assess lactate production, $10~\mu L$ of cell culture supernatant was collected on days 2, 4, and 6 of the DC culture and promptly frozen at $-20~^{\circ}C$ until further analysis. Lactate concentrations were measured using a StatStrip Express Lactate device in combination with StatStrip Lactate test strips, according to the manufacturer's instructions (Nova Biomedical, Boxtel, The Netherlands).

2.4. Seahorse Assay for Mitochondrial Function

Mitochondrial function was assessed on day 6 of DC culture using the Agilent Seahorse XFp Cell Mito Stress Test. Sensor cartridges were hydrated overnight with sterile water, starting the day before the assay. On the day of measurement, DCs were harvested and assessed for viability as described in Section 2.2. Hydrated sensor cartridges were then loaded with Seahorse XF Calibrant and incubated for at least 45 min at 37 $^{\circ}$ C in a non-CO₂ incubator.

Meanwhile, DCs were resuspended in Seahorse XF RPMI assay medium (pH 7.4) supplemented with 10 mM glucose, 1 mM pyruvate, and 2 mM glutamine, and seeded into poly-D-lysine (PDL)-coated Seahorse XFp miniplates that had been pre-equilibrated to 37 °C in a non-CO₂ incubator. Depending on the condition-specific viability, a total of

 5×10^4 – 2×10^5 cells were plated per well. Plates were centrifuged briefly (300× g, 1 min) to ensure cell adherence.

Following drug loading of the sensor cartridges with 1.5 μ M oligomycin (adenosine triphosphate (ATP) synthase inhibitor), 1.5 μ M carbonyl cyanide-p-trifluoromethoxyphenylhydrazone (FCCP; uncoupling agent), and 0.5 μ M rotenone/antimycin A (complex I/III inhibitors), the cartridges were placed into the Seahorse XF Mini Bioanalyzer for calibration. During this time, the cell plates were kept at 37 °C in a non-CO₂ incubator. Once calibration was complete, the cell plate was inserted into the analyzer, and measurements of oxygen consumption rate (OCR) were taken before and after each compound injection. These were used to calculate key mitochondrial parameters reflecting different aspects of mitochondrial respiration, including basal respiration, ATP-linked respiration, proton leak, maximal respiration, spare respiratory capacity, non-mitochondrial respiration, and coupling efficiency. Each condition was tested in technical triplicates. Data were analyzed using the Agilent Seahorse Analytics software (version 1.0.0-749) and normalized to the number of total living DCs per well. All Seahorse-specific equipment and reagents were obtained from Agilent Technologies.

2.5. Allogeneic Mixed Lymphocyte Reaction (Allo-MLR)

To determine the T cell stimulatory capacity of DCs, allogeneic PBLs were co-cultured with DCs in a 10:1 ratio in 24-well plates (Greiner Bio-One), with the number of cells seeded based on live cell counts. PBLs stimulated with 1 µg/mL phytohaemagglutinin (PHA; Merck Life Science) served as a positive control. Furthermore, unstimulated allogeneic PBLs without DCs served as a negative control. Additionally, PBLs from the same donor as the DCs were included to control for potential effects of O₂ deprivation on T cells in the absence of allogeneic stimulation (referred to as the PBL-only control in the results section). The co-cultures were performed in IMDM supplemented with 5% hAB and maintained for five days at 37 °C in a humidified atmosphere with 5% CO₂ under either 21% or 4% O₂ (Figure 1). After this incubation period, the supernatants were collected, frozen, and stored at -20 °C for subsequent testing. As a measure of the T cell stimulatory capacity of DCs, the levels of interferon (IFN)- γ were quantified using a commercially available enzyme-linked immunosorbent assay (ELISA; PeproTech, London, UK) according to the manufacturer's instructions. Each sample was tested in triplicate. Plates were read by measuring absorbance at 405 nm using a Victor³ multilabel plate reader (PerkinElmer, Mechelen, Belgium) and interpolated to the concentration (pg/mL) using MS Office Excel.

2.6. Immunophenotyping of PBLs

To compare the stimulatory capacities of atmospheric and physioxic DCs to elicit allogeneic T cell responses not only based on IFN-γ secretion but also on the surface expression of co-stimulatory ligands and other markers, PBLs were stained with two different antibody panels on the last day of the allo-MLR following a 5-min blocking step (Human TruStain FcX). The first panel was used to distinguish different T cell subsets and contained the following fluorochrome-conjugated monoclonal antibodies: anti-CD45RA-Pacific-Blue, anti-CD8-BV510, anti-CD27-BV605, anti-CD57-BV785, anti-CD4-FITC, anti-CCR7-PE, anti-PD-1-PE-Cy7, anti-CD28-APC, anti-CD3-Spark-Red-718, and LIVE/DEAD fixable Near-Infrared Dead Cell Stain (Table S1). The second panel for T cell exhaustion markers contained the following fluorochrome-conjugated monoclonal antibodies: anti-PD-L2-BV421, anti-CD8-BV510, anti-TIGIT-BV605, anti-TIM-3-BV711, anti-CTLA-4-BV785, anti-CD4-FITC, anti-CD96-PE, anti-LAG-3-PE-Cy7, anti-PD-L1-APC, anti-CD3-Spark-Red-718, and LIVE/DEAD fixable Near-Infrared Dead Cell Stain (Table S1). All antibodies are products of BioLegend, except for CCR7 (Bio-Techne, Abingdon, UK). Samples were

prepared, stained, and acquired as described in Section 2.2, with 5×10^4 live cells recorded per condition. Gating strategy and representative plots for all markers are provided in Supplementary Figure S2.

2.7. Statistical Analysis

Flow cytometric data were analyzed using the FlowJo 10.10.0 software (FlowJo, TreeStar Inc., Ashland, OR, USA). Values are presented as the median, unless otherwise indicated, with the interquartile range (IQR) expressed as median (Q25-Q75). Statistical analyses were performed using GraphPad Prism 10.10.2, with the respective tests outlined in the figure legends. Each dataset was initially tested for normality using the Shapiro-Wilk test. For comparisons between two groups, a two-tailed paired t-test was used for normally distributed data, and the Wilcoxon matched-pairs signed rank test for non-parametric analysis. When comparing three groups, data that did not pass the normality test were analyzed using the Kruskal-Wallis test with Dunn's multiple comparisons due to the inability of the Friedman test for paired data to accommodate datasets with missing values. Normally distributed data were analyzed using a one-way ANOVA (non-paired) with Śidák's multiple comparisons test. For analyses involving multiple levels of grouping, a mixed-effects model with the Geisser-Greenhouse correction and Śidák's multiple comparisons test was employed. Volcano plots for the PBL phenotyping data were generated to visualize fold changes against the Benjamini-Hochberg-adjusted p-values derived from two-tailed paired t-tests. A fold change > 1.0 was classified as upregulation, while a fold change < 1.0 was classified as downregulation. A p-value < 0.05, corresponding to a $-\log$ (adjusted p-value) of 1.30, was considered statistically significant.

3. Results

3.1. Physiological O₂ Levels During the Generation Period Resulted in a Decreased Transformation of Monocytes into DCs

To understand how O₂ influences DC generation and phenotype under physiological conditions, we examined the impact of 4% O₂, referred to hereafter as physioxia, on the generation of mature moDCs in comparison to 21% O₂, which will be referred to as atmospheric O₂ levels or control conditions. We employed two physioxic culture conditions: physioxia during the entire 6-day culture period $(4\% O_2)$ days 0–6) and physioxia only during the maturation phase between days 4 and 6 (4% O_2 D4–6), the latter serving as a maturation-phase-specific comparator to contextualize the effects of continuous low-O₂ exposure. These were compared to continuous culture under 21% O₂ (Figure 1). Our findings demonstrated a significant reduction in the monocyte-to-mDC transformation rate (control: 34.3%, IQR: 26.9–42.4%; 4% O₂ D4–6: 33.4%, IQR: 31.4–40.4%; 4% O₂ D0–6: 24.0%, IQR: 9.3–25.9%) under continuous physioxia compared to atmospheric O_2 levels (p < 0.0001). This was calculated as the number of viable cells on day 6 excluding CD209⁻CD14⁺ monocytes, relative to the number of viable monocytes seeded on day 0. CD14 downregulation and CD209 upregulation was used to distinguish successfully transformed moDCs from undifferentiated monocytes, in line with established phenotypic criteria. The same effect was observed regarding cell viability (p < 0.0001) (Figure 2A). In contrast, no significant differences were observed when comparing control conditions to physioxic maturation conditions. Furthermore, the percentage of monocytes (CD209⁻CD14⁺) was significantly increased upon a full physioxic culture period compared to control conditions (p < 0.0001), whereas no such increase was observed when the cells were exposed to $4\% O_2$ only during the maturation phase (Figure 2B). Taken together, these results suggest that physioxic culture conditions negatively affect DC generation from monocytes when applied throughout the entire culture period.

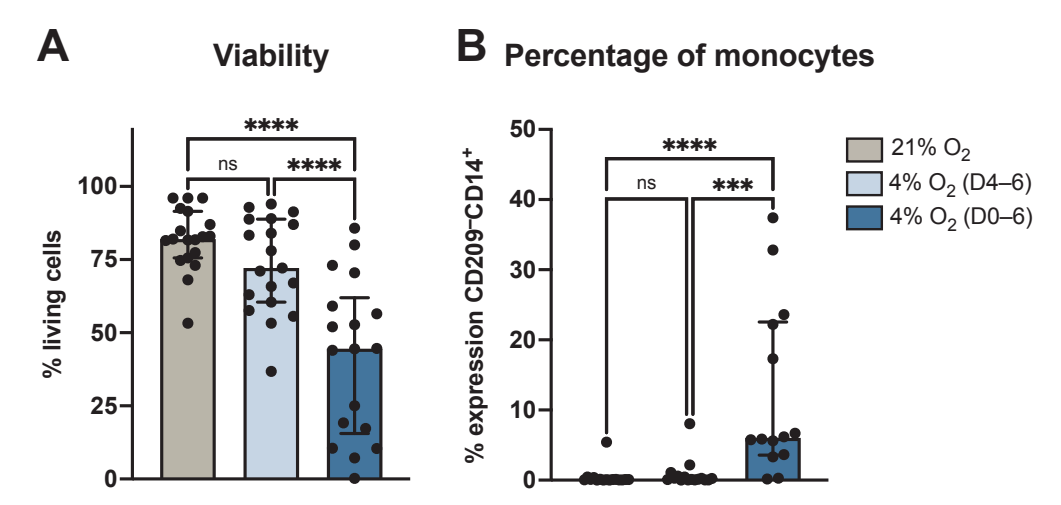


Figure 2. Generation of moDCs under $4\% O_2$ resulted in decreased viability and increased percentage of monocytes. (**A**) Viability of the total cell population on day 6 determined via PI exclusion, prior to DC phenotyping (n = 20). (**B**) Monocyte population represented as the percentage of CD209⁻CD14⁺ cells (n = 16). All cells were cultured under atmospheric O_2 levels, $4\% O_2$ during the entire generation phase (D0–6), or $4\% O_2$ only during the maturation phase (D4–6). Data are shown as median with interquartile range. Statistical analyses were performed using an ordinary one-way ANOVA (**A**) or the Kruskal-Wallis test with Dunn's post-hoc analysis (**B**). Statistical significance is denoted by *, where *** represents p < 0.001 and **** represents p < 0.0001. Abbreviations used: moDCs, monocytederived dendritic cells; O_2 , oxygen; D0–6, days 0 to 6; D4–6, days 4 to 6; PI, propidium iodide; ANOVA, analysis of variance; ns, not significant.

3.2. Physiological O_2 Levels During the Generation Period Resulted in Decreased Surface Expression of Identity and Maturation Markers, and Increased Expression of Tolerance-Associated Marker ILT4

The generation of mDCs from monocytes is typically marked by downregulation of CD14 and upregulation of DC identity and co-stimulatory markers, including CD209, HLA-DR, CD80, CD86, and CD83. To assess the phenotypic status of the cells generated under different O_2 conditions, we analyzed surface marker expression profiles indicative of this immunophenotypic progression. Our study revealed that the proportion of moDCs expressing CD209 and HLA-DR remained high under both physioxic conditions (Figure 3A), indicating preserved cellular integrity (CD209: control: 99.5%, IQR: 99.1–99.8%; 4% O_2 D4–6: 99.2%, IQR: 97.9–99.6%; 4% O_2 D0–6: 93.1%, IQR: 85.7–96.3%; HLA-DR: control: 100.0%, IQR: 99.9–100.0%; 4% O_2 D4–6: 99.9%, IQR: 99.7–100.0%; 4% O_2 D0–6: 99.9%, IQR: 99.7–99.9%). However, significant reductions in the expression levels of CD209 (p < 0.0001) and HLA-DR (p = 0.003), as measured by MFI, were observed under continuous physioxic conditions compared to atmospheric O_2 levels, with significant differences between physioxic maturation and controls for CD209 (p = 0.0104) but not for HLA-DR (Figure 3B).

When examining the maturation markers, we found that the proportion of moDCs expressing CD83 and CD80 was unaffected by physioxia. However, their expression levels were significantly reduced under continuous physioxia compared to atmospheric O_2 levels (CD83: p = 0.0031, CD80: p = 0.0009). Additionally, a significant reduction in CD83 expression was observed under physioxic maturation (p = 0.0344). CD86 was uniformly expressed across all conditions (control: 99.6%, IQR: 99.3–99.8%; 4% O_2 D4–6: 98.9%, IQR: 97.8–99.3%; 4% O_2 D0–6: 99.1%, IQR: 98.5–99.4%; Figure 3A), although expression levels were significantly downregulated under continuous physioxia (p = 0.0002), similar to the other maturation markers (Figure 3B).

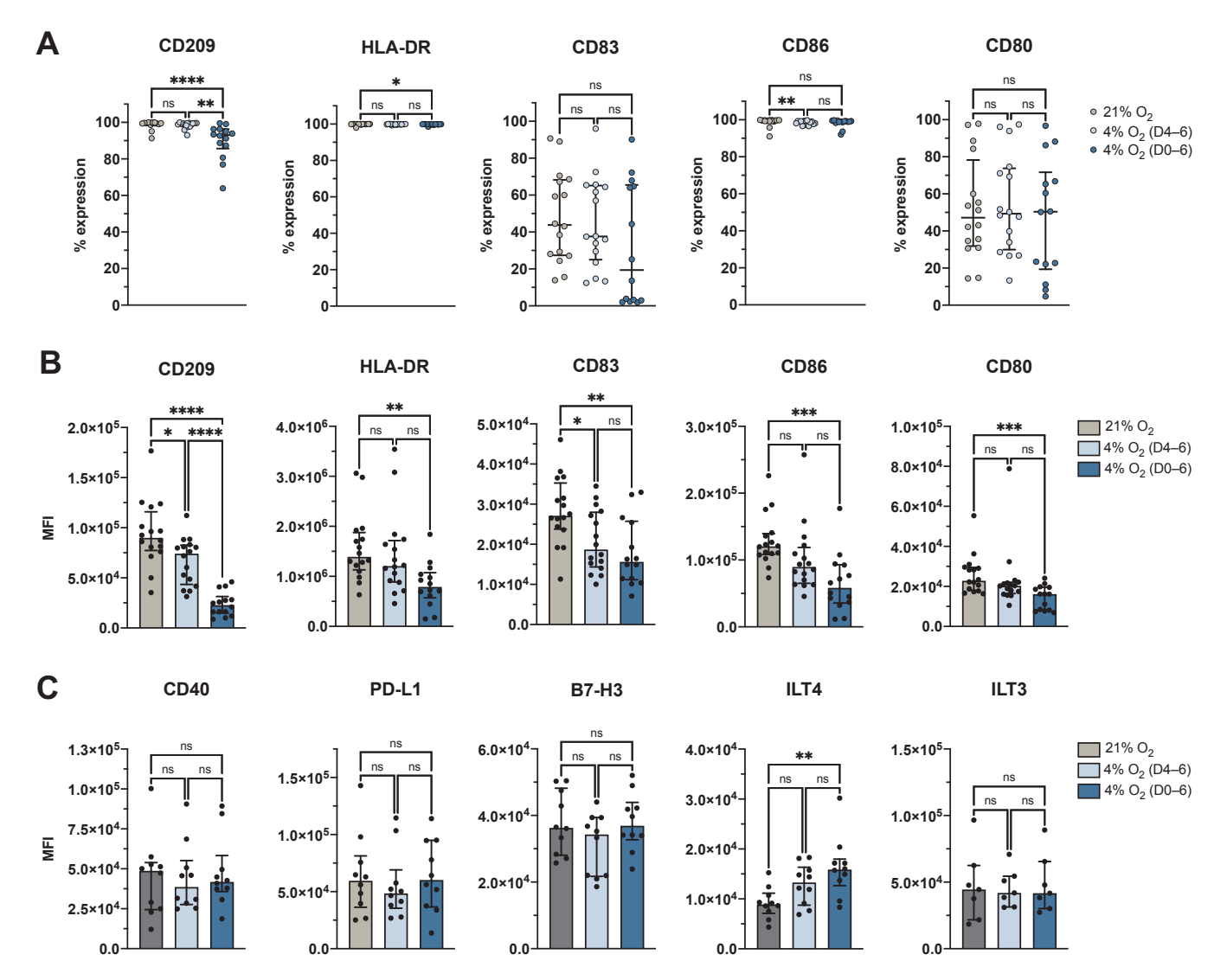


Figure 3. DC generation under 4% O_2 resulted in a decreased surface expression of identity and maturation markers, and an increase of tolerance marker ILT4. (**A**) The percentage of expression for the markers CD209, HLA-DR, CD83, CD86, and CD80 (n = 16). (**B**) The expression levels of the markers CD209, HLA-DR, CD83, CD86, and CD80 presented as MFI of the positive population (n = 16). (**C**) The expression levels of the markers CD40, PD-L1, B7-H3, ILT4, and ILT3 presented as MFI of the positive population (n = 7 for ILT3, n = 10 for all other markers). Cells depicted in all graphs were cultured under atmospheric O_2 levels, 4% O_2 (D4–6), or 4% O_2 (D0–6). Data are shown as median with interquartile range. Statistical analyses were performed using an ordinary one-way ANOVA ((**A**): CD83, CD80; (**B**): CD209, CD83; (**C**): CD40, B7-H3, ILT4, ILT3) or the Kruskal-Wallis test with Dunn's post-hoc analysis ((**A**): CD209, HLA-DR, CD86; (**B**): HLA-DR, CD86, CD80; (**C**): PD-L1). Statistical significance is denoted by *, where * represents p < 0.05, ** represents p < 0.01, and **** represents p < 0.001. Abbreviations used: O_2 , oxygen; D0–6, days 0 to 6; D4–6, days 4 to 6; MFI, mean fluorescence intensity; ANOVA, analysis of variance; CD, cluster of differentiation; HLA-DR, human leukocyte antigen—DR isotype; PD-L1, programmed death-ligand 1; B7-H3, B7 homolog 3; ILT, immunoglobulin-like transcript; ns, not significant.

To further investigate the effect of O_2 levels on tolerance-associated markers, we assessed the expression of CD40, PD-L1, B7-H3, ILT3, and ILT4 on moDCs cultured under atmospheric O_2 , physioxic maturation (4% O_2 D4–6), or continuous physioxia (4% O_2 D0–6). Among the markers tested, only ILT4 showed a statistically significant difference, with expression levels significantly upregulated under continuous physioxia compared to

atmospheric O_2 (p = 0.0051; Figure 3C). No significant differences were observed for CD40, PD-L1, B7-H3, or ILT3 (Figure 3C).

3.3. Physiological O₂ Levels During the Generation Period Increased Lactate Secretion but Largely Preserved Mitochondrial Function

To assess the impact of physiological O_2 levels on DC metabolism, lactate secretion and mitochondrial parameters were evaluated under atmospheric (21% O_2) and physioxic (4% O_2) conditions. While glycolytic activity, as indicated by lactate production, was elevated under physioxia, mitochondrial function remained mostly unaffected (Figure 4).

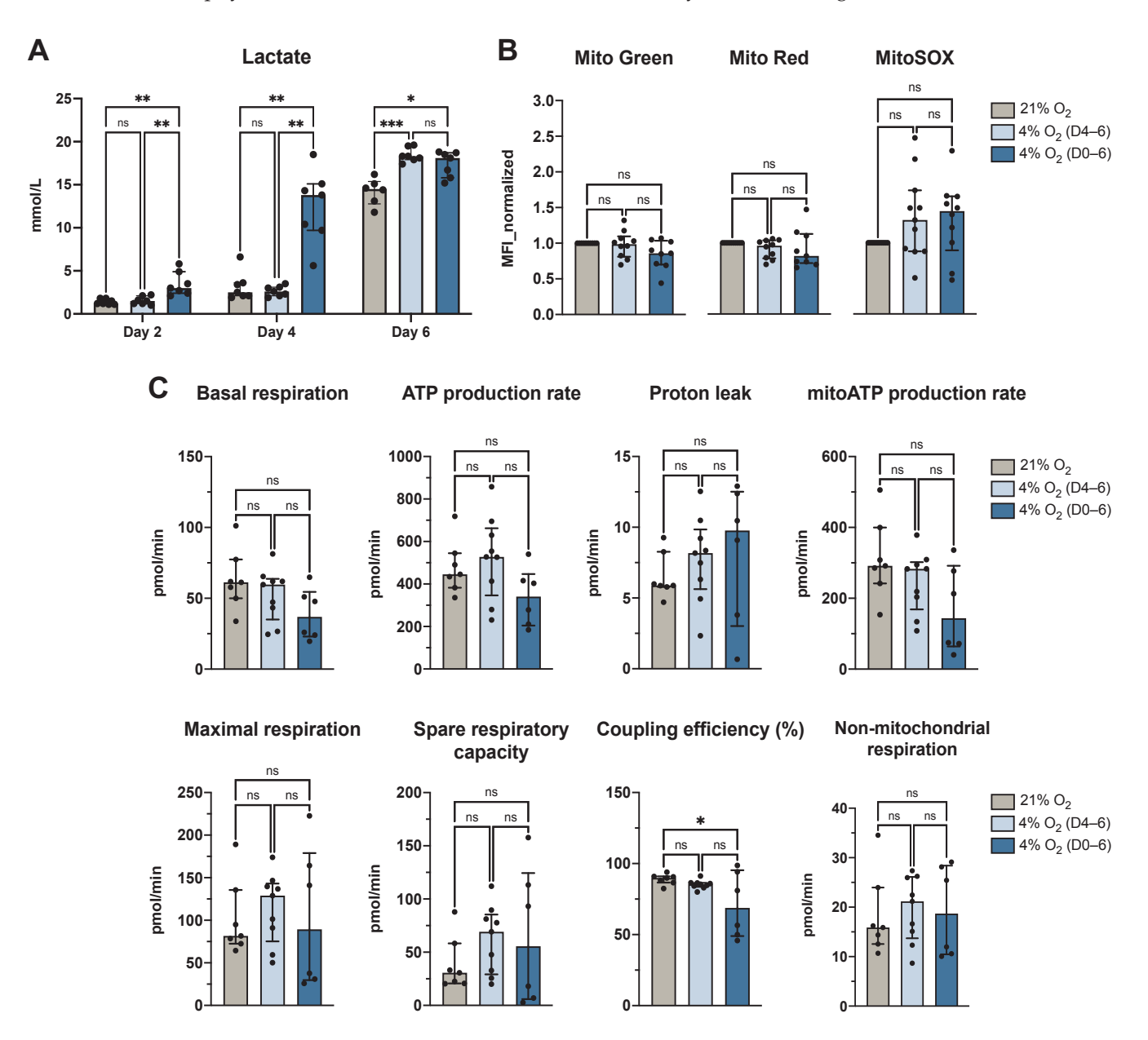


Figure 4. DC generation under 4% O₂ increased lactate production but did not alter mitochondrial function. (**A**) Lactate production by moDCs (n = 7). (**B**) Mitochondrial stainings as indicated by Mitotracker Green (mitochondrial mass), Mitotracker Red (membrane potential), and MitoSOX Red (superoxide production) presented as normalized MFI values (n = 11). (**C**) Seahorse Mito Stress Test analysis of moDCs (n = 9). Mitochondrial parameters shown include basal respiration (OCR under baseline conditions), ATP production rate (portion of OCR used for ATP synthesis, inferred from the drop after oligomycin addition), proton leak (non-ATP-linked OCR following ATP synthase inhibition), mitoATP production rate (absolute ATP output via oxidative phosphorylation), maximal

respiration (peak OCR following FCCP addition), spare respiratory capacity (difference between maximal and basal respiration), coupling efficiency (proportion of basal OCR coupled to ATP production), and non-mitochondrial respiration (residual OCR after inhibition of mitochondrial complexes I and III by rotenone and antimycin A). All cells were cultured under atmospheric O_2 levels, 4% O_2 (D4–6), or 4% O_2 (D0–6). Data are shown as median with interquartile range. Statistical analyses were performed using a mixed-effects model with the Geisser-Greenhouse correction (A), an ordinary one-way ANOVA ((B): Mito Green, Mito Red; (C): basal respiration, ATP production rate, proton leak, mitoATP production rate, maximal respiration, coupling efficiency), or the Kruskal-Wallis test with Dunn's post-hoc analysis ((B): MitoSOX; (C): spare respiratory capacity, non-mitochondrial respiration). Statistical significance is denoted by *, where * represents p < 0.05, ** represents p < 0.01, and *** represents p < 0.001. Abbreviations used: O_2 , oxygen; D0–6, days 0 to 6; D4–6, days 4 to 6; moDCs, monocyte-derived dendritic cells; MFI, mean fluorescence intensity; ANOVA, analysis of variance; OCR, oxygen consumption rate; ATP, adenosine triphosphate; FCCP, carbonyl cyanide-p-trifluoromethoxyphenylhydrazone; ns, not significant.

Lactate measurements revealed a significant increase in secretion by moDCs cultured under continuous physioxia compared to atmospheric O_2 levels on day 2 (p = 0.0063) and day 4 (p = 0.0023; Figure 4A). By day 6, lactate levels were significantly higher in both physioxic culture conditions compared to control cells (D4–6: p = 0.0002, D0–6: p = 0.0163).

Mitochondrial characteristics were assessed using fluorescent dyes (Mitotracker Green, Red, and MitoSOX Red) and Seahorse metabolic flux analysis. Fluorescence-based measurements indicated no significant differences in mitochondrial mass, membrane potential, or mitochondrial superoxide levels between atmospheric and physioxic conditions (Figure 4B), suggesting preserved mitochondrial integrity under both conditions. In parallel, the Seahorse Mito Stress Test evaluated parameters including basal respiration, ATP production rate, proton leak, maximal respiration, spare respiratory capacity, and non-mitochondrial respiration. Most parameters showed no significant differences between physioxic and normoxic culture conditions, aligning with the fluorescence-based findings. Notably, a modest but statistically significant decrease in coupling efficiency was observed under continuous physioxia compared to atmospheric O_2 (p = 0.0489; Figure 4C), indicating reduced efficiency in ATP production relative to total O₂ consumption. Although there was an observed trend towards lower basal respiration and mitochondrial ATP production rate under physioxic conditions, these differences were not statistically significant. Together, these results suggest that while physioxia may slightly reduce respiratory efficiency, mitochondrial health remains uncompromised, and any shifts in ATP production are minimal.

3.4. O₂ Levels During the Allo-MLR Modulate T Cell Responses

To investigate the influence of physiological O_2 levels on DC function in terms of their capacity to stimulate allogeneic T cell responses, we conducted mixed lymphocyte reactions (allo-MLR) under both atmospheric (21% O_2) and physioxic (4% O_2) conditions, evaluating IFN- γ secretion and phenotypic changes of peripheral blood lymphocytes (PBLs) after five days of co-culture (Figures 5 and 6).

As a first step, the effect of O_2 levels during the allo-MLR itself was assessed. DCs cultured under atmospheric O_2 were co-cultured with allogeneic PBLs in either a 21% or 4% O_2 allo-MLR. Under physioxic allo-MLR conditions, these control DCs induced significantly lower levels of IFN- γ secretion compared to atmospheric conditions (p < 0.0001), suggesting that low O_2 leads to T cell hyporesponsiveness in this context (Figure 5). In contrast, no significant differences in IFN- γ secretion were observed when comparing 21% and 4% O_2 allo-MLRs for any of the following: negative control, positive control, PBL-only control, moDCs matured under physioxia (4% O_2 D4–6), or moDCs cultured under continuous physioxia (4% O_2 D0–6). These findings suggest that the reduced IFN- γ levels seen under physioxia may be specific to the combination of atmospheric moDCs and

low O₂ during T cell activation, rather than a general suppression of PBL responsiveness under physioxic conditions.

Allo-MLR (4% vs. 21% O₂)

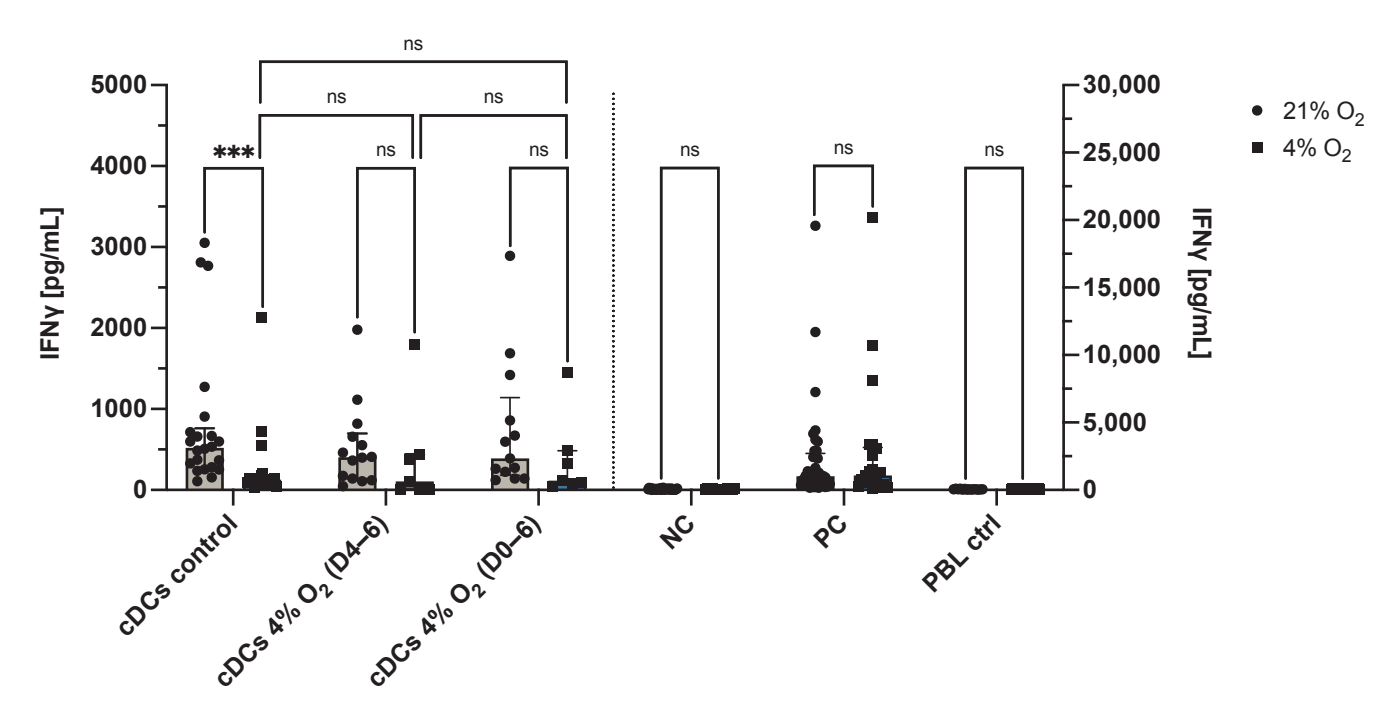


Figure 5. O₂ levels during the allo-MLR modulate T cell responses. IFN- γ secretion (pg/mL) by PBLs stimulated with control moDCs (cultured at 21% O₂), moDCs exposed to physioxia during maturation (4% O₂ D4–6), or moDCs cultured under continuous physioxia (4% O₂ D0–6), as well as NC, PC (PHA-stimulated PBLs), and PBL-only control (autologous PBLs), in 5-day allo-MLRs conducted at either 21% or 4% O₂. Data are shown as median with interquartile range. Comparisons for the three moDC conditions were performed using the Wilcoxon matched-pairs signed rank test. Controls were analyzed using a mixed-effects model with Geisser-Greenhouse correction and Šídák's multiple comparisons test. Statistical significance is denoted by *, where *** represents p < 0.001. Abbreviations used: O₂, oxygen; moDCs, monocyte-derived dendritic cells; D0–6, days 0 to 6; D4–6, days 4 to 6; allo-MLR, allogeneic mixed lymphocyte reaction; IFN- γ , interferon-gamma; PBLs, peripheral blood lymphocytes; NC, negative control; PC, positive control; PHA, phytohemagglutinin; ns, not significant.

Next, the impact of O_2 exposure during DC generation was examined under physioxic allo-MLR conditions. Specifically, IFN- γ secretion was compared across all three DC culture conditions—atmospheric (21% O_2), physioxic maturation (4% O_2 D4–6), and continuous physioxia (4% O_2 D0–6)—in a 4% O_2 allo-MLR. In this setting, no significant differences were observed between the groups (Figure 5), suggesting that preconditioning DCs under physioxia does not markedly alter their IFN- γ -inducing capacity in allogeneic settings.

To gain further insights into how O_2 tension affects T cell phenotypes beyond IFN- γ secretion, flow cytometric profiling was performed on PBLs after five days of allo-MLR. For this, cells were analyzed for memory and exhaustion markers on CD4⁺ and CD8⁺ subsets.

As a baseline comparison, PBLs co-cultured with control DCs (cultured entirely under atmospheric conditions) were analyzed after allo-MLR under either 21% or 4% O_2 . In the CD4⁺ population, significant reductions in MFI were observed for CCR7, TIGIT, and CD45RA under physioxia (Figure 6A). In the CD8⁺ population, MFI of CD57, TIGIT, CD45RA, PD-L2, TIM-3, LAG-3, CTLA-4, CD96, PD-L1, and CCR7 were all significantly decreased under physioxic conditions (Figure 6B). In terms of percentage marker expression,

CD4⁺ cells showed significantly reduced frequencies of CD27⁺CD28⁻, PD-L1⁺, TIGIT⁺, CTLA-4⁺, TIM-3⁺, LAG-3⁺, and CD45RA⁻CCR7⁺ cells (central memory T cells), while CD8⁺ cells showed a decrease in LAG-3⁺, PD-L1⁺, and CCR7⁺ cells, and a corresponding increase in CD27⁺ cells (Figure 6C,D). The control conditions (NC, PC, PBL-only) exhibited minor changes in this setup, limited to MFI shifts in a few markers without significant alterations in the percentage of marker-expressing cells (Figure S3), in line with the IFN- γ secretion data.

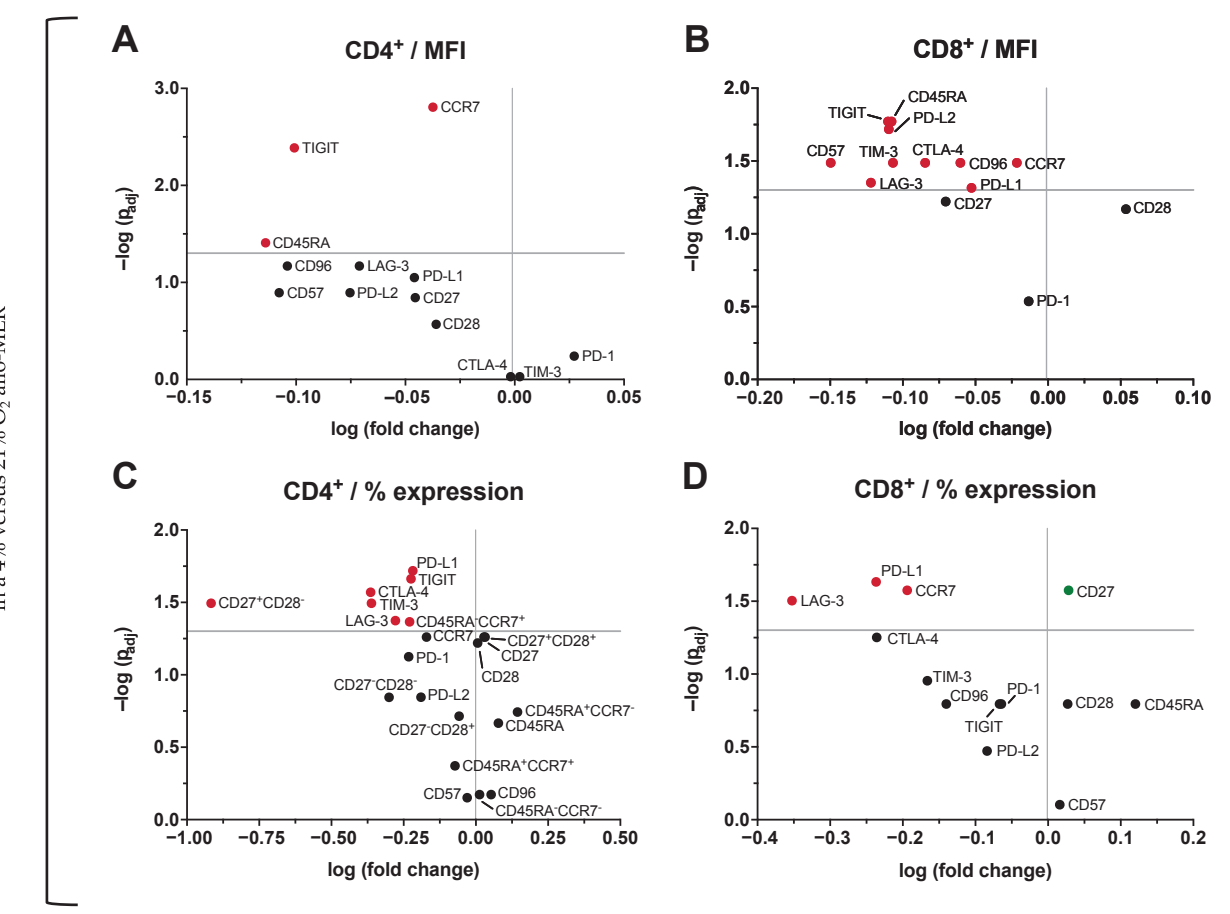


Figure 6. O₂ levels during the allo-MLR modulate T cell phenotypes. Phenotypic analysis of CD4⁺ and CD8⁺ T cell subsets was performed on day 5 of the allo-MLR to evaluate the impact of O₂ tension during T cell activation. Control moDCs cultured at atmospheric O₂ levels were used to stimulate PBLs in either 4% or 21% O₂ allo-MLRs. Significant changes reflect the effect of physioxia (4% O₂) compared to atmospheric conditions (21% O₂). Values represent either MFI (**A,B**) or percentage of expression (**C,D**) in CD4⁺ or CD8⁺ T cell subsets. Data are presented as $-\log$ (Benjamini-Hochberg-adjusted p-value; derived from two-tailed paired t-tests) versus \log (fold change). Statistically significant differences (p < 0.05) are highlighted in red (downregulation) or green (upregulation) (n = 7). Abbreviations used: O₂, oxygen; moDCs, monocyte-derived dendritic cells; D0–6, days 0 to 6; D4–6, days 4 to 6; allo-MLR, allogeneic mixed lymphocyte reaction; PBLs, peripheral blood lymphocytes; CD, cluster of differentiation; MFI, mean fluorescence intensity; TIGIT, T cell immunoreceptor with Ig and ITIM domains; CCR7, C-C chemokine receptor type 7; LAG-3, lymphocyte activation gene 3; PD-L1/2, programmed death-ligand 1/2; CTLA-4, cytotoxic T-lymphocyte-associated protein 4; TIM-3, T cell immunoglobulin and mucin-domain containing-3; PD-1, programmed cell death protein 1.

Next, the influence of O_2 exposure during DC maturation was assessed. When comparing DCs exposed to physioxia during maturation (4% O_2 D4–6) to control DCs (21% O_2) in a 4% O_2 allo-MLR, no significant differences were observed in the expression of any markers on either CD4⁺ or CD8⁺ T cells.

Finally, the effects of continuous physioxia (4% O_2 D0–6) were assessed relative to atmospheric DCs in a 4% O_2 allo-MLR. For CD4⁺ cells, only CD45RA showed a significant reduction in MFI upon physioxic preconditioning (p = 0.034), while no significant differences were observed in CD8⁺ cells. Marker expression frequencies remained unchanged in both T cell subsets.

These results reveal broad downregulation of key exhaustion and memory markers across both CD4⁺ and CD8⁺ T cell subsets along with reduced IFN- γ secretion in response to physioxic allo-MLRs. On the other hand, preconditioning DCs under physioxia alone had limited impact on T cell phenotypes and IFN- γ secretion levels.

4. Discussion

Understanding how O₂ levels influence both DC phenotype and their downstream T cell interactions is crucial for designing more effective immunotherapies and for studying tolerance mechanisms in transplantation and autoimmunity. While most in vitro studies rely on atmospheric O_2 levels (21%), these are far from the physiological conditions that DCs encounter in vivo. Previous research has predominantly focused on exploring DC biology in pathological hypoxia (<2% O₂), relevant for cancer, bacterial infections, arthritis, wound healing, and inflammatory lesions [49]. However, little is known about how physiological O₂ levels affect immune homeostasis. DCs continuously sample antigens in the steady state but avoid full maturation unless activated by PAMPs or DAMPs. The shift from tolerogenic to immunogenic DCs occurs upon encountering inflammatory signals, ensuring that immune responses are mounted only in the presence of a true threat. Understanding the tolerogenic role of DCs under homeostatic conditions has significant implications. Dysregulation of tolerogenic DCs can lead to loss of tolerance and autoimmunity. In addition, tumor microenvironments often exploit tolerogenic mechanisms to suppress DC function and evade immune responses. The main goal of this study was to understand how homeostatic immune responses are generated by mimicking the in vivo conditions of physiological O₂ levels (4% O₂) and comparing them to hyperoxia (21% O₂) typically present in in vitro cell culture. We demonstrated that culturing ex vivo-generated moDCs under physiological O₂ levels leads to reduced monocyte-to-mDC transformation rate and programs the resulting cells toward a tolerogenic phenotype, characterized by increased secretion of lactate, a semi-mature surface marker profile, and altered T cell priming. This suggests a critical role for O_2 in maintaining DC homeostasis, with potential implications for both steady-state and pathological conditions. The observed effects were most pronounced when physioxia was applied throughout the entire culture period, while exposure during the maturation phase only had subtler effects. In vivo, DCs can differentiate from monocytes in inflammatory conditions often characterized by hypoxia [29]. Our experimental setting using physioxia is intended to mimic a homeostatic or steady-state environment. The observed reduction in monocyte-to-mDC transformation rate under physioxia suggests that the metabolic demands in this condition may limit monocyte commitment to the DC lineage in the absence of inflammatory cues, aligning with the physiological scenario under non-inflammatory conditions. The observed reduction in viability under physioxia should be carefully interpreted alongside functional outcomes of the viable DC population. Notably, our assessment on day 6 via PI exclusion reflects the total cell pool before distinguishing between differentiated moDCs and remaining monocytes based on extensive phenotypic profiling. Thus, physioxia affected both overall cell survival and monocyte-to-DC transformation, the latter confirmed by DC lineage markers. This raises the question of why viability decreased under conditions that were intended to mimic physiological O₂ levels. Monocytes were isolated from human blood under standard atmospheric conditions and were then immediately cultured under physioxia. This shift

does not mirror the gradual or tissue-specific O_2 exposure that cells would experience in vivo and highlights the difficulty of mimicking physiological conditions in vitro.

Interestingly, while the percentage of cells expressing key surface molecules remained high (CD209, HLA-DR, CD86) or unchanged (CD80, CD83) under physioxia, their expression levels (as indicated by MFI) were significantly reduced. This discrepancy suggests that although DC identity was preserved, the density of the marker expression on the cell surface declined, which indicates a collective impairment of DC-mediated T cell activation by weakening of co-stimulation (CD86, CD80, CD83), antigen presentation (HLA-DR), and antigen uptake (CD209). Of note, phenotypic profiling was performed on the total viable cell population, capturing not only differentiated DCs but also cells that did not fully commit to the DC lineage. As such, the observed shifts reflect both phenotypic modulation of DCs and impaired monocyte-to-mDC transformation efficiency under physioxia.

The next step for homeostatic DCs in vivo is their potential interaction with T cells under steady-state conditions, where tissue O2 levels are considerably lower than atmospheric. To investigate their functionality in this context, we assessed the capacity of physioxia-conditioned DCs to activate allogeneic T cells under reduced O₂ conditions. We observed no differences in the ability of physioxia-conditioned or atmospheric DCs to induce IFN-γ secretion or to alter the phenotype of PBLs under these conditions. This may suggest that physiological O₂ levels alone do not significantly contribute to shaping immune homeostasis—though the complexity of in vivo interactions cannot be fully recapitulated in this system. However, when we introduced a shift from 21% to $4\% O_2$ during the T cell activation phase, IFN- γ secretion was reduced in control moDC co-cultures. In parallel, we observed a broad downregulation of markers associated with co-inhibitory signaling, memory differentiation, and effector maturation across both CD4+ and CD8+ subsets. This suggests that low O₂ levels at the site of T cell priming may impair effector cytokine production and modulate the quality of T cell responses. Importantly, no difference in IFN- γ secretion was observed between 21% and 4% O_2 in the absence of DCs, highlighting that the O₂ levels did not have a direct effect on T cell function itself but rather attenuated the immunostimulatory capacity of ex vivo-generated DCs during their interaction with T cells. Rather than indicating a classical exhausted phenotype, which would typically involve upregulation of checkpoint molecules and co-inhibitory receptors, the observed profile suggests a hyporesponsive or metabolically restrained T cell state. This is characterized by insufficient activation to induce either effector function or regulatory feedback mechanisms. Markers involved in terminal differentiation (CD57) and lymphoid homing and memory formation (CCR7, CD45RA) were likewise reduced, along with several immune checkpoints and regulatory receptors (PD-1, PD-L1, PD-L2, TIGIT, TIM-3, CTLA-4, LAG-3, CD96). Importantly, our results highlight that immune responses cannot be defined by the absence or presence of individual markers alone but must be instead understood as an integrated functional and phenotypic state. It is important to note that this experimental setup, in which DCs are generated under atmospheric O2 and T cells are activated under physioxic conditions, does not reflect a physiological scenario, as both cell types would naturally co-localize within the same O2 microenvironment in vivo. These insights have implications for immunotherapeutic applications, where ex vivo-generated DCs are administered into low-O₂ tissue environments. Atmospheric O₂ levels are standard during in vitro quality assessments of such cell products, which may not reflect their functional potential in vivo. Our results indicate that physioxia shapes the DC-T cell crosstalk—both in terms of inflammatory cytokine output and T cell phenotypic profile—in a way that does not support robust effector responses. This highlights the need to consider O₂ as a critical environmental regulator of immune activation thresholds.

To better understand the mechanisms underlying the induction of a tolerogenic state under physioxia, we examined cellular metabolism as a potential driver of this phenotype. Immunometabolism is increasingly recognized as a key regulator of immune cell fate, not just in terms of energy production, but also through the integration of environmental signals into functional outcomes. As outlined in our recent review, shifts in cellular respiration stemming from the surrounding O_2 environment can influence whether DCs adopt an immunogenic or tolerogenic profile [49]. This affects features such as cytokine secretion, antigen presentation, and T cell priming. On the metabolic level, we observed that physioxia enhanced lactate production, consistent with a shift toward aerobic glycolysis—also known as the Warburg effect [51]—a hallmark associated with tolerogenic DCs. This metabolite has been shown to influence immune regulation by promoting tolerogenic DC functions, such as the induction of regulatory T cells and suppression of pro-inflammatory cytokines [52-56]. Despite elevated lactate levels, mitochondrial integrity and respiration remained largely intact in physioxia-conditioned DCs. This suggests a metabolic rewiring rather than a collapse of mitochondrial function and may act in concert with the downregulation of co-stimulatory surface molecules, altered cytokine secretion pattern, and changes in antigen uptake or processing capacity to maintain a non-immunogenic profile under steady-state conditions.

Our findings contrast with a study by Futalan et al. (2011), which reported that generation under 5% O_2 did not influence yield, phenotype, or T cell activation of moDCs [57]. Several factors may explain this discrepancy. First, the O_2 level in our study was slightly lower (4% O_2), which may have crossed a functional threshold affecting cellular metabolism and protein expression. Second, the cell isolation methods differed: while we used CD14⁺ immunomagnetic separation to enrich for monocytes, Futalan et al. used adherence-based selection, which may yield a more heterogeneous starting population and influence subsequent differentiation. Furthermore, differences in maturation stimuli, although similar in composition, could have further contributed to the divergence in results. Lastly, our study maintained tighter control of O_2 levels throughout the entire experimental setup and also compared different O_2 levels during the allo-MLR, whereas Futalan et al. performed their co-cultures under atmospheric O_2 conditions. These subtle yet important distinctions highlight the sensitivity of DC generation to microenvironmental parameters and underscore the need for standardization when comparing studies using physiological O_2 levels.

In summary, DCs are central regulators of immune homeostasis, balancing tolerance and immunity through their interaction with T cells and their response to microenvironmental cues. The tolerogenic phenotype of DCs under homeostatic conditions is influenced by cytokines, metabolic signals, and O₂ levels. Our findings point toward a potential link between O₂-sensitive metabolic reprogramming and the establishment of a semi-mature, tolerogenic DC state by limiting robust inflammatory activation, advancing our understanding of immune regulation in health and disease. Physiological O₂ levels may act as a stabilizing factor in steady-state conditions, whereas the hyperoxic conditions typically used in in vitro studies may drive DCs toward an inflammatory state, potentially misrepresenting their behavior in vivo. Recognizing atmospheric O₂ as a state that may drive immunogenicity offers a valuable perspective for future studies seeking to bridge the gap between in vitro models and in vivo immune regulation. Future research should ensure that both DCs and their interacting immune cells are studied under physiologically relevant O₂ conditions to more accurately reflect in vivo scenarios.

Supplementary Materials: The following supporting information can be downloaded at: https://www.mdpi.com/article/10.3390/cells14100736/s1, Table S1: Antibody concentrations; Figure S1: Representative gating strategy for analysis of DC phenotype; Figure S2: Representative gating strategy for analysis of PBL phenotype; Figure S3: Phenotypic analysis of CD4⁺ and CD8⁺ T cell subsets on day 5 of the allo-MLR under the three control conditions.

Author Contributions: Conceptualization, A.P. and N.C.; methodology, A.P., M.V., M.V.D., A.D., S.P., H.D.R. and W.F.A.M.; validation, A.P.; formal analysis, A.P.; investigation, A.P., M.V., M.V.D., A.D., S.P., H.D.R. and W.F.A.M.; data curation, A.P.; writing—original draft preparation, A.P.; writing—review and editing, A.P., Z.N.B. and N.C.; visualization, A.P.; supervision, N.C.; project administration, A.P. and N.C.; funding acquisition, Z.N.B. and N.C. All authors have read and agreed to the published version of the manuscript.

Funding: This project has received funding from the European Union's Horizon 2020 research and innovation programme under the Marie Skłodowska-Curie grant agreement No. 860003 (A.P.), and the Special Research Fund (BOF) of the University of Antwerp (DOCPRO1, PS ID 49061; A.P.). Additional support was provided by the Industrial Research Fund (IOF) of the University of Antwerp (SEP, PS ID 53192; N.C.) and the FWO Hercules infrastructure fund (I010524N). M.V. holds a doctoral scholarship from the BOF (DOCPRO4, PS ID 5114). M.V.D. holds a doctoral fellowship funded by the Flemish Institute for Technological Research (VITO). A.D. receives funding from the Research Foundation—Flanders (FWO—Vlaanderen) under grant agreement No. T002523N. S.P. is supported through the University Hospital Antwerp (UZA) budget 21HMT17, allocated to cancer research. The hypoxia workstation was funded by the FWO—Vlaanderen (G040120N). The Seahorse Bioanalyzer was funded by a BOF infrastructure grant from the University of Antwerp (FN 543600001).

Institutional Review Board Statement: The use of buffy coats for scientific research was approved by the Ethische Commissie Onderzoek UZ/KU Leuven on 20 March 2019, with approval code S62549.

Informed Consent Statement: Anonymized buffy coats were provided by the Blood Transfusion Center of the Red Cross; written informed consent for research use was obtained from all subjects. The study followed the Tenets of Helsinki.

Data Availability Statement: The data presented in this study are available on request from the corresponding author.

Acknowledgments: The authors would like to thank FACSUA, the Flow Cytometry and Cell Sorting Core Facility of the University of Antwerp, for providing access to their equipment and technical support. We also acknowledge the Center for Oncological Research (CORE) for access to the hypoxia workstation, and the Gamete Research Centre (GRC) of the University of Antwerp for use of their Seahorse Bioanalyzer.

Conflicts of Interest: The authors declare no conflict of interest.

Abbreviations

allo-MLR Allogeneic mixed lymphocyte reaction

ATP Adenosine triphosphate
BSA Bovine serum albumin
CCR7 C-C chemokine receptor 7
CD Cluster of differentiation

moDCs Monocyte-derived dendritic cells

CO₂ Carbon dioxide

CTLA-4 Cytotoxic T-lymphocyte-associated protein 4
DAMPs Damage-associated molecular patterns

DCs Dendritic cells
DMSO Dimethyl sulfoxide
FBS Fetal bovine serum

FCCP Carbonyl cyanide-p-trifluoromethoxyphenylhydrazone

FMO Fluorescence-minus-one

FSC Forward scatter

GM-CSF Granulocyte-macrophage colony-stimulating factor

hAB Human AB serum

HLA-DR Human leukocyte antigen-DR iDCs Immature dendritic cells

IL Interleukin

ILT Immunoglobulin-like transcript

 $\begin{array}{ll} \text{IFN-}\gamma & \text{Interferon-gamma} \\ \text{IQR} & \text{Interquartile range} \end{array}$

LAG-3 Lymphocyte activation gene 3
mDCs Mature dendritic cells
MFI Mean fluorescence intensity
moDCs Monocyte-derived dendritic cells

 $\begin{array}{ccc} \text{ns} & \text{Not significant} \\ \text{O}_2 & \text{Oxygen} \end{array}$

OCR Oxygen consumption rate

PAMPs Pathogen-associated molecular patterns

PBLs Peripheral blood lymphocytes
PBS Phosphate-buffered saline
PD-1 Programmed death-1

PD-L1/L2 Programmed death-ligand 1/2

 $\begin{array}{ll} \text{PDL} & \text{Poly-D-lysine} \\ \text{PGE}_2 & \text{Prostaglandin E}_2 \\ \text{PI} & \text{Propidium iodide} \\ \text{SSC} & \text{Side scatter} \end{array}$

Th T helper cell subset

TIGIT T cell immunoreceptor with immunoglobulin and ITIM domain TIGIT T cell immunoreceptor with immunoglobulin and ITIM domain

TNF Tumor necrosis factor Tregs Regulatory T cells

References

- 1. Caux, C.; Massacrier, C.; Vanbervliet, B.; Dubois, B.; Durand, I.; Cella, M.; Lanzavecchia, A.; Banchereau, J. CD34⁺ hematopoietic progenitors from human cord blood differentiate along two independent dendritic cell pathways in response to granulocyte-macrophage colony-stimulating factor plus tumor necrosis factor alpha: II. Functional analysis. *Blood* 1997, 90, 1458–1470. [CrossRef] [PubMed]
- 2. Cravens, P.D.; Melkus, M.W.; Padgett-Thomas, A.; Islas-Ohlmayer, M.; Del P. Martin, M.; Garcia, J.V. Development and activation of human dendritic cells in vivo in a xenograft model of human hematopoiesis. *Stem Cells* **2005**, *23*, 264–278. [CrossRef]
- 3. Patente, T.A.; Pinho, M.P.; Oliveira, A.A.; Evangelista, G.C.M.; Bergami-Santos, P.C.; Barbuto, J.A.M. Human dendritic cells: Their heterogeneity and clinical application potential in cancer immunotherapy. *Front. Immunol.* **2018**, *9*, 3176. [CrossRef]
- 4. Wilson, N.S.; El-Sukkari, D.; Villadangos, J.A. Dendritic cells constitutively present self antigens in their immature state in vivo and regulate antigen presentation by controlling the rates of MHC class II synthesis and endocytosis. *Blood* **2004**, *103*, 2187–2195. [CrossRef] [PubMed]
- 5. Steinman, R.M.; Swanson, J. The endocytic activity of dendritic cells. J. Exp. Med. 1995, 182, 283–288. [CrossRef]
- 6. Skelton, L.; Cooper, M.; Murphy, M.; Platt, A. Human immature monocyte-derived dendritic cells express the G protein-coupled receptor GPR105 (KIAA0001, P2Y14) and increase intracellular calcium in response to its agonist, uridine diphosphoglucose. *J. Immunol.* 2003, 171, 1941–1949. [CrossRef] [PubMed]
- 7. Trombetta, E.S.; Mellman, I. Cell biology of antigen processing in vitro and in vivo. *Annu. Rev. Immunol.* **2005**, 23, 975–1028. [CrossRef] [PubMed]
- 8. Gouwy, M.; Struyf, S.; Leutenez, L.; Pörtner, N.; Sozzani, S.; Van Damme, J. Chemokines and other GPCR ligands synergize in receptor-mediated migration of monocyte-derived immature and mature dendritic cells. *Immunobiology* **2014**, 219, 218–229. [CrossRef]

- 9. Hemmi, H.; Akira, S. TLR signalling and the function of dendritic cells. Chem. Immunol. Allergy 2005, 86, 120–135. [CrossRef]
- 10. Tang, D.; Kang, R.; Coyne, C.B.; Zeh, H.J.; Lotze, M.T. PAMPs and DAMPs: Signal 0s that spur autophagy and immunity. *Immunol. Rev.* 2012, 249, 158–175. [CrossRef]
- 11. Cerboni, S.; Gentili, M.; Manel, N. Diversity of pathogen sensors in dendritic cells. Adv. Immunol. 2013, 120, 211–237. [CrossRef]
- 12. López, C.B.; García-Sastre, A.; Williams, B.R.G.; Moran, T.M. Type I interferon induction pathway, but not released interferon, participates in the maturation of dendritic cells induced by negative-strand RNA viruses. *J. Infect. Dis.* **2003**, *187*, 1126–1136. [CrossRef] [PubMed]
- 13. McIlroy, D.; Tanguy-Royer, S.; Le Meur, N.; Guisle, I.; Royer, P.-J.; Léger, J.; Meflah, K.; Grégoire, M. Profiling dendritic cell maturation with dedicated microarrays. *J. Leukoc. Biol.* **2005**, *78*, 794–803. [CrossRef] [PubMed]
- 14. Dalod, M.; Chelbi, R.; Malissen, B.; Lawrence, T. Dendritic cell maturation: Functional specialization through signaling specificity and transcriptional programming. *EMBO J.* **2014**, *33*, 1104–1116. [CrossRef] [PubMed]
- 15. Allenspach, E.J.; Lemos, M.P.; Porrett, P.M.; Turka, L.A.; Laufer, T.M. Migratory and lymphoid-resident dendritic cells cooperate to efficiently prime naive CD4 T cells. *Immunity* **2008**, *29*, 795–806. [CrossRef]
- 16. Bourque, J.; Hawiger, D. Immunomodulatory Bonds of the Partnership between Dendritic Cells and T Cells. *Crit. Rev. Immunol.* **2018**, *38*, 379–401. [CrossRef]
- 17. Steinman, R.M.; Hawiger, D.; Liu, K.; Bonifaz, L.; Bonnyay, D.; Mahnke, K.; Iyoda, T.; Ravetch, J.; Dhodapkar, M.; Inaba, K.; et al. Dendritic cell function in vivo during the steady state: A role in peripheral tolerance. *Ann. N. Y. Acad. Sci.* **2003**, *987*, 15–25. [CrossRef]
- 18. Cools, N.; Ponsaerts, P.; Van Tendeloo, V.F.I.; Berneman, Z.N. Balancing between immunity and tolerance: An interplay between dendritic cells, regulatory T cells, and effector T cells. *J. Leukoc. Biol.* **2007**, *82*, 1365–1374. [CrossRef]
- 19. Novak, N.; Bieber, T. 2. Dendritic cells as regulators of immunity and tolerance. *J. Allergy Clin. Immunol.* **2008**, 121, S370–S374. [CrossRef]
- 20. Nam, J.-H.; Lee, J.-H.; Choi, S.-Y.; Jung, N.-C.; Song, J.-Y.; Seo, H.-G.; Lim, D.-S. Functional ambivalence of dendritic cells: Tolerogenicity and immunogenicity. *Int. J. Mol. Sci.* **2021**, 22, 4430. [CrossRef]
- 21. Lozano, E.; Dominguez-Villar, M.; Kuchroo, V.; Hafler, D.A. The TIGIT/CD226 axis regulates human T cell function. *J. Immunol.* **2012**, *188*, 3869–3875. [CrossRef] [PubMed]
- 22. Machicote, A.; Belén, S.; Baz, P.; Billordo, L.A.; Fainboim, L. Human CD8⁺HLA-DR⁺ Regulatory T Cells, Similarly to Classical CD4⁺Foxp3⁺ Cells, Suppress Immune Responses via PD-1/PD-L1 Axis. *Front. Immunol.* **2018**, *9*, 2788. [CrossRef]
- 23. Dilek, N.; Poirier, N.; Hulin, P.; Coulon, F.; Mary, C.; Ville, S.; Vie, H.; Clémenceau, B.; Blancho, G.; Vanhove, B. Targeting CD28, CTLA-4 and PD-L1 costimulation differentially controls immune synapses and function of human regulatory and conventional T-cells. *PLoS ONE* **2013**, *8*, e83139. [CrossRef]
- 24. Tekguc, M.; Wing, J.B.; Osaki, M.; Long, J.; Sakaguchi, S. Treg-expressed CTLA-4 depletes CD80/CD86 by trogocytosis, releasing free PD-L1 on antigen-presenting cells. *Proc. Natl. Acad. Sci. USA* **2021**, *118*, e2023739118. [CrossRef]
- 25. Fuse, S.; Obar, J.J.; Bellfy, S.; Leung, E.K.; Zhang, W.; Usherwood, E.J. CD80 and CD86 control antiviral CD8⁺ T-cell function and immune surveillance of murine gammaherpesvirus 68. *J. Virol.* **2006**, *80*, 9159–9170. [CrossRef] [PubMed]
- Koorella, C.; Nair, J.R.; Murray, M.E.; Carlson, L.M.; Watkins, S.K.; Lee, K.P. Novel regulation of CD80/CD86-induced phosphatidylinositol 3-kinase signaling by NOTCH1 protein in interleukin-6 and indoleamine 2,3-dioxygenase production by dendritic cells. J. Biol. Chem. 2014, 289, 7747–7762. [CrossRef]
- 27. Sakaguchi, S.; Yamaguchi, T.; Nomura, T.; Ono, M. Regulatory T cells and immune tolerance. *Cell* **2008**, *133*, 775–787. [CrossRef] [PubMed]
- 28. Iwasaki, A.; Medzhitov, R. Control of adaptive immunity by the innate immune system. *Nat. Immunol.* **2015**, *16*, 343–353. [CrossRef]
- 29. Collin, M.; Bigley, V. Human dendritic cell subsets: An update. Immunology 2018, 154, 3–20. [CrossRef]
- 30. Buck, M.D.; Sowell, R.T.; Kaech, S.M.; Pearce, E.L. Metabolic instruction of immunity. Cell 2017, 169, 570–586. [CrossRef]
- 31. Kim, J. Regulation of immune cell functions by metabolic reprogramming. *J. Immunol. Res.* **2018**, 2018, 8605471. [CrossRef] [PubMed]
- 32. Kedia-Mehta, N.; Finlay, D.K. Competition for nutrients and its role in controlling immune responses. *Nat. Commun.* **2019**, 10, 2123. [CrossRef]
- 33. Gottfried, E.; Kunz-Schughart, L.A.; Ebner, S.; Mueller-Klieser, W.; Hoves, S.; Andreesen, R.; Mackensen, A.; Kreutz, M. Tumor-derived lactic acid modulates dendritic cell activation and antigen expression. *Blood* **2006**, *107*, 2013–2021. [CrossRef] [PubMed]
- 34. Okajima, F. Regulation of inflammation by extracellular acidification and proton-sensing GPCRs. *Cell. Signal.* **2013**, 25, 2263–2271. [CrossRef]
- 35. Cao, L.; Shi, X.; Chang, H.; Zhang, Q.; He, Y. pH-Dependent recognition of apoptotic and necrotic cells by the human dendritic cell receptor DEC205. *Proc. Natl. Acad. Sci. USA* **2015**, *112*, 7237–7242. [CrossRef]

- 36. Hosonuma, M.; Yoshimura, K. Association between pH regulation of the tumor microenvironment and immunological state. *Front. Oncol.* **2023**, *13*, 1175563. [CrossRef]
- 37. Steurer, J.; Hoffmann, U.; Dür, P.; Russi, E.; Vetter, W. Changes in arterial and transcutaneous oxygen and carbon dioxide tensions during and after voluntary hyperventilation. *Respiration* 1997, 64, 200–205. [CrossRef] [PubMed]
- 38. Caldwell, C.C.; Kojima, H.; Lukashev, D.; Armstrong, J.; Farber, M.; Apasov, S.G.; Sitkovsky, M.V. Differential effects of physiologically relevant hypoxic conditions on T lymphocyte development and effector functions. *J. Immunol.* **2001**, 167, 6140–6149. [CrossRef]
- 39. Chow, D.C.; Wenning, L.A.; Miller, W.M.; Papoutsakis, E.T. Modeling pO₂ distributions in the bone marrow hematopoietic compartment. II. Modified Kroghian models. *Biophys. J.* **2001**, *81*, 685–696. [CrossRef]
- 40. Carreau, A.; El Hafny-Rahbi, B.; Matejuk, A.; Grillon, C.; Kieda, C. Why is the partial oxygen pressure of human tissues a crucial parameter? Small molecules and hypoxia. *J. Cell. Mol. Med.* **2011**, *15*, 1239–1253. [CrossRef]
- 41. Keeley, T.P.; Mann, G.E. Defining physiological normoxia for improved translation of cell physiology to animal models and humans. *Physiol. Rev.* **2019**, *99*, 161–234. [CrossRef] [PubMed]
- 42. Chapple, S.J.; Keeley, T.P.; Mastronicola, D.; Arno, M.; Vizcay-Barrena, G.; Fleck, R.; Siow, R.C.M.; Mann, G.E. Bach1 differentially regulates distinct Nrf2-dependent genes in human venous and coronary artery endothelial cells adapted to physiological oxygen levels. *Free Radic. Biol. Med.* **2016**, *92*, 152–162. [CrossRef] [PubMed]
- 43. Ferguson, D.C.J.; Smerdon, G.R.; Harries, L.W.; Dodd, N.J.F.; Murphy, M.P.; Curnow, A.; Winyard, P.G. Altered cellular redox homeostasis and redox responses under standard oxygen cell culture conditions versus physioxia. *Free Radic. Biol. Med.* 2018, 126, 322–333. [CrossRef]
- 44. Stuart, J.A.; Fonseca, J.; Moradi, F.; Cunningham, C.; Seliman, B.; Worsfold, C.R.; Dolan, S.; Abando, J.; Maddalena, L.A. How Supraphysiological Oxygen Levels in Standard Cell Culture Affect Oxygen-Consuming Reactions. *Oxid. Med. Cell. Longev.* 2018, 8238459. [CrossRef] [PubMed]
- Timpano, S.; Guild, B.D.; Specker, E.J.; Melanson, G.; Medeiros, P.J.; Sproul, S.L.J.; Uniacke, J. Physioxic human cell culture improves viability, metabolism, and mitochondrial morphology while reducing DNA damage. FASEB J. 2019, 33, 5716–5728. [CrossRef] [PubMed]
- 46. Shin, D.-Y.; Huang, X.; Gil, C.-H.; Aljoufi, A.; Ropa, J.; Broxmeyer, H.E. Physioxia enhances T-cell development ex vivo from human hematopoietic stem and progenitor cells. *Stem Cells* **2020**, *38*, 1454–1466. [CrossRef]
- 47. Sies, H.; Belousov, V.V.; Chandel, N.S.; Davies, M.J.; Jones, D.P.; Mann, G.E.; Murphy, M.P.; Yamamoto, M.; Winterbourn, C. Defining roles of specific reactive oxygen species (ROS) in cell biology and physiology. *Nat. Rev. Mol. Cell Biol.* **2022**, 23, 499–515. [CrossRef]
- 48. Igarashi, K.J.; Kucinski, I.; Chan, Y.Y.; Tan, T.-K.; Khoo, H.M.; Kealy, D.; Bhadury, J.; Hsu, I.; Ho, P.Y.; Niizuma, K.; et al. Physioxia improves the selectivity of hematopoietic stem cell expansion cultures. *Blood Adv.* **2023**, *7*, 3366–3377. [CrossRef]
- 49. Peter, A.; Berneman, Z.N.; Cools, N. Cellular respiration in dendritic cells: Exploring oxygen-dependent pathways for potential therapeutic interventions. *Free Radic. Biol. Med.* **2025**, 227, 536–556. [CrossRef]
- 50. Van Delen, M.; Janssens, I.; Dams, A.; Roosens, L.; Ogunjimi, B.; Berneman, Z.N.; Derdelinckx, J.; Cools, N. Tolerogenic Dendritic Cells Induce Apoptosis-Independent T Cell Hyporesponsiveness of SARS-CoV-2-Specific T Cells in an Antigen-Specific Manner. *Int. J. Mol. Sci.* 2022, 23, 15201. [CrossRef]
- 51. Vaupel, P.; Multhoff, G. Revisiting the Warburg effect: Historical dogma versus current understanding. *J. Physiol.* **2021**, 599, 1745–1757. [CrossRef] [PubMed]
- 52. Caronni, N.; Simoncello, F.; Stafetta, F.; Guarnaccia, C.; Ruiz-Moreno, J.S.; Opitz, B.; Galli, T.; Proux-Gillardeaux, V.; Benvenuti, F. Downregulation of membrane trafficking proteins and lactate conditioning determine loss of dendritic cell function in lung cancer. *Cancer Res.* 2018, 78, 1685–1699. [CrossRef] [PubMed]
- 53. Marin, E.; Bouchet-Delbos, L.; Renoult, O.; Louvet, C.; Nerriere-Daguin, V.; Managh, A.J.; Even, A.; Giraud, M.; Vu Manh, T.P.; Aguesse, A.; et al. Human Tolerogenic Dendritic Cells Regulate Immune Responses through Lactate Synthesis. *Cell Metab.* **2019**, 30, 1075–1090.e8. [CrossRef]
- 54. Raychaudhuri, D.; Bhattacharya, R.; Sinha, B.P.; Liu, C.S.C.; Ghosh, A.R.; Rahaman, O.; Bandopadhyay, P.; Sarif, J.; D'Rozario, R.; Paul, S.; et al. Lactate Induces Pro-tumor Reprogramming in Intratumoral Plasmacytoid Dendritic Cells. *Front. Immunol.* **2019**, *10*, 1878. [CrossRef] [PubMed]
- 55. Kanemaru, H.; Mizukami, Y.; Kaneko, A.; Tagawa, H.; Kimura, T.; Kuriyama, H.; Sawamura, S.; Kajihara, I.; Makino, K.; Miyashita, A.; et al. A mechanism of cooling hot tumors: Lactate attenuates inflammation in dendritic cells. *iScience* **2021**, 24, 103067. [CrossRef]

- 56. Sanmarco, L.M.; Rone, J.M.; Polonio, C.M.; Fernandez Lahore, G.; Giovannoni, F.; Ferrara, K.; Gutierrez-Vazquez, C.; Li, N.; Sokolovska, A.; Plasencia, A.; et al. Lactate limits CNS autoimmunity by stabilizing HIF-1α in dendritic cells. *Nature* **2023**, 620, 881–889. [CrossRef]
- 57. Futalan, D.; Huang, C.-T.; Schmidt-Wolf, I.G.H.; Larsson, M.; Messmer, D. Effect of oxygen levels on the physiology of dendritic cells: Implications for adoptive cell therapy. *Mol. Med.* **2011**, *17*, 910–916. [CrossRef]

Disclaimer/Publisher's Note: The statements, opinions and data contained in all publications are solely those of the individual author(s) and contributor(s) and not of MDPI and/or the editor(s). MDPI and/or the editor(s) disclaim responsibility for any injury to people or property resulting from any ideas, methods, instructions or products referred to in the content.





Review

Ultraviolet Radiation-Induced Tolerogenic Dendritic Cells in Skin: Insights and Mechanisms

Gelare Ghajar-Rahimi, Nabiha Yusuf * and Hui Xu *

Department of Dermatology, Heersink School of Medicine, University of Alabama, Birmingham, AL 35294, USA * Correspondence: nabihayusuf@uabmc.edu (N.Y.); huixu@uabmc.edu (H.X.)

Abstract: Ultraviolet (UV) radiation has profound effects on the immune system, including the induction of tolerogenic dendritic cells (DCs), which contribute to immune suppression and tolerance. This review explores the roles of conventional CD11c⁺ DCs, as well as cutaneous Langerhans cells and CD11b+ myeloid cells, in UV-induced immune modulation. Two key mechanisms underlying the immunosuppressive relationship between UV and DCs are discussed: the inactivation of DCs and the induction of tolerogenic DCs. DCs serve as a critical link between the innate and adaptive immune systems, serving as professional antigen-presenting cells. In this context, we explore how UV-induced DCs influence the activity of specific T cell subsets, including regulatory T lymphocytes and T helper cells, and shape immune outcomes. Finally, we highlight the implications of UV-induced tolerogenic DCs in select dermatologic pathologies, including cutaneous lupus, polymorphic light eruption, and skin cancer. Understanding the mechanisms by which UV radiation alters DC function offers insights into the complex interplay between environmental factors and immune regulation, providing potential avenues for preventive and therapeutic intervention in UV-induced skin diseases.

Keywords: ultraviolet radiation; skin; tolerogenic dendritic cells; immunology; immunosuppression

1. Introduction

Ultraviolet (UV) radiation, a ubiquitous environmental factor, profoundly influences the immune system, particularly within the skin, where it induces a state of immuno-suppression. Among the cellular mediators of this immunomodulatory effect, dendritic cells (DCs)—the sentinel antigen-presenting cells (APCs) of the immune system—play a pivotal role. UV-induced changes in DC function can impair T cell function, promote immune tolerance, and reshape the skin's immune landscape.

This review focuses on the mechanisms by which UV radiation influences the tolerogenic capacity of DCs in the skin. We explore the roles of various DC subsets, including Langerhans cells (LCs), conventional CD11c⁺ cells, and CD11b⁺ myeloid cells, highlighting their contributions to UV-induced immunosuppression. We also discuss the molecular pathways implicated in the modulation of DC activity, including DNA damage, cytokine signaling, and apoptotic processes. Furthermore, we examine the clinical implications of these findings, highlighting the role of UV-induced DCs in the development of conditions such as cutaneous lupus erythematosus, polymorphic light eruption, and skin cancers. By synthesizing recent advances in the field, this review aims to provide a comprehensive understanding of UV-induced tolerogenic DCs and their broader immunological and clinical significance.

2. Various Cutaneous Immune Cells Implicated in UV-Induced Immune Suppression

This review discusses three broad categories of dendritic cells, reflecting the prevailing trends in the current literature. While the techniques and markers used to define these categories vary somewhat, a summary is provided in Table 1. It is important to note that the classification of immune cells is continually evolving as advancements in molecular techniques, multiparameter imaging, flow cytometry, and transcriptomics drive more specific characterization.

Table 1. Common cellular markers and methods of identification used in the study of UV-induced dendritic cell populations referenced in this review.

	Identification Method	Special Considerations
LCs	 Markers for histologic and immunohistochemical examination: ATPase activity Ia^k and Ia^d CD1a Langerin (CD207) CD103⁻ epidermal LCs vs. CD103⁺ dermal LCs Electron microscopy of ultrastructural appearance and presence of Birbeck granules 	 UV exposure attenuates ATPase staining more so than CD1a and Ia expression [1] LCs are distinguished from dendritic melanocytes by a lack of cytoplasmic pigment granules [2] UV exposure alters LC morphology
cDCs	 Markers for histologic and immunohistochemical examination: CD11c⁺ CD123⁻ CD11c⁺ BDCA3⁺ immunosuppressive subset CD11c⁺ BDCA1⁻ immature, inflammatory 	 UV induces changes to CD11c⁺ populations in the skin, draining lymph nodes and bone marrow Commonly assessed via flow cytometry
CD11b+	 Histologic examination or flow cytometry for the following markers: CD11b+CD36+CD1a- Gr-1 (Ly-6G/Ly-6C) Human: CD11b+ CD1a-HLA-DR+ 	- Commonly assessed via flow cytometry

cDC = conventional dendritic cell, LC = Langerhans cell, UV = ultraviolet, DC = dendritic cell.

2.1. Langerhans Cells

LCs, first described by Paul Langerhans in 1868, were the earliest cells to be identified as DCs, named for their characteristic "tree-like" morphology [3]. LCs are classically considered the tissue-resident macrophages of the skin [4,5]. In healthy skin, these MHC class II-expressing APCs [6,7] reside primarily in the suprabasal epidermis, a depth to which UV penetrates easily. UV radiation has been shown to influence several aspects of LC networks and function. Much of our understanding of the immunosuppressive effects of UV radiation has been elucidated through murine models of contact hypersensitivity (CHS), which is a delayed type of cell-mediated immune response.

Epidermal LCs are essential mediators in the development of CHS responses [8]. The extent of CHS produced in response to a contact allergen correlates with the density of local LCs in the epidermis at the site of initial sensitization. This was first shown in an experiment by Toews et al., in which initial sensitization to the contact allergen 2,4-dinitrofluorobenzene (DNFB) on the abdominal skin, which naturally has a higher density of LCs, triggered a stronger hypersensitivity reaction upon rechallenge compared to sensitization on tail skin, where LCs are relatively scant [8]. Irradiation of the skin with a short course of

290–320 nm UV radiation (UVB) prior to sensitization significantly attenuated the capacity to subsequently develop a CHS response to DNFB. Furthermore, UV-irradiated mice were unable to mount an immune response to re-sensitization to DNFB applied to a distant site at later time points as would be expected in UV-naïve mice, indicating the induction of specific immune tolerance [8]. Later studies by Cruz et al. found that injection of isolated Ia⁺ LCs that had been irradiated and conjugated to hapten ex vivo into normal, wildtype mice resulted in a diminished ability to mount a CHS response, and the development of long-lasting immune tolerance compared to mice injected with non-UV-irradiated LCs [9].

The specific cellular and molecular effects on LCs attributed to UV radiation can be highly variable, based on the dose and range of UV employed and the timing of sampling post-irradiation. Toews et al. found that LCs, as identified by ATPase-positive staining, are transiently depleted at the site of local UVB irradiation. The few ATPase⁺ cells remaining following irradiation exhibit altered morphology [8]. Exposure to high doses of UVB ranging from 400 to 4000 J/m² causes LCs at the site of irradiation to become rounded and swollen, with a reduction in dendritic processes [1,8,10]. Other studies have shown that irradiation with lower doses of UVB 120–2000 J/m² results in LCs with elongated dendritic processes [2,11]. Experiments in murine and human skin by Aberer et al. suggest that the apparent loss of LCs may be reflective of a loss of surface markers (e.g., Ia antigens), rather than a true depletion of LCs [12]. Further immunohistochemistry and electron microscopy has suggested that DCs experience both a change in surface marker expression and cell damage or death in response to UV irradiation [2].

As molecular techniques improve and the classification of DC populations becomes increasingly nuanced, it has become clear that not only are the effects of UV radiation context-dependent, but various cell subpopulations also are impacted in unique ways [13]. Nakagawa et al. have shown that UVB radiation has distinct effects on different LC subpopulations, defined by relative HLA-DR expression [14]. In response to UVB exposure, the relative number of viable HLA-DR^{HI} LCs decreases over time, but this subpopulation exhibits evidence of maturation (downregulation of CD1a; upregulation of CD80, CD86, CD54, CD40, CD83) compared to unexposed controls. UVB potentiates the activity of viable HLA-DR^{HI} LCs through augmented expression of costimulatory molecules, such as TNF- α and proinflammatory cytokines. HLA-DR^{low} LCs, on the other hand, fail to mature in response to UVB, and exhibit robust annexin V binding, indicating apoptosis [14].

While epidermal LCs have been studied extensively, a handful of studies have examined the importance of dermal DCs in UV-induced immunosuppression. Dermal langerin⁺CD103⁺ cells, which constitute two-thirds of langerin⁺ cells in the skin-draining lymph nodes, are derived from the bone marrow, and are constitutively expressed in the dermis [15–17]. Conditional deletion of this population of DCs via radiation reduces the UV-induced suppression of CHS and the suppression of CD8⁺ T cell responses to epicutaneous immunization to OVA [18], suggesting that epidermal langerin⁺ cells are dispensable in the induction of UVB-induced immunosuppression [18]. However, experiments utilizing transgenic mice expressing diphtheria toxin receptors on langerin⁺ cells have suggested that epidermal langerin⁺ cells are required for UVB-induced immune suppression. In these studies, when administered 10 days following diphtheria toxin-mediated depletion of langerin⁺ cells, at which point dermal langerin⁺ cells, but not epidermal langerin⁺ cells, had repopulated, UVB was unable to effectively suppress CHS [19].

2.2. Conventional Dendritic Cells (cDCs)

cDCs that express CD11c and MHC class II antigens have been characterized in mice and humans [20]. Based on their phenotype, they are generally classified into cDC1 and cDC2. In addition to CD11c and MHC class II antigens, murine cDC1 cells express XCR1, IRF8, and CD103, whereas cDC2 cells express CD11b and IRF4. In addition to CD11c and MHC class II antigens, human cDC1 cells express CD304 (BDCA3), CD141 (BDCA4), and XCR1, whereas cDC2 cells express CD1c (BDCA1) and CD11b. cDCs can be detected in the skin, blood, and lymphoid tissues. Many studies investigate the roles of CD11c⁺ DC in UV-induced immune suppression in mice and humans. However, less is known about the specific roles of cDC1 and cDC2 cells in the process.

CD11c⁺ DCs have been implicated in the systemic immunomodulatory effects of UV exposure. In addition to influencing LCs locally at the site of irradiation, UV radiation of the skin leads to functional alterations in distal bone marrow-derived DCs. Cultured bone marrow cells from UV-irradiated BALB/c mice have been shown to produce greater levels of IL-10 and prostaglandin E2 (PGE2), relative to bone marrow cells isolated from non-irradiated controls [21]. When ex vivo bone marrow cell cultures are stimulated with IL-4 and granulocyte macrophage colony stimulating factor (GM-CSF) ex vivo, CD11c⁺ cells are generated. In an adoptive transfer experiment, Ng et al. found that the transfer of bone-marrow-derived CD11c⁺ cells from UV-irradiated mice into naïve recipient mice mitigates CHS responses and confers long-lasting suppression of memory responses to a contact allergen [21]. This mechanism of UV-induced systemic immune suppression was found to be mediated by PGE2, as the effects were blocked by pretreatment with indomethacin [21]. Additional studies have similarly suggested that long-lasting immunosuppressive effects may be epigenetically imprinted in hematopoietic stem cells [22–24].

CD11c⁺ DCs in skin-draining lymph nodes play an important role in UV-mediated suppression of CHS responses. This is thought to be due to their role in IL-12 production. IL-12 has been shown to protect against UV-induced CHS suppression [25–27]. Augmenting IL-12 secretion by CD11c⁺ cells by draining lymph nodes with the Toll-like receptor 7 (TLR7)-agonist Imiquimod prevents UV-induced suppression of hapten sensitization and CHS [28].

Locally, exposure to 2MED of 312 nm narrow-band UVB leads to a significant increase in the number of CD11c⁺ DCs in the dermis of individuals with Fitzpatrick II-III skin [29]. More specifically, the CD11c⁺ DCs seen 24 h following irradiation include immunosuppressive CD11c⁺BDCA3⁺ subsets that have been shown to exert immunosuppressive effects through IL-10 and induction of regulatory T cells [30], as well as immature, inflammatory CD11c⁺BDCA1⁻ BDCA3⁻ subsets that poorly co-localize with dendritic cell lysosomal-associated membrane glycoprotein (DC-LAMP) on immunofluorescence imaging, and express tumor necrosis factor (TNF)- α and TNF-related apoptosis-inducing ligands (TRAILs) [29].

2.3. CD11b⁺ Myeloid Cells

Amongst the inflammatory milieu seen in the skin following UV irradiation are CD11b⁺ myeloid cells [31]. CD11b⁺ myeloid cells can be distinguished from LCs of the skin by the absence of surface CD1a⁺. UV-induced CD36⁺CD11b⁺CD1a⁻ cells are robust producers of IL-10 mRNA and protein [32]. Conversely, UV-exposed keratinocytes and CD1a⁺ LCs express little to no IL-10 mRNA [32]. Further studies show that a ligand of CD11b, iC3b (a complement component C3), is deposited in UV-exposed skin, and is localized in apposition to infiltrating CD11b⁺ myeloid cells. Stimulating CD11b⁺ cells with iC3b significantly induces IL-10 mRNA and protein. In contrast, it suppresses IL-12

mRNA and protein [33]. Mouse studies demonstrate that the depletion of CD11b⁺ cells prevents UV-induced immune suppression [34]. In contrast, the activation of CD11b⁺ cells by complement component C3 is required for UVB-induced CD11b⁺ cell migration into the skin and immune suppression [35]. It is to be noted that cDC2 cells express CD11b⁺ [20]. However, it remains to be determined whether cDC2 cells play a role in UV-induced immune suppression.

3. Mechanisms for UV-Induced Regulation of DC Activity

UV radiation suppresses the immune system by modulating DC function in two main ways: it impairs their antigen-presenting ability, and it promotes tolerance by inducing regulatory, immunosuppressive T cell populations. Together, these effects block immune activation and enhance suppression, resulting in a net immunosuppressive outcome (Figure 1).

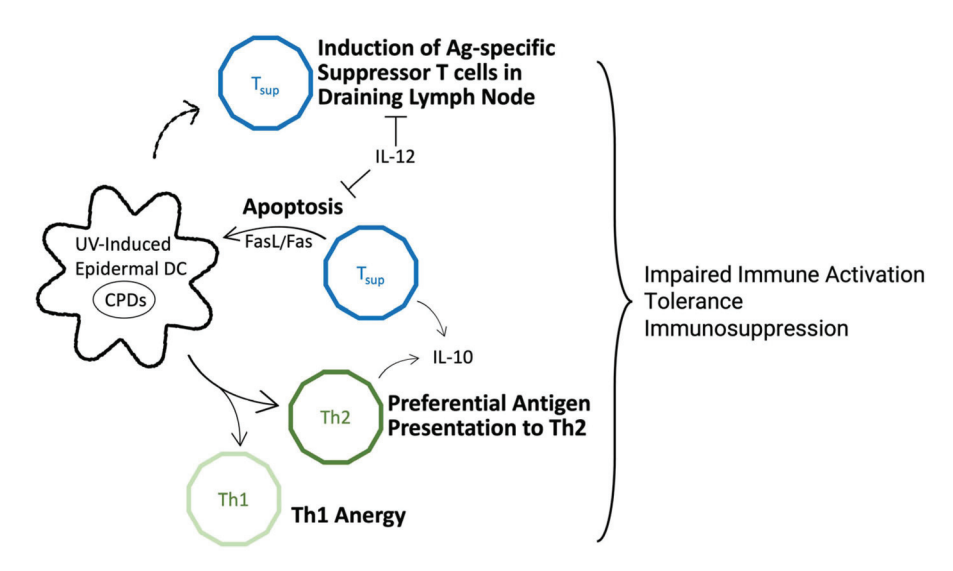


Figure 1. Graphical summary of immunosuppressive actions of UV-induced dendritic cells and T cell populations. Ag = antigen, CPDs = cyclobutene pyrimidine dimers, DC = dendritic cell, Th = T helper cell, Tsup = suppressor T cell.

3.1. Inactivation of DCs

UV-induced DNA damage, particularly the generation of cyclobutane pyrimidine dimers (CPDs), is partially responsible for the impairment of APC function in DCs. Studies have demonstrated that treating UV-irradiated skin with liposomes containing DNA excision repair enzymes, such as T4 endonuclease V, reduces the number of CPD-containing DCs in the draining lymph nodes and restores APC function [36]. In vitro, repairing CPDs using liposomes containing photolyase (a light-activated DNA repair enzyme) also restores the APC function of DCs from UV-irradiated murine skin [37].

UV radiation also disrupts antigen presentation through the induction of DC apoptosis. While controlled apoptosis is essential under normal conditions for maintaining immune homeostasis and self-tolerance [38], UV radiation interferes with this balance. UV radiation prevents the maturation of, and induces apoptotic cell death in, a specific subpopulation of LCs characterized by low HLA-DR expression [14]. Gene knockout mice deficient in pro-apoptotic BH3-interacting death domain protein (Bid) exhibited significant resistance to UV-induced LC depletion, suppression of local CHS responses, and tolerance to haptens. Notably, these mice also displayed reduced CPD accumulation in lymph nodes following UV exposure, compared to wildtype control mice [39]. Additionally, co-culture experiments have demonstrated that hapten-pulsed DCs underwent Fas/FasL-mediated apoptosis when exposed to T cells from UV-irradiated mice. DCs from Lpr and gld

mice, which lacked functional *Fas* and *FasL* genes, were resistant to apoptosis induced by UV-induced T suppressor cells. Notably, interleukin-12 (IL-12) can rescue DCs from Fas/FasL-mediated apoptosis, offering a potential therapeutic pathway [27]. Moreover, apoptotic DCs express CD200 (OX-2), a target of p53, which attenuates proinflammatory cytokine production in response to self-antigens in vitro. In vivo, CD200 is essential for UVB-mediated tolerance to self-antigens, as its absence disrupts this immunosuppressive pathway [40]. CD200R is expressed on myeloid-derived APCs and some T cells, facilitating the immunoregulatory effects mediated by CD200/CD200R signaling [41,42].

3.2. Tolerogenic DCs

Tolerogenic DCs are specialized immunosuppressive APCs that promote immune tolerance, or non-reactivity, to specific antigens. These effects are primarily mediated through interactions with T lymphocytes and the release of anti-inflammatory cytokines. By modulating T cell activity, tolerogenic DCs can induce T cell anergy, promote T cell apoptosis, and facilitate the differentiation of T regulatory (Treg) cells [43].

The activity and function of tolerogenic DCs are not lineage-specific, but are highly influenced by their surrounding microenvironment [43,44]. Notably, UV radiation, particularly UVB, can convert LCs from immunologically active APCs into tolerogenic ones [19]. UV-induced Treg cells are antigen-specific [45]. Treg cells in UV-irradiated skin have been shown to release immunosuppressive IL-10 [46] and express lymph node-homing receptors such as CD62L, while simultaneously lacking skin-homing molecules such as E-selectin or P-selectin [47]. Similarly to naturally occurring, thymic Tregs, UV-induced Tregs express CD25 following hapten sensitization [47]. UV-induced Treg cells also express cytotoxic T-lymphocyte antigen-4 (CTLA-4), which is known to negatively regulate T lymphocyte function [48]. Depleting CLTA-4+ cells or blocking CTLA-4 signaling with a monoclonal antibody blocks the transfer of UV-induced immune suppression in adoptive transfer experiments [48,49].

3.3. DCs and the Development of T Lymphocyte Populations in the Context of UV-Induced Immune Suppression

3.3.1. CD4⁺ Treg Cells

The generation of Tregs following UV exposure involves the migration of LCs exhibiting DNA damage into draining lymph nodes [50]. In experiments in which UV-mediated DNA damage was mitigated by IL-12, the generation of UV-induced Tregs was prevented [25,26,51,52]. In vitro experiments examining DC–Treg interactions in isolation from the influence of surrounding cell types have confirmed that the repair of CPDs in UV-irradiated DCs prevents the induction of suppressor T cells [37]. Unlike the UV-induced suppression of T cells, the induction of Tregs specifically requires the presence of damaged, yet viable, UV-irradiated LCs in the lymph nodes. This distinction is further supported by experiments demonstrating that killing LCs (as opposed to damaging them) with the steroid mometasone inhibits sensitization to contact allergens, but does not lead to Treg production [19].

3.3.2. CD4⁺ T Helper Cells

Under standard biologic conditions, DCs interact with naïve CD4⁺ T cells to promote their differentiation into either type 1 (Th1), type 2 (Th2), or type 17 (Th17) helper cells [53,54]. Th1 cells are generally considered to be inflammatory, as they secrete IFN- γ and aid B lymphocytes in the production of complement-fixing antibodies. The primary effector cytokine of Th2 cells is IL-4, and these cells are associated with allergic, IgE-mediated reactions. Anti-inflammatory IL-10 is also a Th2-type cytokine [55]. UV exposure stimulates the production of Th2 cytokines in the skin-draining lymph nodes more so than Th1

cytokines [56,57]. LCs develop a skewed propensity for presenting to Th2 cells over Th1 cells following UV irradiation [58]. In the setting of *Borrelia burgdorferi* infection, UV irradiation results in diminished levels IgG2a and IgG2b, which typically require functional Th1 activity, and in increased levels of IgG1 antibody, which is supported by Th2 function [59]. Additionally, antigen presentation by UV-irradiated DCs leads to Th1 anergy and tolerance to restimulation with normal antigen-bearing DCs [60]. Th17 cells primarily produce IL-17, which has a wide spectrum of effects on innate and acquired immunity [61,62]. IL-17 is an important inflammatory cytokine for CHS [63]. A deficiency in IL-17-mediated immune responses will suppress CHS [64,65]. UV radiation increases IL-17 production in the skin [66]. Evidence indicates that the knockout of the IL-17 receptor A gene diminishes UVB-induced immune suppression [67]. The mechanisms for such processes are attributed to reduced UVB-induced CD11b+ myeloid cells and Treg cells in the draining lymph nodes. Further studies are required to elucidate these mechanisms.

4. The Role of DCs in UV-Induced Skin Diseases

The dysregulation of immune responses due to UV radiation has profound implications for various skin diseases, three of which will be highlighted here.

4.1. Cutaneous Lupus Erythematous (CLE)

CLE is a subset of lupus erythematous that is characterized by its effects on the skin. CLE is classified into three subtypes: acute, subacute, and chronic. However, clinically, considerable overlap exists amongst these subtypes, often making differentiation challenging [68,69]. CLE may develop as a standalone condition or as a skin-related manifestation of systemic lupus erythematosus [70,71]. UV radiation plays a multifaceted and pleiotropic role in CLE pathogenesis, involving induction of keratinocyte damage, apoptosis, and necrosis. These processes are mechanistically driven by the generation of reactive oxygen species, DNA modifications, and autoantigen expression, which ultimately activate immune pathways—particularly the type I interferon (IFN) system, via cyclic GMP-AMP synthase-stimulator of IFN genes (cGAS-STING) and IFNκ—leading to immune cell recruitment, autoreactivity, and disease flares (reviewed by Patel et al.) [71].

With specific regard to UV-induced DCs, UV exposure induces the accumulation of plasmacytoid DCs (pDCs) via TLR signaling [72,73]. These pDCs are major producers of type I IFNs, which are key mediators in lupus erythematous [72,73]. The number of pDCs in CLE lesions correlates with the degree of immune cell infiltration, highlighting their contribution to disease progression [74]. pDCs in CLE are commonly seen in close association with mature dermal CD208+ DCs or with cytotoxic CD8+ T cells along areas of damage in the dermal-epithelial junction [74]. Mechanistically, pDCs endocytose immune complexes, and the activation of TLR7 and TLR9 leads to type I IFN production [75-77]. In vitro experiments suggest that this process is mediated by the Fc receptor CD32 [78,79]. The humanized IgG1 monoclonal antibody BIIB059 targets blood DC antigen 2 (BDCA2) on the surface of pDCs, effectively downregulating IFN production [80]. In a phase 2 clinical trial, BIIB059 demonstrated significant improvements in clinical endpoints for CLE [81-83]. Other mechanisms, such as the activation of macrophages and cDCs by keratinocyte debris or cell death, have also been proposed as contributors to IFN production [84], further underscoring the complexity of CLE pathophysiology and the interplay between UV exposure and immune activation.

4.2. Polymorphic Light Eruption (PLE)

PLE is a common photodermatitis, characterized by pruritic skin lesions, most often papulovesicular in nature, that develop hours to days after sunlight exposure [85]. The

prevalence of PLE has been shown to correlate with geographic latitude, with higher rates observed in regions farther from the equator [86]. The condition typically manifests within the first three decades of life, and is more commonly reported in females [87,88]. While the lesions typically arise early in the sunny season, repeated UV exposure often leads to a photohardening effect, reducing the likelihood of recurrence as summer progresses. This phenomenon can also be induced through preventive phototherapy [89].

The pathophysiology of PLE remains incompletely understood, but it is believed that patients exhibit resistance to UV-induced immunosuppression, fostering a microenvironment that is conducive to aberrant immune responses to photoinduced stimuli. Specifically, LCs in patients with PLE demonstrate impaired UV-induced mobilization, a defect associated with diminished neutrophil infiltration and reduced expression of key cytokines, such as TNF- α , IL-4, and IL-10, following UV exposure [90–92]. This resistance to tolerogenic signaling likely disrupts immune homeostasis, contributing to the pathological skin responses that are characteristic of PLE.

4.3. Skin Cancer

The role of UV-induced DCs, particularly LCs, in skin cancer pathogenesis is both complex and critical [13]. LCs, under normal circumstances, serve as APCs. UV radiation alters this dynamic by inactivating or modifying LCs, impairing their ability to mount an effective immune response, as discussed above. As posited by Toews et al., if LCs primarily function to present antigens and prevent immunologic tolerance to antigens, their chronic inactivation by UV radiation permits neoantigens from malignantly transformed cells to be perceived as tolerogens [8]. This shift from immune surveillance to tolerance facilitates the unchecked growth of malignant cells, setting the stage for skin cancer development.

Experimental evidence supports this pivotal role of UV-induced changes in LCs in skin cancer pathogenesis. Studies by Kripke and colleagues have demonstrated that UV-irradiated mice fail to reject highly antigenic UV-induced tumors, which would otherwise be eliminated by normal syngeneic recipients [93,94]. This inability to reject tumors correlates with a UV-induced decrease in epidermal LCs, which in turn diminishes antigen-presenting activity in skin-draining lymph nodes. The reduction in DCs within the skin disrupts the immune response, and highlights the importance of LCs in initiating tumor-specific immunity [95].

Moreover, the interaction between LCs and UV-induced carcinogenesis is nuanced. Despite their protective role under normal conditions, LCs may paradoxically augment UV-induced cutaneous carcinogenesis. Studies indicate that epidermal tissues with intact LC networks develop UV-induced tumors more readily than epidermal tissues with scant LCs, independently of CPD formation following UV exposure [96]. This paradox may arise from LCs promoting immune tolerance or fostering an environment that is conducive to tumor growth. Mutant p53 islands, often associated with proliferating mutant keratinocytes, are frequently found in close proximity to LCs, further implicating these cells in tumor progression. Therefore, while LCs play a critical role in immune surveillance, their UV-induced alterations highlight their dual role in the pathogenesis of skin cancer.

5. Conclusions

To conclude, UV radiation profoundly impacts DC function, inducing a tolerogenic state that suppresses immune activation and promotes immune tolerance. This immuno-modulatory effect is mediated by complex cellular and molecular pathways, including alterations in LCs, cDCs, and CD11b⁺ myeloid cells. UV exposure impairs antigen presentation, induces apoptosis, and drives the generation of regulatory T cells, culminating

in the promotion of suppressive immune microenvironments and reactions at both a cutaneous and systemic level.

Insights from studying UV-induced tolerogenic DCs deepen our understanding of the mechanisms underlying immunosuppression, and highlight their clinical relevance in the pathogenesis of autoimmune skin disorders and skin cancers. Significant progress has been made in identifying these tolerogenic DCs and exploring their potential therapeutic implications.

6. Perspective

Our knowledge of the underlying mechanisms of UV-induced immunosuppression remains incomplete. Future research leveraging advanced molecular techniques and single-cell analyses will be crucial for refining our understanding of UV-induced immunosuppression. These approaches will enable the detailed characterization of specific tolerogenic DC subsets, and elucidate the precise pathways by which UV radiation influences DC function and by which UV-induced tolerogenic DCs induce Treg cells and immune tolerance. Furthermore, such advancements will enable innovative strategies in mitigating the adverse effects of UV radiation and harnessing tolerogenic DCs for immunomodulation in therapeutic contexts.

Author Contributions: Conceptualization, H.X., N.Y. and G.G.-R.; investigation, H.X., N.Y. and G.G.-R.; writing—original draft preparation, G.G.-R.; writing—review and editing, H.X., N.Y. and G.G.-R. All authors have read and agreed to the published version of the manuscript.

Funding: This research was supported by R01 AI157398-01 (H.X. and N.Y.) from the National Institute of Allergy and Infectious Diseases, United States.

Data Availability Statement: No new data were created or analyzed in this study.

Conflicts of Interest: The authors declare no conflicts of interest.

Abbreviations

The following abbreviations are used in this manuscript:

APC Antigen-presenting cell BDCA Blood DC antigen

Bid BH3-interacting death domain protein

cDC Conventional dendritic cell CPD Cyclobutene pyrimidine dimer

CHS Contact hypersensitivity

CLE Cutaneous lupus erythematous

DC Dendritic cell

DNFB 2,4-dinitrofluorobenzene

IFN InterferonIL InterleukinLC Langerhans cell

MHC Major histocompatibility complex

pDC Plasmacytoid dendritic cell

Th1 Thelper 1
Th2 Thelper 2
Th17 Thelper 17
Treg Regulatory T cell
UV Ultraviolet
UVB Ultraviolet B

References

- 1. Koulu, L.; Jansen, C.T.; Viander, M. Effect of UVA and UVB irradiation on human epidermal Langerhans cell membrane markers defined by ATPase activity and monoclonal antibodies (OKT 6 and anti-Ia). *Photodermatology* **1985**, *2*, 339–346. [PubMed]
- Obata, M.; Tagami, H. Alteration in Murine Epidermal Langerhans Cell Population by Various UV Irradiations: Quantitative and Morphologic Studies on the Effects of Various Wavelengths of Monochromatic Radiation on Ia-Bearing Cells. J. Investig. Dermatol. 1985, 84, 139–145. [CrossRef] [PubMed]
- 3. Langerhans, P. Über die Nerven der menschlichen Haut. Arch. Pathol. Anat. Physiol. Klin. Med. 1868, 44, 325–337. [CrossRef]
- 4. Stingl, G.; Katz, S.I.; Shevach, E.M.; Rosenthal, A.S.; Green, I. Analogous functions of macrophages and Langerhans cells in the initiation in the immune response. *J. Investig. Dermatol.* **1978**, 71, 59–64. [CrossRef]
- 5. Stingl, G.; Katz, S.I.; Clement, L.; Green, I.; Shevach, E.M. Immunologic functions of Ia-bearing epidermal Langerhans cells. *J. Immunol.* **1978**, 121, 2005–2013. [CrossRef]
- 6. Rowden, G.; Phillips, T.M.; Delovitch, T.L. Expression of ia antigens by murine keratinizing epithelial langerhans cells. *Immunogenetics* **1978**, *7*, 465–478. [CrossRef]
- 7. Stingl, G.; Katz, S.I.; Shevach, E.M.; Wolff-Schreiner, E.; Green, I. Detection of Ia antigens on Langerhans cells in guinea pig skin. *J. Immunol.* **1978**, 120, 570–578. [CrossRef]
- 8. Toews, G.B.; Bergstresser, P.R.; Streilein, J.W. Epidermal Langerhans cell density determines whether contact hypersensitivity or unresponsiveness follows skin painting with DNFB. *J. Immunol.* **1980**, *124*, 445–453. [CrossRef]
- 9. Cruz, P.D., Jr.; Tigelaar, R.E.; Bergstresser, P.R. Langerhans cells that migrate to skin after intravenous infusion regulate the induction of contact hypersensitivity. *J. Immunol.* **1990**, 144, 2486–2492. [CrossRef]
- Noonan, F.P.; Bucana, C.; Sauder, D.N.; De Fabo, E.C. Mechanism of systemic immune suppression by UV irradiation in vivo. II. The UV effects on number and morphology of epidermal Langerhans cells and the UV-induced suppression of contact hypersensitivity have different wavelength dependencies. J. Immunol. 1984, 132, 2408–2416. [CrossRef]
- 11. Orita, M. Effects of ultraviolet irradiation on surface marker expression by epidermal immunocompetent cells and contact sensitization to dinitrofluorobenzene in mice. *Br. J. Dermatol.* **1987**, 117, 721–733. [CrossRef] [PubMed]
- 12. Aberer, W.; Schuler, G.; Stingl, G.; Hönigsmann, H.; Wolff, K. Ultraviolet Light Depletes Surface Markers of Langerhans Cells. *J. Investig. Dermatol.* **1981**, *76*, 202–210. [CrossRef] [PubMed]
- 13. Zhou, L.; Jiang, A.; Veenstra, J.; Ozog, D.M.; Mi, Q.S. The Roles of Skin Langerhans Cells in Immune Tolerance and Cancer Immunity. *Vaccines* **2022**, *10*, 1380. [CrossRef]
- 14. Nakagawa, S.; Koomen, C.W.; Bos, J.D.; Teunissen, M.B.M. Differential Modulation of Human Epidermal Langerhans Cell Maturation by Ultraviolet B Radiation. *J. Immunol.* **1999**, *163*, 5192–5200. [CrossRef]
- 15. Ginhoux, F.; Collin, M.P.; Bogunovic, M.; Abel, M.; Leboeuf, M.; Helft, J.; Ochando, J.; Kissenpfennig, A.; Malissen, B.; Grisotto, M.; et al. Blood-derived dermal langerin+ dendritic cells survey the skin in the steady state. *J. Exp. Med.* **2007**, 204, 3133–3146. [CrossRef]
- 16. Bursch, L.S.; Wang, L.; Igyarto, B.; Kissenpfennig, A.; Malissen, B.; Kaplan, D.H.; Hogquist, K.A. Identification of a novel population of Langerin+ dendritic cells. *J. Exp. Med.* **2007**, 204, 3147–3156. [CrossRef]
- 17. Poulin, L.F.; Henri, S.; de Bovis, B.; Devilard, E.; Kissenpfennig, A.; Malissen, B. The dermis contains langerin+ dendritic cells that develop and function independently of epidermal Langerhans cells. *J. Exp. Med.* **2007**, *204*, 3119–3131. [CrossRef]
- 18. Wang, L.; Jameson, S.C.; Hogquist, K.A. Epidermal Langerhans Cells Are Not Required for UV-Induced Immunosuppression. *J. Immunol.* **2009**, *183*, 5548–5553. [CrossRef]
- 19. Schwarz, A.; Noordegraaf, M.; Maeda, A.; Torii, K.; Clausen, B.E.; Schwarz, T. Langerhans Cells Are Required for UVR-Induced Immunosuppression. *J. Investig. Dermatol.* **2010**, *130*, 1419–1427. [CrossRef]
- 20. Kashem, S.W.; Haniffa, M.; Kaplan, D.H. Antigen-Presenting Cells in the Skin. Annu. Rev. Immunol. 2017, 35, 469–499. [CrossRef]
- 21. Ng, R.L.X.; Bisley, J.L.; Gorman, S.; Norval, M.; Hart, P.H. Ultraviolet Irradiation of Mice Reduces the Competency of Bone Marrow-Derived CD11c+ Cells via an Indomethacin-Inhibitable Pathway. *J. Immunol.* **2010**, *185*, 7207–7215. [CrossRef] [PubMed]
- 22. Ng, R.L.X.; Scott, N.M.; Strickland, D.H.; Gorman, S.; Grimbaldeston, M.A.; Norval, M.; Waithman, J.; Hart, P.H. Altered Immunity and Dendritic Cell Activity in the Periphery of Mice after Long-Term Engraftment with Bone Marrow from Ultraviolet-Irradiated Mice. *J. Immunol.* 2013, 190, 5471–5484. [CrossRef] [PubMed]
- 23. Ng, R.L.; Scott, N.M.; Bisley, J.L.; Lambert, M.J.; Gorman, S.; Norval, M.; Hart, P.H. Characterization of regulatory dendritic cells differentiated from the bone marrow of UV-irradiated mice. *Immunology* **2013**, 140, 399–412. [CrossRef] [PubMed]
- 24. Scott, N.M.; Ng, R.L.; Gorman, S.; Norval, M.; Waithman, J.; Hart, P.H. Prostaglandin E2 imprints a long-lasting effect on dendritic cell progenitors in the bone marrow. *J. Leukoc. Biol.* **2014**, *95*, 225–232. [CrossRef] [PubMed]
- 25. Schmitt, D.A.; Owen-Schaub, L.; Ullrich, S.E. Effect of IL-12 on immune suppression and suppressor cell induction by ultraviolet radiation. *J. Immunol.* **1995**, *154*, 5114–5120. [CrossRef]

- 26. Schwarz, A.; Grabbe, S.; Aragane, Y.; Sandkuhl, K.; Riemann, H.; Luger, T.A.; Kubin, M.; Trinchieri, G.; Schwarz, T. Interleukin-12 prevents ultraviolet B-induced local immunosuppression and overcomes UVB-induced tolerance. *J. Investig. Dermatol.* 1996, 106, 1187–1191. [CrossRef]
- 27. Schwarz, A.; Grabbe, S.; Grosse-Heitmeyer, K.; Roters, B.; Riemann, H.; Luger, T.A.; Trinchieri, G.; Schwarz, T. Ultraviolet Light-Induced Immune Tolerance Is Mediated via the Fas/Fas-Ligand System. *J. Immunol.* 1998, 160, 4262–4270. [CrossRef]
- 28. Thatcher, T.H.; Luzina, I.; Fishelevich, R.; Tomai, M.A.; Miller, R.L.; Gaspari, A.A. Topical Imiquimod Treatment Prevents UV-Light Induced Loss of Contact Hypersensitivity and Immune Tolerance. *J. Investig. Dermatol.* **2006**, 126, 821–831. [CrossRef]
- 29. Crispin, M.K.; Fuentes-Duculan, J.; Gulati, N.; Johnson-Huang, L.M.; Lentini, T.; Sullivan-Whalen, M.; Gilleaudeau, P.; Cueto, I.; Suárez-Fariñas, M.; Lowes, M.A.; et al. Gene profiling of narrow-band UVB-induced skin injury defines cellular and molecular innate immune responses. *J. Investig. Dermatol.* 2013, 133, 692–701. [CrossRef]
- 30. Chu, C.-C.; Ali, N.; Karagiannis, P.; Di Meglio, P.; Skowera, A.; Napolitano, L.; Barinaga, G.; Grys, K.; Sharif-Paghaleh, E.; Karagiannis, S.N.; et al. Resident CD141 (BDCA3)+ dendritic cells in human skin produce IL-10 and induce regulatory T cells that suppress skin inflammation. *J. Exp. Med.* **2012**, 209, 935–945. [CrossRef]
- 31. Cooper, K.D.; Oberhelman, L.; Hamilton, T.A.; Baadsgaard, O.; Terhune, M.; LeVee, G.; Anderson, T.; Koren, H. UV exposure reduces immunization rates and promotes tolerance to epicutaneous antigens in humans: Relationship to dose, CD1a-DR+ epidermal macrophage induction, and Langerhans cell depletion. *Proc. Natl. Acad. Sci. USA* 1992, 89, 8497–8501. [CrossRef] [PubMed]
- 32. Kang, K.; Hammerberg, C.; Meunier, L.; Cooper, K.D. CD11b+ macrophages that infiltrate human epidermis after in vivo ultraviolet exposure potently produce IL-10 and represent the major secretory source of epidermal IL-10 protein. *J. Immunol.* **1994**, 153, 5256–5264. [CrossRef] [PubMed]
- 33. Yoshida, Y.; Kang, K.; Berger, M.; Chen, G.; Gilliam, A.C.; Moser, A.; Wu, L.; Hammerberg, C.; Cooper, K.D. Monocyte Induction of IL-10 and Down-Regulation of IL-12 by iC3b Deposited in Ultraviolet-Exposed Human Skin. *J. Immunol.* 1998, 161, 5873–5879. [CrossRef] [PubMed]
- 34. Hammerberg, C.; Duraiswamy, N.; Cooper, K.D. Reversal of immunosuppression inducible through ultraviolet-exposed skin by in vivo anti-CD11b treatment. *J. Immunol.* **1996**, *157*, 5254–5261. [CrossRef]
- 35. Hammerberg, C.; Katiyar, S.K.; Carroll, M.C.; Cooper, K.D. Activated Complement Component 3 (C3) Is Required for Ultraviolet Induction of Immunosuppression and Antigenic Tolerance. *J. Exp. Med.* 1998, 187, 1133–1138. [CrossRef]
- 36. Vink, A.A.; Strickland, F.M.; Bucana, C.; Cox, P.A.; Roza, L.; Yarosh, D.B.; Kripke, M.L. Localization of DNA damage and its role in altered antigen-presenting cell function in ultraviolet-irradiated mice. *J. Exp. Med.* **1996**, *183*, 1491–1500. [CrossRef]
- 37. Vink, A.A.; Moodycliffe, A.M.; Shreedhar, V.; Ullrich, S.E.; Roza, L.; Yarosh, D.B.; Kripke, M.L. The inhibition of antigen-presenting activity of dendritic cells resulting from UV irradiation of murine skin is restored by in vitro photorepair of cyclobutane pyrimidine dimers. *Proc. Natl. Acad. Sci. USA* 1997, 94, 5255–5260. [CrossRef]
- 38. Sun, L.; Ding, F.; Zhou, L.; Wang, J.; Li, M.; Zhou, P.; Li, J.; Ding, C.; Wang, H.; Xu, Y. Apoptosis of Dendritic Cells and Autoimmune Disease. *Front. Biosci.* **2024**, *29*, 157. [CrossRef]
- 39. Pradhan, S.; Kim, H.K.; Thrash, C.J.; Cox, M.A.; Mantena, S.K.; Wu, J.-H.; Athar, M.; Katiyar, S.K.; Elmets, C.A.; Timares, L. A Critical Role for the Proapoptotic Protein Bid in Ultraviolet-Induced Immune Suppression and Cutaneous Apoptosis. *J. Immunol.* 2008, 181, 3077–3088. [CrossRef]
- 40. Rosenblum, M.D.; Olasz, E.; Woodliff, J.E.; Johnson, B.D.; Konkol, M.C.; Gerber, K.A.; Orentas, R.J.; Sandford, G.; Truitt, R.L. CD200 is a novel p53-target gene involved in apoptosis-associated immune tolerance. *Blood* **2004**, *103*, 2691–2698. [CrossRef]
- 41. Wright, G.J.; Cherwinski, H.; Foster-Cuevas, M.; Brooke, G.; Puklavec, M.J.; Bigler, M.; Song, Y.; Jenmalm, M.; Gorman, D.; McClanahan, T.; et al. Characterization of the CD200 receptor family in mice and humans and their interactions with CD200. *J. Immunol.* 2003, 171, 3034–3046. [CrossRef] [PubMed]
- 42. Wright, G.J.; Puklavec, M.J.; Willis, A.C.; Hoek, R.M.; Sedgwick, J.D.; Brown, M.H.; Barclay, A.N. Lymphoid/neuronal cell surface OX2 glycoprotein recognizes a novel receptor on macrophages implicated in the control of their function. *Immunity* 2000, 13, 233–242. [CrossRef] [PubMed]
- 43. Maldonado, R.A.; von Andrian, U.H. How tolerogenic dendritic cells induce regulatory T cells. *Adv. Immunol.* **2010**, *108*, 111–165. [PubMed]
- 44. Wu, L.; Liu, Y.J. Development of dendritic-cell lineages. *Immunity* 2007, 26, 741–750. [CrossRef]
- 45. Elmets, C.A.; Bergstresser, P.R.; Tigelaar, R.E.; Wood, P.J.; Streilein, J.W. Analysis of the mechanism of unresponsiveness produced by haptens painted on skin exposed to low dose ultraviolet radiation. *J. Exp. Med.* **1983**, *158*, 781–794. [CrossRef]
- 46. Yagi, H.; Tokura, Y.; Wakita, H.; Furukawa, F.; Takigawa, M. TCRV beta 7+ Th2 cells mediate UVB-induced suppression of murine contact photosensitivity by releasing IL-10. *J. Immunol.* **1996**, *156*, 1824–1831. [CrossRef]
- 47. Schwarz, A.; Maeda, A.; Wild, M.K.; Kernebeck, K.; Gross, N.; Aragane, Y.; Beissert, S.; Vestweber, D.; Schwarz, T. Ultraviolet Radiation-Induced Regulatory T Cells Not Only Inhibit the Induction but Can Suppress the Effector Phase of Contact Hypersensitivity. *J. Immunol.* **2004**, *172*, 1036–1043. [CrossRef]

- 48. Freeman, G.J.; Borriello, F.; Hodes, R.J.; Reiser, H.; Hathcock, K.S.; Laszlo, G.; McKnight, A.J.; Kim, J.; Du, L.; Lombard, D.B.; et al. Uncovering of functional alternative CTLA-4 counter-receptor in B7-deficient mice. *Science* **1993**, 262, 907–909. [CrossRef]
- 49. Schwarz, A.; Beissert, S.; Grosse-Heitmeyer, K.; Gunzer, M.; Bluestone, J.A.; Grabbe, S.; Schwarz, T. Evidence for Functional Relevance of CTLA-4 in Ultraviolet-Radiation-Induced Tolerance. *J. Immunol.* **2000**, *165*, 1824–1831. [CrossRef]
- 50. Schwarz, T. Mechanisms of UV-induced immunosuppression. Keio J. Med. 2005, 54, 165–171. [CrossRef]
- 51. Schwarz, A.; Stander, S.; Berneburg, M.; Bohm, M.; Kulms, D.; van Steeg, H.; Grosse-Heitmeyer, K.; Krutmann, J.; Schwarz, T. Interleukin-12 suppresses ultraviolet radiation-induced apoptosis by inducing DNA repair. *Nat. Cell Biol.* **2002**, *4*, 26–31. [CrossRef] [PubMed]
- 52. Meeran, S.M.; Mantena, S.K.; Meleth, S.; Elmets, C.A.; Katiyar, S.K. Interleukin-12-deficient mice are at greater risk of UV radiation-induced skin tumors and malignant transformation of papillomas to carcinomas. *Mol. Cancer Ther.* **2006**, *5*, 825–832. [CrossRef] [PubMed]
- 53. Mosmann, T.R.; Coffman, R.L. TH1 and TH2 Cells: Different Patterns of Lymphokine Secretion Lead to Different Functional Properties. *Annu. Rev. Immunol.* **1989**, *7*, 145–173. [CrossRef] [PubMed]
- 54. Weaver, C.T.; Hatton, R.D.; Mangan, P.R.; Harrington, L.E. IL-17 Family Cytokines and the Expanding Diversity of Effector T Cell Lineages. *Annu. Rev. Immunol.* **2007**, 25, 821–852. [CrossRef]
- 55. Berger, A. Th1 and Th2 responses: What are they? BMJ 2000, 321, 424. [CrossRef]
- 56. Simon, J.C.; Mosmann, T.; Edelbaum, D.; Schopf, E.; Bergstresser, P.R.; Cruz, P.D., Jr. In vivo evidence that ultraviolet B-induced suppression of allergic contact sensitivity is associated with functional inactivation of Th1 cells. *Photodermatol. Photoimmunol. Photomed.* **1994**, *10*, 206–211.
- 57. Araneo, B.A.; Dowell, T.; Moon, H.B.; Daynes, R.A. Regulation of murine lymphokine production in vivo. Ultraviolet radiation exposure depresses IL-2 and enhances IL-4 production by T cells through an IL-1-dependent mechanism. *J. Immunol.* **1989**, 143, 1737–1744. [CrossRef]
- 58. Simon, J.C.; Cruz, P.D., Jr.; Bergstresser, P.R.; Tigelaar, R.E. Low dose ultraviolet B-irradiated Langerhans cells preferentially activate CD4+ cells of the T helper 2 subset. *J. Immunol.* **1990**, 145, 2087–2091. [CrossRef]
- 59. Brown, E.L.; Rivas, J.M.; Ullrich, S.E.; Young, C.R.; Norris, S.J.; Kripke, M.L. Modulation of immunity to Borrelia burgdorferi by ultraviolet irradiation: Differential effect on Th1 and Th2 immune responses. *Eur. J. Immunol.* **1995**, 25, 3017–3022. [CrossRef]
- Simon, J.C.; Tigelaar, R.E.; Bergstresser, P.R.; Edelbaum, D.; Cruz, P.D., Jr. Ultraviolet B radiation converts Langerhans cells from immunogenic to tolerogenic antigen-presenting cells. Induction of specific clonal anergy in CD4+ T helper 1 cells. *J. Immunol.* 1991, 146, 485–491. [CrossRef]
- 61. Veldhoen, M. Interleukin 17 is a chief orchestrator of immunity. Nat. Immunol. 2017, 18, 612–621. [CrossRef] [PubMed]
- 62. Kolls, J.K.; Linden, A. Interleukin-17 family members and inflammation. *Immunity* **2004**, 21, 467–476. [CrossRef] [PubMed]
- 63. Peiser, M. Role of Th17 Cells in Skin Inflammation of Allergic Contact Dermatitis. J. Immunol. Res. 2013, 2013, 261037. [CrossRef]
- 64. He, D.; Wu, L.; Kim, H.K.; Li, H.; Elmets, C.A.; Xu, H. CD8+ IL-17-Producing T Cells Are Important in Effector Functions for the Elicitation of Contact Hypersensitivity Responses. *J. Immunol.* **2006**, 177, 6852–6858. [CrossRef]
- 65. He, D.; Wu, L.; Kim, H.K.; Li, H.; Elmets, C.A.; Xu, H. IL-17 and IFN-{gamma} Mediate the Elicitation of Contact Hypersensitivity Responses by Different Mechanisms and Both Are Required for Optimal Responses. *J. Immunol.* 2009, 183, 1463–1470. [CrossRef]
- 66. MacLeod, A.S.; Rudolph, R.; Corriden, R.; Ye, I.; Garijo, O.; Havran, W.L. Skin-Resident T Cells Sense Ultraviolet Radiation–Induced Injury and Contribute to DNA Repair. *J. Immunol.* **2014**, *192*, 5695–5702. [CrossRef]
- 67. Li, H.; Prasad, R.; Katiyar, S.K.; Yusuf, N.; Elmets, C.A.; Xu, H. Interleukin-17 Mediated Inflammatory Responses Are Required for Ultraviolet Radiation-Induced Immune Suppression. *Photochem. Photobiol.* **2015**, *91*, 235–241. [CrossRef]
- 68. Crowson, A.N.; Magro, C. The cutaneous pathology of lupus erythematosus: A review. J. Cutan. Pathol. 2001, 28, 1–23. [CrossRef]
- 69. Oh, E.H.; Kim, E.J.; Ro, Y.S.; Ko, J.Y. Ten-year retrospective clinicohistological study of cutaneous lupus erythematosus in Korea. *J. Dermatol.* **2018**, 45, 436–443. [CrossRef]
- 70. Jarukitsopa, S.; Hoganson, D.D.; Crowson, C.S.; Sokumbi, O.; Davis, M.D.; Michet, C.J., Jr.; Matteson, E.L.; Maradit Kremers, H.; Chowdhary, V.R. Epidemiology of systemic lupus erythematosus and cutaneous lupus erythematosus in a predominantly white population in the United States. *Arthritis Care Res.* 2015, 67, 817–828. [CrossRef]
- 71. Patel, J.; Borucki, R.; Werth, V.P. An Update on the Pathogenesis of Cutaneous Lupus Erythematosus and Its Role in Clinical Practice. *Curr. Rheumatol. Rep.* **2020**, 22, 69. [CrossRef] [PubMed]
- 72. Yin, Q.; Xu, X.; Lin, Y.; Lv, J.; Zhao, L.; He, R. Ultraviolet B irradiation induces skin accumulation of plasmacytoid dendritic cells: A possible role for chemerin. *Autoimmunity* **2014**, *47*, 185–192. [CrossRef] [PubMed]
- 73. Fitzgerald-Bocarsly, P.; Dai, J.; Singh, S. Plasmacytoid dendritic cells and type I IFN: 50 years of convergent history. *Cytokine Growth Factor Rev.* **2008**, *19*, 3–19. [CrossRef]
- 74. Vermi, W.; Lonardi, S.; Morassi, M.; Rossini, C.; Tardanico, R.; Venturini, M.; Sala, R.; Tincani, A.; Poliani, P.L.; Calzavara-Pinton, P.G.; et al. Cutaneous distribution of plasmacytoid dendritic cells in lupus erythematosus. Selective tropism at the site of epithelial apoptotic damage. *Immunobiology* 2009, 214, 877–886. [CrossRef]

- 75. Means, T.K.; Latz, E.; Hayashi, F.; Murali, M.R.; Golenbock, D.T.; Luster, A.D. Human lupus autoantibody-DNA complexes activate DCs through cooperation of CD32 and TLR9. *J. Clin. Investig.* **2005**, *115*, 407–417. [CrossRef]
- 76. Eloranta, M.L.; Lovgren, T.; Finke, D.; Mathsson, L.; Ronnelid, J.; Kastner, B.; Alm, G.V.; Ronnblom, L. Regulation of the interferon-alpha production induced by RNA-containing immune complexes in plasmacytoid dendritic cells. *Arthritis Rheum*. **2009**, *60*, 2418–2427. [CrossRef]
- 77. Saadeh, D.; Kurban, M.; Abbas, O. Update on the role of plasmacytoid dendritic cells in inflammatory/autoimmune skin diseases. *Exp. Dermatol.* **2016**, 25, 415–421. [CrossRef]
- 78. Bave, U.; Alm, G.V.; Ronnblom, L. The combination of apoptotic U937 cells and lupus IgG is a potent IFN-alpha inducer. *J. Immunol.* **2000**, *165*, 3519–3526. [CrossRef]
- 79. Lovgren, T.; Eloranta, M.L.; Bave, U.; Alm, G.V.; Ronnblom, L. Induction of interferon-alpha production in plasmacytoid dendritic cells by immune complexes containing nucleic acid released by necrotic or late apoptotic cells and lupus IgG. *Arthritis Rheum.* **2004**, *50*, 1861–1872. [CrossRef]
- 80. Chaichian, Y.; Wallace, D.J.; Weisman, M.H. A promising approach to targeting type 1 IFN in systemic lupus erythematosus. *J. Clin. Investig.* **2019**, 129, 958–961. [CrossRef]
- 81. Furie, R.; Werth, V.P.; Merola, J.F.; Stevenson, L.; Reynolds, T.L.; Naik, H.; Wang, W.; Christmann, R.; Gardet, A.; Pellerin, A.; et al. Monoclonal antibody targeting BDCA2 ameliorates skin lesions in systemic lupus erythematosus. *J. Clin. Investig.* **2019**, 129, 1359–1371. [CrossRef] [PubMed]
- 82. Werth, V.P.; Barbey, C.; Franchimont, N. Anti-BDCA2 Antibody for Cutaneous Lupus Erythematosus. N. Engl. J. Med. 2022, 387, 1528–1529. [CrossRef] [PubMed]
- 83. Werth, V.P.; Furie, R.A.; Romero-Diaz, J.; Navarra, S.; Kalunian, K.; van Vollenhoven, R.F.; Nyberg, F.; Kaffenberger, B.H.; Sheikh, S.Z.; Radunovic, G.; et al. Trial of Anti-BDCA2 Antibody Litifilimab for Cutaneous Lupus Erythematosus. N. Engl. J. Med. 2022, 387, 321–331. [CrossRef] [PubMed]
- 84. Biermann, M.H.; Veissi, S.; Maueroder, C.; Chaurio, R.; Berens, C.; Herrmann, M.; Munoz, L.E. The role of dead cell clearance in the etiology and pathogenesis of systemic lupus erythematosus: Dendritic cells as potential targets. *Expert Rev. Clin. Immunol.* **2014**, *10*, 1151–1164. [CrossRef] [PubMed]
- 85. Gruber-Wackernagel, A.; Byrne, S.N.; Wolf, P. Polymorphous Light Eruption: Clinic Aspects and Pathogenesis. *Dermatol. Clin.* **2014**, 32, 315–334. [CrossRef]
- 86. Burfield, L.; Rutter, K.J.; Thompson, B.; Marjanovic, E.J.; Neale, R.E.; Rhodes, L.E. Systematic review of the prevalence and incidence of the photodermatoses with meta-analysis of the prevalence of polymorphic light eruption. *J. Eur. Acad. Dermatol. Venereol.* **2023**, *37*, 511–520. [CrossRef]
- 87. Morison, W.L.; Stern, R.S. Polymorphous light eruption: A common reaction uncommonly recognized. *Acta Derm. Venereol.* **1982**, 62, 237–240. [CrossRef]
- 88. Honigsmann, H. Polymorphous light eruption. Photodermatol. Photoimmunol. Photomed. 2008, 24, 155-161. [CrossRef]
- 89. Lembo, S.; Raimondo, A. Polymorphic Light Eruption: What's New in Pathogenesis and Management. *Front. Med.* **2018**, *5*, 252. [CrossRef]
- 90. Kolgen, W.; van Weelden, H.; Den Hengst, S.; Guikers, K.L.H.; Kiekens, R.C.M.; Knol, E.F.; Bruijnzeel-Koomen, C.A.F.M.; van Vloten, W.A.; de Gruijl, F.R. CD11b+ Cells and Ultraviolet-B-Resistant CD1a+ Cells in Skin of Patients with Polymorphous Light Eruption. *J. Investig. Dermatol.* 1999, 113, 4–10. [CrossRef]
- 91. Kölgen, W.; van Meurs, M.; Jongsma, M.; van Weelden, H.; Bruijnzeel-Koomen, C.A.F.M.; Knol, E.F.; van Vloten, W.A.; Laman, J.; de Grui, F.R. Differential expression of cytokines in uv-b-exposed skin of patients with polymorphous light eruption: Correlation with langerhans cell migration and immunosuppression. *Arch. Dermatol.* **2004**, *140*, 295–302. [CrossRef] [PubMed]
- 92. Schornagel, I.J.; Sigurdsson, V.; Nijhuis, E.H.J.; Bruijnzeel-Koomen, C.A.F.M.; Knol, E.F. Decreased Neutrophil Skin Infiltration After UVB Exposure in Patients with Polymorphous Light Eruption. *J. Investig. Dermatol.* **2004**, 123, 202–206. [CrossRef] [PubMed]
- 93. Kripke, M.L. Antigenicity of murine skin tumors induced by ultraviolet light. *J. Natl. Cancer Inst.* **1974**, *53*, 1333–1336. [CrossRef] [PubMed]
- 94. Kripke, M.L.; Fisher, M.S. Immunologic parameters of ultraviolet carcinogenesis. J. Natl. Cancer Inst. 1976, 57, 211–215. [CrossRef]
- 95. Alcalay, J.; Kripke, M.L. Antigen-presenting activity of draining lymph node cells from mice painted with a contact allergen during ultraviolet carcinogenesis. *J. Immunol.* **1991**, *146*, 1717–1721. [CrossRef]
- 96. Lewis, J.M.; Bürgler, C.D.; Freudzon, M.; Golubets, K.; Gibson, J.F.; Filler, R.B.; Girardi, M. Langerhans Cells Facilitate UVB-induced Epidermal Carcinogenesis. *J. Investig. Dermatol.* **2015**, *135*, 2824–2833. [CrossRef]

Disclaimer/Publisher's Note: The statements, opinions and data contained in all publications are solely those of the individual author(s) and contributor(s) and not of MDPI and/or the editor(s). MDPI and/or the editor(s) disclaim responsibility for any injury to people or property resulting from any ideas, methods, instructions or products referred to in the content.

MDPI AG
Grosspeteranlage 5
4052 Basel
Switzerland

Tel.: +41 61 683 77 34

Cells Editorial Office
E-mail: cells@mdpi.com
www.mdpi.com/journal/cells



Disclaimer/Publisher's Note: The title and front matter of this reprint are at the discretion of the Guest Editors. The publisher is not responsible for their content or any associated concerns. The statements, opinions and data contained in all individual articles are solely those of the individual Editors and contributors and not of MDPI. MDPI disclaims responsibility for any injury to people or property resulting from any ideas, methods, instructions or products referred to in the content.



